SEISMIC RESPONSE OF STRUCTURES WITH COULOMB DAMPING

by

Sanjeev R. Malushte

Dissertation submitted to the Faculty of the

Virginia Polytechnic Institute and State University

in partial fulfillment of the requirements for the degree of

Doctor of Philosophy

in

Engineering Mechanics

APPROVED:

M. P. Singh, Chairman

R. A. Heller

S. M. Holzer

L. Meirovitch

D. T. Mook

February 1989

Blacksburg, Virginia

SEISMIC RESPONSE OF STRUCTURES WITH COULOMB DAMPING

by

Sanjeev R. Malushte

M. P. Singh, Chairman

Engineering Mechanics

(ABSTRACT)

The usefulness of Coulomb (friction) damping in earthquake-resistant design of structures is examined by studying the seismic response characteristics of structures with various arrangements of sliding interfaces. First, three basic arrangements are studied for their effectiveness in reducing lateral displacements of the supporting frame, accelerations of the floor slab and the resulting secondary floor spectra. These are: (1) slab sliding system which has the sliding interface between the floor slab and the supporting frame, (2) double sliding system which consists of sliding interfaces at both top and bottom interfaces (a combination of slab sliding and base sliding), and (3) spring-assisted slab sliding system which is a slab sliding system aided by lateral springs attached to the columns to resist excessive sliding displacement of the slab. The responses are obtained for structures with different frequencies and are presented in response spectrum form. The isolation characteristics of one slab sliding system are compared with those of the base sliding and hysteretic systems. Non-dimensional design parameters defined in terms of the corresponding elastic design spectra are introduced for design purposes and for a consistent presentation of the results. Methods for predicting the important response quantities using the non-dimensional parameters are discussed and their applicability is evaluated.

Next, the response of a simple slab sliding arrangement to simultaneous horizontal and vertical ground motion input is studied to see the effects of the vertical excitation on the isolation effciency of that arrangement. Finally the suitability of adopting such sliding arrangements in multi-story structures is also examined. The seismic responses of multi-story structures with floor slabs sliding at different story levels are obtained and compared with the response of non-sliding structure and base sliding to examine the effectiveness of such sliding arrangement.

Acknowledgements

First, I would like to extend my most sincere gratitude to my Advisor, Prof. M. P. Singh for his leadership, support and patience throughout my graduate studies. I also wish to acknowledge Prof. D. T. Mook and Prof. R. A. Heller, whose guidance and encouragement helped me build a stronger and wider base in different areas of Engineering Mechanics. Prof. Singh, Prof. Mook and Prof. Heller have taught me a great deal and provided me with many opportunities; I am deeply indebted to them for all this.

Thanks are also due to Prof. L. Meirovitch and Prof. S. M. Holzer for agreeing to be on my committee and for the very useful knowledge I learned from their courses.

This research project was sponsored by the National Science Foundation under Grant No. CES-8619306 with Dr. S. C. Liu as the Program Director. This financial support is gratefully acknowledged.

I would like to take this opportunity to thank my wonderful colleagues and friends, especially, , , , and , whose support and friendship has been invaluable to me.

The love, encouragement and strong support of my loving parents and the rest of my family has been the biggest motivating factor for my commitment to the doctorate program. I would like to express my deepest gratitude to God, The Almighty, for giving me such parents, family and friends. The list of acknowledgements will not be complete without the mention of my late friend , whose great friendship made me a stronger person. It is with love and gratefulness that I dedicate this work to my parents and to .

Table of Contents

Chapter I

Introduction

1.1 Background Information

Structures can be designed to behave elastically or inelastically during the occurrence of a design level earthquake. It is a common knowledge that the elastic designs tend to be stiff and cost prohibitive in most cases. Because of this, the designer is prompted to consider inelastic design as an alternative. Experience shows that most structures indeed respond inelastically when subjected to strong eartquake motions. Nonlinear response of structures can result from either inelastic material behavior or large deformations (or both). Alternatively, a structure can be designed to respond nonlinearly by incorporating arrangements that alter system characteristics whenever the excitation becomes severe. The primary purpose of such arrangements is to dissipate the input energy in a manner that the main

structure is protected from the fullest damaging potential of the earthquake. They are referred to as isolation arrangements for this reason.

Dissipation of vibration energy is usually caused by the inherent material or stuctural damping present in the structures. For the purpose of analysis, this damping process is modelled as viscous damping. Viscous damping is the only source of energy dissipation considered in linearly behaving structures. Viscous dissipation of energy is proportional to the square of the relative velocity of the structure and thus a significant dissipation is possible in low and medium frequency structures which have higher values of relative velocity as is evident from the corresponding seismic response spectra. This frequency range is most common for tall structures. Viscous dissipation of energy is, however, rarely adequate. It is, thus, desirable to increase the dissipation of vibration energy by other means. In earthquake structural engineering, the use of vibration isolation and response reduction devices has been increasingly advocated to protect the main structure and its internal components in the event of a major seismic occurence. Williams (32) in his 1973 paper has discussed different types of devices that can be adopted in the earthquake resistant design of structures. Such devices make use of one or more of the following : 1) active control, 2) hysteretic damping, 3) supplementary viscoelastic damping, and 4) Coulomb damping. Of these, the control-based mechanisms are more sophisticated and are being researched actively (18, 33). The remaining three techniques fall under a broad category of passive control. As mentioned earlier, hysteretic behavior of materials can be put to use in dissipating energy by designing members which yield in the case of severe shaking. It can also be used by incorporating a yielding "soft story" (3, 8, 31) in the structure. However, a major disadvantage of utilizing hysteresis in structures is that the residual displacements in such structures are permanent and they can permanently affect the after-event utility of the structure.

Supplemental hysteretic damping can be provided for a base isolation purpose as demonstrated by Skinner, et al (28, 29). The use of viscoelastic dampers acting in parallel with the bracings has also been proposed to provide additional damping and protect the main structural components (2). The advantage of such mechanisms is that they can be retro-fitted to the main structure at any later time, and thus they are being further investigated.

Another category of isolation designs utilizes friction, allowing some parts of the structure to slide relative to others. Friction is routinely used in regulating motion through the process of "braking". Forced vibrations of an oscillator with viscous and Coulomb damping was first studied by Den Hartog (7) in 1931 followed by Levitan (12) in 1960. Since then numerous researchers have studied the effect of Coulomb or friction damping on structures. In the initial stages, researchers studied the response of sliding structures to harmonic excitation. More recent research in earthquake structural engineering has shown that sliding friction can be effectively used to damp out or isolate earthquake induced vibrations, too. Many researchers have studied the behavior of a rigid mass resting on a sliding interface with another mass subjected to harmonic base excitation (9, 34). Response of such sliding structures to stochastic inputs have been reported too (1, 4, 22). Williams (32), Mostaghel, et al (19, 20), Westermo and Udwadia (30) have studied the use of sliding base for dissipation and isolation of input energy. Quamaruddin, et al (26) have reported beneficial results by experimental investigation of such structures. Pall and Marsh (23) have proposed sliding brace mechanisms to damp out excessive vibrations in the super-structure. This makes it possible to distribute the isolation process to many different levels in the structure as opposed to the base isolation. Among the friction devices, the base sliding arrangement seems to have attracted the most research attention.

1.2 Proposed Work

In a multi-degree-of-freedom structure, the base sliding arrangement concentrates the dissipation of energy at the base. Also, once the structure slides, it may be difficult to bring the entire structure back to its original position if desired. These problems can, probably, be alleviated by distributing the sliding interfaces at different levels of a structure. Such arrangement is similar to the sliding brace mechanism in that it will distribute the isolation effort to many levels. To achieve this goal, the authors propose an arrangement in which the slabs at different levels are allowed to slide on friction pads (mounted on the girders of the main frame) so that the slabs can move relative to the main structural frame. This can be achieved by providing openings around the columns to permit, as well as limit, the relative movement of the slabs. This makes the slabs non-monolithic with the frame in this proposed structure; which may, however, have some disadvantages in the design for other loads.

To examine the effectiveness of such an arrangement first a simple one story structure with sliding interface between the frame and supporting slab is examined for horizontal excitation. The analytical formulation and the results of this study are presented in Chapter 2. For comparison, the base sliding system as well as hysteretic systems are also examined.

Since a sliding system with Coulomb damping has no restoring device to bring the' mass back to its original position, it may have large residual relative displacements when the motion ceases. To alleviate this situation a simple spring assisted sliding system has been examined to see under what situation a spring will be effective in reducing the residual displacement. The formulation and results of this study are presented in Chapter 3.

The friction force at an interface depends upon the normal reactions. In the cases of structures subjected to earthquake motions, the normal reaction is likely to be affected by the presence of the vertical ground acceleration. Thus, in Chapter 4, the response of a simple sliding structure simultaneously subjected to horizontal and vertical excitation have been compiled and compared with the results obtained only for the horizontal excitation to study the vertical acceleration effect.

Response of a multi-story structures with sliding interfaces under the floor slabs as well as at the base is examined in Chapter 5. Numerical results are presented for sliding at a single interface as well as for sliding at all floor levels. The response of the slab sliding structure is compared with the response of the corresponding non-sliding and base sliding structures to examine the effectiveness of the slab sliding arrangement. Finally, the concluding remarks on the study are presented in Chapter 6.

Chapter II

Response of a Simple Sliding System

2.1 Introduction

To gain insight into the behavior of sliding systems mentioned in Chapter 1, here we propose to examine the response of a simple single story structure, such as the one shown in Fig. 2.1, when it is subjected to horizontal ground motion. To limit the scope of the study presented in this chapter, the effect of vertical ground motion, though could be important in sliding systems, has not been considered here. This will be considered in Chapter 4.

As mentioned in Chapter 1, the isolation effectiveness of structures provided with sliding interface at their bases has been examined by several investigators in the past. In this chapter, therefore, we also evaluate the performance of our proposed slab sliding scheme vis-a-vis the base sliding scheme by comparing their response for a given ground motion. Since hysteretic behavior is also used to reduce or limit

the response of structures subjected to earthquake loads, a comparison of the hysteretic system with the proposed system has also been presented in this chapter. The numerical results are obtained for different sets of problem parameters and sliding situations.

2.2 *Analytical Formulation*

Here we present the analytical formulation of structure shown in Fig. 2.1 for the cases of (1) only the top mass (slab) sliding against the supporting frame, (2) only the bottom mass or the base slab sliding against the foundation, and (3) both masses sliding against their respective supports. Case 2 has been a subject of several studies (19, 20, 26, 30, 32). The presentation of the analytical formulation for this case here is only to relate this case to the other cases. The third case, where both the top and bottom masses are allowed to slide, is the most general case. In the development of the formulation it is assumed that the frame is massless and the masses are concentrated at the top and bottom. Also, the static and kinetic coefficients fo friction are assumed to be equal. The frame is assumed to behave linearly in this analysis.

2.2.1 Case 1: Slab Sliding Structure

Here two situations are possible : (1) the stick phase where there is no sliding at the interface, and (2) sliding phase when the Coulomb friction comes into play. In the stick phase, the equation of motion can be simply written as

$$\ddot{x}_f + 2\beta_o\omega_o\dot{x}_f + \omega_o^2\ddot{x}_f = -\ddot{x}_g \tag{2.1}$$

where x_f is the relative displacement of the top of the frame with respect to its base, and ω_o and β_o are the nominal frequency and the damping ratio for the system. These are defined as : $\omega_o^2 = k/m_1$ and $\beta_o = c/2\omega_o m_1$, where, m_1 is the top mass, k is the lateral stiffness of the frame, and c is the viscous damping coefficient for system. The above equation is valid as long as the force, F_1, at the interface does not exceed the limiting friction force. That is

$$|F_1| = |m_1(\ddot{x}_g + \ddot{x}_f)| < \mu_1 m_1 g \tag{2.2}$$

where μ_1 is the friction coefficient at the interface of the slab and frame. Equation (2.1) is solved by any standard technique (for example, Nigam and Jennings (21), and the response is tested for condition described by Eq. (2.2).

Sliding occurs at the top interface whenever the response of non-sliding or stick phase violates the above-mentioned condition. During the sliding phase, the interface force remains constant as :

$$F_1 = -\mu_1 m_1 g \,\mathbf{sign}\,(\dot{x}_{s_1}) = -\mu_1 m_1 g\,\varepsilon_1 \tag{2.3}$$

where x_{s_1} is the sliding displacement of the slab relative to the frame and $\mathbf{sign}(\dot{x}_{s_1})$ is the sign of sliding velocity, $\dot{x}_{s_1}$. This sign is denoted as ε_1 and it can be ascertained by knowing the force response at the time sliding is about to begin as

$$\varepsilon_1 = -[\mathbf{sign}(F_1)]_s = -\frac{F_{1_s}}{|F_{1_s}|} \tag{2.4}$$

where the subscript 's' indicates that the force, F_1, in the above equation corresponds to the instant when the slab sliding becomes imminent. The parameter ε_1 was probably first introduced by Mostaghel (20) in his study of the base sliding system. As is evident from Eq. (2.4), the parameter, ε_1 can only take the values of + 1 or − 1.

In terms of the interface force, the equation of equilibrium for the supporting frame can be written as :

$$c\dot{x}_f + kx_f = -F_1 = \mu_1 m_1 g \varepsilon_1 \tag{2.5}$$

Here it is assumed that the frame is massless and the entire mass is concentrated at the slab level. The solution of Eq. (2.5) can be simply written as :

$$x_f(\tau) = x_{f_i} e^{-\frac{\omega_o}{2\beta_o}\tau} + \frac{\mu_1 g}{\omega_o^2}\left(1 - e^{-\frac{\omega_o}{\beta_o}\tau}\right)\varepsilon_1 \tag{2.6}$$

where x_{f_i} is the known frame displacement at any time t_i during the sliding phase and τ is the time measured from t_i.

The equation of motion for the top mass in the sliding phase is :

$$m_1(\ddot{x}_{s_1} + \ddot{x}_f + \ddot{x}_g) = F_1 = -\mu_1 m_1 g \varepsilon_1 \tag{2.7}$$

Substituting for $\ddot{x}_f$ from Eq. (2.6), we obtain

$$\ddot{x}_{s_1} = -\ddot{x}_g - \mu_1 g\,\varepsilon_1 + \frac{\omega_o}{2\beta_o}\dot{x}_{f_i}\, e^{-\frac{\omega_o}{2\beta_o}\tau} \tag{2.8}$$

For ground acceleration $\ddot{x}_g(\tau)$ varying linearly between t_i and t_{i+1}, Eq. (2.8) can be directly integrated twice to give the following solution :

$$x_{s_1}(\tau) = x_{s_{1_i}} + \dot{x}_{s_{1_i}}\tau - \left[w_i \frac{\tau^2}{2} + \frac{w_{i+1} - w_i}{h_i} \frac{\tau^3}{6} \right] \tag{2.9}$$

$$+ \dot{x}_{f_i}\left[\tau - \frac{2\beta_o}{\omega_o}\left(1 - e^{-\frac{\omega_o}{2\beta_o}\tau}\right)\right]; \qquad 0 \le \tau \le h_i$$

where $x_{s_{1_i}}$ and $\dot{x}_{s_{1_i}}$ are the sliding displacement and velocity at the beginning of the i^{th} time-step. Also, $h_i = t_{i+1} - t_i$ = size of the i^{th} time-step and w_i and w_{i+1} are defined in terms of ground acceleration values A_i and A_{i+1} at times t_i and t_{i+1} as :

$$w_i = A_i + \mu_1 g\,\varepsilon_1 \quad \text{and} \quad w_{i+1} = A_{i+1} + \mu_1 g\,\varepsilon_1 \tag{2.10}$$

Eqs. (2.6) and (2.9) provide the complete solution for the sliding phase of the motion. Sliding phase returns to the stick phase whenever $\dot{x}_{s_1}$ becomes zero.

2.2.2 Case 2: Base Sliding Structure

In this case, we assume that there is a sliding interface at the base. When there is no sliding at this interface, the equation of motion remains the same as Eq. (2.1). This equation remains valid as long as the force, F_2, at the sliding interface does not exceed the limiting friction force. This interface force is given by the following equation :

$$F_2 = m_1(\ddot{x}_g + \ddot{x}_f) + m_2\ddot{x}_g = M\ddot{x}_g + m_1\ddot{x}_f \tag{2.11}$$

where M is the total mass of the system, and m_2 is the mass of the bottom slab (base), so that $M = m_1 + m_2$. Sliding does not occur as long as the following condition is satisfied :

$$|F_2| = |M\ddot{x}_g + m_1\ddot{x}_f| < \mu_2 Mg \tag{2.12}$$

Once sliding occurs, the interface force remains constant and opposite to the direction of the sliding velocity as follows :

$$F_2 = -\mu_2 Mg\ \mathbf{sign}(\dot{x}_{s_2}) = -\mu_2 Mg\ \varepsilon_2 \tag{2.13}$$

where ε_2 assigns the proper sign to the force. In this case, it is defined as follows :

$$\varepsilon_2 = -[\mathbf{sign}(F_2)]_s = -\frac{F_{2_s}}{|F_{2_s}|} \tag{2.14}$$

where the subscript 's' indicates that the force, F_2, in the above equation corresponds to the instant when the base sliding becomes imminent. The equation of motion for the combined system of the top and bottom mass can now be written as :

$$m_1(\ddot{x}_{s_2} + \ddot{x}_f + \ddot{x}_g) + m_2(\ddot{x}_{s_2} + \ddot{x}_g) = -\mu_2 Mg\ \varepsilon_2 \tag{2.15}$$

which with some slight simplification can also be written as :

$$\ddot{x}_{s_2} = -\ddot{x}_g - \alpha\ddot{x}_f - \mu_2 g\ \varepsilon_2 \tag{2.16}$$

where α is the ratio of the top mass m_1 to the total mass M. The equation of motion for the top mass can be written as :

$$m_1(\ddot{x}_{s_2} + \ddot{x}_f + \ddot{x}_g) + c\dot{x}_f + kx_f = 0 \tag{2.17}$$

Substituting $\ddot{x}_{s_2}$ from Eq. (2.16) into Eq. (2.17), we obtain

$$m_1(1-\alpha)\ddot{x}_f + c\dot{x}_f + kx_f = \mu_2 m_1 g\, \varepsilon_2 \tag{2.18}$$

It is interesting to note that the equations for the slab sliding case can be obtained from the equations for this case by taking $\alpha = 1$ (or $m_2 = 0$) and replacing μ_2 by μ_1 . Also, the case of a sliding rigid block is obtained by taking $\alpha = 0$ (or $m_1 = 0$), in which case, of course, the consideration of c and k in the equations is irrelevant.

It is noted that Eq. (2.18) is similar to Eq. (2.1), except that the frequency and damping ratio are changed. Thus, its solution can be obtained by any standard approach. This solution is given as :

$$x_f(\tau) = \frac{\mu_2 g\, \varepsilon_2}{\omega_o^2} + e^{-\beta_m \omega_m \tau}\left[\dot{x}_{f_i}\frac{\sin \omega_{md}\tau}{\omega_{md}} + \left(x_{f_i} - \frac{\mu_2 g\, \varepsilon_2}{\omega_o^2}\right)\left(\frac{\beta_m}{\sqrt{1-\beta_m^2}}\sin \omega_{md}\tau + \cos \omega_{md}\tau\right)\right] \tag{2.19}$$

where β_m, ω_m, and ω_{dm} are the modified damping ratio, frequency and damped frequency defined as :

$$\beta_m = \frac{\beta_o}{\sqrt{(1-\alpha)}}\ , \quad \omega_m = \omega_o\sqrt{(1-\alpha)}\ , \quad \omega_{md} = \omega_m\sqrt{1-\beta_m^2} \tag{2.20}$$

Of course, Eqs. (2.19) and (2.20) are not meant to be used for the slab sliding case, that is, when $\alpha = 1$.

Knowing $x_f(\tau)$, Eq. (2.16) can be directly integrated to obtain the sliding displacement, x_{s_2}, and velocity, $\dot{x}_{s_2}$, in terms of x_f and $\dot{x}_f$. The expression for x_{s_2} is

$$x_{s_2}(\tau) = x_{s_{2_i}} - v_i \frac{\tau^2}{2} - \frac{v_{i+1} - v_i}{h_i} \frac{\tau^3}{6} - \alpha [x_f(\tau) - x_{f_i}] + (\dot{x}_{s_{2_i}} + \alpha \dot{x}_{f_i}) \tau \qquad (2.21)$$

where $x_{s_{2_i}}$ and $\dot{x}_{s_{2_i}}$ are the sliding displacement and velocity at the beginning of the i^{th} time-step, and v_i and v_{i+1} are defined in terms of ground acceleration values A_i and A_{i+1} as :

$$v_i = A_i + \mu_2 g \varepsilon_2 \quad \text{and} \quad v_{i+1} = A_{i+1} + \mu_2 g \varepsilon_2 \qquad (2.22)$$

Eqs. (2.19) and (2.21) define the complete solution for this case. The response reverts to the non-sliding phase when $\dot{x}_{s_2}$ becomes zero.

2.2.3 Case 3: Double Sliding Structure

Here we consider the combination of Case 1 and Case 2, thus allowing the top slab and the bottom mass both to slide at their respective interfaces. Of course, we start with the condition when no mass is sliding; the motion in that case is governed by Eq. (2.1). At every step of the calculation, we check whether or not the interface forces F_1 and F_2 given by Eqs. (2.2) and (2.12) are more than the maximum friction forces. The slab sliding occurs first if Eq. (2.2) is violated or the base sliding occurs first if Eq. (2.12) is violated.

Consider the case when the slab starts to slide first. The response in this case is then given by Eqs. (2.6) and (2.9). However, one has to keep checking the magnitude of the force at the bottom interface to see if sliding is likely to begin at that interface. The interface force, F_2 , in this case is defined by the following equation, which is somewhat different from Eq. (2.11).

$$F_2 = -\mu_1 m_1 g\, \varepsilon_1 + m_2 \ddot{x}_g \tag{2.23}$$

Whenever this force exceeds $\mu_2 Mg$, base sliding also occurs. When sliding is occuring at both interfaces, the forces F_1 and F_2 remain constant and are defined by Eqs. (2.3) and (2.13) with ε_1 and ε_2 still defined by Eqs. (2.4) and (2.14).

The equations of motion in this case are :

For the slab,

$$m_1(\ddot{x}_{s_1} + \ddot{x}_{s_2} + \ddot{x}_f + \ddot{x}_g) = -\mu_1 m_1 g\, \varepsilon_1 \tag{2.24}$$

For the frame,

$$c\dot{x}_f + kx_f = \mu_1 m_1 g\, \varepsilon_1 \tag{2.25}$$

For the bottom mass,

$$m_2(\ddot{x}_{s_2} + \ddot{x}_g) = \mu_1 m_1 g\, \varepsilon_1 - \mu_2 Mg\, \varepsilon_2 \tag{2.26}$$

The solution for Eq. (2.25) is given by Eq. (2.6). Eq. (2.26) can be solved by simply integrating it twice to provide

$$x_{s_2}(\tau) = x_{s_{2_i}} + \tau \dot{x}_{s_{2_i}} - \left[u_i \frac{\tau^2}{2} + \frac{u_{i+1} - u_i}{h_i} \frac{\tau^3}{6} \right]; \quad 0 \le \tau \le h_i \tag{2.27}$$

where u_i and u_{i+1} are defined as follows :

$$u_i = A_i + \frac{g}{1-\alpha}(\mu_2\varepsilon_2 - \alpha\mu_1\varepsilon_1) \quad \text{and} \quad u_{i+1} = A_{i+1} + \frac{g}{1-\alpha}(\mu_2\varepsilon_2 - \alpha\mu_1\varepsilon_1) \tag{2.28}$$

Knowing x_f, from Eq. (2.6) and utilizing Eq. (2.26), we obtain :

$$\ddot{x}_{s_1}(\tau) = \frac{g}{1-\alpha}(\mu_2\varepsilon_2 - \mu_1\varepsilon_1) + \frac{\omega_o}{2\beta_o}\dot{x}_{f_i}e^{-\frac{\omega_o}{2\beta_o}\tau} \tag{2.29}$$

Integrating the above equation twice, we obtain :

$$x_{s_1}(\tau) = x_{s_{1_i}} + \dot{x}_{s_{1_i}}\tau + \frac{g}{1-\alpha}(\mu_2\varepsilon_2 - \mu_1\varepsilon_1)\frac{\tau^2}{2} \tag{2.30}$$

$$+ \left[\tau - \frac{2\beta_o}{\omega_o}\left(1 - e^{-\frac{\omega_o}{2\beta_o}\tau}\right)\right]\dot{x}_{f_i}$$

where $x_{s_{1_i}}$ and $\dot{x}_{s_{1_i}}$ are the sliding displacement and velocity for the top mass at the beginning of the time-step. Eqs. (2.6), (2.26), and (2.30) describe the response for the double sliding phase completely.

Another scenario to arrive at the double sliding phase is that the base sliding occurs first followed by the slab sliding. The base sliding occurs first whenever Eq. (2.12) is violated. During the time of base sliding, the system response is given by Eqs. (2.19) and (2.21). However, one has to keep checking the magnitude of the top interface force, F_1, to see if it exceeds the limiting value of $\mu_1 m_1 g$. In this case, the force F_1 is calculated as :

$$F_1 = m_1(\ddot{x}_{s_2} + \ddot{x}_f + \ddot{x}_g) = m_1[(1-\alpha)\ddot{x}_f - \mu_2 g\varepsilon_2] \tag{2.31}$$

Whenever F_1 exceeds its limiting value we arrive at the double sliding case; the equation of motion and the corresponding solution of which were discussed earlier.

2.3 Non-Dimensional System Parameters

The main aim of introducing Coulomb damping was to reduce the response of the primary system as well as supported secondary systems. The response of primary system can be defined in terms of the frame deformation, which is directly proportional to the forces in the frame if it remains linear. The reduction in the frame forces achieved by introduction of Coulomb friction is characterized by a parameter δ, herein called as the *reduction factor* . This parameter is defined as follows :

$$\delta = \frac{x_{f_{max}}}{\mathbf{RSD}} \tag{2.32}$$

where **RSD** is the spectral displacement which is equal to the deformation of the frame if the system has no Coulomb damping and remains linear. Thus a $\delta = 0.40$ implies that the deformation of the frame, and hence the force in the frame are reduced by 60% of what they would be if the system were elastic.

Another parameter of interest relates the maximum accelerations of the slab in systems with and without sliding interface. The ratio of these two accelerations is a measure of the effectiveness of the sliding interface in reducing the acceleration level of the floor - - a quantity of immediate interest in the design of secondary systems. Herein, this parameter is referred to as the *isolation factor* . Since the maximum acceleration of the slab is directly proportional to the friction force at the interface, its

value is limited to $\mu_1 g$. The corresponding maximum acceleration in the system with no sliding interface is equal to the absolute acceleration response spectrum value at the system frequency and damping ratio, denoted by **ASA**. Thus the isolation factor, denoted by γ, is defined as :

$$\gamma = \frac{\mu_1 g}{\mathbf{ASA}} \tag{2.33}$$

A value of $\gamma = 0.40$ implies that the acceleration of the slab in the sliding system is reduced by 60%, when compared to the acceleration in the corresponding non-sliding (elastic) system.

It was observed (15) numerically that for a slab sliding system, the two parameters discussed above were almost equal. Now, this is also evident from the equations of motion developed for this case. From Eq. (2.6), it is seen that the relative velocity of the frame with respect to the ground, $\dot{x}_f$, diminishes very fast as soon as the sliding begins because of the term $e^{-(\omega_o/2\beta_o)\tau}$. As a result, from Eq. (2.5), frame deformation simplifies to $x_f = \mu_1 m_1 g/k$, and the response reduction factor δ becomes

$$\delta = \frac{x_{f_{max}}}{\mathbf{RSD}} \cong \frac{\mu_1 m_1 g}{k\,\mathbf{RSD}} = \frac{\mu_1 g}{\omega_o^2\,\mathbf{RSD}} \cong \frac{\mu_1 g}{\mathbf{ASA}} = \gamma \tag{2.34}$$

Where use has been made of the fact that absolute acceleration response spectrum value, **ASA**, is approximately equal to ω_o^2 **RSD**, which is the pseudo acceleration response spectrum value. For the damping ratio values of practical interest, this assumption is known to be quite accurate.

Here, in the case of slab sliding systems, these two factors are used as the parameters of the systems in liu of the coefficient of friction, μ. That is, a slab sliding system will be characterized by δ or γ. A set of results obtained for different δ or γ

will be compared. The advantages of using these factors as parameters will also be pointed out while discussing the results. Since these two factors are also equal, they are used interchangeably while presenting the results for slab sliding case. It is, however, noted that these two factors are not equal to each other for a base sliding system.

2.4 Numerical Results

The numerical results are presented in spectrum form where the response of several systems with different frequencies have been considered. To obtain these results, five earthquake ground motions of (1) 1940 El Centro, S90W component (Motion 1), (2) 1951 Ferndale City Hall, S44W component (Motion 2), (3) 1971 Lake Hughes, Array Station No. 1, N21E component (Motion 3), (4) 1971 Lake Hughes, Array Station No. 4, S21W component (Motion 4), and (5) 1971 Lake Hughes, Array Station No. 09, N69W component (Motion 5), chosen arbitrarily and normalized to a peak ground acceleration of 0.50 G were considered. Out of the five ground motions selected herein, the first one corresponds to a soft site condition, the second to a medium stiff site and the rest three were recorded on hard sites. The last three records (Motions 3, 4 and 5) possess similar characteristics as far as site stiffness, magnitude and epicentral distance are concerned. The details about the duration, peak ground motion values, site location and stifness, etc, for each of the above earthquake motions are presented in Appendix 1. Different ground motions were considered to examine qualitatively the response variability due to the type of ground motion, since

these factors are known to affect the shape and magnitude of the response spectra for linear oscillators (16).

2.4.1 Slab Sliding Displacements

Fig. 2.2(a) shows the spectra for slab sliding displacements in the slab sliding system (SSS) subjected to Motion No. 5 (hard site) for three different values of reduction factor parameters. It may be noted that a constant value of δ does not mean that the friction coefficient, μ_1 is constant. In fact, the values of friction coefficient required to achieve a constant reduction in the frame response over the range of frequencies are shown in Fig. 2.2(b) for three values of δ . These μ —spectrum curves are simply obtained by multiplying the elastic absolute acceleration (**ASA**) spectrum by δ/g. From Fig. 2.2(a), it is observed that the displacements are rather large in the low frequency range. As one would expect, smaller sliding displacements are obtained for higher δ values, that is for higher coefficient of friction values. Fig. 2.3(a) and (b) show sliding displacement spectra for Ground Motions 3 and 4 (both hard sites, too) for different values of δ. Again, it is seen that lower values of δ (causing higher reduction in response) produce larger sliding displacements in both cases. However, in the case of these two earthquakes the shape of the spectra is somewhat different than the one seen in Fig. 2.2(a) for Ground Motion 5. Also, the magnitudes of the spectra are seen to be highly variable from one earthquake to another.

It is of interest to compare the sliding displacement spectra caused by different earthquake motions. Figs. 2.4(a) and (b) compare the sliding displacement spectra due to the three hard ground motions considered in this study for $\delta = 0.10$ and $\delta = 0.20$, respectively. It is observed that the shape of the spectra are

similar for Ground Motions 3 and 4, but remarkably different for Ground Motion 5 in the high period (low frequency range), as demonstrated by the sharply rising values in that region. Fig. 2.5 shows a similar comparison for all the ground motions considered in this study for $\delta = 0.30$. The figure shows that the El Centro earthquake (referred to as Ground Motion 1) recorded on a soft site causes rather high sliding displacements in the low frequency range, especially in comparison to the rest of the ground motions considered herein. The sliding displacement spectrum due to the Ground Motion 2 recorded on medium stiff site is generally of much lower magnitude compared to the other ground motions. It is, however, noted that the observations about the shapes and magnitudes of the slab sliding displacement spectra can not be genralized, since the number of ground motions considered in this study is too small to make any sweeping conclusions.

In all the cases, however, it seems that the sliding displacement values are in practical range for high and medium frequency structures. This is encouraging, since the sliding displacements show the amount of clearance required to permit free slab movement. Also, the residual slab displacement at the end of the earthquake motion, a quantity of design interest, was observed to be about the same as the maximum sliding displacement indicating that there is no significant recovery process in such sliding systems to bring them to their original position. Results were also obtained for other damping ratio values. It was observed that for the practical range of interest of damping ratio values, the sliding displacements did not differ much from each other.

2.4.2 Effect on Floor Response Spectra

As mentioned earlier, because of the sliding interface, the maximum acceleration of the slab is limited to $\mu_1 g = \gamma$ **ASA**. This reduction in the acceleration is of direct relevance in the design of secondary system supported on the slab. Besides a reduction in the maximum acceleration, it is also of interest to examine the frequency response characteristics of the slab motion, represented in terms of the floor response spectra.

Figs. 2.6(a) and (b) show the floor acceleration response spectra for two slab sliding systems of different frequencies resulting from their response to Ground Motion No. 4. The floor spectra in Fig. 2.6(a) are for a primary structure of 20 cps frequency, and in Fig. 2.6(b) for a primary structure of 4 cps frequency. In both figures, floor spectra for two values of isolation parameters ($\gamma = 0.10$ and $\gamma = 0.20$) are compared with the spectra of the non-sliding system. These two values of isolation parameters correspond to the coefficient of friction values of 0.063 and 0.126 for the system in Fig. 2.6(a), and 0.1236 and 0.2472 for the systems in Fig. 2.6(b). A marked reduction in the secondary system response for a system with sliding interface, especially at the frequency of the primary system, is noted. Also, the response at frequencies higher than the resonance frequency is significantly reduced. The same observations are found to be true for other Ground Motions, too. This is evident from Figs. 2.7(a) & (b) and 2.8(a) & (b), which have been drawn for the same cases as in Fig. 2.6(a) & (b), but for Ground Motions 5 and 1, respectively. Thus it can be seen that the secondary systems placed on a sliding floor will experience a greatly reduced level of input motion and response.

Here it is now relevant to mention a distinct advantage of utilizing γ or δ as the system parameters, in lieu of the coefficient of friction, in the presentation of the results for slab sliding case. These results have been obtained for a maximum ground acceleration of 0.50 G. If this maximum ground acceleration is doubled to a value of 1.0 G, then the above response spectrum values will also be doubled. That is, to obtain the results for any level of peak ground acceleration, a direct linear interpolation of the results obtained for constant value of γ is possible. Such linear interpolation of the results obtained for a constant friction coefficient will, of course, not be possible.

2.4.3 Slab Sliding System Versus Bilinear Hysteretic System

There are important similarities between the slab sliding system and the bilinear hysteretic system (BLH). For example, the maximum forces acting on the masses are limited to a fixed value of $\mu_1 m_1 g$ in a slab sliding system and to a value of kx_y, where k is the primary stiffness and x_y is the yield displacement in an elasto-plastic (E-P) oscillator. In the sliding system, the hysteresis loop is rectangular in shape with the force plotted against sliding displacement and in a bilinear hysteretic system, the loop is a parallelogram with the force plotted against the (inelastic) displacement of the oscillator. In the hysteretic system, the maximum deformation of members is of design interest as it defines the ductility requirement. Likewise, in a sliding system, the maximum sliding displacement of the mass is of interest as the system must be able to accomodate it to reduce the force response. Beyond these similarities, however, the sliding system has a definite advantage in that the sliding

displacements are recoverable, whereas the residual displacements in hysteretic systems are permanent and thus they can affect the after-event utility of the structure.

Because of the aforementioned similarities, it is also possible to define the response reduction factor, δ, for a hysteretic system also as the ratio of the yield displacement to the maximum displacement which would be obtained if the force resisting element were elastic. That is,

$$\delta = \frac{x_y}{\mathbf{RSD}} \tag{2.35}$$

where x_y = the yield displacement of the spring, and **RSD** = displacement response spectrum value. This reduction factor has precisely the same meaning as it had for the slab sliding system. Thus $\delta = 0.20$ implies that the yield force in the hysteretic system will be 20% of the force if the system remained elastic. It is, however, noted that for the hysteretic system, δ is not equal to the isolation factor, γ, as it was for the slab sliding system. That is, the acceleration of the mass is not reduced by the same amount as the reduction in the forces. The author used his previous work on the hysteretic systems to compute their response spectra (13) for different δ values. Fig. 2.9(a) shows this isolation factor for an elasto-plastic and two bilinear hysteretic systems with post-yielding stiffnesses of 5% and 10% of the pre-yielding stiffness for a response reduction factor of 0.20. Also shown is the isolation factor for the slab sliding system which remains constant. It is noted that for the hysteretic systems, accelerations are reduced in the low to medium frequency ranges, but there may actually be an amplification in the high frequency range. Of course, the isolation factor spectrum is constant for the slab sliding system, being equal to the response reduction factor. It is also seen to be smaller than that for the hysteretic systems.

In Fig. 2.9(b), the maximum displacement values of the hysteretic system, with $\delta = 0.20$, are compared with the sliding displacement for the slab sliding system with the same δ value. It is interesting to note that these displacement values in the two systems are nearly same, particularly in the high and medium frequency ranges. In the low frequency range, the sliding displacements can be much larger. The figure shows the displacements which the systems must accomodate to achieve a response reduction value of 0.20 or in other words, reduce the response by 80%. For the slab sliding system, it indicates the clearance one should provide for an unobstructed sliding of the slab. Whereas for the hysteretic systems, they indicate how much the stiffness element should be able to deform without breaking; that is, they define the ductility requirement of the stiffness element. Although, the displacement values of the hysteretic system are about the same as those of the slab sliding system, the corresponding ductility requirements are rather too high to be achievable in practice. This can be seen from the ductility ratio curves corresponding to the displacement curves of the hysteretic systems, the scale for which is shown on the right side of the figure. The corresponding sliding displacements, however, seem to be reasonable, except may be for flexible (low frequency) structures.

Fig. 2.10 compares the spectra for energy dissipation per unit mass (15) for slab sliding and three cases of bilinear hysteretic (including the elasto-palstic case) systems. It is interesting to note that the values for energy dissipation are about the same for all the four systems considered herein, this being especially, for the slab sliding and elasto-plastic systems. This indicates that the cumulative sliding displacement of the slab sliding system and the cumulative hysteretic displacement of the elasto-plastic system are of the same order. It was shown (15) that in case of the slab sliding system, most of the dissipation is caused due to friction damping. However, for the bilinear hysteretic systems, larger viscous dissipation is caused due

to increased velocities and accelerations in the high frequency range, as can be seen in Fig. 2.9(a). Consequently, this leads to slightly higher dissipation in that frequency range for the bilinear hysteretic oscillartors as compared to the slab sliding system.

2.4.4 Slab Sliding and Base Sliding Systems

In this section, we compare the response characteristics of the slab sliding system, where only the top mass slides against the supporting frame, and the base sliding system (BSS), where sliding occurs between the base mass and the foundation. In the case of base sliding system, the parameters γ and δ are not as meaningful as they are in the case of slab sliding system. They are also not equal to each other for the base sliding system. Thus, here for the comparison of results between the slab sliding and base sliding systems, the coefficient of friction is chosen as a parameter in stead of δ or γ. The results are presented for a given value of the coefficient of friction ($\mu_1 = \mu_2 = \mu$) and different values of mass ratio parameter, α. Here, it is recalled that the case of $\alpha = 1$ corresponds to the slab sliding system.

Fig. 2.11(a) shows the spectra for the absolute acceleration values of the slab for different values of α. Also shown in the figure is the spectrum for the non-sliding case, referred to as the elastic spectrum. The results for $\alpha = 1$ refer to the slab sliding system. As one would expect, in the case of slab sliding system, the slab acceleration spectrum is a line parallel to the horizontal axis at a constant level of μg. The spectrum curves for other values of α, of course, belong to the base sliding system with different slab to the total system mass ratios. The curve for $\alpha = 0.25$, for example, corresponds to the case when the slab mass is 1/3 of the base mass. It is noted that higher acceleration values are obtained for the base sliding system when

compared to the value of μg for the slab sliding system. Also, lower the mass ratio, α, higher are the accelerations.

Fig. 2.11(b) compares the displacement of the frame at top. This displacement is directly proportional to the forces in the frame. Again, it is noted that the forces in the slab sliding system will be significantly smaller than those in the base sliding system for the same value of μ. As was the case with slab accelerations, relatively higher displacements are obtained for lower mass ratios. It is of interest to note the easy predictability of the slab sliding system response which is defined by a straight line (on a log-log plot); the equation of this straight line is $x_{f_{max}} = (\mu g/\omega_o^2)$.

Fig. 2.12 shows the sliding displacement spectra for the two types of sliding systems for the El Centro earthquake ground motion. It is interesting to note that the sliding displacements are not sensitive to α values for stiff and medium stiff systems. For softer systems, the sliding displacements are higher for the slab sliding system and there is a significant variation in the displacement values with different mass ratios. As noted earlier, the sliding displacements can be rather large for flexible systems; that is, larger clearances will be required to permit unobstructed movement of the sliding masses.

As an example of comparison of slab sliding system, base sliding system and elasto-plastic system, we chose to compare their secondary floor spectra in Figs. 2.13(a) and (b). In Fig. 2.13(a), the frequency of the primary structure is 20 cps. The slab sliding and elasto-plastic systems both have the same $\delta = 0.10$. This value of δ corresponds to a coefficient of friction value of 0.063 at the sliding interface of the slab sliding system. The same value of friction coefficient has been used at the interface of the base sliding system. Similarly, Fig. 2.13(b) is for the primary structure of frequency 4 cps with $\delta = 0.10$ and $\mu = 0.1236$. The damping ratio of the primary system is $\beta_o = 0.05$. The damping ratio of the secondary system, β_s is 0.02 in Fig.

2.13(a) and 0.05 in Fig. 13(b). A significant difference between the secondary spectra of the slab sliding and base sliding systems is seen. The reason for this difference is attributable to the effect shown in Fig. 2.11(a), which showed that the slab sliding system causes lower slab acceleration values compared to the base sliding system. The spectrum for the elasto-plastic system is seen to be very close to the spectrum for the slab sliding system in one case and quite different in the other. However, in general, the spectrum for the slab sliding case is lower than the spectra for the other two systems.

2.4.5 Results for Double Sliding System

It is of natural interest to see if one can provide additional protection for the frame of the structure as well as the secondary systems supported on the slab by introducing sliding interfaces at both the top and bottom interfaces. Herein, such structure is referred to as a double sliding structure (DSS). Indeed, if the slab is also allowed to slide in a base sliding system, one can further reduce the lateral force in the frame as well as acceleration of the slab. Any desired level of reduction in the force and acceleration can be achieved by a proper selection of μ_1, as discussed in the slab sliding case. The results in Figs. 2.14(a) and (b) are obtained for a 90% reduction in the force and acceleration; that is, for $\delta = 0.10$. Three different combinations of the friction coefficients at the top and bottom, related by $\nu = \mu_2/\mu_1$, have been considered. For example, a value of $\nu = 2.0$ means that the friction coefficient at the bottom is two times the friction coefficient at the top. Figs. 2.14(a) and (b) show the sliding displacements at the top and bottom, respectively. We note from Fig. 2.14(a) that by reducing μ_2 the slab sliding displacements are also reduced.

That is required clearance to allow the slab to move freely can be reduced by appropriately reducing the coefficient of friction at the base. This lowering of the coefficient of friction at the base, however, leads to higher sliding displacements of the base as is seen from Fig. 2.14(b). Thus, there is a trade off involved in the choice of appropriate coefficient of friction values to achieve a design where the sliding displacements at top and bottom are equitably distributed.

2.5 *Concluding Remarks*

To study the effect of Coulomb damping, simple structures with sliding interfaces at top (slab sliding system) or at bottom (base sliding system), are analyzed for earthquake induced horizontal ground motion. The response spectrum values for sliding displacements, force in the supporting frame and absolute acceleration of the slab are obtained for the two systems to compare their effectiveness. Dimensionless parameters of response reduction factor and isolation factor are introduced which help in a more convenient presentation of the results of the proposed slab sliding system. The comparison of the results of the slab sliding, base sliding and hysteretic systems indicates a better effectiveness of the slab sliding system with regard to its response reduction and isolation of seismic motion. The clearances required for the uninterrupted slab movement in the slab sliding system do not seem to be too large to be accommodated in practice, except may be for flexible structures. However, it is felt that a large number of recorded motions need to be considered to obtain more conclusive results about the sliding displacements, a quantity of interest in the design of sliding systems.

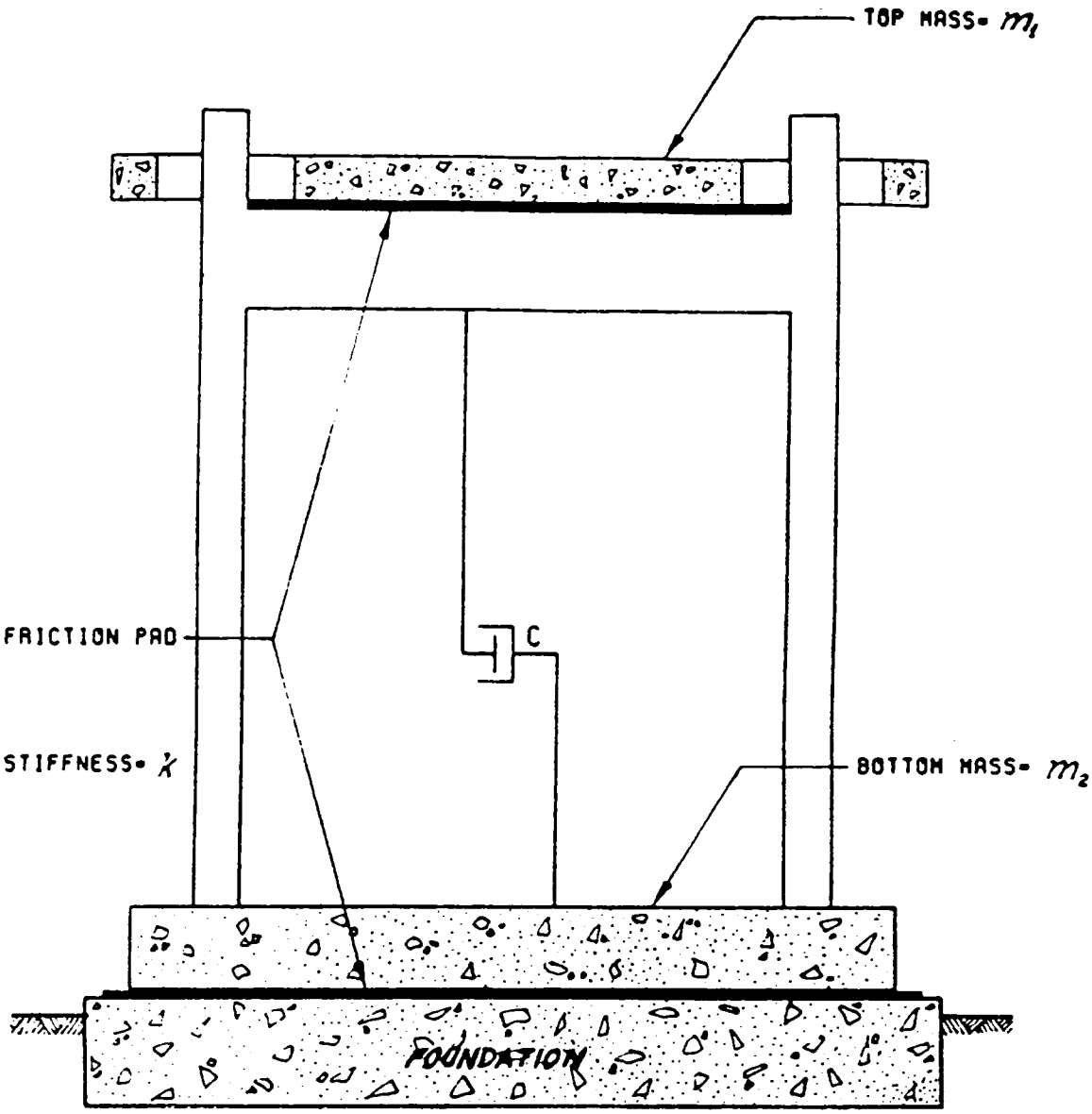

FIG. 2.1 PROPOSED SLIDING SYSTEM

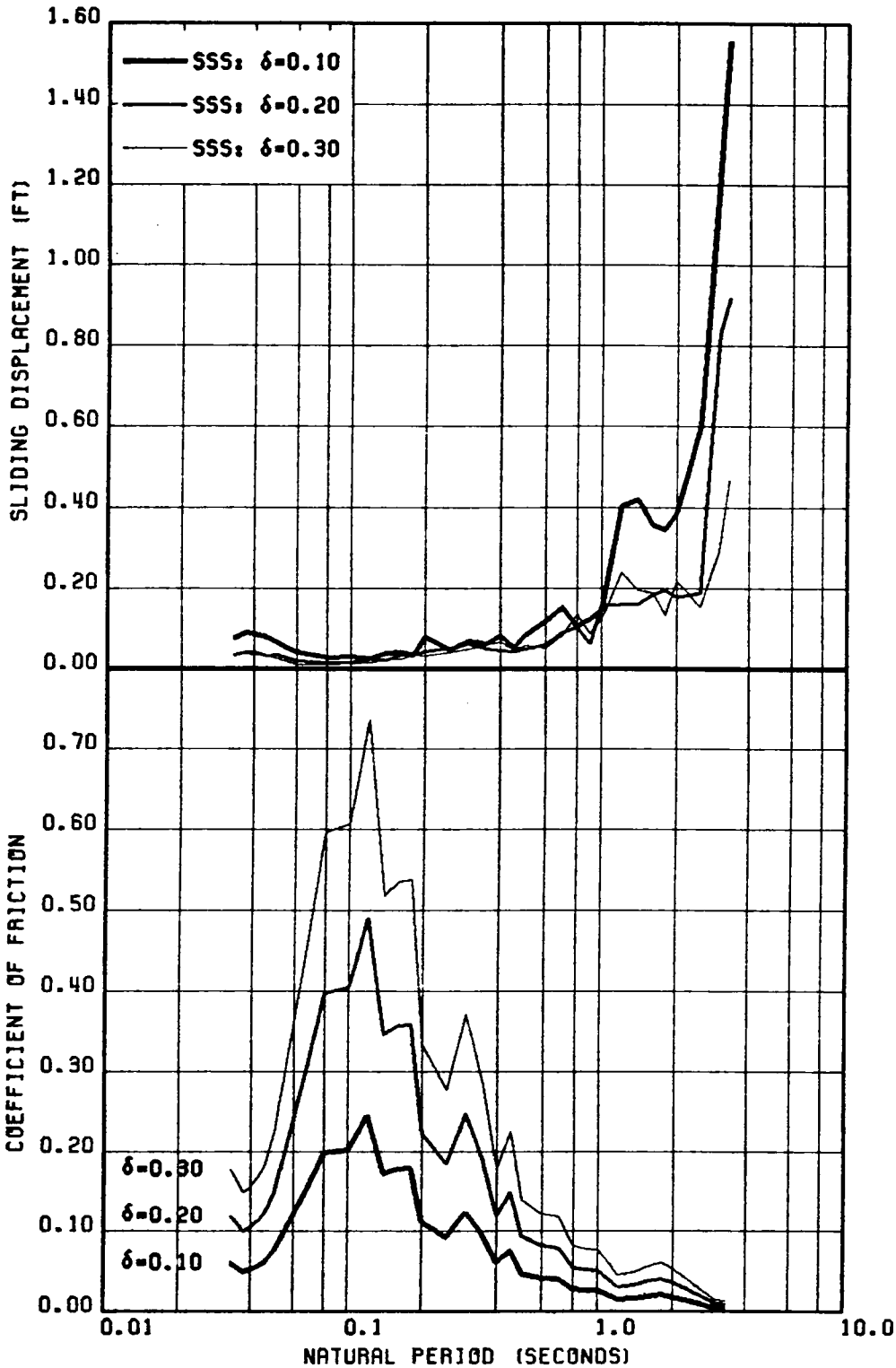

FIG. 2.2 SPECTRA FOR (a) SLAB SLIDING DISPLACEMENT AND (b) REQUIRED FRICTION COEFFICIENT; δ = 0.10, 0.20 AND 0.30, β_o = 0.02, GROUND MOTION 5.

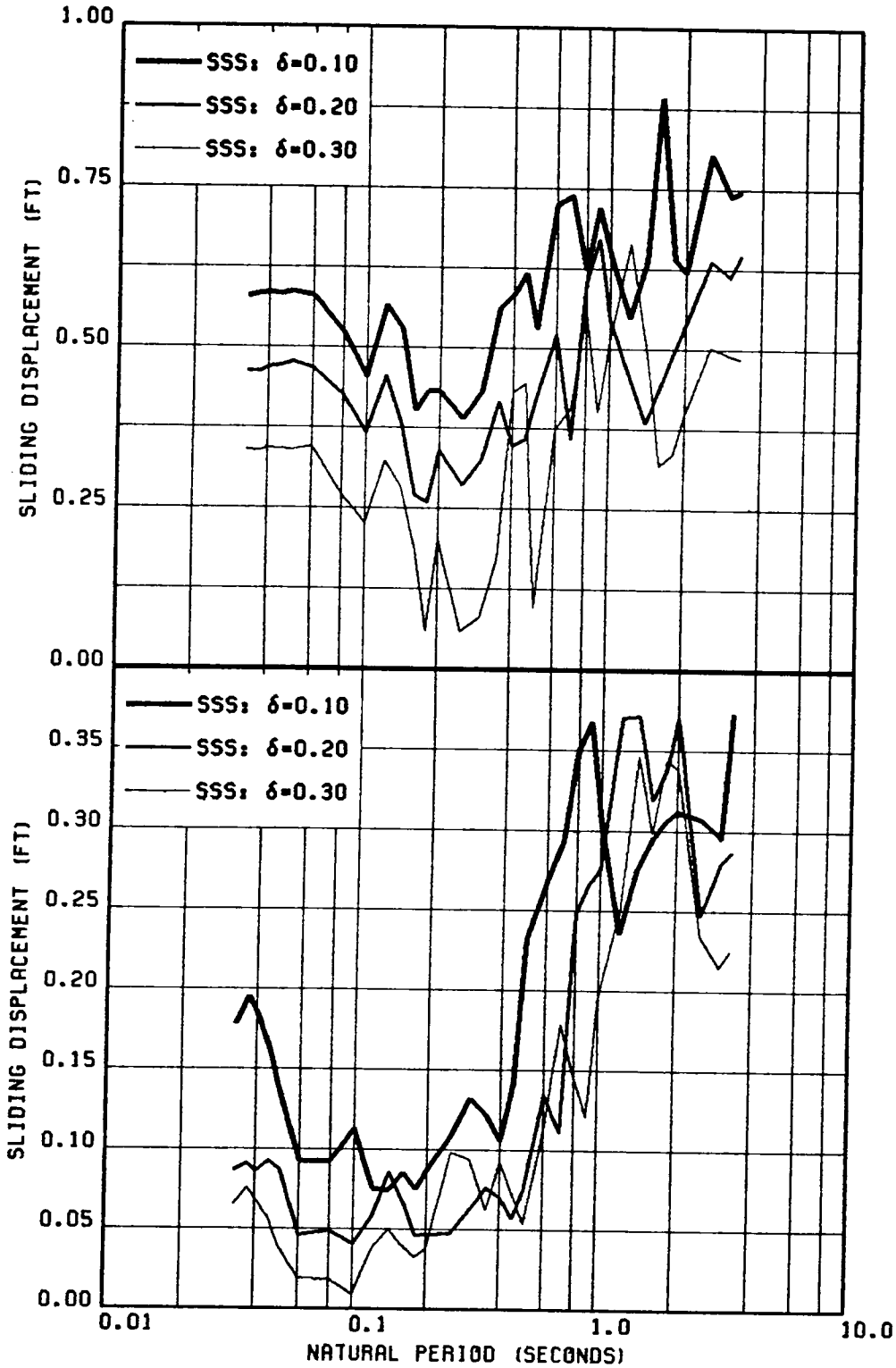

FIG. 2.3 SPECTRA OF SLAB SLIDING DISPLACEMENT FOR (a) GROUND MOTION 3 AND (b) GROUND MOTION 4; δ= 0.10, 0.20 AND 0.30, β_o = 0.02.

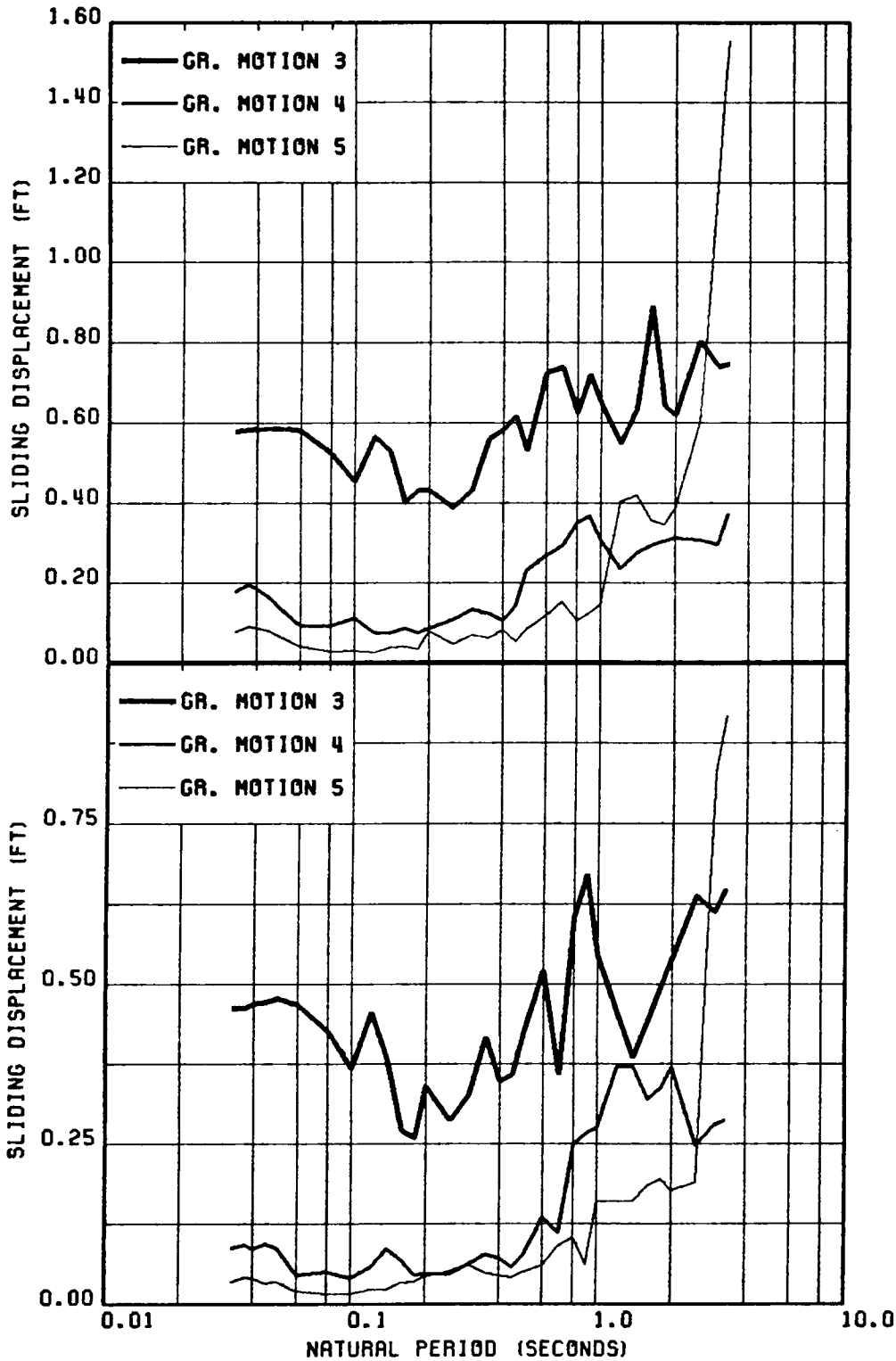

FIG. 2.4 COMPARISON OF SLAB SLIDING DISPLACEMENT SPECTRA FOR DIFFERENT GROUND MOTIONS WITH (a) $\delta = 0.10$ AND (b) $\delta = 0.20$; $\beta_o = 0.02$.

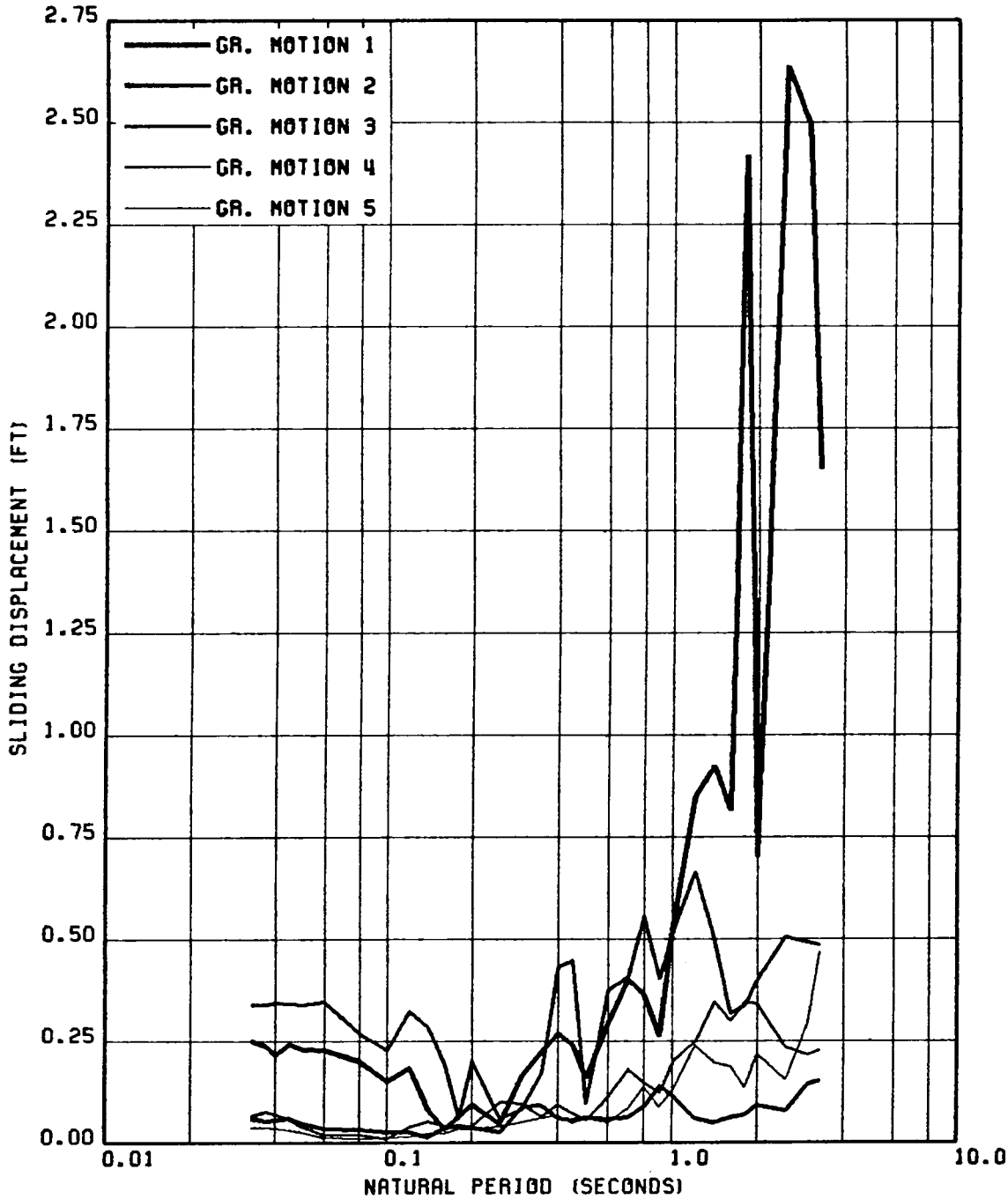

FIG. 2.5 COMPARISON OF SLAB SLIDING DISPLACEMENT SPECTRA FOR DIFFERENT GROUND MOTIONS; $\delta = 0.30$, $\beta_o = 0.02$.

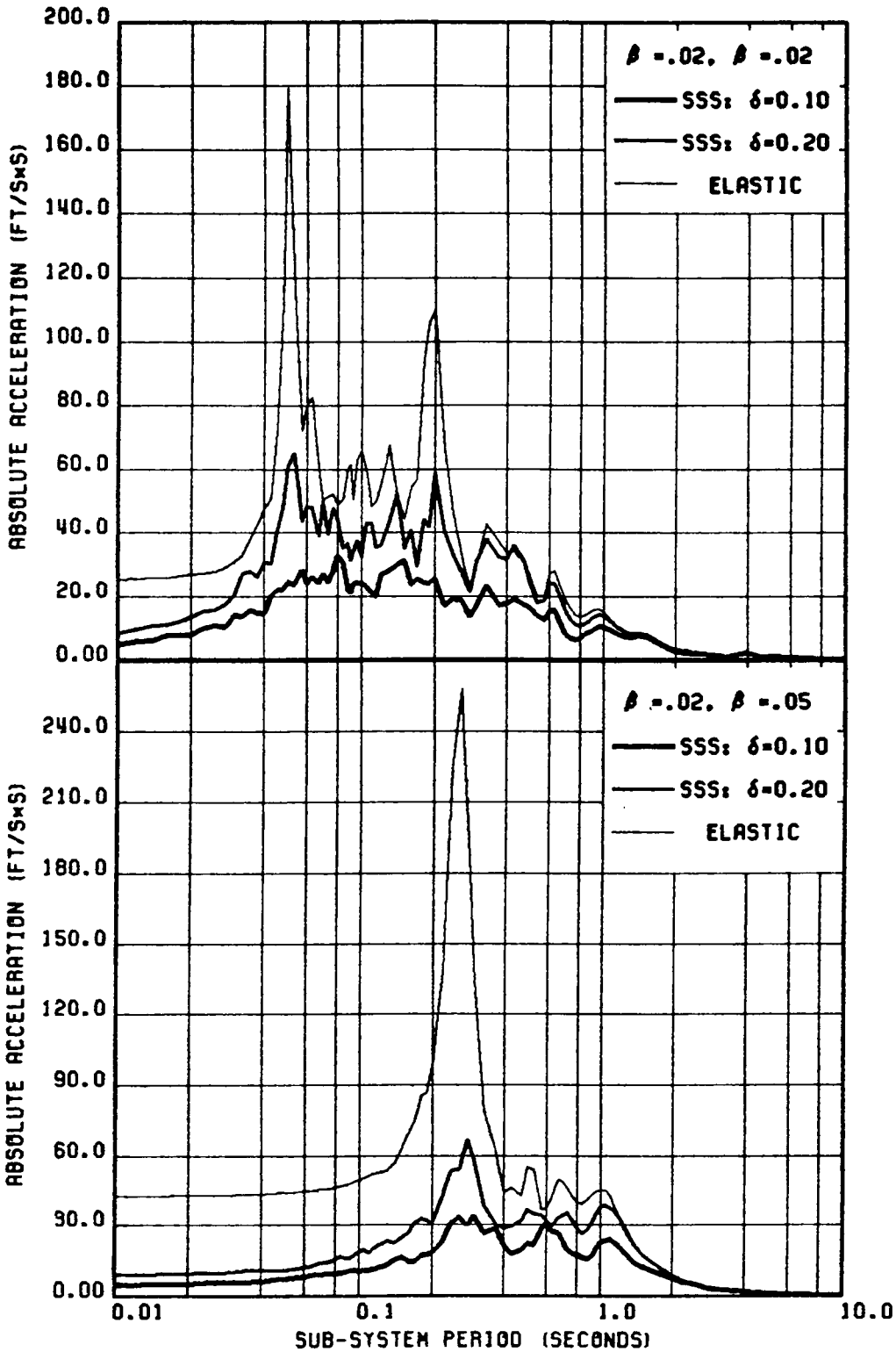

FIG. 2.6 FLOOR SPECTRA FOR TWO PRIMARY STRUCTURES WITH FREQUENCIES EQUAL TO (a) 20 CPS AND (b) 4 CPS FOR β_s/β = .1, .2, 1. (ELASTIC), GR. MOTION 4.

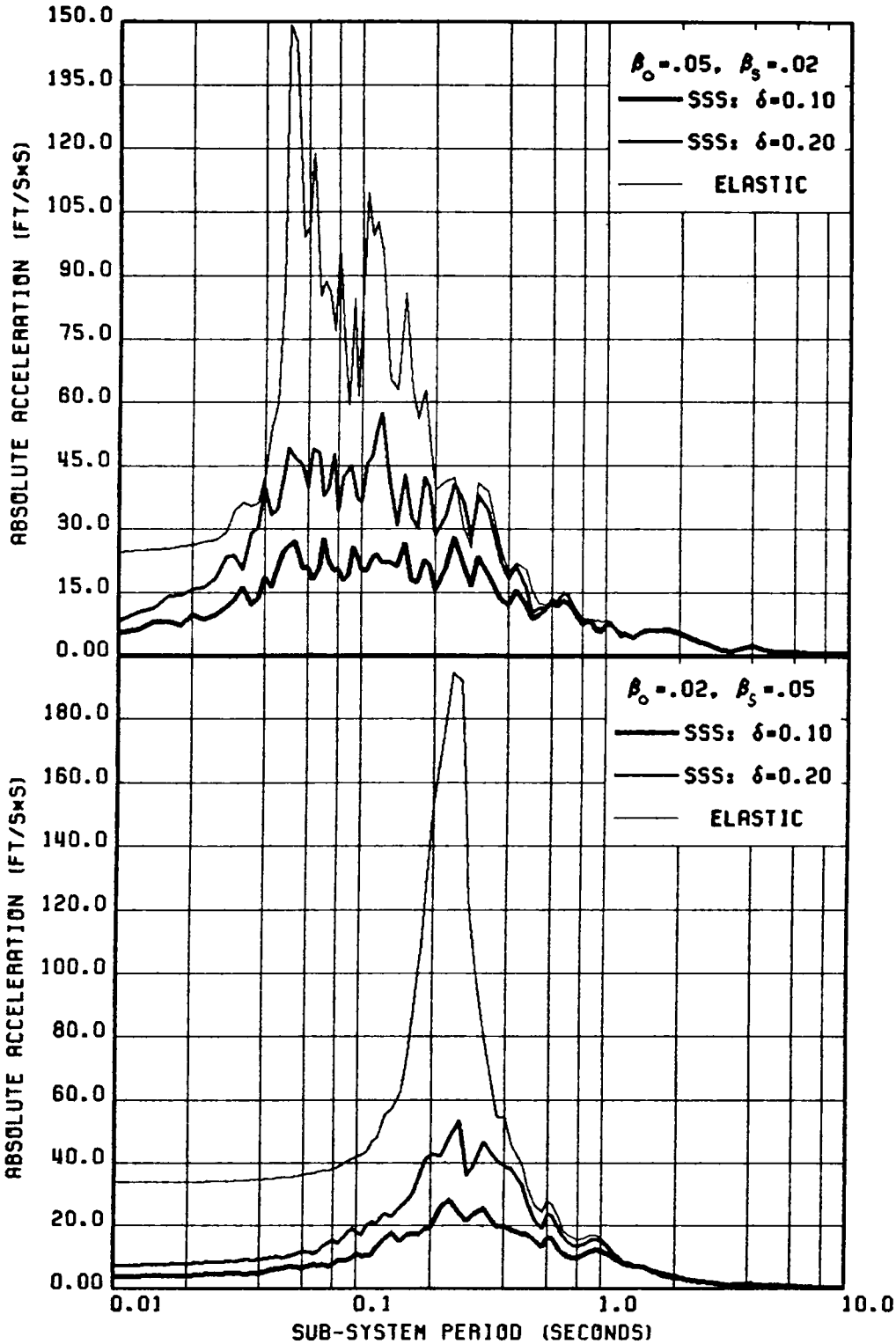

FIG. 2.7 FLOOR SPECTRA FOR TWO PRIMARY STRUCTURES WITH FREQUENCIES EQUAL TO (a) 20 CPS AND (b) 4 CPS FOR δ = .1, .2, 1. (ELASTIC), GR. MOTION 5.

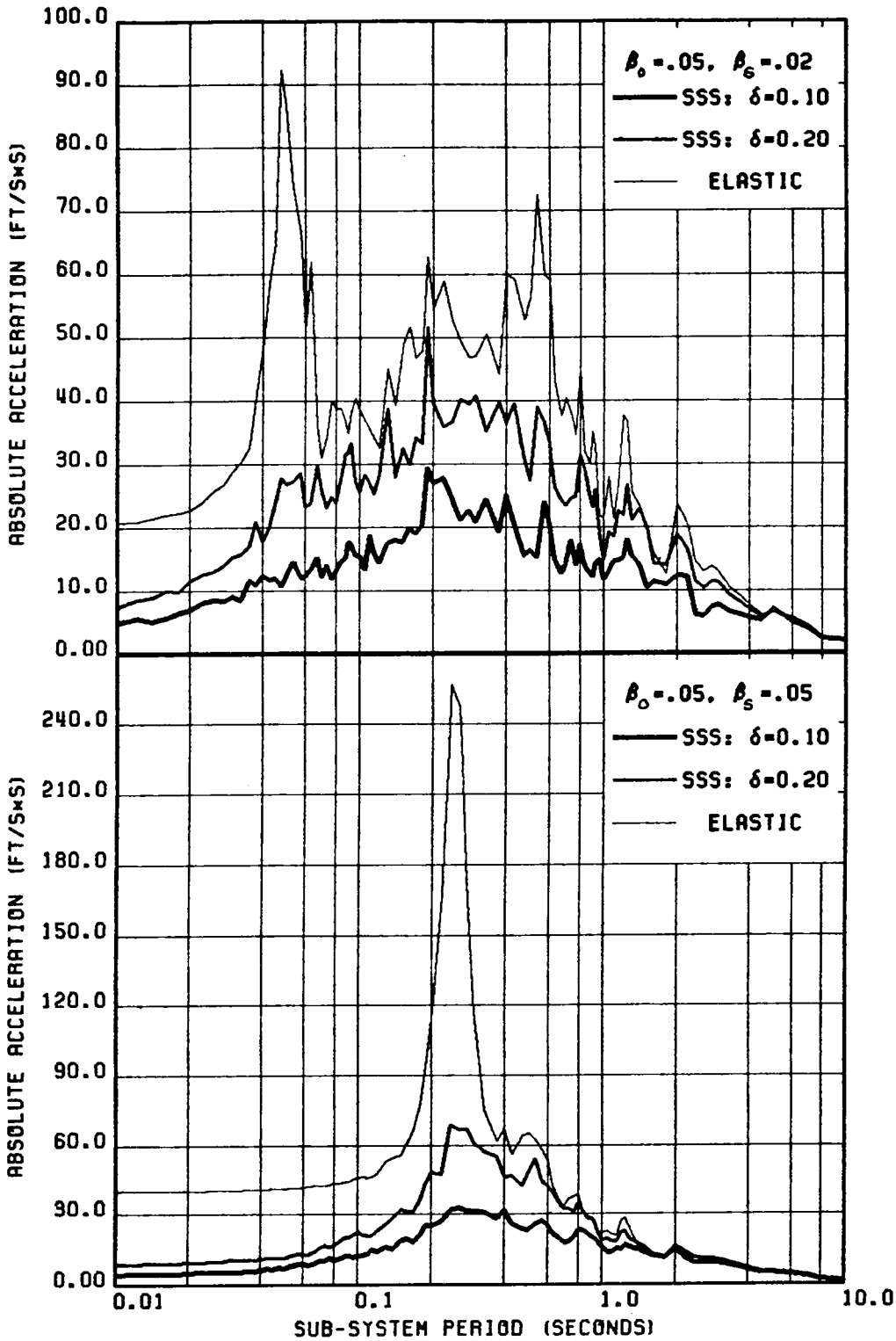

FIG. 2.8 FLOOR SPECTRA FOR TWO PRIMARY STRUCTURES WITH FREQUENCIES EQUAL TO (a) 20 CPS AND (b) 4 CPS FOR ζ = .1, .2, 1. (ELASTIC), GR. MOTION 1.

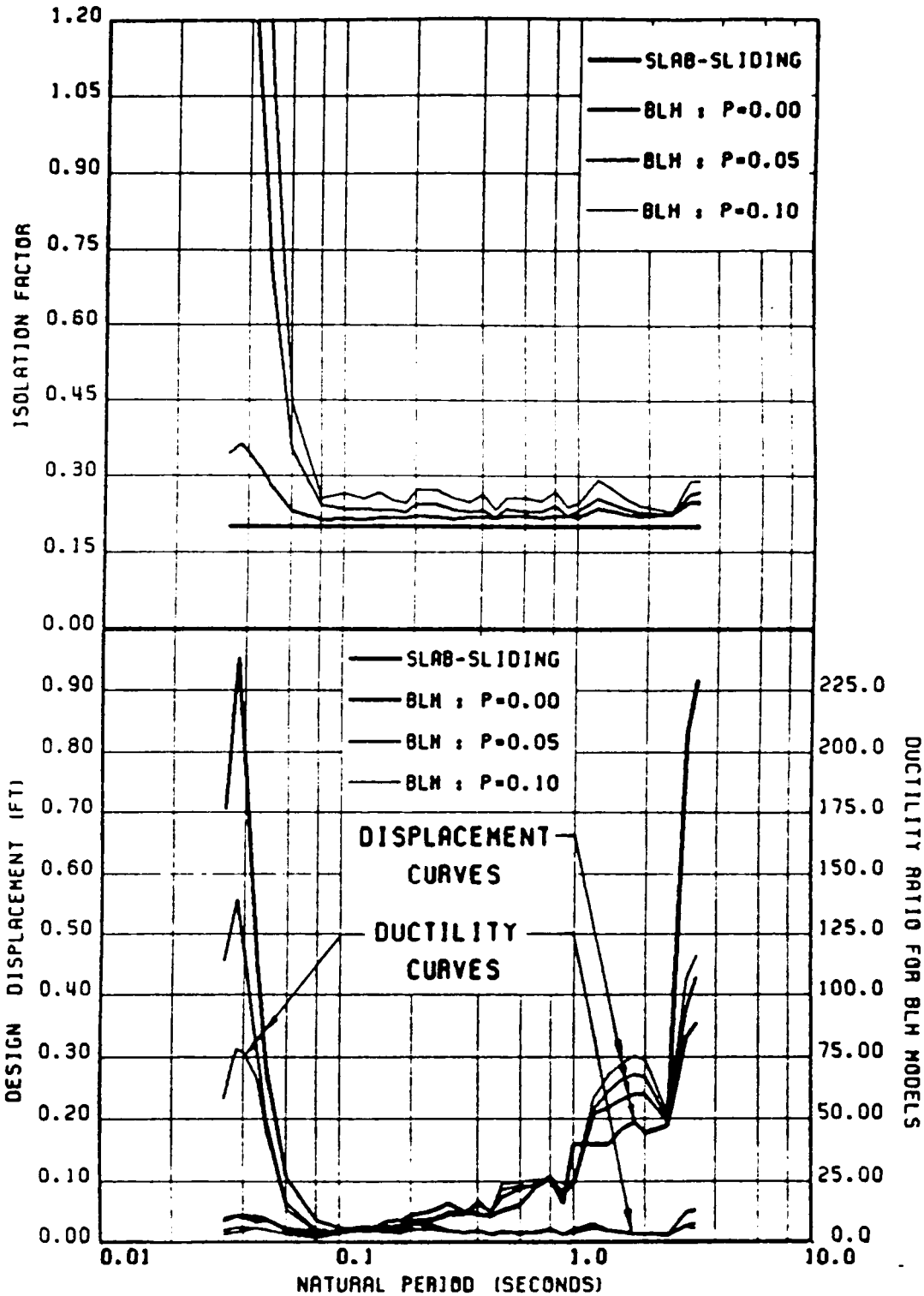

FIG. 2.9 COMPARISON OF SPECTRA OF (a) ISOLATION FACTOR AND (b) DESIGN DISPLACEMENT OF SLAB SLIDING SYSTEM AND DIFFERENT BILINEAR HYSTERETIC SYSTEMS; δ = 0.20, β = 0.02, GROUND MOTION 5.

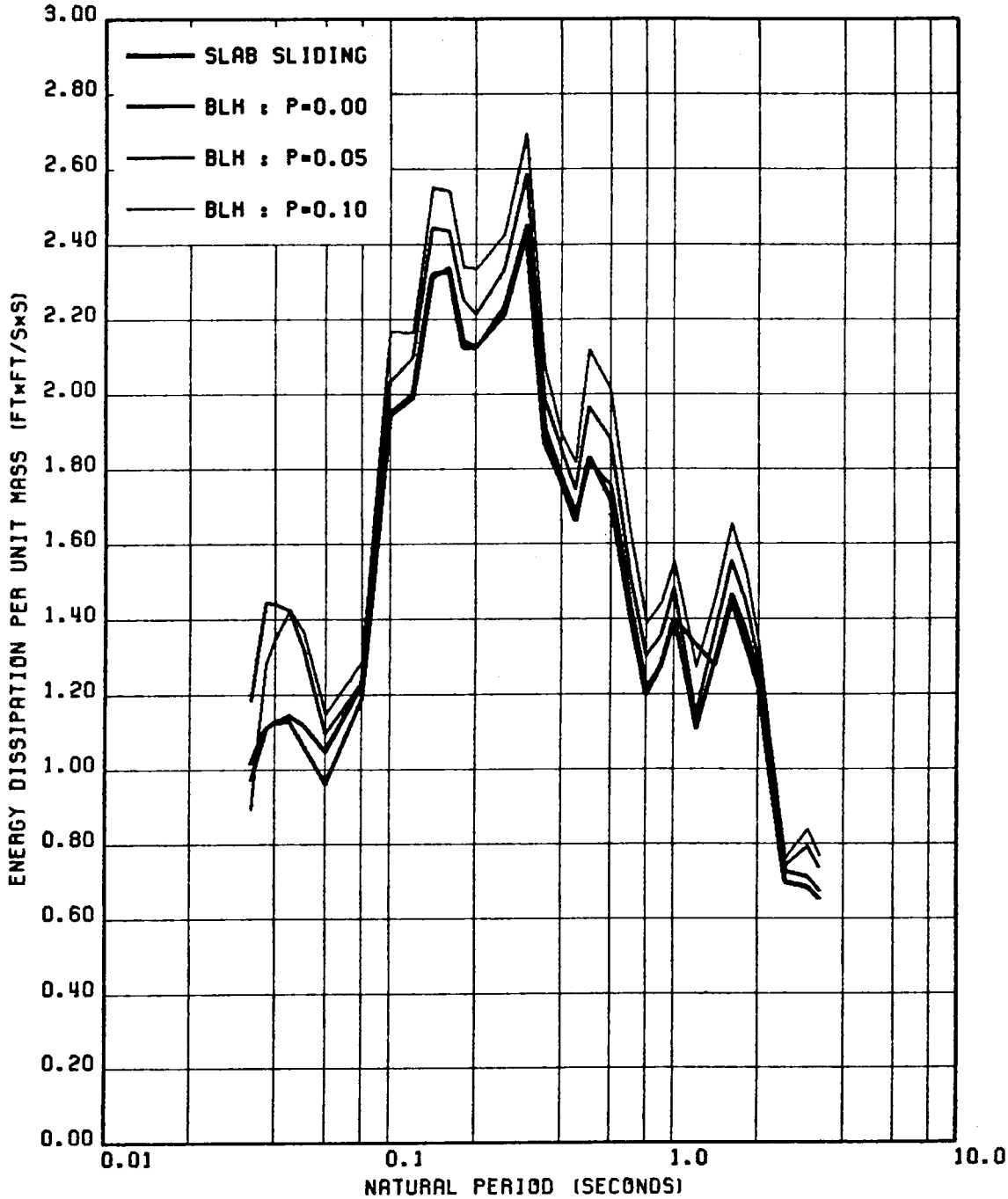

FIG. 2.10 COMPARISON OF SPECTRA OF ENERGY DISSIPATION PER UNIT MASS FOR SLAB SLIDING SYSTEM AND DIFFERENT BILINEAR HYSTERETIC SYSTEMS; δ = 0.20, β_o = 0.02, GROUND MOTION 5.

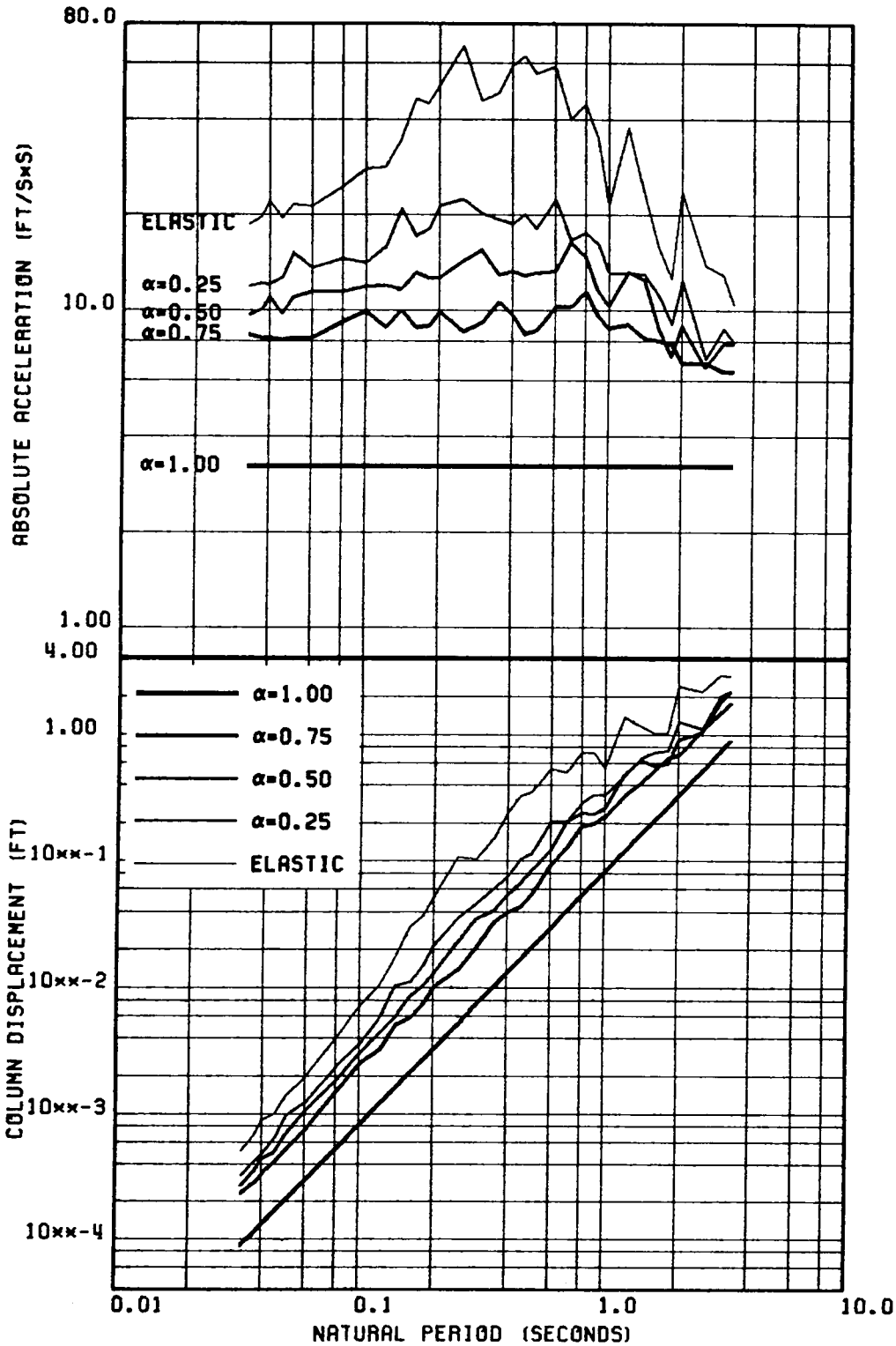

FIG. 2.11 COMPARISON OF SPECTRA OF (a) MAXIMUM SLAB ACCELERATION & ( ) FRAME DEFORMATION FOR SLAB SLIDING (α=1.0) & VARIOUS BASE SLIDING SYSTEMS (α=0.75, 0.50 & 0.25); μ = 0.10, β_o = 0.02, GROUND MOTION 1.

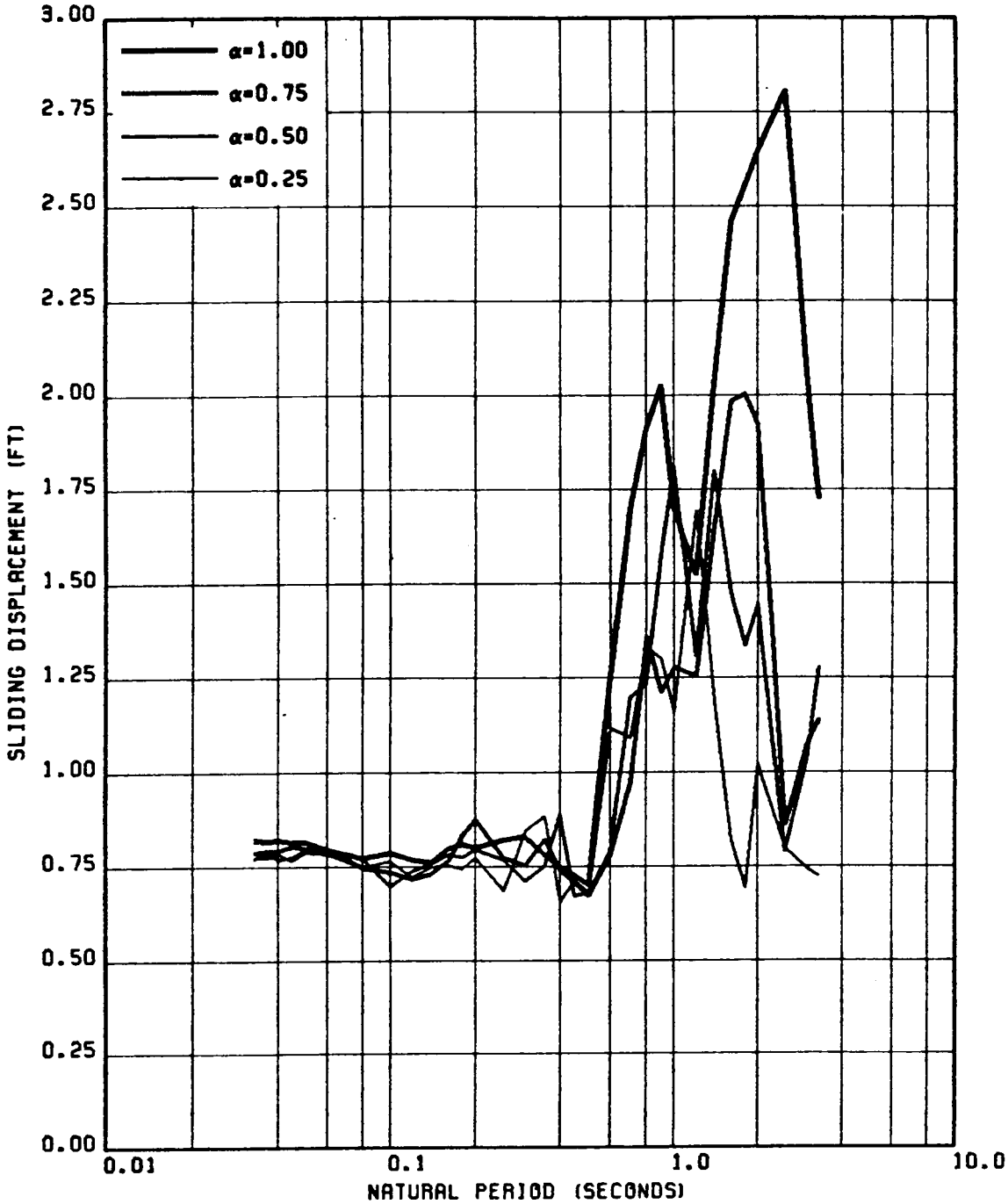

FIG. 2.12 COMPARISON OF SLIDING DISPLACEMENT SPECTRA OF SLAB SLIDING SYSTEM (α=1.0) & DIFFERENT BASE SLIDING SYSTEMS (α=0.75, 0.50 AND 0.25); μ = 0.10, β_o = 0.05, GROU D MOTION 1.

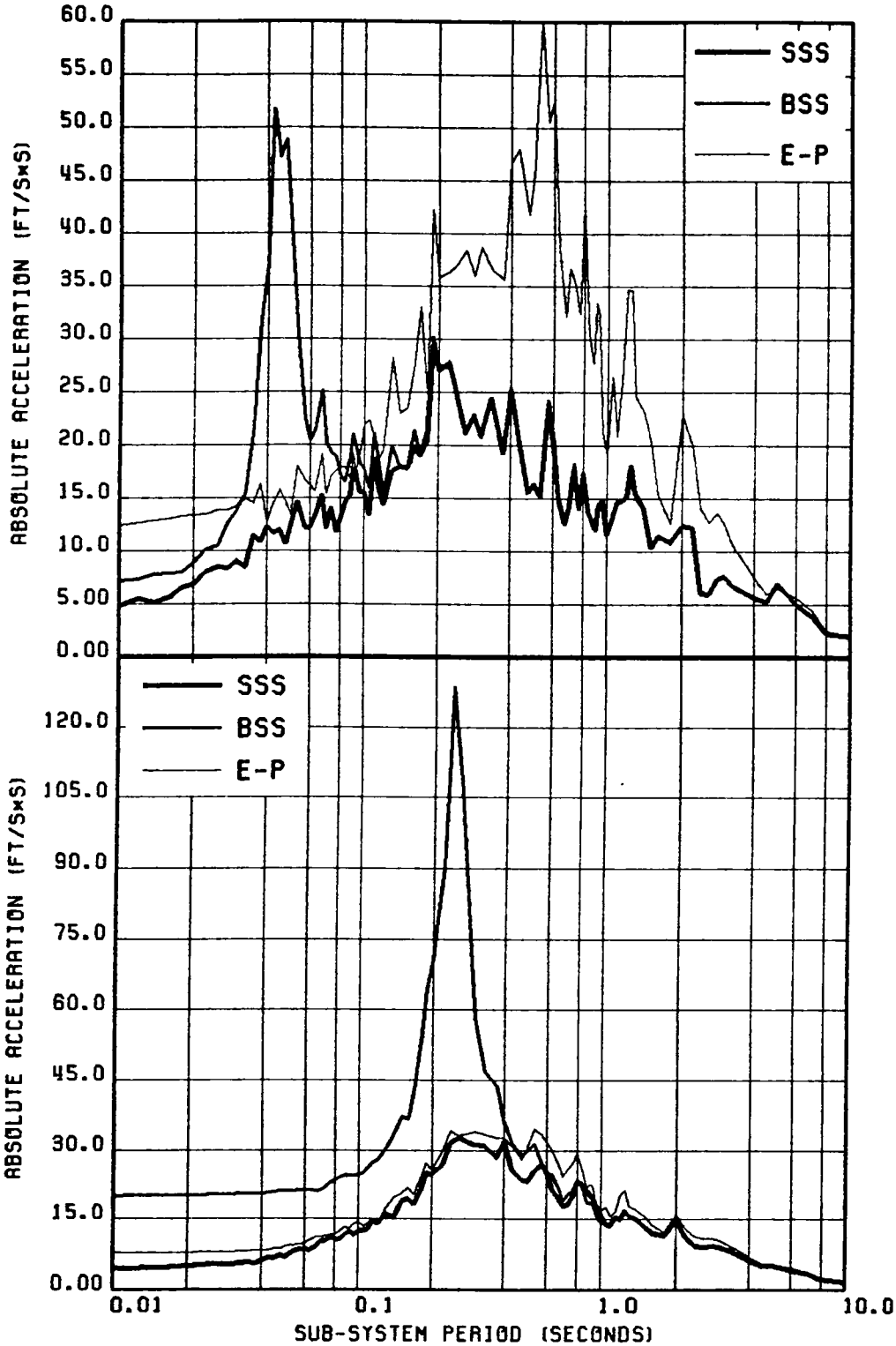

FIG. 2.13 COMPARISON OF FLOOR SPECTRA FOR SLAB SLAB SLIDING, BASE SLIDING & ELASTO-LPASTIC SYSTEMS WITH (a) T=0.05 SEC, β_o =0.02 & μ=0.063 AND (b) T=0.25 SEC, β_o =0.05 & μ=0.123-ALSO, β_s =0.05, GROUND MOTION 1.

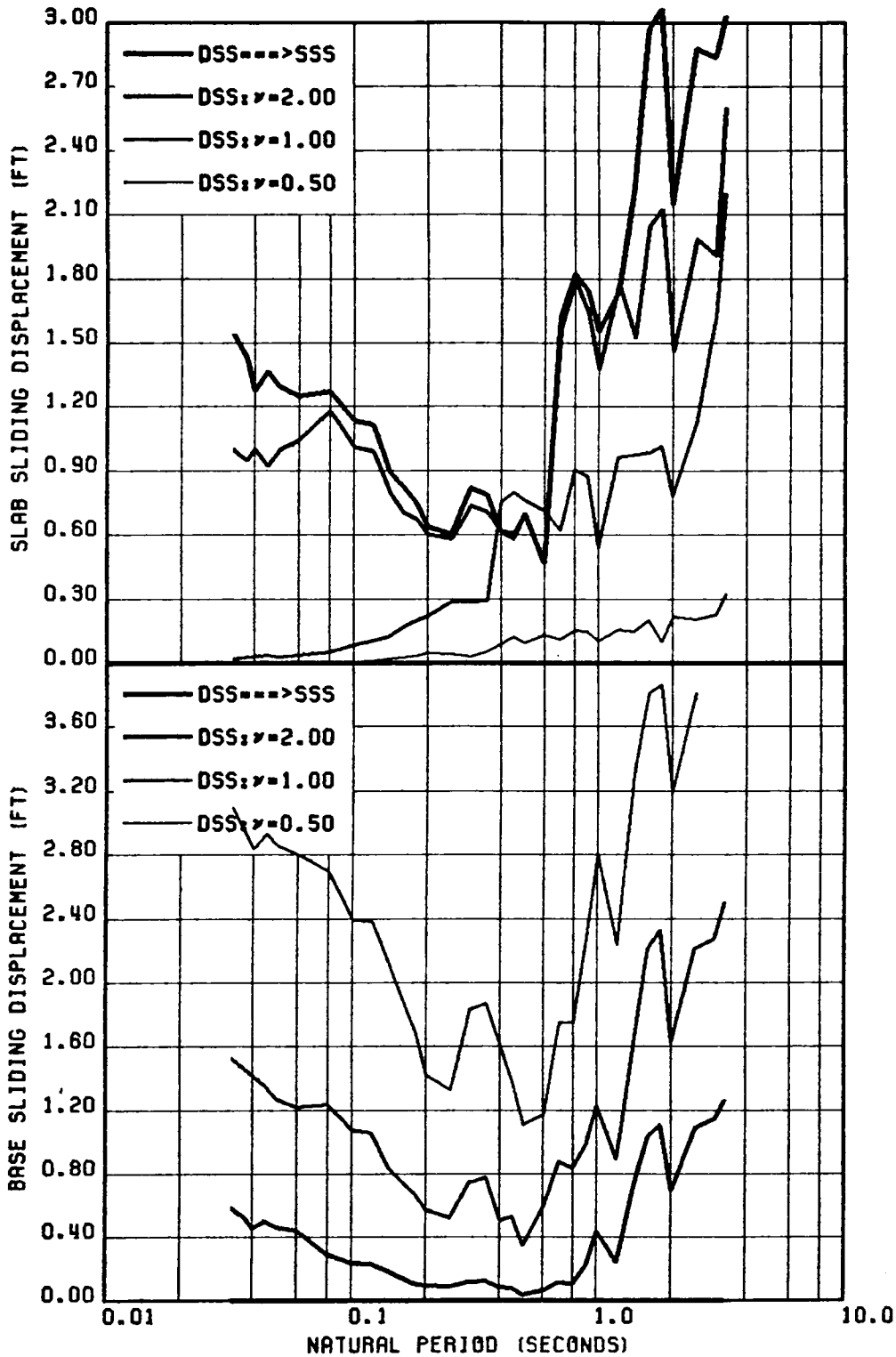

FIG. 2.14 (a) SLAB SLIDING DISPLACEMENT & (b) BASE SLIDING DISPLACEMENT SPECTRA FOR DOUBLE SLIDING SYSTEMS WITH DIFFERENT FRICTION COEFFICIENT RATIOS (γ VALUES); δ = 0.10, β = 0.05, GROUND MOTION 1.

Chapter III

Spring-Assisted Sliding System

3.1 Introduction

In Chapter II it was demonstrated that by permitting the slab mass to slide on the frame, the frictional damping at the interface can be effectively utilized to reduce the forces in the frame and the acceleration of the slab. However, for the proposed sliding system to be effective, it was necessary that the mass be permitted to slide without any obstruction. For stiff structures, the sliding displacements were small enough such that they could be easily accommodated in practice, but for flexible structures these displacements were rather on the high side.

This large sliding displacement requirement could be reduced by introducing a sliding interface at the base. However, this can only achieved at the cost of increased sliding displacements at the base. Thus the problem was only transferred from one place to another and not resolved. It was also observed that the residual

displacement of the sliding mass after the motion ceased was almost the same as the maximum sliding displacement at the interface. This indicated that no recovery or restoring mechanism was available in the system to bring the sliding mass to its original position.

This motivated us to examine the sliding systems which are provided with some recovery mechanism at the sliding interface. This recovery mechanism can be introduced simply by providing a spring between the supporting frame and the sliding mass. This arrangement is shown in Fig. 15. In this arrangement, the lateral spring would resist the relative motion of the slab with respect to the frame. This, of course, would lead to an increased lateral force transfer to the frame and also larger accelerations in the floor slab. It is of interest to examine the suitability of such an arrangement in bringing about a reduction in the sliding displacements without a large increase in the forces and accelerations. The analytical formulation describing the derivation of the equations of motion and their solution approach are presented for a spring-assisted sliding system. Numerical results for various response quantities of interest are obtained and compared to examine the suitability of the proposed scheme.

3.2 *Analytical Formulation*

Fig. 3.1 shows a schematic representation of the proposed spring-assisted system. The frame and springs are assumed to be massless. The damping in the frame and springs is modelled as viscous damping. The entire mass is assumed to be concentrated in the slab. The stiffness of the lateral spring is assumed to be pk,

where k is the stiffness the supporting frame. The damping coefficient associated with the spring is taken as qc, where c is the damping coefficient for the frame. Again, only the response to unidirectional horizontal ground motion is considered.

During excitation of the structure, two possible situations can occur : (1) the non-sliding (stick) phase, and (2) sliding phase during which the slab slides against the frame. The motion at the interface is opposed by the friction force and the lateral springs as well. In the stick phase, the equation of motion can be written as

$$\ddot{x}_f + 2\beta_o\omega_o\dot{x}_f + \omega_o^2 x_f = -\ddot{x}_g \tag{3.1}$$

The above equation is identical with Eq. (2.1), where again x_f = lateral displacement of the frame top with respect to the ground, $\omega_o = \sqrt{k/m_1}$ = nominal frequency of the frame, and $\beta_o = c/(2\omega_o m_1)$ = damping ratio for the frame. This equation is valid as long as the force, F_1, at the interface does not exceed the limiting friction force. That is

$$|F_1| = |m_1(\ddot{x}_g + \ddot{x}_f) + pkx_{res}| < \mu_1 m_1 g \tag{3.2}$$

where x_{res} is the residual sliding displacement of the slab, which is the distance between the current position of the slab and the stiffness center of the frame. (Here, it is assumed that the mass and the stiffness centers were coincident and that the lateral spring was unstretched before the motion started.) Eq. (3.1) can be solved by any standard technique (for example, Nigam and Jennings (20), and then whether or not the system is in the stick or sliding phase can be tested according to the condition described by Eq. (3.2).

Sliding occurs at the top interface whenever the response of non-sliding or stick phase violates the condition in Eq. (3.2). During the sliding phase, the interface force remains constant as :

$$F_1 = -\mu_1 m_1 g \, \mathbf{sign}\,(\dot{x}_{s_1}) = -\mu_1 m_1 g \, \varepsilon_1 \tag{3.3}$$

where x_{s_1} is the sliding displacement of the slab relative to the frame and $\mathbf{sign}(\dot{x}_{s_1})$ is the sign of sliding velocity, $\dot{x}_{s_1}$. This sign is denoted as ε_1. It can be ascertained by knowing the force response at the time sliding is about to begin as

$$\varepsilon_1 = -[\mathbf{sign}(F_1)]_s = -\frac{F_{1_s}}{|F_{1_s}|} \tag{3.4}$$

where the subscript 's' indicates that the force, F_1, in the above equation corresponds to the instant at which the slab sliding is imminent. The above equation is identical to Eq. (2.4).

To derive the equations of motion for the sliding phase, we choose to apply the Lagrange equation approach. We choose x_{s_1} and x_f as the generalized coordinates. The kinetic energy, T and the potential energy, V can then be expressed as follows :

$$T = \frac{1}{2} m_1 (\dot{x}_g + \dot{x}_f + \dot{x}_{s_1})^2 \tag{3.5a}$$

$$V = \frac{1}{2} k x_f^2 + \frac{1}{2} p k x_{s_1}^2 \tag{3.5b}$$

The Langrangian, L is then given by

$$L = T - V = \frac{1}{2} m_1 (\dot{x}_g + \dot{x}_f + \dot{x}_{s_1})^2 - \frac{1}{2} k x_f^2 - \frac{1}{2} p k x_{s_1}^2 \tag{3.6}$$

The friction force, $\mu_1 m_1 g \varepsilon_1$, and the force pkx_{res} in the lateral spring (due to the residual displacement x_{res}) are included as the generalized forces. The parameter ε_1 identifies the direction of the friction force. The viscous dissipation is included through the Raleigh's dissipation function, which is defined as

$$F = \frac{1}{2} c\dot{x}_f^2 + \frac{1}{2} qc\dot{x}_{s_1}^2 \tag{3.7}$$

Finally, the governing equations of motion are obtained from :

$$\frac{\mathrm{d}}{\mathrm{dt}}\left(\frac{\partial L}{\partial \dot{x}_f}\right) - \frac{\partial L}{\partial x_f} + \frac{\partial F}{\partial \dot{x}_f} = 0 \tag{3.8a}$$

$$\frac{\mathrm{d}}{\mathrm{dt}}\left(\frac{\partial L}{\partial \dot{x}_{s_1}}\right) - \frac{\partial L}{\partial x_{s_1}} + \frac{\partial F}{\partial \dot{x}_{s_1}} = -\mu_1 m_1 g \varepsilon_1 - pkx_{res} \tag{3.8b}$$

Substituting Eqs. (3.6) and (3.7) in Eqs. (3.8a) and (3.8b), we get the equations of motion as

$$m_1(\ddot{x}_{s_1} + \ddot{x}_f + \ddot{x}_g) + kx_f + c\dot{x}_f = 0 \tag{3.9a}$$

$$m_1(\ddot{x}_{s_1} + \ddot{x}_f + \ddot{x}_g) + pkx_{s_1} + qc\dot{x}_{s_1} = -\mu_1 m_1 g \varepsilon_1 - pkx_{res} \tag{3.9b}$$

We will further modify these equations for the convenience of subsequent treatment. Subtracting Eq. (3.9a) from (3.9b) and rearranging the terms, we get

$$qc\dot{x}_{s_1} + pkx_{s_1} - c\dot{x}_f - kx_f = -\mu_1 m_1 g \varepsilon_1 - -pkx_{res} \tag{3.10}$$

and with slight rearrangement of terms in Eq. (3.9a), we obtain

$$m_1\ddot{x}_{s_1} + m_1\ddot{x}_f + c\dot{x}_f + kx_f = -m_1\ddot{x}_g \tag{3.11}$$

Eqs. (3.10) and (3.11) are coupled differential equations. For a given ground motion time history, it will be convinient to solve them by the state vector approach. Depending upon the choice of the state vector variables, one can get different forms of the state vector equations. Here, we choose to define the state vector variables as $\dot{x}_t$, x_t and x_{s_1}, where x_t is the total displacement of the slab with respect to the ground displacement and is thus defined as

$$x_t = x_f + x_{s_1} \tag{3.12}$$

As will be seen later, this choice of the variables and the following manipulations lead to an analytically more convinientform of the state vector equations than what would have been obtained otherwise.

Substituting Eq. (3.12) in Eqs. (3.10) and (3.11), we get the following governing equations of motion in terms of x_t and x_{s_1} :

$$(1+q)c\dot{x}_{s_1} + (1+p)kx_{s_1} - c\dot{x}_t - kx_t = -pkx_{res} - \mu_1 m_1 g\varepsilon_1 \tag{3.13}$$

$$m_1\ddot{x}_t + c\dot{x}_t - c\dot{x}_{s_1} + kx_t - kx_{s_1} = -m_1\ddot{x}_g \tag{3.14}$$

To define these equations in terms of frequency parameter ω_o and damping ratio β_o, we divide the above equations by m_1 to obtain the following

$$\dot{x}_{s_1} = \frac{1}{1+q}\left[\dot{x}_t + \frac{\omega_o}{2\beta_o}x_t - \frac{\omega_o}{2\beta_o}(1+p)x_{s_1} - \frac{p\omega_o}{2\beta_o}x_{res} - \frac{\mu_1 g\varepsilon_1}{2\beta_o\omega_o}\right] \tag{3.15}$$

$$\ddot{x}_t = -2\beta_o\omega_o\dot{x}_t + 2\beta_o\omega_o\dot{x}_{s_1} - \omega_o^2 x_t + \omega_o^2 x_{s_1} - \ddot{x}_g \tag{3.16}$$

Furthermore, we can eliminate $\dot{x}_{s_1}$ from Eq. (3.16) by substituting Eq. (3.15) as follows

$$\ddot{x}_t = \frac{1}{1+q}\left[-q\omega_o^2 x_t + (q-p)\omega_o^2 x_{s_1} - 2\beta_o\omega_o q\dot{x}_t - p\omega_o^2 x_{res} - \mu_1 g\varepsilon_1 - (1+q)\ddot{x}_g \right] \tag{3.17}$$

Eqs. (3.15) and (3.17) can now be written as a system of first order differential equations as

$$\{\dot{y}\} = [A]\{y\} + \{f\} \tag{3.18}$$

where the state vector $\{y\}$, the system matrix $[A]$ and the force vector $\{f\}$ are defined as

$$\{y\} = \{y_1 \;\; y_2 \;\; y_3\}^T = \{x_t \;\; x_{s_1} \;\; \dot{x}_t\}^T \tag{3.19}$$

$$[A] = \begin{bmatrix} 0 & 0 & 1 \\ \dfrac{\omega_o}{2\beta_o(1+q)} & -\dfrac{\omega_o(1+p)}{2\beta_o(1+q)} & \dfrac{1}{1+q} \\ -\dfrac{\omega_o^2 q}{1+q} & -\dfrac{\omega_o^2(p-q)}{1+q} & -\dfrac{2\beta_o\omega_o q}{1+q} \end{bmatrix} \tag{3.20}$$

$$\{f\} = \begin{Bmatrix} 0 \\ -\dfrac{p\omega_o^2 x_{res} + \mu_1 g\varepsilon_1}{2\beta_o\omega_o(1+q)} \\ -\dfrac{\ddot{x}_g(1+q) + p\omega_o^2 x_{res} + \mu_1 g\varepsilon_1}{1+q} \end{Bmatrix} \tag{3.21}$$

In the development of Eq. (3.18), the following auxiliary equation has been added

$$\dot{y}_1 = \dot{x}_t = y_3 \tag{3.22}$$

If we were to use $\dot{x}_f$ and x_f instead of $\dot{x}_t$ and x_t as the state vector variables, then the resulting state vector equation will also contain a coefficient matrix on the left hand side of Eq. (3.18). Obviously, Eq. (3.18) is more convenient to solve in this case since there is no matrix on its left side.

3.3 *Solution of Equations of Motion*

The system of equations in Eq. (3.18) can be solved by an approximate step-by-step approach for a given ground motion time history. Here, however, we present a method to obtain the exact solution by decoupling the equations of motion.

The decoupling of Eq. (3.18) can be conviniently effected by utilizing the eigenvalues and eigenvectors of the system matrix $[A]$ and $[A]^T$. These characteristics are obtained as the solutions of the following conjugate eigenvalue problems :

$$\begin{aligned} [A][\xi] &= [\xi][\Lambda] \\ [A]^T[\rho] &= [\rho][\Lambda] \end{aligned} \tag{3.23}$$

where $[\Lambda]$ is the diagonal matrix containing the eigenvalues, and $[\xi]$ and $[\rho]$ are the matrices of the right and left eigenvectors of matrix $[A]$. It is well known that the two eigenvalue problems have the same eigenvalues.

Without any loss of generality, we assume that $p = q$. For this case, the characteristic equation of matrix $[A]$ is given by

$$\left(\frac{\omega_o}{2\beta_o} + \lambda \right) \left[\lambda^2 + 2\beta_o\omega_o \frac{p}{1+p} \lambda + \frac{p}{1+p} \omega_o^2 \right] = 0 \qquad (3.24)$$

The solution of the above equation provides the three eigenvalues as

$$\begin{aligned} \lambda_1 &= -\frac{\omega_o}{2\beta_o} \\ \lambda_2 &= -r\omega_o + i\theta \\ \lambda_3 &= -r\omega_o + i\theta \end{aligned} \qquad (3.25)$$

where,

$$\begin{aligned} r &= \frac{p}{1+p} \\ \theta &= r\omega_o \sqrt{\frac{1}{r\beta_o} - 1} \end{aligned} \qquad (3.26)$$

Note that for normal ranges of r and β, there are one real and two complex conjugate eigenvalues. For each of these eigenvalues, the corresponding eigenvectors can be easily obtained. It is expedient to biorthonormalize the left and right eigenvectors as

$$\begin{aligned} [\rho]^T [\xi] &= [I] \\ [\rho]^T [A] [\xi] &= [\Lambda] \end{aligned} \qquad (3.27)$$

where [I] is the identity matrix. These normalized eigenvector matrices are as follows :

$$[\xi] = \begin{bmatrix} 0 & \frac{\omega_o}{2(\omega_o + \beta_o\lambda_2)} & \frac{\omega_o}{2(\omega_o + \beta_o\lambda_2^*)} \\ -\frac{1}{1+p} & \frac{\omega_o}{2(1+p)(\omega_o + \beta_o\lambda_2)} & \frac{\omega_o}{2(1+p)(\omega_o + \beta_o\lambda_2^*)} \\ 0 & \frac{\omega_o\lambda_2}{2(\omega_o + \beta_o\lambda_2)} & \frac{\omega_o\lambda_2^*}{2(\omega_o + \beta_o\lambda_2^*)} \end{bmatrix} \tag{3.28}$$

$$[\rho] = \begin{bmatrix} 1 & 1 & 1 \\ -(1+p) & 0 & 0 \\ 0 & -\frac{(1+p)\lambda_2}{p\omega_o^2} & -\frac{(1+p)\lambda_2^*}{p\omega_o^2} \end{bmatrix} \tag{3.29}$$

Substituting the following transformation

$$\{y\} = [\xi]\{z\} \tag{3.29}$$

into Eq. (3.18) and premultiplying by $\{\rho\}^T$, we obtain

$$[\rho]^T[\xi]\{\dot{z}\} = [\rho]^T[A][\xi]\{z\} + [\rho]^T\{f\} \tag{3.30}$$

Utilizing the biorthonormal properties of the eigenvector matrices, as stated in Eq. (3.27), we obtain

$$\{\dot{z}\} = [\ \lambda\ ]\{z\} + \{\zeta\} \tag{3.31}$$

where the force vector in the generalized coordinates is defined as

$$\{\zeta\} = [\rho]^T\{f\} = \begin{Bmatrix} \dfrac{\mu_1 g\varepsilon_1 + p\omega_o^2 x_{res}}{2\beta_o\omega_o} \\ \dfrac{\lambda_2}{p\omega_o^2}\left[\ \mu_1 g\varepsilon_1 + p\omega_o^2 x_{res} + (1+p)\ddot{x}_g\ \right] \\ \dfrac{\lambda_3}{p\omega_o^2}\left[\ \mu_1 g\varepsilon_1 + p\omega_o^2 x_{res} + (1+p)\ddot{x}_g\ \right] \end{Bmatrix} \tag{3.32}$$

Eqs. (3.31) are decoupled equations, the solution of which will define the principal coordinates z_1, z_2 and z_3. For the ground acceleration $\ddot{x}_g(t)$ varying linearly from A_i to A_{i+1} during a time interval t_i to t_{i+1}, the solution of these equations can be written as :

$$\begin{aligned} z_1 &= a_1 e^{\lambda_1\tau} + \frac{\mu_1 g\varepsilon_1 + p\omega_o^2 x_{res}}{\omega_o^2} \\ z_2 &= a_2 e^{\lambda_2\tau} - V_i - \frac{V_{i+1} - V_i}{\lambda_2 h_i} - \frac{V_{i+1} - V_i}{h_i}\tau \\ z_3 &= a_3 e^{\lambda_3\tau} - V_i - \frac{V_{i+1} - V_i}{\lambda_2 h_i} - \frac{V_{i+1} - V_i}{h_i}\tau \end{aligned} \tag{3.33}$$

where, $\tau = t - t_i$ and $h_i = t_{i+1} - t_i$ = the interval size. The constants V_i and V_{i+1} corresponding to times t_i and t_{i+1} are defined as follows :

$$V_i = \frac{1}{p\omega_o^2}\left[\mu_1 g\varepsilon_1 + p\omega_o^2 x_{res} + (1+p)A_i\right]$$
$$V_{i+1} = \frac{1}{p\omega_o^2}\left[\mu_1 g\varepsilon_1 + p\omega_o^2 x_{res} + (1+p)A_{i+1}\right] \tag{3.34}$$

The constants of integration a_1, a_2 and a_3 are obtained by applying the initial conditions on the response vector $\{y\}$ which is defined in terms of the principal coordinates $\{z\}$ by Eq. (3.29). These initial conditions are :

$$\begin{aligned} x_t(\tau = 0) &= x_{t_i} \\ x_{s_1}(\tau = 0) &= x_{s_{1_i}} \\ \dot{x}_t(\tau = 0) &= \dot{x}_{t_i} \end{aligned} \tag{3.35}$$

Substituting the above conditions in Eq. (3.33), we get the following for a_1, a_2 and a_3 :

$$\begin{aligned} a_1 &= x_{t_i} - (1+p)x_{s_{1_i}} - \frac{\mu_1 g\varepsilon_1 + p\omega_o^2 x_{res}}{\omega_o^2} \\ a_2 &= X_i + \lambda_2 Y_i \\ a_3 &= X_i + \lambda_2^* Y_i \end{aligned} \tag{3.36}$$

where,

$$\begin{aligned} X_i &= x_{t_i} + V_i + \frac{V_{i+1} - V_i}{\lambda_1 h_i} \\ Y_i &= -\frac{1+p}{p\omega_o^2}\left(\dot{x}_{t_i} + \frac{V_{i+1} - V_i}{h_i}\right) \end{aligned} \tag{3.37}$$

It is noted that $a_3 = a_2^*$. Substituting for a_1, a_2 and a_3 in Eq. (3.33) and then finally substituting for $\{z\}$ in Eq. (3.29) along with some lengthy algebraic manipulations, we get the following expressions for the desired displacements and velocities :

$$
\begin{aligned}
x_{s_1}(\tau) = {} & \frac{1}{1+p} e^{-\frac{\omega_o}{2\beta_o}\tau} x_{t_i} + e^{-\frac{\omega_o}{2\beta_o}\tau} x_{s_{1_i}} \\
& - \frac{1}{1+p}\left(1 - e^{-\frac{\omega_o}{2\beta_o}\tau}\right) \frac{\mu_1 g \varepsilon_1 + p\omega_o^2 x_{res}}{\omega_o^2} \\
& + \frac{1}{1+p}\left[-1 + \frac{\tau}{h_i} - \frac{2\beta_o}{\omega_o h_i} \right] V_i + \frac{1}{1+p}\left[\frac{2\beta_o}{\omega_o h_i} - \frac{\tau}{h_i} \right] V_{i+1} \\
& + \frac{e^{-r\omega_o\tau}}{1+p}\left[\frac{\theta\beta_o \sin(\theta\tau)}{\omega_o(1-r\beta_o)} + \cos(\theta\tau) \right] X_i + \frac{e^{-r\omega_o\tau}}{1+p}\left[-\frac{\theta \sin(\theta\tau)}{1-r\beta_o} \right] Y_i
\end{aligned}
\tag{3.38a}
$$

$$
\begin{aligned}
\dot{x}_{s_1}(\tau) = {} & \frac{\omega_o}{2\beta_o(1+p)} e^{-\frac{\omega_o}{2\beta_o}\tau} x_{t_i} - \frac{\omega_o}{2\beta_o} e^{-\frac{\omega_o}{2\beta_o}\tau} x_{s_{1_i}} \\
& - e^{-\frac{\omega_o}{2\beta_o}\tau}\left[\frac{\mu_1 g \varepsilon_1 + p\omega_o^2 x_{res}}{2\beta_o\omega_o(1+p)} \right] + \frac{1}{(1+p)h_i} V_i - \frac{1}{(1+p)h_i} V_{i+1} \\
& + \frac{e^{-r\omega_o\tau}}{1+p}\left[-\frac{\theta \sin(\theta\tau)}{1-r\beta_o} \right] X_i + \frac{r\omega_o^2 e^{-r\omega_o\tau}}{1+p}\left[\frac{\theta \sin(\theta\tau)}{\omega_o(1-r\beta_o)} - \frac{\cos(\theta\tau)}{\beta_o} \right] Y_i
\end{aligned}
\tag{3.38b}
$$

and

$$
x_t(\tau) = (1+p)x_{s_1}(\tau) + a_1 e^{-\frac{\omega_o}{2\beta_o}\tau} + \frac{\mu_1 g \varepsilon_1 + p\omega_o^2 x_{res}}{\omega_o^2} \tag{3.39a}
$$

$$
\dot{x}_t(\tau) = (1+p)\dot{x}_{s_1}(\tau) - \frac{\omega_o}{2\beta_o} e^{-\frac{\omega_o}{2\beta_o}\tau} \tag{3.39b}
$$

Eqs. (3.38) and (3.39) define the response of the system during any sliding phase occuring between t_i and t_{i+1}. It is noted that $0 \leq \tau \leq (t_{i+1} - t_i)$. The displacement response of the frame which is directly proportional to the forces in the frame can be calculated from :

$$
x_f(\tau) = x_t(\tau) - x_{s_1}(\tau) \tag{3.40}
$$

The response at time t_{i+1} (at the end of the time step) is obtained by replacing τ with $h_i = t_{i+1} - t_i$. Sliding ceases to occur if the sliding velocity, $\dot{x}_{s_1}(\tau)$ becomes zero.

3.4 Numerical Results

The numerical results obtained for a sliding system without lateral spring indicated that a significant reduction in the accelerations of the slab and corresponding reduction in the forces in the frame can be achieved by permitting the slab mass to slide at the interface with the frame. However, to realize these advantages it was necessary that the slab be able to slide uninterrupted to dissipate energy by Coulomb damping. The amount by which the slab should be able to slide depended upon the frequency of the structure. The sliding displacements in the low frequency structures were observed to be on rather high size. To see if the provision of a lateral spring can be effective in reducing the sliding displacement without any significant increase in the accelerations and forces, these response quantities have been obtained for structures of varying frequencies and are presented in the response spectrum form. Five different ground motions recorded on soft, medium stiff and hard sites have been used as the seismic inputs in the numerical calculations. These motions have been enumerated in Chapter 2.

In the earlier study presented in Chapter 2, an isolation or response reduction parameter was introduced to define the frictional characteristics of the sliding interface rather than the friction coefficient. This parameter was then used to show the effect of slab sliding or the Coulomb damping on the response of structures of different frequencies. This parameter was defined by :

$$\delta = \frac{\mu_1 g}{\mathbf{ASA}} \tag{3.41}$$

where **ASA** = absolute acceleration spectrum value for the corresponding elastic oscillator and μ_1 = friction coefficient at the interface between the slab and frame.

It was then observed that for a given value of this parameter the normalized slab acceleration and frame displacement responses (normalized with respect to the response of a corresponding non-sliding elastic structure) were both equal to the parameter δ for all structures of different frequencies. That is, in a slab sliding structure if δ were equal to 0.2, the maximum slab acceleration and forces in the supporting frame will be only 20% of these response quantities in a the corresponding non-sliding elastic structure; also this fraction will remain the same for all structures of different frequencies. Thus the choice of this parameter enabled us to compare and study different structures of different frequencies more consistently. Therefore, to demonstrate the effectiveness of providing a lateral spring, we have again chosen this parameter to characterize the sliding interfaces of structures with different frequencies. Of course, now with the introduction of a lateral spring, the normalized system response will not be equal to the δ parameter. This is because the lateral spring introduces additional forces on the mass and the frame.

Fig. 3.2 is for structures with δ parameter = 0.2, and shows the spectra for the normalized slab acceleration (normalized with respect to the acceleration of the slab in a non-sliding elastic structure) for different values of stiffness ratio p. The spectrum for p = 0. corresponds to the case of a slab sliding system with no lateral spring. As mentioned earlier, this spectrum is a horizontal line at the level = 0.20. The spectra for spring-assisted systems with different values of ratio p are seen to merge with the spectrum for p = 0. at the medium to low frequencies (that is, period

> 0.20 sec). In the high frequency range, however, the accelerations in the spring-assisted systems can be significantly higher than those obtained in the elastic system. Also, as one would expect, the acceleration spectra for higher values of p are higher. Thus introduction of a lateral spring does not significantly change the acceleration of medium to low frequency structures, but it can amplify the accelerations of a high frequency structure.

Similar observations can also be made about the displacement response of the supporting frame, which is directly proportional to the forces in the frame. Fig. 3.3 shows the displacement spectrum values, normalized with respect to the displacement of the elastic system. These results are for structures with the same δ parameter and stiffness ratios and with the same ground motion as in Fig. 3.2. Although it was not immediately apparent before these results were plotted, the spectra in this figure are almost identical to the acceleration spectra in Fig. 3.2. Thus based on these results one leads to the same conclusions as in the previous paragraph regarding the effect of the lateral spring.

To ascertain the effectiveness of a lateral spring in reducing the sliding displacements, the response spectrum of this quantity is plotted in Fig. 3.4. These results are also for the same δ-parameter, stiffness ratios and ground motion as those used in Figs. 3.2 and 3.3. It is observed from this figure that by provision of a lateral spring the sliding displacements are indeed reduced for the low frequency structures. Also, the stiffer the lateral spring (that is, the larger spring ratio p), the smaller the sliding displacement. The reduction in the sliding displacement is also observed in the case of the high frequency structures, but as observed from Figs. 3.2 and 3.3, this reduction is associated with a significant increase in the slab acceleration and frame deformation responses which obviously is undesirable. Thus, the lateral spring does

not help the high frequency structures but is quite helpful with flexible structures in reducing the sliding displacement requirement.

To examine the effectiveness of a lateral spring in the recovery of the sliding displacement at the end of the motion, Fig. 3.5 showing the residual displacement spectra is presented. Here again, the δ –parameter, stiffness ratios and ground motion are the same as in the previous figures. If there is no lateral spring, then the residual displacement is usually the same as the sliding displacement, as it can be seen from the curves for $p = 0$ in Fig. 3.5. However, for the other values of the stiffness ratios, we observe that the residual displacements are less than the sliding displacements. Furthermore, this difference is more for the stiffer lateral springs. Also a system with stiffer spring will have a smaller residual displacement. This indicates that a lateral spring does provide some displacement recovery mechanism which tries to bring the sliding mass back to its original position.

Figs. 3.6 to 3.8 show secondary floor spectra comparison for elastic, slab sliding and spring-assisted slab sliding systems. Fig. 3.6 is for a primary structure frequency of 5 cps subjected to Ground Motion 5. The figure shows that the provision of the lateral spring in the spring-assisted systems does not lead to any significant increase in the resulting secondary spectra. In fact, the spectra corresponding to the slab sliding and spring-assisted slab sliding systems almost overlap each other. This also shows that the spring-assisted system is equally effective in reducing the resonance effect that takes place when the frequencies of the primary and secondary structures coincide. Fig. 3.7 corresponds to a primary structure frequency of 0.50 cps subjected to Ground Motion 5. Here too, the same observations made concerning Fig. 3.6 are seen to be valid. In fact, the overlapping of the spectra corresponding to sliding systems is almost total, so that they can not be distinguished from each other. This observation is important, because a slight increase in the level of peak acceleration

response of the slab in the spring-assisted systems does not seem to result in increased magnitudes of secondary spectra of primary structures in the low and medium frequency ranges. However, the same is not true for structures in the high frequency range. It may be recalled from Fig. 3.3 that in this frequency range, there is in fact an increase in the level of acceleration response over and above the corresponding elastic response. It can be seen in Fig. 3.8 that this translates into increased levels of secondary spectra. Fig. 3.8 correponds to a primary structure of frequency 20 cps, subjected to Ground Motion 1. It shows that though the spring-assisted systems are successful in alleviating the resonance effect, overall, they are not effective in reducing the secondary floor spetra. They lead to higher levels of secondary spectra in the high frequency end of the spectrum and also, they seem to cause a shift in the resonance frequency region.

Figs. 3.9 to 3.11 are similar to Figs. 3.2, 3.4 and 3.5, respectively. They show the spectra for the same response quantities as in Figs. 3.2, 3.4 and 3.5, but now these spectra correspond to Ground Motion 5 (recorded on a hard site) as the input. Also, they are obtained for a lower value of the δ –parameter. The information from these figures substantiates our earlier observations. That is, the introduction of a lateral spring is again seen to reduce the sliding displacement without any significant increase in the slab acceleration and frame displacement response, especially for medium to low frequency structures. For high frequency structures, the use of a lateral spring is not helpful as it leads to an amplification of the acceleration and frame displacement response.

Figs. 3.12 to 3.14 are shown to study the effect of the site stiffness (viz. soft, medium stiff and hard) on the response of the spring-assisted system. Response spectra for normalized slab acceleration, normalized frame deformation and sliding displacement of the slab are compared for Ground Motions 1, 2 and 5. They

correspond to soft, medium stiff, and hard site conditions, respectively. Fig. 3.12 shows that irrespective of the site stiffness, the normalized slab acceleration levels are about the same in low and medium frequency ranges. However, in the high frequency range, the spectrum corresponding to hard site exhibits a different characteristic than the spectra for the other two site condidtions. Fig. 3.13 shows a similar comparison for normalized frame displacement. As expected, the spectra in here are almost identical as the ones in Fig. 3.12 and thus the same observations are true for this case, too. It is noted that in both Figs. 3.12 and 3.13, the spectra shown are normalized with respect to their respective elastic (non-sliding) spectra. Also, it is important to point out that the observations made here regarding the possible influence of the site stiffness can not be considered general, since the number of ground motions used in this study is too few. Fig. 3.14 shows comparison of sliding displacement spectra for various site conditions. Here, just as for the case of simple slab sliding system, the sliding displacements for the soft ground motion are generally larger than the other two ground motions. It is also seen that the sliding displacement spectrum for the hard site ground motion is generally of the lowest magnitude among the three considered herein. For all the site types, the spectrum curves follow a rather consistent pattern in that they all start low in the high frequenccy range and rise somewhat sharply in the low frequency ends of the spectra. Again, it is mentioned that these observations may not be considered general.

Figs. 3.15 and 30 are similar to Figs. 3.12 and 3.14, but they are drawn for Ground Motions 3, 4 and 5. Here, the purpose is to see the variability in the response spectra for ground motions recorded on the sites with the same stifness characteristic. Fig. 3.15 shows the spectra for normalized slab acceleration. It is seen that the Ground Motions 4 and 5 produce very similar spectra, however, the spectrum corresponding

to Ground Motion 3 is markedly different than the other two in the high frequency range. The comparison of the sliding displacement spectra in Fig. 3.16 shows that the curves for Ground Motions 4 and 5 are in closer agreement with each other than compared to the curve for Ground Motion 3. These observations indicate that a large ensemble of ground motions may be necessary to arrive at more substantive conclusions regarding the effects of ground motion characteristics.

3.5 *Concluding Remarks*

In the study of slab sliding structures, it was observed that by permitting the slab to slide one can significantly reduce the acceleration of the slab as well as the forces in the lateral force carrying members. However, for low frequency structures this arrangement required a fairly large amount of unobstructed sliding displacement. To reduce this sliding displacement requirement, here the provision of a lateral spring between the supporting frame and a sliding slab is proposed. To investigate the effectiveness of providing a lateral spring, the equations of motion of the slab, frame and lateral spring system are developed. This leads to a set of two coupled linear differential equation when the slab is sliding. Explicit solution of this coupled set is obtained in the state vector form by the utilization of the eigenvalues and eigenvectors of the system matrix. Numerical results are obtained for two ground motion time histories. In particular, the response quantities of the slab acceleration, frame deformation and sliding and residual displacements are obtained for structures of different frequencies and presented in response spectrum form.

From these results it is observed that, in the medium to low frequency structures, the provision of a rather weak spring can be effective in reducing the sliding displacement requirements of a slab sliding system without any significant increase in the slab accelerations and frame forces. In the high frequency structures, however, the introduction of a weak spring can in fact amplify the slab accelerations and frame forces significantly. That is, the introduction of even a weak spring can be detrimental to a high frequency structure. However, as was mentioned earlier the high frequency structures did not need any help or modification as the sliding displacements for such structures were quite low to start with and thus could be accommodated easily in practice. For the large sliding displacements in the low frequency structures, this study shows that the provision of a flexible lateral spring between the frame and slab can alleviate this problem to some extent.

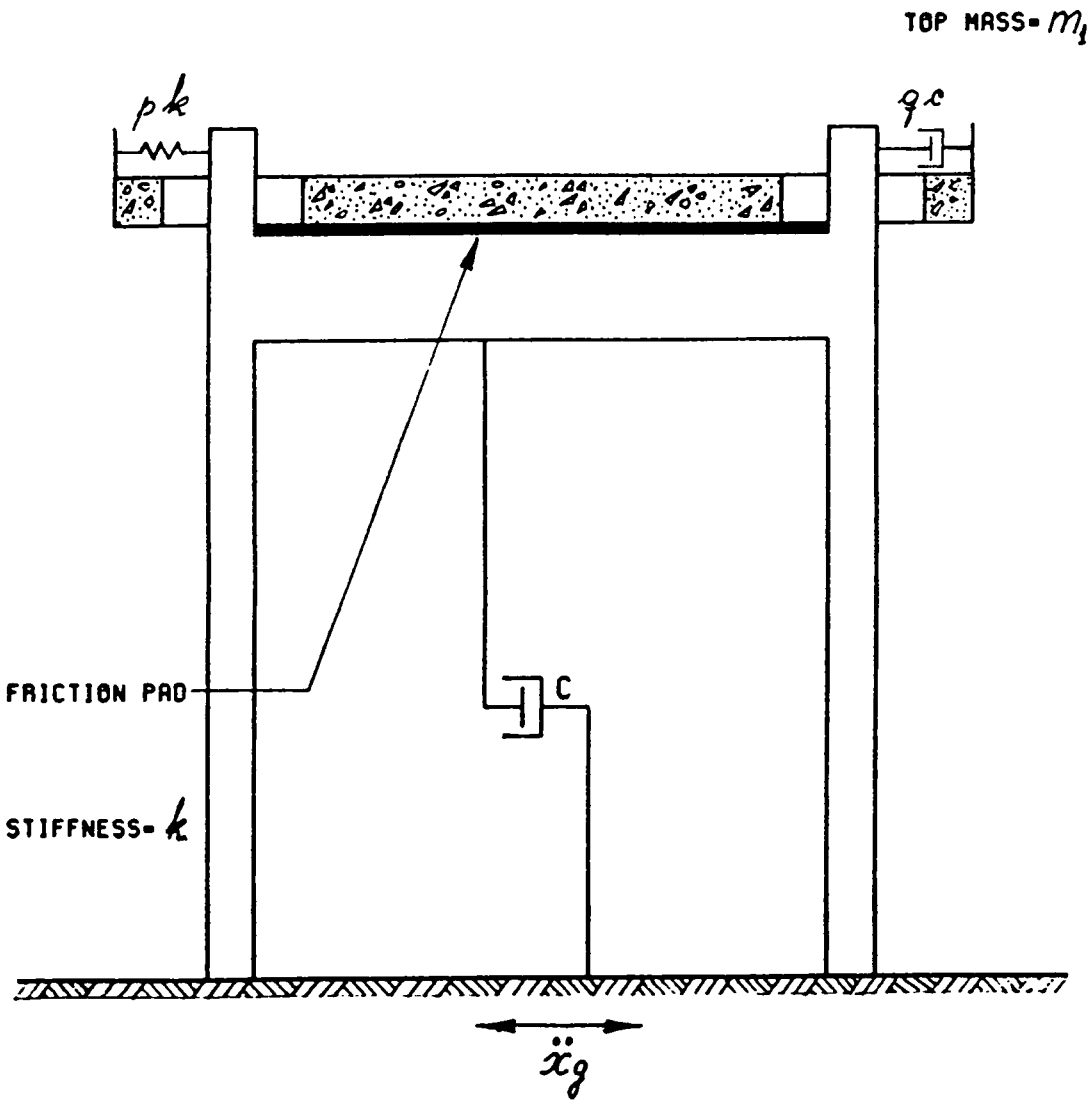

FIG. 3.1 PROPOSED SPRING-ASSISTED SLAB SLIDING SYSTEM

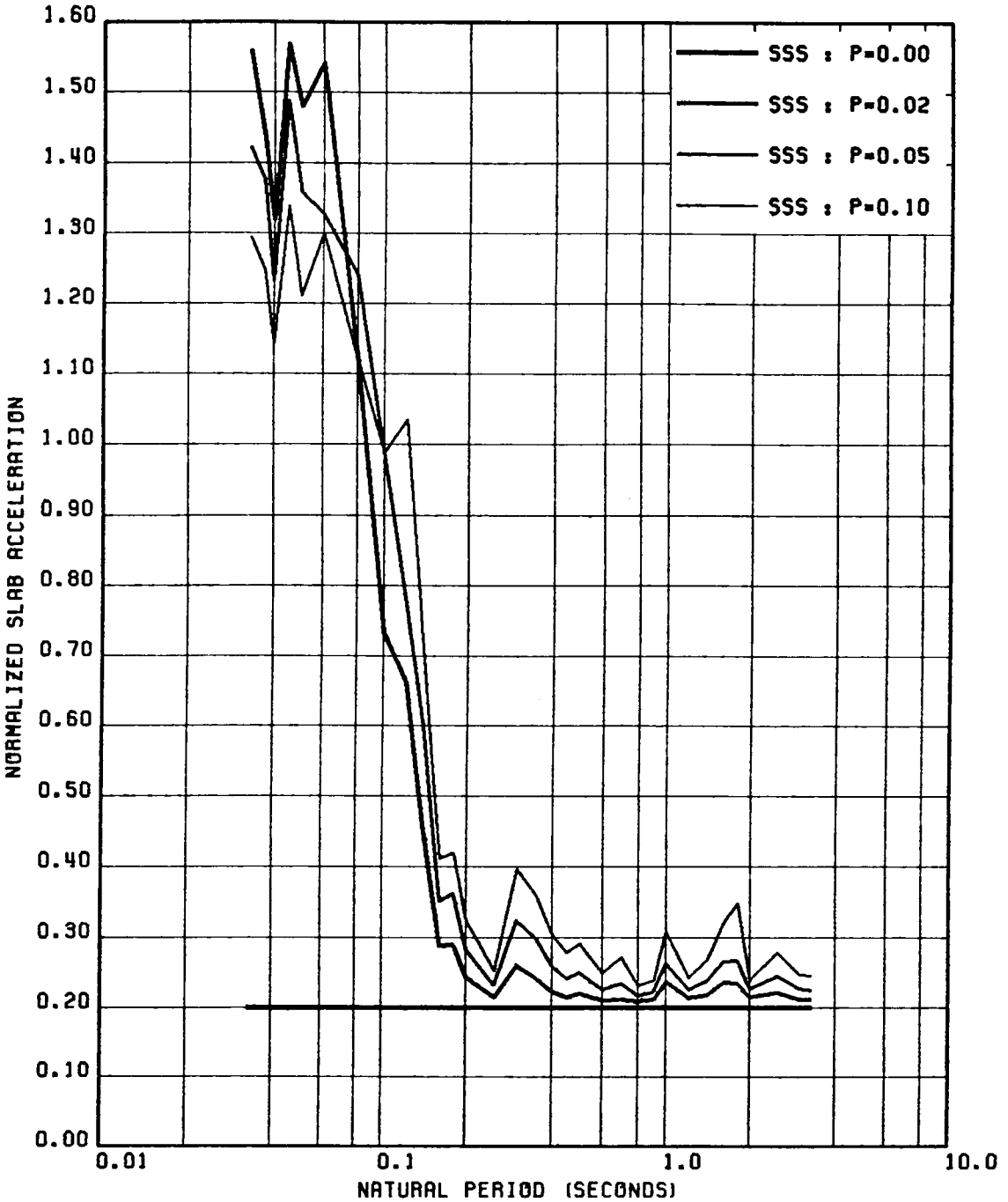

FIG. 3.2 SLAB ACCELERATION SPECTRA (NORMALIZED WITH RESPECT TO THE CORRESPONDING NON-SLIDING ASA SPECTRUM) FOR VARIOUS SPRING-ASSISTED SLAB SLIDING SYSTEMS; GROUND MOTION 1, β_o = 0.02 AND δ = 0.20.

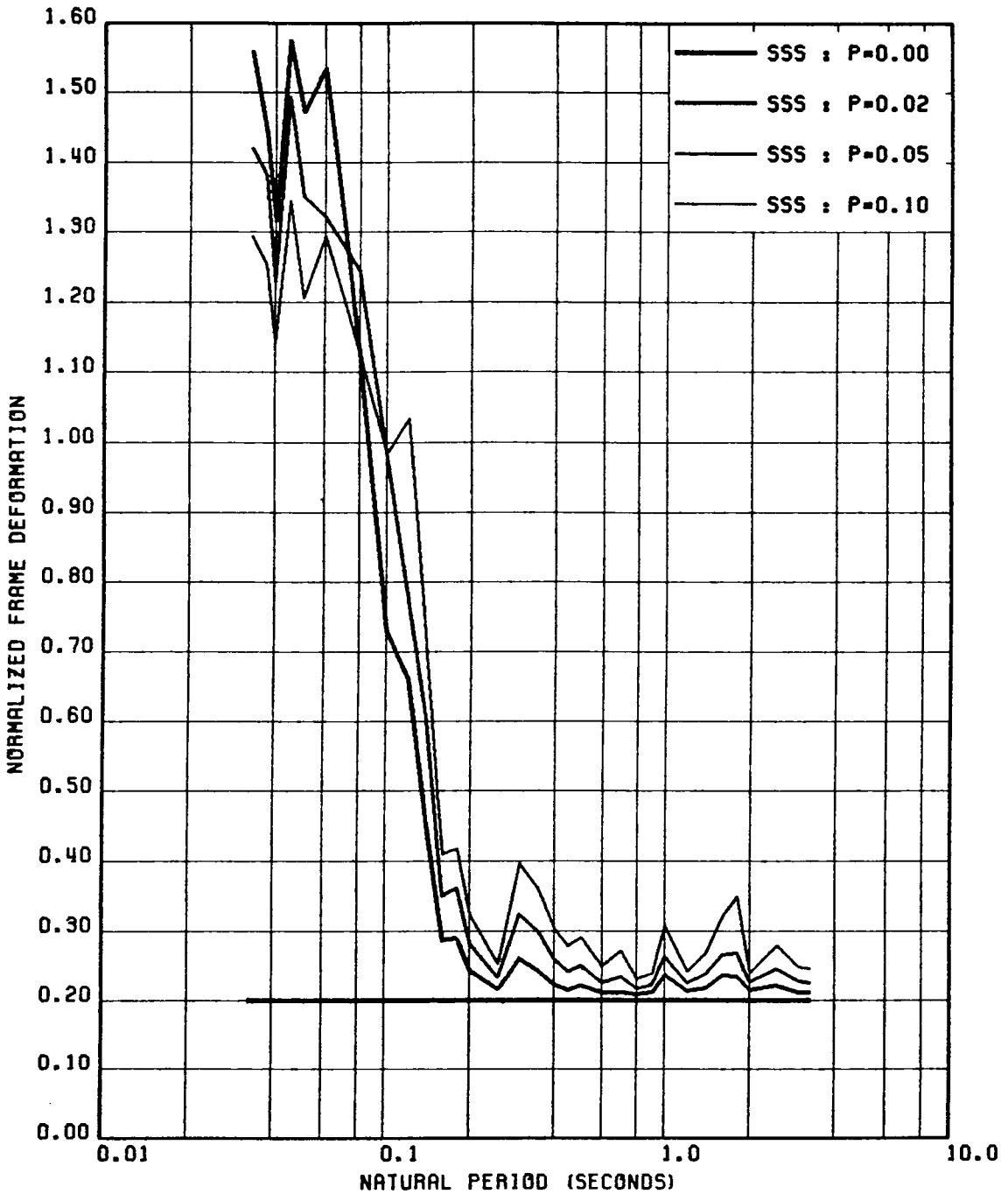

FIG. 3.3 FRAME DEFORMATION SPECTRA (NORMALIZED WITH RESPECT TO THE CORRESPONDING NON-SLIDING ASA SPECTRUM) FOR VARIOUS SPRING-ASSISTED SLAB SLIDING SYSTEMS; GROUND MOTION 1, β_o = 0.02 AND δ = 0.20.

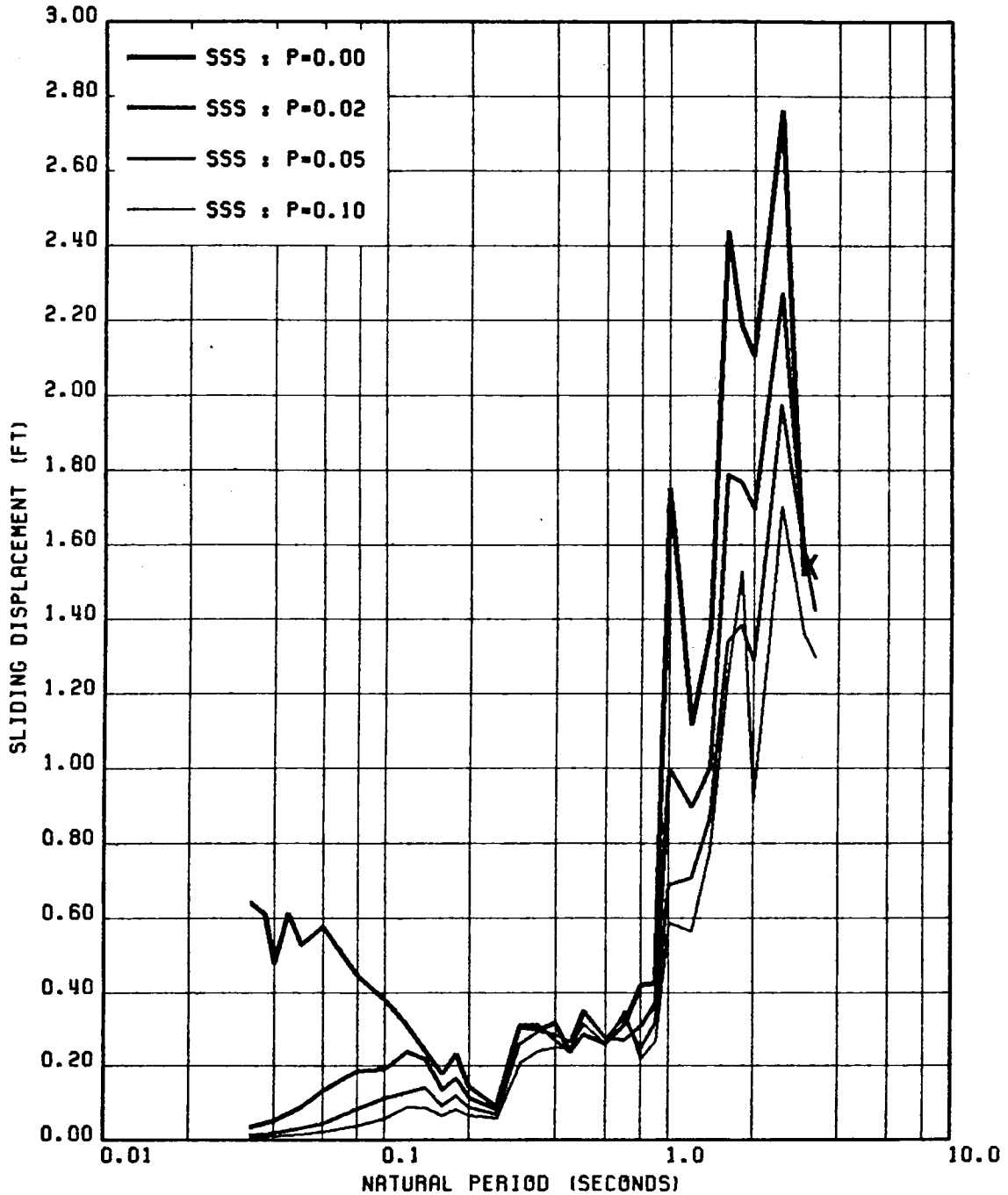

FIG. 3.4 SLAB SLIDING DISPLACEMENT SPECTRA OF SLAB SLIDING & VARIOUS SPRING ASSISTED SLIDING SYSTEMS SUBJECTED TO GR MOTION 1; β_o=0.02, δ=0.20.

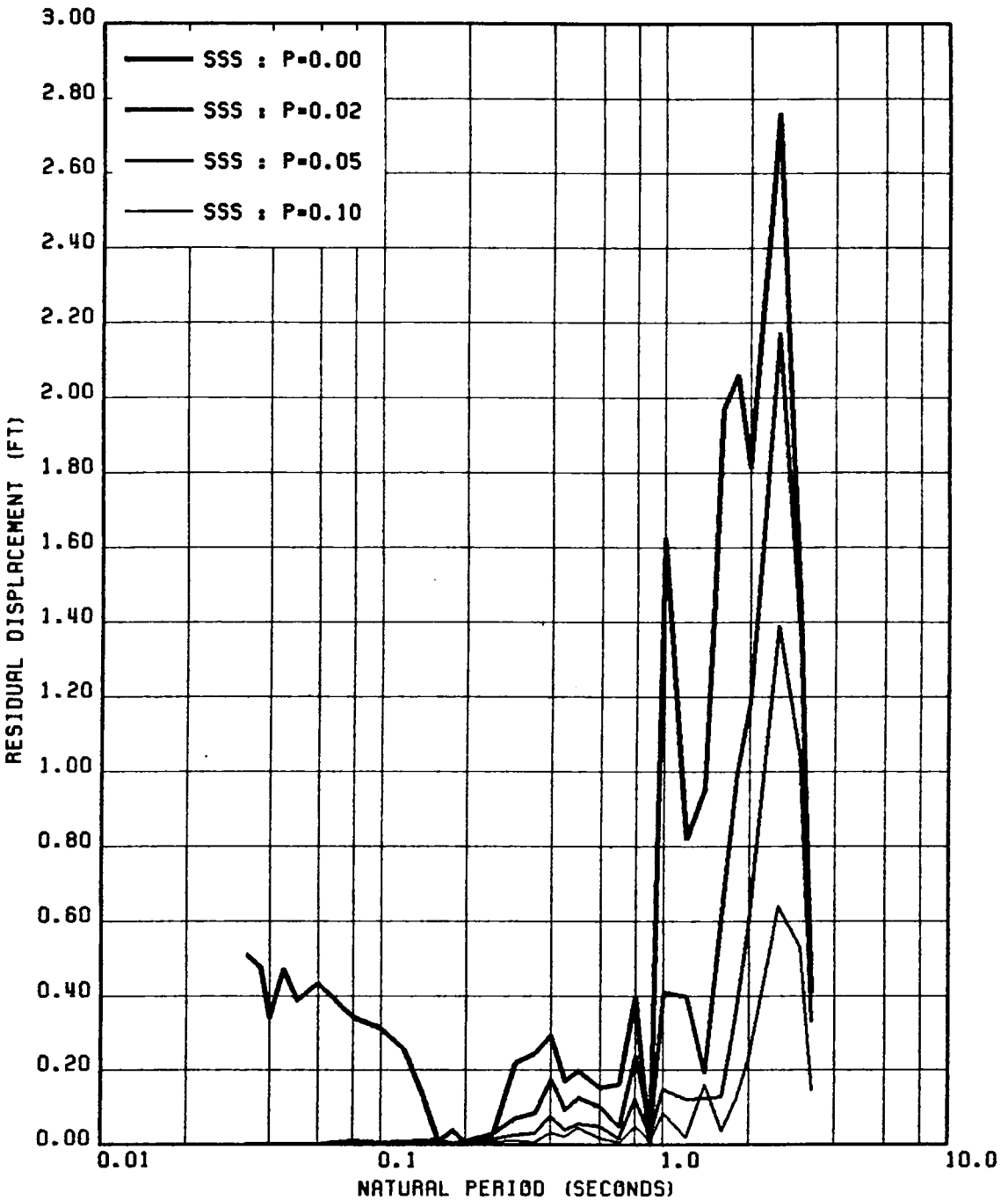

FIG. 3.5 SPECTRA OF RESIDUAL DISPLACEMENT FOR SLAB SLIDING & VARIOUS SPRING ASSISTED SLIDING SYSTEMS SUBJECTED TO GR MOTION 1; β_o=0.02, δ=0.20.

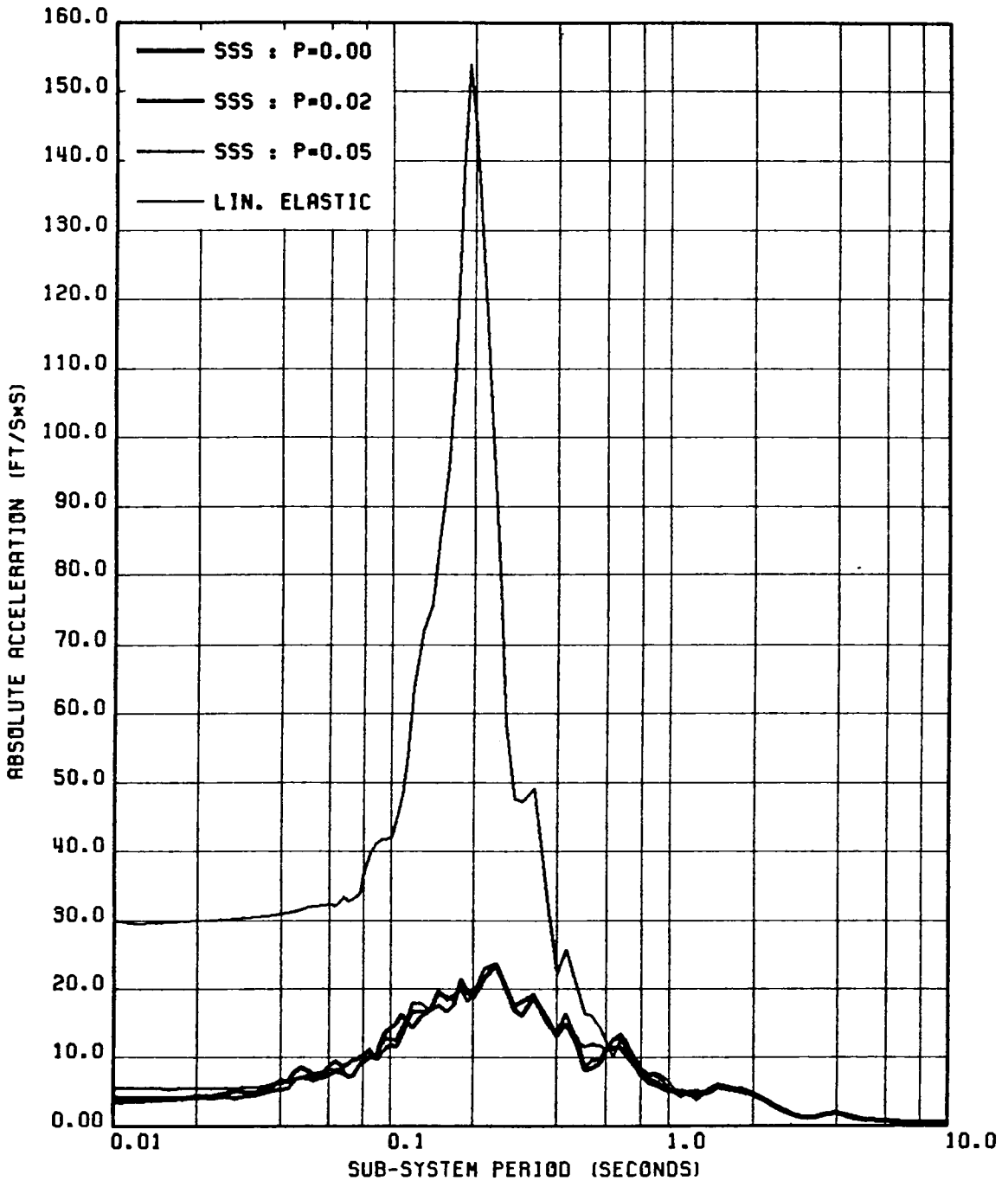

FIG. 3.6 COMPARISON OF SECONDARY FLOOR SPECTRA FOR ELASTIC, SLAB SLIDING & SPRING-ASSISTED SYSTEMS-GR. MOTION 5, F=5 CPS, β_a , β_s =0.05, δ=0.10.

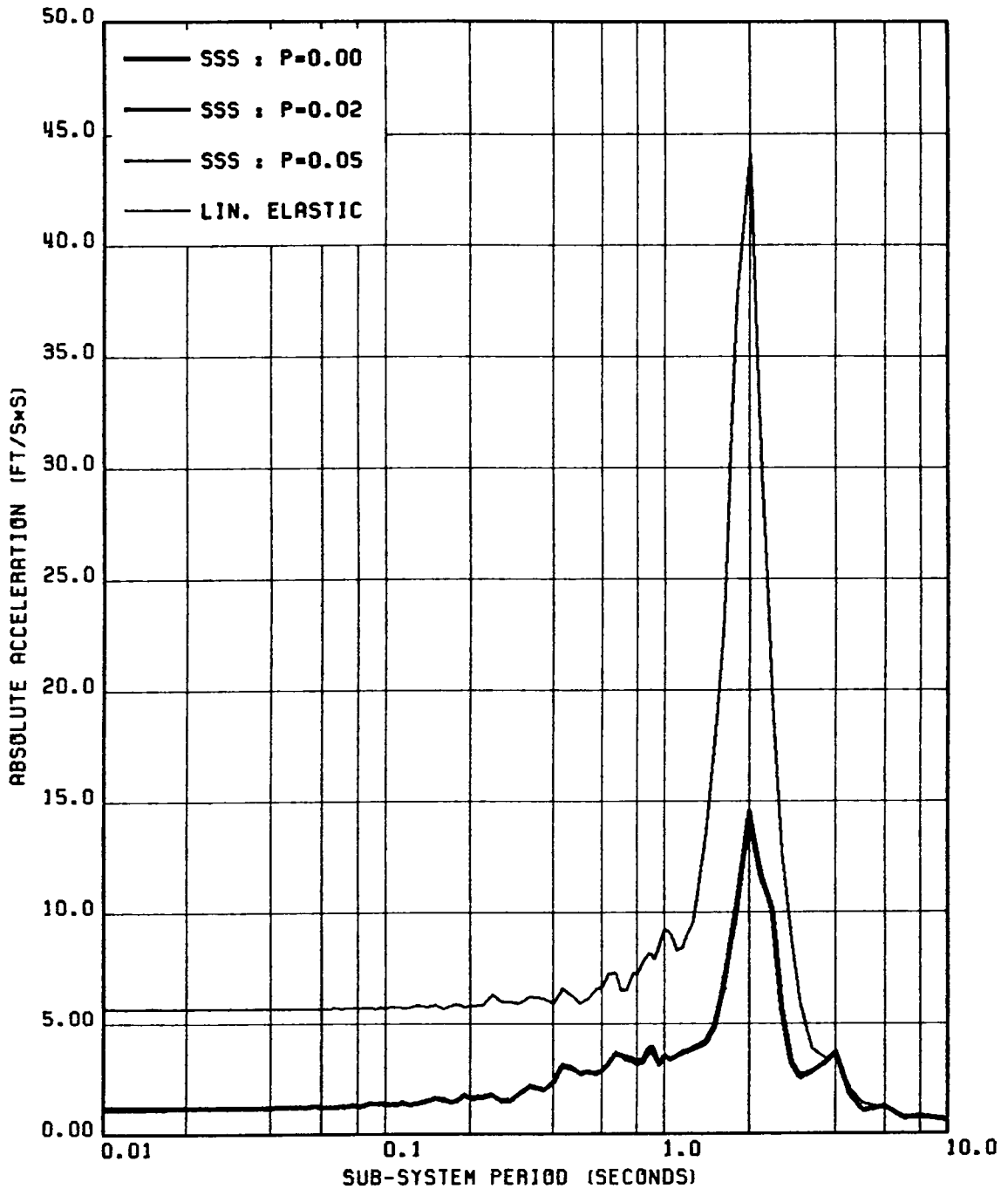

FIG. 3.7 COMPARISON OF SECONDARY FLOOR SPECTRA FOR ELASTIC, SLAB SLIDING & SPRING-ASSISTED SYSTEMS-GR MOTION 5, F=.5 CPS, β_o , β_s =0.05, δ=0.20.

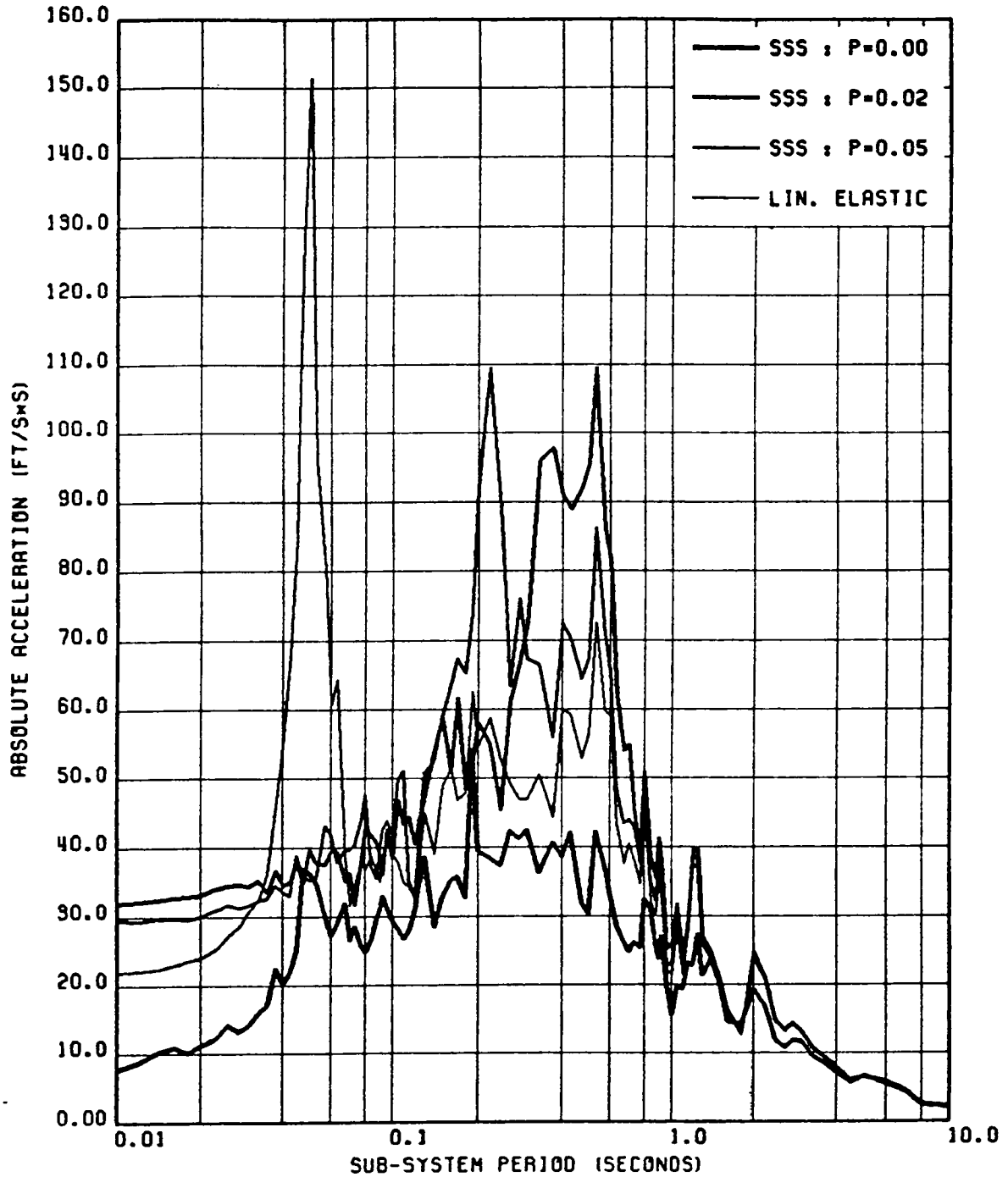

FIG. 3.8 COMPARISON OF SECONDARY FLOOR SPECTRA FOR ELASTIC, SLAB SLIDING AND SPRING-ASSISTED SYSTEMS-GR. MOTION 1, F=20 CPS, β β =0.02, δ=0.10.

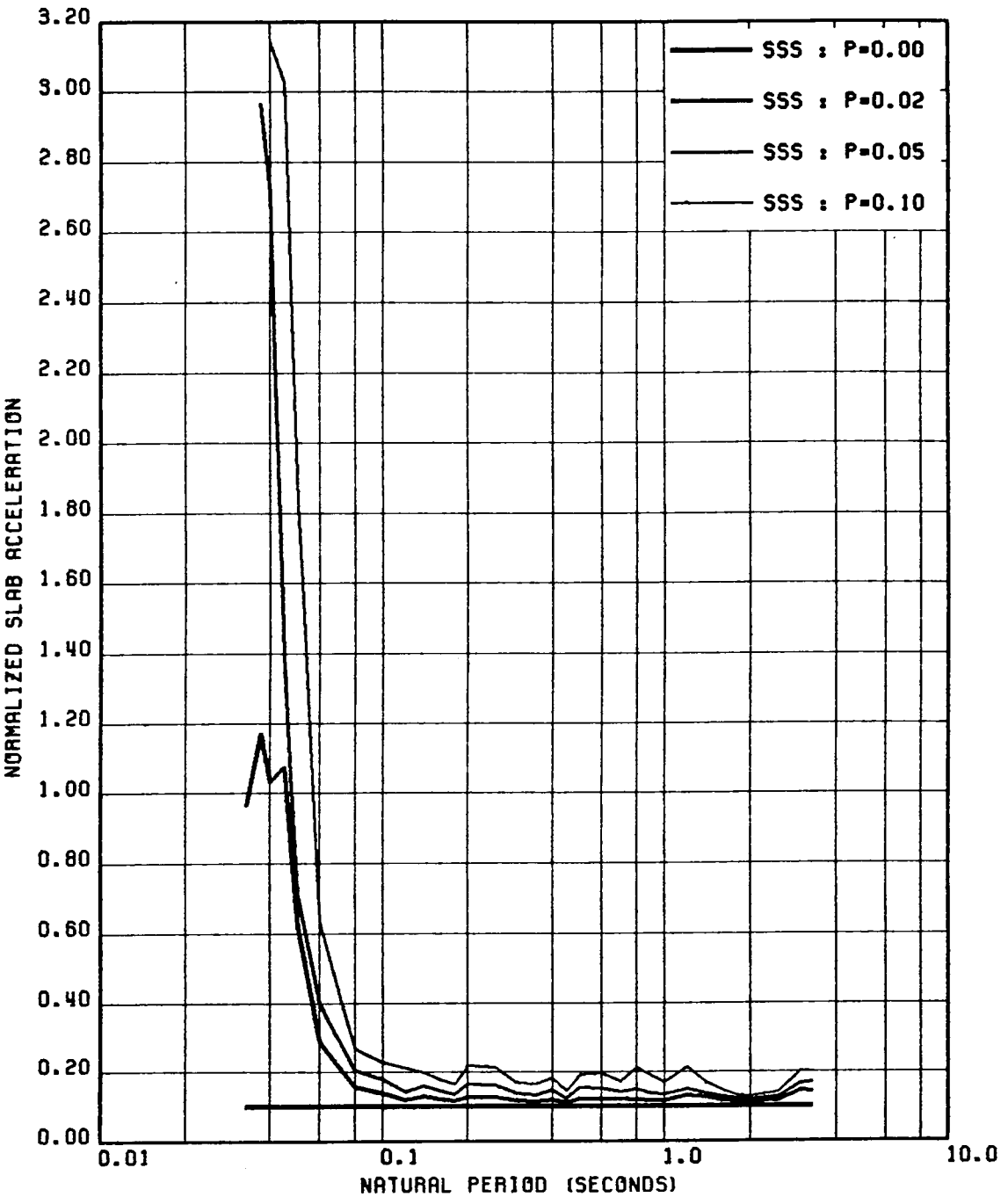

FIG. 3.9 SLAB ACCELERATION SPECTRA (NORMALIZED WITH RESPECT TO THE CORRESPONDING NON-SLIDING ASA SPECTRUM) FOR VARIOUS SPRING-ASSISTED SLAB SLIDING SYSTEMS; GROUND MOTION 5, β_o = 0.02 AND δ = 0.10.

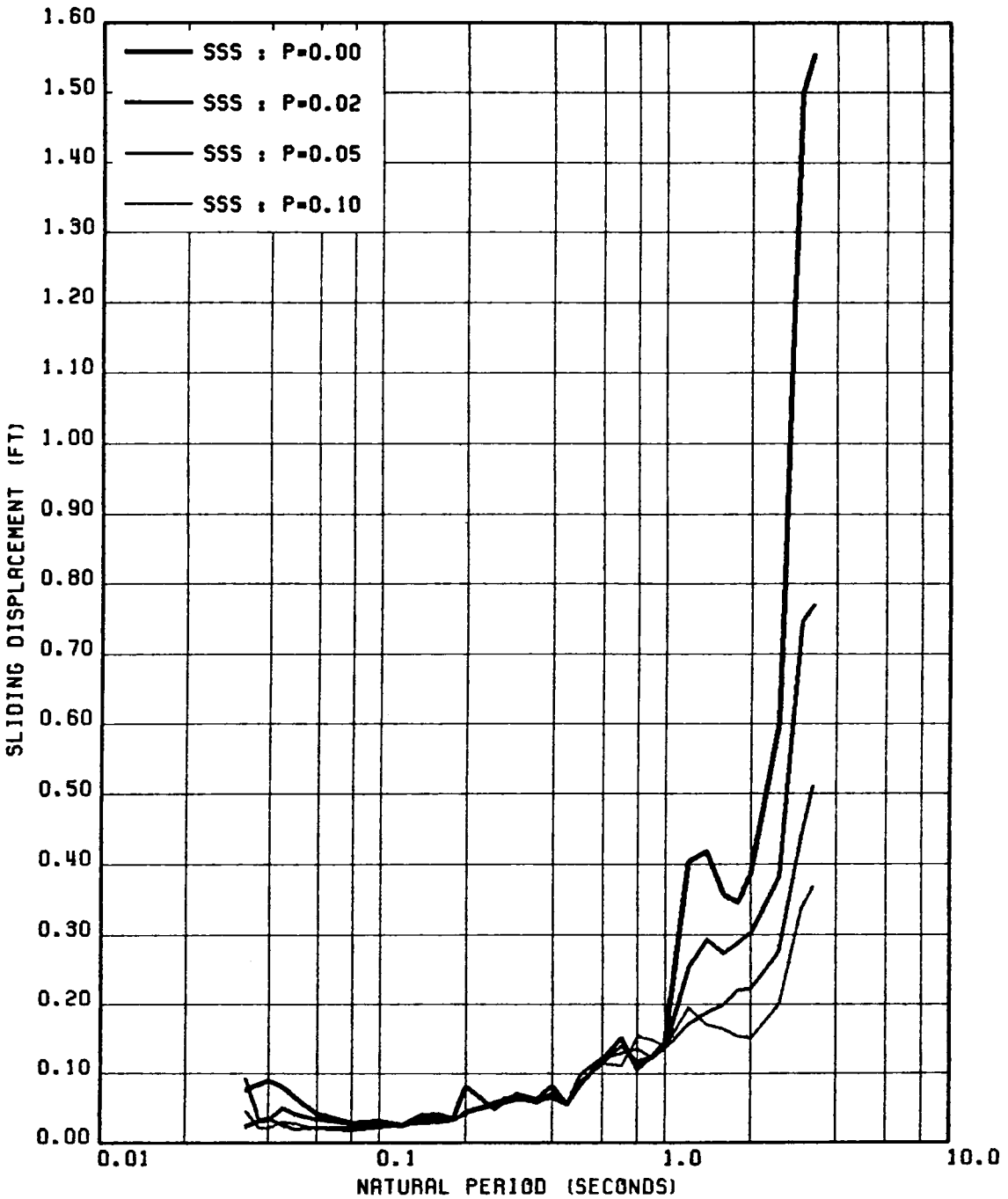

FIG. 3.10 SLAB SLIDING DISPLACEMENT SPECTRA OF SLAB SLIDING AND DIFFERENT SPRING-ASSISTED SLIDING SYSTEMS; GR. MOTION 5; β_o=0.02, δ=0.10.

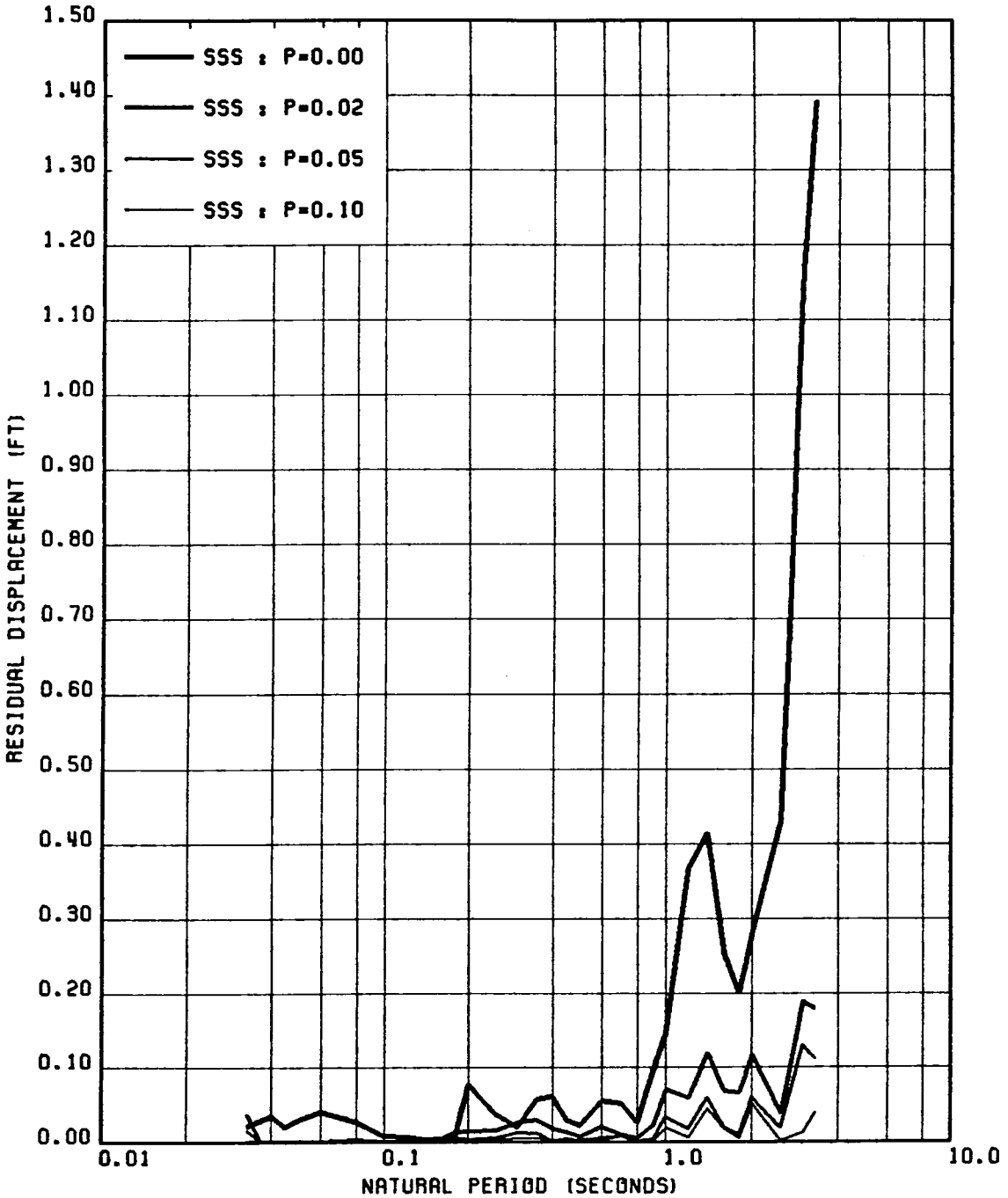

FIG. 3.11 SPECTRA OF RESIDUAL DISPLACEMENT FOR SLAB SLIDING AND DIFFERENT SPRING-ASSISTED SLIDING SYSTEMS; GR. MOTION 5; β_o=0.02, δ=0.10.

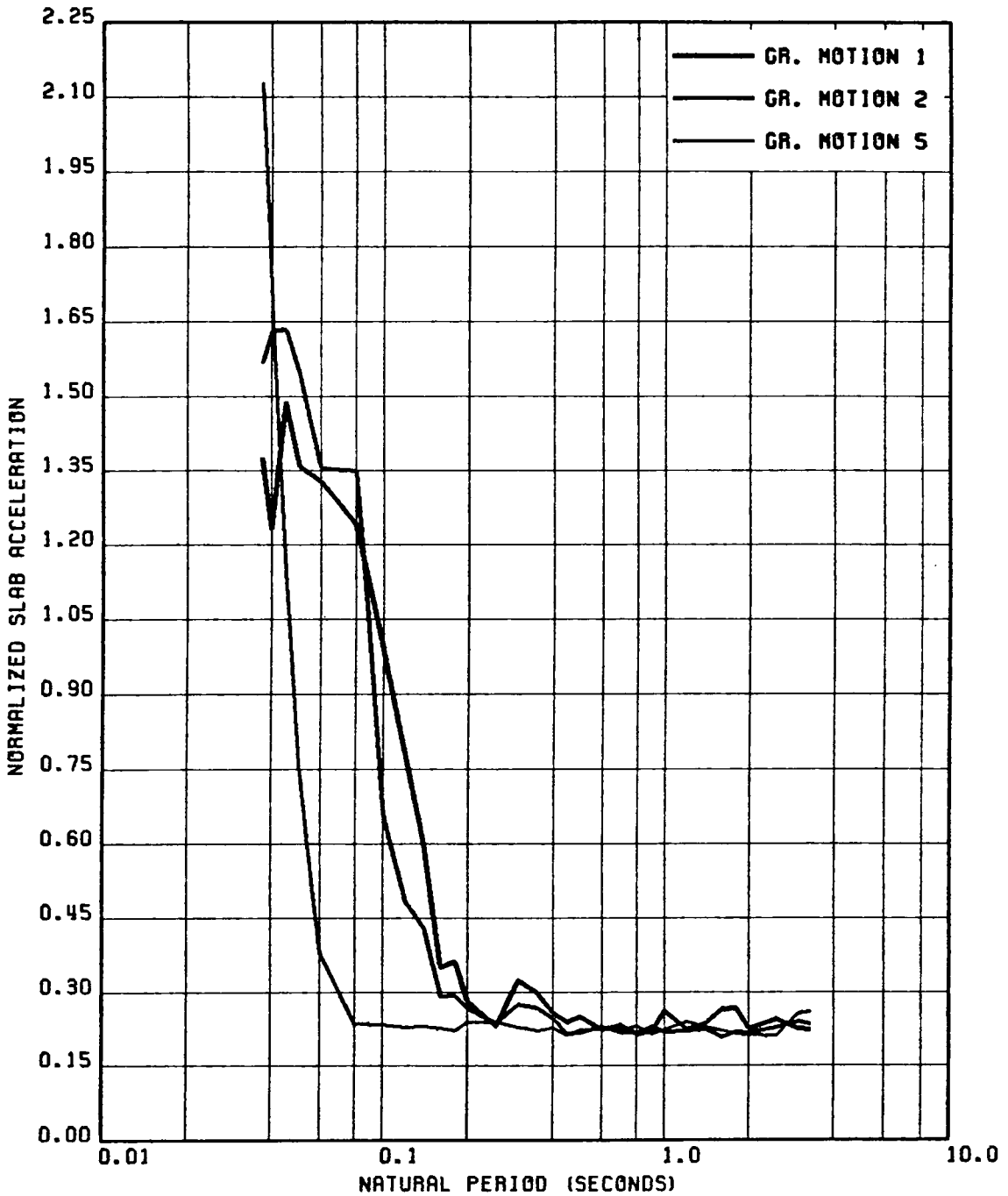

FIG. 3.12 COMPARISON OF SLAB ACCELERATION SPECTRA (NORMALIZED W.R.T. CORRESPONDING NON-SLIDING ASA SPECTRA) FOR GROUND MOTIONS 1, 2 & 5; OF THE SPRING-ASSISTED SLIDING SYSTEM WITH p=0.05, β_o=0.02 & δ=0.20.

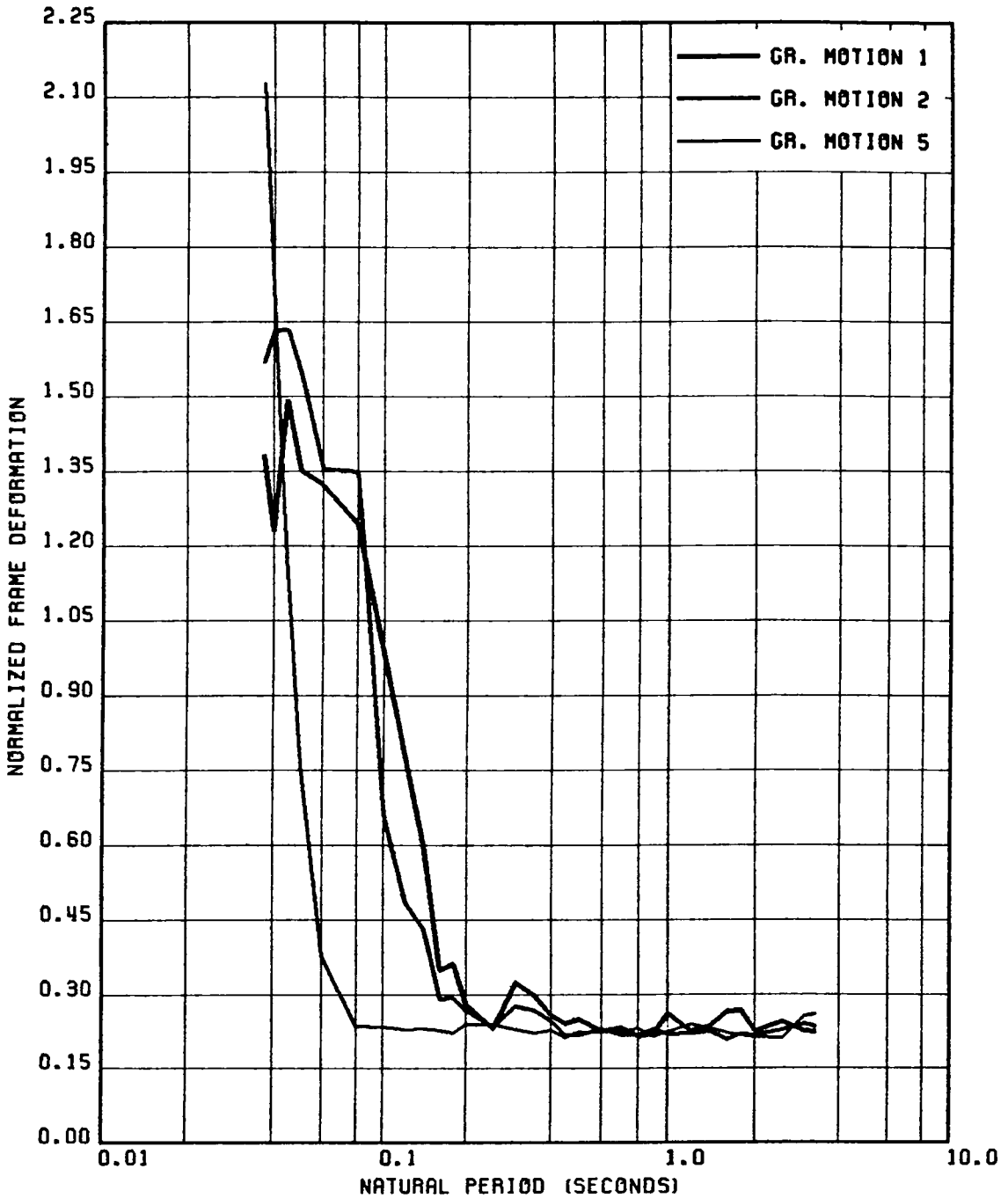

FIG. 3.13 COMPARISON OF FRAME DEFORMATION SPECTRA (NORMALIZED W.R.T. CORRESPONDING NON-SLIDING ASA SPECTRA) FOR GROUND MOTIONS 1, 2 & 5; OF THE SPRING-ASSISTED SLIDING SYSTEM WITH p=0.05, β_o=0.02 & δ=0.20.

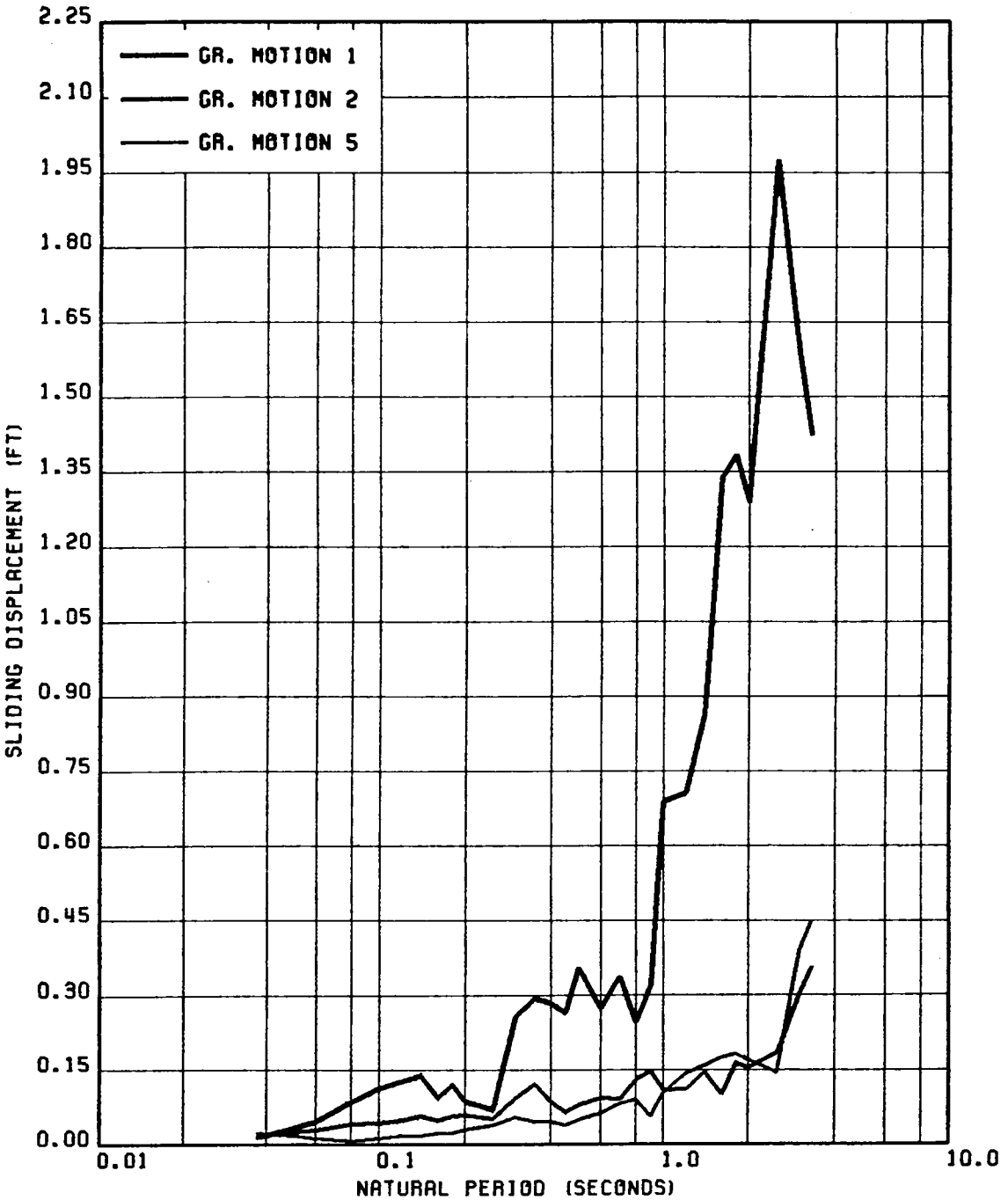

FIG. 3.14 COMPARISON OF SLAB SLIDING DISPLACEMENT SPECTRA FOR GROUND MOTION 1, 2 & 5 FOR SPRING-ASSISTED SYSTEM WITH ρ=0.05, β_o=0.02, δ=0.20.

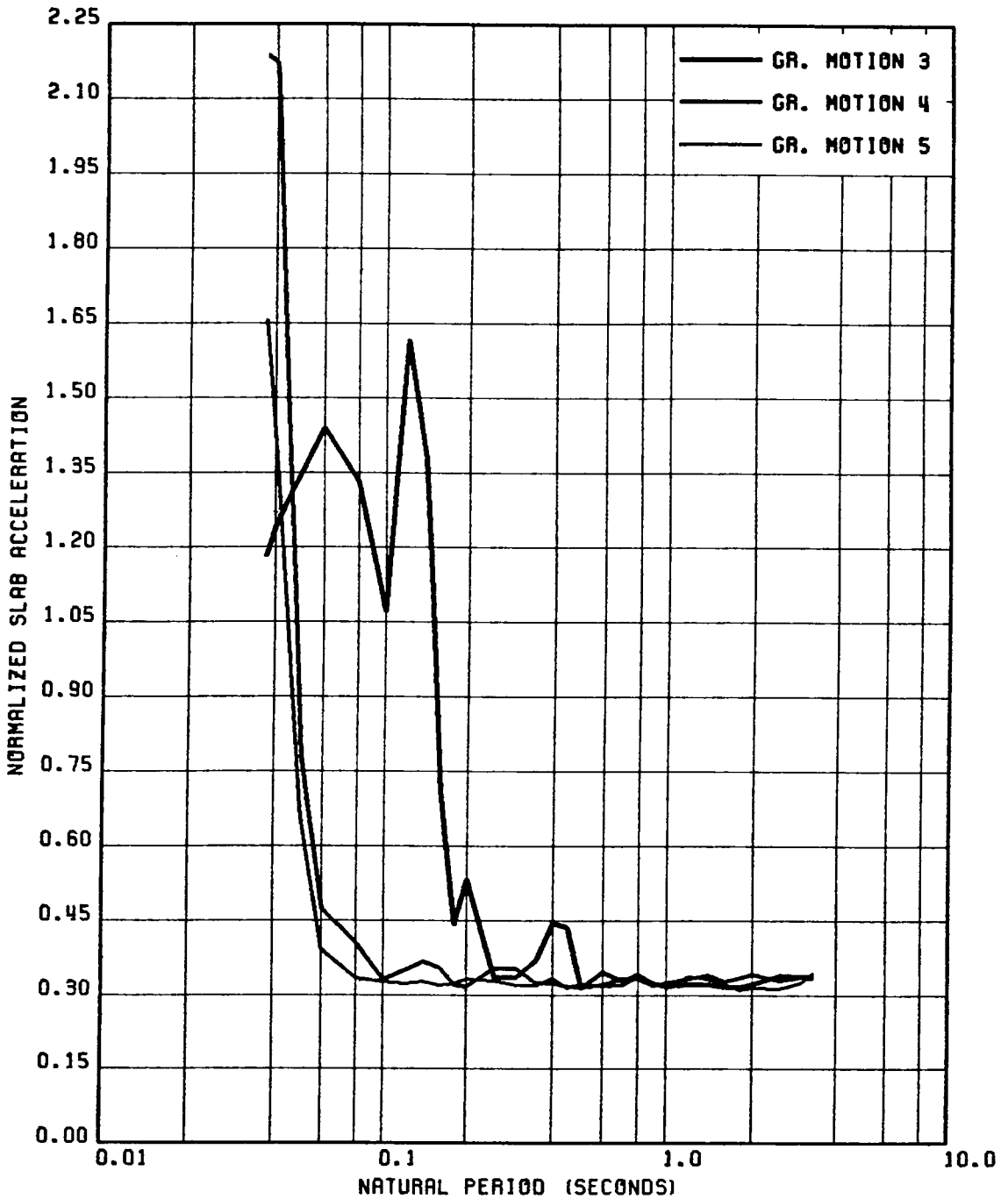

FIG. 3.15 COMPARISON OF SLAB ACCELERATION SPECTRA (NORMALIZED W.R.T. CORRESPONDING NON-SLIDING ASA SPECTRA) FOR GROUND MOTIONS 3, 4 & 5; OF THE SPRING-ASSISTED SLIDING SYSTEM WITH p=0.05, β_o=0.02 & δ=0.30.

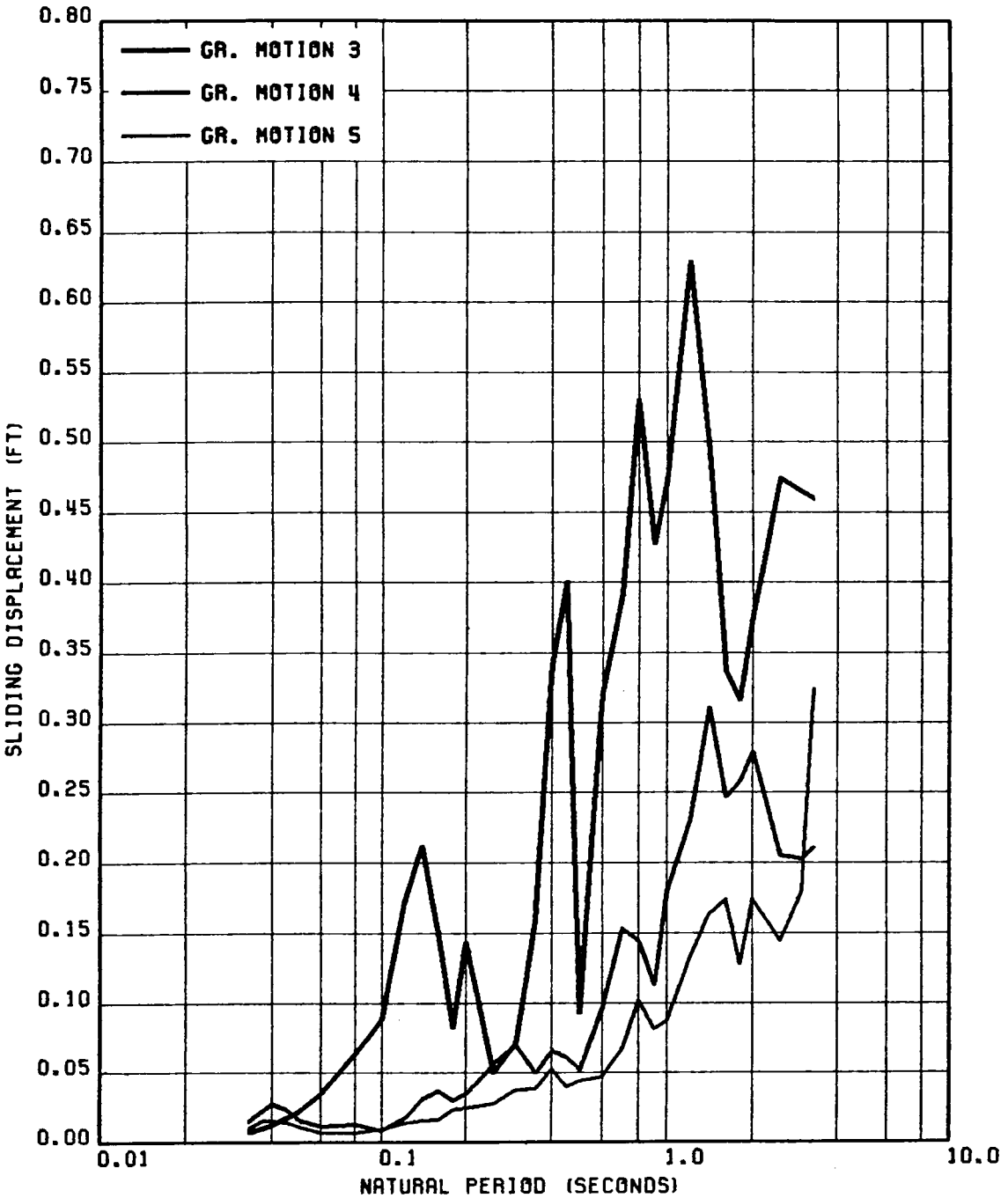

FIG. 3.16 COMPARISON OF SLAB SLIDING DISPLACEMENT SPECTRA FOR GROUND MOTION 3, 4 & 5 FOR SPRING-ASSISTED SYSTEM WITH $p=0.05$, $\beta_o=0.02$, $\delta=0.20$.

Chapter IV

Response of Proposed Sliding Systems to Vertical Excitation

4.1 Introduction

In Chapters 2 and 3, we studied the response of the basic slab sliding system and spring-assisted slab sliding systems subjected to only horizontal ground motion. Since the friction force is proportional to the normal reaction at the interface, which is directly affected by the normal acceleration, it is very important and very relevant to study the effect of the vertical ground motion on the response of a sliding system. A few other researchers (13, 18, 20) have also studied the response of the base sliding systems to simultaneous horizontal and vertical excitation. Herein we propose to extend such studies to the slab sliding and spring assisted slab sliding systems subjected to simultaneous horizontal and vertical excitations.

It is relevant to point out that under vertical excitation, the vertical acceleration of the slab can be more than the gravitational acceleration in some cases. Thus, there is a likelihood of loss of contact between the frame and the slab. Such separation will requiere a good deal of amplification of the vertical motion by the structure, which is only likely when the vertical stiffness is rather small compared to what is usually provided in civil structures. As most civil structures are relatively very stiff in the vertical direction, their vertical accelerations are the same as the ground acceleration. Here, therefore, it is assumed that such separation does not occur.

4.2 Analytical Formulation

To evaluate the effect of vertical acceleration, herein the (1)base sliding system, (2)basic slab sliding system, and (3)spring-assisted slab sliding system are studeied. The equations of motion are developed and their solution approach is presented. In all the three cases, the governing equations are are very similar to the case of no vertical excitation, except that now the presence of the vertical ground motion modifies the forcing function terms during the sliding phase.

4.2.1 Base Sliding Structure

In this case, during the non-sliding phase, the equation of motion and the interface force F_2 are still defined by Eqs. (2.1) and (2.11) as for the case of only horizontal ground motion. However, now the condition for changing to sliding phase is altered

because of the presence of the vertical ground motion. Thus Eq. (2.12) is changed to the following form :

$$|F_2| = |M\ddot{x}_g + m_1\ddot{x}_f| < \mu_2 M(g + \ddot{z}_g) \tag{4.1}$$

where $\ddot{z}_g$ is the vertical ground motion input, considered positive upward and μ_2 is the coefficient of friction at the base. Whenever the above condition is not satisfied, the response changes to the sliding phase. Thus in this case now the interface force F_2 does not remain constant during the sliding phase because of the influence of the vertical excitation. The following equation defines the interface force during the sliding phase :

$$F_2 = -\mu_2 M\varepsilon_2 (g + \ddot{z}_g) \tag{4.2}$$

The parameter ε_2 is defined by Eq. (2.14) as before. During the sliding phase, the equation of motion for the entire system consisting of the two masses is given as:

$$m_1 (\ddot{x}_{s_2} + \ddot{x}_f + \ddot{x}_g) + m_2 (\ddot{x}_{s_2} + \ddot{x}_g) = -\mu_2 M\varepsilon_2 (g + \ddot{z}_g) \tag{4.3}$$

Which can be simplified as follows :

$$\ddot{x}_{s_2} = -\alpha\ddot{x}_f - [\ddot{x}_g + \mu_2\varepsilon_2 (g + \ddot{z}_g)] \tag{4.4}$$

where α is the mass ratio of the base mass to the total mass of the structure as defined in Chapter 2. The equation of motion for the top mass is given by Eq. (2.17). Substituting Eq. (4.4) into Eq. (2.17) and dividing through by m_1, we get

$$(1-\alpha)\ddot{x}_f + 2\beta_o\omega_o\dot{x}_f + \omega_o^2 x_f = \mu_2\varepsilon_2(g + \ddot{z}_g) \tag{4.5}$$

The term $\ddot{z}_g$ in Eqs. (4.3) and (4.5) can be assumed to vary linearly during any time interval between two digitized steps of the ground motion record as:

$$\ddot{z}_g(t - t_i) = \ddot{z}_g(\tau) = Z_i + \frac{Z_{i+1} - Z_i}{h_i}\tau ; \quad h_i = t_{i+1} - t_i \text{ and } 0 \leq \tau \leq h_i \quad (4.6)$$

where Z_i and Z_{i+1} are the known vertical acceleration values recorded at times t_i and t_{i+1}, respectively. For this linear variation of $\ddot{z}_g$, the solution to Eq. (4.5) can be obtained by using any standard approach, such as by Nigam and Jennings' approach (20). The sliding response, $x_{s_2}(\tau)$ is still given by Eq. (2.21), but now the terms v_i and v_{i+1} are defined as follows :

$$v_i = A_i + \mu_2\varepsilon_2(g + Z_i) \text{ and } v_{i+1} = A_{i+1} + \mu_2\varepsilon_2(g + Z_{i+1}) \quad (4.7)$$

The sliding phase reverts back to non-sliding whenever the sliding velocity, $\dot{x}_{s_2}$ becomes zero.

4.2.2 Slab Sliding Structure

Again, in this case, the non-sliding response is governed by the same equation, that is Eq. (2.1), which gives the response for the case of undirectional horizontal excitation. However, the condition for change to sliding phase is different and is given by the following equation :

$$|F_1| = |m_1(\ddot{x}_g + m_1\ddot{x}_f)| < \mu_1 m_1(g + \ddot{z}_g) \quad (4.8)$$

Sliding begins whenever the above condition is not satisfied. During the sliding phase, the interface force, F_1 is given as follows :

$$F_1 = -\mu_1 m_1 \varepsilon_1 (g + \ddot{z}_g) \tag{4.9}$$

As before, the parameter ε_1 is still given by Eq. (2.4). During sliding, the following equation governs the response of the supporting frame :

$$c\dot{x}_f + kx_f = -F_1 = \mu_1 m_1 \varepsilon_1 (g + \ddot{z}_g) \tag{4.10}$$

where x_f is the frame deformation. The response to the above equation is as follows

$$\begin{aligned} x_f(\tau) = {} & x_{f_i} e^{-\frac{\omega_o}{2\beta_o}\tau} + u_i \left(1 - e^{-\frac{\omega_o}{2\beta_o}\tau}\right) + (u_{i+1} - u_i)\frac{\tau}{h_i} \\ & - \frac{2\beta_o}{\omega_o h_i}(u_{i+1} - u_i)\left(1 - e^{-\frac{\omega_o}{2\beta_o}\tau}\right) \end{aligned} \tag{4.11}$$

where the terms u_i and u_{i+1} are now defined as :

$$u_i = \frac{\mu_1 \varepsilon_1}{\omega_o^2}(g + Z_i) \text{ and } u_{i+1} = \frac{\mu_1 \varepsilon_1}{\omega_o^2}(g + Z_{i+1}) \tag{4.12}$$

During the sliding phase, The equation of motion for the top mass can be written as

$$m_1(\ddot{x}_{s_1} + \ddot{x}_f + \ddot{x}_g) = F_1 = -\mu_1 m_1 \varepsilon_1 (g + \ddot{z}_g) \tag{4.13}$$

Differentiating Eq. (4.11) twice and substituting the result in the above equation, we obtain :

$$\ddot{x}_{s_1} = -\left[\ddot{x}_g + \mu_1 \varepsilon_1 (g + \ddot{z}_g)\right] + \frac{\omega_o}{2\beta_o}\dot{x}_{f_i} e^{-\frac{\omega_o}{2\beta_o}\tau} \tag{4.14}$$

The above equation can simply be integrated twice to obtain x_{s1} the same expression as Eq. (2.9) but with the terms w_i and w_{i+1} being defined as :

$$w_i = A_i + \mu_1\varepsilon_1(g + Z_i) \text{ and } w_{i+1} = A_{i+1} + \mu_1\varepsilon_1(g + Z_{i+1}) \qquad (4.15)$$

The response changes to non-sliding if the sliding velocity $\dot{x}_{s_1}(\tau)$ becomes zero.

4.2.3 Spring-Assisted Slab Sliding Structure

The non-sliding response in this case is again given by Eq. (3.1), which is the governing differential equation for response to horizontal ground motion, except that now the condition described by Eq. (3.2) is modified to include the vertical excitation as follows :

$$|F_1| = | m_1(\ddot{x}_g + m_1\ddot{x}_f) + pkx_{res} | < \mu_1 m_1(g + \ddot{z}_g) \qquad (4.15)$$

The response changes to sliding phase whenever the above condition is not satisfied. During sliding, the interface force F_1 is given by Eq. (4.9), and as before, the parameter ε_1 is still given by Eq. (2.4).

Due to the change in the expression for F_1, Eqs. (3.15) and (3.17) now take the following form :

$$\dot{x}_{s_1} = \frac{1}{1+q}\left[\dot{x}_t + \frac{\omega_o}{2\beta_o}x_t - \frac{\omega_o}{2\beta_o}(1+p)x_{s_1} - \frac{p\omega_o}{2\beta_o}x_{res} - \frac{\mu_1\varepsilon_1(g + \ddot{z}_g)}{2\beta_o\omega_o}\right] \qquad (4.16)$$

and

$$\ddot{x}_t = \frac{1}{1+q}\Big[-q\omega_o^2 x_t + (q-p)\omega_o^2 x_{s_1} - 2\beta_o\omega_o q\dot{x}_t - p\omega_o^2 x_{res} - \mu_1\varepsilon_1(g + \ddot{z}_g) - (1+q)\ddot{x}_g \Big] \tag{4.17}$$

Proceeding in the same manner as in Chapter 3, the equations of motion can now be written in the state vector form as : different from Eq. (3.20b) :

$$\begin{Bmatrix} \dot{y}_1 \\ \dot{y}_2 \\ \dot{y}_3 \end{Bmatrix} = \begin{bmatrix} 0 & 0 & 1 \\ \dfrac{\omega_o}{2\beta_o(1+q)} & -\dfrac{\omega_o(1+p)}{2\beta_o(1+q)} & \dfrac{1}{1+q} \\ -\dfrac{\omega_o^2 q}{1+q} & -\dfrac{\omega_o^2(p-q)}{1+q} & -\dfrac{2\beta_o\omega_o q}{1+q} \end{bmatrix} \begin{Bmatrix} y_1 \\ y_2 \\ y_3 \end{Bmatrix} + \begin{Bmatrix} 0 \\ -\dfrac{p\omega_o^2 x_{res} + \mu_1\varepsilon_1(g + \ddot{z}_g)}{2\beta_o\omega_o(1+q)} \\ -\dfrac{\ddot{x}_g(1+q) + p\omega_o^2 x_{res} + \mu_1\varepsilon_1(g + \ddot{z}_g)}{1+q} \end{Bmatrix} \tag{4.18}$$

This equation is different from Eq. (3.21) in its forcing function term which now includes the effect of the vertical excitation. The coefficient matrix [A] is still the same as Eq. (3.20b). Thus the eigenvalues and eigenvectors of [A] are still given by Eqs. (3.25) to (3.29) in Chapter 3. With the transformation of Eq. (4.18), the decoupled differential equations of motion are obtained as follows:

$$\begin{Bmatrix} \dot{z}_1 \\ \dot{z}_2 \\ \dot{z}_3 \end{Bmatrix} = \begin{Bmatrix} \lambda_1 z_1 \\ \lambda_2 z_2 \\ \lambda_3 z_3 \end{Bmatrix} + \begin{Bmatrix} \dfrac{\mu_1 \varepsilon_1 (g + \ddot{z}_g) + p\omega_o^2 x_{res}}{2\beta_o \omega_o} \\ \dfrac{\lambda_2}{p\omega_o^2}\left[\mu_1 \varepsilon_1 (g + \ddot{z}_g) + p\omega_o^2 x_{res} + (1+p)\ddot{x}_g \right] \\ \dfrac{\lambda_3}{p\omega_o^2}\left[\mu_1 \varepsilon_1 (g + \ddot{z}_g) + p\omega_o^2 x_{res} + (1+p)\ddot{x}_g \right] \end{Bmatrix} \quad (4.19)$$

For linearly varying ground acceleration values between two recordings t_i to t_{i+1}, the solution to the above set of differential equations can then be written as :

$$\begin{Bmatrix} z_1 \\ z_2 \\ z_3 \end{Bmatrix} = \begin{Bmatrix} a_1 e^{\lambda_1 \tau} - W_i - \dfrac{W_{i+1} - W_i}{\lambda_1 h_i} - \dfrac{W_{i+1} - W_i}{h_i}\tau \\ a_2 e^{\lambda_2 \tau} - V_i - \dfrac{V_{i+1} - V_i}{\lambda_2 h_i} - \dfrac{V_{i+1} - V_i}{h_i}\tau \\ a_3 e^{\lambda_3 \tau} - V_i - \dfrac{V_{i+1} - V_i}{\lambda_2 h_i} - \dfrac{V_{i+1} - V_i}{h_i}\tau \end{Bmatrix} \quad (4.20)$$

where a_1, a_2 and a_3 can be determined from the initial conditions given in Chapter 3. W_i, W_{i+1}, V_i and V_{i+1} are defined as :

$$\begin{aligned} W_i &= -\frac{1}{\omega_o^2}\left[\mu_1 \varepsilon_1 (g + Z_i) + p\omega_o^2 x_{res} \right] \\ W_{i+1} &= -\frac{1}{\omega_o^2}\left[\mu_1 \varepsilon_1 (g + Z_{i+1}) + p\omega_o^2 x_{res} \right] \end{aligned} \quad (4.21a)$$

$$\begin{aligned} V_i &= -\frac{1}{p\omega_o^2}\left[\mu_1 \varepsilon_1 (g + Z_i) + p\omega_o^2 x_{res} + (1+p)A_i \right] \\ V_{i+1} &= -\frac{1}{\omega_o^2}\left[\mu_1 \varepsilon_1 (g + Z_{i+1}) + p\omega_o^2 x_{res} + (1+p)A_{i+1} \right] \end{aligned} \quad (4.21b)$$

Applying the initial conditions as in Chapter 3, we obtain the following expressions for the constants a_1, a_2 and a_3 :

$$\begin{Bmatrix} a_1 \\ a_2 \\ a_3 \end{Bmatrix} = [\rho]^T \begin{Bmatrix} x_{s_{1_i}} - \dfrac{W_i}{1+p} - \dfrac{W_{i+1}-W_i}{(1+p)\lambda_1 h_i} + \dfrac{V_i}{1+p} + \dfrac{V_{i+1}-V_i}{(1+p)\lambda_1 h_i} \\ x_{t_i} + V_i + \dfrac{V_{i+1}-V_i}{\lambda_1 h_i} \\ \dot{x}_{t_i} + \dfrac{V_{i+1}-V_i}{h_i} \end{Bmatrix} \quad (4.22)$$

Finally, knowing the initial constants and the solution for the principal coordinates in Eq (4.20), the elements of the state vector are obtained from Eq. (3.29) as :

$$\begin{aligned} x_{s_1}(\tau) = & -\frac{1}{1+p} e^{-\frac{\omega_o}{2\beta_o}\tau} x_{t_i} + e^{-\frac{\omega_o}{2\beta_o}\tau} x_{s_{1_i}} \\ & + \frac{1}{1+p}\left(1 - e^{-\frac{\omega_o}{2\beta_o}\tau}\right)\left[W_i + \frac{W_{i+1}-W_i}{\lambda_1 h_i} \right] + \frac{W_{i+1}-W_i}{(1+p)h_i}\tau \\ & + \frac{1}{1+p}\left[-1 + \frac{\tau}{h_i} - \frac{2\beta_o}{\omega_o h_i} \right] V_i + \frac{1}{1+p}\left[\frac{2\beta_o}{\omega_o h_i} - \frac{\tau}{h_i} \right] V_{i+1} \\ & + \frac{e^{-r\omega_o\tau}}{1+p}\left[\frac{\theta\beta_o \sin(\theta\tau)}{\omega_o(1-r\beta_o)} + \cos(\theta\tau) \right] X_i + \frac{e^{-r\omega_o\tau}}{1+p}\left[-\frac{\theta \sin(\theta\tau)}{1-r\beta_o} \right] Y_i \end{aligned} \quad (4.23a)$$

$$\begin{aligned} \dot{x}_{s_1}(\tau) = & \frac{\omega_o}{2\beta_o(1+p)} e^{-\frac{\omega_o}{2\beta_o}\tau} x_{t_i} - \frac{\omega_o}{2\beta_o} e^{-\frac{\omega_o}{2\beta_o}\tau} x_{s_{1_i}} \\ & + \frac{\omega_o}{2\beta_o} e^{-\frac{\omega_o}{2\beta_o}\tau} W_i + \frac{W_{i+1}-W_i}{(1+p)h_i}\left[1 - e^{-\frac{\omega_o}{2\beta_o}\tau} \right] \\ & + \frac{1}{(1+p)h_i} V_i - \frac{1}{(1+p)h_i} V_{i+1} \\ & + \frac{e^{-r\omega_o\tau}}{1+p}\left[-\frac{\theta \sin(\theta\tau)}{1-r\beta_o} \right] X_i + \frac{r\omega_o^2 e^{-r\omega_o\tau}}{1+p}\left[\frac{\theta \sin(\theta\tau)}{\omega_o(1-r\beta_o)} - \frac{\cos(\theta\tau)}{\beta_o} \right] Y_i \end{aligned} \quad (4.23b)$$

$$x_t(\tau) = (1+p)x_{s_1}(\tau) + a_1 e^{-\frac{\omega_o}{2\beta_o}\tau} - W_i - \frac{W_{i+1} - W_i}{\lambda_1 h_i} - \frac{W_{i+1} - W_i}{h_i}\tau \quad (4.24a)$$

$$\dot{x}_t(\tau) = (1+p)\dot{x}_{s_1}(\tau) - \frac{\omega_o}{2\beta_o} e^{-\frac{\omega_o}{2\beta_o}\tau} - \frac{W_{i+1} - W_i}{h_i} \quad (4.24b)$$

Eqs. (4.23) and (4.24) define the response of the system completely. The system reverts to non-sliding if the sliding velocity $\dot{x}_{s_1}$ becomes zero.

4.3 Numerical Results

Here the numerical results are obtained to examine the effect of vertical excitation on the three sliding systems under consideration. The response quantities of the absolute acceleration of the slab, frame deformation and sliding displacement are obtained and presented in response spectrum form. To study the frequency characteristics of the slab motion, the floor response spectra are also obtained, and compared for the three different sliding systems. Three different sets of horizontal and accompanying vertical accelerograms, recorded at three different sites are used as seismic inputs. The peak horizontal acceleration of each input is normalized to 0.05 G; the vertical ground acceleration record is also accordingly adjusted. For instance, for Ground Motion 3, the peak acceleration value for the horizontal component was 0.142 G. To normalize this ground motion record, such that the peak value is 0.5 G, all acceleration readings of this record need to be multiplied by a factor of (0.50 G / 0.142 G). The same factor is then used to normalize the corresponding vertical acceleration time-history. The vertical acceleration

time-history for this motion has the peak value of 0.094 G. The peak value of the normalized vertical motion will then be (0.094 G $\times$ 0.50 G /0.142 G) = 0.324 G . The same approach was used to normalize the other ground motions used in this study. The response quantities of slab acceleration and frame deformation are normalized with respect to the corresponding elastic spectrum values. This provides a uniform and convinient basis for comparison of the respective spectral quantities. Also, the spectra were obtained for the δ-parameter in Chapter 3. It may be recalled that δ is the friction coefficient value normalized with respect to the corresponding absolute acceleration spectrum value expressed in g-units, for the system frequency. The choice of the parameter δ is a convinient one for comparison; choosing a value smaller than 1.0 guarantees sliding response for the slab sliding and spring-assisted slab sliding systems. For the slab sliding systems, this parameter is also a direct measure of reduction in response when compared with the response of the corresponding non-sliding system.

Figs. 4.1 to 4.10 are presented to study the sensitivity of the three sliding systems to the presence of vertical acceleration as input. That is, here the response spectra with and without the presence of vertical excitation are compared. Figs. 4.11 to 4.14, on the other hand, compare the effectiveness of various sliding systems with each other in the presence of vertical excitation.

Fig. 4.1 and 4.2 are for the base sliding system. Fig. 4.1 shows the spectra for the response quantities of slab acceleration and frame displacement, whereas Fig. 4.2 shows the spectra for base sliding displacement both with and without vertical motion. The figures clearly show that these spectra are only slightly affected. That is the response spectra for the case of excitation due to just horizontal ground motion is almost the same as those obtained for simultaneous horizontal and vertical excitation. The same observations were found to be true for other earthquake ground

motions, too. Thus, this system is observed to be unsensitive to the presence of vertical motion.

Figs. 4.3 to 4.6 are presented to study the sensitivity of the slab sliding system to the presence of vertical ground acceleration. Figs. 4.3 and 4.4 compare the normalized deformations and accelerations spectra for two different earthquake ground motions. Fig. 4.3 is for Ground Motion 4 and $\delta = 0.10$, whereas Fig. 4.4 is for Ground Motion 5 and $\delta = 0.30$. Both figures indicate that the slab sliding response spectra of normalized slab acceleration and frame deformation are sensitive to the presence of vertical acceleration. Furthermore, these spectra are also more or less of constant magnitude, just like the ones corresponding to case of horizontal excitation (in which case, these spectra were indeed of constant magnitude). It is possible to appreciate the reason for the shape of these spectra if one studies Eqs. (4.10) and (4.13). They indicate that the maximum possible value of the interface force F_1 is equal to $\mu_1 m_1(g + \ddot{z}^+_{g_{max}})$, where $\ddot{z}^+_{g_{max}}$ is maximum positive acceleration value of the vertical ground motion time-history. This in turn, stipulates that the maximum possible slab acceleration would be $\mu_1(g + \ddot{z}^+_{g_{max}})$ Thus, the maximum possible normalized acceleration can be obtained from:

$$
\begin{aligned}
(\text{Normalized Acceleration})_{max} &= \frac{\text{Maximum Acceleration}}{\textbf{ASA}} \\
&= \frac{\mu_1 g\left(1 + \dfrac{\ddot{z}^+_{g_{max}}}{g}\right)}{\textbf{ASA}} \\
&= \frac{\mu_1 g}{\textbf{ASA}}\left(1 + \frac{\ddot{z}^+_{g_{max}}}{g}\right) \\
&= \delta\left(1 + \frac{\ddot{z}^+_{g_{max}}}{g}\right)
\end{aligned}
\tag{4.25}
$$

Thus for a given values of δ and $\ddot{z}_{g\,max}$, the maximum possible value of the normalized acceleration is fixed, according to Eq. 4.25. It is, however, noted that maximum normalized acceleration of the slab will be equal to the maximum possible normalized acceleration, given by Eq. 4.25, only when the peak positive vertical acceleration occurs during the sliding phase. In some cases it may not happen, that is, there may not be any sliding at the instant the peak positive acceleration occurs in the vertical motion. It is for this reason we observe that the acceleration and displacement spectra in Figs. 4.3 and 4.4 are not of constant value, but are nearly equal to the value given by Eq. 4.25.

It is of interest to see if the increase in normalized acceleration levels would cause any increase in the resulting secondary floor spectra. To check this, we have presented Figs. 4.5 to 4.7 showing the comparison of secondary spectra for three structures subjected to just the horizontal and both horizontal and vertical components of Ground Motion 5, respecetively. In Fig. 4.5, the natural period of the primary structure is 0.05 sec (stiff structure). For this case, it is seen that there is hardly any change in the floor spectrum magnitude in the presence of vertical acceleration, except a small difference toward the end of high frequency region. Here, as one may expect, the response spectrum value is simply equal to the maximum acceleretion of the primary structure which in itself increases in the presence of vertical acceleration (as seen in Figs. 4.3 and 4.4). However, this difference is localized to the end of the high frequency region only. In Fig. 4.6, secondary spectra are shown for a primary structure with a period of 0.20 sec (medium stiff structure). Here also, it is noted that the spectra for the conditions of excitation input are in close agreement except toward the end of the high frequency region. Fig. 4.7 is for a primary structure with a period of 2.0 sec (flexible structure). Here it is seen that there is a difference in the floor spectra for the two excitation

conditions. This difference is mainly confined to the high frequency region. Further inspection reveals that this difference is approximately to the difference in magnitudes of slab accelerations of the primary structure when it is subjected to the two cases of excitation conditions under consideration.

It is pointed out that increase in the level of ground acceleration (that is, increasing $\ddot{x}_{g\,max}$ and $\ddot{z}_{g\,max}$) would increase the normalized acceleration and displacement spectra, thereby further reducing the effectiveness of the slab sliding model in producing a response reduction in those quantities. It is added that this increase in the magnitude of maximum slab acceleration may not be tantamount to any consequent increase in the secondary floor spectra, since the system responds to this higher acceleration response only momentarily.

Figs. 4.8 and 4.9 compare the for sliding displacement spectra of slab sliding system, obtained with and without vertical excitation, for two sets of ground motions Fig. 4.8 is for $\delta = 0.10$ and Ground Motion 4, whereas Fig. 4.9 is for $\delta = 0.30$ and Ground Motion 5. Both the figures clearly show that the sliding displacement spectra are relatively unaffected by the presence of vertical component in the ground motion.

Figs. 4.10 to 4.13 are for the spring assisted slab sliding system. Fig. 4.10 shows the normalized acceleration and frame deformation spectra, whereas Figs. 4.12 and 4.13 show the sliding displacement spectra, obtained with and without vertical motion for two sets of recorded ground motions. As in the case of the base sliding system, it is observed that the spring-assisted slab sliding system is also not sensitive to the vertical ground motion component. That is, the spectra for the cases of horizontal excitation and simultaneous horizontal and vertical excitation are almost equal to each other. This observation was found to be true for all the three earthquake ground motions considered herein and for different levels δ .

Figs. 4.14 to 4.17 compare the performances of slab sliding, base sliding and spring-assisted slab sliding systems when they are subjected to simultaneous horizontal and vertical excitation. Figs. 4.14 and 4.15 compare the normalized acceleration and frame displacement spectra for two different earthquakes. Figs. 4.16 and 4.17, on the other hand, compare the sliding displacement spectra for two different earthquakes. Figs. 4.14 and 4.15 show that the slab sliding system, though sensitive to the presence of vertical ground motion component, still provides the best isolation for slab acceleration and frame displacement responses when compared with the other two systems. The spring-assisted slab sliding system also provides about the same level of isolation as the slab sliding system, but only in the low and medium frequency ranges. In high frequency range, however, the spring-assisted system is very ineffective in bringing about any reduction in the acceleration and frame displacement response. This was also observed to be the case in Chapter 3, where the response characteristics were reported for response to just the horizontal ground motion only. Figs. 4.14 and 4.15 also show that the base sliding system is not as effective as the slab sliding system in reducing the accleration and frame displacement response.

Figs. 4.16 and 4.17 compare the sliding displacement spectra for the three types of sliding systems. It is seen the slab sliding system has the largest sliding diplacement spectra. Again, as demonstrated in Chapter 3, the spring-assisted slab sliding system seems to reasonably effective in reducing the levels of sliding displacement response when compared to the slab sliding system response.

4.4 Concluding Remarks

In this chapter, the response characteristics of different sliding systems are studied to investigate the effect of the presence of the vertical acceleration on response quantities of interest. The results show that the base sliding and spring-assisted slab sliding structures are insensitive to the presence of the vertical acceleration. However, the pure sliding structure is observed to experience increased levels of slab accelerations and frame deformations, regardless of the frequency of the structure. It is shown that such increase in the acceleration and deformation response is directly related to $\ddot{z}_{g_{max}}^{+}$, the maximum value of positive vertical ground acceleration value, and that the increase can be estimated fairly accurately knowing the value of $\ddot{z}_{g_{max}}^{+}$. Furthermore, it is observed that the increase in acceleration values affects the resulting secondary spectrum only in the high frequency end of the spectrum.

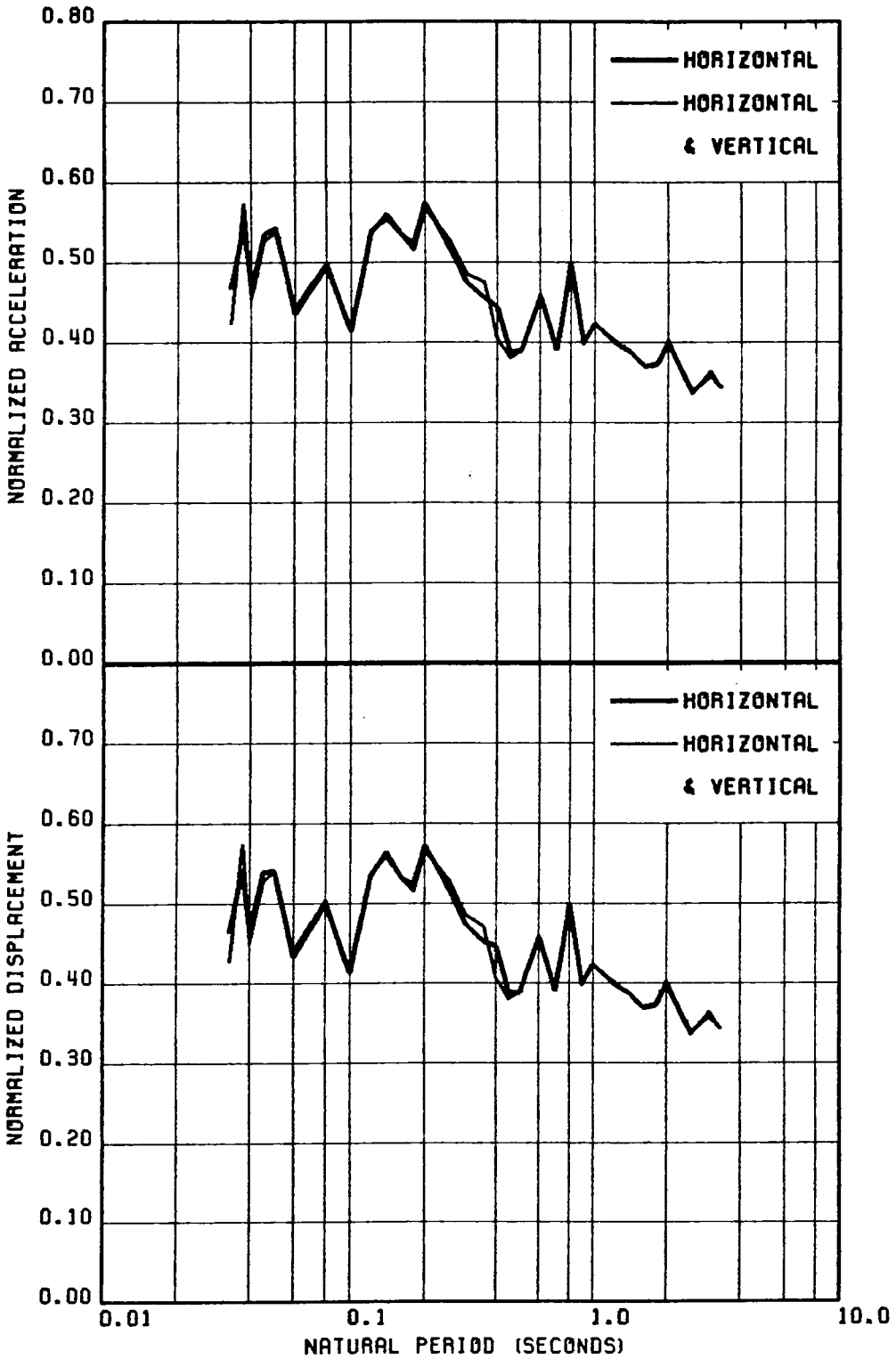

FIG. 4.1 COMPARISON OF SPECTRA OF (a) NORMALIZED ACCELERATION, (b) NORMALIZED DISPLACEMENT-STUDY OF THE EFFECT OF COMBINED HORIZONTAL & VERTICAL ACCELERATION ON BSS RESPONSE-GR. MOTION 5, α=0.25, β_0=0.02 & δ=0.10

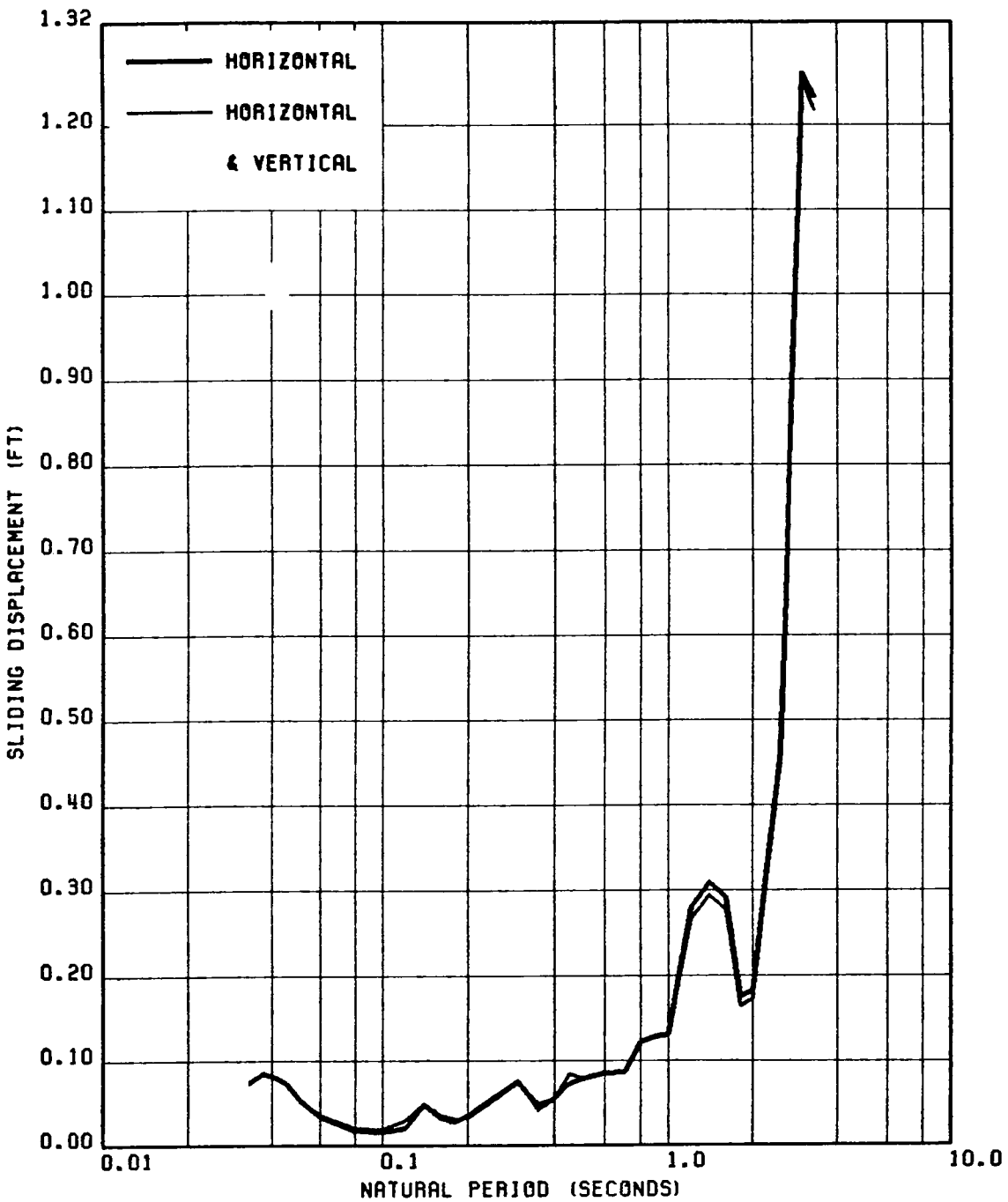

FIG. 4.2 COMPARISON OF BASE SLIDING DISPLACEMENT SPECTRA TO SHOW THE EFFECT OF COMBINED HORIZONTAL & VERTICAL GROUND ACCELERATION ON RESPONSE OF BSS FOR GROUND MOTION 5, α=0.25, β_o=0.02 AND δ=0.10

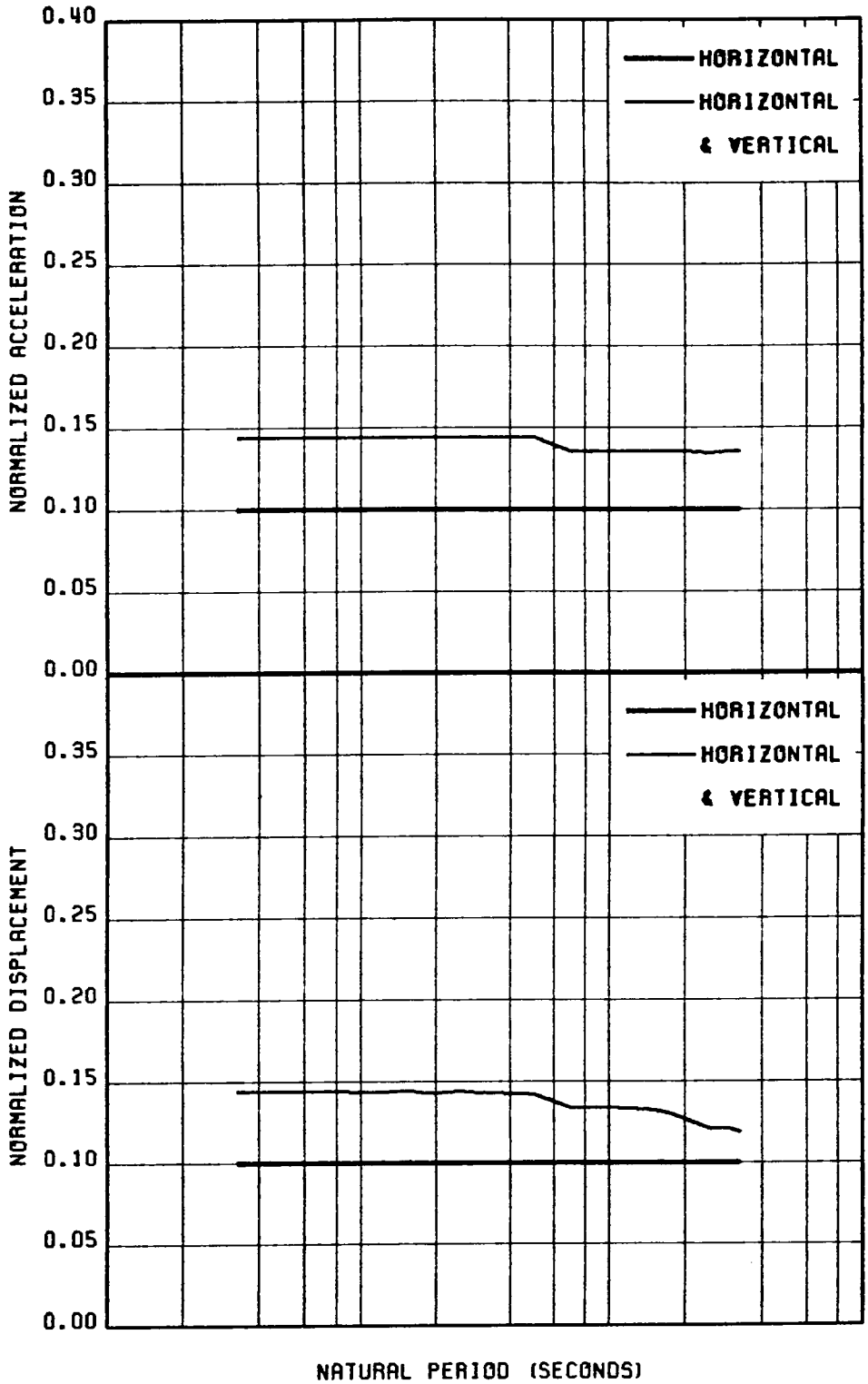

FIG. 4.3 COMPARISON OF SPECTRA OF (a) NORMALIZED ACCELERATION, (b) NORMALIZED DISPLACEMENT TO STUDY THE EFFECT OF COMBINED HORIZONTAL & VERTICAL ACCELERATION ON RESPONSE OF SSS; GROUND MOTION 4, β_o=0.02 & δ=0.10

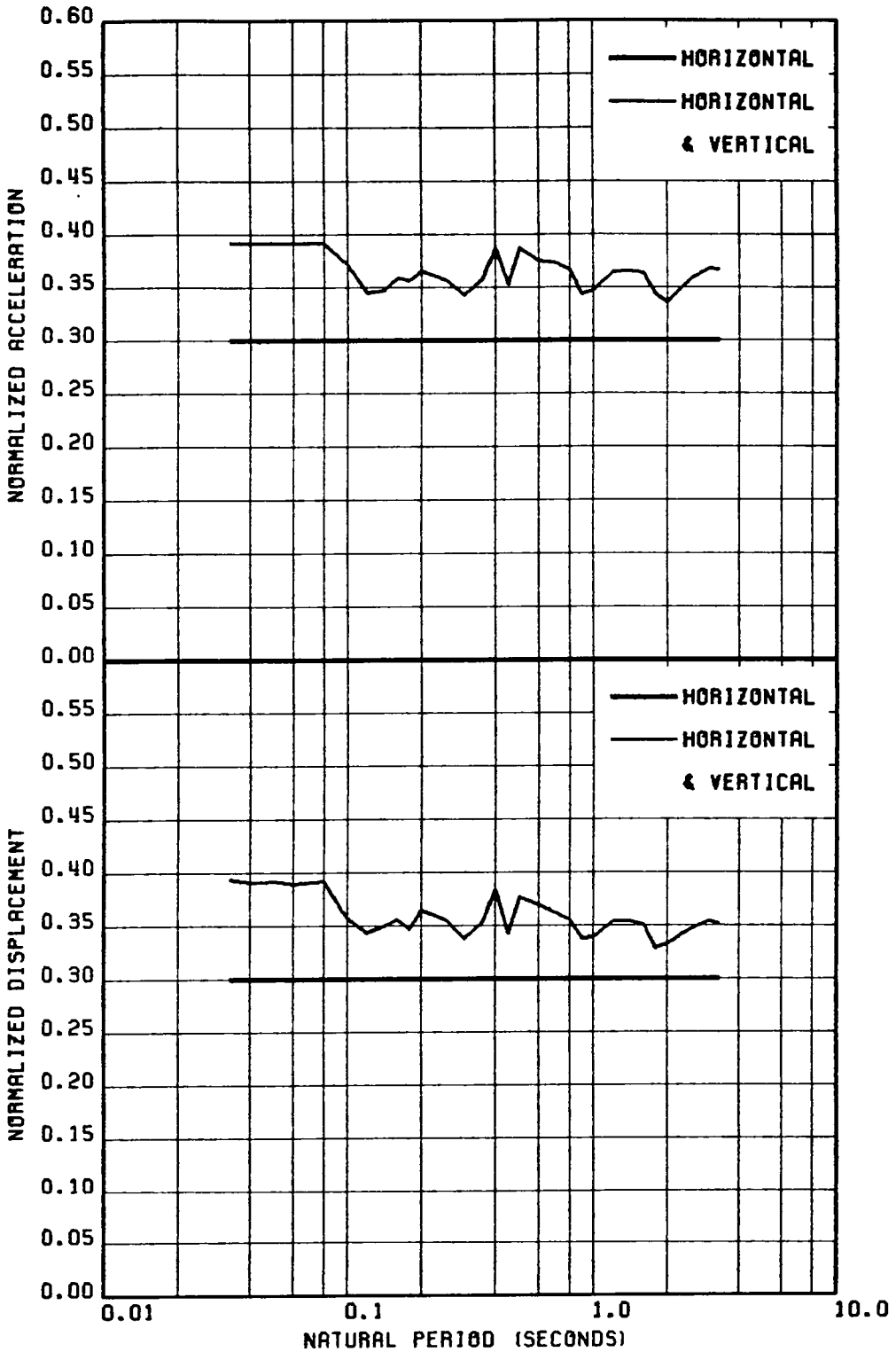

FIG. 4.4 COMPARISON OF SPECTRA OF (a) NORMALIZED ACCELERATION, (b) NORMALIZED DISPLACEMENT TO STUDY THE EFFECT OF COMBINED HORIZONTAL & VERTICAL ACCELERATION ON RESPONSE OF SSS; GROUND MOTION 5, β_o =0.02 & δ=0.30

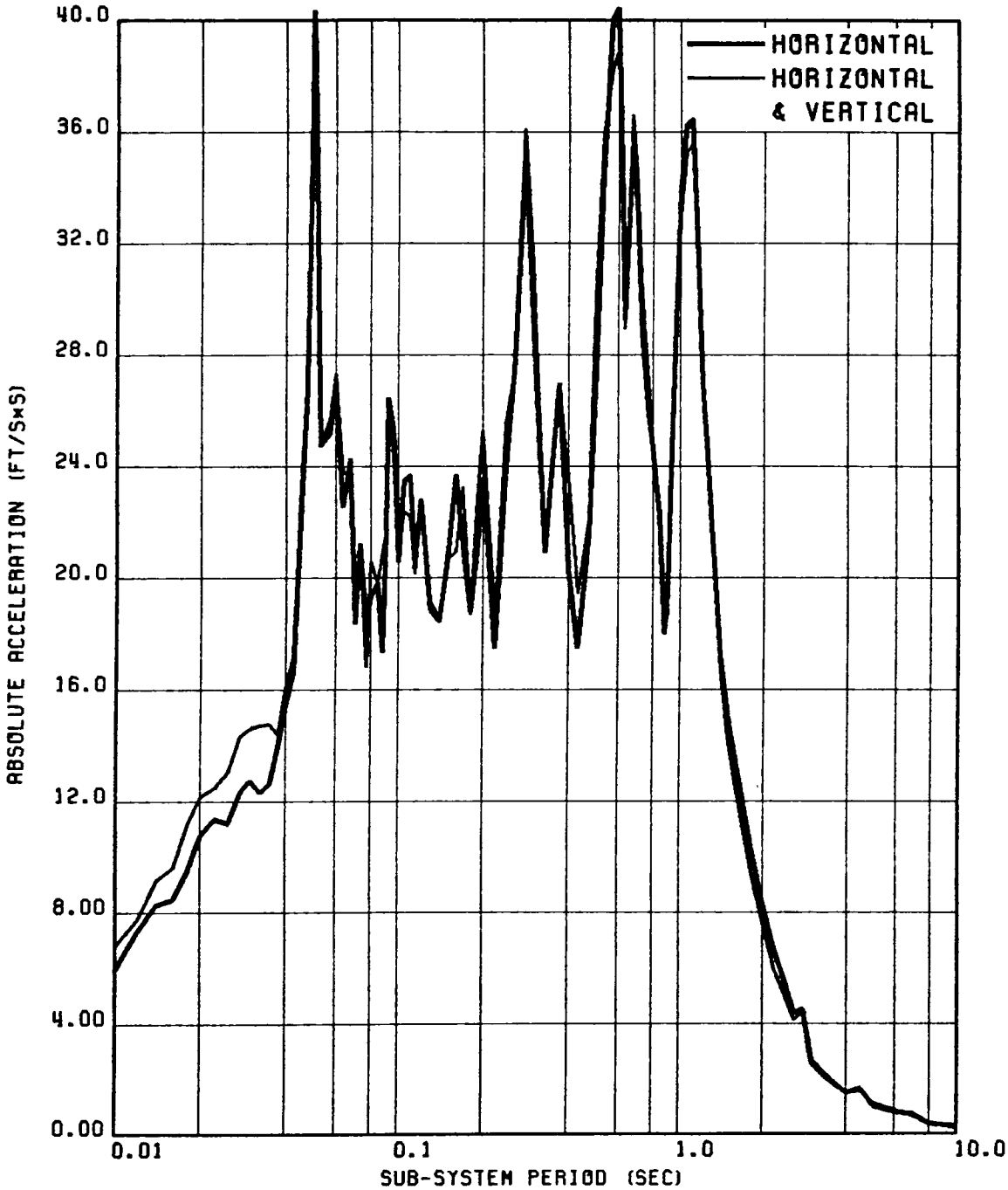

FIG. 4.5 EFFECT OF VERTICAL ACCELERATION ON THE SECONDARY FLOOR SPECTRA OF A PRIMARY STRUCTURE WITH T=0.05 SEC, $\beta_p = \beta_s = 0.02$, $\delta = 0.10$, MOTION 5.

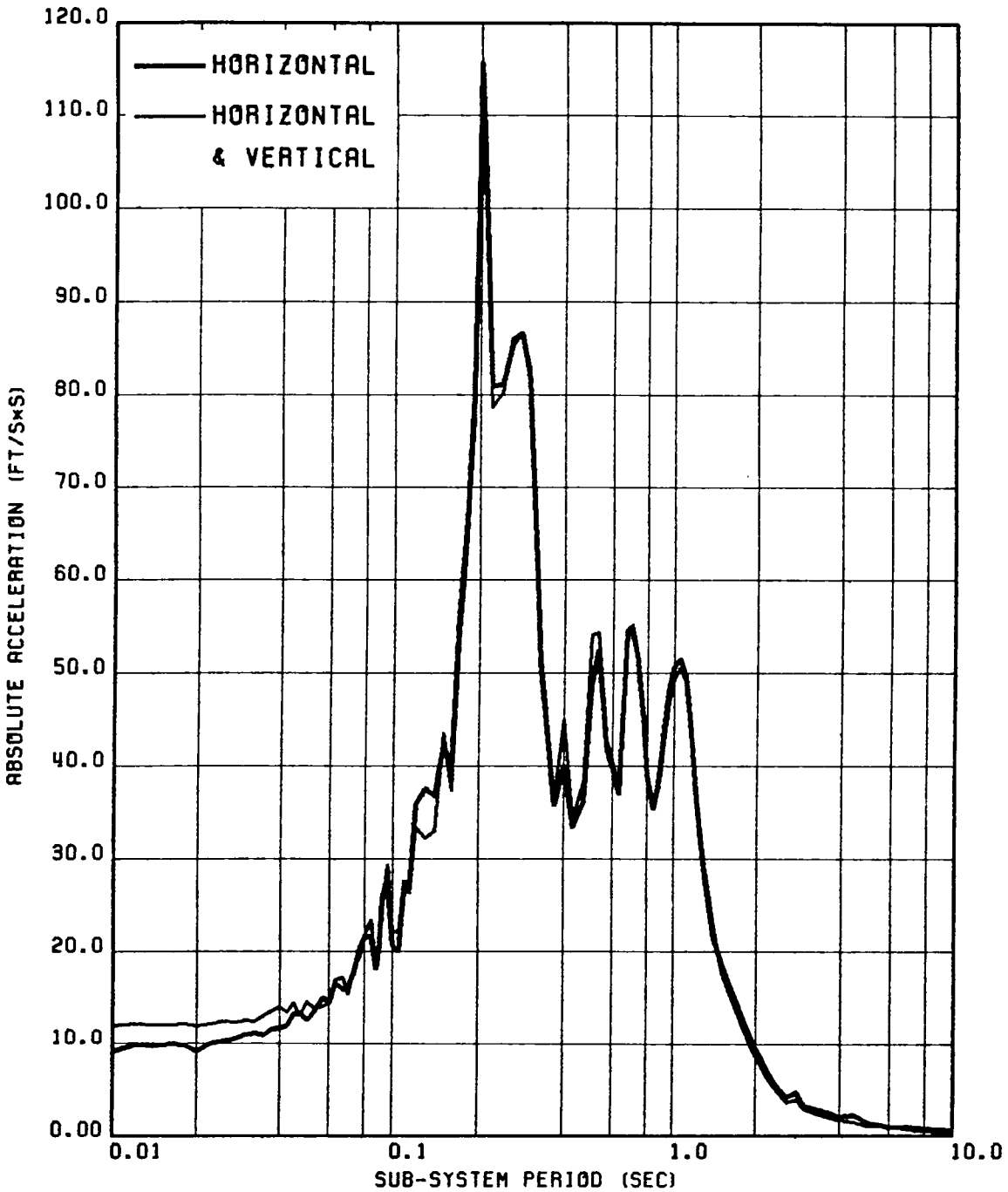

FIG. 4.6 EFFECT OF VERTICAL ACCELERATION ON THE SECONDARY FLOOR SPECTRA OF A PRIMARY STRUCTURE WITH T=0.20 SEC, $\beta_o = \beta_s$=0.02, δ=0.10, MOTION 5.

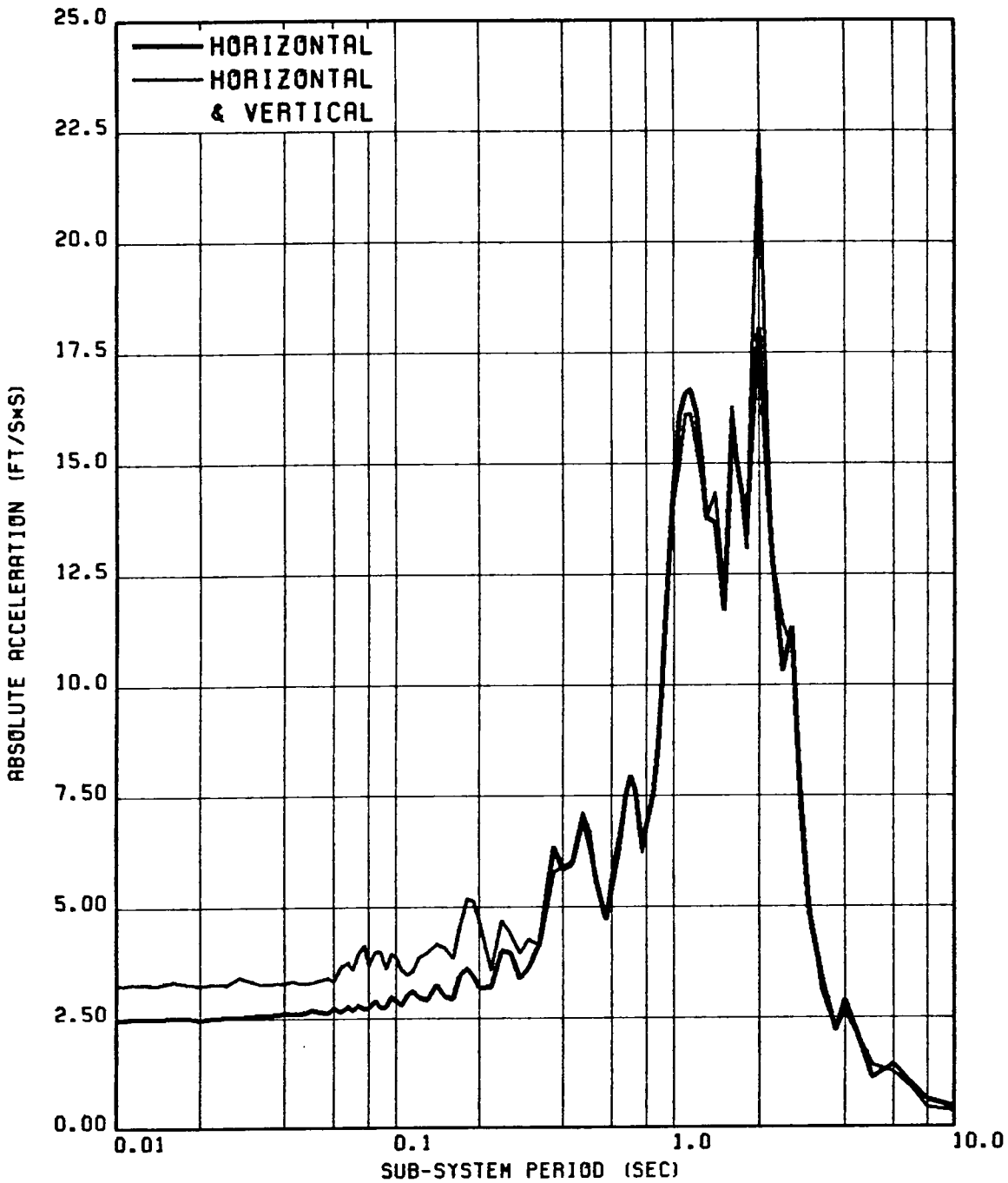

FIG. 4.7 EFFECT OF VERTICAL ACCELERATION ON THE SECONDARY FLOOR SPECTRA OF A PRIMARY STRUCTURE WITH T=2.00 SEC, $\beta_p = \beta_s = 0.02$, $\delta = 0.10$, MOTION 5.

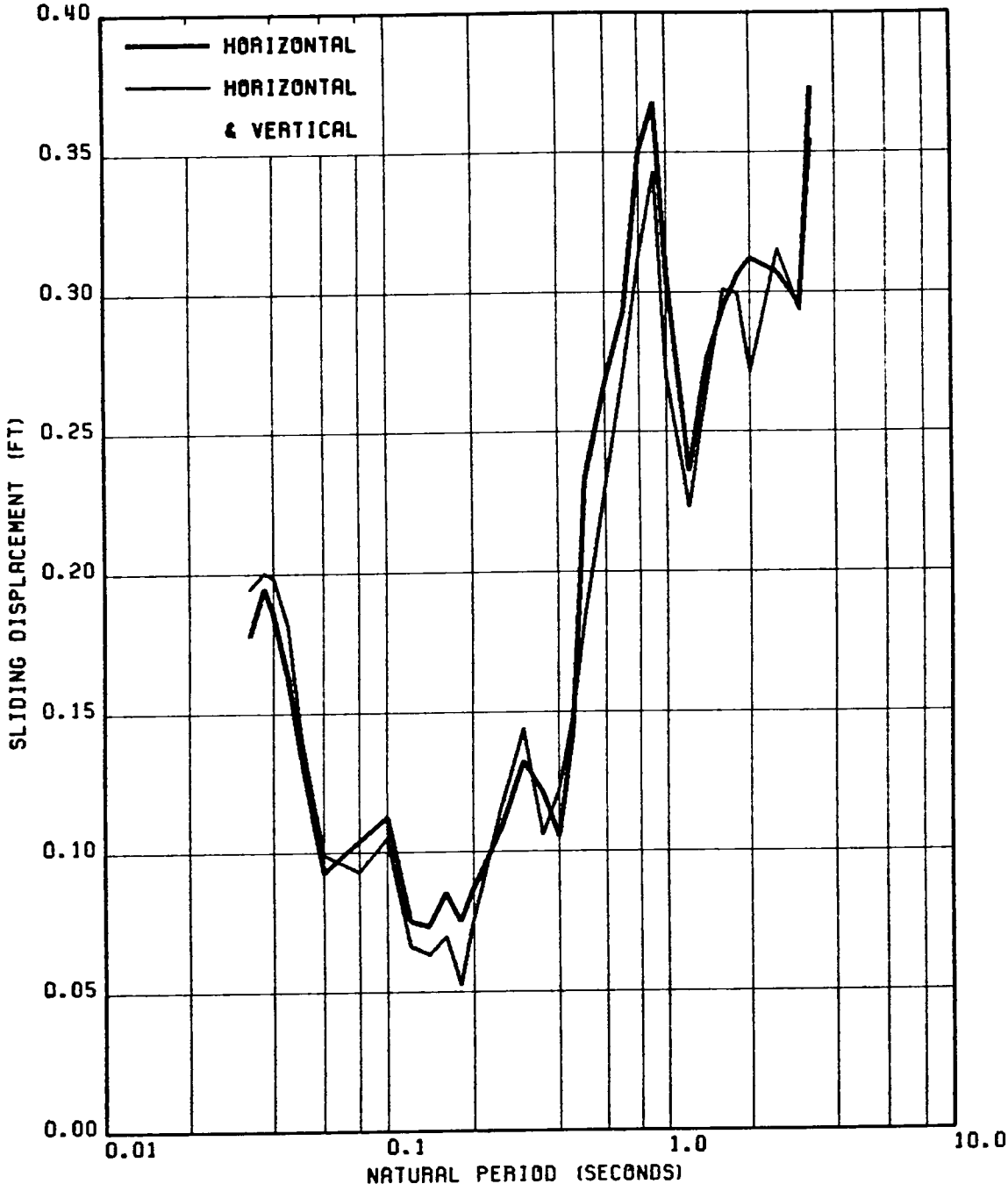

FIG. 4.8 COMPARISON OF SLAB SLIDING DISPLACEMENT SPECTRA TO SHOW THE EFFECT OF COMBINED HORIZONTAL & VERTICAL GROUND ACCELERATION ON RESPONSE OF SSS FOR GROUND MOTION 4, β_o=0.02 AND δ=0.10

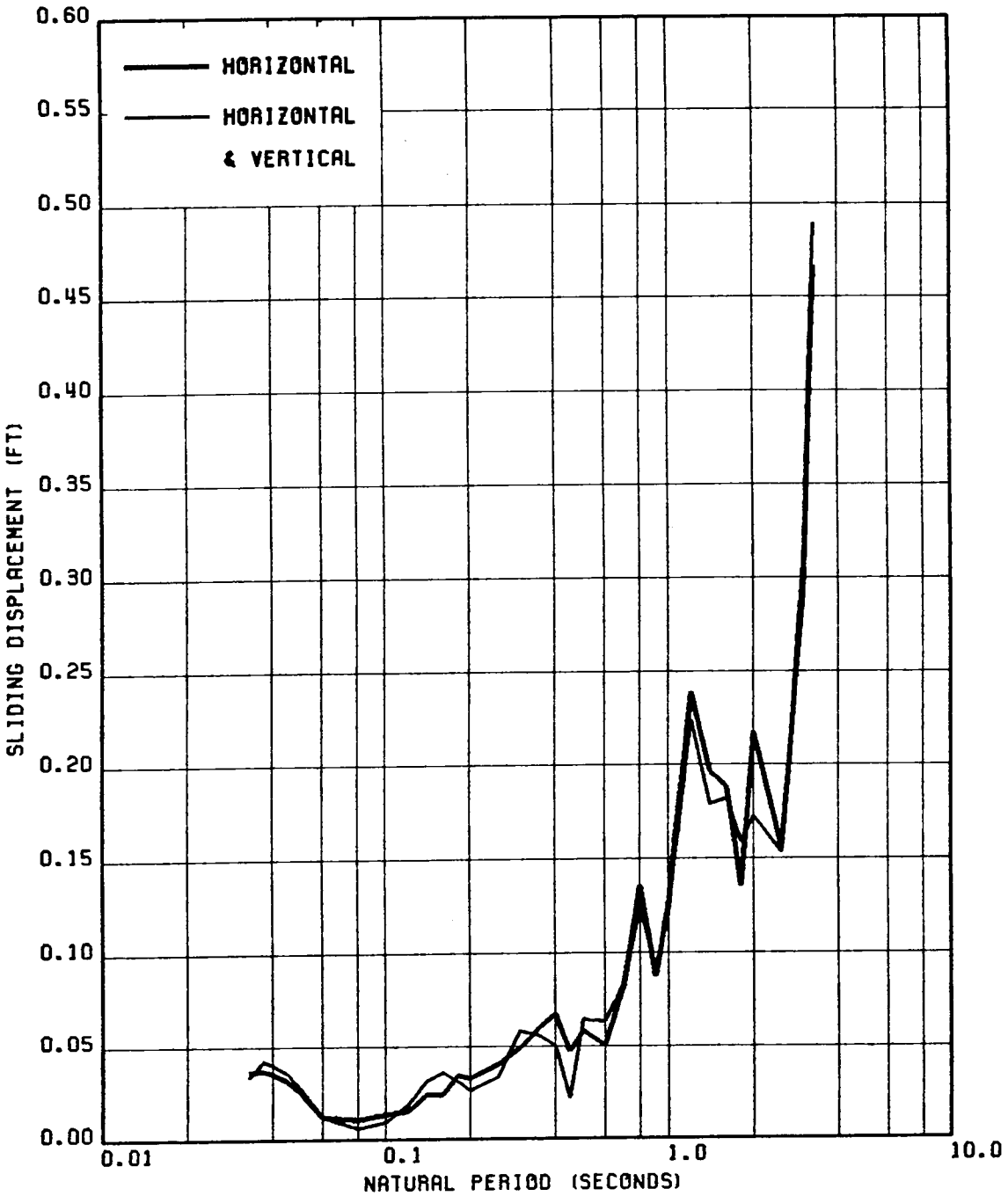

FIG. 4.9 COMPARISON OF SLAB SLIDING DISPLACEMENT SPECTRA TO SHOW THE EFFECT OF COMBINED HORIZONTAL & VERTICAL GROUND ACCELERATION ON RESPONSE OF SSS FOR GROUND MOTION 5, β_o=0.02 AND δ=0.30

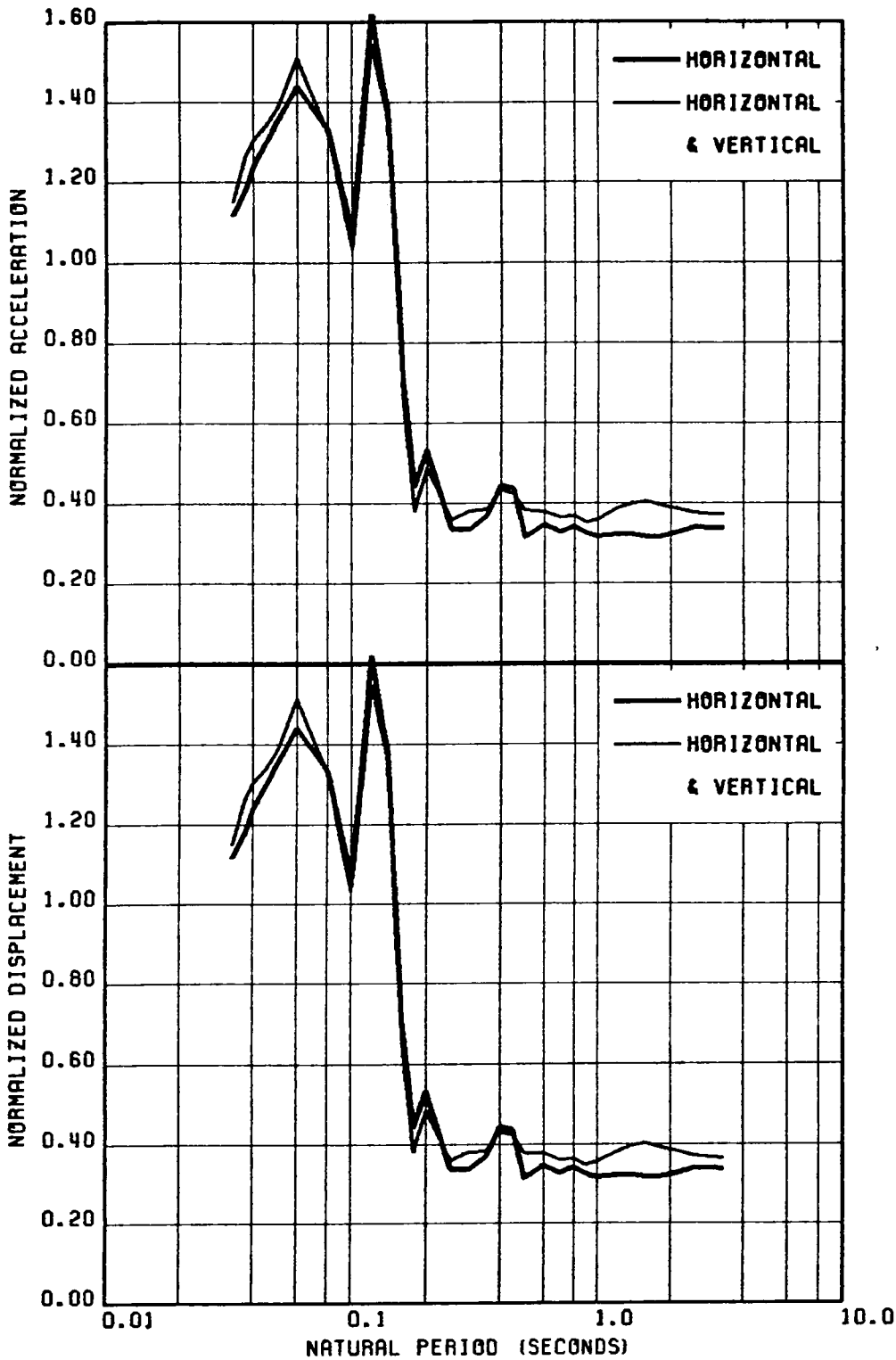

FIG. 4.10 COMPARISON OF SPECTRA OF (a) NORMALIZED ACCELERATION (b) NORMALIZED DISPLACEMENT RS SHOW THE EFFECT OF COMBINED HORIZONTAL & VERTICAL ACCELERATION ON SPRING-SSS RESPONSE; GR MOTION 3, P=0.02 & δ=0.30

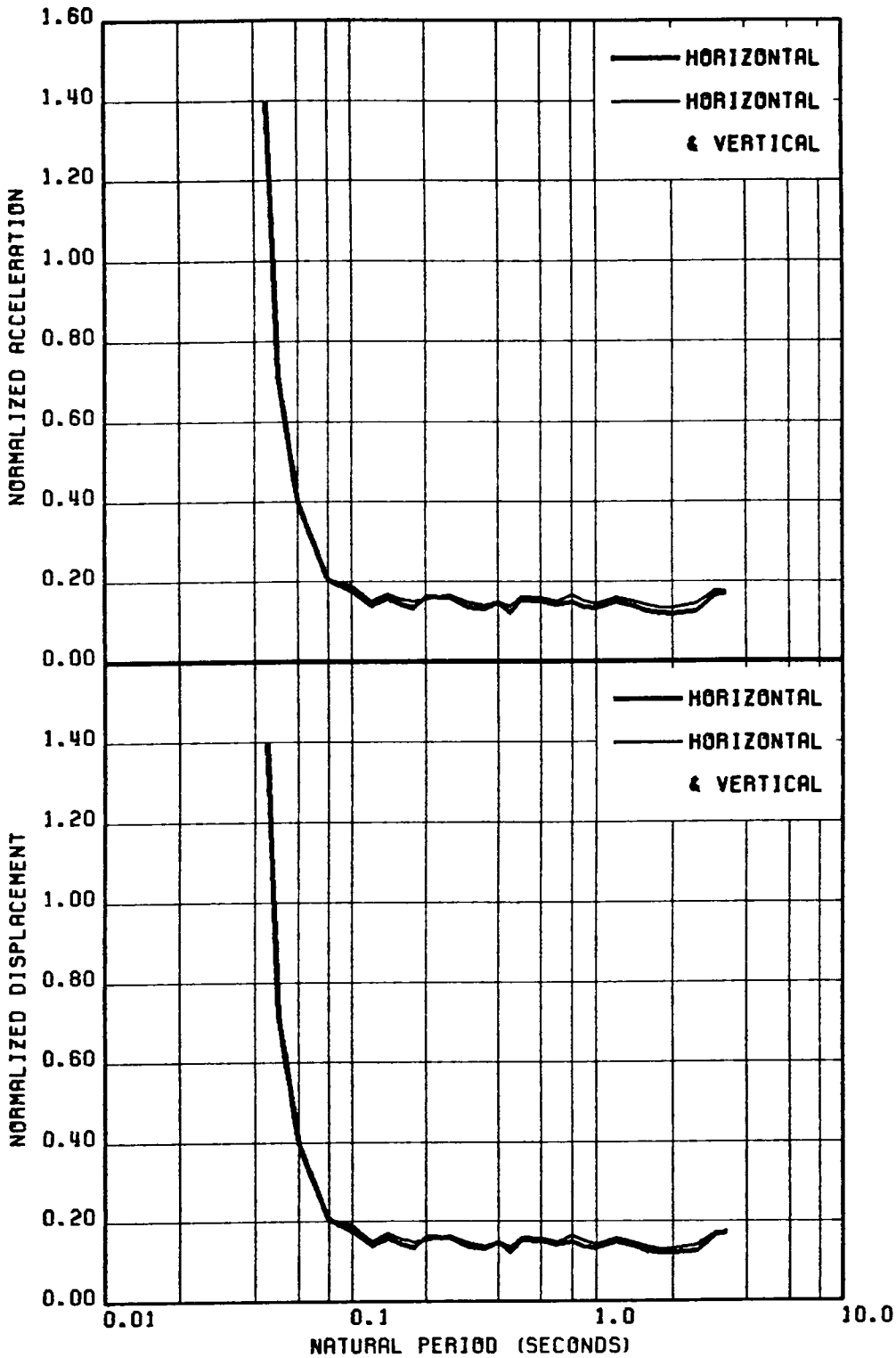

FIG. 4.11 COMPARISON OF SPECTRA OF (a) NORMALIZED ACCELERATION (b) NORMALIZED DISPLACEMENT RS SHOW THE EFFECT OF COMBINED HORIZONTAL & VERTICAL ACCELERATION ON SPRING-SSS RESPONSE; GR MOTION 5, P=0.02 & δ=0.10

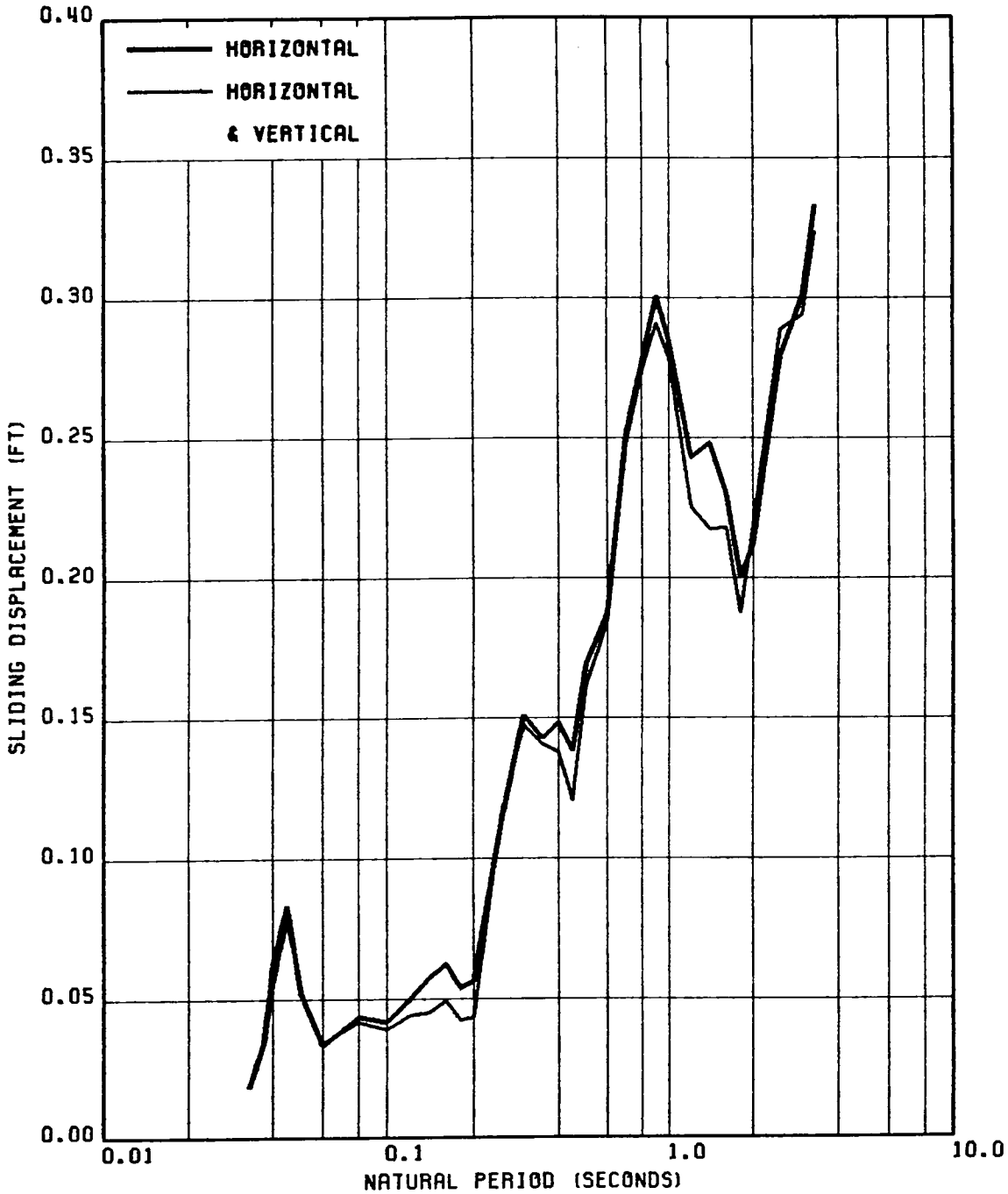

FIG. 4.12 COMPARISON OF SLAB SLIDING DISPLACEMENT SPECTRA TO SEE THE EFFECT OF COMBINED HORIZONTAL & VERTICAL GROUND ACCELERATION ON RESPONSE OF SPRING-ASSISTED SSS FOR GROUND MOTION 4, P=0.02 AND δ=0.10.

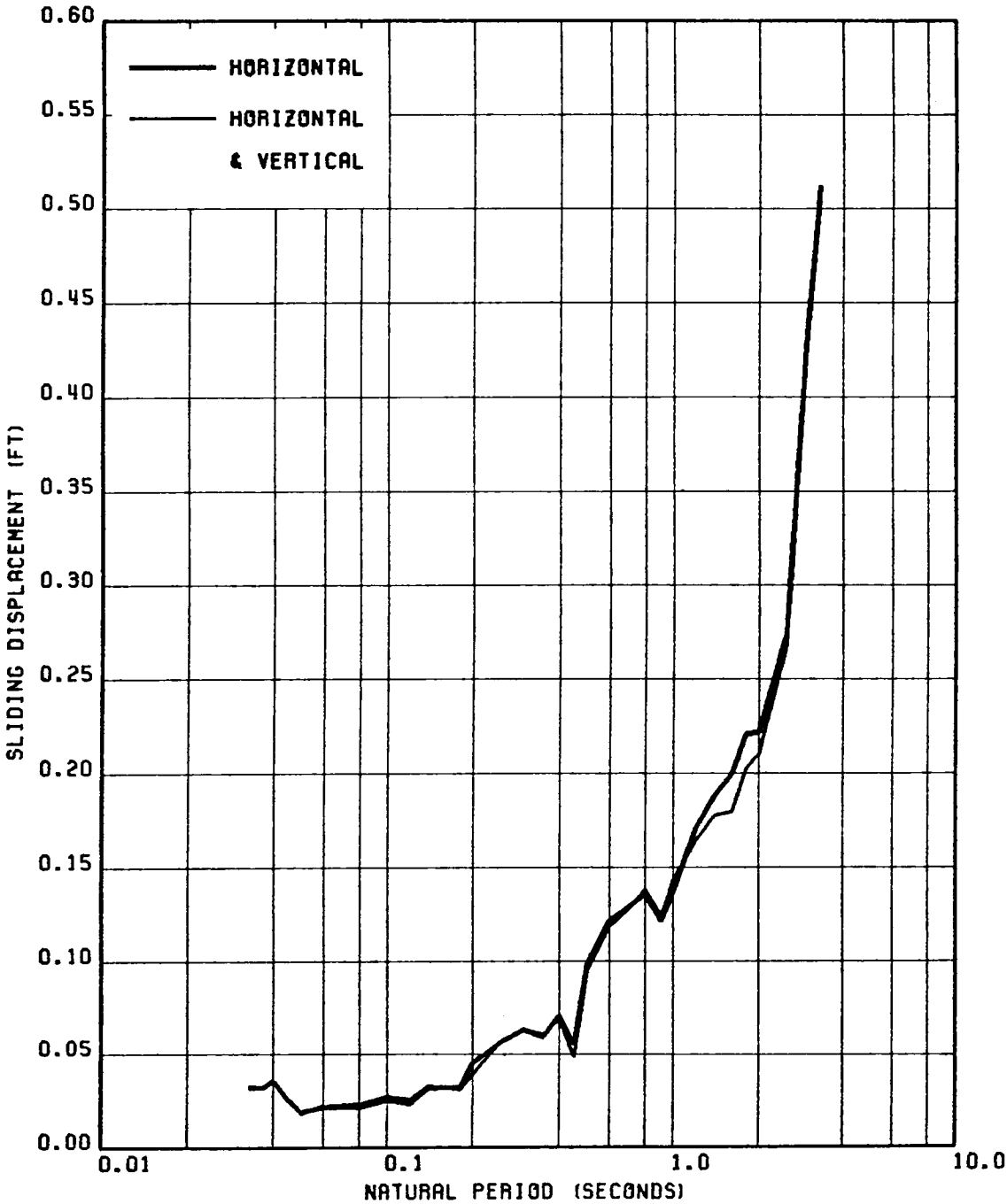

FIG. 4.13 COMPARISON OF SLAB SLIDING DISPLACEMENT SPECTRA TO SEE THE EFFECT OF COMBINED HORIZONTAL & VERTICAL GROUND ACCELERATION ON RESPONSE OF SPRING-ASSISTED SSS FOR GROUND MOTION 5, P=0.02 AND δ=0.10.

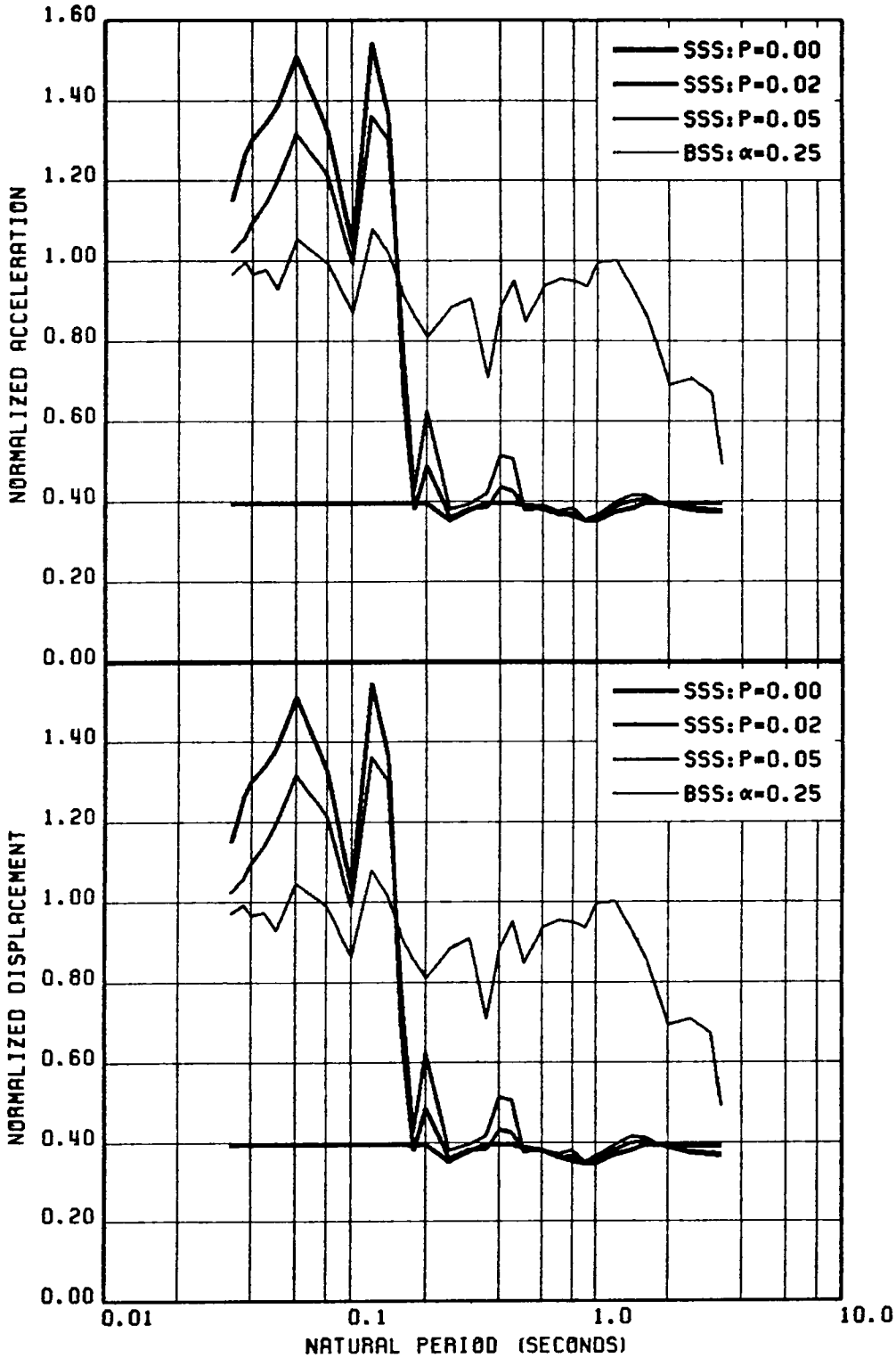

FIG. 4.14 COMPARISON OF SPECTRA OF (a) NORMALIZED ACCELERATION (b) NORMALIZED DISPLACEMENT FOR SSS, BSS & SPRING-ASSISTED SSS FOR SIMULTANEOUS HORIZONTAL & VERTICAL EXCITATION; GR. MOTION 3 β_o =0.02 & δ= 0.30

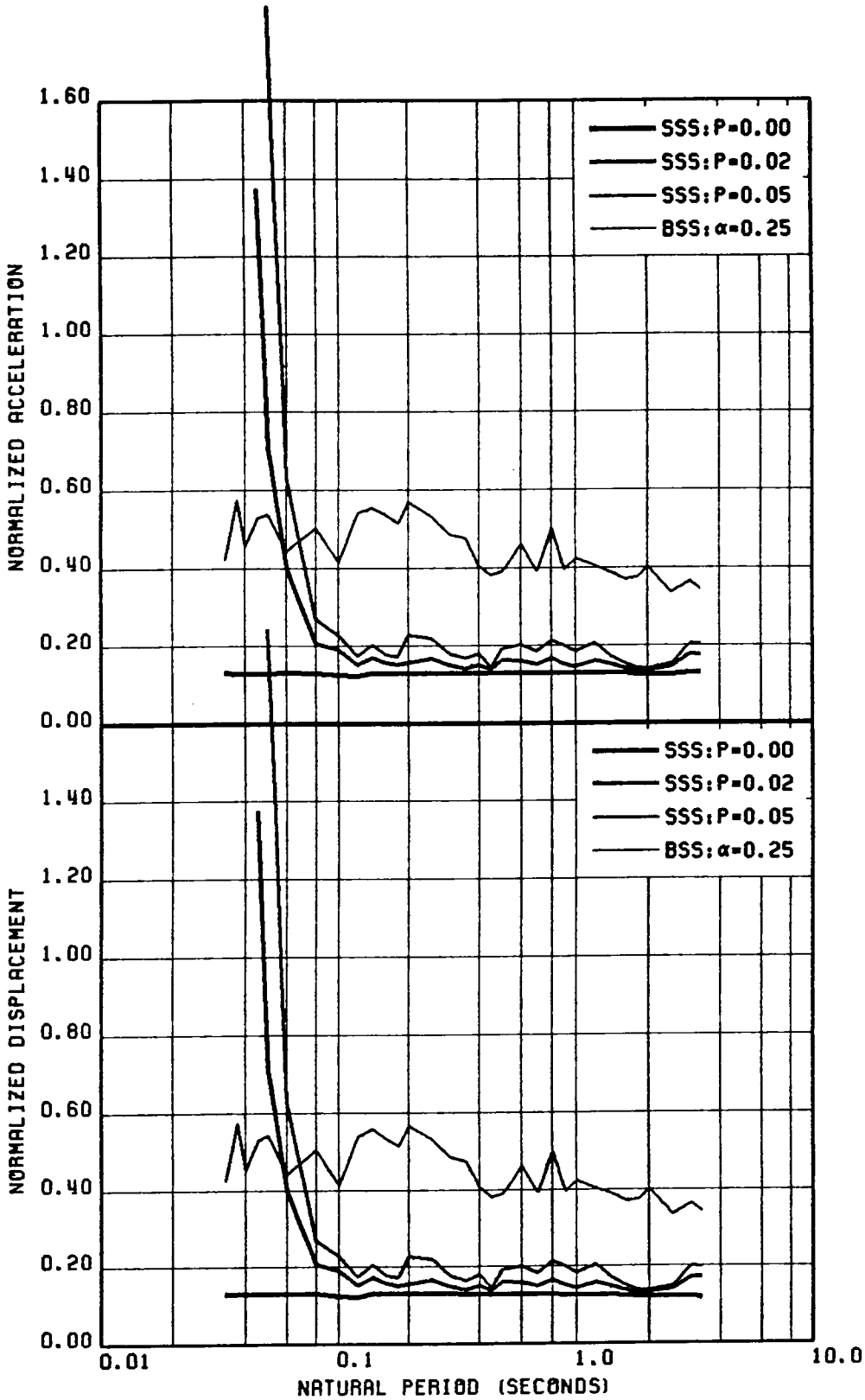

FIG. 4.15 COMPARISON OF SPECTRA OF (a) NORMALIZED ACCELERATION (b) NORMALIZED DISPLACEMENT FOR SSS, BSS & SPRING-ASSISTED SSS FOR SIMULTANEOUS HORIZONTAL & VERTICAL EXCITATION; GR. MOTION 5 β_o=0.02 & δ= 0.10

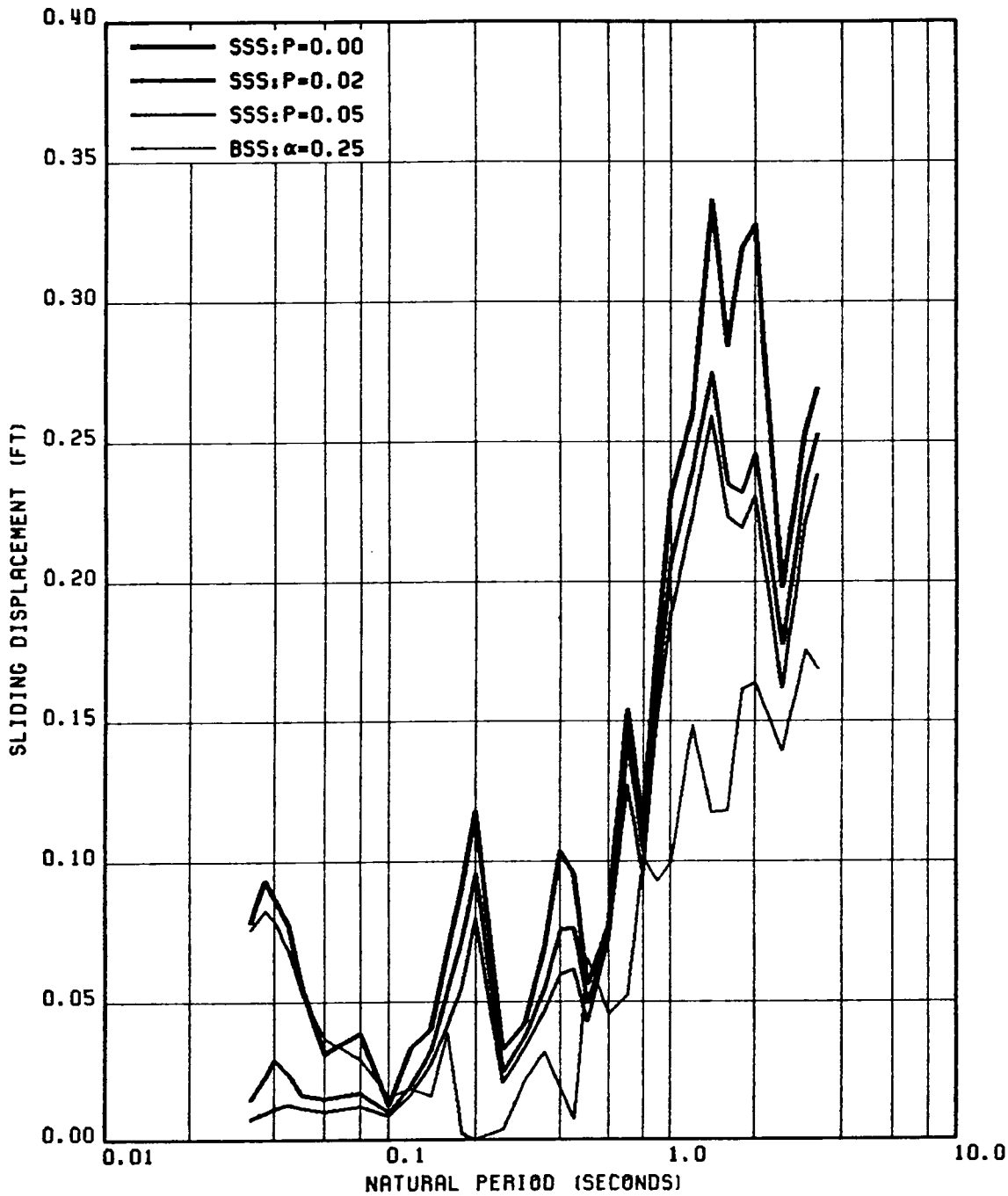

FIG. 4.16 COMPARISON OF THE SPECTRA OF SLIDING DISPLACEMENT FOR BSS, SSS & SPRING-ASSISTED SLAB SLIDING SYSTEMS FOR SIMULTANEOUS HORIZONTAL AND VERTICAL EXCITATION FROM GROUND MOTION 4, δ=0.02 AND δ=0.30.

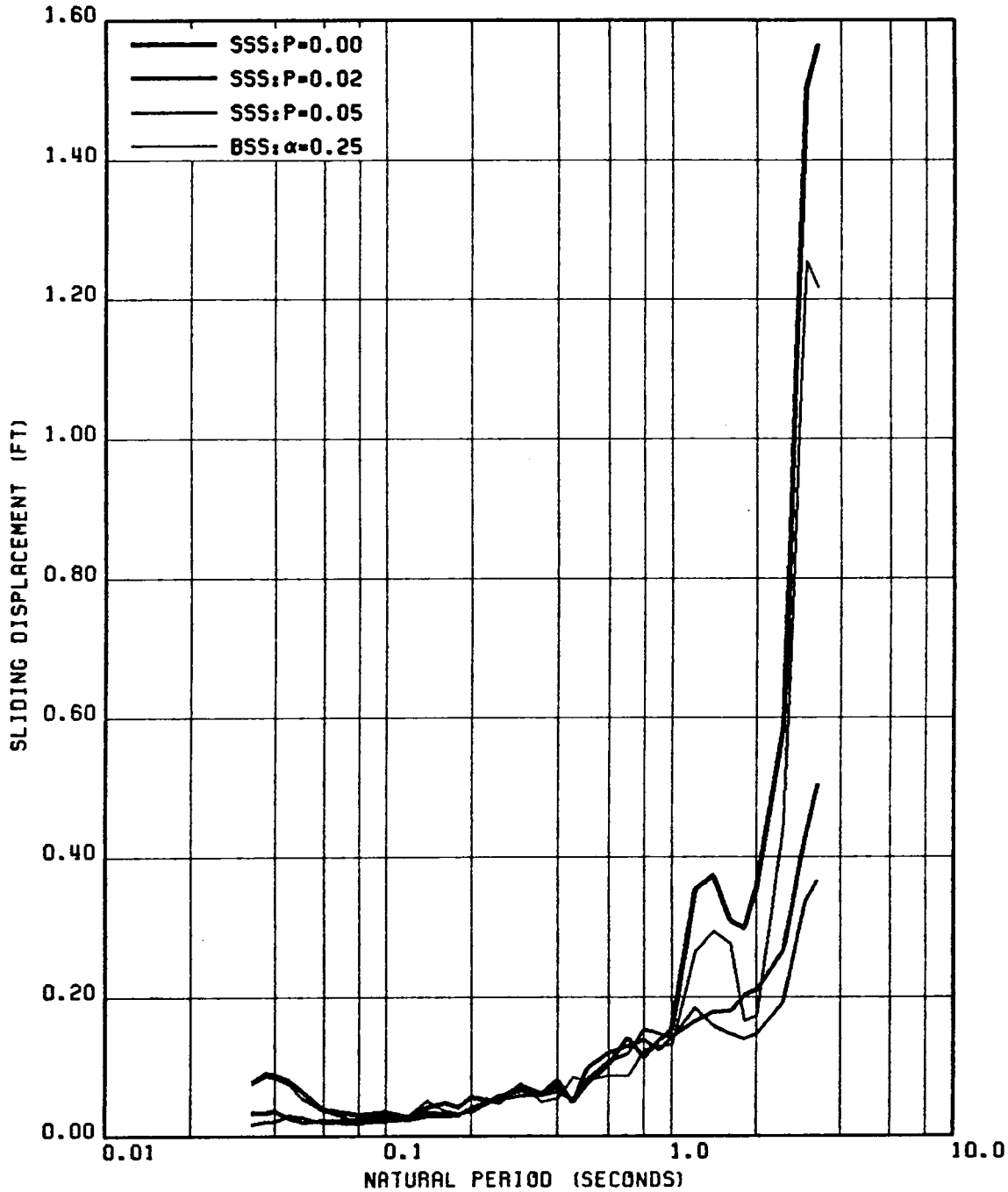

FIG. 4.17 COMPARISON OF THE SPECTRA OF SLIDING DISPLACEMENT FOR BSS, SSS & SPRING-ASSISTED SLAB SLIDING SYSTEMS FOR SIMULTANEOUS HORIZONTAL AND VERTICAL EXCITATION FROM GROUND MOTION 5, δ=0.02 AND δ=0.10.

Chapter V

Seismic Response of MDOF Sliding Structures

5.1 Introduction

In Chapters 2, 3 and 4, we have studied the seismic response characteristics of single-story structures fitted with different sliding arrangements. The observations made about the behavior of the single-story sliding structure were significant, and perhaps indicative of the response characteristics for a multi-story sliding structure. We now extend the analysis to multi-degree of freedom structures in this chapter. The formulation for vibration response of a multi-story sliding structure is presented. Numerical results are obtained and compared to the response of non-sliding structures to show the benefits achieved due to the provision of sliding interfaces at various floor levels.

5.2 *Analytical Formulation*

In this section the equations of motion are developed for multi-story structures, shown in Figs. 5.1 and 5.2, modeled as shear beam structures. Fig. 5.1 shows the proposed slab sliding arrangement, wherein a sliding interface can be provided at any one or all the floor levels. Fig. 5.2 shows a base sliding arrangement. The analytical formulation for the slab sliding arrangement is presented first, followed by the formulation for the base sliding arrangement.

5.2.1 Formulation for Slab Sliding Arrangement

In this case, the floor slabs are allowed to slide on the frame. Therefore, the equations for both the sliding and non-sliding cases are developed.

For the non-sliding case, the equation of motion for an i^{th} floor level can be written as:

$$m_i(\ddot{x}_{f_i} + \ddot{x}_g) = -k_i(x_{f_i} - x_{f_{i-1}}) + k_{i+1}(x_{f_{i+1}} - x_{f_i}), \quad i = 1,2,.....,n \qquad (5.1)$$

where n is the number of floors, $x_{f_{i-1}}$, x_{f_i} and $x_{f_{i+1}}$ denote the horizontal nodal displacements (relative to the ground) of the frame at the $(i-1)^{th}$, i^{th} and $(i+1)^{th}$ floor levels, respectively; m_i is the mass of the i^{th} floor slab; and k_i and k_{i+1} are the lateral stiffnesses of the columns immediately below and above the i^{th} floor slab, respectively. The horizontal ground acceleration input is denoted by $\ddot{x}_g$ The above set of equations can be put in a standard matrix form as floows :

$$[M]\{\ddot{x}_f\} + [K]\{x_f\} = \{\ddot{X}_g\} \tag{5.2}$$

where $[M]$ is the diagonal mass matrix and $[K]$ is the stiffness matrix of the structure. For the case of a shear structure the stiffness matrix is of tridiagonal form. These and the load vector, $\{\ \ddot{X}_g\ \}$ are given in the Appendix.

For the non-sliding case, these equations can be solved by modal analysis approach for a given ground motion input. At each step of the solution, the possibility of sliding of the floor masses at different levels is checked. The sliding occurs whenever the interface force, F_i , which is equal to mass times the absolute acceleration, exceeds the maximum friction force. This condition for sliding can be stated as follows:

$$| F_i | = | m_i(\ddot{x}_{f_i} + \ddot{x}_g) | \geq \mu_i m_i(g + \ddot{z}_g); \quad 1 \leq i \leq n \tag{5.3}$$

where μ_i is the friction coefficient for the sliding interface at the i^{th} level and $\ddot{z}_g$ is the vertical acceleration of the mass. Here it is assumed that this vertical acceleration is the same as the ground acceleration; that is, no filtering or amplification of the vertical motion through the structure is expected. This is usually the case, since most civil structures are relatively very stiff in the vertical direction.

Whenever Eq. (5.3) is satisfied, sliding initiates at the respective interface. In this case, the equation of motion of the mass can be simply written by applying Newton's Law as follows:

$$m_i(\ddot{x}_{s_i} + \ddot{x}_{f_i} + \ddot{x}_g) = -\mu_i m_i \varepsilon_i (g + \ddot{z}_g) \tag{5.4}$$

where x_{s_i} is the sliding displacement of the slab mass with respect to the position of the frame at the i^{th} floor level on which it is supported. Also,

$$\varepsilon_i = \text{sign}\,(\dot{x}_{s_i}) = -\frac{(F_i)_s}{|F_i|_s} \tag{5.5}$$

where the subscript 's' denotes that the quantity F_i appearing in the above equation is evaluated at the instant sliding is imminent.

For an assumed linear variation of the ground motion values between two consecutive time steps t_k and t_{k+1}, Eq. (5.4) can be directly integrated to obtain x_{s_i} as follows:

$$x_{s_i}(\tau) = -\frac{\tau^2}{6h_k}(2W_{i_k} + W_{i_{k+1}}) - [x_{f_i}(\tau) - x_{f_{i_k}}] + \tau \dot{x}_{f_{i_k}} \tag{5.6}$$

where, $x_{f_{i_k}}$ and $\dot{x}_{f_{i_k}}$, respectively, are the frame displacement and velocity values at the i^{th} floor level and time t_k. The quantities W_{i_k} and $W_{i_{k+1}}$ are as follows :

$$\begin{aligned} W_k^i &= A_k + \mu_i \varepsilon_i (g + Z_k) \\ W_{k+1}^i &= A_{k+1} + \mu_i \varepsilon_i (g + Z_{k+1}) \end{aligned} \tag{5.7}$$

In which A_k and A_{k+1} are the horizontal acceleration values at times t_k and t_{k+1} respectively. Also Z_k and Z_{k+1} are the corresponding vertical acceleration values at these two time steps.

From Eq. (5.6), it is seen that the sliding displacement response x_{s_i} and corresponding velocity can be calculated if $x_{f_{i_k}}$ and $\dot{x}_{f_{i_k}}$ are known. These latter quantities can be obtained from the solution of the equation of motion of the frame as explained below.

We will consider a general case when l number of floor masses are sliding. Correspondingly, there will be $(n-l)$,non-sliding floor masses. The equations of motion for the non-sliding masses remain the same as Eq. (5.1); there will $(n-l)$ such

equations, one for each non-sliding mass. Also, at a floor level which is sliding, the force transmitted from the sliding slab to the frame is equal to $\mu_i m_i \varepsilon_i (g + \ddot{z}_g)$. The equation of equilibrium of the frame node at this level is as follows (see the free body diagrams in Fig. 5.1)

$$k_i (x_{f_i} - x_{f_{i-1}}) - k_{i+1} (x_{f_{i+1}} - x_{f_i}) + \mu_i m_i \varepsilon_i (g + \ddot{z}_g) = 0 \tag{5.8}$$

The two sets of equation for sliding and non-sliding masses can now be combined and written in matrix form as follows:

$$\begin{bmatrix} \underline{M}_{nn} & \underline{0} \\ \underline{0} & \underline{0} \end{bmatrix} \begin{Bmatrix} \ddot{\underline{X}}_f^n \\ \ddot{\underline{X}}_f^s \end{Bmatrix} + \begin{bmatrix} \underline{C}_{nn} & \underline{C}_{ns} \\ \underline{C}_{sn} & \underline{C}_{ss} \end{bmatrix} \begin{Bmatrix} \dot{\underline{X}}_f^n \\ \dot{\underline{X}}_f^s \end{Bmatrix} + \begin{bmatrix} \underline{K}_{nn} & \underline{K}_{ns} \\ \underline{K}_{sn} & \underline{K}_{ss} \end{bmatrix} \begin{Bmatrix} \underline{X}_f^n \\ \underline{X}_f^s \end{Bmatrix} = \begin{Bmatrix} F_n \\ F_s \end{Bmatrix} \tag{5.9}$$

where the supscripts "n" and "s" identify the quantities associated with non-sliding and sliding masses. Thus $\underline{M}_{nn}$, $\underline{C}_{nn}$ and $\underline{K}_{nn}$ are the mass, damping and stiffness sub-matrices associated with the non-sliding masses. $\underline{K}_{ss}$ likewise is the stiffness sub-matrix associated with the nodes where sliding occurs. Notice that a damping matrix [C] (in a properly partitioned form) is introduced in the above equation. This matrix is used to account for the inherent material and structural damping in the structure, modelled as viscous damping. For a general configuration of the damping matrix, one may have to resort to the state vector approach to obtain the response of the structure. The cross sub-matrices $\underline{K}_{sn}$ and $\underline{K}_{ns}$ are the matrices which couple the two different sets of nodes. Similar definition applies to the sub-matrices of the mass and damping matrices. The vectors $\underline{X}_f^n$ and $\underline{X}^s suff$ contain the displacements of the non-sliding and sliding nodes of the structure, respectively. The force vector pertaining to the non-sliding nodes contains terms like $m_i \ddot{x}_g$, whereas the vector pertaining to the sliding nodes contains terms such as $-\mu_j m_j \varepsilon_j (g + \ddot{z}_g)$.

At every step of the calculation, the sliding and non-sliding masses are identified and knowing this, one can properly partition the mass, damping and stiffness matrices corresponding to the partitioned frame displacement and force vectors as shown in Eq. (5.9).

We need to solve Eq. (5.9) to obtain the response of the non-sliding masses, as well as displacement and velocity quantities x_{f_i} and $\dot{x}_{f_i}$, which are required in Eq. (5.6).

Although, it is possible to solve the case of a general damping matrix (which will involve complex algebra), we will now assume that the damping matrix is directly proportional to the stiffness matrix. This simplifies the algebra considerably and at the same time will enable us to evaluate the effect of the friction damping in structure response. With this assumption, the equation can now be written as:

$$\begin{bmatrix} \underline{M}_{nn} & \underline{0} \\ \underline{0} & \underline{0} \end{bmatrix} \begin{Bmatrix} \ddot{\underline{X}}_f^n \\ \ddot{\underline{X}}_f^s \end{Bmatrix} + h \begin{bmatrix} \underline{K}_{nn} & \underline{K}_{ns} \\ \underline{K}_{sn} & \underline{K}_{ss} \end{bmatrix} \begin{Bmatrix} \dot{\underline{X}}_f^n \\ \dot{\underline{X}}_f^s \end{Bmatrix} + \begin{bmatrix} \underline{K}_{nn} & \underline{K}_{ns} \\ \underline{K}_{sn} & \underline{K}_{ss} \end{bmatrix} \begin{Bmatrix} \underline{X}_f^n \\ \underline{X}_{sf} \end{Bmatrix} = \begin{Bmatrix} F_n \\ F_s \end{Bmatrix} \quad (5.10)$$

where h is the constant of proportionality. Eq. (5.10) is equivalent to the following two sets of equations:

$$[M_{nn}]\{\ddot{x}_f^n\} + [K_{nn}]\{h\dot{\underline{X}}_f^n + \underline{X}_f^n\} + [K_{ns}]\{h\dot{\underline{X}}_f^s + \underline{X}_f^s\} = \{F_n\} \quad (5.11a)$$

$$[K_{ss}]\{h\dot{\underline{X}}_f^s + \underline{X}_f^s\} + [K_{sn}]\{h\dot{\underline{X}}_f^n + \underline{X}_f^n\} = \{F_s\} \quad (5.11b)$$

Substituting for $\{h\dot{\underline{X}}_f^s + \underline{X}_f^s\}$ from Eq. (5.11b) into Eq. (5.11a), we obtain the following condensed equation of motion:

$$[M_c]\{\ddot{\underline{X}}_f^n\} + [C_c]\{\dot{\underline{X}}_f^n\} + [K_c]\{\underline{X}_f^n\} = \{F_c\} \quad (5.12)$$

where the subscript c defines the condensed quantities defined as follows:

$$
\begin{aligned}
[M_c] &= [M_{nn}] \\
[K_c] &= [K_{nn} - K_{ns} K_{ss}^{-1} K_{sn}] \\
[C_c] &= h[K_c] \\
\{F_c\} &= \{F_n\} - [K_{ss}]^{-1} [K_{sn}] \{F_s\}
\end{aligned}
\tag{5.13}
$$

It is noted that $[K_c]$ is a symmetric matrix. Futhermore, the condensed damping matrix is proportional to the condensed stiffness matrix. This will enable us to use the normal mode approach to solve the condensed equations of motion.

Knowing the response of these condensed equation, we can now proceed to solve the second set of Eqs. (5.11b). It can now be rewritten as follows:

$$
\{\dot{X}_f^s\} + \gamma \{X_f^s\} = - [K_{ss}]^{-1} [K_{sn}] \{\dot{X}_f^n + \gamma X_f^n\} + \gamma [K_{ss}]^{-1} \{F_s\} \tag{5.14}
$$

where, $\gamma = 1/h$. The above is a set of decoupled first order differential equations and the solution for the decoupled degrees of freedom can be easily found for the forcing function on the right side.

At the end of each time step, the sliding condition in Eq. (5.3) is checked at other non-sliding interface. Also whenever the sliding velocity of a sliding mass become zero that mass ceases to slide. The change from non-sliding to sliding as well as from sliding to non-sliding at any floor level changes the equations of motion. Thus it is necessary to keep track of the changes that are likely to occur as the solution progresses.

It is noted that the order or the degree of freedom of the problem to be solved changes whenever there is a change in the sliding structure. For a n-floor structure where all floor are allowed to slide the number of the degrees of freedom could be 2n. It is also noted that there are 2^n different possible combinations of sliding and

non-sliding mass configurations, each with its own set of governing differential equations.

5.2.2 Formulation for Base Sliding Arrangement

The provision of a sliding interface at the bottom of a multi-story structure is yet another interesting possibility for seismic isolation. Here, it is intended to compare the response of the base sliding structures with the response of the slab sliding structures. The derivation of the equations of motion for a multi-story base sliding structure is now presented.

Consider, for example, a shear beam model of the structure as discussed in the previous section. In that case, the non-sliding response is still governed by the Eq. (5.2). However, here one checks for the possibility of sliding at the bottom interface by applying the following condition :

$$| F_b | = | M\ddot{x}_g + m_1\ddot{x}_{f_1} + m_2\ddot{x}_{f_2} + ... + m_n\ddot{x}_{f_n} | \leq \mu_b M (g + \ddot{z}_g) \qquad (5.15)$$

where $M = m_b + \sum m_i$ = the total mass of the structure, including the mass of the auxiliary base slab, denoted by m_b and μ_b = the friction coefficient at the base sliding interface; and x_{f_i} = displacement of the floor at i^{th} floor level with respect to the base. Sliding initiates at the bottom interface if the above condition is not satisfied.

During the base sliding phase, the equation of dynamic equilibrium for the entire structure can be written as follows:

$$M (\ddot{x}_s + \ddot{x}_g) + m_1\ddot{x}_{f_1} + ... + m_n\ddot{x}_{f_n} = -\mu_b M\varepsilon (g + \ddot{z}_g) \qquad (5.16)$$

where x_s is the sliding displacement of the base with respect to ground, and

$$\varepsilon = \mathbf{sign}\,(\dot{x}_s) = - \frac{(F_b)_s}{|F_b|_s} \tag{5.17}$$

where the subscript s indicates that the quantities in the above equation are evaluated at the time sliding becomes imminent. Eq. (5.16) can be rewritten as follows:

$$\ddot{x}_s = -\mu_b g\varepsilon - \ddot{x}_g - \sum_{i=1}^{n} \frac{m_i}{M}\,\ddot{x}_{f_i} \tag{5.18}$$

The sliding response x_s can be obtained exactly if the $\{x_f\}$ response is known in closed form. The following is the solution for x_s response :

$$\begin{aligned} x_s(\tau) = {} & x_{s_k} + \dot{x}_{s_k}\tau - V_k\tau - \frac{V_{k+1} - V_k}{h_k}\,\frac{\tau^2}{2} \\ & - \sum_{i=1}^{n} \frac{m_i}{M}\left(x_{f_i}(\tau) - x_{f_{i_k}} - \dot{x}_{f_{i_k}}\tau\right) \end{aligned} \tag{5.19}$$

In order to obtain the solution for the x_f's, we can write the equation for dynamic equilibrium of i^{th} floor slab mass as follows:

$$m_i\left(\ddot{x}_{f_i} + \ddot{x}_s + \ddot{x}_g\right) = k_i x_{f_{i-1}} - (k_i + k_{i+1})\,x_{f_i} + k_{i+1}\,x_{f_{i+1}} \tag{5.20}$$

Substituting Eq. (5.18) into Eq. (5.20), and dividing the subsequent equation by M, we obtain:

$$\sum_{k=1}^{n}\left(m_i - \frac{m_i m_k}{M}\ddot{x}_{f_k}\right) - k_i x_{f_{i-1}} + (k_i + k_{i+1})x_{f_i} - k_{i+1}x_{f_{i+1}} - \mu_b m_i g\varepsilon = 0 \quad (5.21)$$

where $i = 1,2,.....,n$. The above equations can be conviniently expressed by the following matrix equation:

$$[\overline{M}]\{\ddot{X}_f^s\} + [C]\{\dot{X}_f^s\} + [K]\{X_f^s\} = [M]\{I\}\mu_b\varepsilon(g + \ddot{z}_g) \quad (5.22)$$

where $\{X_f^s\}$ is the frame deformation vector for the case of base sliding. Matrices $[K]$ and $[M]$ have been defined in the earlier section and the new mass matrix $[\overline{M}]$ and the influence vector $\{I\}$ are defined as follows:

$$[\overline{M}] = \begin{bmatrix} m_1(1-\frac{m_1}{M}) & -\frac{m_1 m_2}{M} & . & -\frac{m_1 m_n}{M} \\ -\frac{m_2 m_1}{M} & m_2(1-\frac{m_2}{M}) & . & . \\ . & . & . & . \\ . & . & . & -\frac{m_{n-1}m_n}{M} \\ -\frac{m_n m_1}{M} & -\frac{m_n m_2}{M} & . & m_n(1-\frac{m_n}{M}) \end{bmatrix} \quad (5.23)$$

$$\{I\} = \{1 \;\; 1 \;\; .... \;\; 1 \;\; 1\}^T \quad (5.24)$$

In Eq. (5.22), we have introduced the damping matrix to account for the viscous dissipation energy. We will again assume that it is proportional to the stiffness matrix

$[K]$. Thus, the method of modal analysis can be applied to obtain the x_f 's during sliding. The base sliding ceases to occur if the base sliding velocity $\dot{x}_s$ becomes zero at any time during sliding.

5.3 Numerical Results

To examine the effect of providing sliding interfaces under various slabs, here numerical results are obtained for three three-story structures modeled as shear beams. Figs. 5.1 and 5.2 show the structure with slab sliding and base sliding arrangements, respectively. The mass and stiffness distribution of the super-structure is identical in both cases and it is indicated in Figs. 5.1 and 5.2. It may be noted that the base sliding arrangement in Fig. 5.2 requires an auxiliary mass at the base of the structure. The natural frequencies of the structure depend on the ratio k/m, since in Figs. 5.1 and 5.2, the mass and stiffness distribution for the structure is expressed in terms of m and k, respectively. Herein, three different pairs for values of m and k were considered. This resulted in study of three structures with varying frequency distribution. The natural frequencies of Structure 1 are in the medium range. Structure 2 is stiffer, whereas Structure 3 is more flexible than Structure 1. The frequencies of these structures are given in Tables 5.1 to 5.3. The damping matrix is chosen to be proportional to the stiffness matrix. The modal damping ratios for each structure are also furnished in Tables 5.1 to 5.3.

Three ground motions used in this study are Motion Nos. 1, 2 and 3, listed in Chapter 2. It is recalled that Ground Motion 1 was recorded on a soft site, Motion 2 on a medium stiff site and Motion 3 on a stiff site. Responses are obtained for purely

horizontal excitation as well as for the case of simultaneous horizontal and vertical excitation.

For the case of slab sliding structures, responses have been obtained two cases: (1)only one sliding interface, and (2)three sliding interfaces with the possibility of simultaneous sliding at all interfaces. To evaluate the effectiveness of sliding interfaces, these responses have been compared with the responses of a corresponding elastic (non-sliding) structure. For comparison, the responses for the base sliding structure have also been obtained. The response quantities of interest are the accelerations of each floor slab, deformation of the frame at each floor level and the sliding and residual displacements of each slab mass. In most cases, the slab accelerations and frame deformations, normalized with respect to the corresponding maximum response for the equivalent non-sliding structure, are presented. Thus a normalized value less than unity implies a reduction in the response. For example, a value of 0.80 means that the response has been reduced by 20% because of the provision of a sliding arrangement.

Tables 5.1 to 5.3 give the maximum response values of the frame displacements and slab accelerations for the three structures without any sliding interface. As one would expect, the Structure 2, being the most stiff has the smallest deformations and Structure 3, being the most flexible has the largest deformations.

5.3.1 Response of Base Sliding Structure

In Tables 5.4 to 5.9 are given the results for the response of the three structures considered in this study when they are provided with a sliding interface at their bases and subjected to Ground Motion 1. The mass of the auxiliary base slab is taken as

one third of the total mass of the structures in all the cases. The maximum response values presented in these tables are normalized with respect to the corresponding response values of the structure with no sliding interface. Several coefficient of friction values ranging from 0.05 onwards have been considered. Tables 5.4, 5.5 and 5.6 are for Structures 1, 2 and 3, respectively, when they are subjected to the horizontal component of Ground Motion 1. It is observed from these tables that base sliding arrangement is generally effective in reducing the frame deformation response for low values of friction coefficient. The corresponding base sliding displacements seem reasonable except for friction coeffcient of 0.05. It is noted however, that the base sliding arrangement is not very effective in reducing the slab acceleration. In fact, they actually amplify the response in comparison to the non-sliding response, as seen from the normalized acceleration values larger than 1.0. These observations are similar to the ones made for one-story base sliding structures in Chapter 2. It is noted that in Table 5.6, base sliding did not occur for friction coefficients larger than 0.30, thus the resulting response values for these cases are same as the elastic response.

Tables 5.7, 5.8 and 5.9 provide results similar to those in Tables 5.4, 5.5, 5.6 for the case when the same structures are also subjected to the vertical component along with the horizontal component of Ground Motion 1. Comparing the results presented in these tables with the corresponding results from the tables for just horizontal input, it is noted that the presence of vertical acceleration does not affect the response significantly. Again, this observation is the same as that made for the case of one-story base sliding structure.

5.3.2 Response of Structures With Only One Sliding Slab

The results for the case when only the first floor slab is allowed to slide are given in Tables 5.10 and 5.11. Table 5.10 is for excitation due to just the horizontal component and Table 5.11 for both the horizontal and vertical components of excitation. The friction coefficient is varied from 0.10 to 0.80, in increments of 0.05. It is noted that no sliding would occur for a value of friction coefficient larger than the acceleration (in G-units) of the first floor slab for the non-sliding case. From the results, it is observed that first floor sliding arrangement does reduce the frame deformation response, but not as much as the base sliding arrangement. This arrangement also reduces accelerations at other floor levels. Although for some values of friction coefficients, a slight amplification in acceleration of floor 2 is observed. The accompanying sliding displacements also seem to be reasonable.

The results in Table 5.11 show that presence of vertical acceleration does increase the value of acceleration at the first floor slab. One can estimate the possible maximum value of the first floor slab acceleration as $\mu_1 (g + \ddot{z}^+_{g_{max}})$. This effect of vertical acceleration is the same as discussed in Chapter 4, where a similar increase was observed for the case of one-story slab sliding structure. However, it is noted that this increase in the acceleration does not seem to affect the other responses significantly.

Tables 5.12 and 5.13 are similar to Tables 5.10 and 5.11, but with the sliding interface now being provided at the second floor level. Friction coefficient values ranging from 0.10 to 1.50 in increments of 0.10 are considered. It is observed that the provision of sliding interface at the second floor is more effective than the interface at first floorin reducing the frame deformation response. For some high friction

coefficient values, however, an increase in the acceleration of the first floor is observed, although acceleration at floor 3 is reduced. Comparison of the results in Table 5.13, where the vertical component of the input motion is also considered, with the results in Table 5.12 shows that the vertical motion does not significantly affect the response characteristics.

The response results for the case when only the top floor is permitted to slide are given in Tables 5.14 and 5.15. Again, Table 5.14 is for only the horizontal componenet of the input and Table 5.15 is for the horizontal as well as vertical components of the ground motion. The friction coefficient values ranging from 0.15 to 2.25, in increments of 0.15 have been considered. From the results in these tables, it is seen that this sliding arrangement is the most effective when compared to first and second floor slab sliding arrangements in reducing the frame deformations. In this respect, however, the base sliding arrangement at the third floor level does not appear to be as effective does seem to be slightly more effective in reducing the frame deformations. It is also observed that unlike the base sliding arrangement (Tables 5.4 and 5.7), sliding at the third floor level does not cause any acceleration amplication. The accelerations are consistently reduced at all floor levels for the case of third floor slab sliding arrangement. The sliding displacements as shown in the last columns of Tables 5.14 and 5.15 are not unreasonably large.

5.3.3 Results for a Multiple-Slab-Sliding

It now is of interest to see if the provision of more than one sliding interface can further reduce the frame deformation and slab acceleration responses, without causing large sliding displacements. With this in mind; many several sets of results

are generated for the case of multiple-slab-sliding, which we have also referred to as "multi-sliding" cases. Fig. 5.1 shows a multi-sliding arrangement in which sliding interfaces are provided at all the floor levels.

Numerical results for three different cases are presented. In the first case, the coefficient of friction is taken to be the same at all sliding interfaces. In the second case, the friction coefficient values at the interfaces are chosen such that a desired level of maximum acceleration response is effected. In the third case, the chice of friction coefficient values is made such that a predecided level of frame deformation response is achieved. The methods to select the required friction coefficient values in each case are also discussed in the respective sections.

Multiple-Slab-Sliding With Equal Friction Coefficient

The main purpose of presenting these results is to compare the effectiveness of the multi-sliding system vis-a-vis the base sliding system, both provided with the same friction coefficient at the sliding interfaces. To ensure that sliding does take place in the multi-sliding case, the friction coefficient should be at the most equal to the minimum floor acceleration value (expressed in G-units), obtained for the corresponding non-sliding case. In fact, to really ensure that sliding does occur at all interfaces, the friction coefficient should be significantly smaller than the above mentioned value.

The response values are obtained for the floor acceleration, frame deformation, sliding and residual slab displacements and secondary floor response spectra. The floor accelerations and frame deformation values have been normalized with respect to the corresponding values for the non-sliding structure. As mentioned earlier, the latter values are given in Tables 5.1 to 5.3.

The response results are presented in tabular as well as graphical forms. There is some duplication in the information presented. The tabular representation provides a better quantitative description of many response quantities at the same time. The graphical representation, on the other hand, is more expressive about the qualitative character of the individual response quantities. Thus, even at the risk of some duplication, both the forms of presentation have been retained.

The numerical results for the slab sliding cases with equal friction coefficient are presented in Tables 5.16 to 5.21. The comparisons of these multi-sliding results with the corresponding base sliding results are shown in Figs. 5.3 to 5.18. Base sliding systems with two different mass ratios of 1/3 (Base-Sliding-1) and 1/2 (Base-Sliding-2) have been considered. This mass ratio is the ratio of the mass of the auxiliary base slab to the total mass of the structure. As mentioned earlier, the results for mass ratio = 1/3 have been given in Tables 5.4 to 5.9.

Figs. 5.3 to 5.5 compare the normalized floor accelerations of the multi-sliding and the two different base sliding structures for the first, second and third floor levels, respectively. Here, the comparison of base sliding with multi-sliding results clearly reveals that the multi-sliding structure is better in causing reduction in floor slab accelerations. This difference is seen to increase for higher friction coefficients. To show the effect of adding vertical excitation to the input, Figs. 5.11 to 5.13 are presented for the same response quantities. It is seen that the presence of vertical acceleration increases the floor accelerations for the multi-sliding case, whereas the acceleration in the base sliding cases remain relatively unaffected. However, in spite of this, the multi-sliding arrangement still provides a better reduction in the floor accelerations than the base sliding cases. The maximum possible of the floor acceleration in the multi-sliding case is changed to $\mu\,(g + \ddot{z}^{+}_{g_{max}})$ in the presence of vertical acceleration.

Figs. 5.6 to 5.8 compare the normalized frame deformation at the first, second and third floors, respectively for the base sliding and multi-sliding cases. Again, it is seen that the multi-sliding case is more effective in this regard too. It is interesting to note that for the multi-sliding case, there is an almost linear relationship between the friction coefficient and the frame deformations. The same relationship is also more or less linear for base sliding cases also, but not to the same degree as for the multi-sliding case. Figs. 5.14 to 5.16 show the effect of adding vertical acceleration input for the same response quantities. It is seen that vertical accleleration does not cause any appreciable change in these response for both multi-sliding and base sliding cases.

Table 5.16 shows the magnitudes of sliding displacements required to achieve the acceleration and deformation reduction. It is seen that these displacements for the multi-sliding arrangement are reasonable and their magnitudes compare well with the base sliding displacements, given in Table 5.4. Figs. 5.9 compares the sliding displacements for the multi-sliding and base sliding structures for horizontal excitation. As mentioned earlier, the sliding displacements are not large for both types of sliding arrangements. Fig. 5.17 shows the effect of adding vertical acceleration input. This effect is observed to be insignificant.

Comparison of the residual displacements is shown in Figs. 5.10 and 5.18 for just the horizontal component and combined horizontal and vertical excitations, respectively. It is observed that for base sliding as well as multi-sliding cases, the residual displacements are substantially smaller than the corresponding maximum sliding displacements. As is seen from Fig. 5.18, the presence of vertical acceleration seems to change the residual displacement values at times, but its effect does not seem to change the overall shape of the residual displacement curves.

Besides the effect of sliding on floor acceleration levels, it is also of interest to study its effect on the frequency content of the floor motions. To show this, the secondary floor response spectra have been obtained at the three floor levels. Figs. 5. 19 to 5.30 compare the secondary floor spectra for non-sliding, base sliding (mass ratio = 1/3) and multi-sliding structures. All figures correspond to Ground Motion 3 as the input and a friction coefficient of 0.10. A damping ratio of 0.02 was used to obtain the secondary spectra. Figs. 5.19 to 5.21 are the secondary spectra for the first, second and third floor levels of Structure 1, respectively. From these figures, it is seen that the floor spectra for the multi-sliding case are of the lowest magnitude. It is noticed that the base sliding causes a shift in the dominant frequency of the floor spectra. This is probably because sliding changes the frequency characteristics of the input at the base of the structure to coincide with the higher mode of the structure. This frequency shift is, however, absent in the secondary floor spectra for the multi-sliding case.

Figs. 5.22 to 5.24 show the effect of icluding the vertical ground motion component on the secondary spectra for Structure 1. Of course, vertical acceleration does not change the non-sliding response and hence the secondary spectra corresponding to this case are unchanged. As observed before, the base sliding causes a shift in the dominant frequency of the floor spectra. Again, the multi-sliding case produces the lowest secondary spectra. Comparison of Figs. 5.19 to 5.21 which were generated for only horizontal component with Figs. 5.22 to 5.24 reveals that vertical acceleraration though increases the maximum floor accelerations for the multi-sliding cases, it does not change the floor spectrum values significantly. The spectra for base sliding structure, however, are seen to be affected slightly more than the multi-sliding case, especially on the high frequency range.

Figs. 5.25 to 5.27 show secondary spectra for Structure 2, with the horizontal component of Ground Motion 3 as the input. Since this structure is more stiff than Structure 1, the peaks in its secondary spectra for the non-sliding case occur in the high frequency region. Just as for Structure 1, the secondary spectra for the multi-sliding case are the lowest. Again, a shift in the dominant frequency of the floor spectra is noted for the base sliding case.

Similar floor response spectra results are shown in Figs. 5.28 to 5.30 for Structure 3 subjected to the horizontal component of Ground Motion 3. Since this is a flexible structure, the peaks in its secondary spectra are in the low frequency region. Other than that, the floor response spectra characteristics for thsi structure are similar to those of the other two structures.

After having established the effectiveness of multi-sliding arrangement in reducing structural response, we now turn our attention to show the effect of friction on the frame deformations and sliding displacements at different floor levels. Fig. 5.31 shows the effect of friction coefficient on the normalized frame deformation responses. As mentioned earlier, the variation of frame deformation with friction coefficient is remarkably linear. This is similar to the case of one-story slab sliding structure, where the maximum frame deformation approaches a value of $\mu_1 m_1 g/k$, thereby making the frame deformation response linearly proportional to the friction level. Here also, this linear variation can be explained by an examination of Eq. (5.14). For the case when all slabs are sliding, Eq. (5.14) can be specialized as follows:

$$\dot{\underline{X}}_f^s + \gamma \underline{X}_f^s = - \underline{K}^{-1} \gamma (g + \ddot{z}_g) \underline{M} \{ \mu_1 \varepsilon_1, \mu_2 \varepsilon_2, \mu_3 \varepsilon_3 \}^T \qquad (5.25)$$

For low viscous damping ratios, γ is a large number ($\gamma = 1/h = \omega_1/\beta_1$). Due to this, the transient response arising for the above case is mainly governed by the loading function on the right side of the above equation, and the effect of initial conditions becomes insignificant very fast. In absence of the vertical acceleration, the the response for this case can be written as:

$$\underset{\sim}{X}_f^s = - g \, \underline{K}^{-1} \{ m_1\mu_1\varepsilon_1, \; m_2\mu_2\varepsilon_2, \; m_3\mu_3\varepsilon_3 \}^T \tag{5.26}$$

Obviously, $\underset{\sim}{X}_f^s$ values will be maximum when all the sliding orientations are the same. That is, when all ε_i's are of the same sign. Clearly, for equal coefficient of friction at all floor levels, the maximum frame deformation response would then be directly proportional to the value of the friction coefficient. This explains why the variation of normalized frame deformation with the friction coefficient is linear as seen in Fig. 5.31. For very high friction coefficient values, there may not be any sliding at some floor/s, in which case, Eq. (5.26) will not be applicable. It will be seen later (Figs. 5.37 and 5.40) that this does happen, indeed.

In the presence of vertical acceleration, the maximum possible values of response could be obtained by replacing g with $(g + \ddot{z}_{g_{max}}^+)$ in Eq. (5.25). Again, the response will increase linearly with μ if the $\ddot{z}_{g_{max}}^+$ occurs during the sliding of all masses. If this does not happen then the response might be slightly less, as seen in Fig. 5.34.

Figs. 5.32 and 5.35 show the effect of friction on the slab sliding displacements. Fig. 5.32 is for excitation only in the horizontal direction, whereas Fig. 5.35 is for excitation both in the horizontal and vertical directions. As one may expect, lower friction coefficient values cause higher sliding displacements, which decrease very rapidly with higher values of friction coefficient. As will be seen later, this is not always the norm and that sometimes higher value of friction can cause larger sliding

displacements at some floor level/s. Comparison of Figs. 5.32 and 5.35 shows that there is no appreciable effect on the sliding displacements due to the presence vertical acceleration.

Figs. 5.33 and 5.36 show the effect of friction on residual displacements for excitation due to just horizontal and both horizontal and vertical components of Ground Motion 1. It is observed that in both cases, the values of residual diaplacements are quite small and they are substantially smaller than the corresponding maximum sliding displacement values.

Figs. 5.37 to 5.39 are similar to Figs. 5.31 to 5.33, but they are for Structure 2. Also, Figs. 5.40 to 5.42 are similar to the earlier four figures, but they are for Structure 3. All these figures show the same kind of results as those made for Structure 1 in Figs. 5.31 and 5.32. However, it is interesting to note from Fig. 5.41 that the slab sliding displacement for the third floor is not of monotonically decreasing nature with increase in the friction level. Also, for Structure 2 (stiff structure), there seems to be a more monotonic variation of sliding and residual displacements than for the case of the other two structures. Also, there seems to be a larger difference in the levels of residual and sliding displacement values for the case of the stiff structure.

Multiple-Slab-Sliding With Desired Acceleration Reduction

As it was possible for a single degree of freedom structure, one can also reduce the acceleration of various floors of a multi-story structure to any desired level by providing appropriate friction at the interfaces. For example, if the acceleration of the i^{th} floor is required to be reduced to r_i times its value in a non-sliding case, then the friction coefficient at its interface with the frame should be chosen equal to $\mu_i = r_i A_i/g$, where A_i is the maximum acceleration of the floor in the non-sliding case.

The factor r_i will be referred to as the *acceleration reduction factor*. The choice of the friction coefficient value in the manner described above will ensure that the acceleration of the floor will not exceed $\mu_i g$, irrespective of what friction coefficients are chosen at the other sliding interfaces. In the presence of vertical acceleration, the maximum floor acceleration may be increased to a value of $\mu_i (g + \ddot{z}^+_{g_{max}})$. This means that the normalized acceleration value will be increased to

$$\begin{aligned} \text{Norm. Acceleration} &= \frac{\mu_i g\,(1 + \ddot{z}^+_{g_{max}}/g)}{A_i} \\ &= r_i (1 + \ddot{z}^+_{g_{max}}/g) \end{aligned} \tag{5.27}$$

It is, however, noted that this will be the maximum possible value of the normalized acceleration in the presence of vertical excitation.

It is of interest to see how the frame deformation and sliding displacements are affected when a desired level of acceleration reduction is imposed on the structure. For this, we have generated numerical results for equal reduction in the accelerations of all the floors; that is, the acceleration reduction factor $r_i = r$. These results are presented in Tables 5.22 to 5.27 for the three structures with Ground Motion 2 as the input. Some of these results are also presented in graphical form in Figs. 5.43 to 5.60. The acceleration reduction factor values in the range of 0.10 to 0.80, in increments of 0.05 are used.

Figs. 5.43 to 5.45 show the plots for frame deformation, sliding displacement and residual displacement, respectively, for horizontal excitation of Structure 1. Fig. 5.43 shows that the variation of the normalized frame deformations at the three floor levels is more or less linear with the acceleration reduction parameter. This is to be expected, as an increase in the level of acceleration reduction parameter means that the loading vector on the right side of Eq. (5.26) is increased proportionately, which

in turn leads to a corresponding increase in the frame deformation values. However, it is interesting to note that the normalized frame deformations, though linearly proportional to the acceleration reduction parameter, are usually of higher magnitudes than the acceleration reduction parameter (this is indicated by the slope of the lines in Figs. 5.43 which is greater than unity). This means that the reduction in the frame deformations is smaller than the specified reduction in the acceleration response.

Fig. 5.44 shows the variation of sliding displacements at the three floor levels with acceleration reduction parameter. Here, the sliding displacements for floor levels 1 and 2 are seen to decrease with an increase in acceleration levels (as signified by higher values of acceleration reduction parameters). However, this is not the case with floor level 3, where the sliding displacements are seen to be increasing for intermediate values of the acceleration reduction factor. Figs. 5.45 shows the variation of residual displacement response. It is observed that they are usually smaller than the corresponding sliding displacements.

The set of the next three figures, Figs. 5.46 to 5.48, show the effect of vertical acceleration on the three response quantities of interest. All these response quantities are increased somewhat, but not significantly.

The set of the next six figures, Figs. 5.49 to 5.54, is for Structure 2. They show similar response results as the previous set six figures for Structure 1. It is seen from Fig. 5.49 that the variation of the normalized frame deformations with the acceleration reduction parameter is again linear. Furthermore, the lines corresponding to the three floor levels almost coincide with each other and they have a slope of 1.0. This means that the level of reduction in the frame deformation is the same as the reduction in slab accelerations. This observation is different from the observation made for Structure 1. A possible qualitative explanation for this behavior in Structure

2 is that this structure being a stiff structure, the acceleration and displacement responses are in phase for all floor levels. For more flexible structures, this probably is not the case as different modes affect the responses of structure such that they cause a phase difference in the acceleration and deformation responses. Fig. 5.50 and 5.51 show the sliding and residual displacements. These are seen to decrease monotoncally for higher values of acceleration reduction parameters. Comparison of Figs. 5.52 with 5.49 shows that the frame deformation values are increased by about $\ddot{z}^{+}_{g_{max}}/g$ due to the presence of vertical excitation. Figs. 5.53 and 5.54 show that the sliding and residual displacements values are almost unchanged despite the presence of vertical accelration.

Similar results for the soft structure, Structure 3, are shown in Figs. 5.55 to 5.60. Increase in the frame deformation with acceleration reduction parameter (factor) is not as linear as it was before for the other two structures. This indicates that for the friction coefficient values chosen according to the desired level of acceleration reduction does not necessarily produce sliding at all floors, particularly in the case of this structure. Of course, the floor accelerations and frame deformations are accordingly smaller than the estimated upper bounds. It is also interesting to note that the slope of the curves showing the variation of normalized frame deformation in Fig. 5.55 is now larger than unity. This means that for a chosen level of reduction in the floor accelerations, the corresponding reduction in the the frame deformation will be less. As discussed earlier, this is because this structure is more flexible than the other two structures. Comparison of Figs. 5.57 and 5.60 with Figs. 5.56 and 5.59 shows that for this flexible structure, the residual displacements are generally not much smaller than the corresponding sliding displacement values.

Multiple-Slab-Sliding With Frame Deformation Control

In the previous section, the maximum acceleration responses of the slabs were controlled at predecided levels. The effect of such control on the frame deformation and sliding and residual displacements of different slabs was studied. In this section, we plan to control the deformation levels in the frame and study the effect of this control on the slab accelerations and sliding and residual displacement responses.

Let us consider a case when the frame deformations are to be reduced to the levels of δ_1, δ_2 and δ_3 of their respective values in the non-sliding case at the first, second and third floor levels, respectively. One can then obtain the required coefficient of friction values to achieve these desired levels of reduction in the frame deformation response from Eq. (5.26) as:

$$\begin{Bmatrix} m_1\mu_1 \\ m_2\mu_2 \\ m_3\mu_3 \end{Bmatrix} = \frac{1}{g} K \begin{Bmatrix} \delta_1 x_{f_1}^{ns} \\ \delta_2 x_{f_2}^{ns} \\ \delta_3 x_{f_3}^{ns} \end{Bmatrix} \tag{5.28}$$

In Eq. (5.28), $x_{f_1}^{ns}$, $x_{f_2}^{ns}$ and $x_{f_2}^{ns}$ are the maximum frame deformation values at the first, second and third floor levels, respectively, in the non-sliding case.

In the following, we will present several sets of results for an equal reduction in the frame deformations at all floor levels. That is, the following results are for $\delta_1 = \delta_2 = \delta_2$. These results are given in Tables 5.28 to 5. 45. The variations of the floor accelerations and sliding and residual displacement with frame deformation reduction parameter δ are also diplayed graphically in Figs. 5.61 to 5.114. In these figures, this parameter has been referred to as the *Frame Deformation Reduction Factor* . The responses of the three structures subjected to three different ground motions are presented. Furthermore, to

investigate the effect of vertical motion, responses with and without the vertical components of the ground motions have been obtained. Thus for each structure, there are sisx tables: three for only horizontal component of the earthquakes and an additional three for the horizontal plus vertical components of the same earthquake motions.

In all the tables and plots, the frame deformation reduction parameter is varied from 0.10 to 0.80, in increments of 0.05. It is mentioned that the choice of the friction coefficient values according to Eq. (5.28) ensures that the frame deformations remain below the (preselcted) δ times the deformations in the non-sliding case. The actual value in fact be smaller than this upper bound. The deformation would reach this level only when the case of all slabs sliding occurs. However, it is likely that the friction coefficient at a certain floor level may be rather high to bring about this occurence. In such a case, the frame deformation response would be actually be smaller than the attempted level of reduction at that floor level.

Table 5.28 lists the responses of Structure 1 for excitations due to just the horizontal component of Ground Motion 1. In Table 5.28, it is observed that the normalized frame deformation vlues at the three floor levels are simply equal to chosen frame deformation reduction parameters, indicating that sliding does occur at all floor levels. Fig. 5.61 shows the variation of normalized slab accelerations. It is seen that the normalized accelerations at the three floor levels vary linearly with the frame deformation reduction parameter. However, now the slope of these lines is lesser than equal to unity, implying that the extent of reduction in the floor accelerations is greater than the extent of reduction in frame deformation response. (See the earlier discussion on this in the previous section, where results for controlled floor accelerations were discussed). Fig. 5.62 shows that the accompanying sliding displacements for this case are not large and thus reasonable.

Also, Fig. 5.63 shows that the residual displacements are quite smaller than the corresponding sliding displacement values.

Table 5.29 lists the results for when both the horizontal and vertical components are applied. The effect on the normalized frame displacements is predicatable in that they could be increased to a maximum value of $\delta\,(g + \ddot{z}^{+}_{g_{max}})/g$ if the maximum vertical acceleration occurs during a sliding phase. However, since the values of the normalized frame deformation values, as given in the first three columns of Table 5.29, did not increase to the maximum amount. Obviously, not all slabs slided when the value $\ddot{z}^{+}_{g_{max}}$ occured in the vertical acceleration time history. These effects of vertical acceleration can be seen in Fig. 5.64.

Fig. 5.65 shows the slab sliding displacements in the presence of vertical acceleration. Comparing it with the correponding values in Fig. 5.62, which are for only horizontal excitation, it is observed that vertical acceleration did not change sliding displacements significantly. Fig. 5.66 shows that residual displacements are somewhat larger in the presence of vertical acceleration (compared to their values when only the horizontal component was applied, as can be seen in Fig. 5.63). However, they are still relatively smaller than the corresponding sliding displacement values in Fig. 5.65.

Tables 5.30 to 5.33 show tables similar to 5.28 and 5.29, but for Ground Motions 2 and 3. The significant observation for these cases is that the sliding displacements for these ground motions are relatively significantly smaller than the ones for Ground Motion 1. This is more evident when one compares the corresponding plots. Figs. 5.68 shows that the maximum sliding displacements when subjected to Ground Motion 2 are about 0.20 ft only, whereas these are about 1.25 ft for Ground Motio 1. This is probably due to the fact that Ground Motion 1 corresponds to a soft site and

is of longer duration. In Fig. 5.74, the maximum sliding displacements for Ground Motion 3 are about 0.60 Ft, about half that for Ground Motion 1.

Results in Figs. 5.70 to 5.72 and Figs. 5.76 to 5.78 are for the combined horizontal and vertical excitations due to Ground Motions 2 and 3, respectively. Comparing these results withthe corresponding results for the cases of only horizontal excitation, one can see that the effect of the vertical excitation on the sliding and residual displacement responses is not very significant. Some changes do occur in the frame deformation and floor acceleration responses when the vertical excitation is also applied, but these changes are easily predictable.

Tables 5.34 to 5.39 are similar to Tables 5.28 to 5.33. They correspond to the Structure 2, which is stiff. The most notable thing in these tables and corresponding figures (Figs. 5.79, 5.85, and 5.91) is that the normalized slab accelerations are almost equal to the value of frame reduction parameters (slope $\simeq$ = 1.0). Of course, in some cases, especially for higher values of frame reduction parameters in the neighborhood of 0.70 onwards, the normalized frame deformation and slab acceleration values are sometimes smaller than the frame reduction parameters due to reasons mentioned earlier. It is interesting to note that the slab sliding displacements for Structure 2 are not too different than the corresponding sliding displacements in case of Structure 1. However, for the case of Structure 2, the sliding displacements vary in a smooth monotonic fashion, whereas this was not always true for Structure 1. Comparing Figs. 5. 50 and 5.86, it is observed that the sliding displacements for Structure 2 are almost identical for the cases of equal acceleration reduction and equal deformation reduction. This is to be expected because, in case of Structure 2, the acceleration levels and hence the corresponding μ's are almost equal for both these methods. It is observed in Figs. 5.81, 5.87 and 5.93 that the residual displacements for Structure 2 are uniformaly varying and their magnitudes

are smaller than the corresponding sliding displacement values in Figs. 5.80, 5.86 and 5.92, respectively. Finally, for Strcture 2 also, the effect of vertical acceleration on the response quantities of interest is similar to its effect on Structure 1, described in earlier paragraphs.

Tables 5.40 to 5.45 and Figs. 5.97 to 5.114 are for Structure 3, which is a flexible structure. Here, it is observed that in this case, the choice of friction coefficient values to effect a desired reduction in frame deformation causes a relatively large reduction in the levels of floor acclerations. In particular, in Table 5.40, the normalized second floor accelerations are much smaller than the normalized floor accelerations at floor levels 1 and 3. In the first row of Table 5.40, it is seen that for frame deformation reduction parameter of 0.10, one obtains a normalized second floor accleration of 0.0112, meaning that a reduction in the frame deformations by a factor of 10 causes a corresponding reduction by a factor of approximately 90 in the second floor acceleration magnitude. Also, this only happens at the second floor and not at the first and third floors. This means that the friction coefficient for the sliding interface at the second floor level, calculated according to Eq. (5.28), is very small, in comparison to the friction coefficients at first and third floor sliding interfaces. It is also this reason that very large sliding displacements at this interface are encountered (Fig. 5.98, corresponding to Ground Motion 1). A similar effect is seen in Table 5.42 and Fig. 5.104, for the case of excitation due to Ground Motion 2. However, comparison of Fig. 5.104 with the corresponding Fig. 5.56 for the case of equal acceleration reduction reveals that such an effect is completely absent in Fig. 5.56, wherein the sliding displacements are distributed far more equitably at the three sliding interfaces. Also, comparison of Fig. 5.55 with Fig. 5.103 shows that the frame deformation reductions in Fig. 5.55 for the case of equal acceleration reduction are distributed rather uniformly across the three floors, whereas the same is not true in

Fig. 5.103 for the case of equal deformation reduction, where it is noted that the normalized acceleration of floor 2 is reduced drastically compared to the reduction for the other two floors. Fig. 5.109 for the response of Structure 3 to Ground Motion 3, however shows that such is not always the case. Herein, although the magnitudes of normalized floor accelerations at the three floor levels are not quite close to each other, they are not as significantly different as observed for Figs. 5.97 and 5.103. Comparison of Fig. 5.110 with Figs. 5.98 and 5.104 also shows that the sliding displacements at the three floor levels for Ground Motion 3 are more uniformly distributed than the displacements for Ground Motions 1 and 2. The residual displacements for Structure 3 (flexible) are smaller than their corresponding sliding displacement values, but not as much smaller as they were in the case of Structure 2 (a stiff structure). The effects of vertical acceleration on the response of Structure 3 is also seen to be similar to those for Structures 1 and 2.

5.4 *Concluding Remarks*

In this chapter, the seismic response of three three-story structures was studied for various sliding arrangements. Structure 1 is medium stiff, Structure 2 is stiff and Structure 3 is flexible. Response of these structures was obtained for three ground motion records, with and without the presence of vertical acceleration.

Comparison of base sliding and the proposed multi-sliding arrangement showed that for the same values of friction coefficient, the multi-sliding arrangement was more effective in reducing the frame deformations, slab accelerations and the resulting secondary floor spectra. Also, for the case of multi-sliding arrangement, it

was shown that the frame deformation response can be accurately estimated. Comparison of the sliding displacements showed that they are usually reasonable for most cases. Comparison of residual displacements showed that they are significantly smaller than the maximum sliding displacements values, for both base sliding and multi-sliding arrangements, except for the (flexible) Structure 3.

The study showed that base sliding arrangement is insensitive to the presence of vertical acceleration. For the multi-sliding case, there usually occurs a slight increase in the frame deformation and slab acceleration responses. This increase, however, be estimated fairly accurately. It was found that this increase in accelerations did not change the secondary floor spectra and the sliding displacement characteristics significantly. The effect of vertical acceleration on the residual displacements seems to be harder to characterize, since there was no pattern detected for this response quantity. However, it is mentioned that the residual displacements are affected in the presence of vertical acceleration and frequently, the change was seen to be noticeable.

As in the case of one-story sliding structures, here too, it was considered advantageous to use friction coefficent values normalized according to some useful criteria. For the case of multi-sliding multi-story structures, one can choose friction coefficients such that the maximum slab acceleration values of non-sliding case are reduced to a desired factor called as the acceleration reduction parameter (factor). The friction coefficient values can be selected by knowing the maximum floor accelerations of the non-sliding structure. It was found that the friction coefficients obtained in this manner insure that the normalized floor accelerations will at the most be equal to the value of the acceleration reduction parameter. For a predecided level of reduction in the accelerations, the corresponding reductions in the frame deformations were usually smaller. But the variation of frame deformation with

respect to the acceleration reduction parameter was found to be linear. For high frquency structures, it was found that the the acceleration reduction approach yields the same level of reduction in frame deformations.

One can also choose to limit the frame deformations to specified values, as defined by the deformation reduction parameter. For prescribed values of deformation reduction parameters, one can calculate the required values of friction coefficients from Eq. (5.28). It was observed that the friction coefficients obtained in this manner will ensure that the normalized frame deformations and floor accelerations are at the most equal to the value of the deformation reduction parameter. For flexible structures (Structure 3), and even for Structure 1, the normalized slab acceleration values for Structure 3 (soft structure) were sometimes smaller than the corresponding normalized deformation values. This meant that the required friction coefficients for achieving a desired state of deformation reduction were unevenly distributed across the different floor levels., causing different levels of actual reduction in response at different floor levels. In general, however, the magnitudes of sliding displacements and residual displacements were observed to be within a reasonable range.

This study was performed for three recorded ground motions. It was observed that the magnitudes of maximum sliding displacements and hence the corresponding residual displacements depend on the stiffness of the site on which the ground motion is recorded, probably because this influences the frequency constitution of the input. It was noticed that sliding displacements were generally a lot higher for the El Centro ground motion, which is one of the more intense earthquakes recorded on a soft site.

TABLE 5.1

NON-SLIDING RESPONSE OF STRUCTURE 1

$\omega_1 = 14.08$ Rad/Sec, $\beta_1 = 0.0200$

$\omega_2 = 30.70$ Rad/Sec, $\beta_2 = 0.0436$

$\omega_3 = 46.83$ Rad/Sec, $\beta_3 = 0.0665$

Ground Motion No.	First Floor Accln. (Ft/S*S)	Second Floor Accln. (Ft/S*S)	Third Floor Accln. (Ft/S*S)	Frame Def. @ First Floor (Ft)	Frame Def. @ Second Floor (Ft)	Frame Def. @ Third Floor (Ft)
1	30.859	56.883	89.877	0.1256D+00	0.2787D+00	0.4471D+00
2	31.973	52.864	70.356	0.1013D+00	0.2063D+00	0.3094D+00
3	18.989	30.043	42.024	0.6128D-01	0.1299D+00	0.2047D+00

TABLE 5.2

NON-SLIDING RESPONSE OF STRUCTURE 2

ω_1 = 56.32 Rad/Sec, β_1 = 0.0200

ω_2 = 122.80 Rad/Sec, β_2 = 0.0436

ω_3 = 187.30 Rad/Sec, β_3 = 0.0665

Ground Motion No.	First Floor Accln. (Ft/S*S)	Second Floor Accln. (Ft/S*S)	Third Floor Accln. (Ft/S*S)	Frame Def. @ First Floor (Ft)	Frame Def. @ Second Floor (Ft)	Frame Def. @ Third Floor (Ft)
1	20.079	29.291	40.600	0.4315D-02	0.8976D-02	0.1373D-01
2	25.051	33.797	43.043	0.5032D-02	0.1013D-01	0.1507D-01
3	18.050	21.203	26.567	0.3236D-02	0.6405D-02	0.9518D-02

TABLE 5.3

NON-SLIDING RESPONSE OF STRUCTURE 3

$\omega_1 = 3.52$ Rad/Sec, $\beta_1 = 0.0200$

$\omega_2 = 7.68$ Rad/Sec, $\beta_2 = 0.0436$

$\omega_3 = 11.71$ Rad/Sec, $\beta_3 = 0.0665$

Ground Motion No.	First Floor Accln. (Ft/S*S)	Second Floor Accln. (Ft/S*S)	Third Floor Accln. (Ft/S*S)	Frame Def. @ First Floor (Ft)	Frame Def. @ Second Floor (Ft)	Frame Def. @ Third Floor (Ft)
1	16.473	20.549	24.563	0.4649D+00	0.8434D+00	0.1508D+01
2	7.093	8.052	11.102	0.2049D+00	0.3553D+00	0.6534D+00
3	14.119	19.412	27.125	0.3376D+00	0.7769D+00	0.1406D+01

TABLE 5.4

SLIDING RESPONSE OF STRUCTURE 1 TO HORIZONTAL COMPONENT OF GROUND MOTION NO. 1

The Following Results Correspond to Base Sliding Arrangement with Mass Ratio = 1/3.

Friction Coeff.	Norm. First Floor Accln.	Norm. Second Floor Accln.	Norm. Third Floor Accln.	Norm. First Floor Def.	Norm. Second Floor Def.	Norm. Third Floor Def.	Sliding Disp. @ Base Level (Ft)
0.05	0.5571	0.2974	0.1708	0.0594	0.0605	0.0708	1.86704
0.10	0.6917	0.4810	0.2654	0.1214	0.1323	0.1313	0.73214
0.15	0.8935	0.6586	0.4445	0.1543	0.1737	0.2036	0.41298
0.20	1.0947	0.7596	0.5278	0.2263	0.2449	0.2614	0.37913
0.25	1.2419	0.9331	0.6131	0.2703	0.2771	0.3008	0.32036
0.30	1.2884	0.9289	0.7529	0.3139	0.3258	0.3685	0.30577
0.35	1.6009	1.0311	0.7670	0.3648	0.3833	0.4014	0.30177
0.40	1.7784	1.0937	0.8878	0.4325	0.4336	0.4660	0.33186
0.45	1.8889	1.2291	0.8754	0.4626	0.4736	0.4760	0.21448

TABLE 5.5

SLIDING RESPONSE OF STRUCTURE 1 TO HORZ. AND VERT. COMPONENTS OF GROUND MOTION NO. 1

The Following Results Correspond to Base Sliding Arrangement with Mass Ratio = 1/3.

Friction Coeff.	Norm. First Floor Accln.	Norm. Second Floor Accln.	Norm. Third Floor Accln.	Norm. First Floor Def.	Norm. Second Floor Def.	Norm. Third Floor Def.	Sliding Disp. @ Base Level (Ft)
0.05	0.5667	0.2999	0.1786	0.0604	0.0620	0.0711	1.88234
0.10	0.6874	0.4305	0.3298	0.1106	0.1260	0.1262	0.71205
0.15	0.9422	0.6478	0.4389	0.1565	0.1730	0.2021	0.44474
0.20	1.1478	0.7935	0.5376	0.2288	0.2476	0.2623	0.34701
0.25	1.3520	0.9225	0.6657	0.2760	0.2766	0.3093	0.37485
0.30	1.4084	0.9371	0.7603	0.3217	0.3294	0.3538	0.37348
0.35	1.5011	1.0409	0.8289	0.3753	0.3938	0.4416	0.34256
0.40	1.7541	1.1573	0.8765	0.4158	0.4282	0.4334	0.32925
0.45	1.8864	1.2118	1.0071	0.4801	0.4683	0.5055	0.28802

TABLE 5.6

SLIDING RESPONSE OF STRUCTURE 1 TO HORIZONTAL COMPONENT OF GROUND MOTION NO. 1

The Following Results Correspond to Base Sliding Arrangement with Mass Ratio = 1/3.

Friction Coeff.	Norm. First Floor Accln.	Norm. Second Floor Accln.	Norm. Third Floor Accln.	Norm. First Floor Def.	Norm. Second Floor Def.	Norm. Third Floor Def.	Sliding Disp. @ Base Level (Ft)
0.05	0.8144	0.6094	0.4340	0.0874	0.1002	0.1109	1.83302
0.10	0.8762	0.7091	0.5701	0.1809	0.2009	0.2143	0.77435
0.15	1.2641	0.9899	0.8745	0.2804	0.2867	0.3555	0.35068
0.20	1.4361	1.0669	0.9627	0.3617	0.3684	0.4358	0.19699
0.25	1.6494	1.2691	1.0039	0.4278	0.4428	0.4741	0.15589
0.30	1.7937	1.4825	1.3015	0.5268	0.5320	0.5832	0.08633
0.35	2.3405	1.6731	1.2683	0.5655	0.5849	0.6484	0.04821
0.40	2.2298	1.9088	1.3477	0.6516	0.6587	0.6836	0.02732
0.45	2.5409	2.0611	1.6543	0.7226	0.7304	0.8106	0.02101

TABLE 5.7

SLIDING RESPONSE OF STRUCTURE 2 TO HORZ. AND VERT. COMPONENTS OF GROUND MOTION NO. 1

The Following Results Correspond to Base Sliding Arrangement with Mass Ratio = 1/3.

Friction Coeff.	Norm. First Floor Accln.	Norm. Second Floor Accln.	Norm. Third Floor Accln.	Norm. First Floor Def.	Norm. Second Floor Def.	Norm. Third Floor Def.	Sliding Disp. @ Base Level (Ft)
0.05	0.8170	0.5861	0.4386	0.0888	0.1010	0.1133	1.85550
0.10	0.9607	0.7387	0.6032	0.2007	0.1920	0.2234	0.75686
0.15	1.3010	1.0244	0.8923	0.3101	0.3094	0.3682	0.35518
0.20	1.3751	1.2590	1.1117	0.4060	0.4055	0.4943	0.23548
0.25	1.7803	1.3384	1.1772	0.4912	0.5368	0.5834	0.18024
0.30	1.8013	1.5921	1.3253	0.5184	0.5735	0.6142	0.11945
0.35	2.2962	1.7219	1.2389	0.5863	0.5902	0.6360	0.04801
0.40	2.3634	2.0006	1.4949	0.6802	0.7120	0.7383	0.03701
0.45	2.5959	2.1113	1.6530	0.7622	0.7944	0.8170	0.02719

TABLE 5.8

SLIDING RESPONSE OF STRUCTURE 3 TO HORIZONTAL COMPONENT OF GROUND MOTION NO. 1

The Following Results Correspond to Base Sliding Arrangement with Mass Ratio = 1/3.

Friction Coeff.	Norm. First Floor Accln.	Norm. Second Floor Accln.	Norm. Third Floor Accln.	Norm. First Floor Def.	Norm. Second Floor Def.	Norm. Third Floor Def.	Sliding Disp. @ Base Level (Ft)
0.05	0.8491	0.6447	0.6402	0.2320	0.2813	0.2682	1.65709
0.10	1.2018	0.9916	0.8198	0.5579	0.5765	0.4746	0.96976
0.15	1.0822	1.3290	1.0177	0.5793	0.7338	0.6472	0.31641
0.20	1.6428	1.4443	1.6092	0.8186	0.9723	0.8572	0.46950
0.25	2.1535	1.7237	1.4374	0.9660	1.0046	0.8783	0.16587
0.30	2.1781	1.6102	1.0875	0.9955	1.0279	0.9983	0.18382
0.35	1.0000	1.0000	1.0000	1.0000	1.0000	1.0000	0.00000
0.40	1.0000	1.0000	1.0000	1.0000	1.0000	1.0000	0.00000
0.45	1.0000	1.0000	1.0000	1.0000	1.0000	1.0000	0.00000

TABLE 5.9

SLIDING RESPONSE OF STRUCTURE 3 TO HORZ. AND VERT. COMPONENTS OF GROUND MOTION NO. 1

The Following Results Correspond to Base Sliding Arrangement with Mass Ratio = 1/3.

Friction Coeff.	Norm. First Floor Accln.	Norm. Second Floor Accln.	Norm. Third Floor Accln.	Norm. First Floor Def.	Norm. Second Floor Def.	Norm. Third Floor Def.	Sliding Disp. @ Base Level (Ft)
0.05	0.8617	0.6534	0.6402	0.2272	0.2769	0.2634	1.69584
0.10	1.1176	0.9097	0.7773	0.3739	0.4340	0.3998	1.17538
0.15	1.0487	1.2846	1.0544	0.5532	0.7055	0.6490	0.27231
0.20	1.6771	1.3974	1.7072	0.8136	0.8991	0.9031	0.34142
0.25	1.9241	1.6395	1.7040	1.0127	1.0237	0.9442	0.22823
0.30	2.1122	1.5752	1.0584	0.9910	0.9716	0.9730	0.22219
0.35	1.0000	1.0000	1.0000	1.0000	1.0000	1.0000	0.00000
0.40	1.0000	1.0000	1.0000	1.0000	1.0000	1.0000	0.00000
0.45	1.0000	1.0000	1.0000	1.0000	1.0000	1.0000	0.00000

TABLE 5.10

SLIDING RESPONSE OF STRUCTURE 1 TO HORIZONTAL COMPONENT OF GROUND MOTION NO. 1

The Following Results Correspond to Provision of Sliding Interface at First Floor.

First Floor Accln. Ft/S*S	Second Floor Accln. Ft/S*S	Third Floor Accln. Ft/S*S	Norm. First Floor Def.	Norm. Second Floor Def.	Norm. Third Floor Def.	Sliding Disp. @ First Floor (Ft)
3.220	35.030	53.360	0.5205	0.5682	0.5750	1.08848
4.831	35.837	52.957	0.5082	0.5453	0.5612	0.56889
6.441	39.061	55.306	0.5474	0.5804	0.5754	0.47435
8.051	42.979	59.167	0.5976	0.6280	0.6082	0.25855
9.661	46.722	61.333	0.6428	0.6699	0.6435	0.27733
11.271	49.972	61.789	0.6865	0.7100	0.6800	0.35430
12.881	52.682	67.549	0.7307	0.7508	0.7268	0.36044
14.491	54.947	72.371	0.7747	0.7912	0.7601	0.27909
16.101	57.918	75.231	0.8203	0.8337	0.7980	0.18437
17.710	61.005	77.705	0.8619	0.8714	0.8585	0.12358
19.320	62.602	81.706	0.9108	0.9175	0.9114	0.07852
20.930	61.539	83.213	0.9563	0.9597	0.9446	0.04896
22.540	57.923	85.356	0.9779	0.9751	0.9633	0.02337
24.150	55.160	87.566	0.9921	0.9830	0.9787	0.01190
25.760	54.699	89.172	0.9932	0.9889	0.9899	0.00753

TABLE 5.11

SLIDING RESPONSE OF STRUCTURE 1 TO HORZ. AND VERT. COMPONENTS OF GROUND MOTION NO. 1

The Following Results Correspond to Provision of Sliding Interface at First Floor.

First Floor Accln. Ft/S*S	Second Floor Accln. Ft/S*S	Third Floor Accln. Ft/S*S	Norm. First Floor Def.	Norm. Second Floor Def.	Norm. Third Floor Def.	Sliding Disp. @ First Floor (Ft)
4.679	35.116	53.159	0.5205	0.5675	0.5740	0.99329
7.018	35.344	53.700	0.5004	0.5380	0.5599	0.61013
8.343	38.360	54.519	0.5436	0.5747	0.5699	0.51940
10.429	41.849	58.012	0.5955	0.6228	0.6048	0.29878
12.515	45.377	60.258	0.6416	0.6652	0.6414	0.31905
14.600	48.514	61.563	0.6865	0.7054	0.6829	0.37045
16.686	51.259	68.244	0.7325	0.7468	0.7298	0.34293
18.145	54.864	72.885	0.7794	0.7930	0.7622	0.27176
20.161	59.415	75.461	0.8271	0.8337	0.8040	0.18711
22.177	62.361	78.753	0.8727	0.8734	0.8651	0.12661
24.193	63.470	83.061	0.9215	0.9182	0.9175	0.08828
26.209	61.867	84.030	0.9640	0.9583	0.9483	0.06100
26.816	58.303	85.759	0.9860	0.9746	0.9658	0.03618
26.939	55.356	87.589	0.9941	0.9846	0.9803	0.01842
27.853	54.825	89.038	0.9952	0.9912	0.9909	0.00840

TABLE 5.12

SLIDING RESPONSE OF STRUCTURE 1 TO HORIZONTAL COMPONENT OF GROUND MOTION NO. 1

The Following Results Correspond to Provision of Sliding Interface at Second Floor.

First Floor Accln. Ft/S*S	Second Floor Accln. Ft/S*S	Third Floor Accln. Ft/S*S	Norm. First Floor Def.	Norm. Second Floor Def.	Norm. Third Floor Def.	Sliding Disp. @ Second Floor (Ft)
25.718	3.221	45.945	0.4058	0.3500	0.4103	1.18251
28.260	6.441	47.694	0.4536	0.3834	0.4359	0.83944
28.031	9.661	43.515	0.4454	0.3764	0.4131	0.88281
25.499	12.881	41.953	0.4692	0.3979	0.4140	0.56466
29.671	16.101	45.542	0.5686	0.4772	0.4857	0.44572
34.283	19.321	54.884	0.6449	0.5466	0.5635	0.44459
36.440	22.540	63.644	0.6943	0.6045	0.6354	0.35525
37.230	25.761	68.851	0.7116	0.6489	0.6881	0.24523
39.035	28.981	68.842	0.7703	0.6748	0.7039	0.18648
41.879	32.200	73.262	0.8464	0.7226	0.7518	0.14199
42.670	35.420	76.198	0.9052	0.7871	0.8062	0.08535
39.494	38.640	81.077	0.9308	0.8415	0.8620	0.03936
34.039	41.860	84.926	0.9368	0.8863	0.9058	0.04749
32.613	45.080	87.750	0.9603	0.9248	0.9424	0.04445
33.729	48.300	89.348	0.9836	0.9526	0.9675	0.02792

TABLE 5.13

SLIDING RESPONSE OF STRUCTURE 1 TO HORZ. AND VERT. COMPONENTS OF GROUND MOTION NO. 1

The Following Results Correspond to Provision of Sliding Interface at Second Floor.

First Floor Accln. Ft/S*S	Second Floor Accln. Ft/S*S	Third Floor Accln. Ft/S*S	Norm. First Floor Def.	Norm. Second Floor Def.	Norm. Third Floor Def.	Sliding Disp. @ Second Floor (Ft)
26.148	4.679	45.543	0.4067	0.3521	0.4099	1.19462
28.020	8.504	47.606	0.4556	0.3873	0.4372	0.85267
27.545	12.515	43.507	0.4474	0.3826	0.4160	0.95592
26.093	16.686	42.235	0.4738	0.4042	0.4197	0.69280
30.210	20.858	47.347	0.5788	0.4849	0.4964	0.53987
34.144	23.793	55.370	0.6415	0.5433	0.5608	0.45090
37.394	27.758	63.659	0.6909	0.5960	0.6249	0.34890
38.255	31.724	69.710	0.7225	0.6404	0.6788	0.24003
40.918	33.961	69.474	0.7865	0.6688	0.6984	0.20627
43.417	36.185	72.583	0.8606	0.7382	0.7530	0.18783
43.247	39.592	76.160	0.9137	0.8024	0.8185	0.13062
39.312	43.191	79.776	0.9346	0.8543	0.8658	0.05712
34.316	46.790	82.668	0.9431	0.8978	0.9045	0.02280
32.016	50.390	85.253	0.9608	0.9364	0.9394	0.03560
32.544	53.989	86.839	0.9837	0.9645	0.9642	0.02446

TABLE 5.14

SLIDING RESPONSE OF STRUCTURE 1 TO HORIZONTAL COMPONENT OF GROUND MOTION NO. 1

The Following Results Correspond to Provision of Sliding Interface at Third Floor.

First Floor Accln. Ft/S*S	Second Floor Accln. Ft/S*S	Third Floor Accln. Ft/S*S	Norm. First Floor Def.	Norm. Second Floor Def.	Norm. Third Floor Def.	Sliding Disp. @ Third Floor (Ft)
23.296	32.240	4.830	0.3932	0.3215	0.2206	1.01596
24.142	33.141	9.661	0.4424	0.3750	0.2743	0.99731
25.925	39.076	14.491	0.5440	0.4687	0.3530	0.59562
23.732	37.228	19.321	0.5333	0.4721	0.3753	0.53368
26.460	40.480	24.151	0.5561	0.4982	0.4119	0.42925
30.174	45.176	28.981	0.6147	0.5632	0.4727	0.31039
32.462	50.220	33.811	0.7168	0.6523	0.5484	0.23105
30.140	53.563	38.641	0.7663	0.7123	0.6061	0.19101
29.399	53.382	43.471	0.7792	0.7358	0.6410	0.14295
29.308	50.980	48.301	0.7889	0.7422	0.6653	0.12725
30.195	49.021	53.131	0.8269	0.7707	0.7033	0.11331
31.893	50.419	57.961	0.8540	0.8054	0.7452	0.08851
32.707	54.781	62.791	0.8740	0.8314	0.7816	0.06790
32.209	58.746	67.620	0.9164	0.8886	0.8375	0.07220
29.975	61.712	72.451	0.9531	0.9445	0.8927	0.06999

TABLE 5.15

SLIDING RESPONSE OF STRUCTURE 1 TO HORZ. AND VERT. COMPONENTS OF GROUND MOTION NO. 1

The Following Results Correspond to Provision of Sliding Interface at Third Floor.

First Floor Accln. Ft/S*S	Second Floor Accln. Ft/S*S	Third Floor Accln. Ft/S*S	Norm. First Floor Def.	Norm. Second Floor Def.	Norm. Third Floor Def.	Sliding Disp. @ Third Floor (Ft)
23.357	32.372	7.018	0.3929	0.3218	0.2214	1.00332
23.985	32.995	12.714	0.4466	0.3798	0.2853	0.95755
25.570	38.197	18.415	0.5473	0.4734	0.3662	0.68081
24.210	36.127	25.029	0.5332	0.4745	0.3901	0.58635
25.531	38.482	30.357	0.5506	0.4967	0.4288	0.46193
28.185	42.142	35.479	0.6039	0.5491	0.4743	0.32276
34.091	46.994	40.107	0.7078	0.6290	0.5307	0.26218
32.305	50.276	43.320	0.7424	0.6806	0.5826	0.20839
29.464	51.914	48.735	0.7612	0.7162	0.6244	0.18163
29.401	52.137	54.150	0.7801	0.7410	0.6595	0.17760
30.985	50.257	59.388	0.8014	0.7562	0.6918	0.15999
31.785	49.935	64.787	0.8354	0.7920	0.7423	0.13167
31.390	51.728	70.161	0.8608	0.8177	0.8018	0.09895
29.828	55.337	75.440	0.9015	0.8708	0.8571	0.07889
29.685	57.462	80.483	0.9405	0.9182	0.9074	0.05265

TABLE 5.16

SLIDING RESPONSE OF STRUCTURE 1 TO HORIZONTAL COMPONENT OF GROUND MOTION NO. 1

These Results are for Multi-Sliding Arrangement With Equal Friction Coefficient Approach.

First Floor Accln. Ft/S*S	Second Floor Accln. Ft/S*S	Third Floor Accln. Ft/S*S	Norm. First Floor Def.	Norm. Second Floor Def.	Norm. Third Floor Def.	Sliding Disp. @ First Floor (Ft)	Sliding Disp. @ Second Floor (Ft)	Sliding Disp. @ Third Floor (Ft)
1.610	1.611	1.610	0.0321	0.0271	0.0236	1.87312	1.93517	1.98257
3.220	3.220	3.220	0.0641	0.0542	0.0473	0.75593	0.80022	0.79339
4.830	4.830	4.830	0.0962	0.0812	0.0709	0.37426	0.53617	0.83143
6.440	6.440	6.440	0.1282	0.1083	0.0945	0.23185	0.39226	0.68025
8.050	8.050	8.050	0.1603	0.1354	0.1182	0.24692	0.31220	0.60417
9.661	9.660	9.660	0.1923	0.1625	0.1418	0.18698	0.36207	0.52494
11.270	11.270	11.270	0.2244	0.1895	0.1654	0.10915	0.46478	0.51564
12.880	12.880	12.880	0.2564	0.2166	0.1891	0.06883	0.38809	0.49904
14.490	14.490	14.490	0.2885	0.2437	0.2127	0.06954	0.25075	0.55663
16.100	16.100	16.101	0.3205	0.2708	0.2363	0.05376	0.17315	0.56956
17.710	17.710	17.710	0.3526	0.2978	0.2600	0.03574	0.13784	0.53266
19.320	19.321	19.321	0.3846	0.3249	0.2836	0.02233	0.11433	0.47572
20.930	20.930	20.931	0.4167	0.3520	0.3072	0.01382	0.10349	0.39923
22.540	22.540	22.541	0.4488	0.3791	0.3308	0.00873	0.09314	0.35299
24.150	24.151	24.151	0.4808	0.4061	0.3545	0.00716	0.08492	0.32905
25.760	25.760	25.760	0.5129	0.4332	0.3781	0.00408	0.07880	0.31266

TABLE 5.17

SLIDING RESPONSE OF STRUCTURE 1 TO HORZ. AND VERT. COMPONENTS OF GROUND MOTION NO. 1

These Results are for Multi-Sliding Arrangement With Equal Friction Coefficidnt Approach.

First Floor Accln. Ft/S*S	Second Floor Accln. Ft/S*S	Third Floor Accln. Ft/S*S	Norm. First Floor Def.	Norm. Second Floor Def.	Norm. Third Floor Def.	Sliding Disp. @ First Floor (Ft)	Sliding Disp. @ Second Floor (Ft)	Sliding Disp. @ Third Floor (Ft)
2.339	2.339	2.339	0.0463	0.0391	0.0341	1.89243	1.89392	2.03728
4.679	4.679	4.679	0.0926	0.0782	0.0683	0.70009	0.81165	0.81515
6.944	6.816	6.816	0.1327	0.1126	0.0984	0.36729	0.49635	0.75267
8.343	8.902	9.088	0.1552	0.1345	0.1215	0.23180	0.37349	0.64822
10.429	10.195	11.360	0.1940	0.1639	0.1431	0.17449	0.29036	0.58000
12.082	12.515	12.714	0.2329	0.1967	0.1717	0.16483	0.33655	0.50941
14.600	13.879	14.112	0.2717	0.2295	0.2003	0.10168	0.35761	0.52571
16.686	15.862	16.206	0.3105	0.2622	0.2289	0.08631	0.31430	0.53039
17.845	17.845	18.372	0.3493	0.2950	0.2575	0.05096	0.22282	0.56161
19.676	19.827	20.353	0.3857	0.3268	0.2855	0.03724	0.16431	0.57083
21.165	21.810	22.943	0.4163	0.3541	0.3102	0.02806	0.13786	0.53805
22.383	23.764	25.029	0.4413	0.3769	0.3319	0.02183	0.11062	0.48088
23.197	25.548	27.115	0.4614	0.3991	0.3540	0.01817	0.09044	0.42499
23.166	27.291	29.201	0.4775	0.4233	0.3771	0.01344	0.08472	0.35524
24.213	28.992	30.357	0.4971	0.4476	0.4002	0.01062	0.08179	0.31266
25.699	30.652	31.392	0.5192	0.4710	0.4228	0.00692	0.07959	0.28296

TABLE 5.18

SLIDING RESPONSE OF STRUCTURE 2 TO HORIZONTAL COMPONENT OF GROUND MOTION NO. 1

These Results are for Multi-Sliding Arrangement With Equal Friction Coefficient Approach.

First Floor Accln. Ft/S*S	Second Floor Accln. Ft/S*S	Third Floor Accln. Ft/S*S	Norm. First Floor Def.	Norm. Second Floor Def.	Norm. Third Floor Def.	Sliding Disp. @ First Floor (Ft)	Sliding Disp. @ Second Floor (Ft)	Sliding Disp. @ Third Floor (Ft)
1.611	1.611	1.611	0.0583	0.0525	0.0481	1.81742	1.83113	1.83607
3.221	3.221	3.221	0.1166	0.1051	0.0962	0.78579	0.77455	0.83186
4.832	4.831	4.831	0.1749	0.1576	0.1443	0.37686	0.37146	0.38713
6.441	6.442	6.441	0.2332	0.2102	0.1924	0.22998	0.23105	0.32536
8.051	8.052	8.051	0.2915	0.2627	0.2405	0.13228	0.17036	0.21089
9.661	9.662	9.661	0.3498	0.3153	0.2886	0.06773	0.08373	0.09731
11.271	11.271	11.271	0.4081	0.3678	0.3367	0.03006	0.04931	0.06808
12.881	12.881	12.881	0.4664	0.4204	0.3848	0.00962	0.02193	0.04228
14.491	14.491	14.492	0.5247	0.4729	0.4329	0.00256	0.01024	0.02685
16.101	16.101	16.101	0.5830	0.5255	0.4810	0.00104	0.00571	0.01869
17.711	17.711	17.711	0.6413	0.5780	0.5291	0.00053	0.00333	0.01255
19.320	19.321	19.321	0.6996	0.6306	0.5772	0.00018	0.00204	0.00895

TABLE 5.19

SLIDING RESPONSE OF STRUCTURE 2 TO HORZ. AND VERT. COMPONENTS OF GROUND MOTION NO. 1

These Results are for Multi-Sliding Arrangement With Equal Friction Coefficient Approach.

First Floor Accln. Ft/S*S	Second Floor Accln. Ft/S*S	Third Floor Accln. Ft/S*S	Norm. First Floor Def.	Norm. Second Floor Def.	Norm. Third Floor Def.	Sliding Disp. @ First Floor (Ft)	Sliding Disp. @ Second Floor (Ft)	Sliding Disp. @ Third Floor (Ft)
2.339	2.339	2.339	0.0846	0.0762	0.0698	1.83419	1.84395	1.84140
4.679	4.679	4.679	0.1678	0.1502	0.1369	0.66697	0.68955	0.69435
6.891	6.872	7.018	0.2491	0.2244	0.2057	0.35756	0.35999	0.37783
9.248	9.051	9.358	0.3261	0.2933	0.2702	0.23447	0.22792	0.29883
10.502	10.429	10.429	0.3764	0.3393	0.3106	0.16155	0.19981	0.23077
11.896	12.503	12.515	0.4290	0.3944	0.3644	0.09415	0.11231	0.13150
13.879	13.879	13.879	0.5005	0.4511	0.4129	0.04394	0.06047	0.07884
15.862	15.862	15.862	0.5720	0.5155	0.4719	0.01614	0.03021	0.05284
16.533	17.845	17.845	0.6192	0.5681	0.5232	0.00617	0.01399	0.02897
17.508	18.353	19.797	0.6320	0.5698	0.5286	0.00277	0.00806	0.01921
19.210	20.188	20.276	0.6937	0.6256	0.5728	0.00155	0.00499	0.01271
20.780	21.534	22.060	0.7515	0.6778	0.6209	0.00072	0.00449	0.00965

TABLE 5.20

SLIDING RESPONSE OF STRUCTURE 3 TO HORIZONTAL COMPONENT OF GROUND MOTION NO. 1

These Results are for Multi-Sliding Arrangement With Equal Friction Coefficient Approach.

First Floor Accln. Ft/S*S	Second Floor Accln. Ft/S*S	Third Floor Accln. Ft/S*S	Norm. First Floor Def.	Norm. Second Floor Def.	Norm. Third Floor Def.	Sliding Disp. @ First Floor (Ft)	Sliding Disp. @ Second Floor (Ft)	Sliding Disp. @ Third Floor (Ft)
1.610	1.610	1.610	0.1385	0.1432	0.1121	1.86809	2.15966	2.77690
3.220	3.220	3.220	0.2770	0.2863	0.2242	1.63467	2.63892	2.52219
4.830	4.830	4.830	0.4155	0.4295	0.3363	0.59825	1.28287	2.00472
6.440	6.440	6.440	0.5541	0.5727	0.4484	0.25722	0.83508	0.82368
8.050	8.050	8.050	0.6926	0.7159	0.5605	0.10149	0.22347	2.01313
9.660	9.660	9.660	0.8074	0.8460	0.6653	0.05322	0.24570	2.70516
11.270	11.270	11.270	0.7879	0.8544	0.7020	0.03190	0.07132	2.15438
12.880	12.880	12.880	0.8392	0.9319	0.7774	0.01082	0.05115	1.46961
13.230	14.490	14.490	0.8319	0.9515	0.8204	0.00000	0.05385	1.06905
13.230	16.100	16.100	0.8617	0 9354	0.8434	0.00000	0.04637	0.74977

TABLE 5.21

SLIDING RESPONSE OF STRUCTURE 3 TO HORZ. AND VERT. COMPONENTS OF GROUND MOTION NO. 1

These Results are for Multi-Sliding Arrangement With Equal Friction Coefficient Approach.

First Floor Accln. Ft/S*S	Second Floor Accln. Ft/S*S	Third Floor Accln. Ft/S*S	Norm. First Floor Def.	Norm. Second Floor Def.	Norm. Third Floor Def.	Sliding Disp. @ First Floor (Ft)	Sliding Disp. @ Second Floor (Ft)	Sliding Disp. @ Third Floor (Ft)
2.339	2.339	2.339	0.1945	0.2010	0.1574	1.93844	2.28564	2.78648
4.679	4.679	4.679	0.3873	0.3997	0.3119	1.48696	2.31714	2.27335
5.948	5.641	7.018	0.4648	0.4778	0.3894	0.73773	1.30583	1.98152
7.931	7.353	8.348	0.5892	0.5986	0.4753	0.35297	0.80009	0.96767
9.687	9.192	9.487	0.6930	0.7233	0.5694	0.15168	0.41069	1.98322
10.858	11.030	11.384	0.7952	0.8421	0.6684	0.06609	0.10273	2.57569
12.112	12.815	13.281	0.7775	0.8444	0.6964	0.04750	0.06768	2.25150
12.995	14.419	15.178	0.8353	0.9227	0.7727	0.01673	0.06581	1.48279
13.226	16.268	16.815	0.8305	0.9410	0.8166	0.00329	0.07026	1.13725
13.230	17.577	18.323	0.8404	0.9346	0.8470	0.00000	0.06102	0.90212

TABLE 5.22

SLIDING RESPONSE OF STRUCTURE 1 TO HORIZONTAL COMPONENT OF GROUND MOTION NO. 2

These Results are for Multi-Sliding Arrangement With Equal Acceleration Reduction Method.

Norm. First Floor Def.	Norm. Second Floor Def.	Norm. Third Floor Def.	Norm. First Floor Accln.	Norm. Second Floor Accln.	Norm. Third Floor Accln.	Sliding Disp. @ First Floor (Ft)	Sliding Disp. @ Second Floor (Ft)	Sliding Disp. @ Third Floor (Ft)
0.1197	0.1228	0.1245	0.1000	0.1000	0.1000	0.13054	0.06928	0.10498
0.1796	0.1842	0.1868	0.1500	0.1500	0.1500	0.06486	0.05940	0.12009
0.2395	0.2456	0.2490	0.2000	0.2000	0.2000	0.03515	0.04759	0.11698
0.2994	0.3070	0.3113	0.2500	0.2500	0.2500	0.02488	0.02867	0.11975
0.3592	0.3684	0.3736	0.3000	0.3000	0.3000	0.01666	0.01555	0.13614
0.4191	0.4298	0.4358	0.3500	0.3500	0.3500	0.01503	0.02126	0.15473
0.4790	0.4912	0.4981	0.4000	0.4000	0.4000	0.00963	0.01747	0.15217
0.5387	0.5525	0.5603	0.4500	0.4500	0.4500	0.00549	0.02065	0.14738
0.5805	0.6050	0.6166	0.5000	0.5000	0.5000	0.00477	0.02375	0.13201
0.6440	0.6682	0.6801	0.5500	0.5500	0.5500	0.00192	0.02158	0.11545
0.7166	0.7358	0.7465	0.5964	0.6000	0.6000	0.00000	0.01536	0.09674
0.7780	0.7980	0.8093	0.6500	0.6500	0.6500	0.00043	0.01298	0.08133
0.8318	0.8546	0.8674	0.7000	0.7000	0.7000	0.00001	0.01003	0.07163
0.8641	0.8855	0.8910	0.7500	0.7500	0.7500	0.00096	0.00943	0.05327
0.8945	0.9134	0.9107	0.8000	0.8000	0.8000	0.00168	0.00846	0.03736

TABLE 5.23

SLIDING RESPONSE OF STRUCTURE 1 TO HORZ. AND VERT. COMPONENTS OF GROUND MOTION NO. 2

These Results are for Multi-Sliding Arrangement With Equal Acceleration Reduction Method.

Norm. First Floor Def.	Norm. Second Floor Def.	Norm. Third Floor Def.	Norm. First Floor Accln.	Norm. Second Floor Accln.	Norm. Third Floor Accln.	Sliding Disp. @ First Floor (Ft)	Sliding Disp. @ Second Floor (Ft)	Sliding Disp. @ Third Floor (Ft)
0.1350	0.1384	0.1403	0.1129	0.1128	0.1128	0.14523	0.07844	0.12591
0.2024	0.2076	0.2105	0.1694	0.1692	0.1692	0.06181	0.05927	0.13652
0.2699	0.2768	0.2807	0.2259	0.2256	0.2256	0.04455	0.04457	0.13523
0.3367	0.3453	0.3501	0.2820	0.2815	0.2820	0.03380	0.03326	0.14418
0.4040	0.4143	0.4202	0.3384	0.3378	0.3384	0.01528	0.02962	0.16093
0.4706	0.4828	0.4898	0.3935	0.3948	0.3948	0.01140	0.02743	0.17686
0.5244	0.5449	0.5548	0.4239	0.4512	0.4512	0.00638	0.02540	0.17426
0.5510	0.5939	0.6116	0.4640	0.5076	0.5076	0.00658	0.01129	0.16165
0.5894	0.6492	0.6727	0.5086	0.5628	0.5640	0.00539	0.00676	0.14433
0.6576	0.7143	0.7401	0.5594	0.6176	0.6204	0.00350	0.00596	0.12728
0.7290	0.7776	0.8062	0.5825	0.6601	0.6767	0.00000	0.00298	0.12509
0.7831	0.8254	0.8444	0.5785	0.7182	0.7015	0.00000	0.00155	0.10079
0.8298	0.8655	0.8703	0.6341	0.7746	0.7191	0.00000	0.00202	0.07911
0.8703	0.8999	0.8927	0.6999	0.8280	0.7571	0.00000	0.00186	0.06086
0.9052	0.9289	0.9123	0.7661	0.8799	0.8013	0.00000	0.00119	0.04536

TABLE 5.24

SLIDING RESPONSE OF STRUCTURE 2 TO HORIZONTAL COMPONENT OF GROUND MOTION NO. 2

These Results are for Multi-Sliding Arrangement With Equal Acceleration Reduction Method.

Norm. First Floor Def.	Norm. Second Floor Def.	Norm. Third Floor Def.	Norm. First Floor Accln.	Norm. Second Floor Accln.	Norm. Third Floor Accln.	Sliding Disp. @ First Floor (Ft)	Sliding Disp. @ Second Floor (Ft)	Sliding Disp. @ Third Floor (Ft)
0.1008	0.1010	0.1014	0.1000	0.1000	0.1000	0.18079	0.15235	0.12364
0.1512	0.1515	0.1521	0.1501	0.1500	0.1500	0.13785	0.10809	0.09071
0.2016	0.2020	0.2028	0.2000	0.2000	0.2000	0.12200	0.09224	0.07413
0.2018	0.2020	0.2028	0.2500	0.2500	0.2500	0.09716	0.07358	0.05603
0.3024	0.3030	0.3042	0.3001	0.3000	0.3000	0.07367	0.05140	0.03785
0.3528	0.3535	0.3549	0.3500	0.3500	0.3500	0.05457	0.04188	0.03420
0.4032	0.4039	0.4056	0.4001	0.4000	0.4000	0.04256	0.03703	0.03344
0.4536	0.4544	0.4563	0.4500	0.4500	0.4500	0.03265	0.03130	0.03188
0.5040	0.5049	0.5070	0.5000	0.5000	0.5000	0.02371	0.02313	0.02455
0.5544	0.5554	0.5577	0.5500	0.5500	0.5500	0.01674	0.01675	0.01816
0.6048	0.6059	0.6084	0.6000	0.6000	0.6000	0.01152	0.01197	0.01326
0.6552	0.6564	0.6591	0.6500	0.6500	0.6500	0.00764	0.00831	0.00907
0.7056	0.7069	0.7099	0.7000	0.7000	0.7000	0.00476	0.00539	0.00524
0.7560	0.7574	0.7606	0.7500	0.7500	0.7500	0.00289	0.00321	0.00237
0.8064	0.8079	0.8113	0.8000	0.8000	0.8000	0.00151	0.00132	0.00253

TABLE 5.25

SLIDING RESPONSE OF STRUCTURE 2 TO HORZ. AND VERT. COMPONENTS OF GROUND MOTION NO. 2

These Results are for Multi-Sliding Arrangement With Equal Acceleration Reduction Method.

Norm. First Floor Def.	Norm. Second Floor Def.	Norm. Third Floor Def.	Norm. First Floor Accln.	Norm. Second Floor Accln.	Norm. Third Floor Accln.	Sliding Disp. @ First Floor (Ft)	Sliding Disp. @ Second Floor (Ft)	Sliding Disp. @ Third Floor (Ft)
0.1428	0.1439	0.1443	0.1129	0.1129	0.1129	0.17040	0.14801	0.12004
0.1707	0.1710	0.1718	0.1694	0.1694	0.1694	0.13201	0.10196	0.08482
0.2277	0.2281	0.2290	0.2259	0.2259	0.2259	0.11658	0.08483	0.06842
0.2846	0.2851	0.2863	0.2823	0.2823	0.2823	0.09273	0.06115	0.04837
0.3415	0.3421	0.3435	0.3388	0.3388	0.3388	0.06851	0.04564	0.03320
0.3984	0.3991	0.4008	0.3953	0.3953	0.3953	0.04966	0.03651	0.02747
0.4553	0.4561	0.4580	0.4518	0.4518	0.4518	0.03781	0.03178	0.02749
0.5122	0.5131	0.5153	0.5082	0.5082	0.5082	0.02843	0.02670	0.02654
0.5691	0.5702	0.5725	0.5647	0.5647	0.5647	0.02043	0.01966	0.02013
0.6260	0.6272	0.6298	0.6212	0.6212	0.6212	0.01421	0.01470	0.01448
0.6813	0.6830	0.6860	0.6772	0.6776	0.6776	0.00900	0.00876	0.00830
0.6990	0.7188	0.7283	0.6889	0.7341	0.7341	0.00571	0.00535	0.00431
0.7467	0.7499	0.7664	0.7419	0.7789	0.7905	0.00344	0.00295	0.00365
0.7980	0.7994	0.8027	0.7948	0.7948	0.8406	0.00192	0.00150	0.00408
0.8497	0.8512	0.8547	0.8478	0.8465	0.8850	0.00108	0.00081	0.00391

TABLE 5.26

SLIDING RESPONSE OF STRUCTURE 3 TO HORIZONTAL COMPONENT OF GROUND MOTION NO. 2

These Results are for Multi-Sliding Arrangement With Equal Acceleration Reduction Method.

Norm. First Floor Def.	Norm. Second Floor Def.	Norm. Third Floor Def.	Norm. First Floor Accln.	Norm. Second Floor Accln.	Norm. Third Floor Accln.	Sliding Disp. @ First Floor (Ft)	Sliding Disp. @ Second Floor (Ft)	Sliding Disp. @ Third Floor (Ft)
0.1643	0.1869	0.1526	0.1000	0.1000	0.1000	0.18936	0.18579	0.13858
0.2464	0.2804	0.2289	0.1500	0.1500	0.1500	0.13739	0.23533	0.11233
0.3285	0.3739	0.3052	0.2000	0.2000	0.2000	0.17267	0.17558	0.10977
0.4101	0.4667	0.3809	0.2500	0.2500	0.2500	0.15322	0.12694	0.09512
0.4535	0.5321	0.4403	0.3000	0.3000	0.3000	0.12128	0.10354	0.13398
0.4969	0.5919	0.4968	0.3500	0.3500	0.3500	0.08439	0.11518	0.16760
0.5518	0.6589	0.5578	0.4000	0.4000	0.4000	0.07072	0.12231	0.21911
0.6089	0.7300	0.6215	0.4500	0.4500	0.4500	0.06773	0.11141	0.26350
0.6491	0.7903	0.6792	0.5000	0.5000	0.5000	0.06416	0.09304	0.28738
0.6719	0.8376	0.7302	0.5500	0.5500	0.5500	0.05941	0.06760	0.28954
0.7008	0.8891	0.7849	0.6000	0.6000	0.6000	0.05007	0.04491	0.25353
0.7470	0.9272	0.8326	0.6500	0.6500	0.6500	0.04051	0.02349	0.22134
0.7943	0.9523	0.8695	0.7000	0.7000	0.7000	0.03180	0.01295	0.19198
0.8405	0.9713	0.9027	0.7500	0.7500	0.7500	0.02354	0.01051	0.16091
0.8856	0.9815	0.9315	0.8000	0.8000	0.8000	0.01648	0.01012	0.12478

TABLE 5.27

SLIDING RESPONSE OF STRUCTURE 3 TO HORZ. AND VERT. COMPONENTS OF GROUND MOTION NO. 2

These Results are for Multi-Sliding Arrangement With Equal Acceleration Reduction Method.

Norm. First Floor Def.	Norm. Second Floor Def.	Norm. Third Floor Def.	Norm. First Floor Accln.	Norm. Second Floor Accln.	Norm. Third Floor Accln.	Sliding Disp. @ First Floor (Ft)	Sliding Disp. @ Second Floor (Ft)	Sliding Disp. @ Third Floor (Ft)
0.1708	0.1944	0.1587	0.1128	0.1120	0.1090	0.19292	0.17512	0.12102
0.2563	0.2916	0.2381	0.1692	0.1674	0.1589	0.13914	0.23828	0.11770
0.3405	0.3874	0.3159	0.2256	0.2195	0.2119	0.15869	0.18558	0.10451
0.4116	0.4689	0.3853	0.2820	0.2734	0.2648	0.14645	0.13761	0.09985
0.4547	0.5338	0.4422	0.3384	0.3281	0.3178	0.10846	0.11290	0.13535
0.4969	0.5923	0.4986	0.3948	0.3828	0.3708	0.06969	0.12474	0.14567
0.5486	0.6576	0.5594	0.4512	0.4374	0.4237	0.05608	0.13004	0.19222
0.6156	0.7389	0.6292	0.5076	0.4921	0.4759	0.05160	0.13774	0.23369
0.6473	0.7910	0.6833	0.5640	0.5468	0.5221	0.04904	0.10998	0.26959
0.6700	0.8395	0.7352	0.6204	0.6015	0.5721	0.04791	0.08932	0.27610
0.7059	0.8946	0.7936	0.6761	0.6562	0.6241	0.04195	0.06216	0.24862
0.7524	0.9326	0.8410	0.7309	0.7108	0.6761	0.03692	0.03799	0.21655
0.8014	0.9571	0.8778	0.7782	0.7655	0.7281	0.02743	0.01876	0.18561
0.8493	0.9752	0.9113	0.7976	0.8202	0.7801	0.01928	0.01205	0.15267
0.8958	0.9835	0.9399	0.8484	0.8749	0.8322	0.01400	0.00527	0.11440

TABLE 5.28

SLIDING RESPONSE OF STRUCTURE 1 TO HORIZONTAL COMPONENT OF GROUND MOTION NO. 1

These Results are for Multi-Sliding Arrangement With Equal Deformation Reduction Method.

Norm. First Floor Def.	Norm. Second Floor Def.	Norm. Third Floor Def.	Norm. First Floor Accln.	Norm. Second Floor Accln.	Norm. Third Floor Accln.	Sliding Disp. @ First Floor (Ft)	Sliding Disp. @ Second Floor (Ft)	Sliding Disp. @ Third Floor (Ft)
0.1000	0.1000	0.1000	0.0730	0.0970	0.0999	1.24793	0.40289	0.49658
0.1500	0.1500	0.1500	0.1095	0.1455	0.1499	0.83618	0.32372	0.33410
0.2000	0.2000	0.2000	0.1460	0.1940	0.1998	0.60725	0.31660	0.33460
0.2500	0.2500	0.2500	0.1825	0.2426	0.2498	0.39394	0.27620	0.28149
0.3000	0.3000	0.3000	0.2190	0.2911	0.2997	0.34530	0.21785	0.22017
0.3500	0.3500	0.3500	0.2555	0.3396	0.3497	0.26449	0.17773	0.17357
0.4000	0.4000	0.4000	0.2920	0.3881	0.3996	0.27899	0.16540	0.16950
0.4500	0.4500	0.4500	0.3285	0.4366	0.4496	0.33000	0.16488	0.17321
0.5000	0.5000	0.5000	0.3649	0.4851	0.4995	0.37095	0.17552	0.14439
0.5500	0.5500	0.5500	0.4014	0.5336	0.5495	0.37252	0.16405	0.12234
0.6000	0.6000	0.6000	0.4379	0.5821	0.5994	0.33091	0.13232	0.09486
0.6500	0.6500	0.6500	0.4744	0.6306	0.6494	0.27712	0.09507	0.07164
0.7000	0.7000	0.7000	0.5109	0.6791	0.6993	0.20943	0.05293	0.05227
0.7500	0.7500	0.7500	0.5474	0.7276	0.7493	0.15205	0.01558	0.03794
0.8000	0.8000	0.8000	0.5839	0.7762	0.7992	0.11111	0.03033	0.02743

TABLE 5.29

SLIDING RESPONSE OF STRUCTURE 1 TO HORZ. AND VERT. COMPONENTS OF GROUND MOTION NO. 1

These Results are for Multi-Sliding Arrangement With Equal Deformation Reduction Method.

Norm. First Floor Def.	Norm. Second Floor Def.	Norm. Third Floor Def.	Norm. First Floor Accln.	Norm. Second Floor Accln.	Norm. Third Floor Accln.	Sliding Disp. @ First Floor (Ft)	Sliding Disp. @ Second Floor (Ft)	Sliding Disp. @ Third Floor (Ft)
0.1295	0.1283	0.1258	0.1060	0.1369	0.1270	1.26027	0.40140	0.49437
0.1816	0.1816	0.1816	0.1591	0.1792	0.1845	0.74475	0.30409	0.31682
0.2421	0.2421	0.2421	0.2121	0.2514	0.2461	0.52866	0.29655	0.26363
0.3006	0.3003	0.2994	0.2333	0.2987	0.3041	0.37302	0.26474	0.26407
0.3560	0.3556	0.3541	0.2837	0.3584	0.3581	0.31974	0.16002	0.18341
0.4057	0.4049	0.4023	0.3309	0.4159	0.4063	0.30264	0.14676	0.13917
0.4492	0.4475	0.4454	0.3782	0.4551	0.4465	0.33138	0.12970	0.13079
0.4991	0.4991	0.4991	0.4255	0.4941	0.5011	0.35199	0.15617	0.13417
0.5532	0.5531	0.5532	0.4728	0.5383	0.5551	0.37415	0.15229	0.13111
0.6043	0.6040	0.6053	0.5200	0.5842	0.6091	0.35761	0.14992	0.13021
0.6532	0.6517	0.6547	0.5673	0.6218	0.6601	0.31412	0.12843	0.09742
0.6978	0.6949	0.6984	0.5941	0.6778	0.7047	0.27477	0.09642	0.07053
0.7410	0.7365	0.7369	0.6397	0.7353	0.7376	0.21761	0.06385	0.04933
0.7847	0.7785	0.7757	0.6854	0.7891	0.7717	0.16249	0.02827	0.02959
0.8283	0.8211	0.8175	0.7311	0.8417	0.8130	0.12411	0.02887	0.01310

TABLE 5.30

SLIDING RESPONSE OF STRUCTURE 1 TO HORIZONTAL COMPONENT OF GROUND MOTION NO. 2

These Results are for Multi-Sliding Arrangement With Equal Deformation Reduction Method.

Norm. First Floor Def.	Norm. Second Floor Def.	Norm. Third Floor Def.	Norm. First Floor Accln.	Norm. Second Floor Accln.	Norm. Third Floor Accln.	Sliding Disp. @ First Floor (Ft)	Sliding Disp. @ Second Floor (Ft)	Sliding Disp. @ Third Floor (Ft)
0.1000	0.1000	0.1000	0.0940	0.0809	0.0781	0.18271	0.15883	0.16925
0.1500	0.1500	0.1500	0.1411	0.1214	0.1172	0.08033	0.06614	0.13279
0.2000	0.2000	0.2000	0.1881	0.1618	0.1563	0.05155	0.05936	0.12801
0.2500	0.2500	0.2500	0.2351	0.2023	0.1954	0.03765	0.04378	0.12227
0.3000	0.3000	0.3000	0.2821	0.2428	0.2344	0.02372	0.02679	0.12809
0.3500	0.3500	0.3500	0.3291	0.2832	0.2735	0.01483	0.01781	0.13765
0.4000	0.4000	0.4000	0.3761	0.3237	0.3126	0.00850	0.01672	0.16376
0.4500	0.4500	0.4500	0.4231	0.3641	0.3516	0.00344	0.01877	0.16821
0.4891	0.4946	0.4964	0.4701	0.4046	0.3907	0.00192	0.01734	0.16667
0.5272	0.5327	0.5345	0.5172	0.4450	0.4298	0.00176	0.01206	0.16616
0.5582	0.5663	0.5775	0.5642	0.4855	0.4689	0.00056	0.01513	0.15505
0.5838	0.6152	0.6268	0.6015	0.5260	0.5079	0.00000	0.01616	0.14224
0.6381	0.6696	0.6797	0.5925	0.5664	0.5470	0.00000	0.01522	0.12380
0.6993	0.7251	0.7334	0.5675	0.6069	0.5861	0.00000	0.01232	0.10482
0.7568	0.7788	0.7859	0.6227	0.6473	0.6251	0.00000	0.01005	0.09170

TABLE 5.31

SLIDING RESPONSE OF STRUCTURE 1 TO HORZ. AND VERT. COMPONENTS OF GROUND MOTION NO. 2

These Results are for Multi-Sliding Arrangement With Equal Deformation Reduction Method.

Norm. First Floor Def.	Norm. Second Floor Def.	Norm. Third Floor Def.	Norm. First Floor Accln.	Norm. Second Floor Accln.	Norm. Third Floor Accln.	Sliding Disp. @ First Floor (Ft)	Sliding Disp. @ Second Floor (Ft)	Sliding Disp. @ Third Floor (Ft)
0.1127	0.1127	0.1127	0.1062	0.0913	0.0883	0.19020	0.19021	0.18563
0.1690	0.1690	0.1690	0.1593	0.1369	0.1322	0.07625	0.07374	0.15158
0.2254	0.2254	0.2254	0.2124	0.1825	0.1763	0.04687	0.06120	0.14325
0.2817	0.2817	0.2817	0.2655	0.2282	0.2203	0.03403	0.04746	0.14144
0.3372	0.3372	0.3373	0.3182	0.2731	0.2644	0.02180	0.03727	0.15164
0.3929	0.3929	0.3931	0.3699	0.3194	0.3085	0.01370	0.03627	0.16165
0.4373	0.4428	0.4448	0.3987	0.3651	0.3525	0.00632	0.03257	0.18705
0.4660	0.4855	0.4917	0.4484	0.4107	0.3966	0.00646	0.02561	0.18607
0.4914	0.5264	0.5380	0.4627	0.4563	0.4407	0.00492	0.02579	0.18422
0.5151	0.5653	0.5828	0.4855	0.5020	0.4847	0.00372	0.01577	0.17845
0.5470	0.6081	0.6303	0.5296	0.5457	0.5288	0.00245	0.00590	0.16544
0.6024	0.6547	0.6802	0.5722	0.5890	0.5729	0.00140	0.00413	0.15008
0.6569	0.7052	0.7326	0.6129	0.6261	0.6170	0.00040	0.00243	0.13128
0.7114	0.7615	0.7888	0.5740	0.6609	0.6610	0.00000	0.00203	0.12933
0.7602	0.8049	0.8310	0.5747	0.7081	0.7002	0.00000	0.00042	0.11406

TABLE 5.32

SLIDING RESPONSE OF STRUCTURE 1 TO HORIZONTAL COMPONENT OF GROUND MOTION NO. 3

These Results are for Multi-Sliding Arrangement With Equal Deformation Reduction Method.

Norm. First Floor Def.	Norm. Second Floor Def.	Norm. Third Floor Def.	Norm. First Floor Accln.	Norm. Second Floor Accln.	Norm. Third Floor Accln.	Sliding Disp. @ First Floor (Ft)	Sliding Disp. @ Second Floor (Ft)	Sliding Disp. @ Third Floor (Ft)
0.1000	0.1000	0.1000	0.0784	0.0833	0.0949	0.54808	0.49480	0.52173
0.1500	0.1500	0.1500	0.1177	0.1249	0.1423	0.42589	0.50987	0.35148
0.2000	0.2000	0.2000	0.1569	0.1666	0.1898	0.51404	0.41430	0.46914
0.2500	0.2500	0.2500	0.1961	0.2082	0.2372	0.50600	0.30339	0.30704
0.3000	0.3000	0.3000	0.2353	0.2499	0.2846	0.44946	0.37688	0.22882
0.3500	0.3500	0.3500	0.2745	0.2915	0.3321	0.40487	0.42266	0.19052
0.4000	0.4000	0.4000	0.3137	0.3331	0.3795	0.31190	0.34650	0.11680
0.4500	0.4500	0.4500	0.3529	0.3748	0.4270	0.42323	0.27035	0.06644
0.5000	0.5000	0.5000	0.3921	0.4164	0.4744	0.44847	0.21307	0.07101
0.5500	0.5500	0.5500	0.4313	0.4581	0.5218	0.41533	0.13459	0.07053
0.6000	0.6000	0.6000	0.4706	0.4997	0.5693	0.34117	0.09191	0.09246
0.6500	0.6500	0.6500	0.5098	0.5413	0.6167	0.23990	0.07607	0.08958
0.7000	0.7000	0.7000	0.5490	0.5830	0.6642	0.18320	0.06452	0.07344
0.7500	0.7500	0.7500	0.5882	0.6246	0.7116	0.15412	0.06742	0.05460
0.8000	0.8000	0.8000	0.6274	0.6663	0.7590	0.10759	0.05918	0.04134

TABLE 5.33

SLIDING RESPONSE OF STRUCTURE 1 TO HORZ. AND VERT. COMPONENTS OF GROUND MOTION NO. 3

These Results are for Multi-Sliding Arrangement With Equal Deformation Reduction Method.

Norm. First Floor Def.	Norm. Second Floor Def.	Norm. Third Floor Def.	Norm. First Floor Accln.	Norm. Second Floor Accln.	Norm. Third Floor Accln.	Sliding Disp. @ First Floor (Ft)	Sliding Disp. @ Second Floor (Ft)	Sliding Disp. @ Third Floor (Ft)
0.1310	0.1310	0.1310	0.1035	0.1099	0.1245	0.57564	0.41412	0.54171
0.1865	0.1865	0.1865	0.1552	0.1648	0.1878	0.43132	0.57310	0.26556
0.2487	0.2487	0.2487	0.2070	0.2170	0.2504	0.55322	0.46158	0.33871
0.3177	0.3184	0.3191	0.2580	0.2747	0.3130	0.54691	0.34167	0.22934
0.3872	0.3872	0.3868	0.3076	0.3297	0.3697	0.49615	0.22634	0.19385
0.4603	0.4603	0.4602	0.3622	0.3846	0.4382	0.45442	0.22704	0.13552
0.5272	0.5272	0.5272	0.4139	0.4396	0.5008	0.39183	0.18741	0.13885
0.5930	0.5929	0.5929	0.4657	0.4945	0.5634	0.26040	0.17213	0.13494
0.6587	0.6586	0.6585	0.5174	0.5495	0.6260	0.27256	0.12328	0.12257
0.7207	0.7206	0.7202	0.5691	0.6044	0.6863	0.26852	0.10422	0.11996
0.7647	0.7631	0.7600	0.6209	0.6594	0.7191	0.21989	0.08326	0.13787
0.7928	0.7849	0.7668	0.6726	0.6926	0.6980	0.13825	0.09473	0.12473
0.7800	0.7585	0.7526	0.7244	0.7000	0.7071	0.08559	0.10085	0.09315
0.7760	0.7411	0.7313	0.7761	0.7148	0.7055	0.09358	0.10804	0.07032
0.7773	0.7726	0.7724	0.8279	0.7323	0.7361	0.08125	0.10021	0.06044

TABLE 5.34

SLIDING RESPONSE OF STRUCTURE 2 TO HORIZONTAL COMPONENT OF GROUND MOTION NO. 1

These Results are for Multi-Sliding Arrangement With Equal Deformation Reduction Method.

Norm. First Floor Def.	Norm. Second Floor Def.	Norm. Third Floor Def.	Norm. First Floor Accln.	Norm. Second Floor Accln.	Norm. Third Floor Accln.	Sliding Disp. @ First Floor (Ft)	Sliding Disp. @ Second Floor (Ft)	Sliding Disp. @ Third Floor (Ft)
0.1000	0.1000	0.1000	0.0924	0.1001	0.0998	1.51404	0.86200	0.51716
0.1500	0.1500	0.1500	0.1386	0.1501	0.1498	0.90363	0.43506	0.26027
0.2000	0.2000	0.2000	0.1848	0.2001	0.1996	0.55578	0.27823	0.15379
0.2500	0.2500	0.2500	0.2311	0.2502	0.2496	0.38023	0.17249	0.08211
0.3000	0.3000	0.3000	0.2772	0.3003	0.2995	0.30273	0.10978	0.03789
0.3500	0.3500	0.3500	0.3234	0.3503	0.3494	0.24052	0.06820	0.01697
0.4000	0.4000	0.4000	0.3696	0.4002	0.3993	0.18439	0.04258	0.01592
0.4500	0.4500	0.4500	0.4158	0.4502	0.4492	0.11710	0.01836	0.01170
0.5000	0.5000	0.5000	0.4620	0.5002	0.4991	0.08511	0.01041	0.00545
0.5500	0.5500	0.5500	0.5082	0.5502	0.5491	0.05634	0.00642	0.00457
0.6000	0.6000	0.6000	0.5544	0.6002	0.5990	0.03327	0.00405	0.00429
0.6500	0.6500	0.6500	0.6006	0.6503	0.6489	0.02822	0.00362	0.00472
0.7000	0.7000	0.7000	0.6468	0.7003	0.6988	0.02036	0.00386	0.00470
0.7500	0.7500	0.7500	0.6929	0.7503	0.7487	0.01229	0.00341	0.00437
0.8000	0.8000	0.8000	0.7391	0.8003	0.7986	0.00836	0.00238	0.00325

TABLE 5.35

SLIDING RESPONSE OF STRUCTURE 2 TO HORZ. AND VERT. COMPONENTS OF GROUND MOTION NO. 1

These Results are for Multi-Sliding Arrangement With Equal Deformation Reduction Method.

Norm. First Floor Def.	Norm. Second Floor Def.	Norm. Third Floor Def.	Norm. First Floor Accln.	Norm. Second Floor Accln.	Norm. Third Floor Accln.	Sliding Disp. @ First Floor (Ft)	Sliding Disp. @ Second Floor (Ft)	Sliding Disp. @ Third Floor (Ft)
0.1451	0.1451	0.1451	0.1342	0.1454	0.1450	1.51585	0.86125	0.49317
0.2170	0.2170	0.2170	0.2013	0.2170	0.2169	0.91122	0.46657	0.31291
0.2746	0.2714	0.2638	0.2685	0.2907	0.2622	0.61966	0.28811	0.18405
0.3132	0.3124	0.3105	0.3356	0.3240	0.3130	0.42841	0.22325	0.09523
0.3723	0.3706	0.3682	0.3633	0.3888	0.3688	0.28076	0.13709	0.04958
0.4281	0.4281	0.4281	0.4189	0.4312	0.4297	0.24840	0.08556	0.02071
0.4555	0.4554	0.4556	0.4788	0.4928	0.4572	0.20998	0.05511	0.01925
0.5122	0.5122	0.5122	0.5386	0.5544	0.5143	0.15510	0.02755	0.01457
0.5691	0.5691	0.5691	0.5865	0.6160	0.5699	0.11402	0.01586	0.00597
0.6129	0.6164	0.6183	0.6258	0.6282	0.6269	0.07628	0.00897	0.00448
0.6675	0.6684	0.6702	0.6827	0.6820	0.6839	0.04896	0.00582	0.00347
0.7216	0.7232	0.7239	0.7396	0.7356	0.7409	0.02861	0.00345	0.00249
0.7751	0.7775	0.7787	0.7965	0.7893	0.7977	0.01475	0.00167	0.00267
0.8260	0.8302	0.8321	0.8534	0.8420	0.8447	0.00948	0.00201	0.00301
0.8778	0.8782	0.8783	0.9102	0.8884	0.8869	0.00621	0.00188	0.00259

TABLE 5.36

SLIDING RESPONSE OF STRUCTURE 2 TO HORIZONTAL COMPONENT OF GROUND MOTION NO. 2

These Results are for Multi-Sliding Arrangement With Equal Deformation Reduction Method.

Norm. First Floor Def.	Norm. Second Floor Def.	Norm. Third Floor Def.	Norm. First Floor Accln.	Norm. Second Floor Accln.	Norm. Third Floor Accln.	Sliding Disp. @ First Floor (Ft)	Sliding Disp. @ Second Floor (Ft)	Sliding Disp. @ Third Floor (Ft)
0.1000	0.1000	0.1000	0.1000	0.0999	0.0978	0.18172	0.15175	0.12734
0.1500	0.1500	0.1500	0.1500	0.1498	0.1467	0.13946	0.10867	0.09130
0.2000	0.2000	0.2000	0.1999	0.1998	0.1956	0.12258	0.09230	0.07651
0.2500	0.2500	0.2500	0.2499	0.2497	0.2445	0.09899	0.06754	0.05492
0.3000	0.3000	0.3000	0.2999	0.2996	0.2934	0.07387	0.05134	0.03935
0.3500	0.3500	0.3500	0.3499	0.3496	0.3422	0.05462	0.04139	0.03470
0.4000	0.4000	0.4000	0.3998	0.3995	0.3911	0.04240	0.03657	0.03439
0.4500	0.4500	0.4500	0.4498	0.4495	0.4400	0.03245	0.03111	0.03302
0.5000	0.5000	0.5000	0.4998	0.4994	0.4889	0.02383	0.02350	0.02622
0.5500	0.5500	0.5500	0.5498	0.5493	0.5378	0.01678	0.01703	0.01939
0.6000	0.6000	0.6000	0.5997	0.5993	0.5867	0.01152	0.01222	0.01424
0.6500	0.6500	0.6500	0.6497	0.6492	0.6356	0.00763	0.00854	0.00986
0.7000	0.7000	0.7000	0.6997	0.6991	0.6845	0.00473	0.00561	0.00587
0.7500	0.7500	0.7500	0.7496	0.7490	0.7334	0.00284	0.00339	0.00272
0.8000	0.8000	0.8000	0.7996	0.7990	0.7822	0.00176	0.00198	0.00265

TABLE 5.37

SLIDING RESPONSE OF STRUCTURE 2 TO HORZ. AND VERT. COMPONENTS OF GROUND MOTION NO. 2

These Results are for Multi-Sliding Arrangement With Equal Deformation Reduction Method.

Norm. First Floor Def.	Norm. Second Floor Def.	Norm. Third Floor Def.	Norm. First Floor Accln.	Norm. Second Floor Accln.	Norm. Third Floor Accln.	Sliding Disp. @ First Floor (Ft)	Sliding Disp. @ Second Floor (Ft)	Sliding Disp. @ Third Floor (Ft)
0.1129	0.1129	0.1129	0.1129	0.1128	0.1104	0.17970	0.14775	0.12432
0.1694	0.1694	0.1694	0.1693	0.1692	0.1656	0.13382	0.10234	0.08497
0.2258	0.2258	0.2258	0.2258	0.2256	0.2213	0.11772	0.10022	0.06009
0.2823	0.2823	0.2823	0.2822	0.2820	0.2761	0.09354	0.06124	0.04928
0.3388	0.3388	0.3388	0.3386	0.3384	0.3313	0.06867	0.04551	0.03463
0.3952	0.3952	0.3952	0.3951	0.3948	0.3865	0.04970	0.03608	0.02817
0.4517	0.4517	0.4517	0.4515	0.4512	0.4417	0.03746	0.03127	0.02794
0.5081	0.5081	0.5081	0.5080	0.5076	0.4969	0.02827	0.02639	0.02758
0.5646	0.5646	0.5646	0.5644	0.5639	0.5521	0.02056	0.02004	0.02167
0.6210	0.6210	0.6210	0.6209	0.6203	0.6074	0.01395	0.01383	0.01488
0.6766	0.6770	0.6772	0.6773	0.6767	0.6626	0.00914	0.00965	0.00905
0.6962	0.7132	0.7193	0.6885	0.7331	0.7178	0.00574	0.00571	0.00504
0.7414	0.7456	0.7580	0.7415	0.7822	0.7730	0.00342	0.00324	0.00369
0.7922	0.7922	0.7921	0.7945	0.7938	0.8243	0.00190	0.00172	0.00424
0.8434	0.8434	0.8432	0.8474	0.8443	0.8703	0.00108	0.00081	0.00410

TABLE 5.38

SLIDING RESPONSE OF STRUCTURE 2 TO HORIZONTAL COMPONENT OF GROUND MOTION NO. 3

These Results are for Multi-Sliding Arrangement With Equal Deformation Reduction Method.

Norm. First Floor Def.	Norm. Second Floor Def.	Norm. Third Floor Def.	Norm. First Floor Accln.	Norm. Second Floor Accln.	Norm. Third Floor Accln.	Sliding Disp. @ First Floor (Ft)	Sliding Disp. @ Second Floor (Ft)	Sliding Disp. @ Third Floor (Ft)
0.1000	0.1000	0.1000	0.0957	0.0972	0.0999	0.56709	0.50437	0.41194
0.1500	0.1500	0.1500	0.1436	0.1458	0.1499	0.42651	0.45246	0.39079
0.2000	0.2000	0.2000	0.1916	0.1944	0.1998	0.44699	0.38813	0.26393
0.2500	0.2500	0.2500	0.2393	0.2773	0.2498	0.38159	0.29487	0.25038
0.3000	0.3000	0.3000	0.2872	0.2917	0.2998	0.29407	0.22875	0.16882
0.3500	0.3500	0.3500	0.3350	0.3403	0.3497	0.21269	0.17855	0.14251
0.4000	0.4000	0.4000	0.3829	0.3889	0.3997	0.18275	0.13378	0.08497
0.4500	0.4500	0.4500	0.4307	0.4375	0.4496	0.14034	0.11527	0.05900
0.5000	0.5000	0.5000	0.4786	0.4861	0.4996	0.13024	0.09828	0.02207
0.5500	0.5500	0.5500	0.5265	0.5347	0.5496	0.11165	0.06121	0.00470
0.6000	0.6000	0.6000	0.5743	0.5833	0.5995	0.09001	0.03618	0.00481
0.6500	0.6500	0.6500	0.6222	0.6319	0.6495	0.06301	0.01520	0.00422
0.7000	0.7000	0.7000	0.6700	0.6805	0.6994	0.04146	0.00391	0.00341
0.7500	0.7500	0.7500	0.7179	0.7291	0.7494	0.02376	0.00308	0.00291
0.8000	0.8000	0.8000	0.7657	0.7777	0.7993	0.01066	0.00236	0.00235

TABLE 5.39

SLIDING RESPONSE OF STRUCTURE 2 TO HORZ. AND VERT. COMPONENTS OF GROUND MOTION NO. 3

These Results are for Multi-Sliding Arrangement With Equal Deformation Reduction Method.

Norm. First Floor Def.	Norm. Second Floor Def.	Norm. Third Floor Def.	Norm. First Floor Accln.	Norm. Second Floor Accln.	Norm. Third Floor Accln.	Sliding Disp. @ First Floor (Ft)	Sliding Disp. @ Second Floor (Ft)	Sliding Disp. @ Third Floor (Ft)
0.1319	0.1319	0.1319	0.1263	0.1283	0.1318	0.57845	0.51884	0.39996
0.1927	0.1928	0.1928	0.1895	0.1924	0.1978	0.41006	0.46089	0.45787
0.2638	0.2638	0.2638	0.2526	0.2566	0.2637	0.45830	0.42580	0.32357
0.3298	0.3298	0.3298	0.3158	0.3207	0.3296	0.42334	0.33147	0.19745
0.3957	0.3957	0.3957	0.3789	0.3848	0.3955	0.33058	0.22634	0.09718
0.4617	0.4617	0.4617	0.4421	0.4490	0.4615	0.24919	0.16241	0.06367
0.5277	0.5277	0.5277	0.5052	0.5131	0.5274	0.19493	0.13604	0.03104
0.5936	0.5936	0.5936	0.5684	0.5772	0.5933	0.14342	0.07673	0.02318
0.6596	0.6596	0.6596	0.6315	0.6414	0.6592	0.08958	0.02899	0.01575
0.6977	0.6906	0.6742	0.6947	0.7055	0.6402	0.04080	0.01630	0.00629
0.7366	0.7238	0.6956	0.7578	0.7605	0.6533	0.02276	0.01025	0.00534
0.7322	0.7100	0.6921	0.8059	0.7304	0.6932	0.01305	0.00711	0.00295
0.7503	0.7222	0.7177	0.8343	0.7525	0.7134	0.00825	0.00482	0.00267
0.7683	0.7551	0.7488	0.8456	0.7794	0.7451	0.00497	0.00453	0.00211
0.8056	0.8017	0.7956	0.8659	0.8192	0.7858	0.00268	0.00373	0.00217

TABLE 5.40

SLIDING RESPONSE OF STRUCTURE 3 TO HORIZONTAL COMPONENT OF GROUND MOTION NO. 1

These Results are for Multi-Sliding Arrangement With Equal Deformation Reduction Method.

Norm. First Floor Def.	Norm. Second Floor Def.	Norm. Third Floor Def.	Norm. First Floor Accln.	Norm. Second Floor Accln.	Norm. Third Floor Accln.	Sliding Disp. @ First Floor (Ft)	Sliding Disp. @ Second Floor (Ft)	Sliding Disp. @ Third Floor (Ft)
0.1000	0.1000	0.1000	0.0774	0.0112	0.0902	2.47030	6.06535	2.45637
0.1500	0.1500	0.1500	0.1162	0.0168	0.1353	2.05221	5.22850	1.94409
0.2000	0.2000	0.2000	0.1549	0.0225	0.1804	1.99959	4.91377	1.32546
0.2500	0.2500	0.2500	0.1936	0.0281	0.2255	1.36644	4.32615	0.61184
0.3000	0.3000	0.3000	0.2323	0.0337	0.2706	0.84297	4.15772	0.53474
0.3500	0.3500	0.3500	0.2711	0.0393	0.3157	0.49750	3.93978	0.58496
0.4000	0.4000	0.4000	0.3098	0.0449	0.3608	0.31098	3.66391	0.57700
0.4500	0.4500	0.4500	0.3485	0.0505	0.4059	0.29211	3.41442	0.67696
0.5000	0.5000	0.5000	0.3872	0.0562	0.4510	0.25707	3.17252	0.75160
0.5499	0.5499	0.5498	0.4259	0.0618	0.4961	0.19280	2.94073	0.78921
0.5807	0.5758	0.5735	0.4647	0.0674	0.5412	0.22100	3.07104	0.66689
0.6018	0.5882	0.5803	0.5034	0.0730	0.5863	0.25648	2.86859	0.52523
0.6185	0.5951	0.5949	0.5421	0.0786	0.6314	0.27544	2.43485	0.38029
0.6209	0.5955	0.6368	0.5808	0.0842	0.6765	0.20904	2.20285	0.23601
0.6202	0.5958	0.6674	0.6195	0.0898	0.7216	0.16440	2.05824	0.11222

TABLE 5.41

SLIDING RESPONSE OF STRUCTURE 3 TO HORZ. AND VERT. COMPONENTS OF GROUND MOTION NO. 1

These Results are for Multi-Sliding Arrangement With Equal Deformation Reduction Method.

Norm. First Floor Def.	Norm. Second Floor Def.	Norm. Third Floor Def.	Norm. First Floor Accln.	Norm. Second Floor Accln.	Norm. Third Floor Accln.	Sliding Disp. @ First Floor (Ft)	Sliding Disp. @ Second Floor (Ft)	Sliding Disp. @ Third Floor (Ft)
0.1266	0.1263	0.1267	0.1125	0.0162	0.1311	2.50323	5.96793	1.81272
0.1864	0.1849	0.1898	0.1688	0.0243	0.1966	1.87321	5.21918	1.61076
0.2449	0.2423	0.2443	0.2251	0.0326	0.2556	1.94909	4.86094	1.33723
0.2916	0.2848	0.2826	0.2813	0.0396	0.2647	1.39111	4.27679	0.61622
0.3501	0.3253	0.3213	0.3376	0.0484	0.3022	0.86900	4.16223	0.53289
0.3812	0.3780	0.3748	0.3368	0.0571	0.3533	0.61420	3.96053	0.45468
0.4220	0.4189	0.4184	0.3849	0.0653	0.4005	0.39017	3.70739	0.59870
0.4687	0.4665	0.4648	0.4166	0.0734	0.4437	0.29125	3.45428	0.64903
0.5165	0.5127	0.5094	0.4592	0.0816	0.4904	0.25847	3.21919	0.70049
0.5584	0.5555	0.5525	0.5034	0.0897	0.5394	0.24418	2.99557	0.76471
0.5798	0.5747	0.5696	0.5461	0.0979	0.5836	0.29761	2.80203	0.69679
0.5994	0.5887	0.5796	0.5879	0.1061	0.6313	0.34779	2.77054	0.59222
0.6155	0.5958	0.5884	0.6285	0.1142	0.6799	0.37051	2.42725	0.45246
0.6267	0.6015	0.6278	0.6538	0.1224	0.7244	0.34404	2.25252	0.31828
0.6305	0.6052	0.6572	0.6917	0.1305	0.7441	0.30652	2.10961	0.18397

TABLE 5.42

SLIDING RESPONSE OF STRUCTURE 3 TO HORIZONTAL COMPONENT OF GROUND MOTION NO. 2

These Results are for Multi-Sliding Arrangement With Equal Deformation Reduction Method.

Norm. First Floor Def.	Norm. Second Floor Def.	Norm. Third Floor Def.	Norm. First Floor Accln.	Norm. Second Floor Accln.	Norm. Third Floor Accln.	Sliding Disp. @ First Floor (Ft)	Sliding Disp. @ Second Floor (Ft)	Sliding Disp. @ Third Floor (Ft)
0.1000	0.1000	0.1000	0.0886	0.0008	0.0895	0.24461	5.16327	0.17020
0.1500	0.1500	0.1500	0.1328	0.0012	0.1343	0.14716	3.94209	0.12469
0.2000	0.2000	0.2000	0.1771	0.0016	0.1791	0.20120	3.50567	0.16952
0.2500	0.2500	0.2500	0.2213	0.0021	0.2238	0.24133	3.23478	0.23873
0.3000	0.3000	0.3000	0.2656	0.0025	0.2686	0.19472	3.07820	0.24022
0.3500	0.3500	0.3500	0.3099	0.0029	0.3134	0.16832	2.87985	0.18361
0.4000	0.4000	0.4000	0.3541	0.0033	0.3581	0.14819	2.66458	0.10986
0.4500	0.4500	0.4500	0.3984	0.0037	0.4029	0.13701	2.40706	0.12518
0.5000	0.5000	0.5000	0.4427	0.0041	0.4477	0.11651	2.01325	0.13115
0.5500	0.5500	0.5500	0.4869	0.0045	0.4924	0.10386	1.98862	0.11920
0.5999	0.5999	0.5999	0.5312	0.0049	0.5372	0.10086	1.83025	0.09860
0.6431	0.6401	0.6381	0.5754	0.0053	0.5820	0.09729	1.68513	0.12031
0.6841	0.6770	0.6725	0.6197	0.0057	0.6267	0.08156	1.58616	0.12928
0.7269	0.7167	0.7102	0.6640	0.0061	0.6715	0.08077	1.68119	0.14080
0.7617	0.7448	0.7340	0.7082	0.0065	0.7163	0.07439	1.68169	0.12565

TABLE 5.43

SLIDING RESPONSE OF STRUCTURE 3 TO HORZ. AND VERT. COMPONENTS OF GROUND MOTION NO. 2

These Results are for Multi-Sliding Arrangement With Equal Deformation Reduction Method.

Norm. First Floor Def.	Norm. Second Floor Def.	Norm. Third Floor Def.	Norm. First Floor Accln.	Norm. Second Floor Accln.	Norm. Third Floor Accln.	Sliding Disp. @ First Floor (Ft)	Sliding Disp. @ Second Floor (Ft)	Sliding Disp. @ Third Floor (Ft)
0.1064	0.1064	0.1064	0.1000	0.0009	0.0967	0.24627	5.15766	0.15503
0.1560	0.1560	0.1560	0.1498	0.0014	0.1421	0.13620	3.93140	0.12037
0.2080	0.2080	0.2080	0.1997	0.0018	0.1895	0.21634	3.30654	0.15161
0.2580	0.2580	0.2580	0.2496	0.0023	0.2371	0.25516	3.25106	0.22065
0.3096	0.3096	0.3096	0.2995	0.0028	0.2845	0.22252	3.07254	0.26116
0.3611	0.3611	0.3611	0.3494	0.0032	0.3239	0.17935	2.87351	0.18134
0.4123	0.4123	0.4123	0.3994	0.0037	0.3699	0.16666	2.66866	0.11112
0.4638	0.4638	0.4638	0.4494	0.0041	0.4108	0.16212	2.45670	0.13129
0.5000	0.4999	0.4999	0.4992	0.0046	0.4623	0.15834	2.24040	0.12541
0.5496	0.5495	0.5495	0.5491	0.0050	0.5046	0.15266	2.05444	0.10823
0.5993	0.5992	0.5992	0.5990	0.0055	0.5548	0.14741	1.85913	0.09977
0.6429	0.6401	0.6384	0.6490	0.0060	0.6011	0.12862	1.70995	0.12284
0.6837	0.6770	0.6727	0.6989	0.0064	0.6473	0.11103	1.62101	0.13153
0.7239	0.7075	0.7058	0.7488	0.0069	0.6936	0.09032	1.69881	0.12609
0.7628	0.7470	0.7368	0.7987	0.0073	0.7398	0.08018	1.71204	0.12172

TABLE 5.44

SLIDING RESPONSE OF STRUCTURE 3 TO HORIZONTAL COMPONENT OF GROUND MOTION NO. 3

These Results are for Multi-Sliding Arrangement With Equal Deformation Reduction Method.

Norm. First Floor Def.	Norm. Second Floor Def.	Norm. Third Floor Def.	Norm. First Floor Accln.	Norm. Second Floor Accln.	Norm. Third Floor Accln.	Sliding Disp. @ First Floor (Ft)	Sliding Disp. @ Second Floor (Ft)	Sliding Disp. @ Third Floor (Ft)
0.1000	0.1000	0.1000	0.0190	0.0321	0.0773	0.68278	0.83013	0.67016
0.1500	0.1500	0.1500	0.0285	0.0482	0.1160	0.66726	0.58316	0.46713
0.2000	0.2000	0.2000	0.0380	0.0643	0.1547	0.65482	0.50099	0.35772
0.2500	0.2500	0.2500	0.0475	0.0804	0.1933	0.66081	0.44788	0.26743
0.3000	0.3000	0.3000	0.0570	0.0964	0.2320	0.64359	0.53702	0.32606
0.3500	0.3500	0.3500	0.0665	0.1125	0.2706	0.61728	0.55183	0.38415
0.4000	0.4000	0.4000	0.0759	0.1286	0.3093	0.58898	0.58922	0.43116
0.4500	0.4500	0.4500	0.0854	0.1446	0.3480	0.55883	0.57759	0.46617
0.5000	0.5000	0.5000	0.0949	0.1607	0.3866	0.53644	0.52151	0.39143
0.5500	0.5500	0.5500	0.1044	0.1768	0.4253	0.51670	0.46916	0.32603
0.6000	0.6000	0.6000	0.1139	0.1928	0.4639	0.49897	0.40094	0.26599
0.6500	0.6500	0.6500	0.1234	0.2089	0.5026	0.48077	0.32887	0.20667
0.7000	0.7000	0.7000	0.1329	0.2249	0.5413	0.46135	0.27523	0.14345
0.7500	0.7500	0.7500	0.1424	0.2410	0.5799	0.43763	0.22137	0.07736
0.8000	0.8000	0.8000	0.1519	0.2571	0.6186	0.40682	0.16870	0.01575

TABLE 5.45

SLIDING RESPONSE OF STRUCTURE 3 TO HORZ. AND VERT. COMPONENTS OF GROUND MOTION NO. 3

These Results are for Multi-Sliding Arrangement With Equal Deformation Reduction Method.

Norm. First Floor Def.	Norm. Second Floor Def.	Norm. Third Floor Def.	Norm. First Floor Accln.	Norm. Second Floor Accln.	Norm. Third Floor Accln.	Sliding Disp. @ First Floor (Ft)	Sliding Disp. @ Second Floor (Ft)	Sliding Disp. @ Third Floor (Ft)
0.1310	0.1310	0.1310	0.0250	0.0424	0.1020	0.69860	0.93280	0.87006
0.1965	0.1965	0.1965	0.0376	0.0636	0.1530	0.75392	0.61504	0.47877
0.2618	0.2618	0.2617	0.0501	0.0848	0.2041	0.76321	0.52068	0.38790
0.3246	0.3244	0.3240	0.0626	0.1060	0.2518	0.71223	0.43829	0.30967
0.3862	0.3858	0.3848	0.0751	0.1272	0.2976	0.67156	0.47047	0.24035
0.4484	0.4477	0.4460	0.0877	0.1484	0.3447	0.65616	0.49959	0.18833
0.5111	0.5102	0.5081	0.1002	0.1696	0.3924	0.63542	0.48447	0.22226
0.5747	0.5737	0.5717	0.1127	0.1908	0.4416	0.61219	0.43782	0.23617
0.6389	0.6378	0.6363	0.1252	0.2120	0.4921	0.58752	0.37034	0.24278
0.7013	0.7001	0.6981	0.1377	0.2332	0.5399	0.56660	0.32996	0.21940
0.7600	0.7582	0.7546	0.1503	0.2544	0.5822	0.55303	0.25335	0.15270
0.8058	0.8023	0.7944	0.1628	0.2756	0.6091	0.53003	0.20350	0.09057
0.8268	0.8200	0.8024	0.1753	0.2964	0.6067	0.49739	0.16534	0.04419
0.8423	0.8314	0.8094	0.1878	0.3014	0.6076	0.46461	0.13573	0.00505
0.8540	0.8386	0.8171	0.2004	0.3215	0.6171	0.43255	0.11154	0.00000

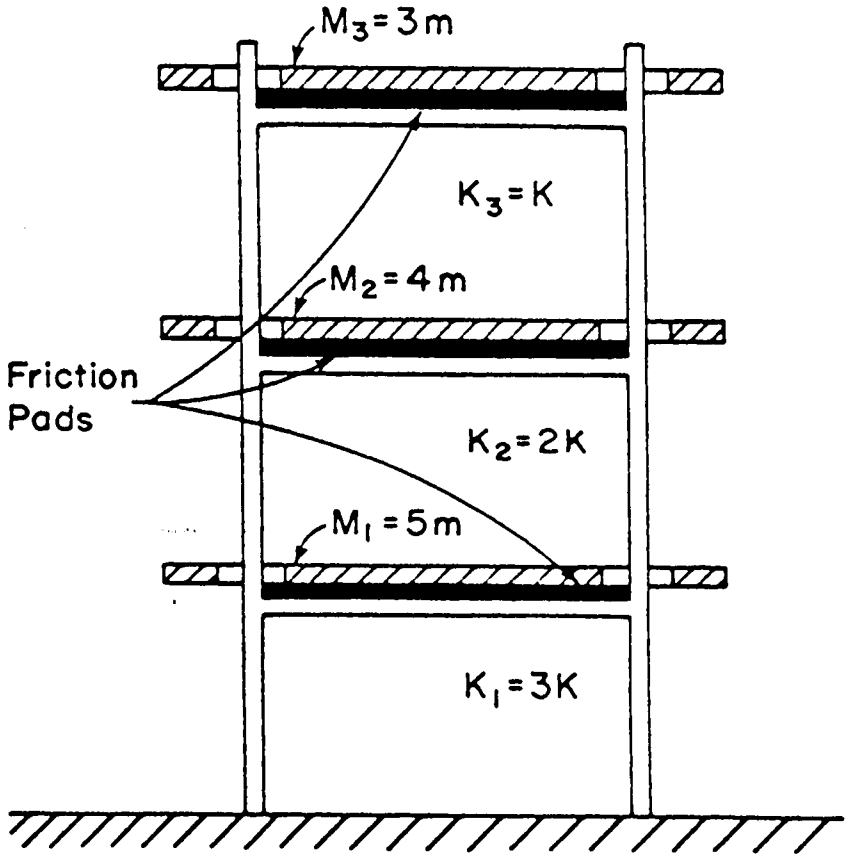

FIG. 5.1 PROPOSED MULTI-SLIDING STRUCTURE

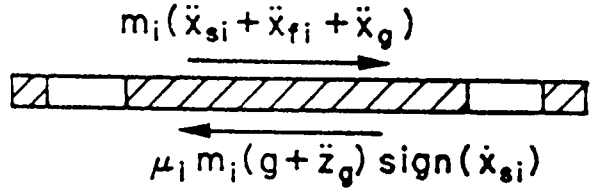

FREE BODY DIAGRAM OF SLIDING SLAB

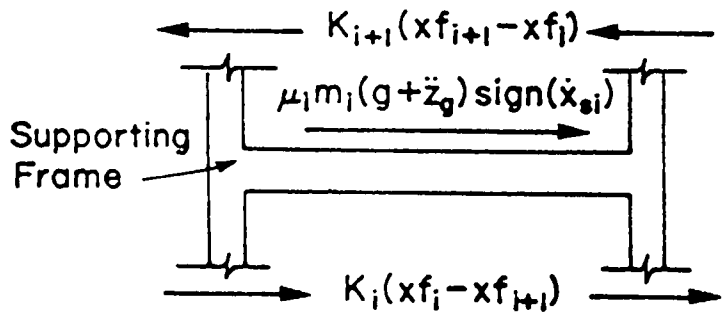

FREE BODY DIAGRAM OF FRAME NODE

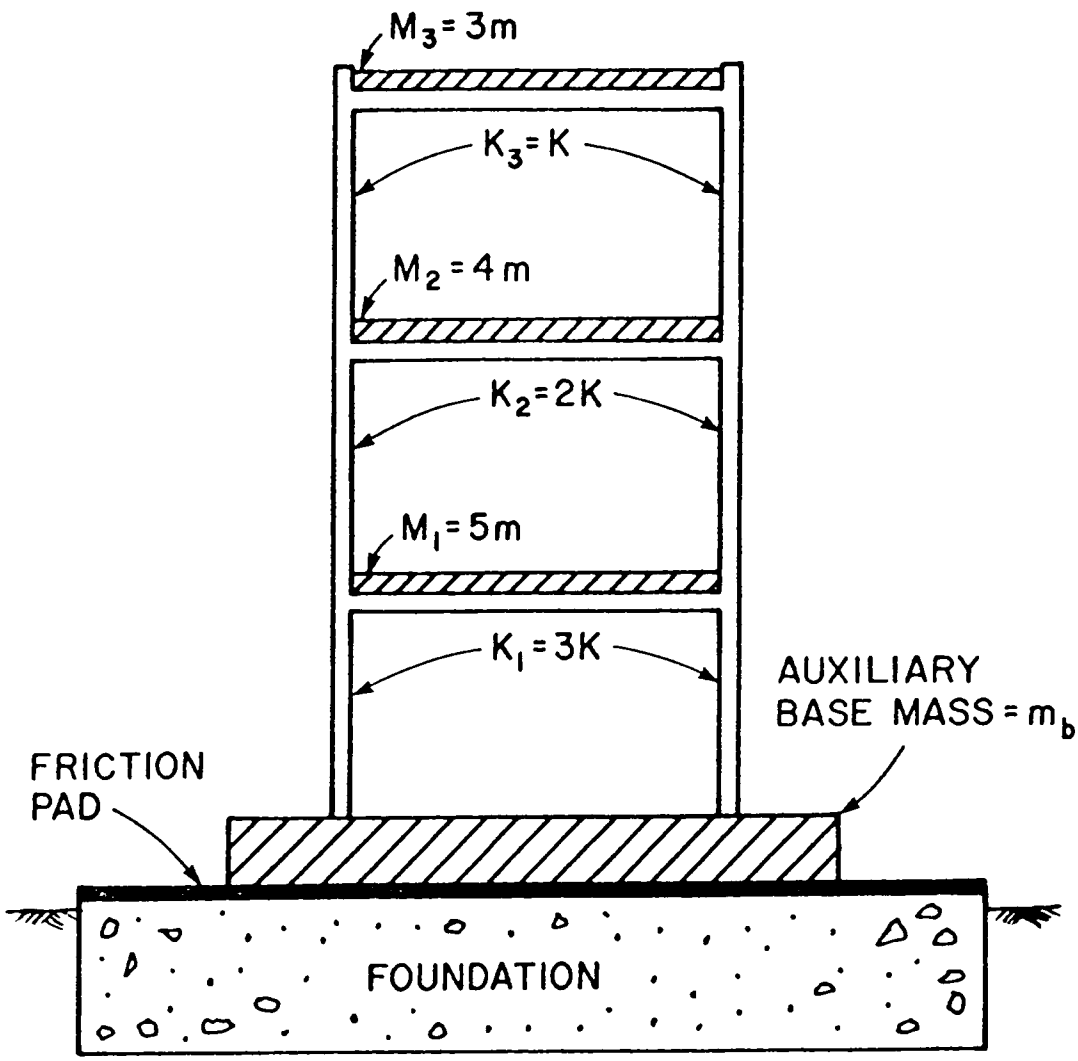

FIG. 5.2 BASE SLIDING STRUCTURE

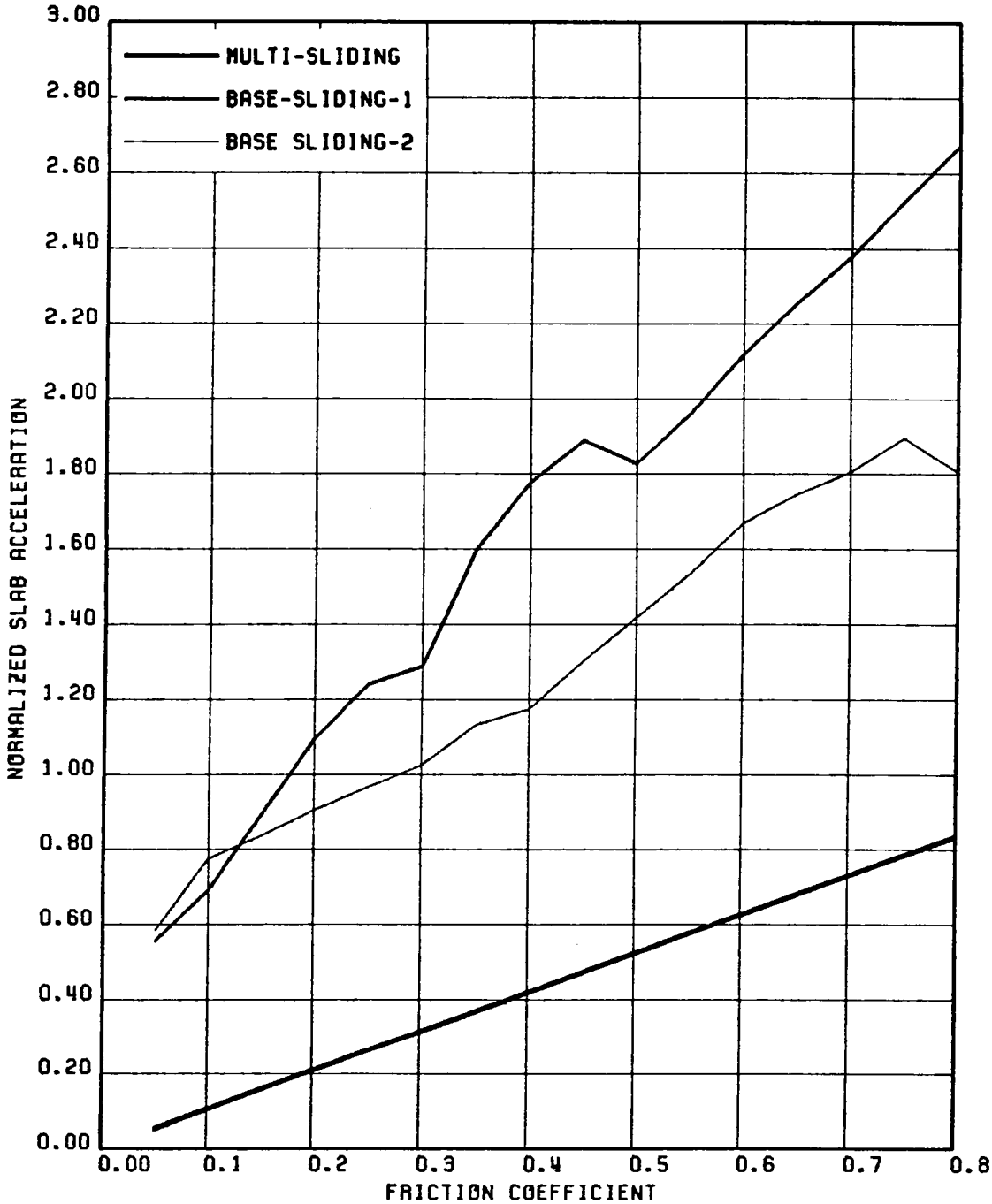

FIG. 5.3 COMPARISON OF NORMALIZED ACCELERATION OF FIRST FLOOR (NORMALIZED W.R.T. THE CORRESPONDING NON-SLIDING RESPONSE) FOR BASE SLIDING & MULTI-SLIDING CASES; STRUCTURE 1, GR MOTION 1-HZ COMPONENT

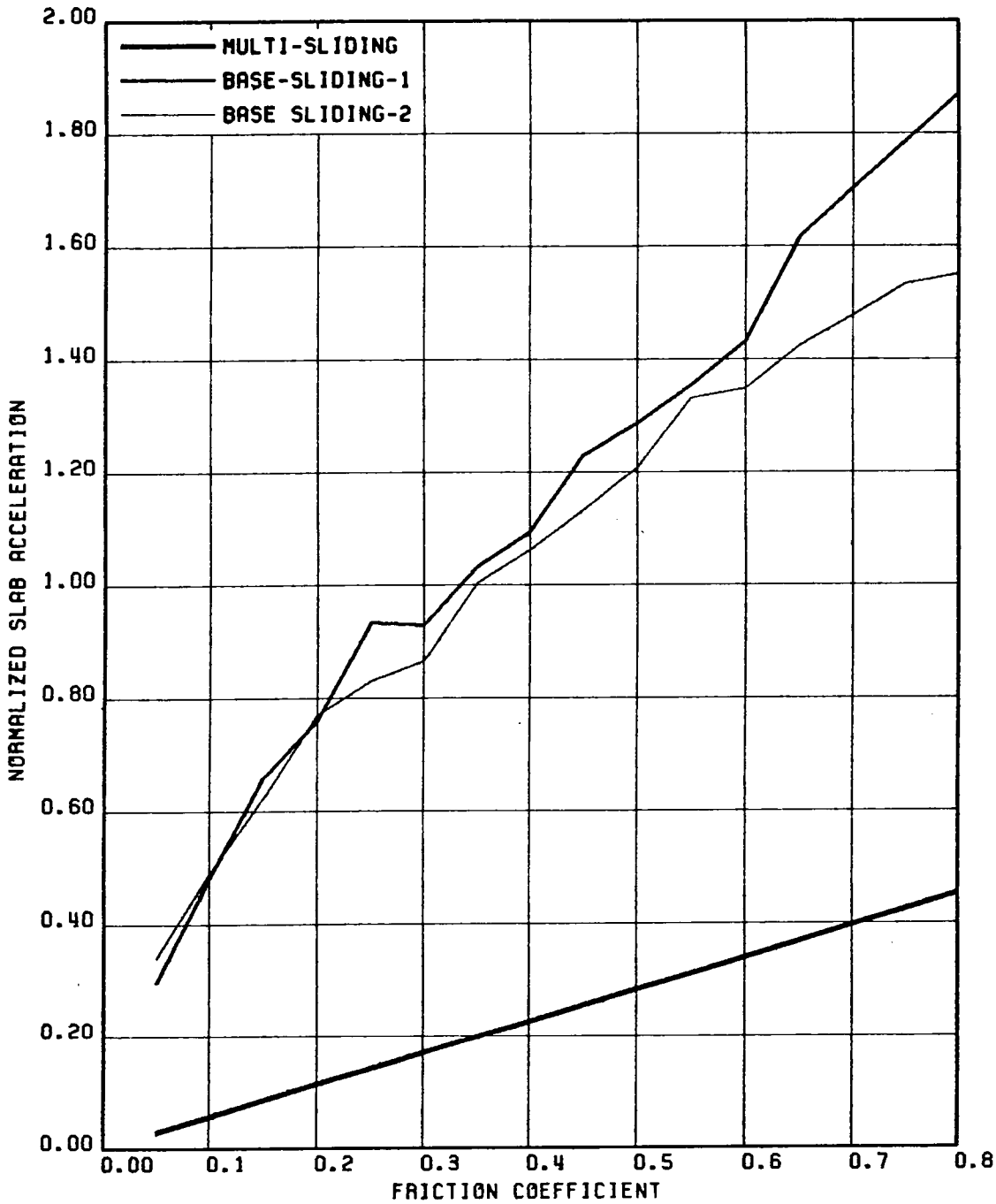

FIG. 5.4 COMPARISON OF NORMALIZED ACCELERATION OF SECOND FLOOR (NORMALIZED W.R.T. THE CORRESPONDING NON-SLIDING RESPONSE) FOR BASE SLIDING & MULTI-SLIDING CASES; STRUCTURE 1, GR MOTION 1-HZ COMPONENT

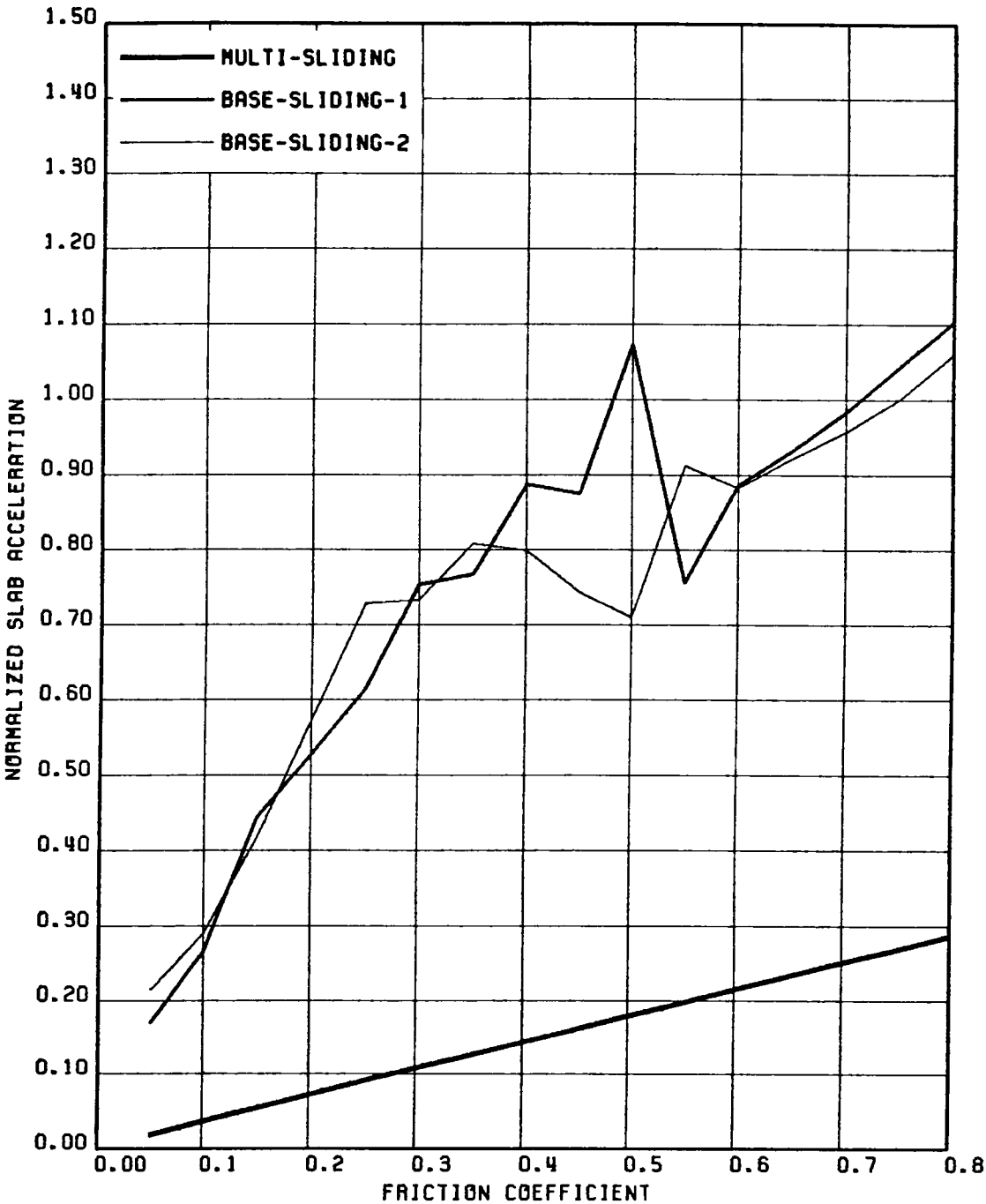

FIG. 5.5 COMPARISON OF NORMALIZED ACCELERATION OF THIRD FLOOR (NORMALIZED W.R.T. THE CORRESPONDING NON-SLIDING RESPONSE) FOR BASE SLIDING & MULTI-SLIDING CASES; STRUCTURE 1, GR MOTION 1-HZ COMPONENT

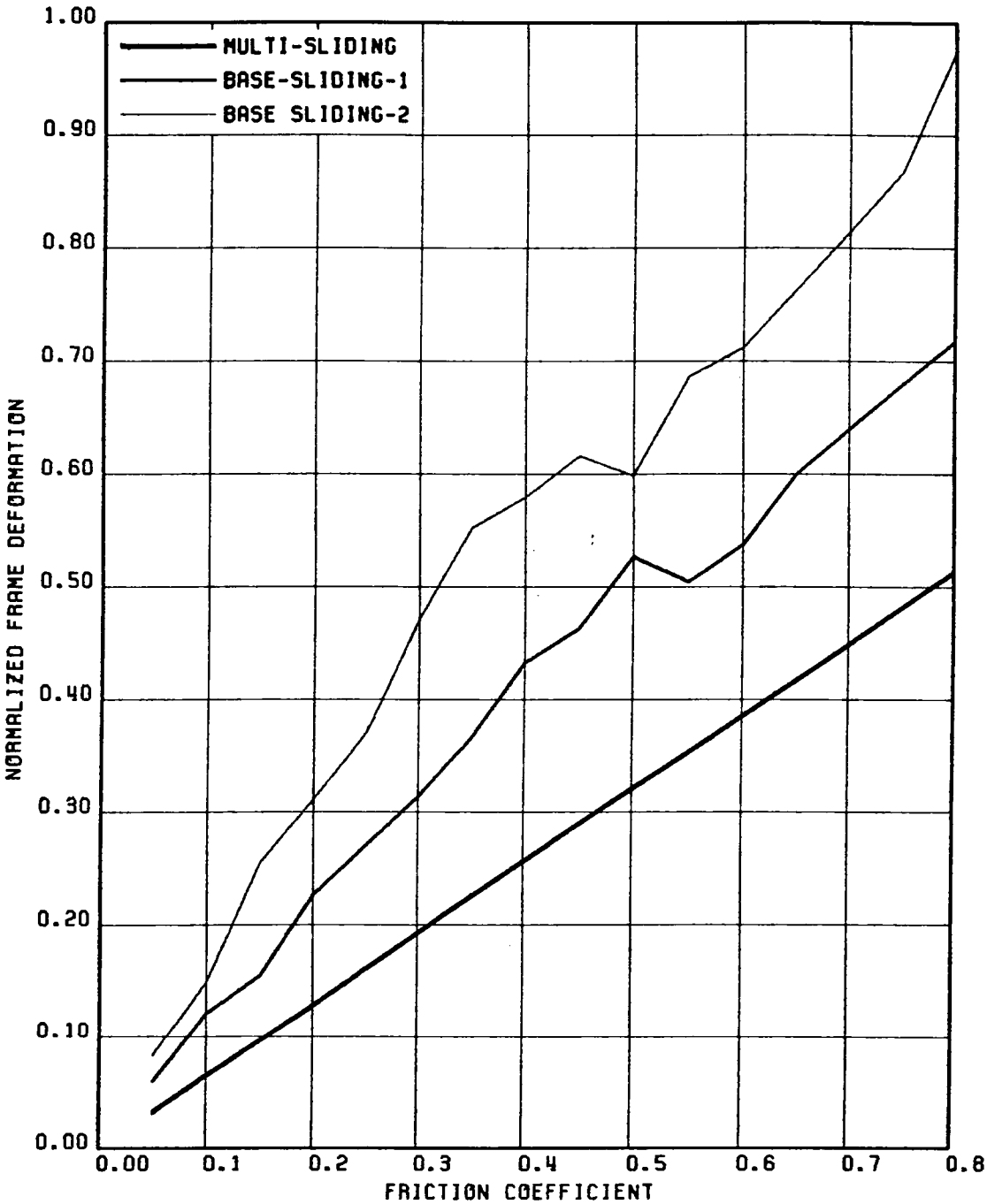

FIG. 5.6 COMPARISON OF NORMALIZED DEFORMATION AT FIRST FLOOR (NORMALIZED W.R.T. THE CORRESPONDING NON-SLIDING RESPONSE) FOR BASE SLIDING & MULTI-SLIDING CASES; STRUCTURE 1, GR MOTION 1-HZ COMPONENT

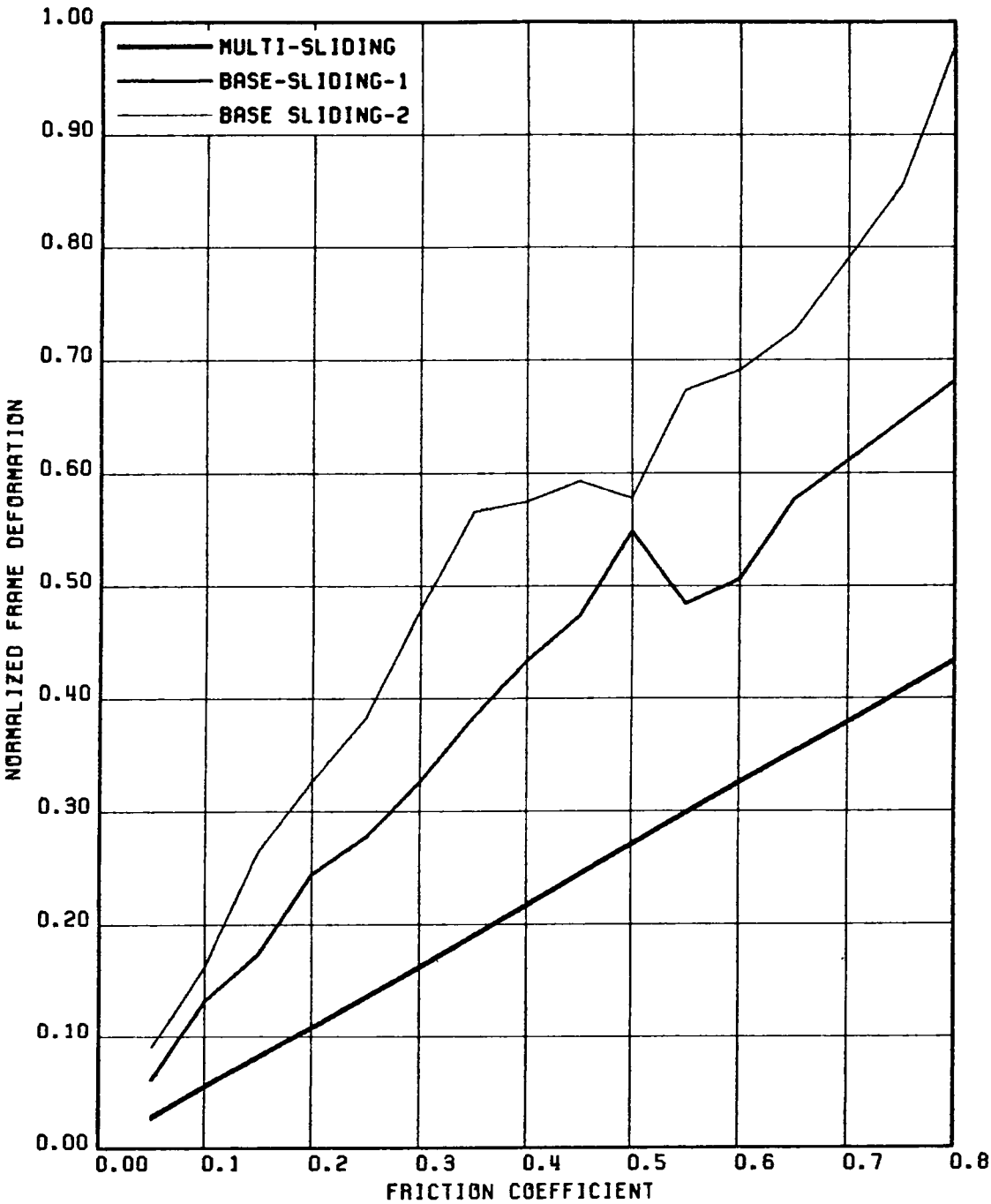

FIG. 5.7 COMPARISON OF NORMALIZED DEFORMATION AT SECOND FLOOR (NORMALIZED W.R.T. THE CORRESPONDING NON-SLIDING RESPONSE) FOR BASE SLIDING & MULTI-SLIDING CASES; STRUCTURE 1, GR MOTION 1-HZ COMPONENT

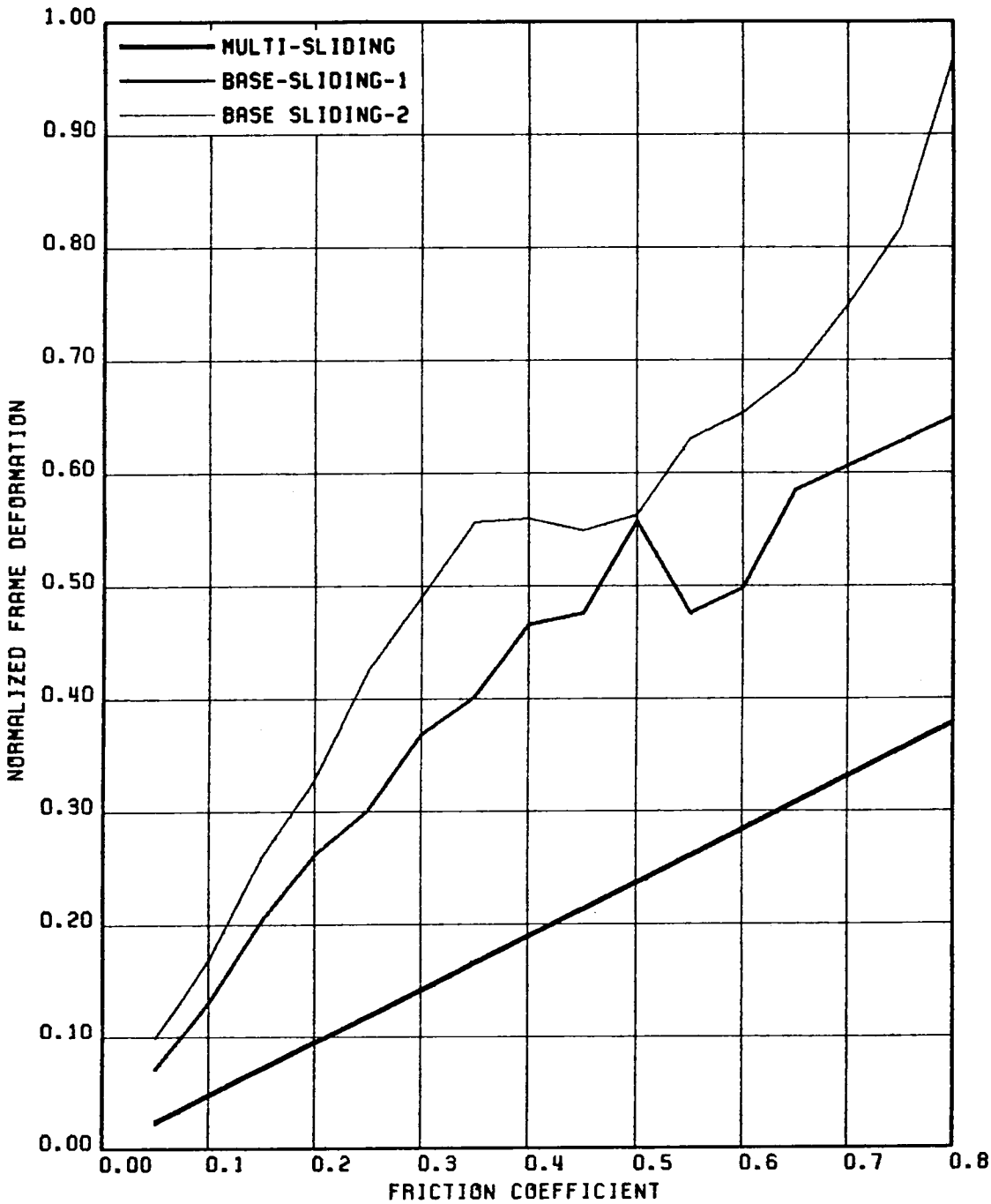

FIG. 5.8 COMPARISON OF NORMALIZED DEFORMATION AT THIRD FLOOR (NORMALIZED W.R.T. THE CORRESPONDING NON-SLIDING RESPONSE) FOR BASE SLIDING & MULTI-SLIDING CASES; STRUCTURE 1, GR MOTION 1-HZ COMPONENT

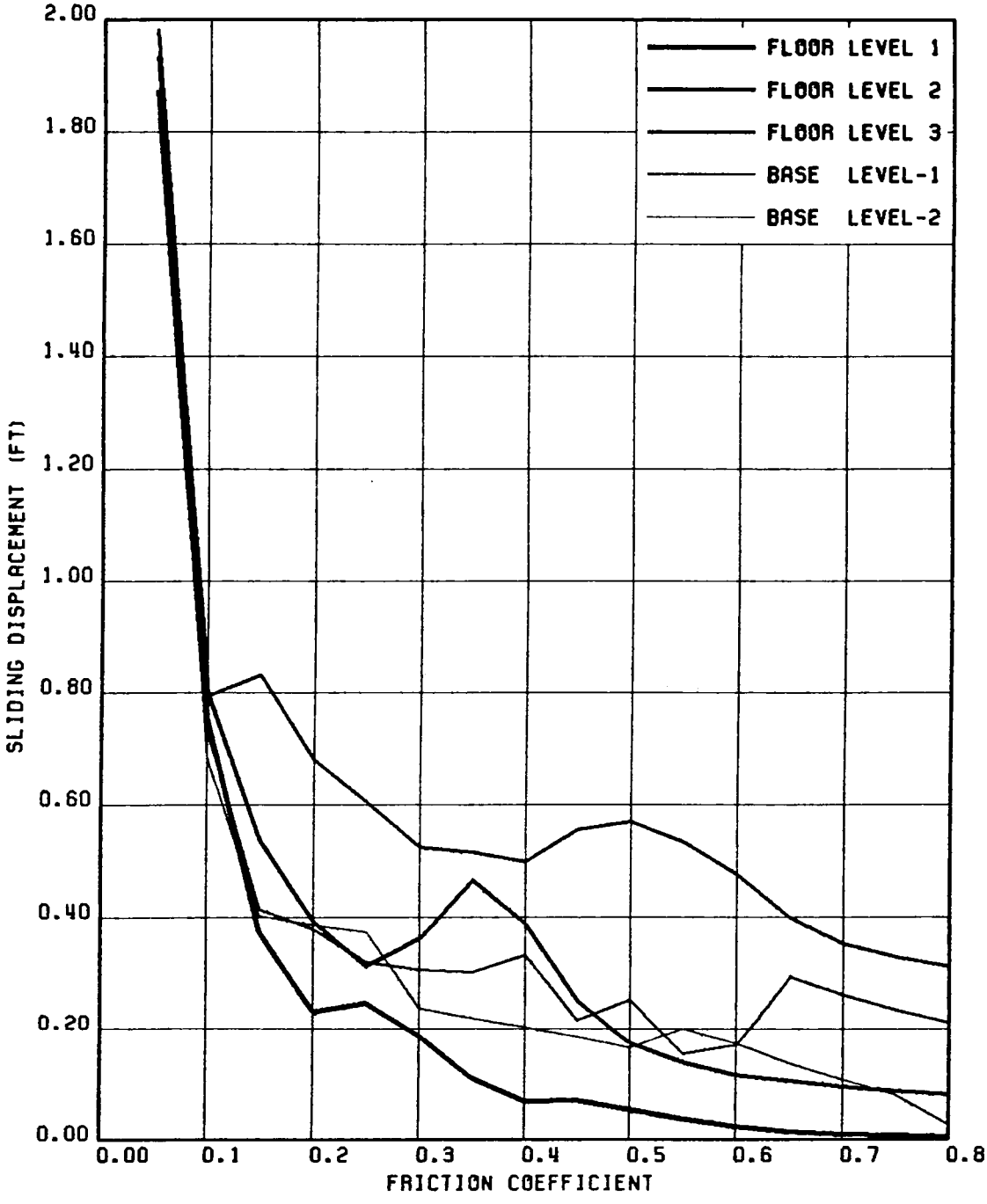

FIG. 5.9 COMPARISON OF MAXIMUM SLIDING DISPLACEMENTS FOR BASE SLIDING AND MULTI-SLIDING CASES; STRUCTURE 1, GR MOTION 1-HZ COMPONENT

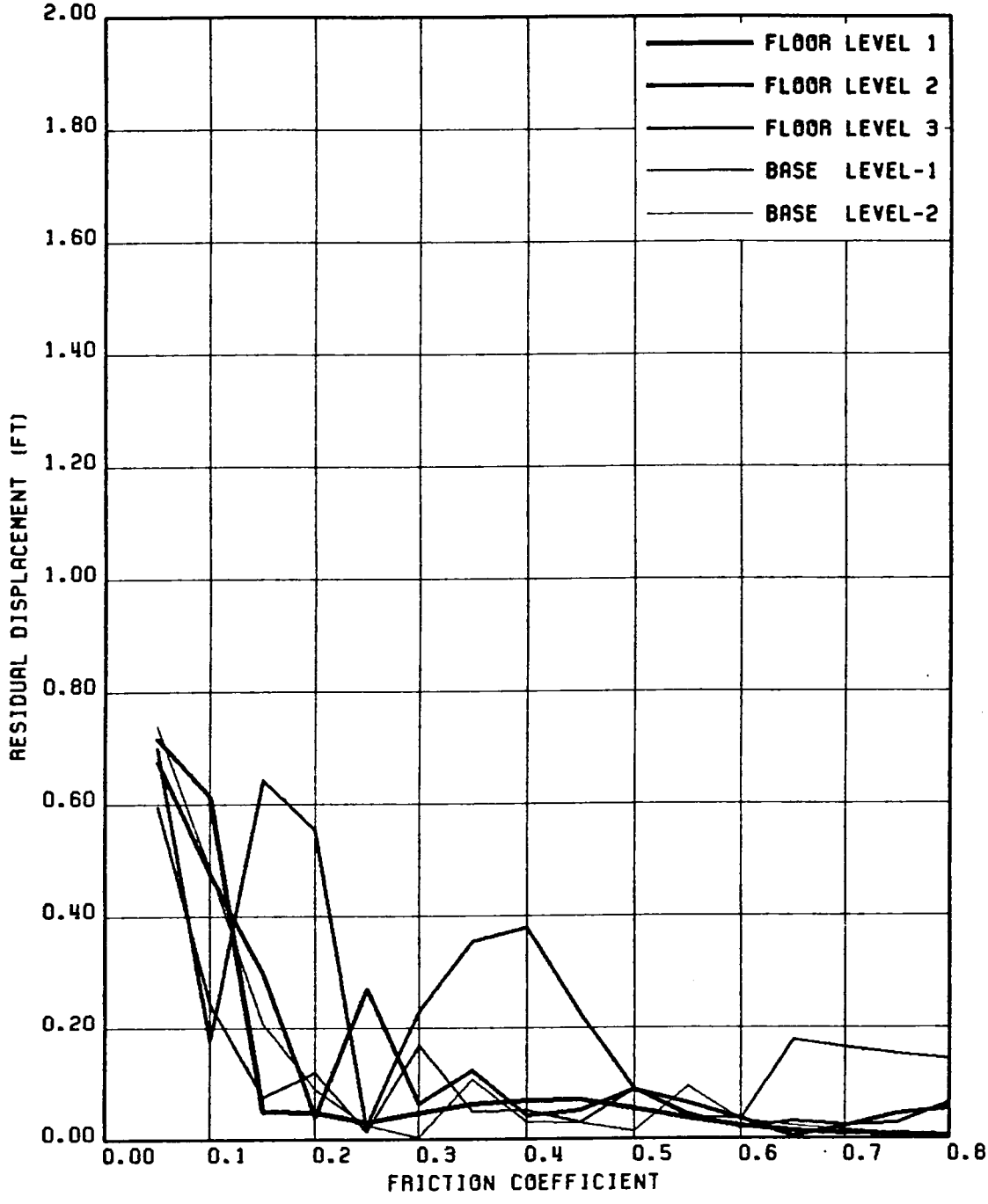

FIG. 5.10 COMPARISON OF RESIDUAL SLIDING DISPLACEMENTS FOR BASE SLIDING AND MULTI-SLIDING CASES; STRUCTURE 1, GR MOTION 1-HZ COMPONENT

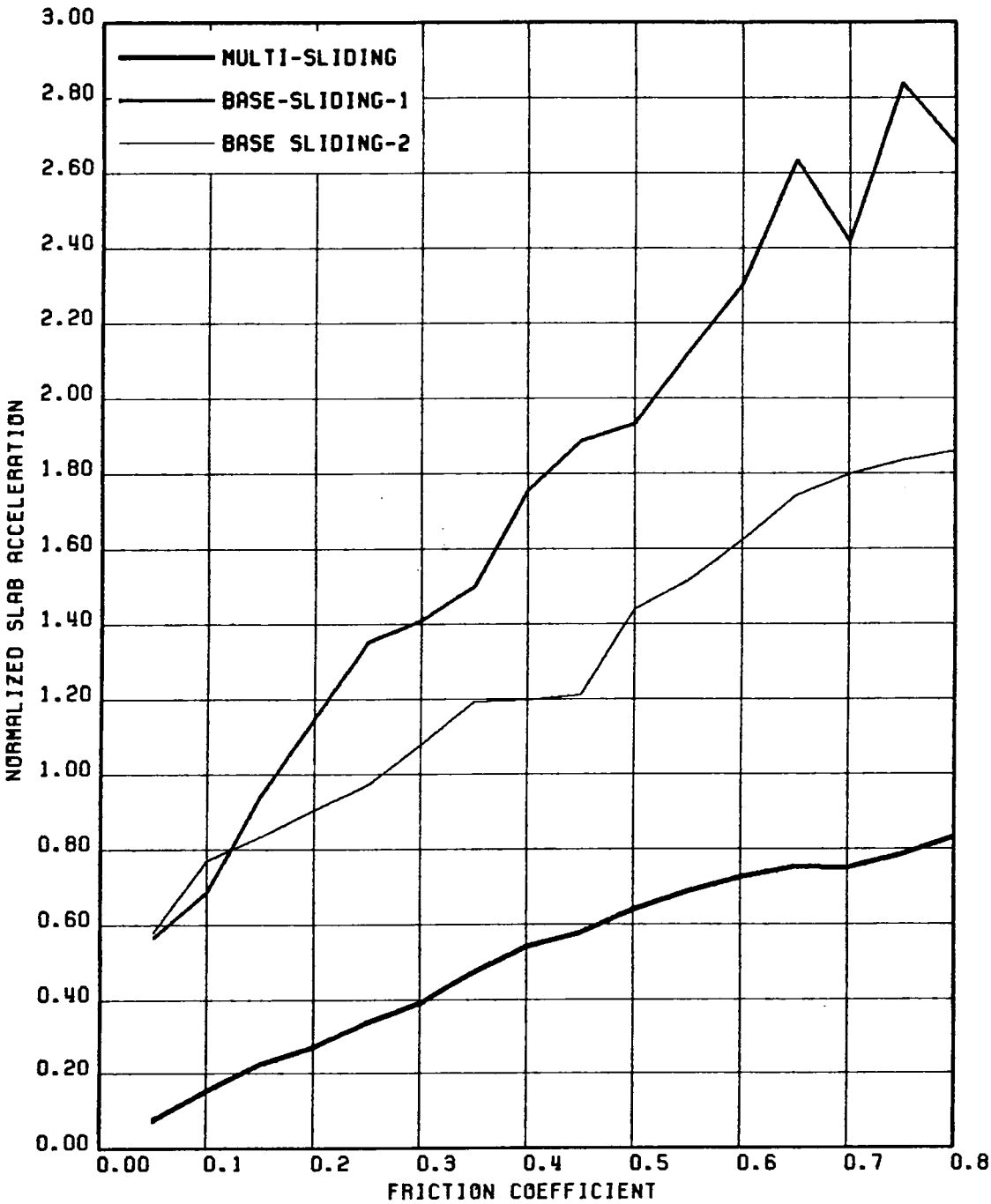

FIG. 5.11 COMPARISON OF NORMALIZED ACCELERATION OF FIRST FLOOR (NORMALIZED W.R.T. THE CORRESPONDING NON-SLIDING RESPONSE) FOR BASE SLIDING & MULTI-SLIDING CASES; STRUCTURE 1, GR MOTION 1-HZ & VT COMPONENT

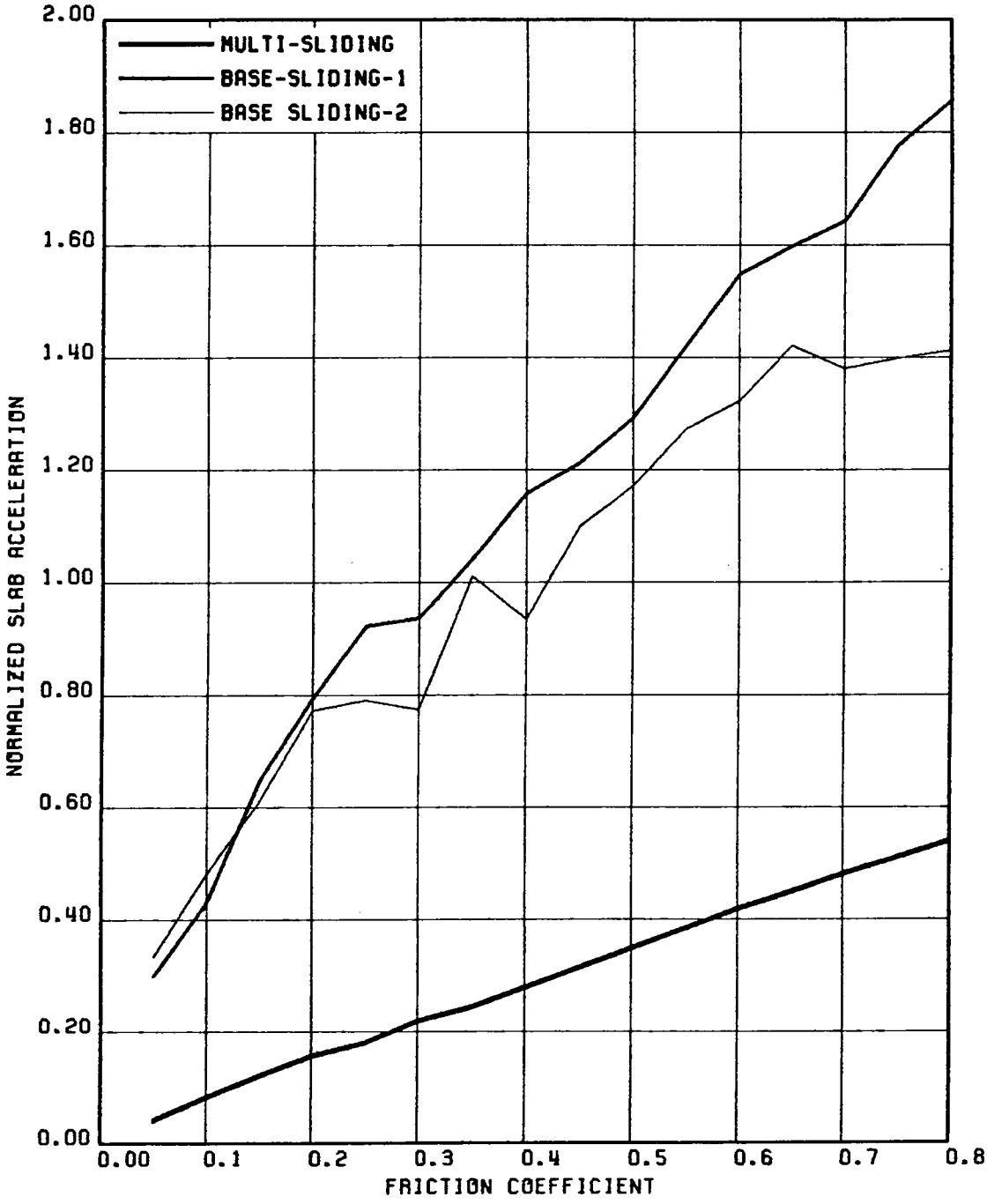

FIG. 5.12 COMPARISON OF NORMALIZED ACCELERATION OF SECOND FLOOR (NORMALIZED W.R.T. THE CORRESPONDING NON-SLIDING RESPONSE) FOR BASE SLIDING & MULTI-SLIDING CASES; STRUCTURE 1, GR MOTION 1-HZ & VT COMPONENT

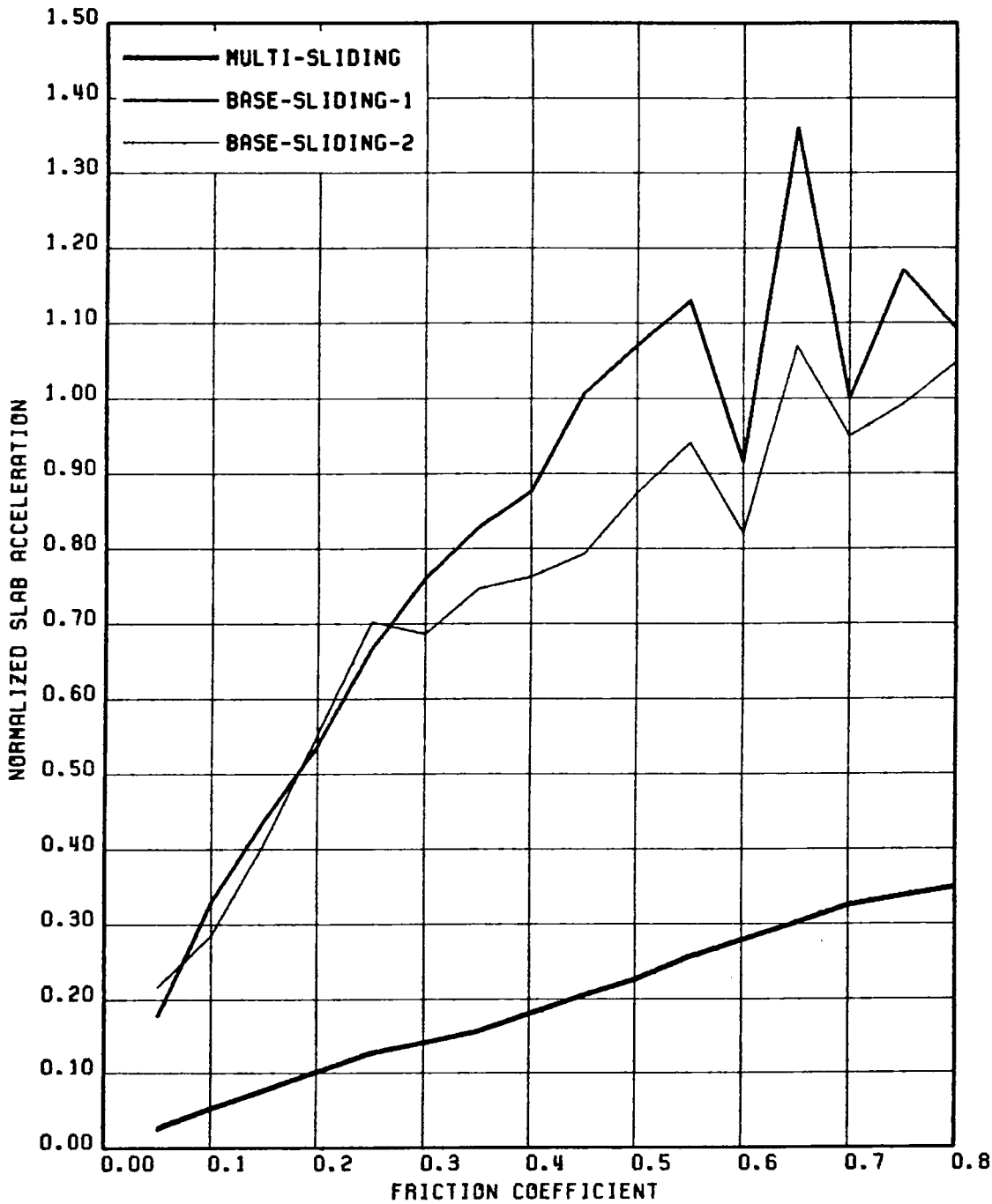

FIG. 5.13 COMPARISON OF NORMALIZED ACCELERATION OF THIRD FLOOR (NORMALIZED W.R.T. THE CORRESPONDING NON-SLIDING RESPONSE) FOR BASE SLIDING & MULTI-SLIDING CASES; STRUCTURE 1, GR MOTION 1-HZ & VT COMPONENT

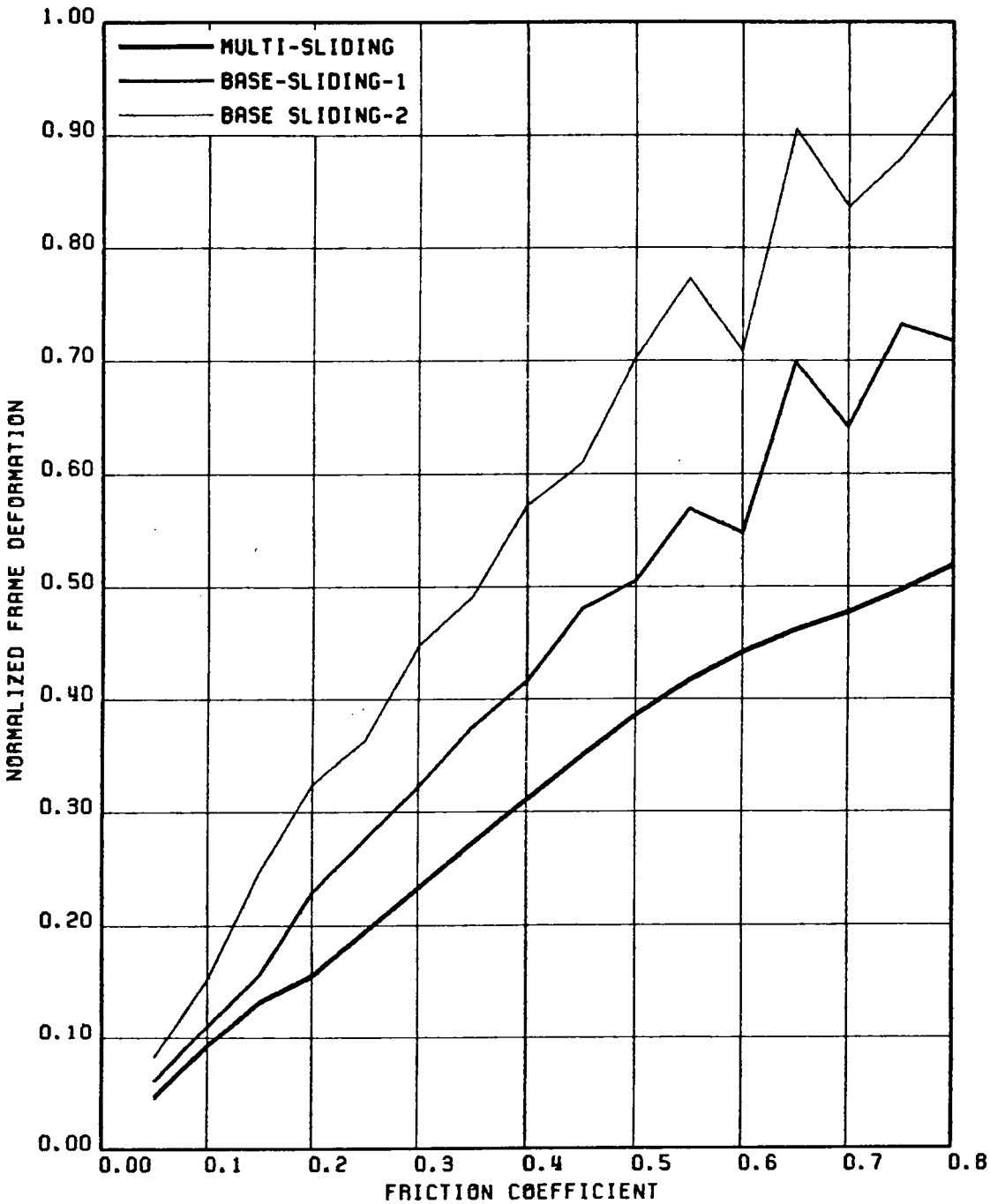

FIG. 5.14 COMPARISON OF NORMALIZED DEFORMATION AT FIRST FLOOR (NORMALIZED W.R.T. THE CORRESPONDING NON-SLIDING RESPONSE) FOR BASE SLIDING & MULTI-SLIDING CASES; STRUCTURE 1, GR MOTION 1-HZ & VT COMPONENT

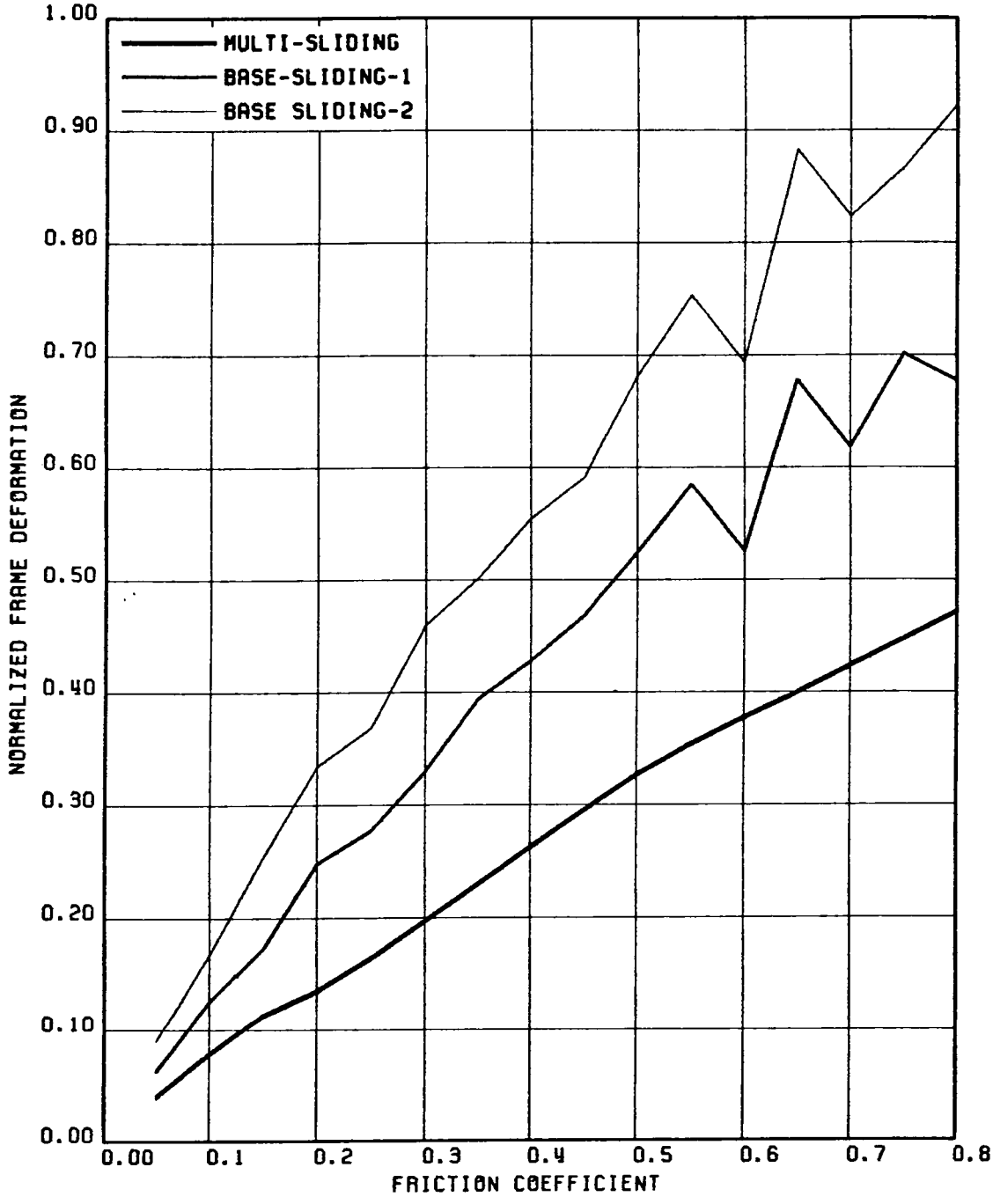

FIG. 5.15 COMPARISON OF NORMALIZED DEFORMATION AT SECOND FLOOR (NORMALIZED W.R.T. THE CORRESPONDING NON-SLIDING RESPONSE) FOR BASE SLIDING & MULTI-SLIDING CASES; STRUCTURE 1, GR MOTION 1-HZ & VT COMPONENT

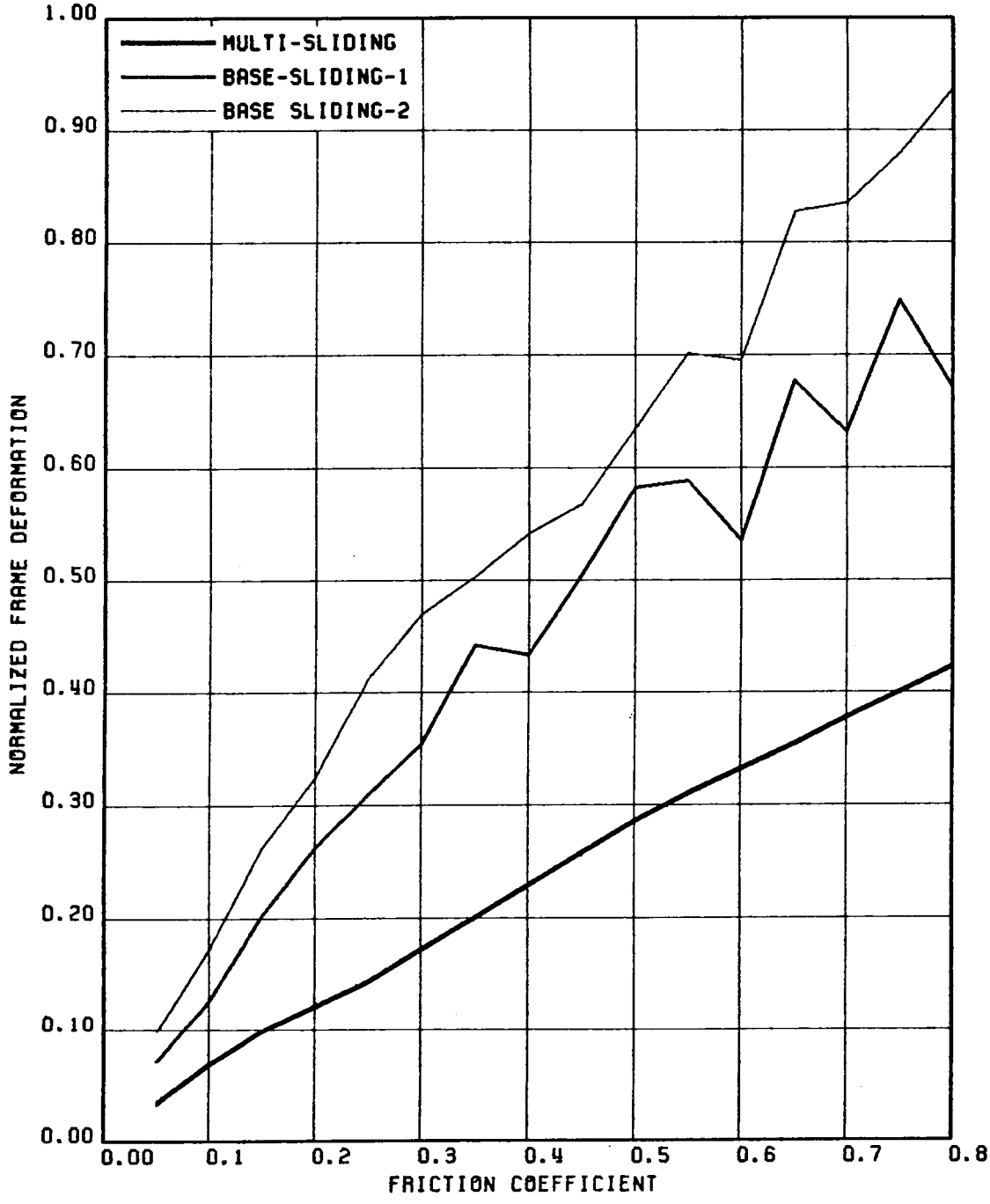

FIG. 5.16 COMPARISON OF NORMALIZED DEFORMATION AT THIRD FLOOR (NORMALIZED W.R.T. THE CORRESPONDING NON-SLIDING RESPONSE) FOR BASE SLIDING & MULTI-SLIDING CASES; STRUCTURE 1, GR MOTION 1-HZ & VT COMPONENT

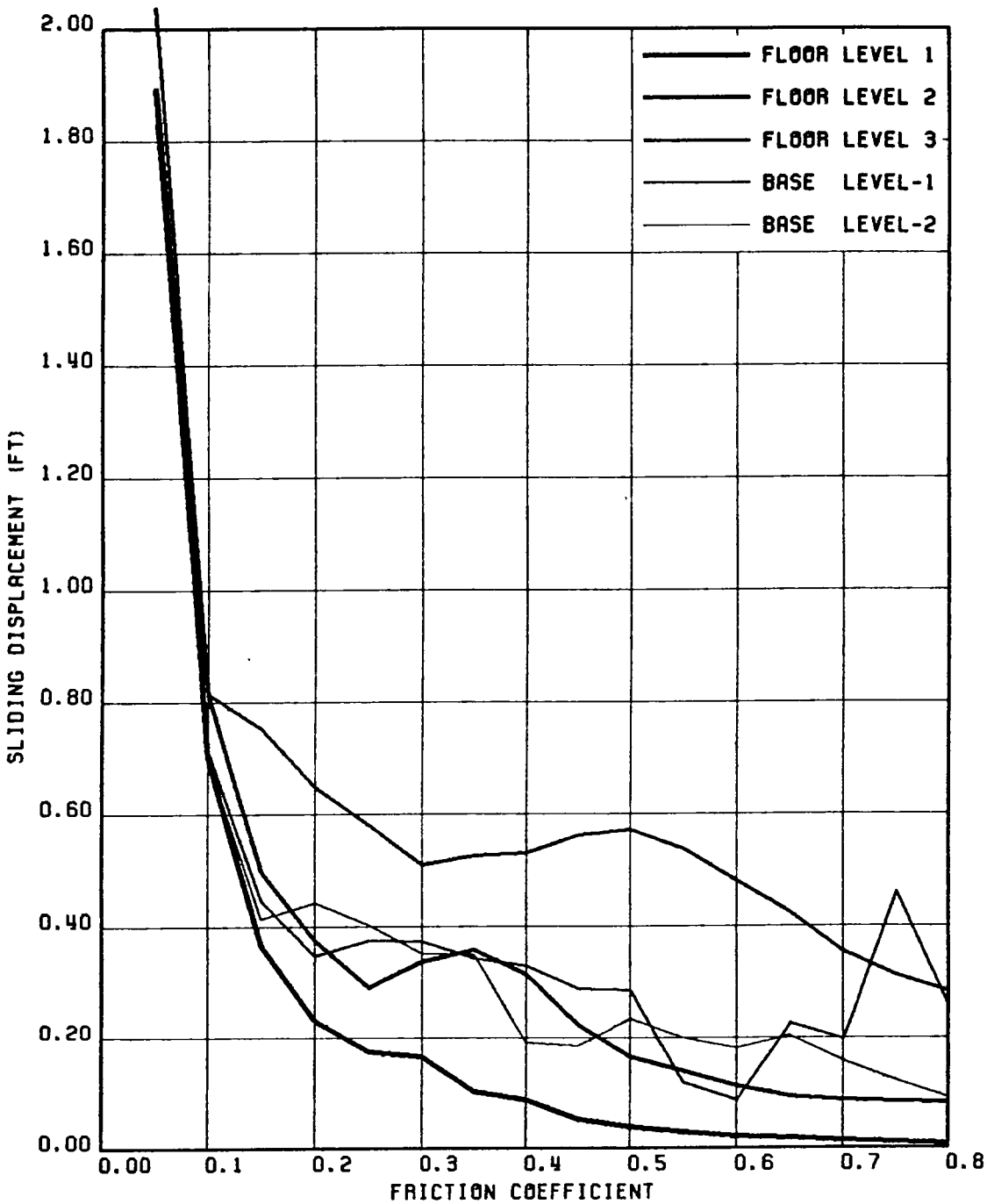

FIG. 5.17 COMPARISON OF MAXIMUM SLIDING DISPLACEMENTS FOR BASE SLIDING AND MULTI-SLIDING CASES; STRUCTURE 1, GR MOTION 1-HZ & VT COMPONENT

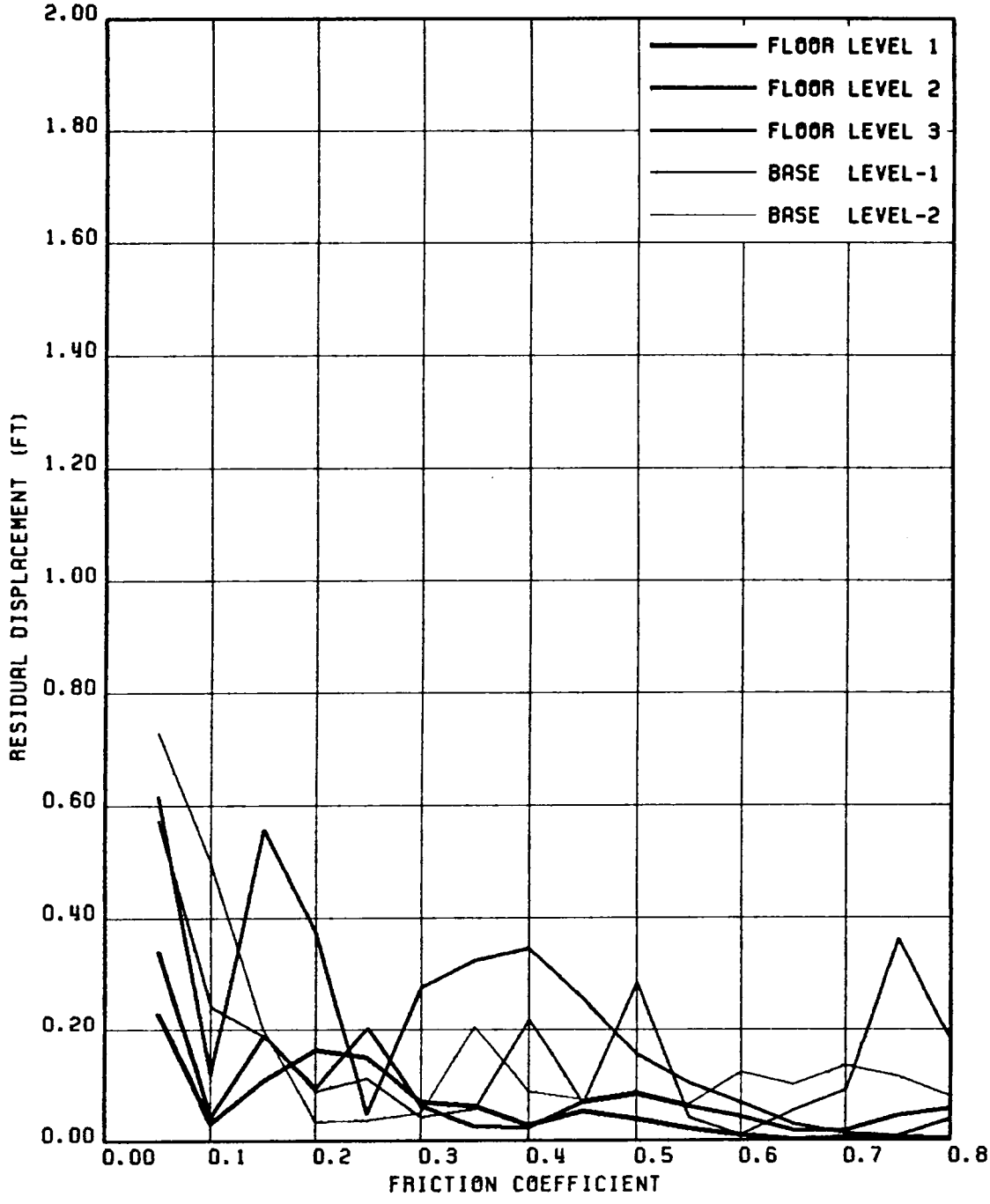

FIG. 5.18 COMPARISON OF RESIDUAL SLIDING DISPLACEMENTS FOR BASE SLIDING AND MULTI-SLIDING CASES; STRUCTURE 1, GR MOTION 1-HZ & VT COMPONENT

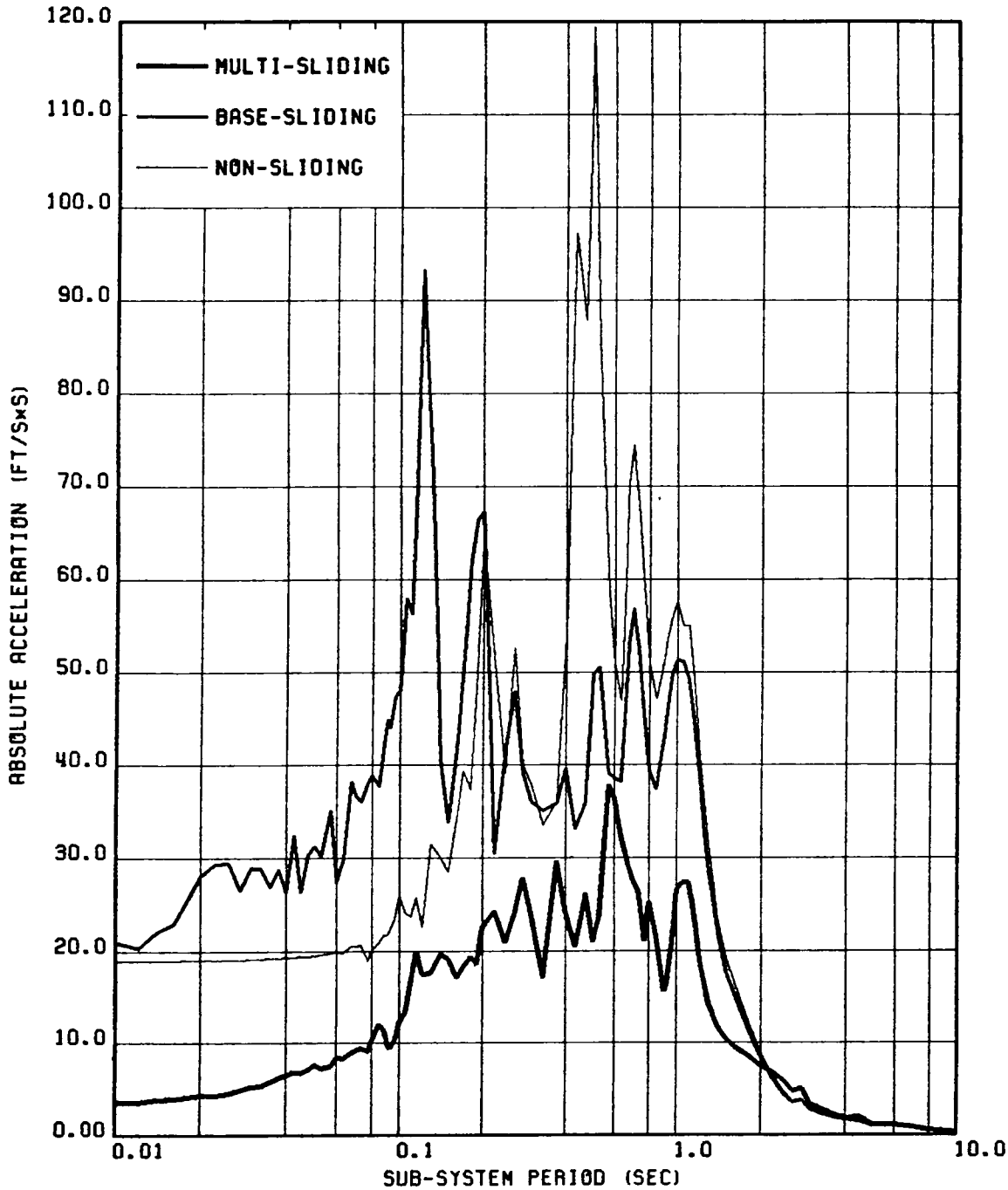

FIG. 5.19 SECONDARY FLOOR SPECTRA OF ABSOLUTE ACCELERATION FOR OSCILLATORS ON THE FIRST FLOOR; STRUCTURE 1, GR MOTION 3-HZ COMPONENT

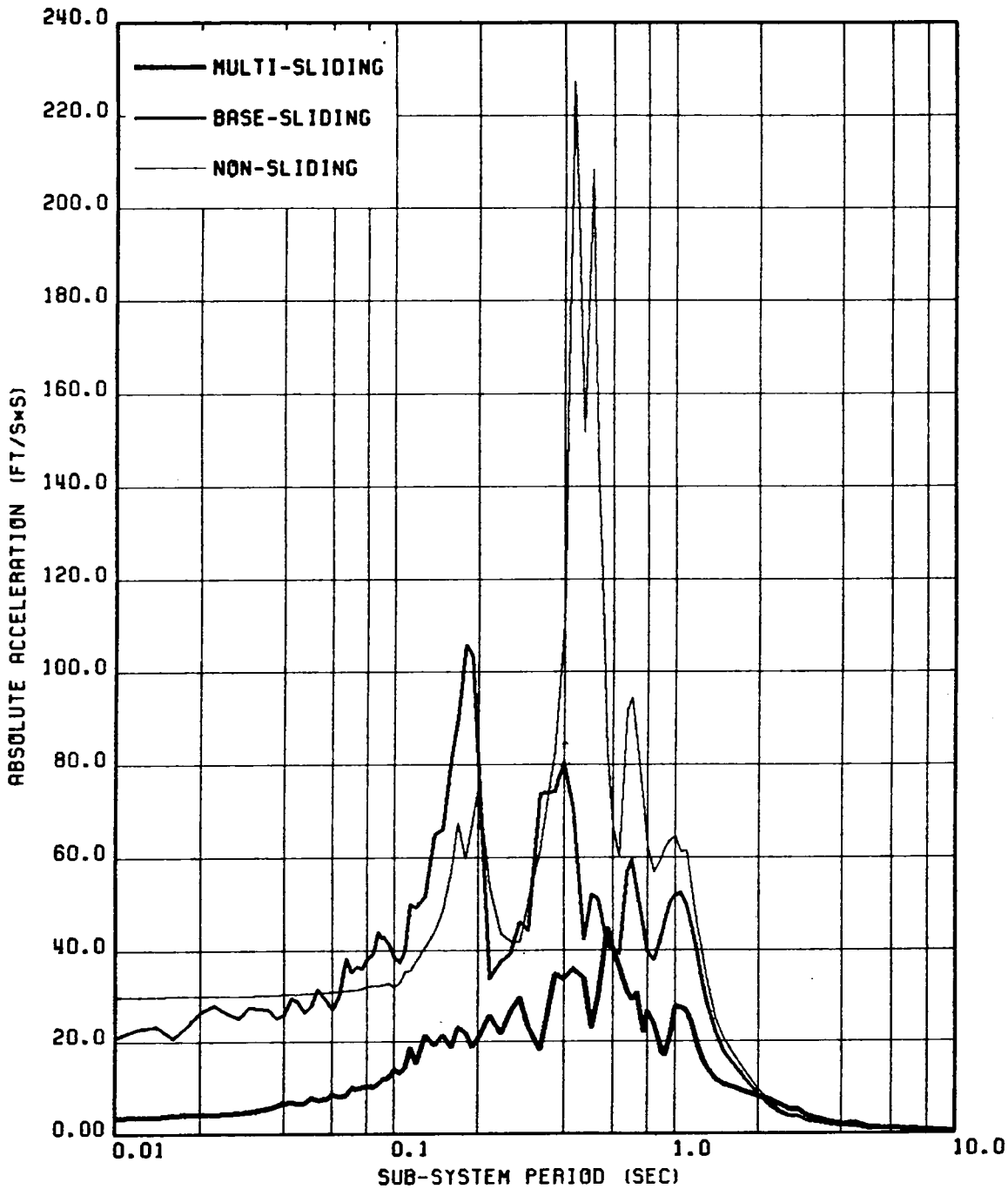

FIG. 5.20 SECONDARY FLOOR SPECTRA OF ABSOLUTE ACCELERATION FOR OSCILLATORS ON THE SECOND FLOOR; STRUCTURE 1, GR MOTION 3-HZ COMPONENT

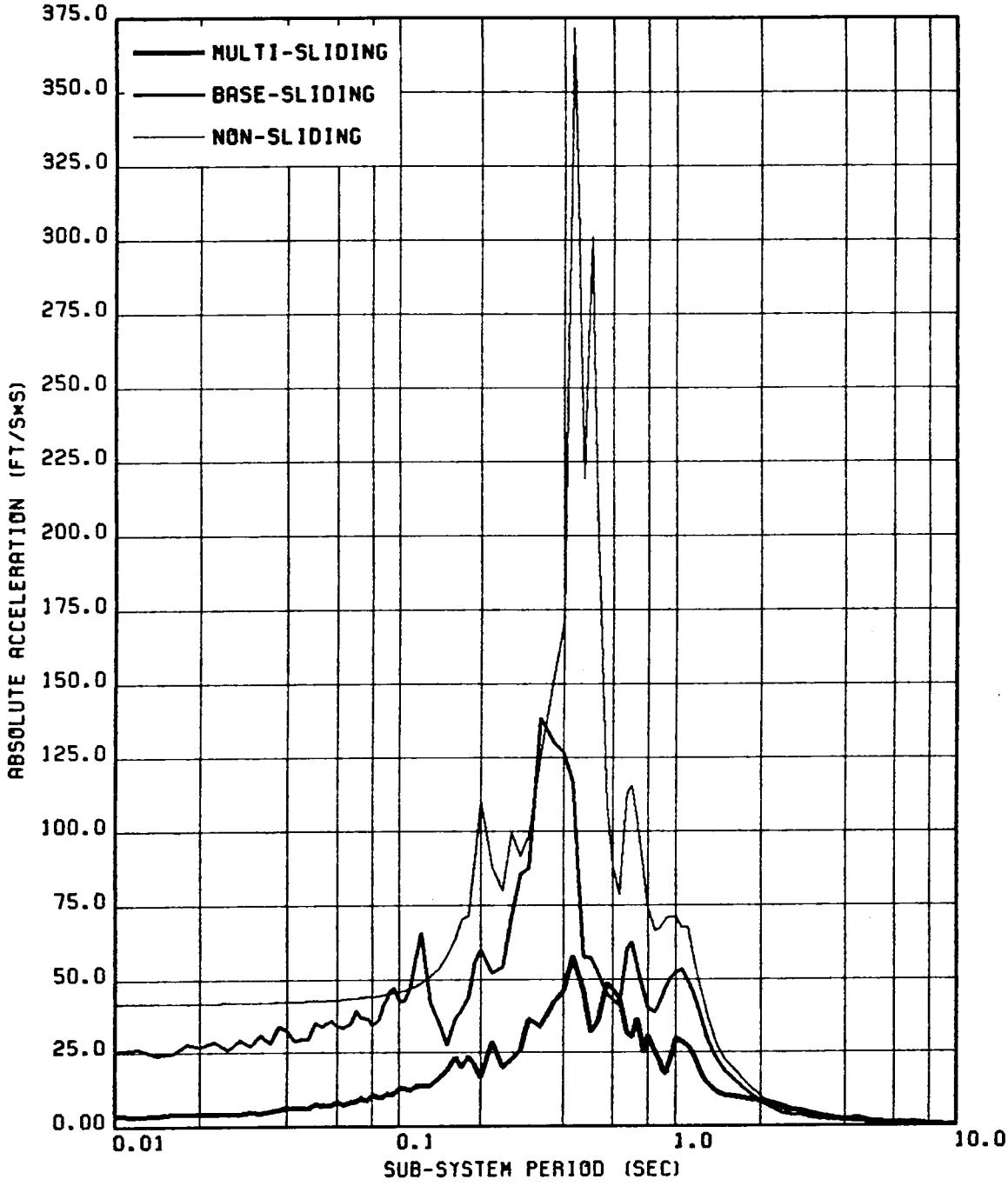

FIG. 5.21 SECONDARY FLOOR SPECTRA OF ABSOLUTE ACCELERATION FOR OSCILLATORS ON THE THIRD FLOOR; STRUCTURE 1, GR MOTION 3-HZ COMPONENT

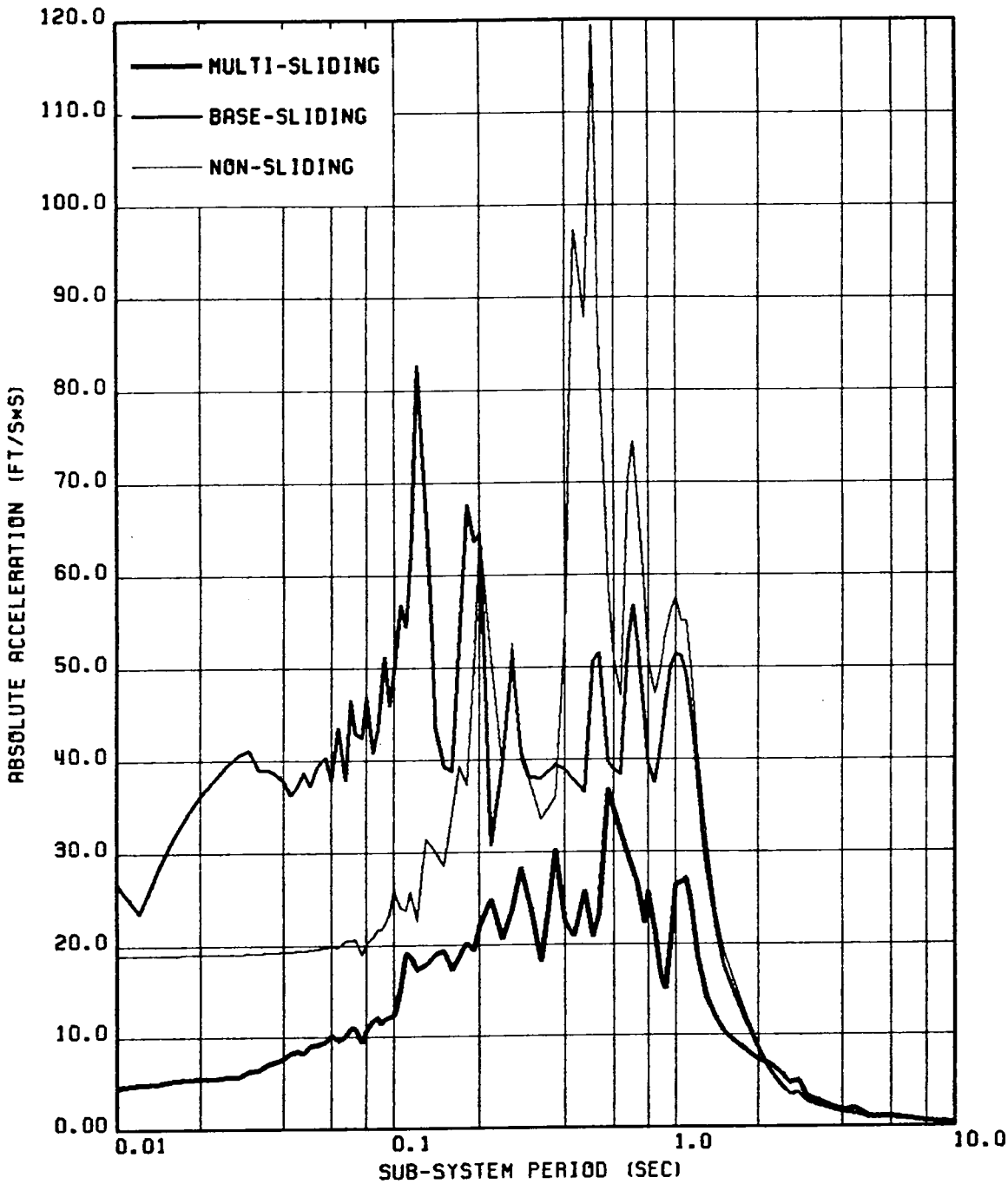

FIG. 5.22 SECONDARY FLOOR SPECTRA OF ABSOLUTE ACCELERATION FOR OSCILLATORS ON THE FIRST FLOOR; STRUCTURE 1, GR MOTION 3-HZ & VT COMPONENT

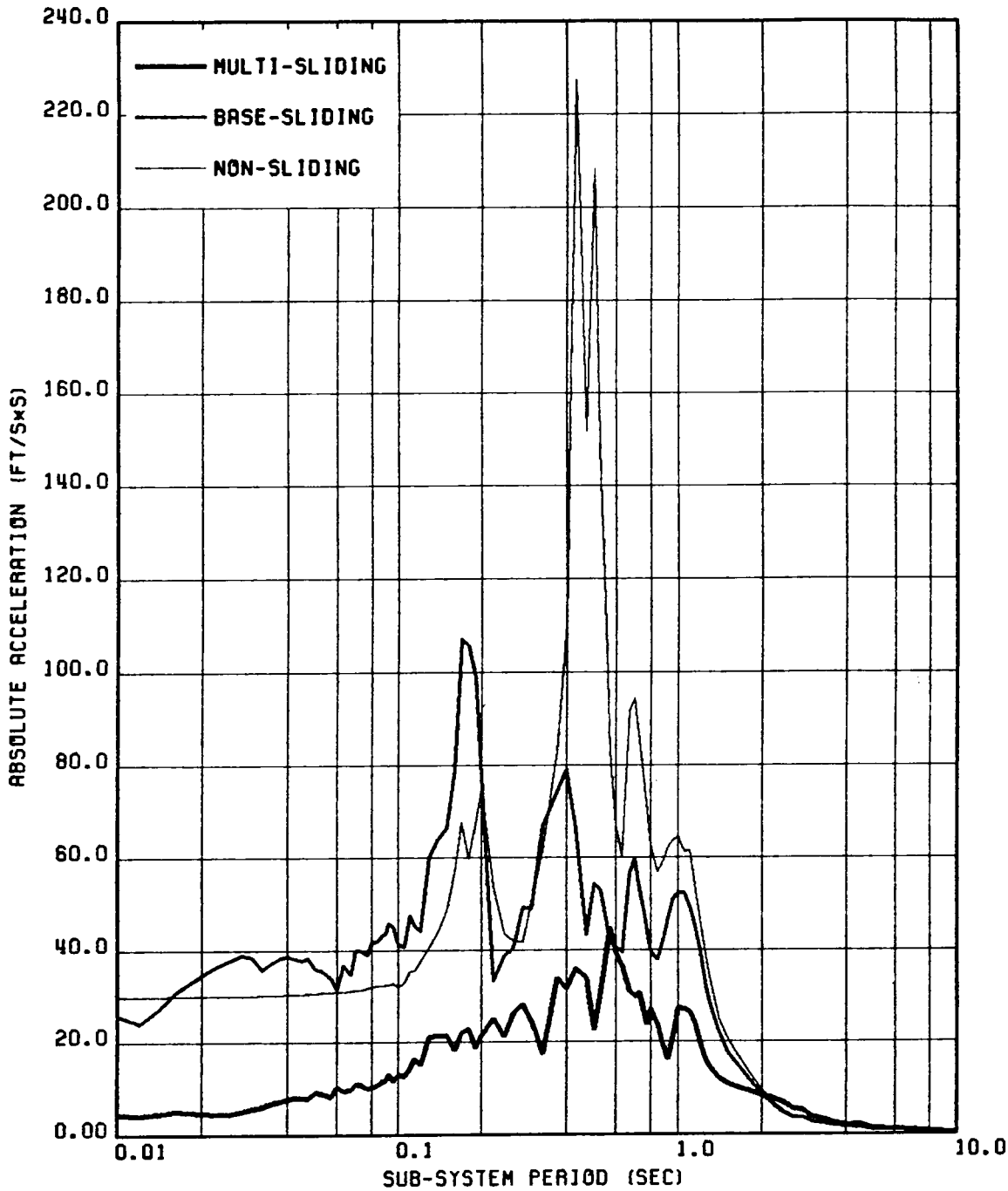

FIG. 5.23 SECONDARY FLOOR SPECTRA OF ABSOLUTE ACCELERATION FOR OSCILLATORS ON THE SECOND FLOOR; STRUCTURE 1, GR MOTION 3-HZ & VT COMPONENT

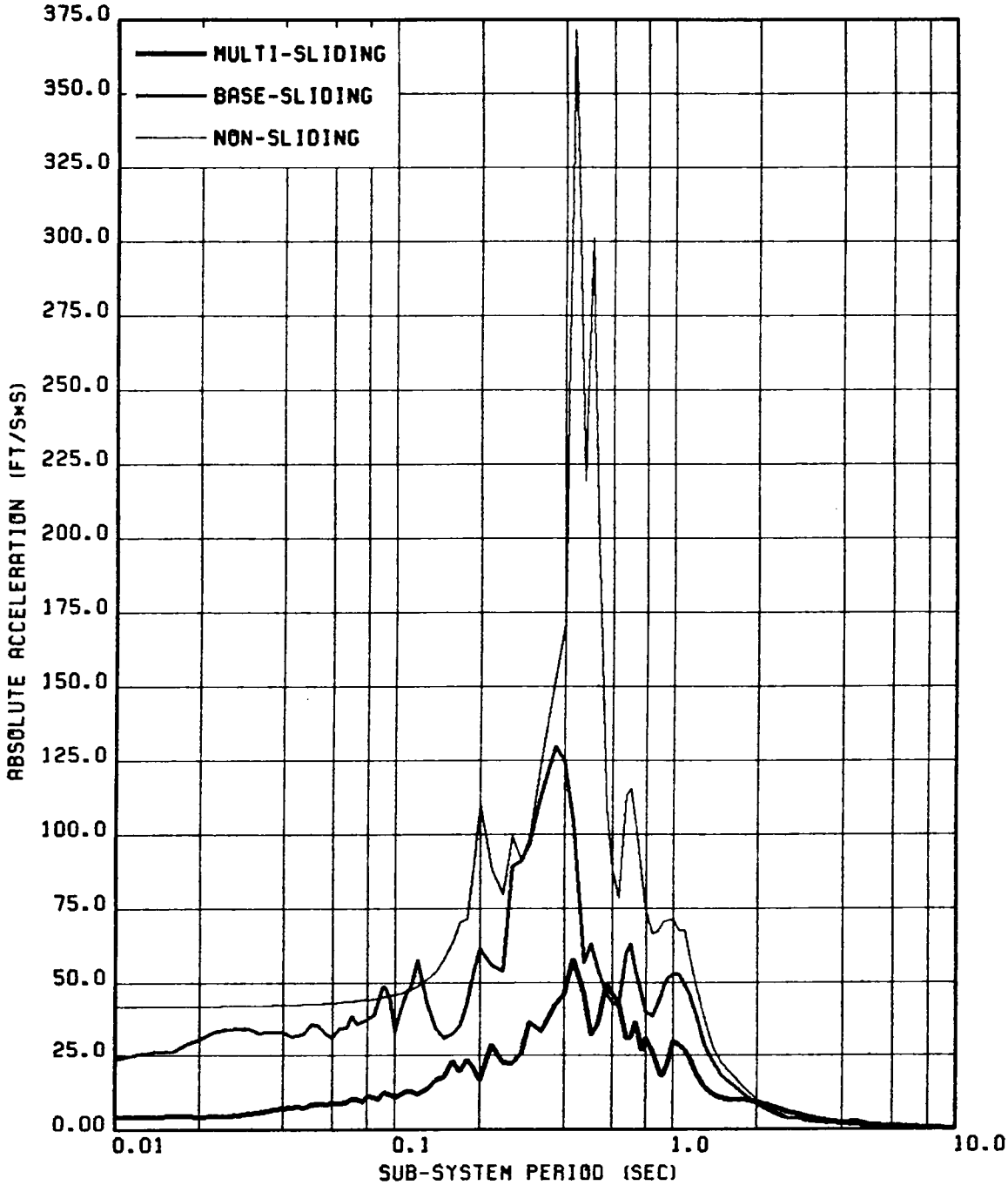

FIG. 5.24 SECONDARY FLOOR SPECTRA OF ABSOLUTE ACCELERATION FOR OSCILLATORS ON THE THIRD FLOOR; STRUCTURE 1, GR MOTION 3-HZ & VT COMPONENT

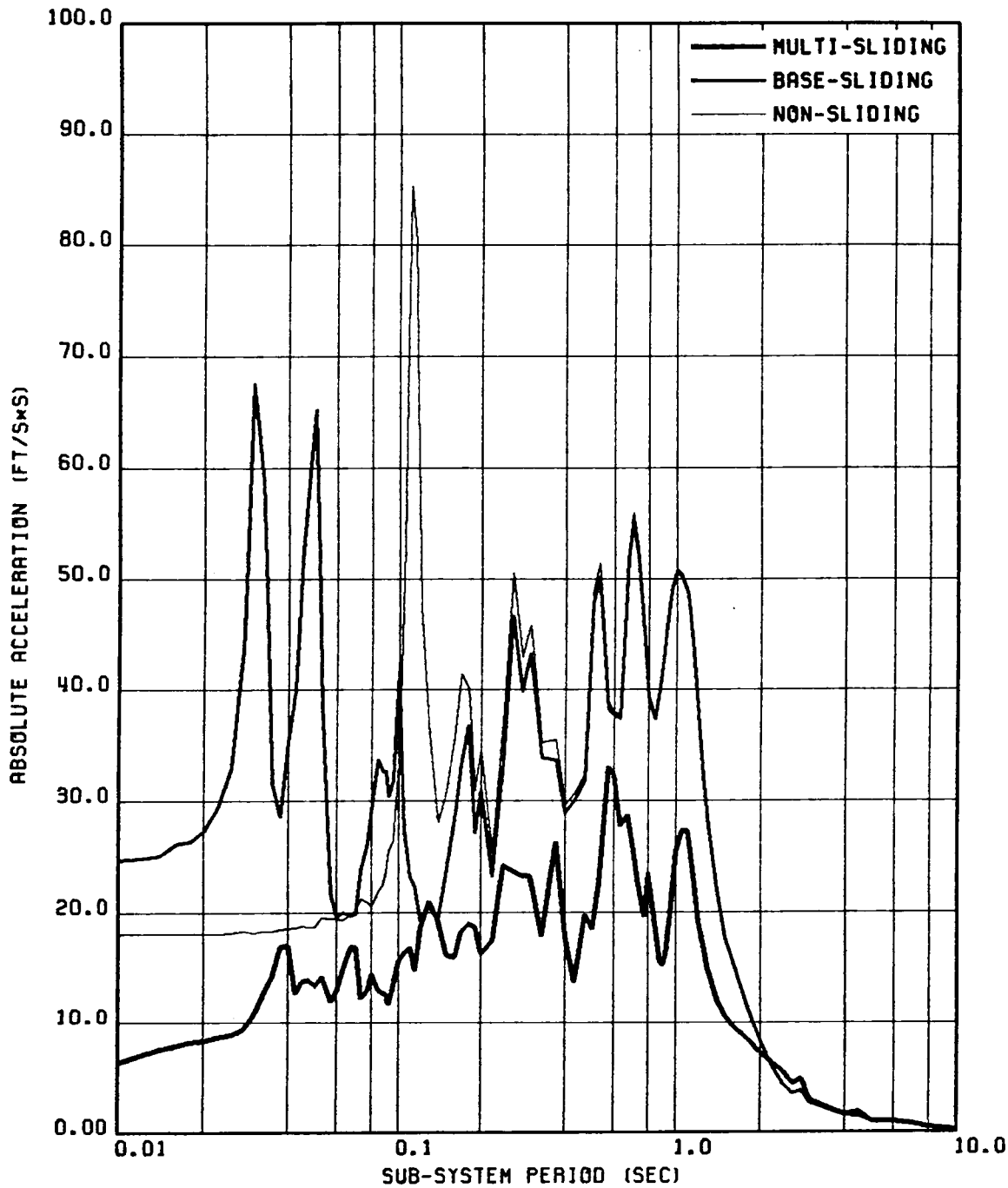

FIG. 5.25 SECONDARY FLOOR SPECTRA OF ABSOLUTE ACCELERATION FOR OSCILLATORS ON THE FIRST FLOOR; STRUCTURE 2, GR MOTION 3-HZ COMPONENT

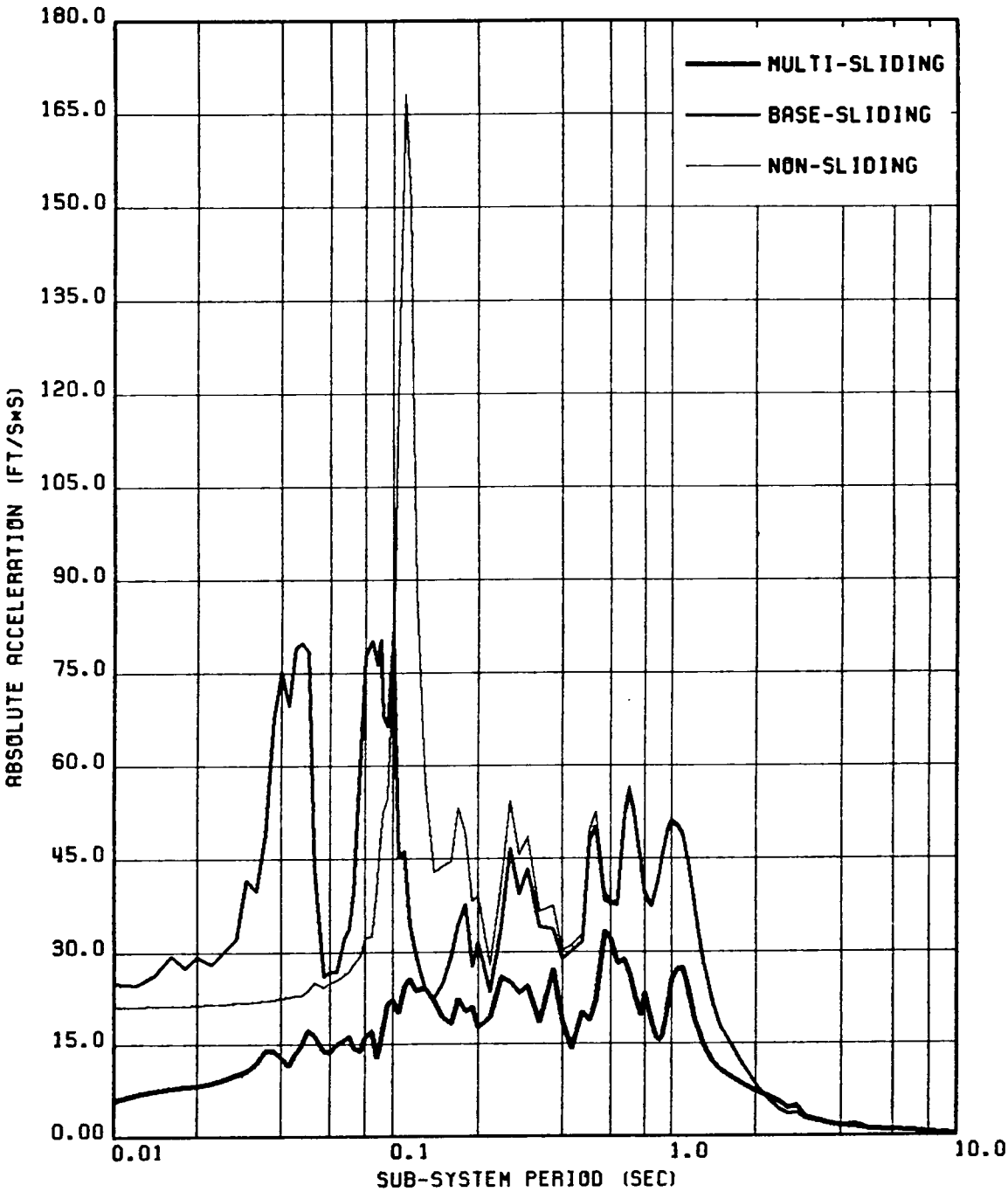

FIG. 5.26 SECONDARY FLOOR SPECTRA OF ABSOLUTE ACCELERATION FOR OSCILLATORS ON THE SECOND FLOOR; STRUCTURE 2, GR MOTION 3-HZ COMPONENT

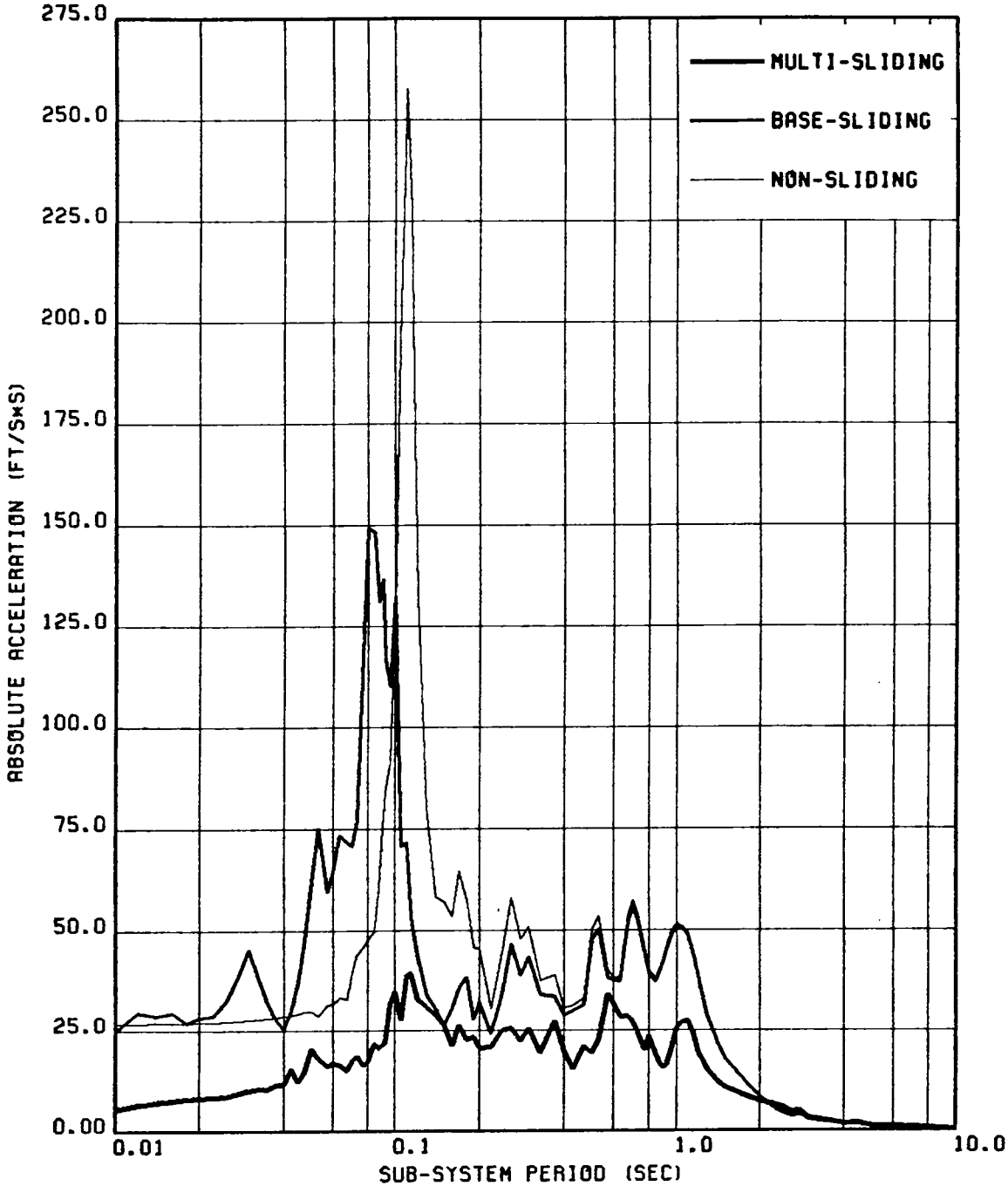

FIG. 5.27 SECONDARY FLOOR SPECTRA OF ABSOLUTE ACCELERATION FOR OSCILLATORS ON THE THIRD FLOOR; STRUCTURE 2, GR MOTION 3-HZ COMPONENT

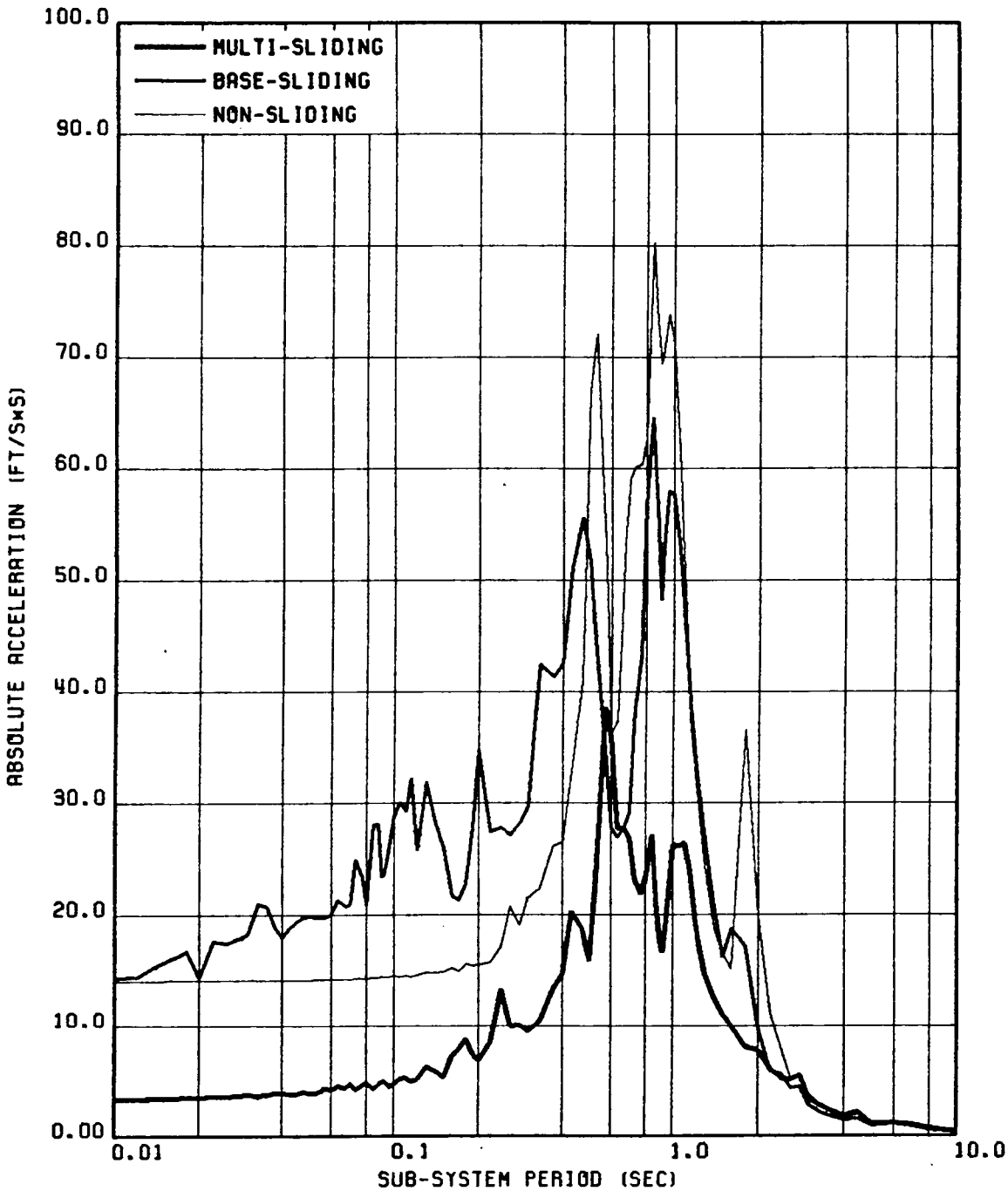

FIG. 5.28 SECONDARY FLOOR SPECTRA OF ABSOLUTE ACCELERATION FOR OSCILLATORS ON THE FIRST FLOOR; STRUCTURE 3, GR MOTION 3-HZ COMPONENT

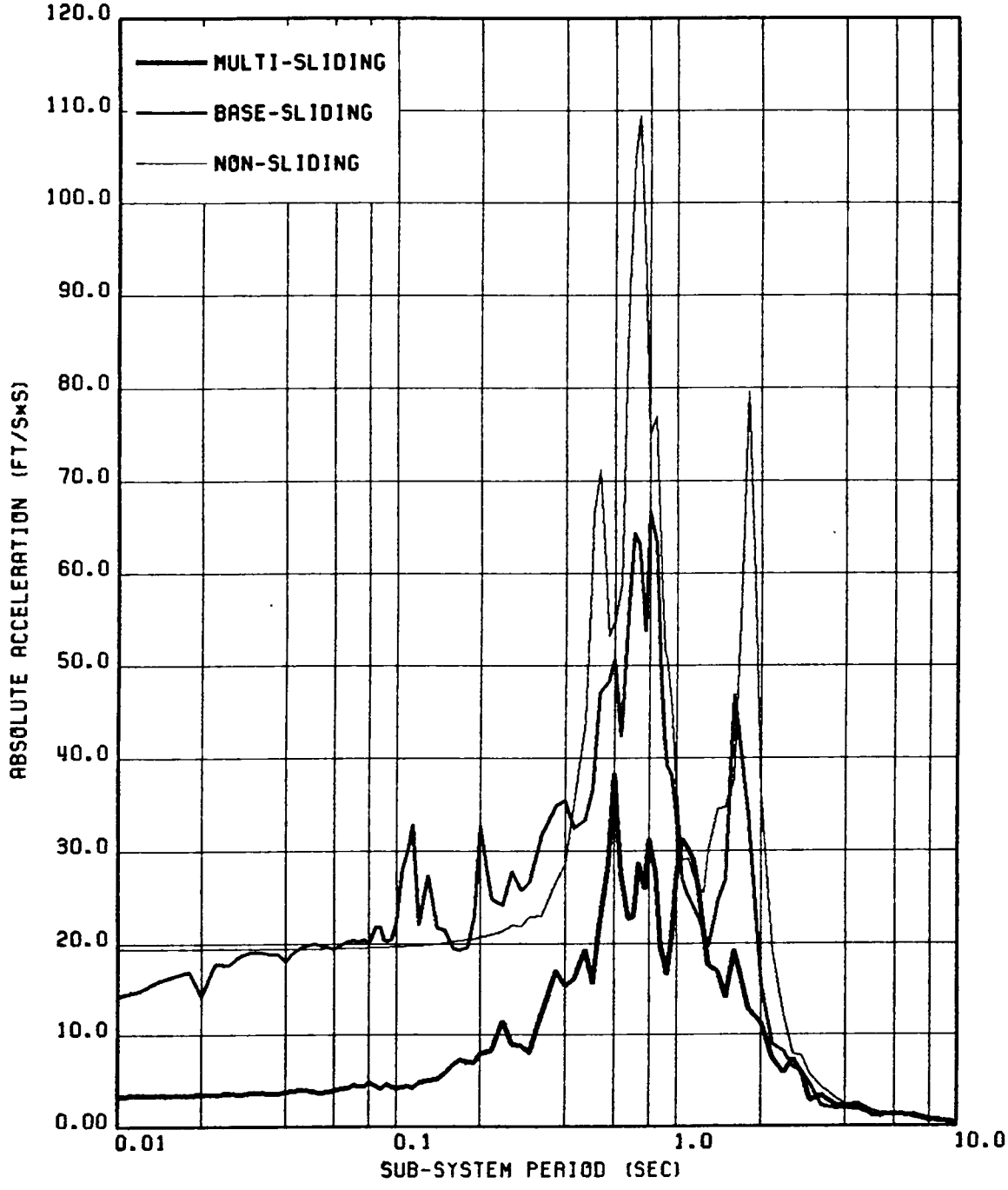

FIG. 5.29 SECONDARY FLOOR SPECTRA OF ABSOLUTE ACCELERATION FOR OSCILLATORS ON THE SECOND FLOOR; STRUCTURE 3, GR MOTION 3-HZ COMPONENT

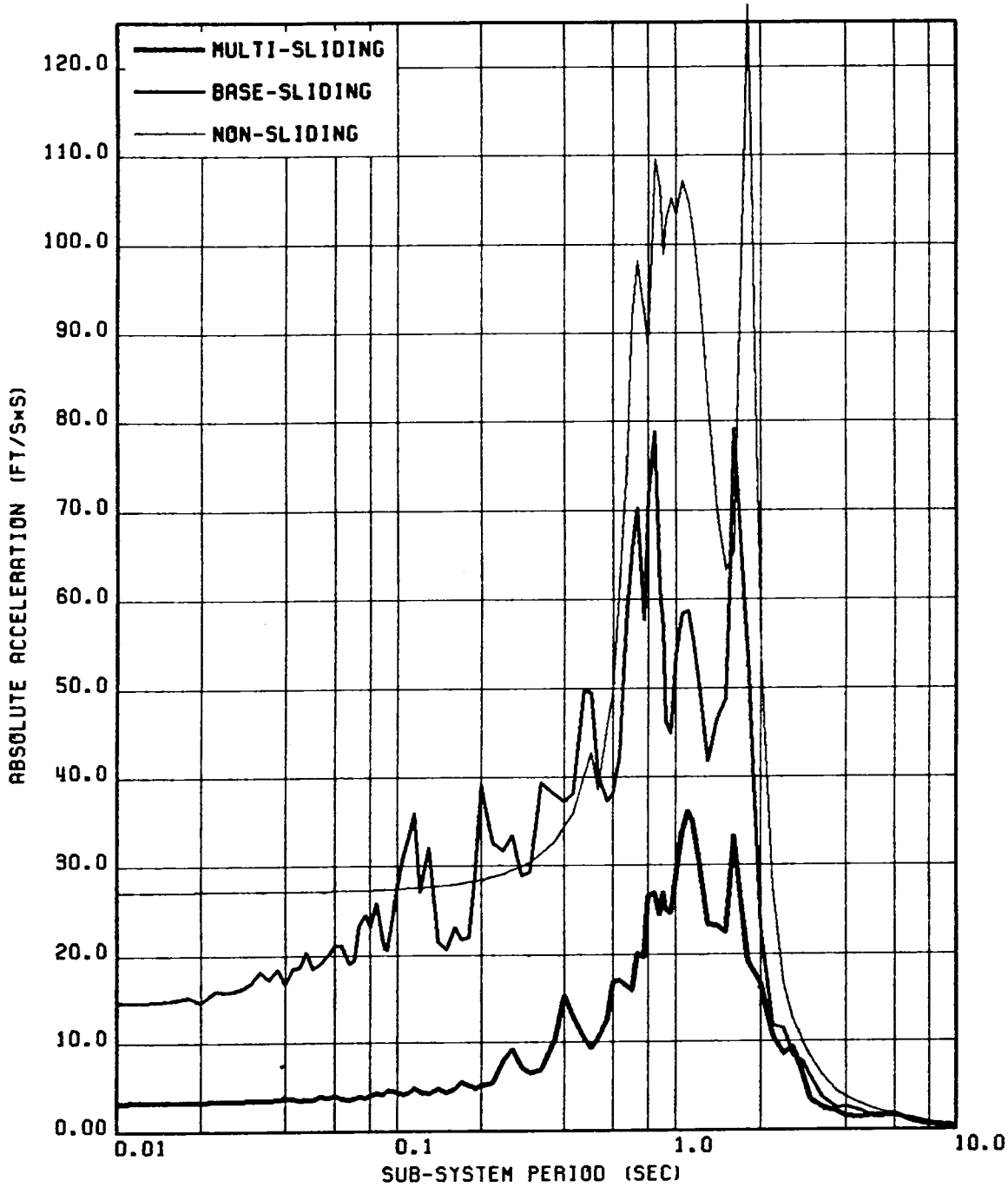

FIG. 5.30 SECONDARY FLOOR SPECTRA OF ABSOLUTE ACCELERATION FOR OSCILLATORS ON THE THIRD FLOOR; STRUCTURE 3, GR MOTION 3-HZ COMPONENT

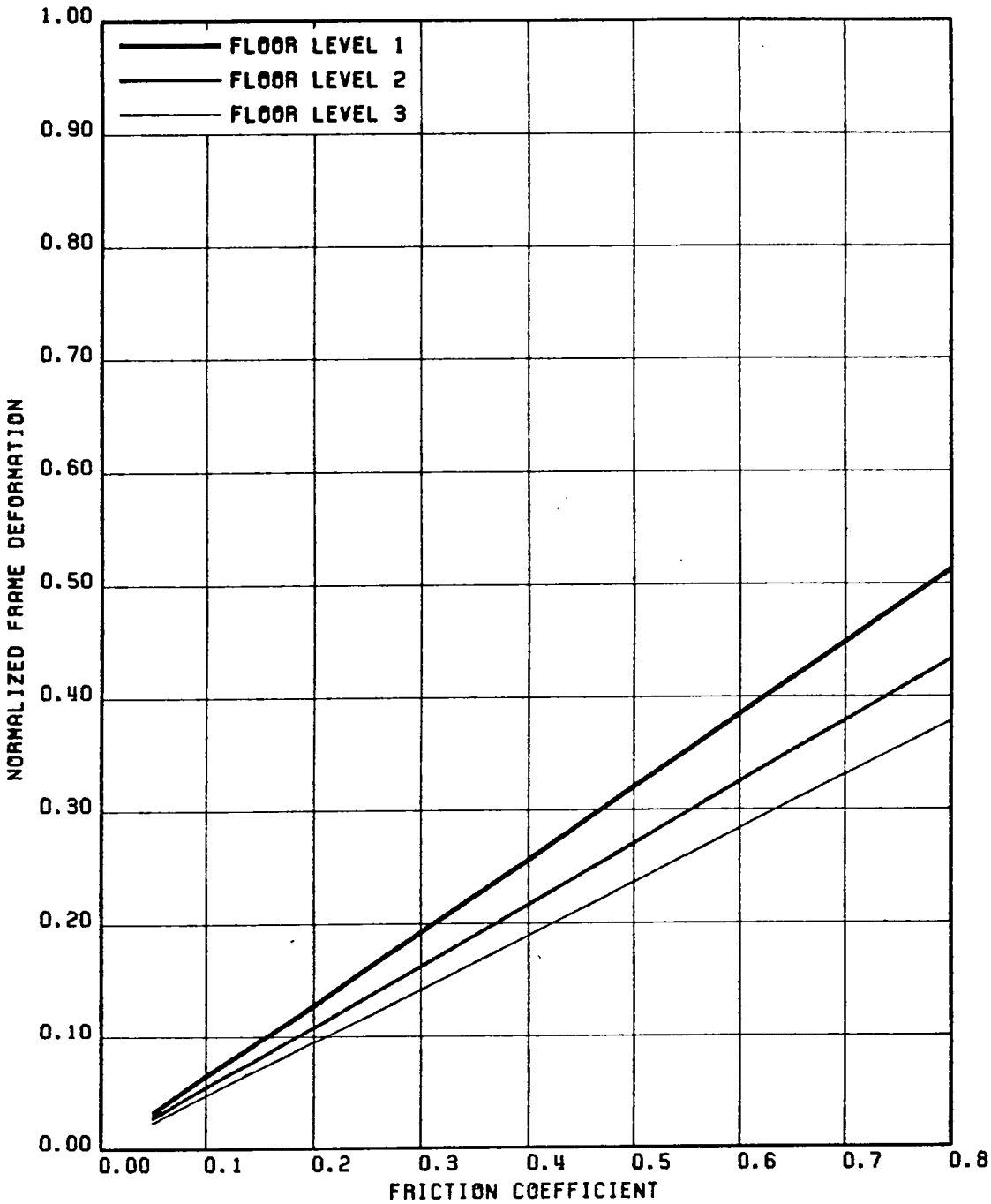

FIG. 5.31 VARIATION OF NORMALIZED FRAME DEFORMATION (NORMALIZED W.R.T. THE CORRESPONDING NON-SLIDING DEFORMATION RESPONSE) WITH THE UNIFORM FRICTION COEFFICIENT; STRUCTURE 1, GR MOTION 1-HZ COMPONENT

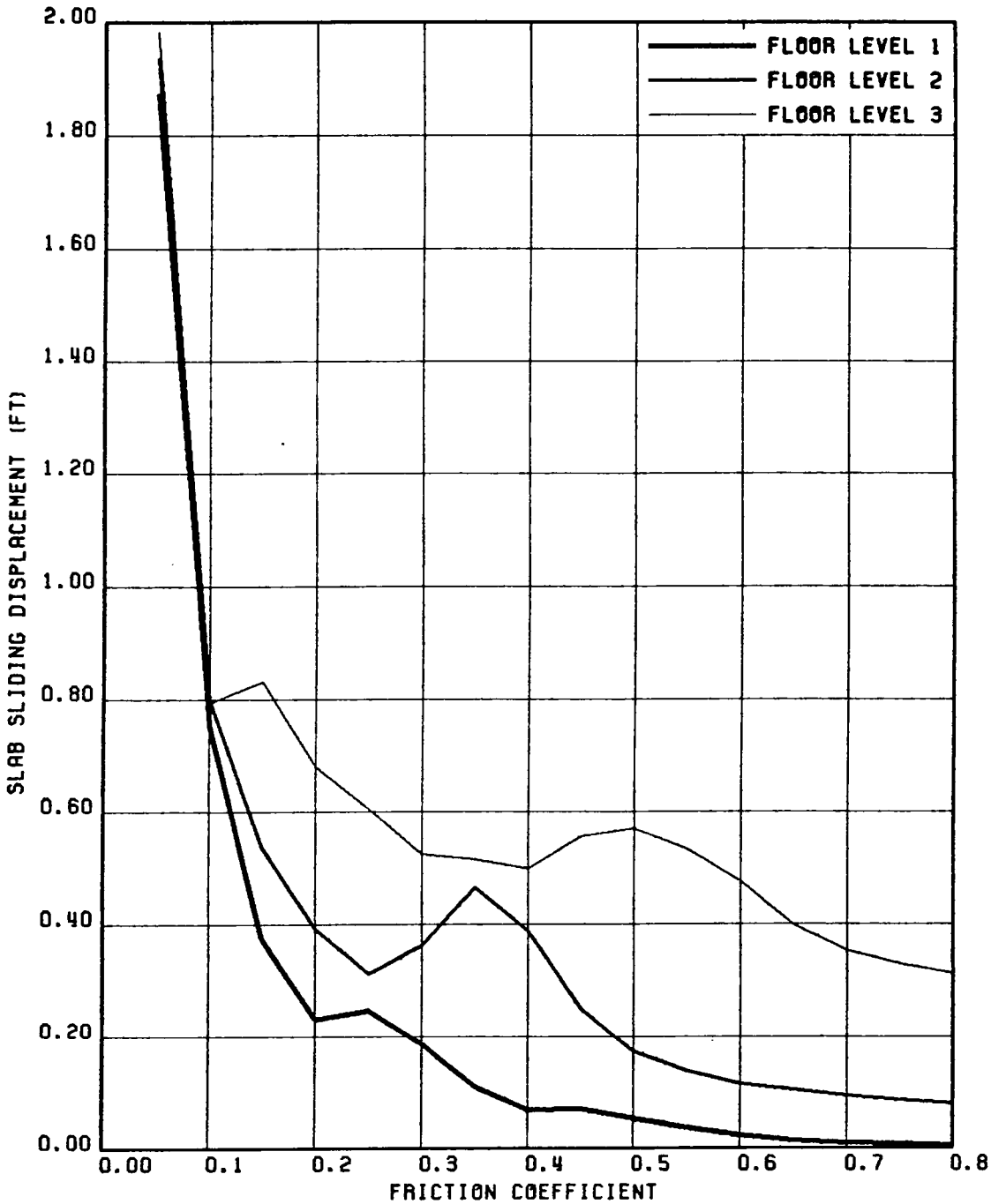

FIG. 5.32 VARIATION OF MAXIMUM SLAB SLIDING DISPLACEMENTS WITH THE UNIFORM FRICTION COEFFICIENT; STRUCTURE 1, GR MOTION 1-HZ COMPONENT

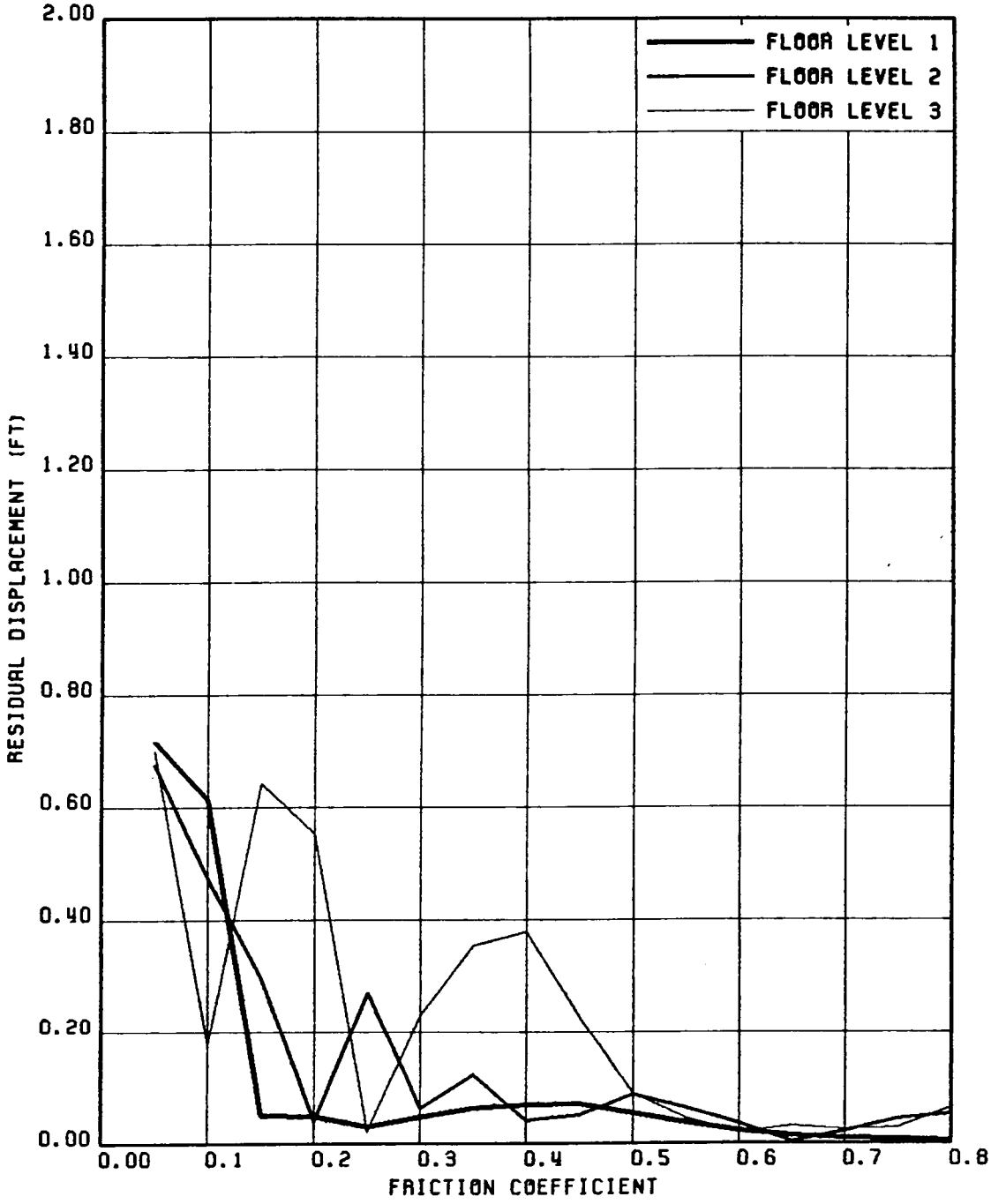

FIG. 5.33 VARIATION OF RESIDUAL SLAB SLIDING DISPLACEMENTS WITH THE UNIFORM FRICTION COEFFICIENT; STRUCTURE 1, GR MOTION 1-HZ COMPONENT

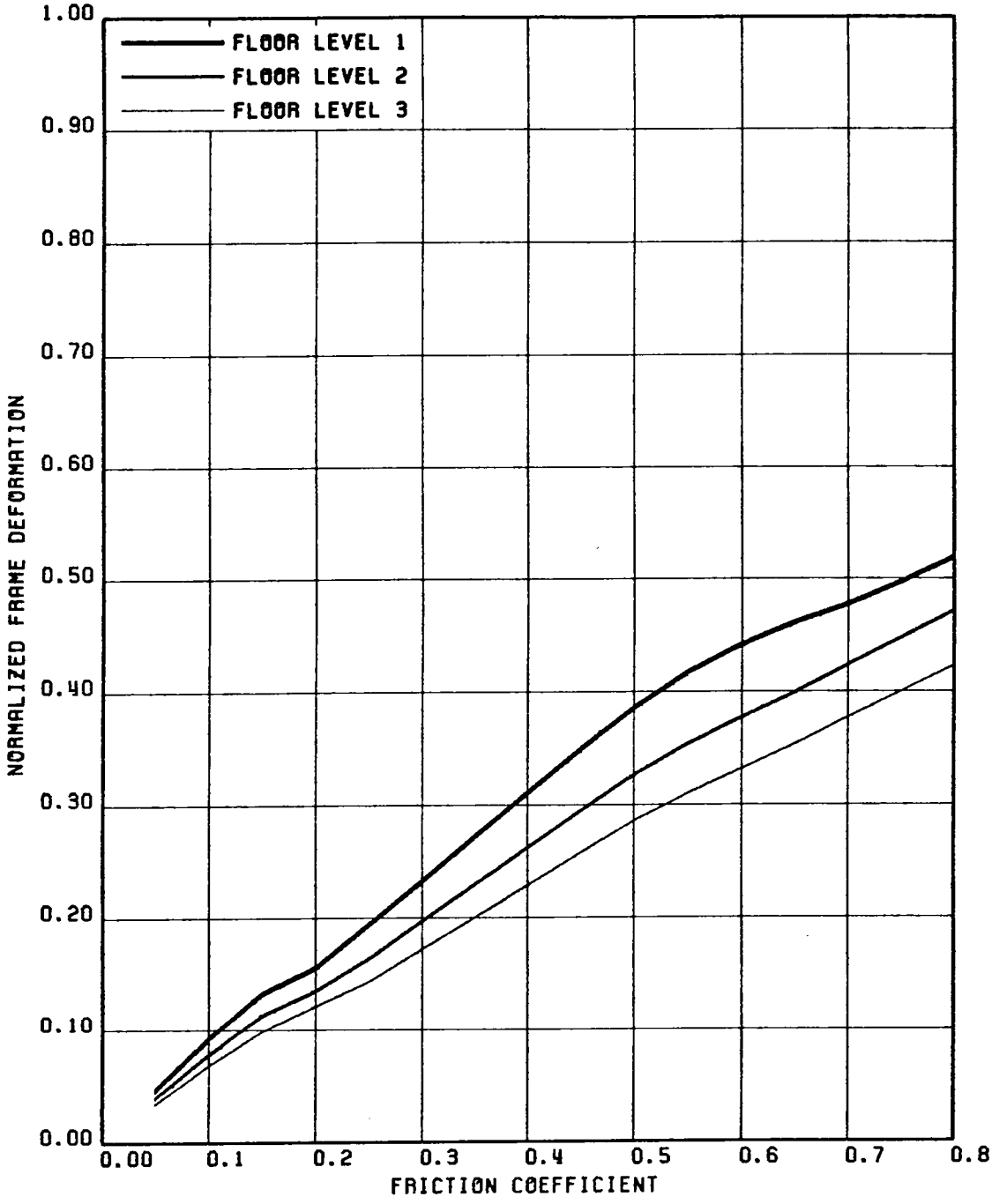

FIG. 5.34 VARIATION OF NORMALIZED FRAME DEFORMATION (NORMALIZED W.R.T. THE CORRESPONDING NON-SLIDING DEFORMATION RESPONSE) WITH THE UNIFORM FRICTION COEFFICIENT; STRUCTURE 1, GR MOTION 1-HZ & VT COMPONENT

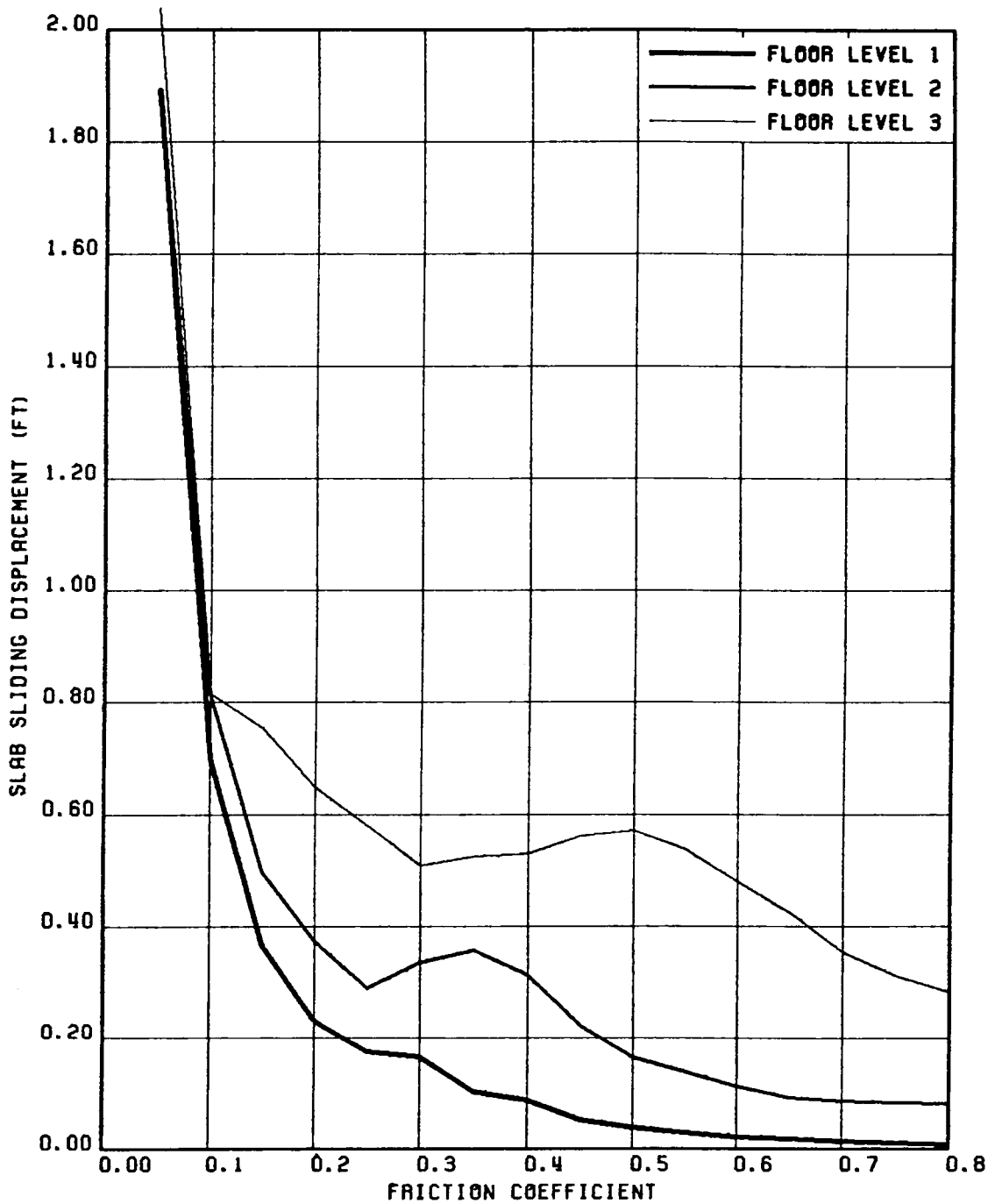

FIG. 5.35 VARIATION OF MAXIMUM SLAB SLIDING DISPLACEMENTS WITH THE UNIFORM FRICTION COEFFICIENT; STRUCTURE 1, GR MOTION 1-HZ & VT COMPONENT

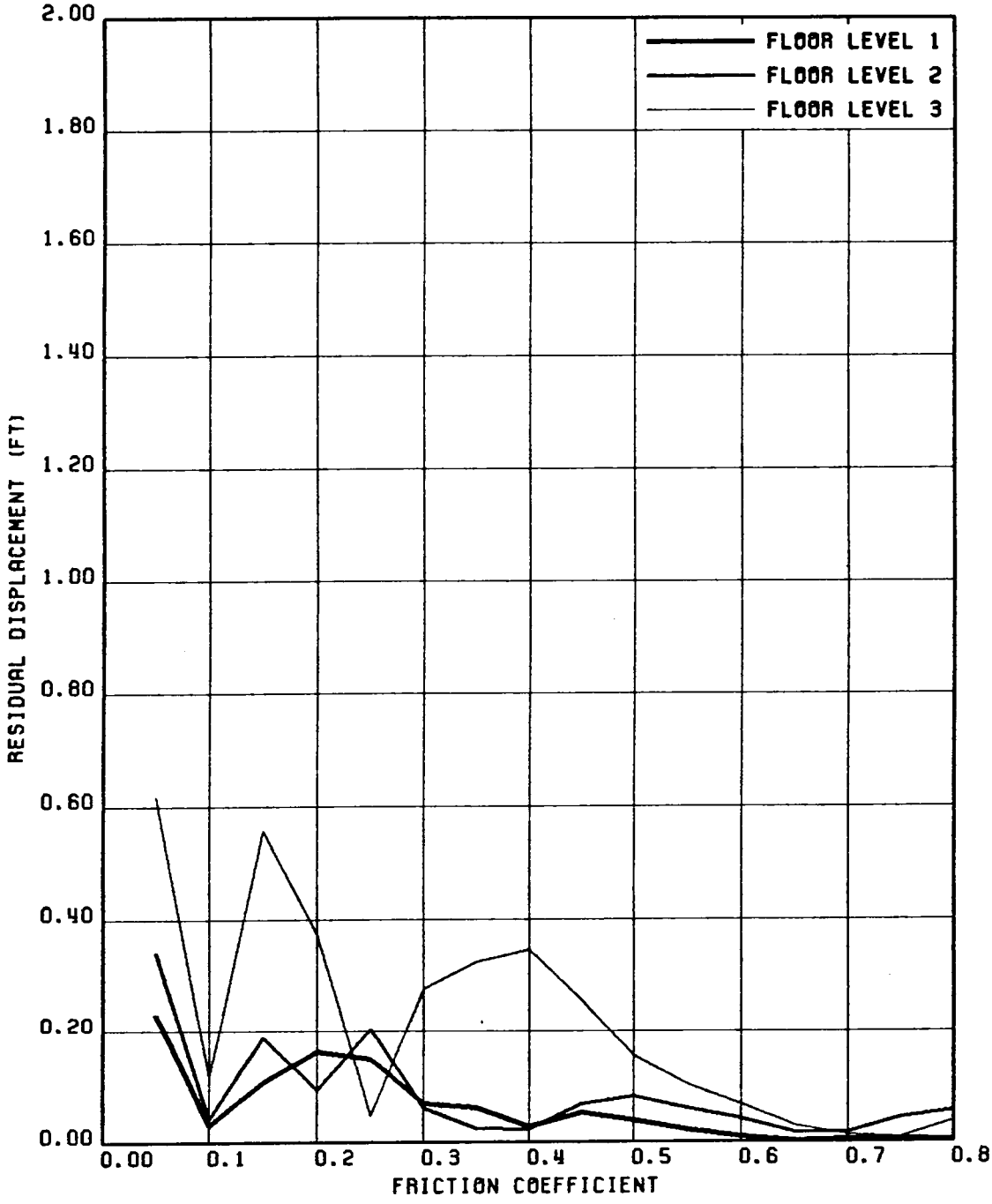

FIG. 5.36 VARIATION OF RESIDUAL SLAB SLIDING DISPLACEMENTS WITH THE UNIFORM FRICTION COEFFICIENT; STRUCTURE 1, GR MOTION 1-HZ & VT COMPONENT

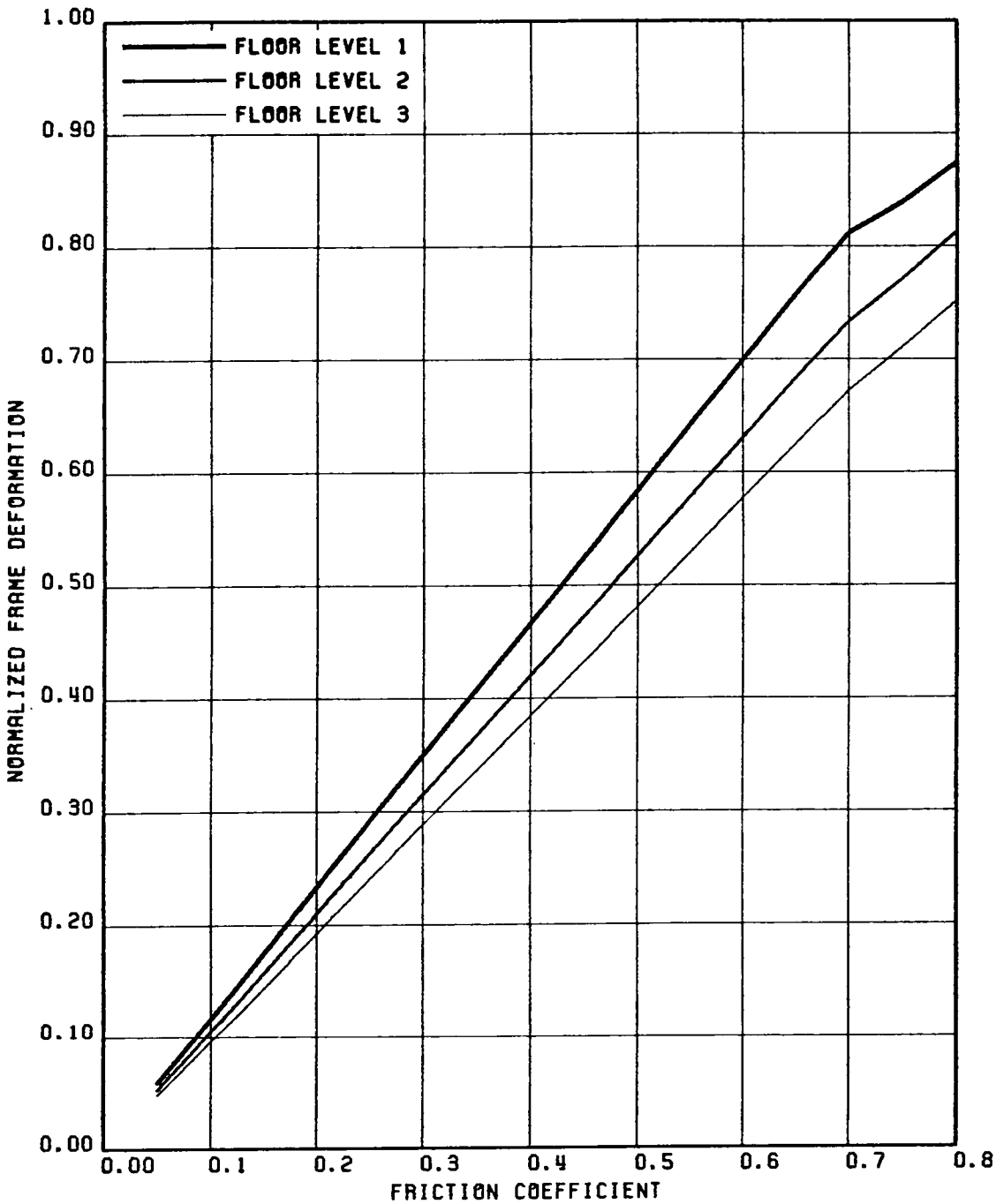

FIG. 5.37 VARIATION OF NORMALIZED FRAME DEFORMATION (NORMALIZED W.R.T. THE CORRESPONDING NON-SLIDING DEFORMATION RESPONSE) WITH THE UNIFORM FRICTION COEFFICIENT; STRUCTURE 2, GR MOTION 1-HZ COMPONENT

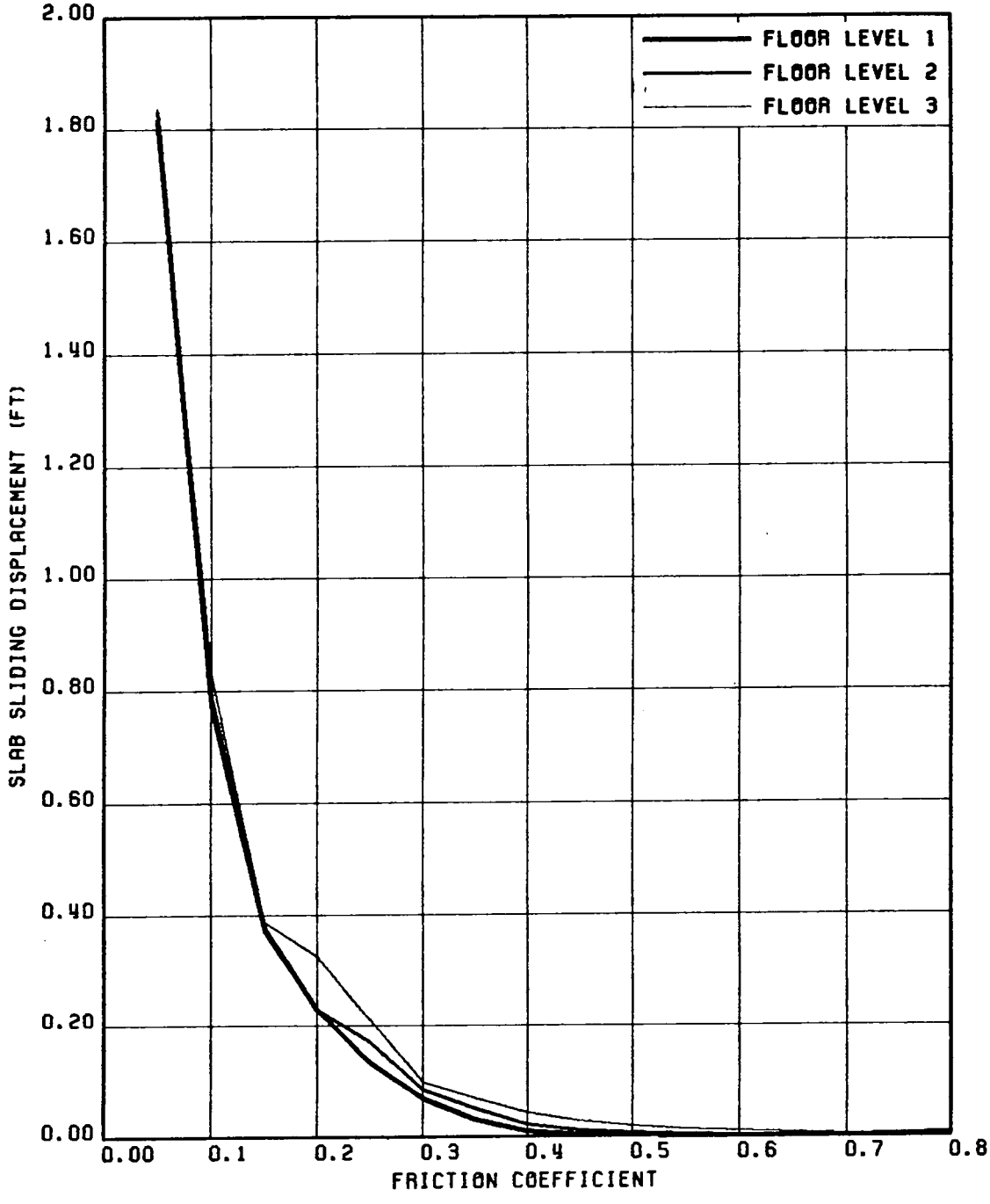

FIG. 5.38 VARIATION OF MAXIMUM SLAB SLIDING DISPLACEMENTS WITH THE UNIFORM FRICTION COEFFICIENT; STRUCTURE 2, GR MOTION 1-HZ COMPONENT

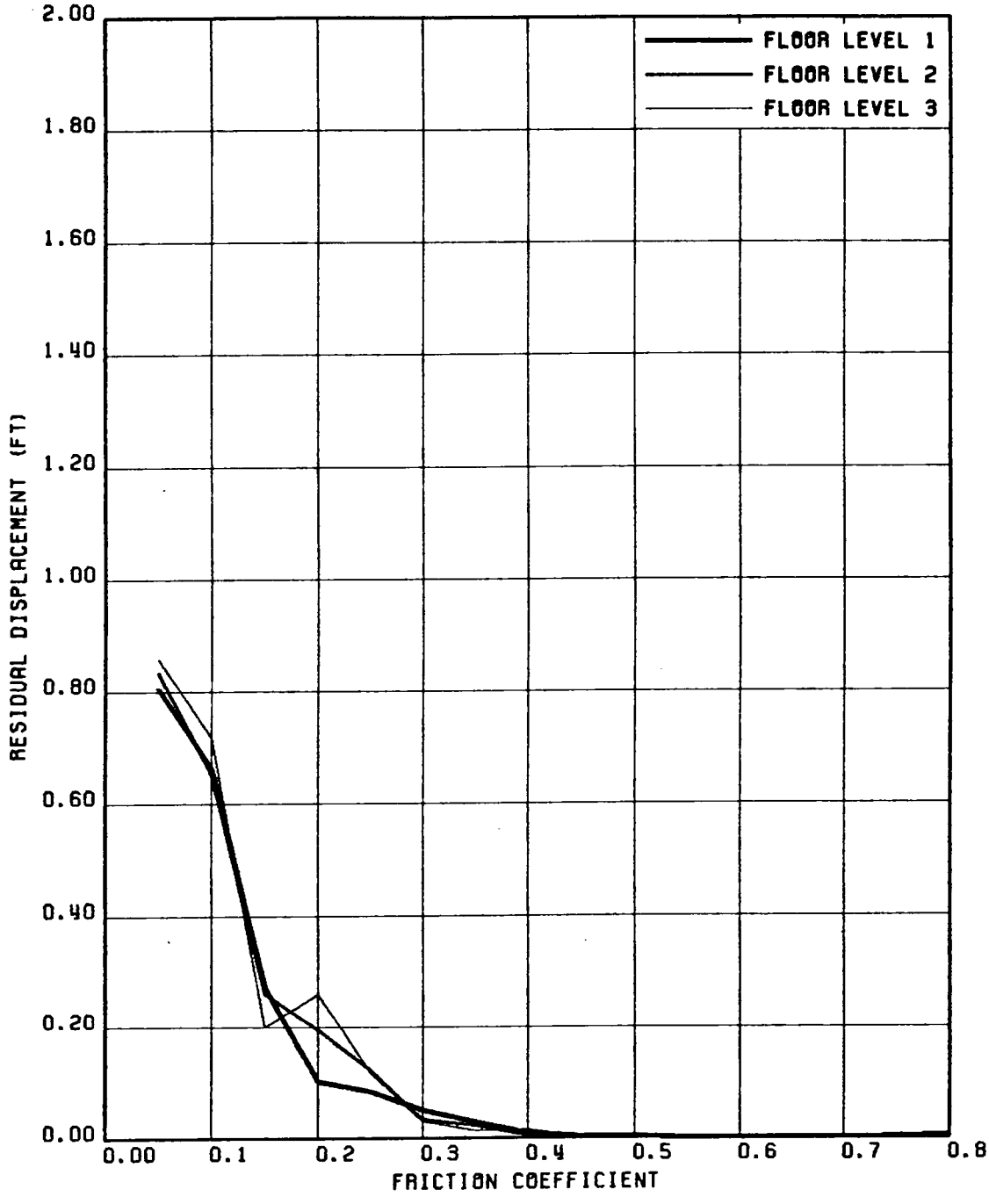

FIG. 5.39 VARIATION OF RESIDUAL SLAB SLIDING DISPLACEMENTS WITH THE UNIFORM FRICTION COEFFICIENT; STRUCTURE 2, GR MOTION 1-HZ COMPONENT

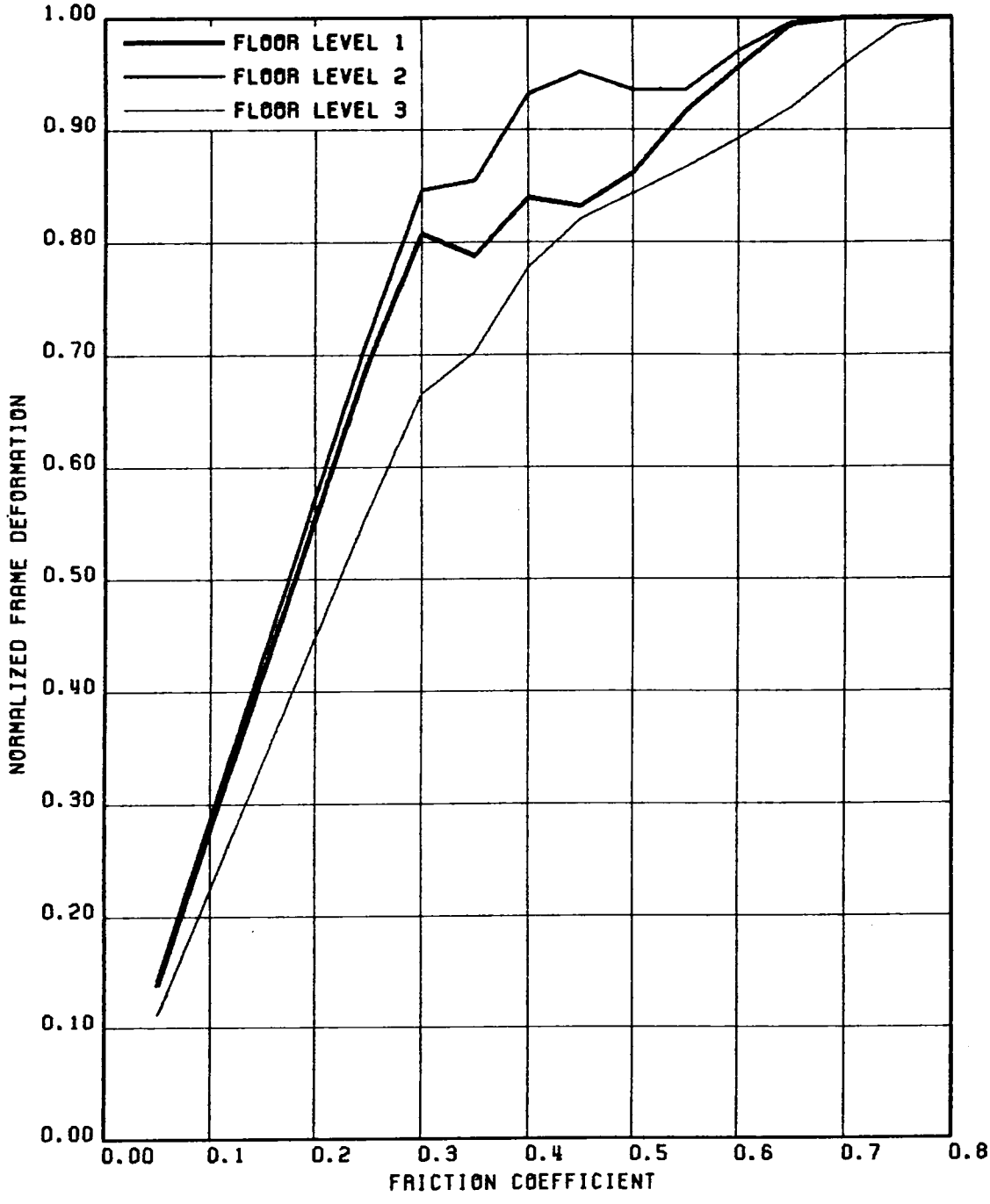

FIG. 5.40 VARIATION OF NORMALIZED FRAME DEFORMATION (NORMALIZED W.R.T. THE CORRESPONDING NON-SLIDING DEFORMATION RESPONSE) WITH THE UNIFORM FRICTION COEFFICIENT; STRUCTURE 3, GR MOTION 1-HZ COMPONENT

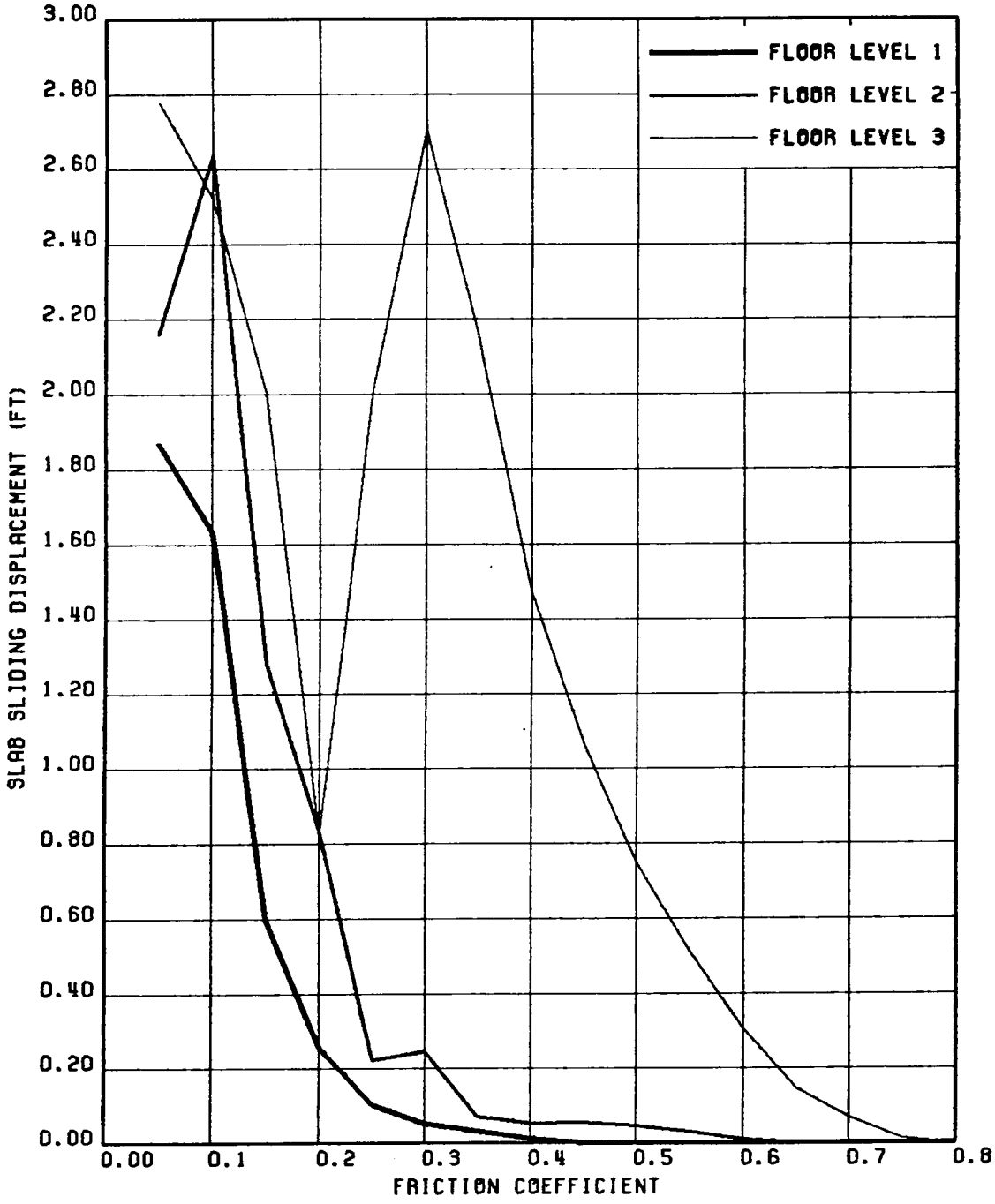

FIG. 5.41 VARIATION OF MAXIMUM SLAB SLIDING DISPLACEMENTS WITH THE UNIFORM FRICTION COEFFICIENT; STRUCTURE 3, GR MOTION 1-HZ COMPONENT

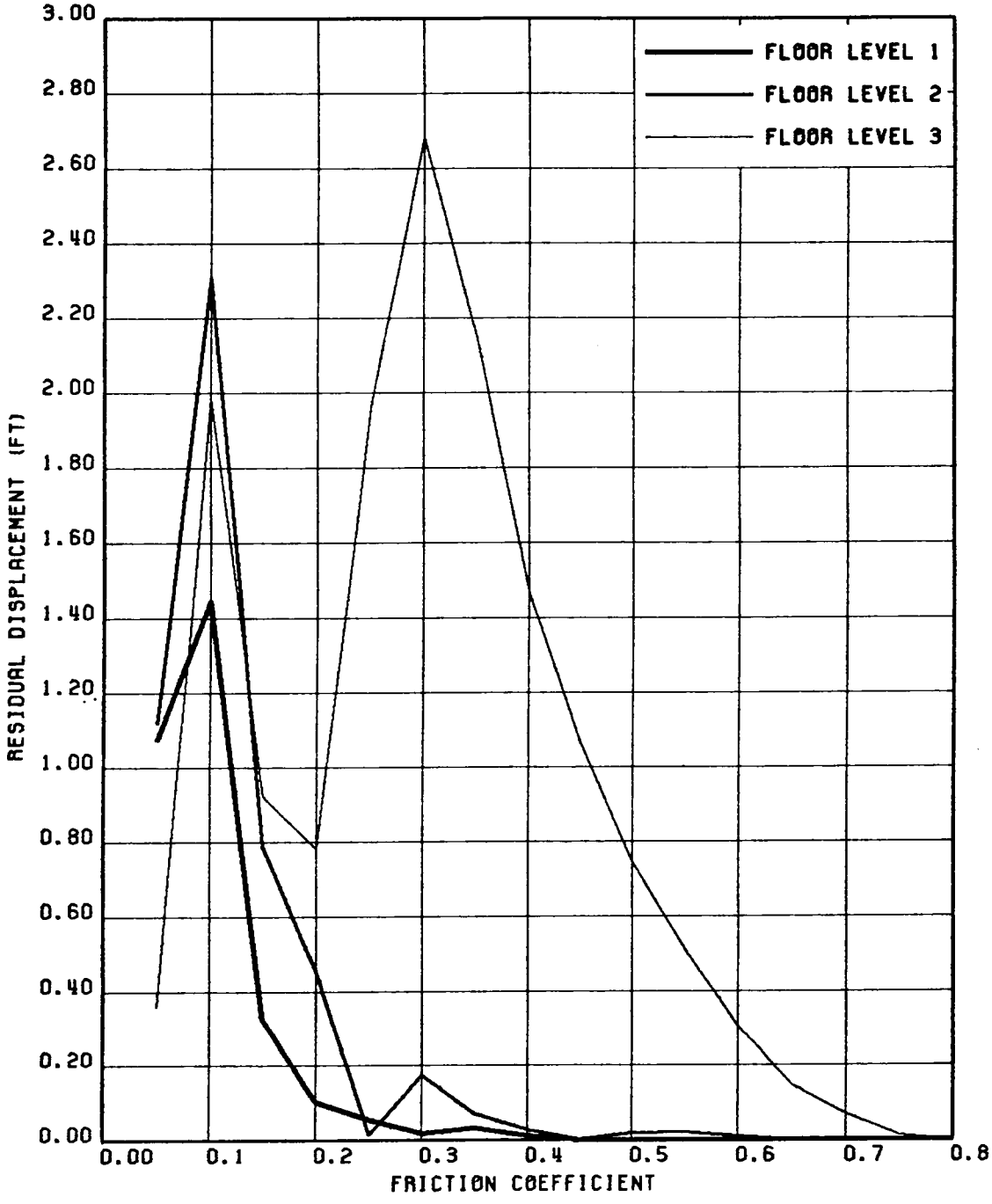

FIG. 5.42 VARIATION OF RESIDUAL SLAB SLIDING DISPLACEMENTS WITH THE UNIFORM FRICTION COEFFICIENT; STRUCTURE 3, GR MOTION 1-HZ COMPONENT

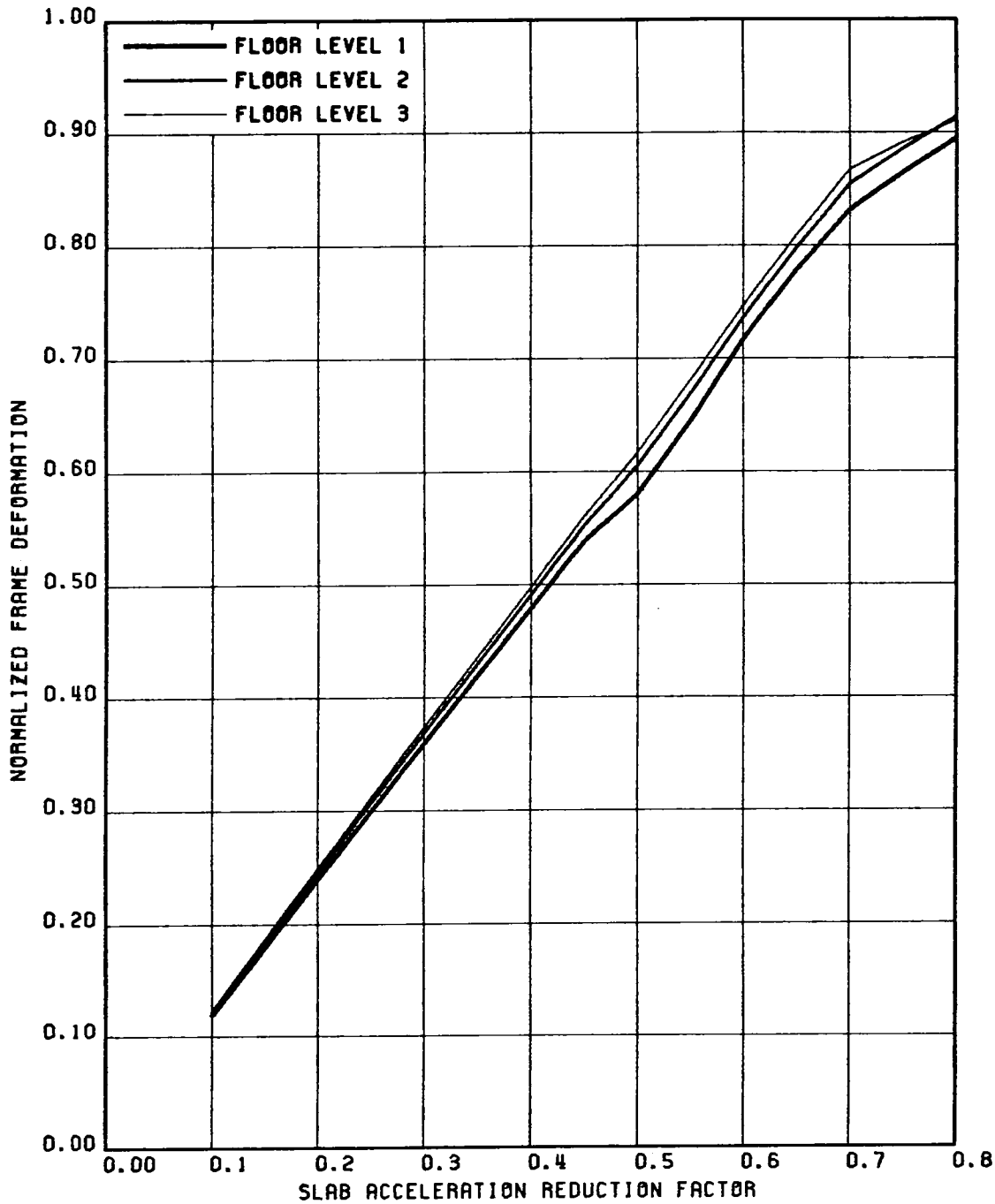

FIG. 5.43 VARIATION OF NORMALIZED FRAME DEFORMATION (NORMALIZED W.R.T. THE CORRESPONDING NON-SLIDING DEFORMATION RESPONSE) WITH SLAB ACCELERATION REDUCTION FACTOR; STRUCTURE 1, GR MOTION 2-HZ COMPONENT

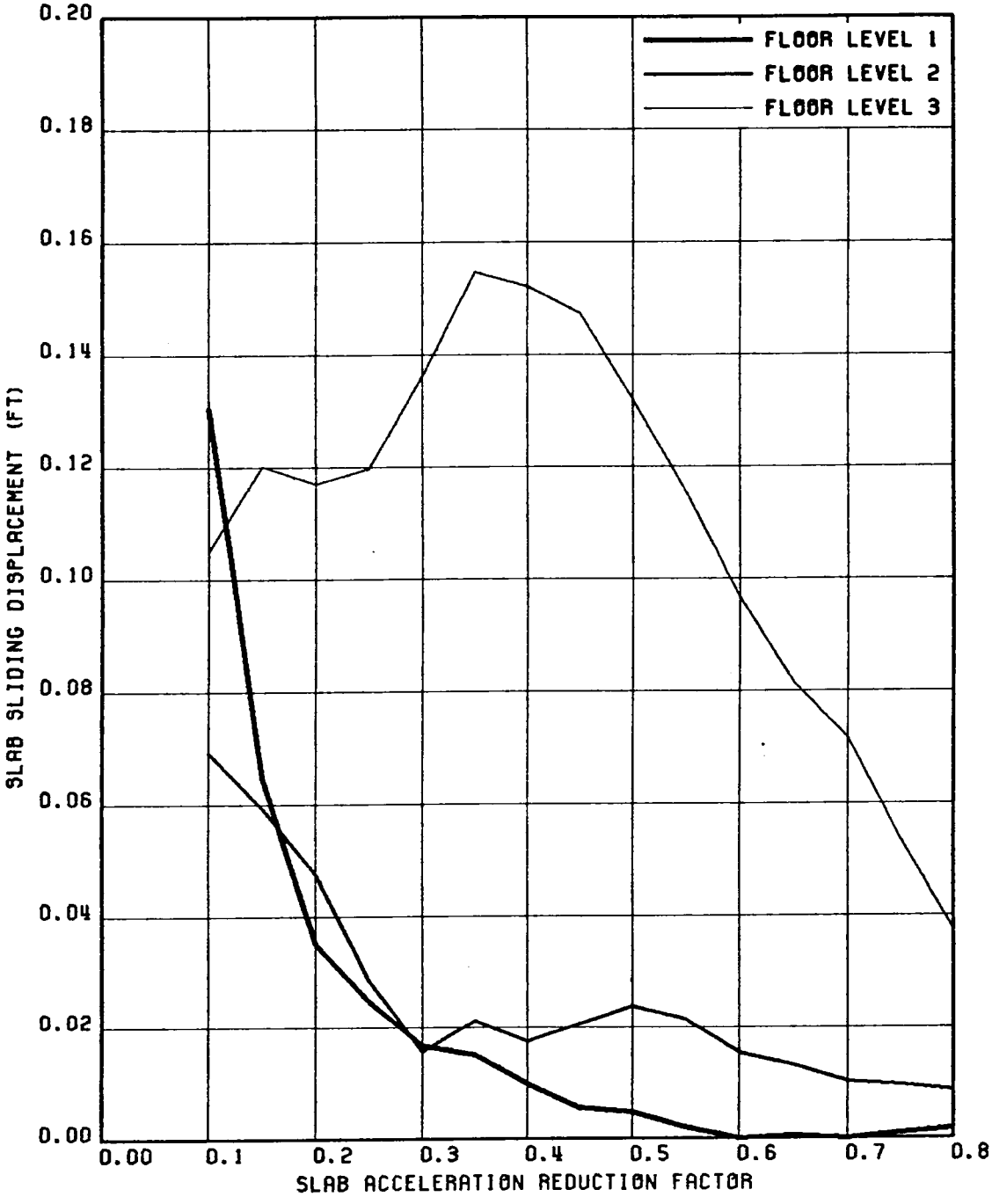

FIG. 5.44 VARIATION OF MAXIMUM SLAB SLIDING DISPLACEMENTS WITH SLAB ACCELERATION REDUCTION FACTOR; STRUCTURE 1, GR MOTION 2-HZ COMPONENT

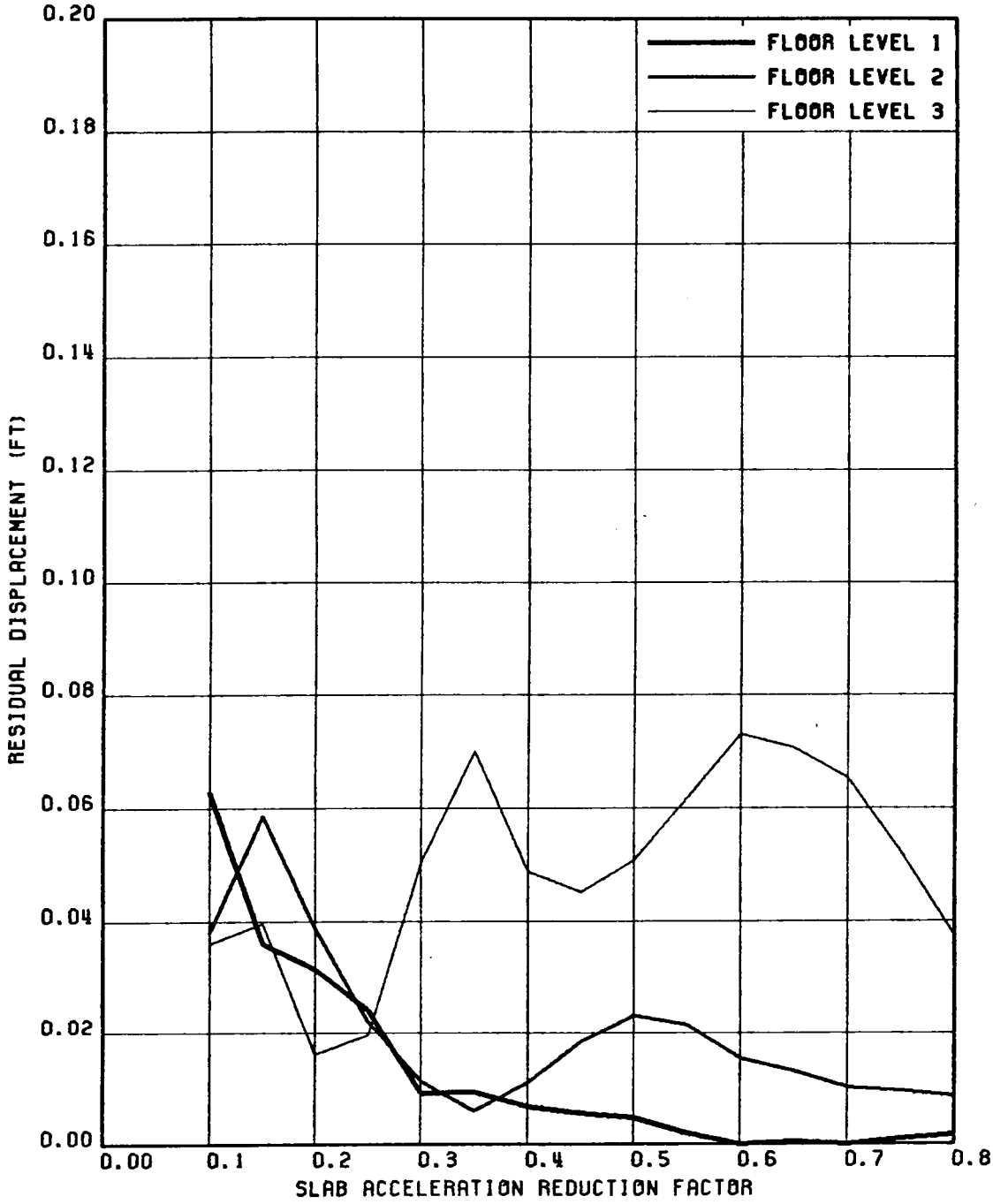

FIG. 5.45 VARIATION OF RESIDUAL SLAB SLIDING DISPLACEMENTS WITH SLAB ACCELERATION REDUCTION FACTOR; STRUCTURE 1, GR MOTION 2-HZ COMPONENT

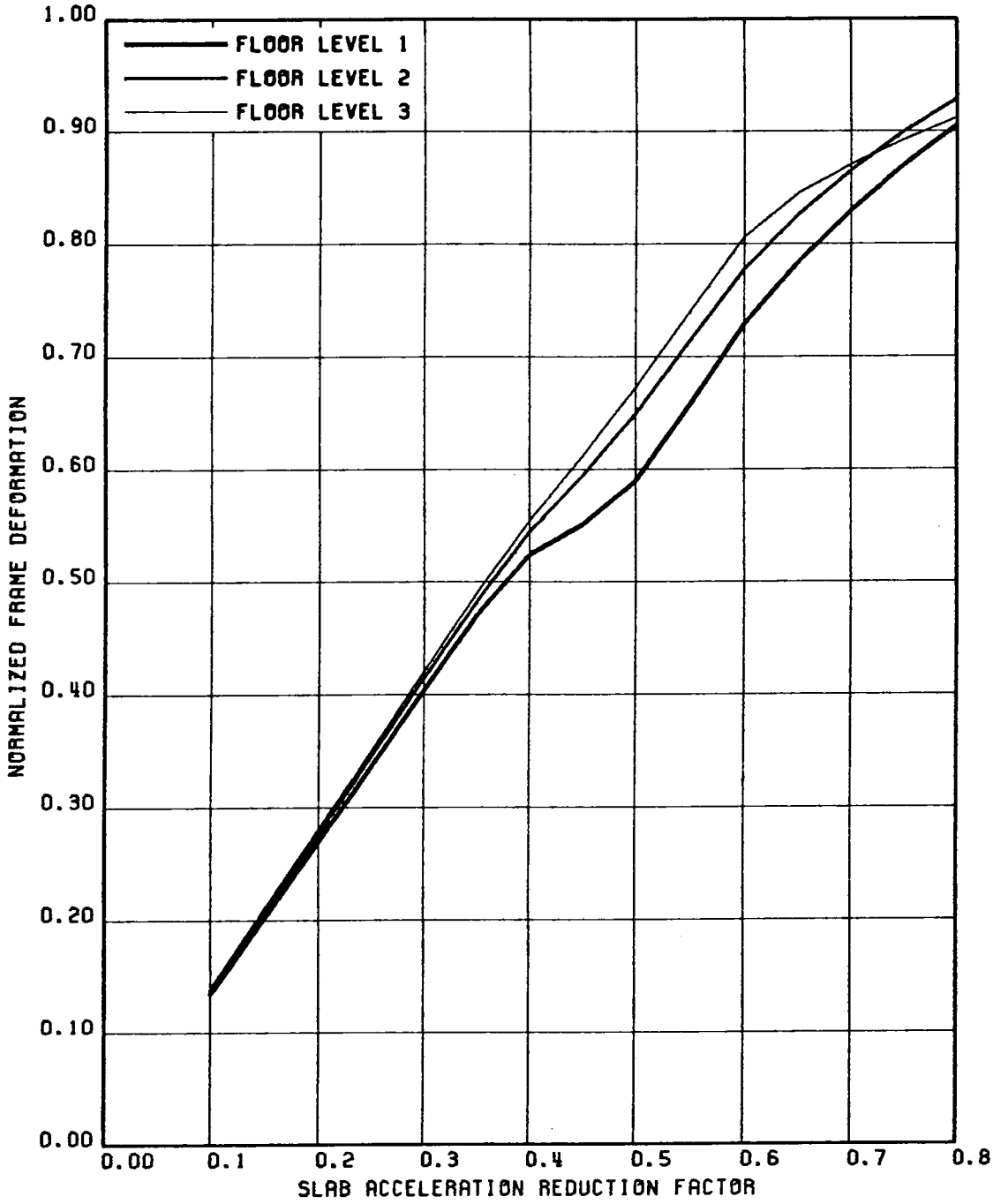

FIG. 5.46 VARIATION OF NORMALIZED FRAME DEFORMATION (NORMALIZED W.R.T. THE CORRESPONDING NON-SLIDING DEFORMATION RESPONSE) WITH SLAB ACCELERATION REDUCTION FACTOR; STRUCTURE 1, GR MOTION 2-HZ & VT COMP

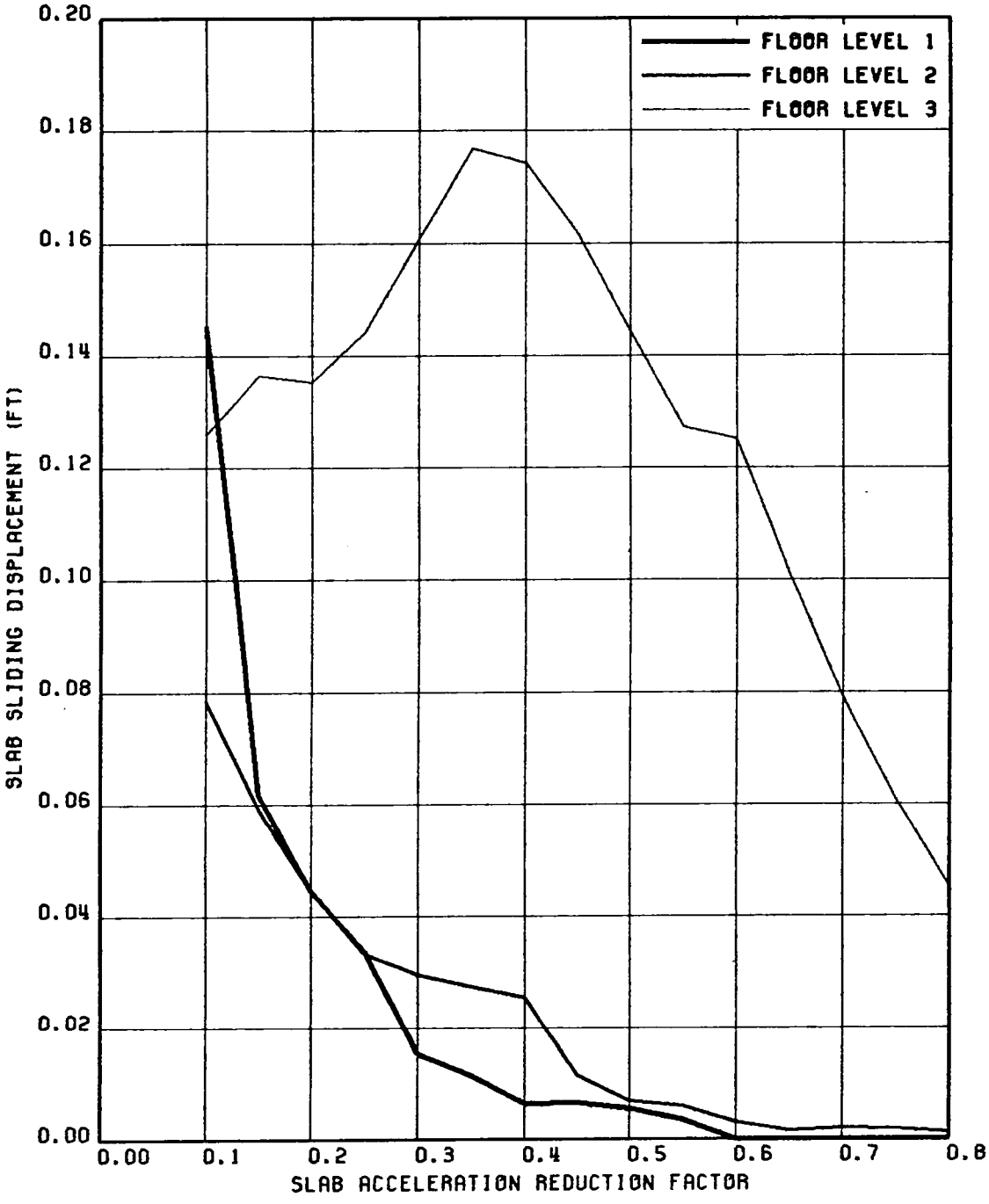

FIG. 5.47 VARIATION OF MAXIMUM SLAB SLIDING DISPLACEMENTS WITH SLAB ACCELERATION REDUCTION FACTOR; STRUCTURE 1, GR MOTION 2-HZ & VT COMP

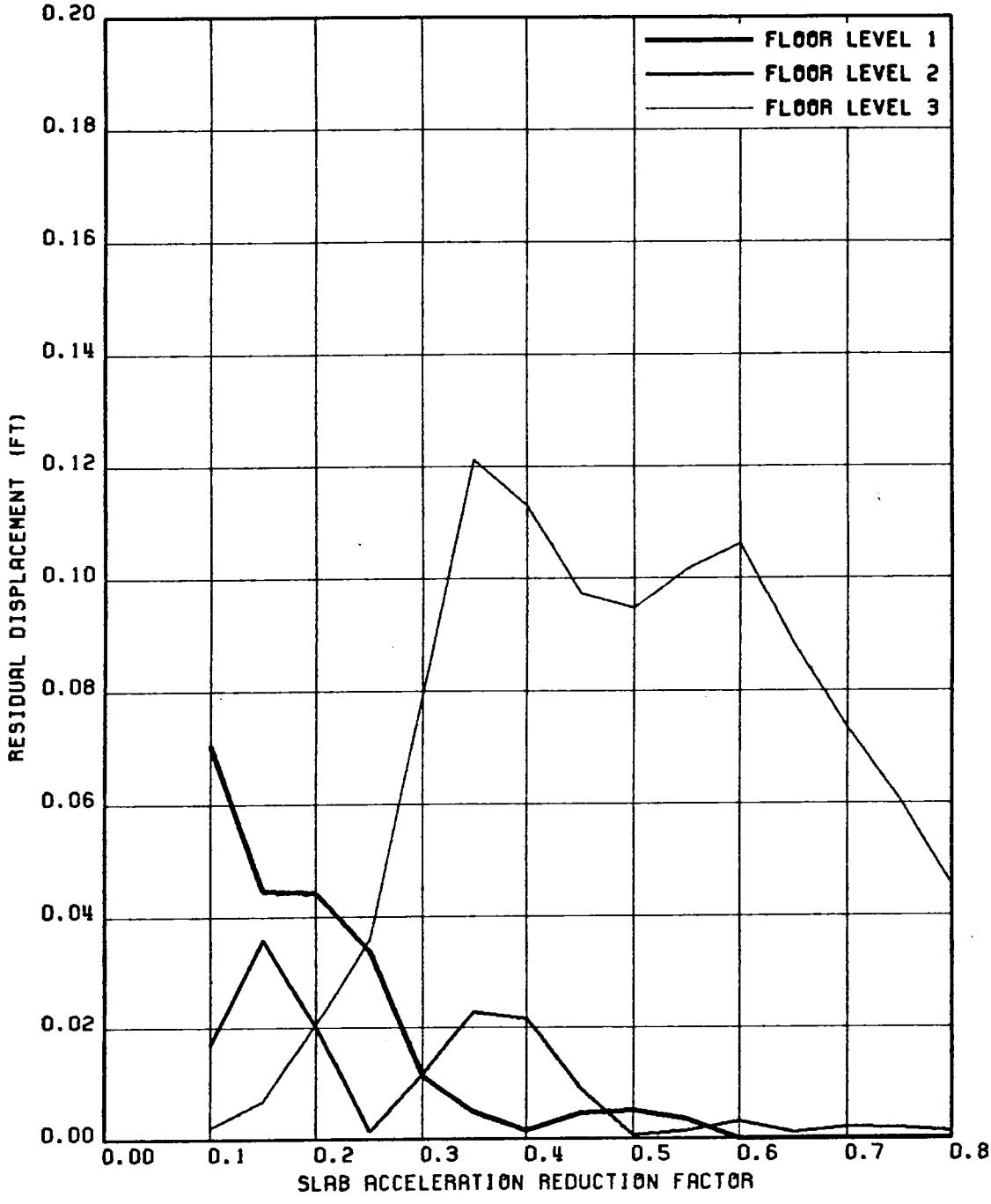

FIG. 5.48 VARIATION OF RESIDUAL SLAB SLIDING DISPLACEMENTS WITH SLAB ACCELERATION REDUCTION FACTOR; STRUCTURE 1, GR MOTION 2-HZ & VT COMP

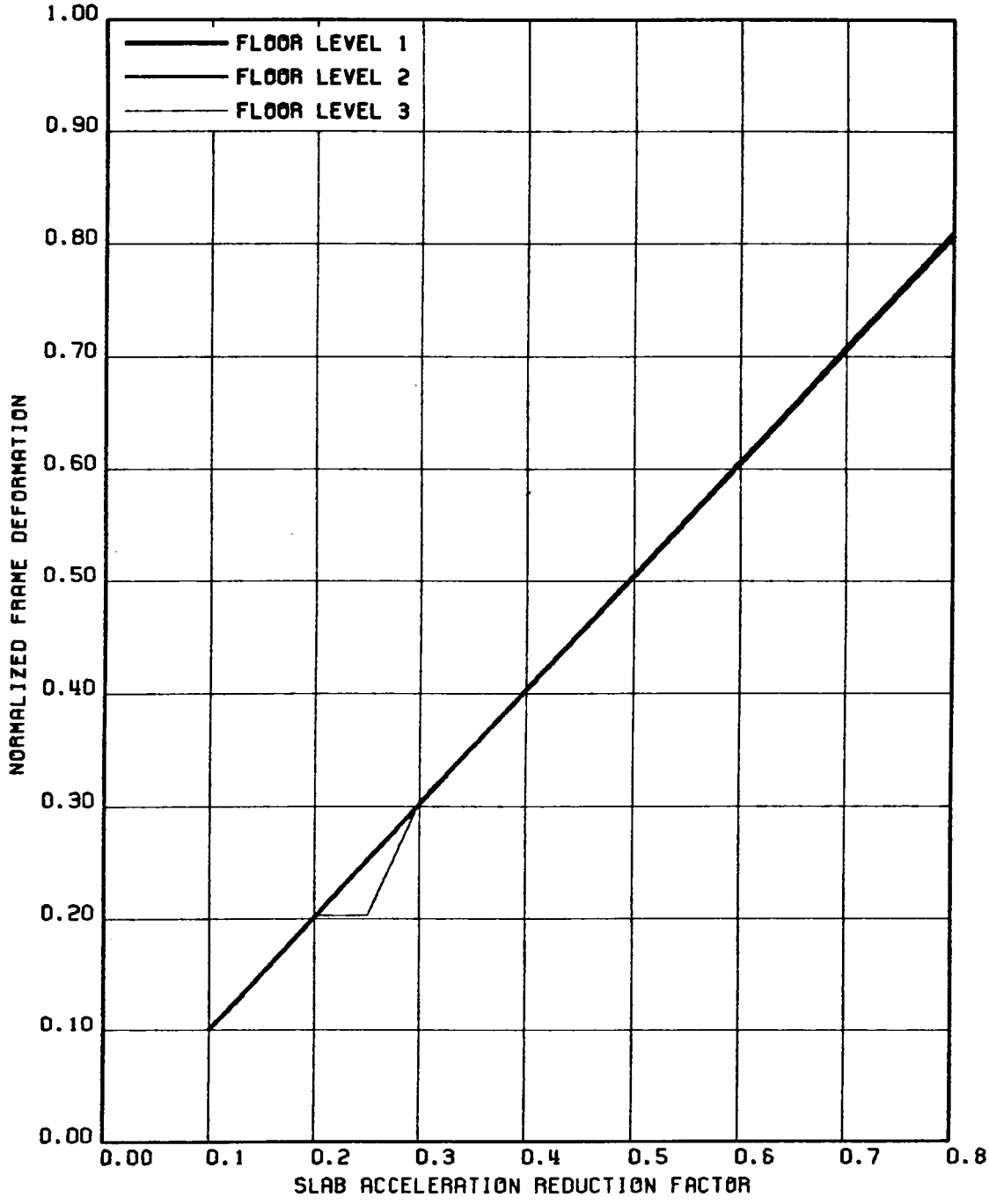

FIG. 5.49 VARIATION OF NORMALIZED FRAME DEFORMATION (NORMALIZED W.R.T. THE CORRESPONDING NON-SLIDING DEFORMATION RESPONSE) WITH SLAB ACCELERATION REDUCTION FACTOR; STRUCTURE 2, GR MOTION 2-HZ COMPONENT

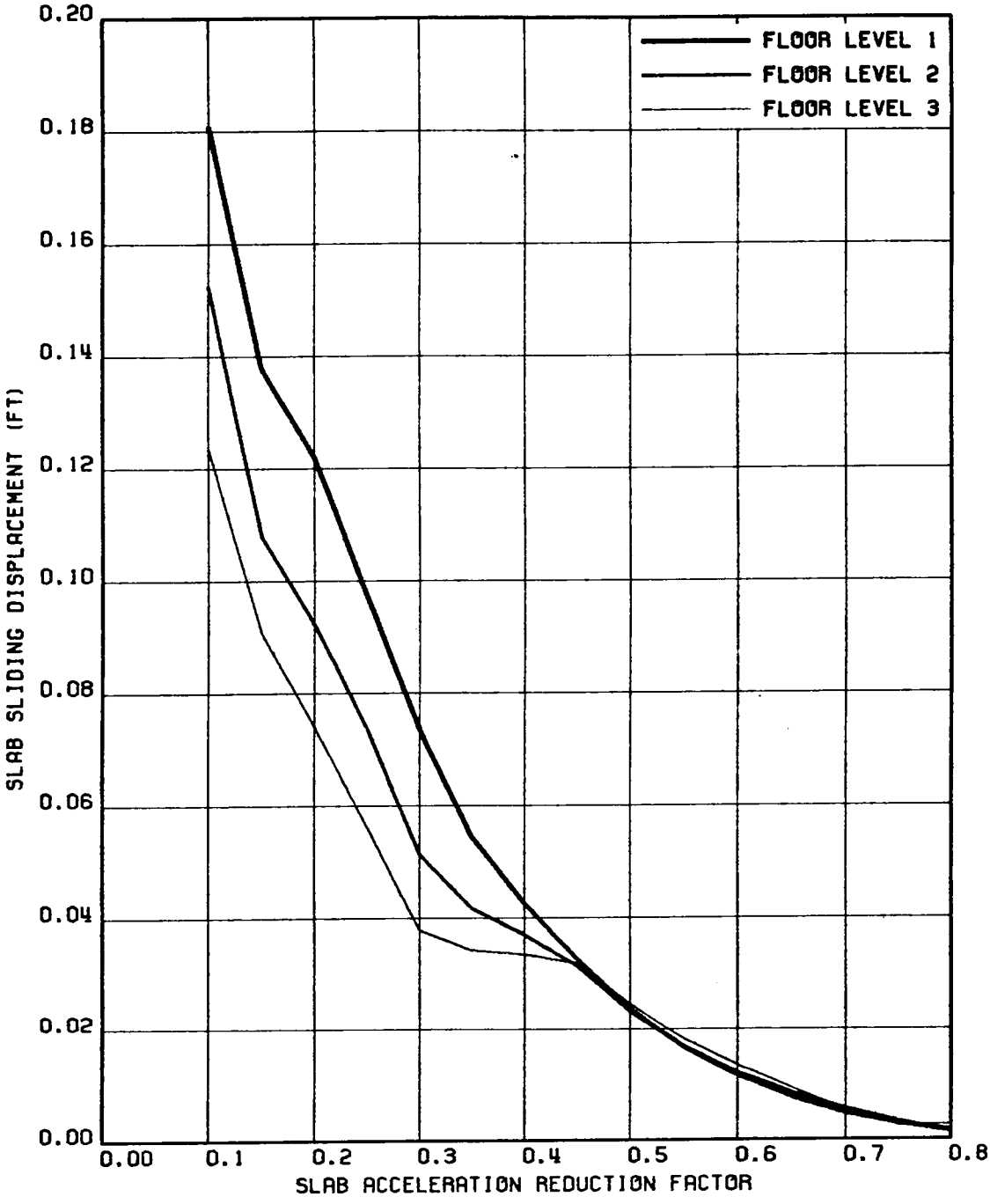

FIG. 5.50 VARIATION OF MAXIMUM SLAB SLIDING DISPLACEMENTS WITH SLAB ACCELERATION REDUCTION FACTOR; STRUCTURE 2, GR MOTION 2-HZ COMPONENT

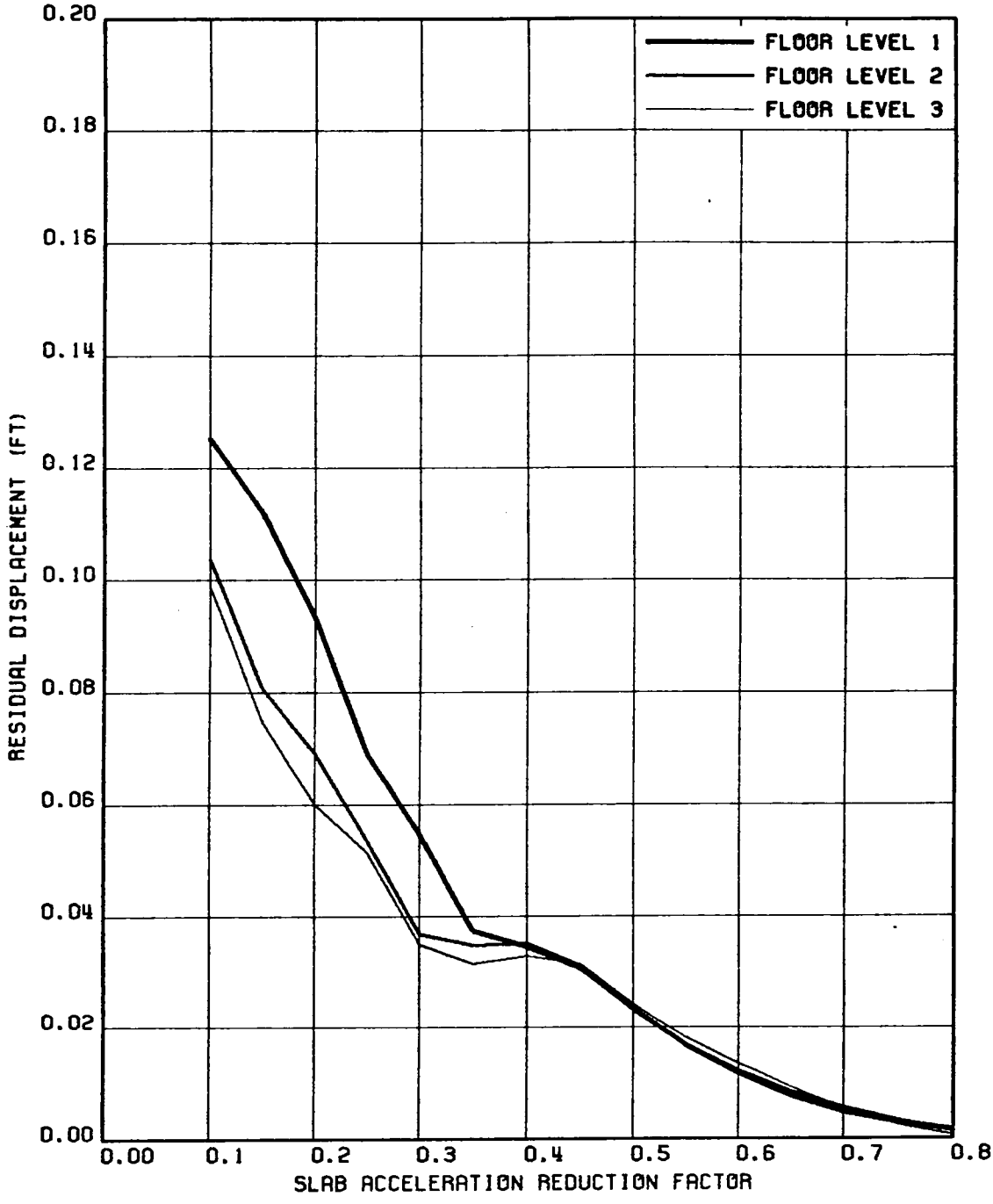

FIG. 5.51 VARIATION OF RESIDUAL SLAB SLIDING DISPLACEMENTS WITH SLAB ACCELERATION REDUCTION FACTOR; STRUCTURE 2, GR MOTION 2-HZ COMPONENT

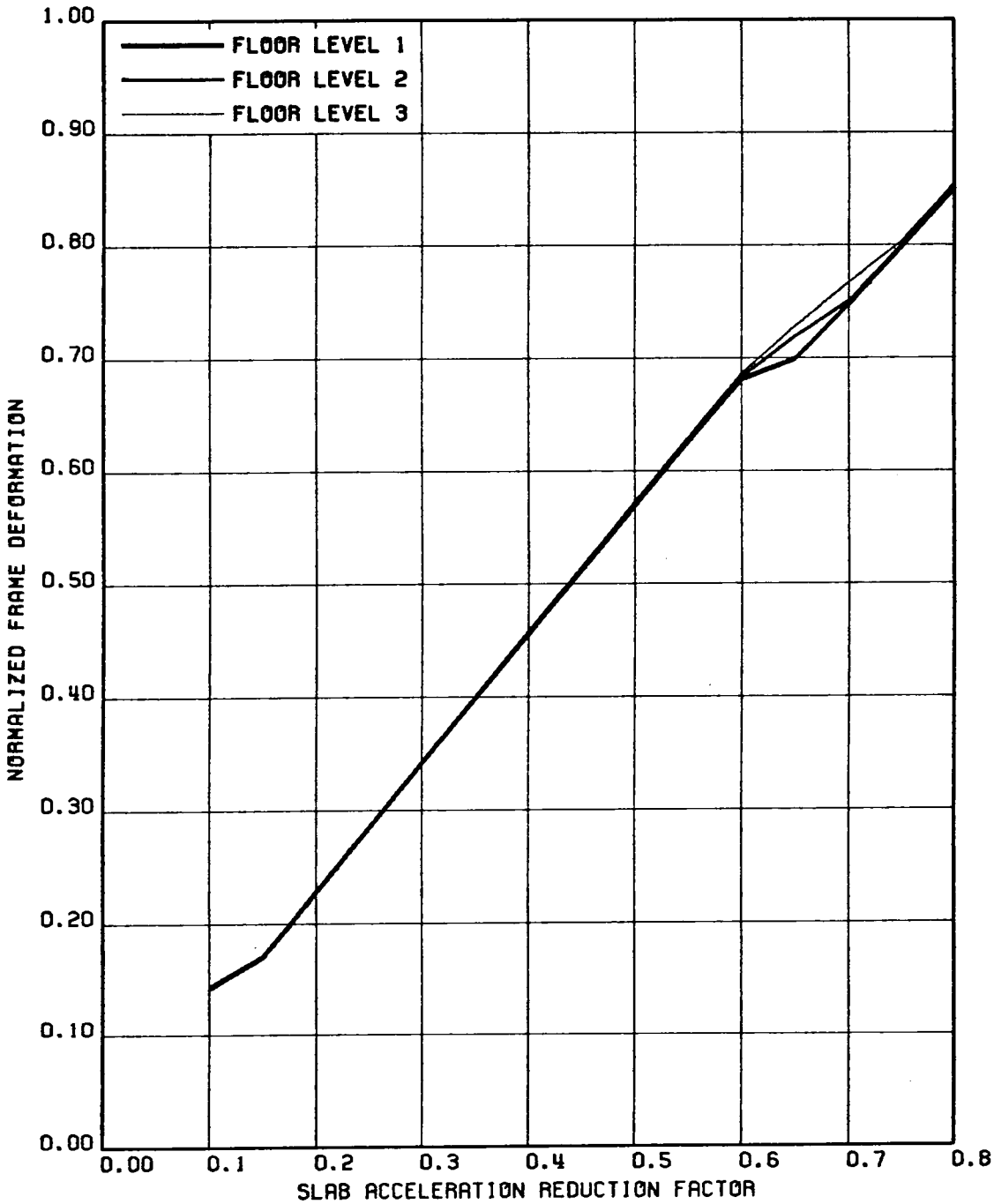

FIG. 5.52 VARIATION OF NORMALIZED FRAME DEFORMATION (NORMALIZED W.R.T. THE CORRESPONDING NON-SLIDING DEFORMATION RESPONSE) WITH SLAB ACCELERATION REDUCTION FACTOR; STRUCTURE 2, GR MOTION 2-HZ & VT COMP

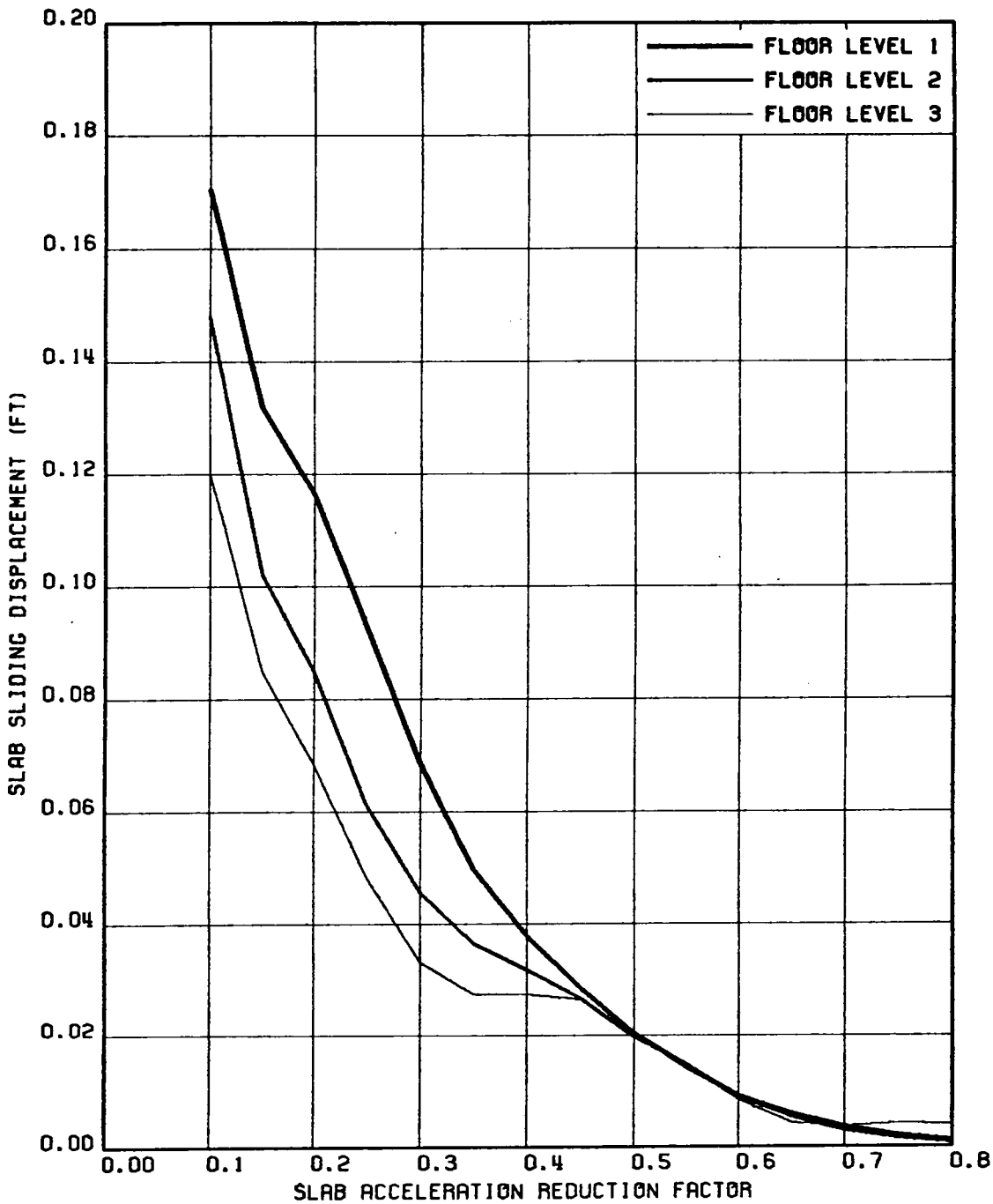

FIG. 5.53 VARIATION OF MAXIMUM SLAB SLIDING DISPLACEMENTS WITH SLAB ACCELERATION REDUCTION FACTOR; STRUCTURE 2, GR MOTION 2-HZ & VT COMP

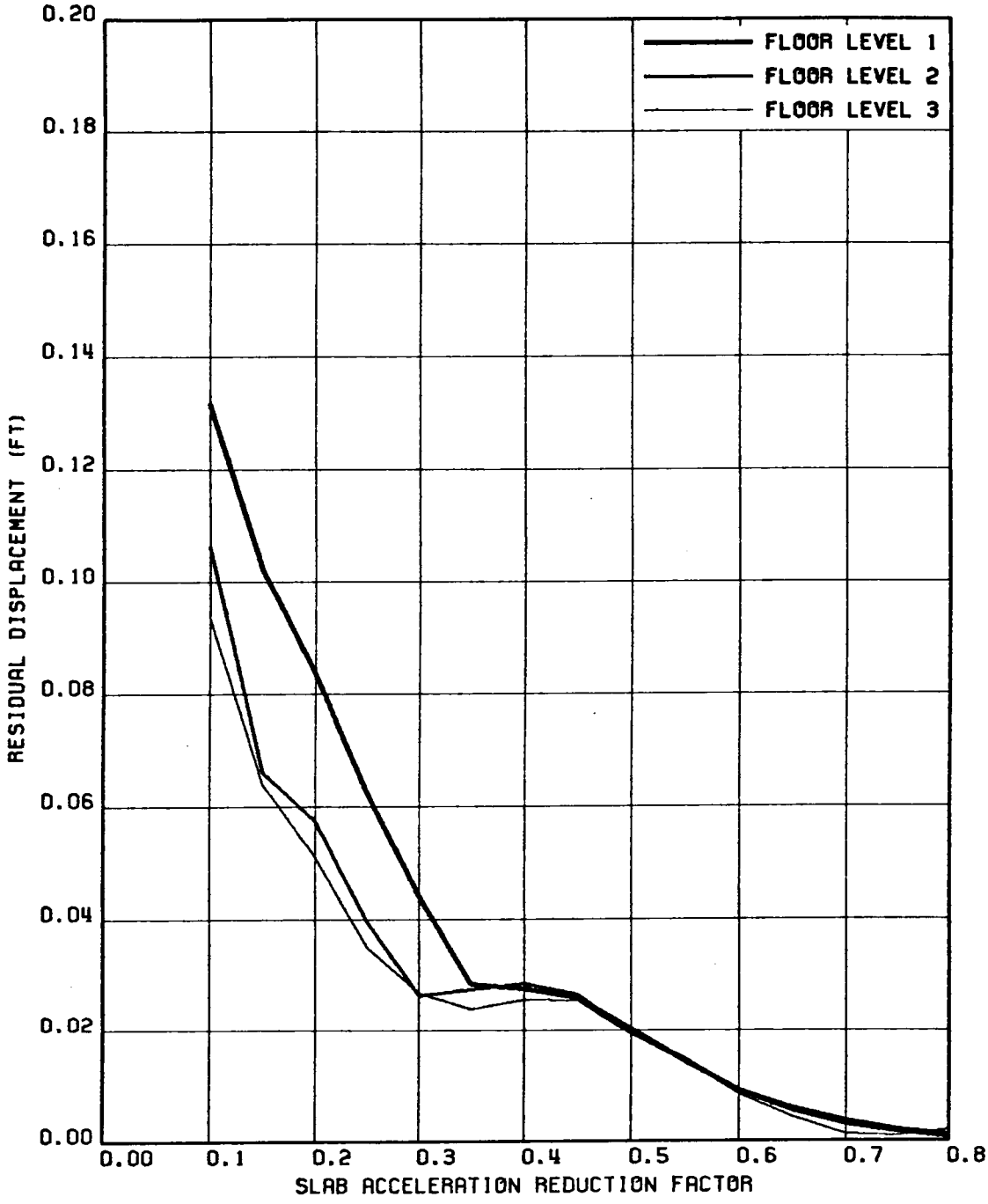

FIG. 5.54 VARIATION OF RESIDUAL SLAB SLIDING DISPLACEMENTS WITH SLAB ACCELERATION REDUCTION FACTOR; STRUCTURE 2, GR MOTION 2-HZ & VT COMP

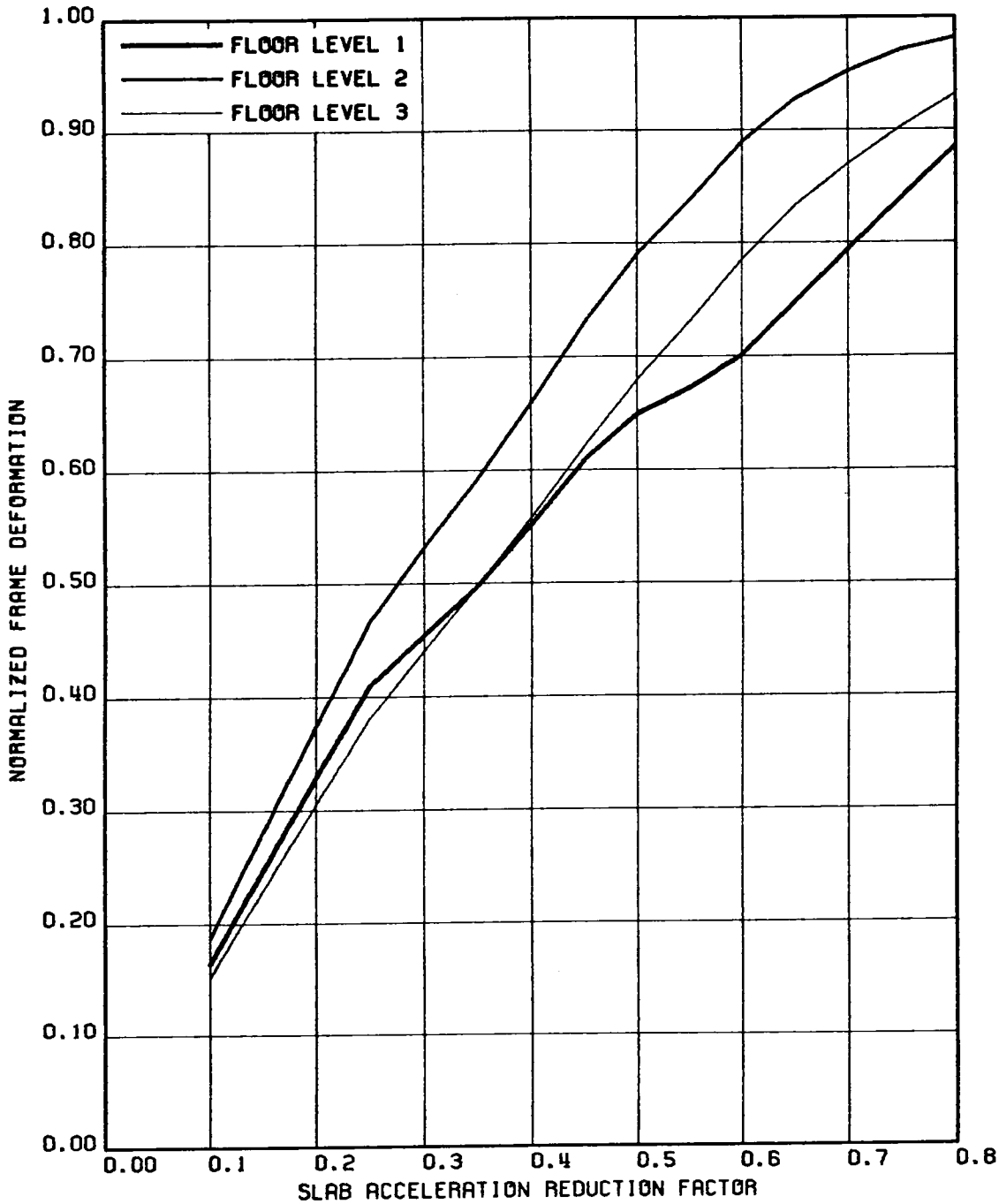

FIG. 5.55 VARIATION OF NORMALIZED FRAME DEFORMATION (NORMALIZED W.R.T. THE CORRESPONDING NON-SLIDING DEFORMATION RESPONSE) WITH SLAB ACCELERATION REDUCTION FACTOR; STRUCTURE 3, GR MOTION 2-HZ COMPONENT

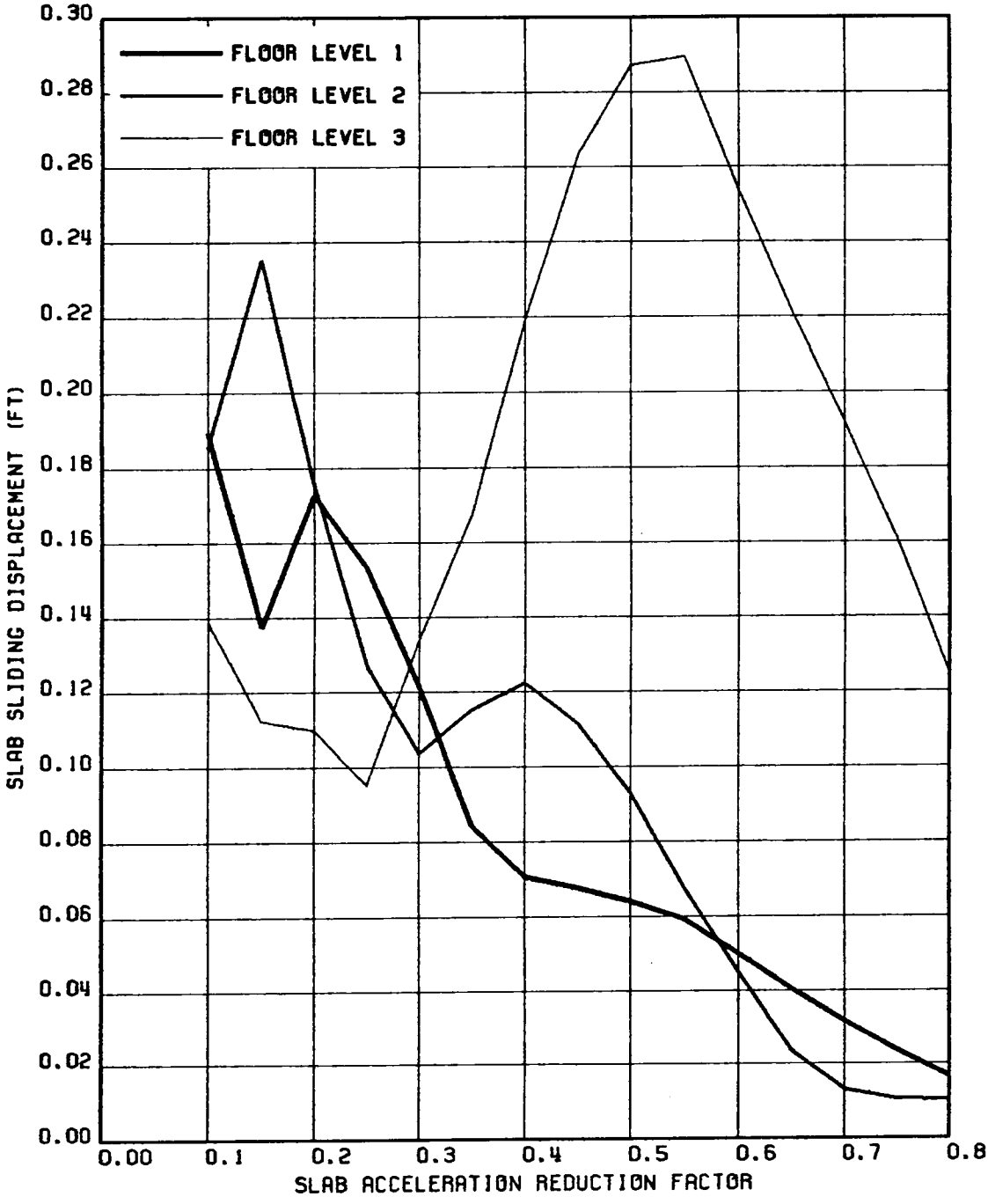

FIG. 5.56 VARIATION OF MAXIMUM SLAB SLIDING DISPLACEMENTS WITH SLAB ACCELERATION REDUCTION FACTOR; STRUCTURE 3, GR MOTION 2-HZ COMPONENT

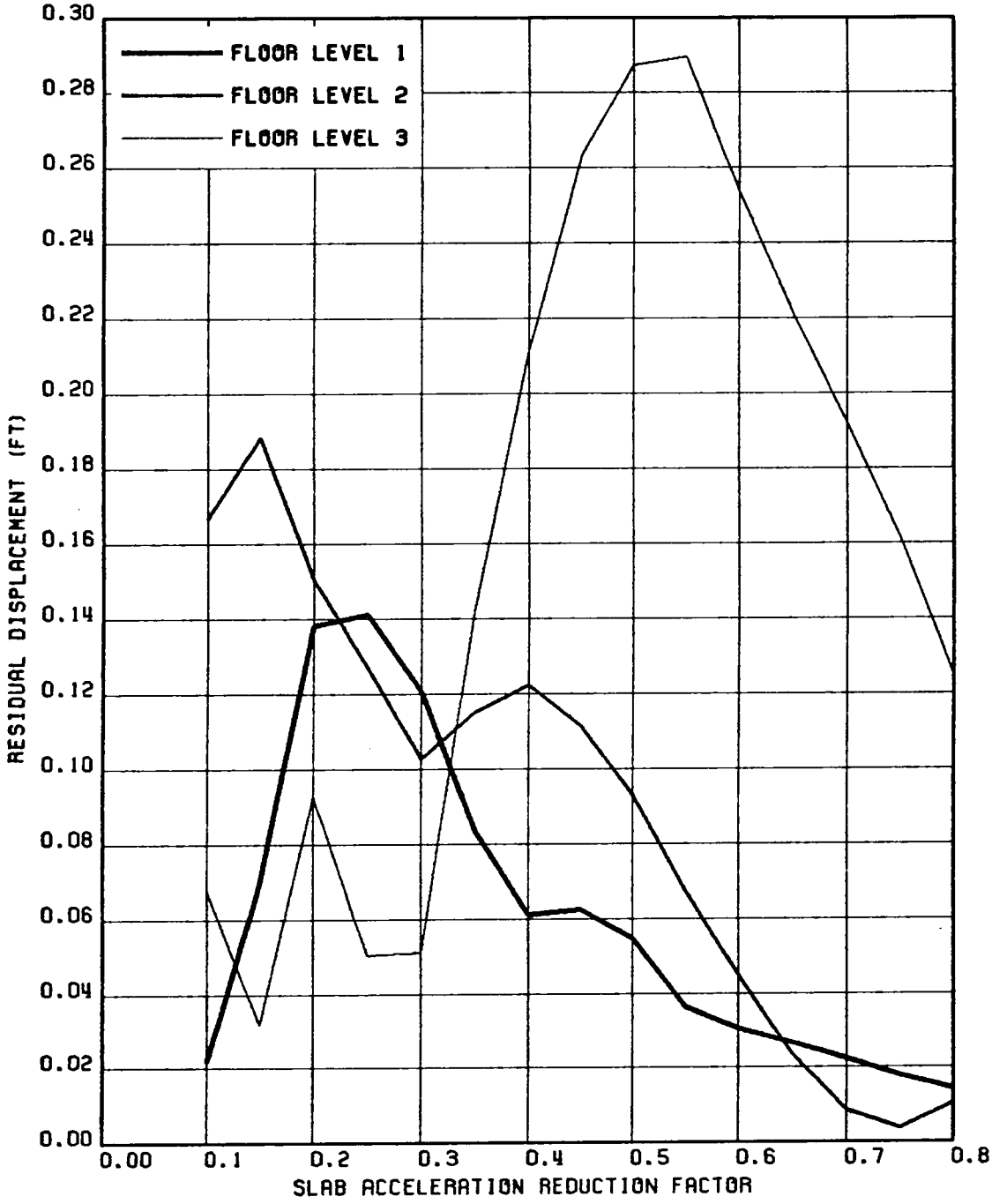

FIG. 5.57 VARIATION OF RESIDUAL SLAB SLIDING DISPLACEMENTS WITH SLAB ACCELERATION REDUCTION FACTOR; STRUCTURE 3, GR MOTION 2-HZ COMPONENT

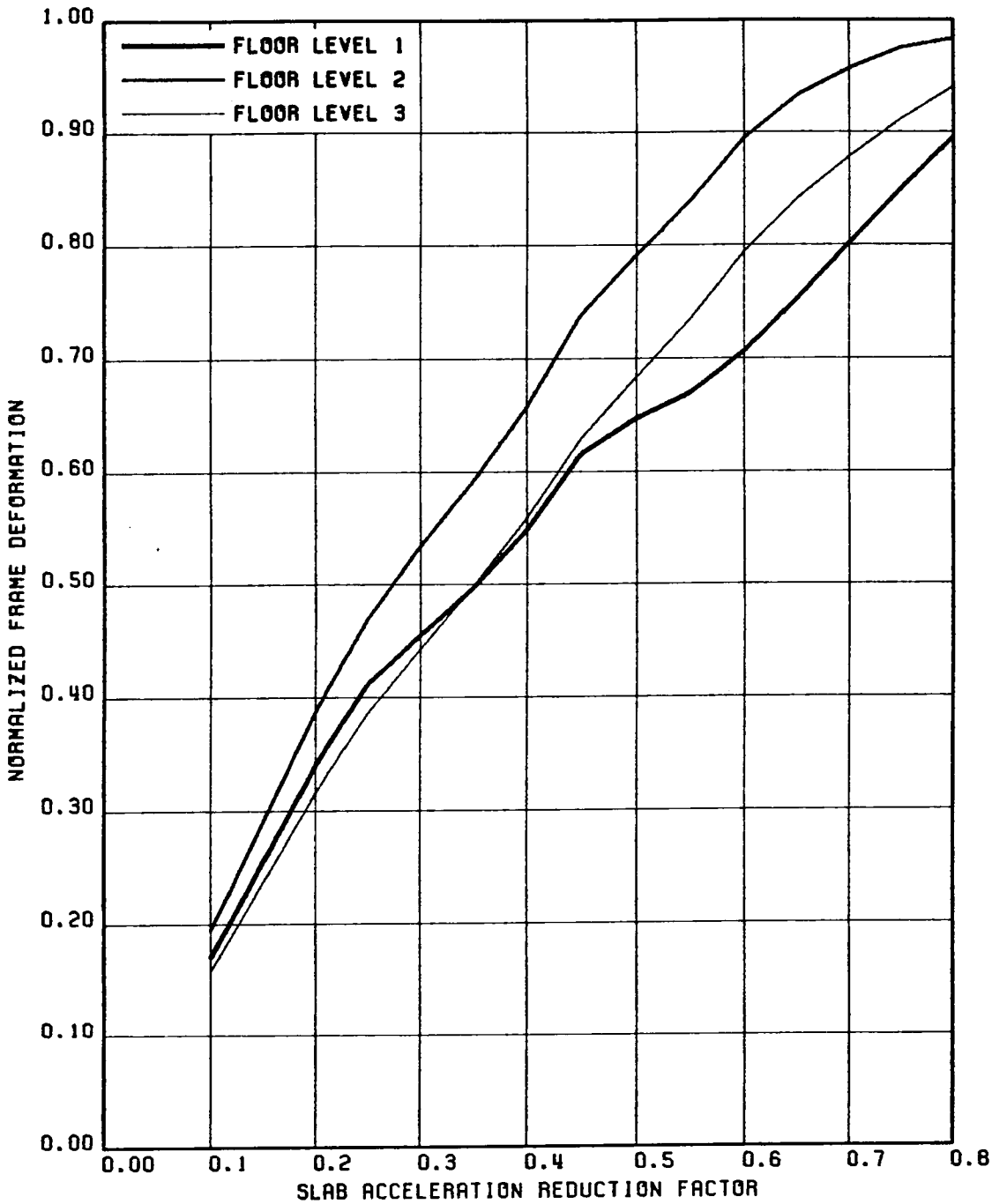

FIG. 5.58 VARIATION OF NORMALIZED FRAME DEFORMATION (NORMALIZED W.R.T. THE CORRESPONDING NON-SLIDING DEFORMATION RESPONSE) WITH SLAB ACCELERATION REDUCTION FACTOR; STRUCTURE 3, GR MOTION 2-HZ & VT COMP

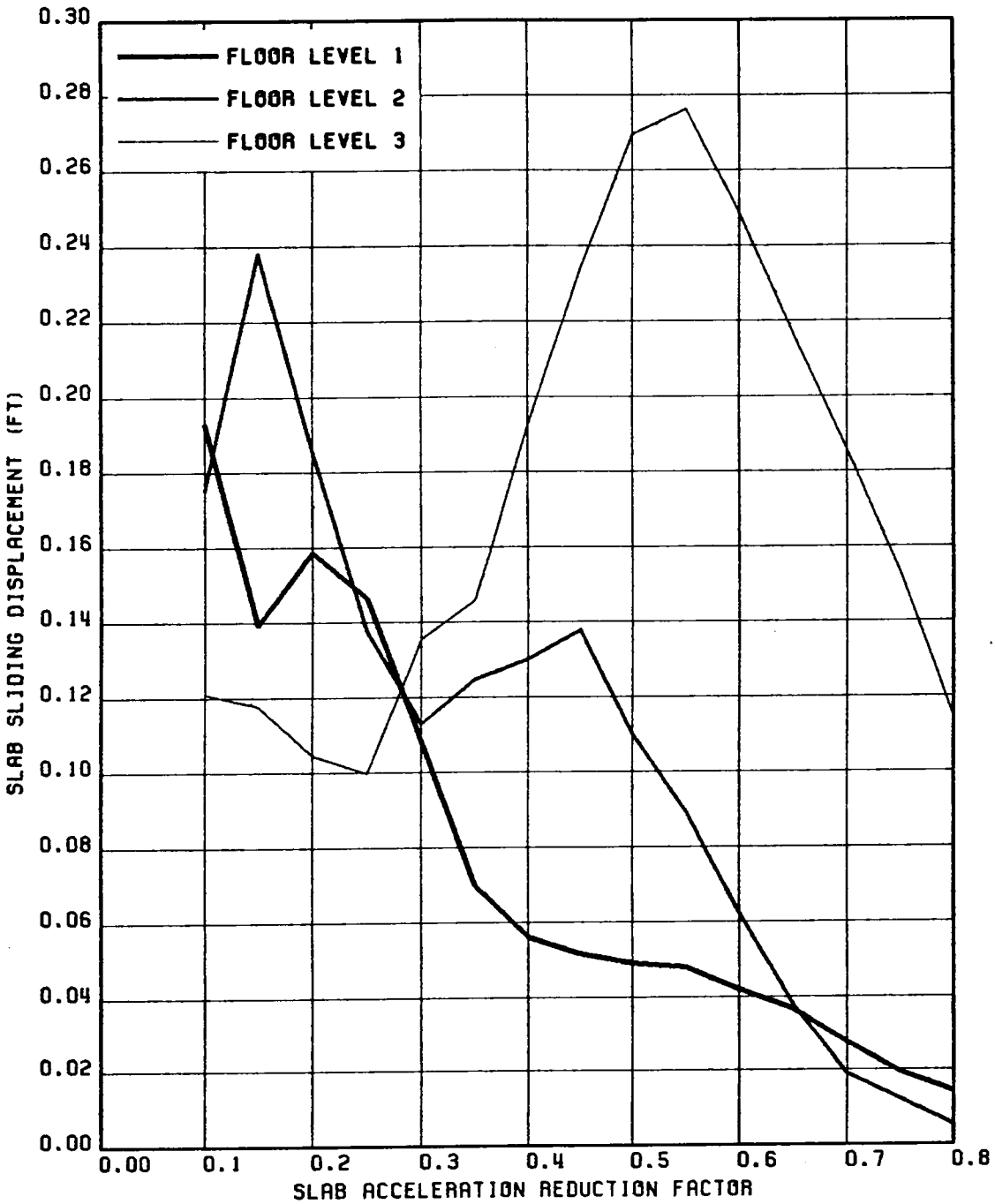

FIG. 5.59 VARIATION OF MAXIMUM SLAB SLIDING DISPLACEMENTS WITH SLAB ACCELERATION REDUCTION FACTOR; STRUCTURE 3, GR MOTION 2-HZ & VT COMP

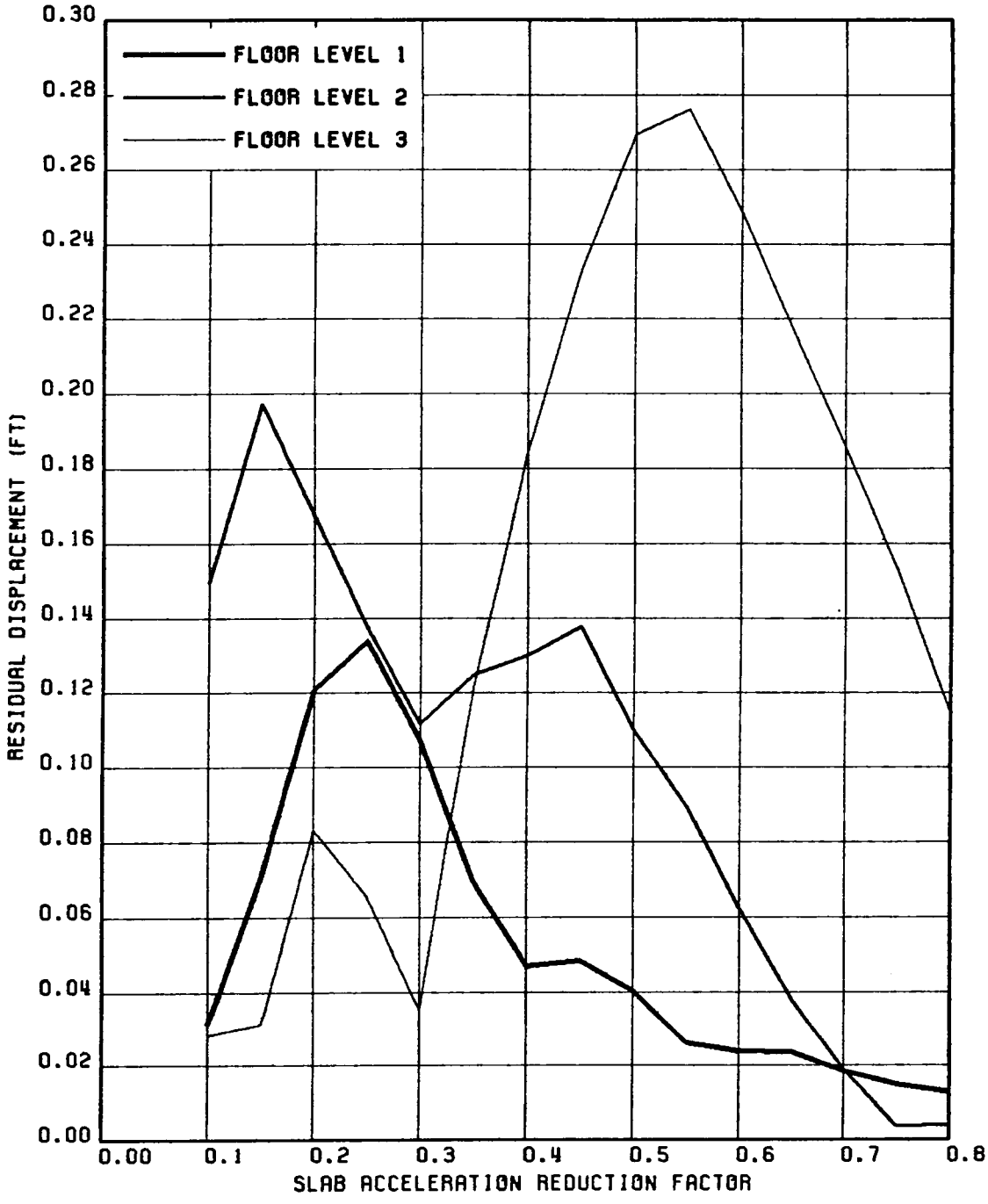

FIG. 5.60 VARIATION OF RESIDUAL SLAB SLIDING DISPLACEMENTS WITH SLAB ACCELERATION REDUCTION FACTOR; STRUCTURE 3, GR MOTION 2-HZ & VT COMP

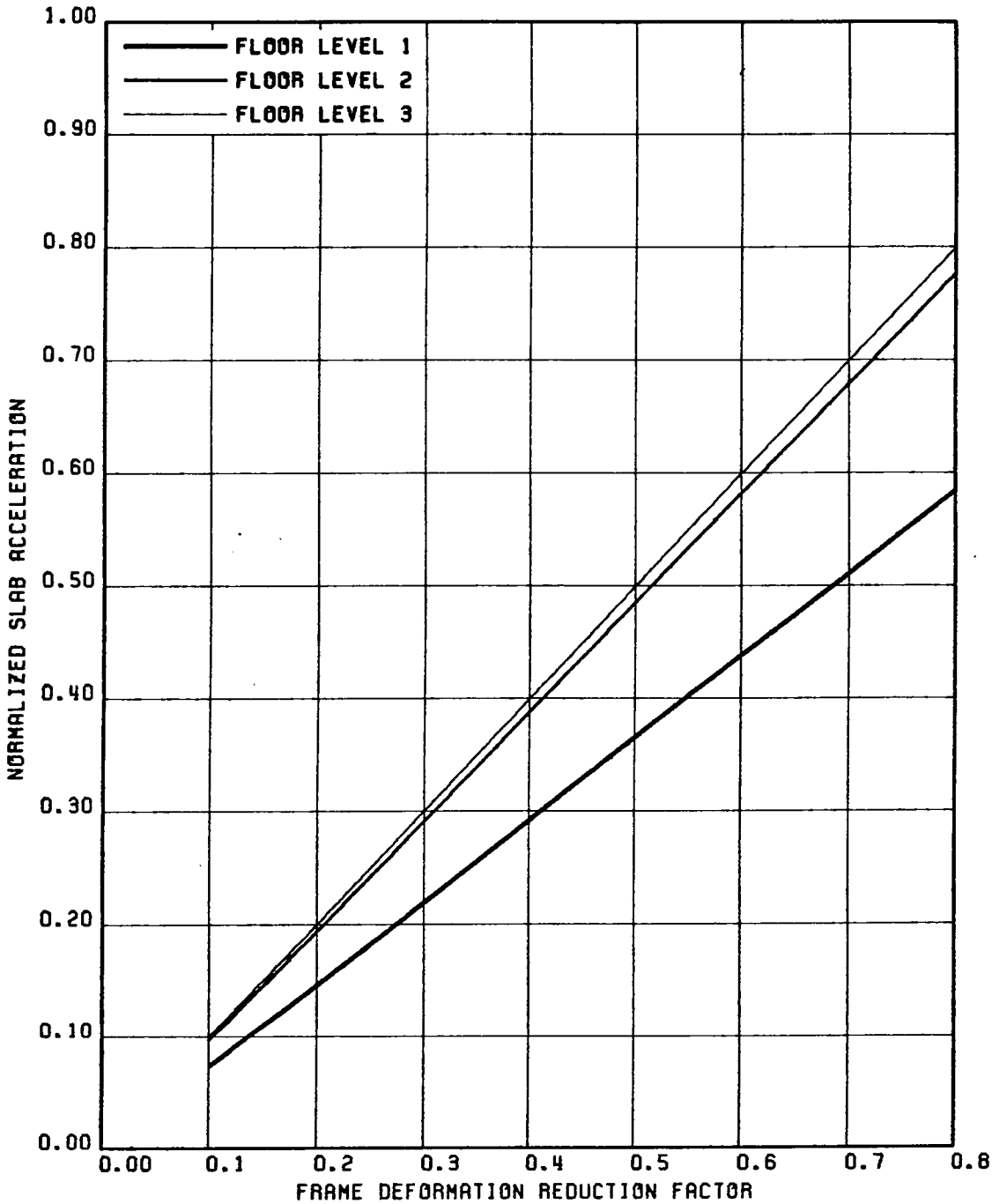

FIG. 5.61 VARIATION OF NORMALIZED SLAB ACCELERATION (NORMALIZED W.R.T. THE CORRESPONDING NON-SLIDING ACCELERATION RESPONSE) WITH FRAME DEFORMATION REDUCTION FACTOR; STRUCTURE 1, GR MOTION 1-HZ COMPONENT

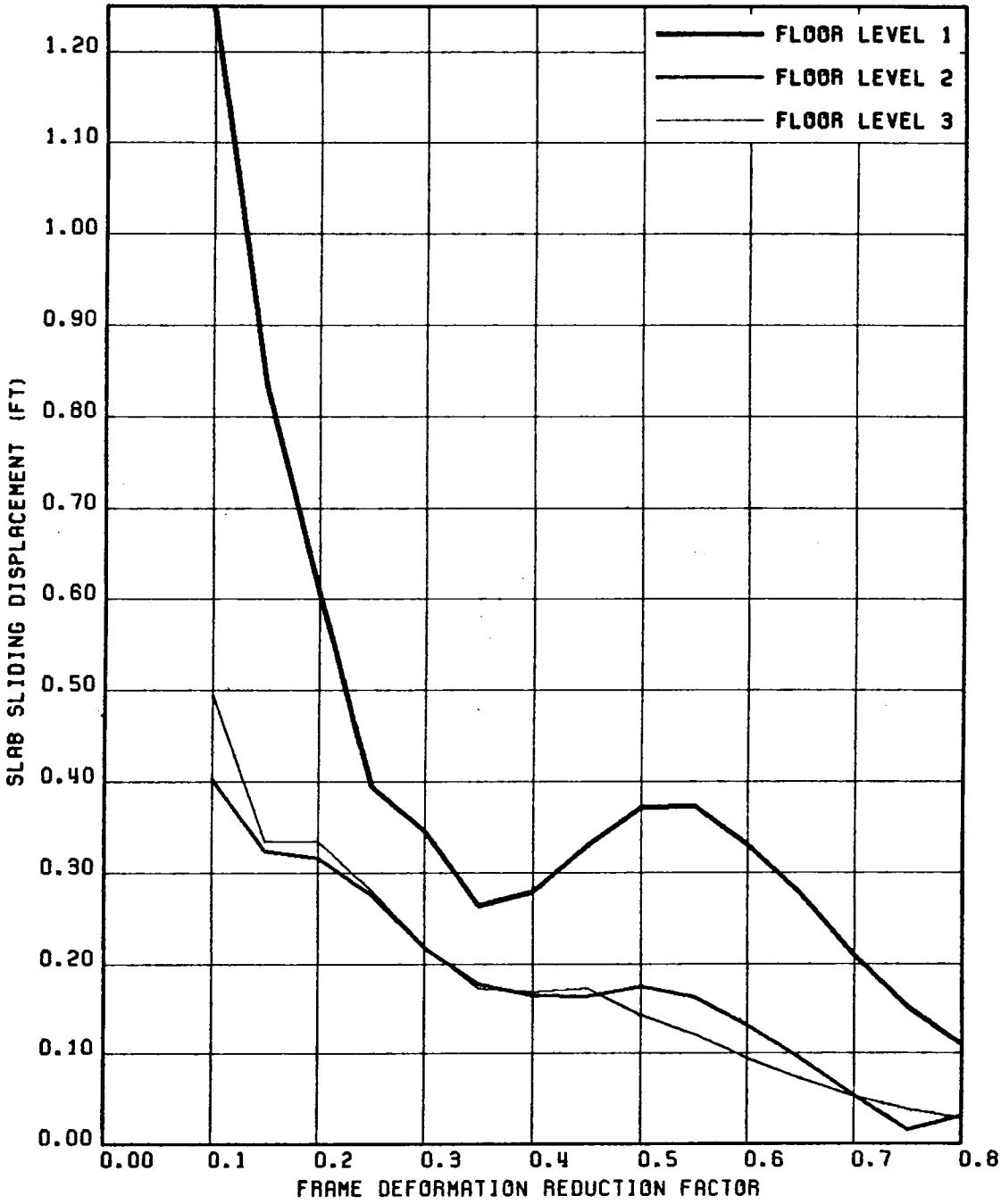

FIG. 5.62 VARIATION OF MAXIMUM SLAB SLIDING DISPLACEMENTS WITH FRAME DEFORMATION REDUCTION FACTOR; STRUCTURE 1, GR MOTION 1-HZ COMPONENT

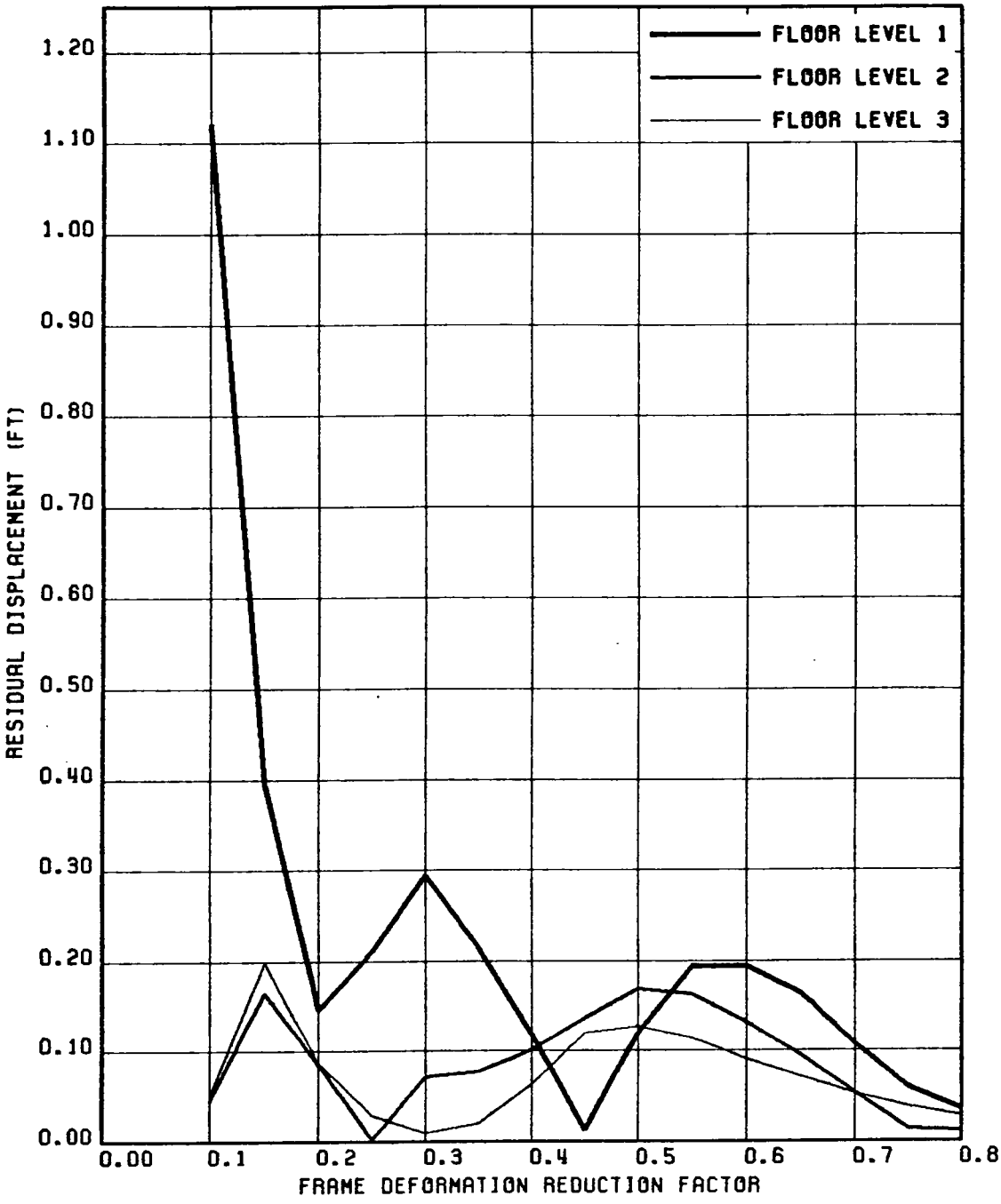

FIG. 5.63 VARIATION OF RESIDUAL SLAB SLIDING DISPLACEMENTS WITH FRAME DEFORMATION REDUCTION FACTOR; STRUCTURE 1, GR MOTION 1-HZ COMPONENT

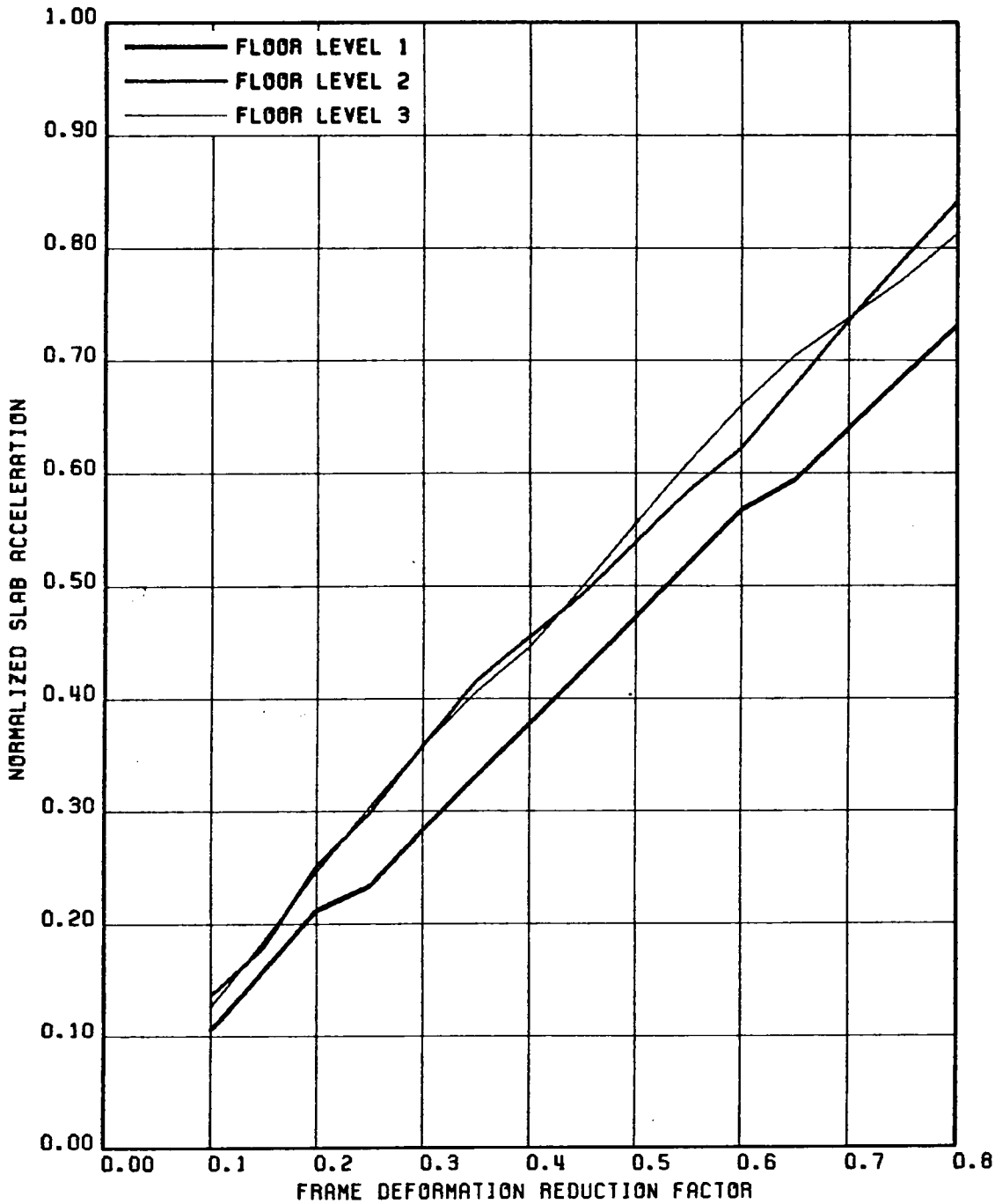

FIG. 5.64 VARIATION OF NORMALIZED SLAB ACCELERATION (NORMALIZED W.R.T. THE CORRESPONDING NON-SLIDING ACCELERATION RESPONSE) WITH FRAME DEFORMATION REDUCTION FACTOR; STRUCTURE 1, GR MOTION 1-HZ & VT COMP

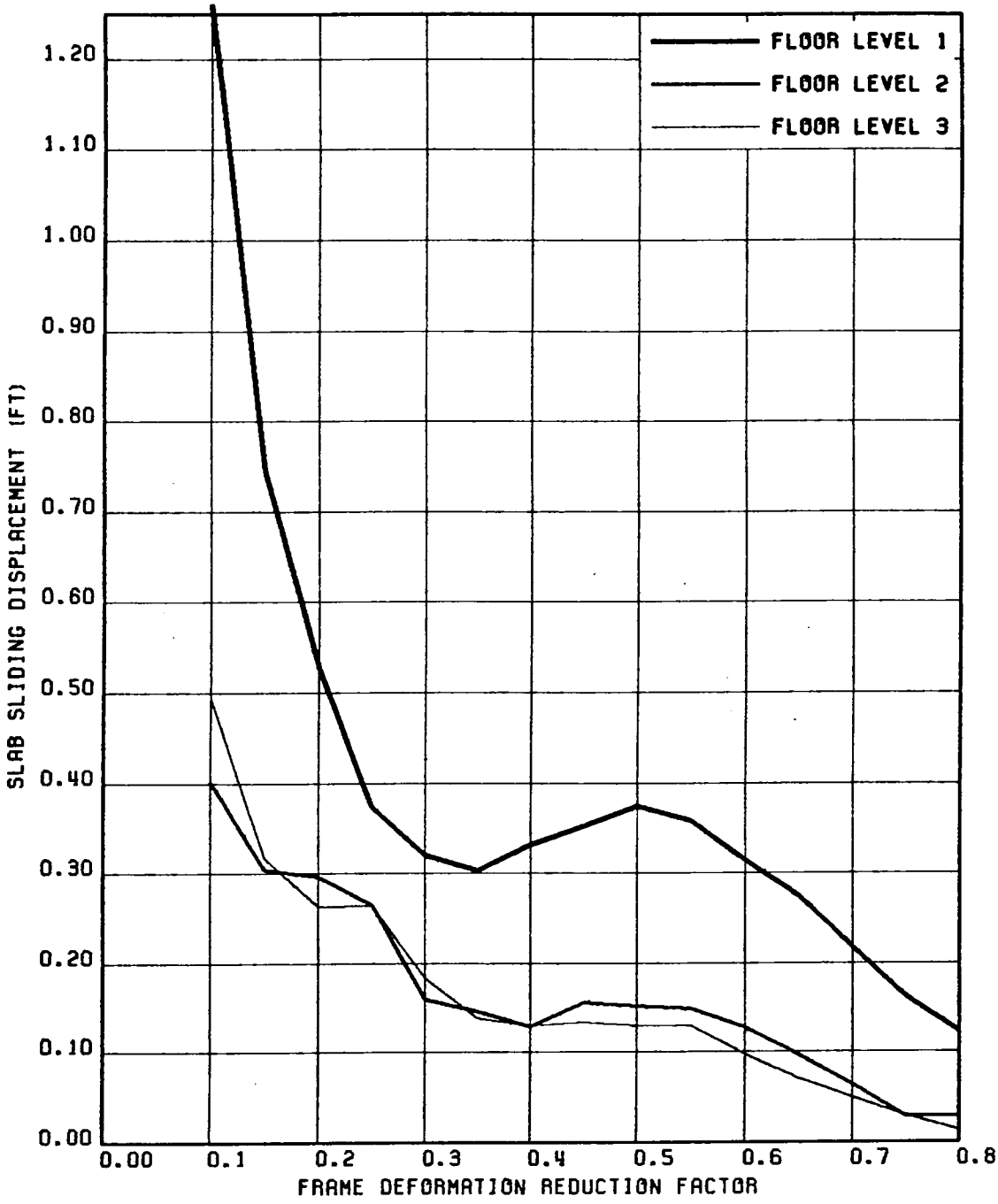

FIG. 5.65 VARIATION OF MAXIMUM SLAB SLIDING DISPLACEMENTS WITH FRAME DEFORMATION REDUCTION FACTOR; STRUCTURE 1, GR MOTION 1-HZ & VT COMP

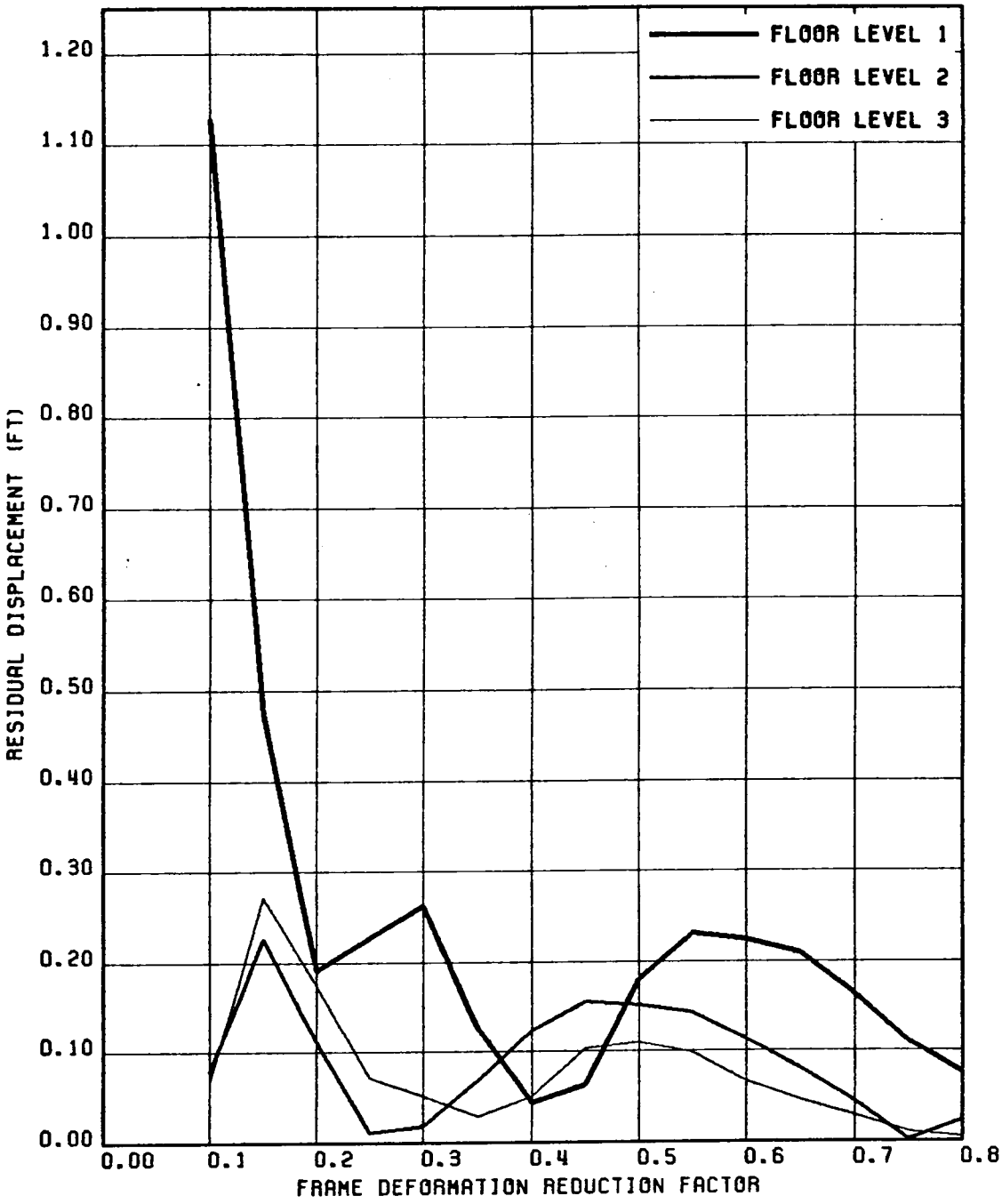

FIG. 5.66 VARIATION OF RESIDUAL SLAB SLIDING DISPLACEMENTS WITH FRAME DEFORMATION REDUCTION FACTOR; STRUCTURE 1, GR MOTION 1-HZ & VT COMP

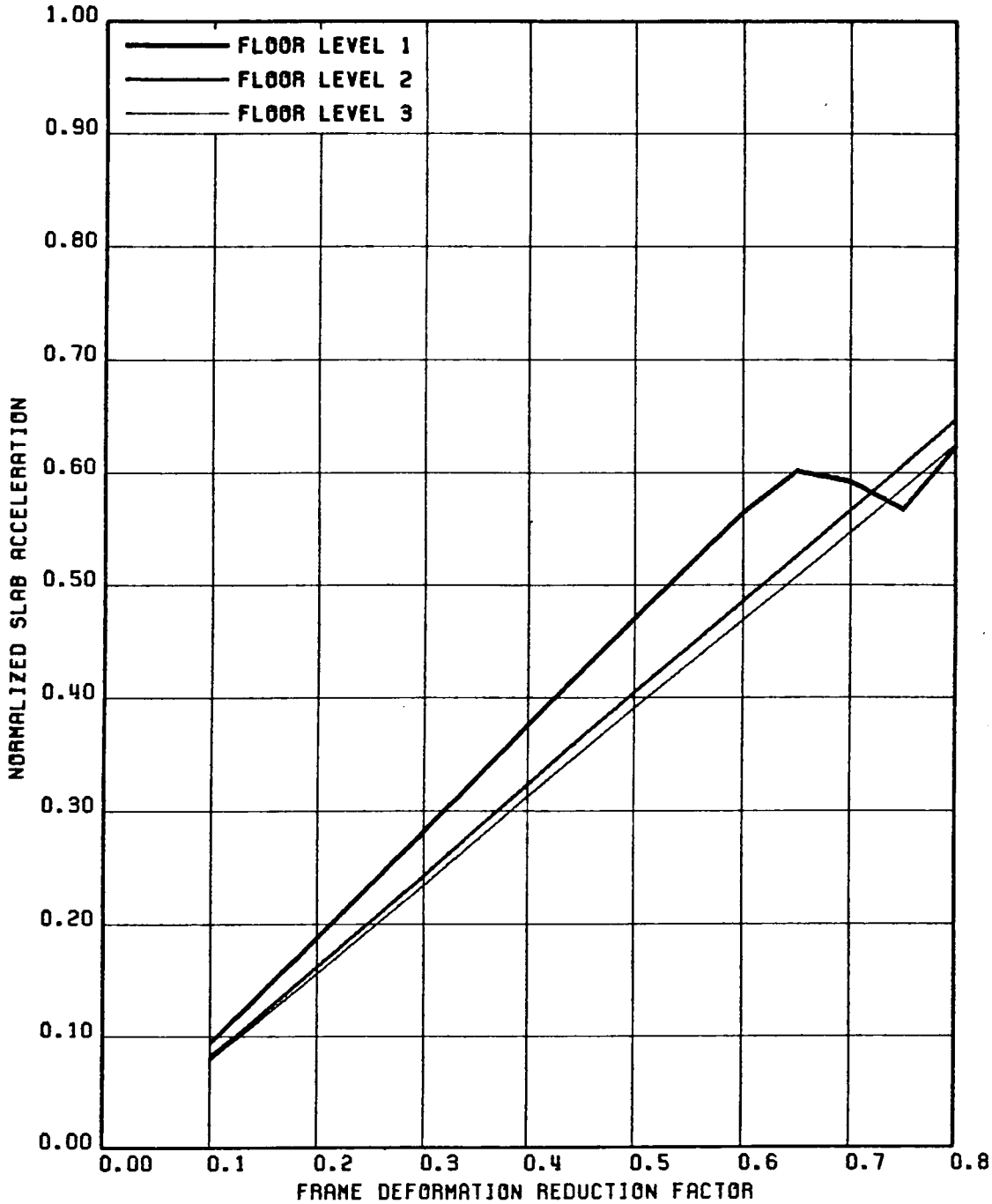

FIG. 5.67 VARIATION OF NORMALIZED SLAB ACCELERATION (NORMALIZED W.R.T. THE CORRESPONDING NON-SLIDING ACCELERATION RESPONSE) WITH FRAME DEFORMATION REDUCTION FACTOR; STRUCTURE 1, GR MOTION 2-HZ COMPONENT

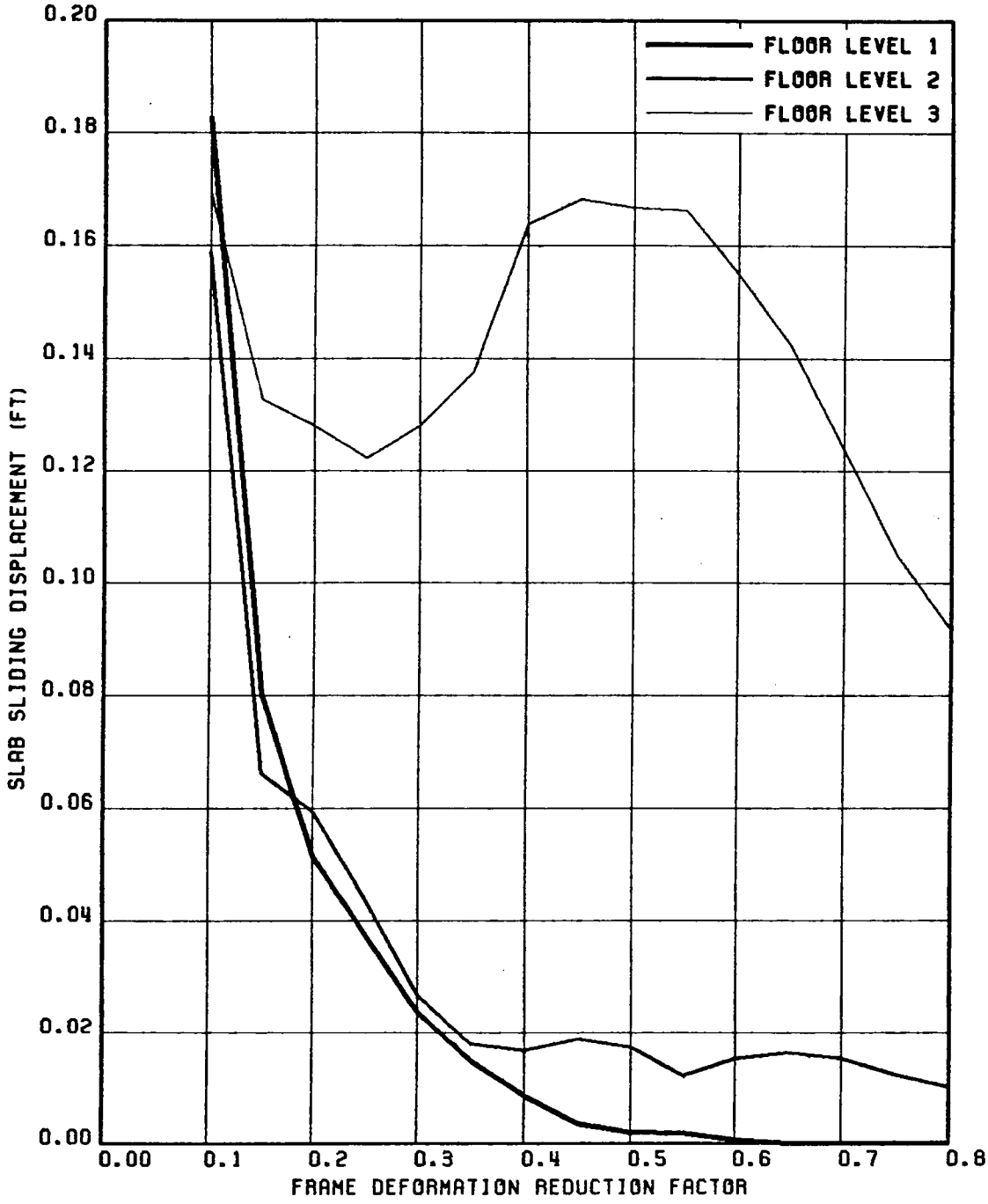

FIG. 5.68 VARIATION OF MAXIMUM SLAB SLIDING DISPLACEMENTS WITH FRAME DEFORMATION REDUCTION FACTOR; STRUCTURE 1, GR MOTION 2-HZ COMPONENT

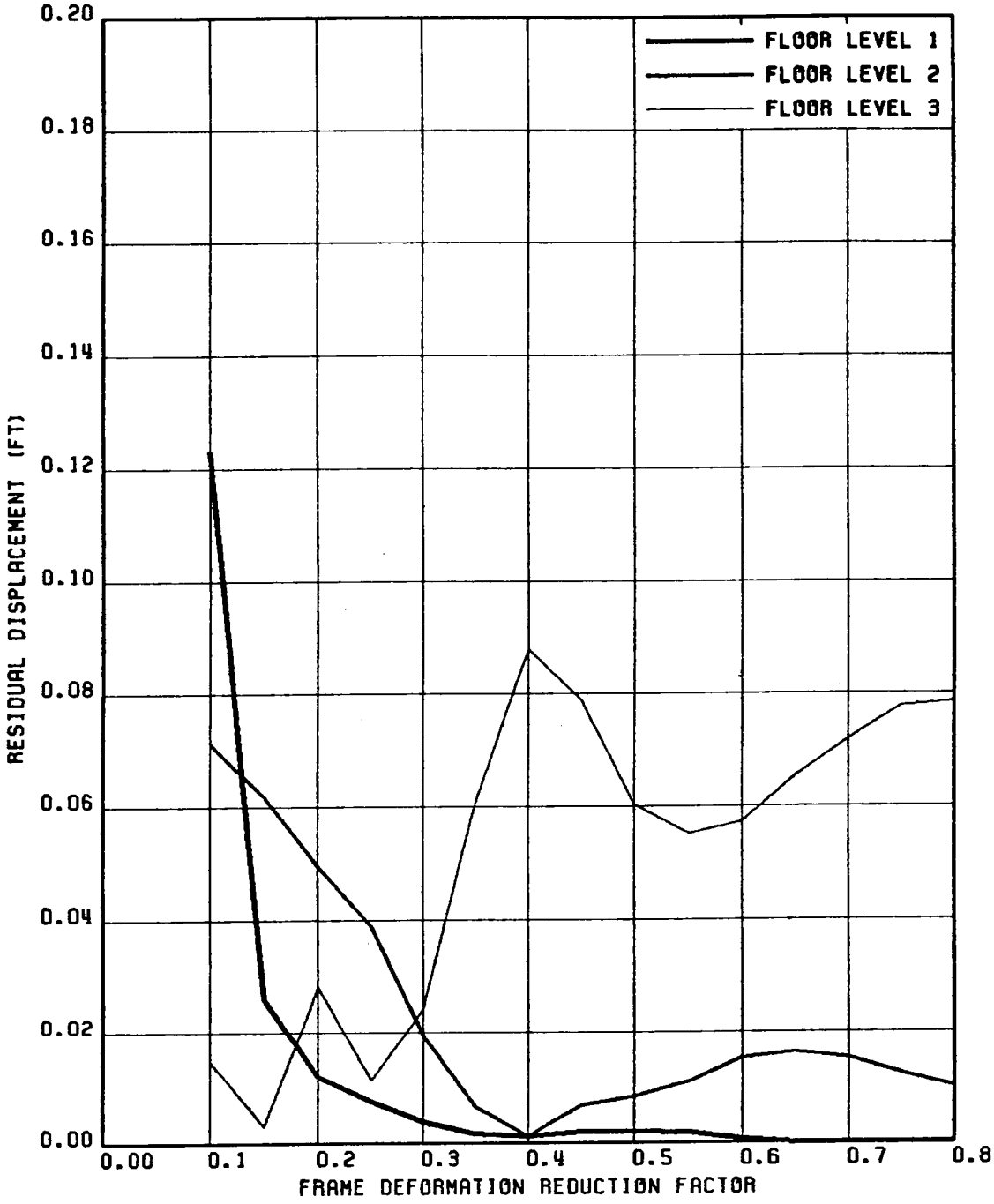

FIG. 5.69 VARIATION OF RESIDUAL SLAB SLIDING DISPLACEMENTS WITH FRAME DEFORMATION REDUCTION FACTOR; STRUCTURE 1, GR MOTION 2-HZ COMPONENT

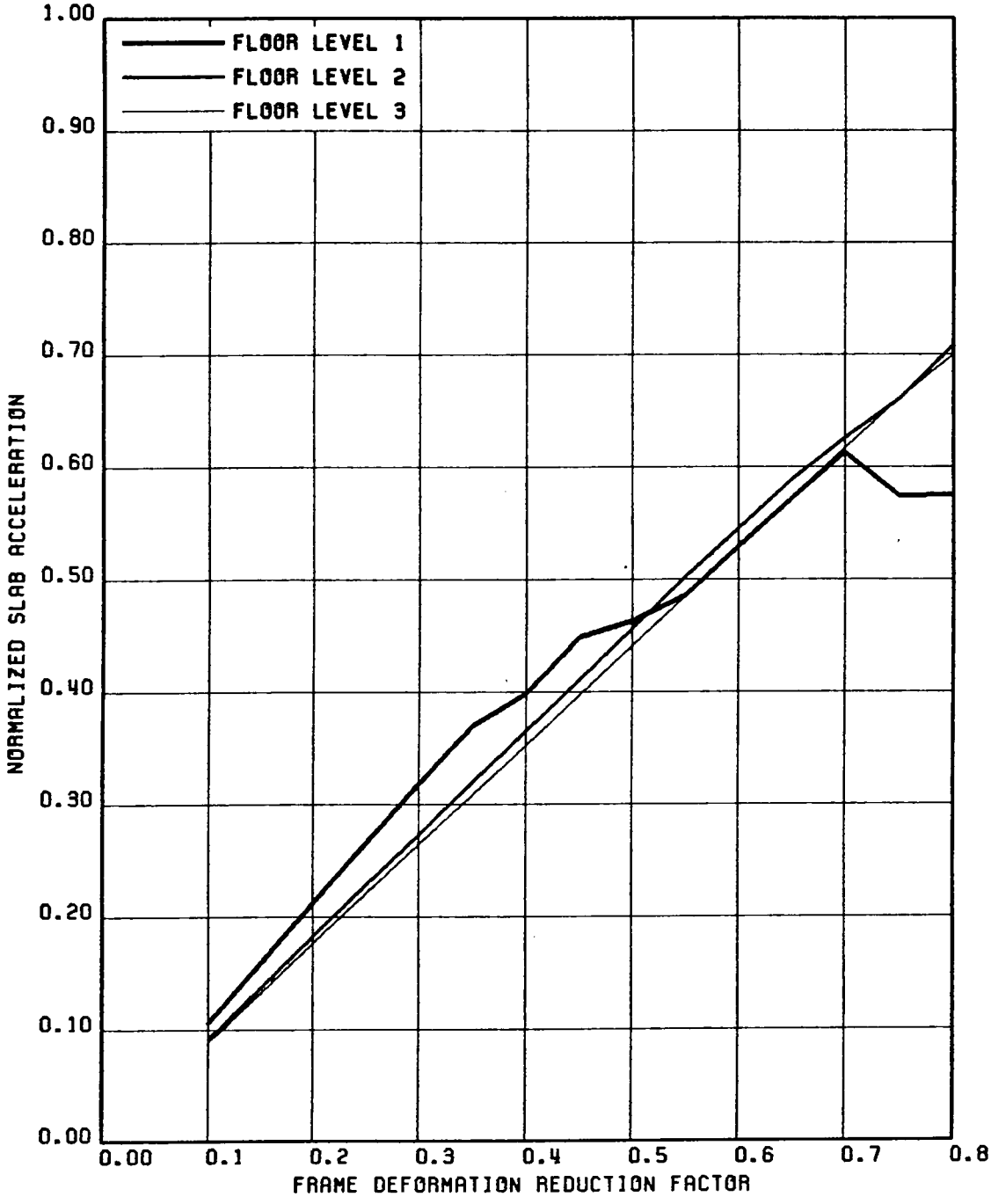

FIG. 5.70 VARIATION OF NORMALIZED SLAB ACCELERATION (NORMALIZED W.R.T. THE CORRESPONDING NON-SLIDING ACCELERATION RESPONSE) WITH FRAME DEFORMATION REDUCTION FACTOR; STRUCTURE 1, GR MOTION 2-HZ & VT COMP

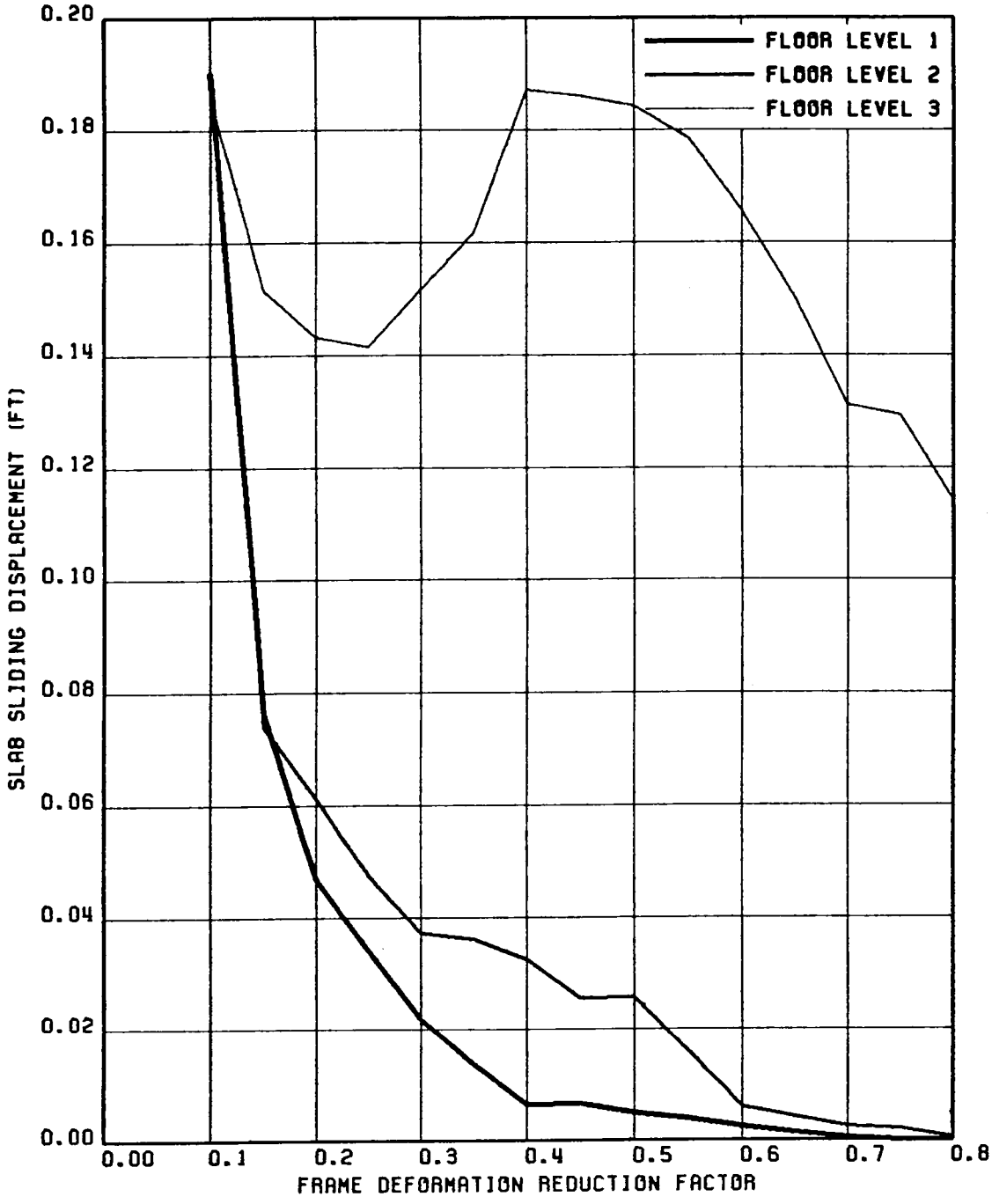

FIG. 5.71 VARIATION OF MAXIMUM SLAB SLIDING DISPLACEMENTS WITH FRAME DEFORMATION REDUCTION FACTOR; STRUCTURE 1, GR MOTION 2-HZ & VT COMP

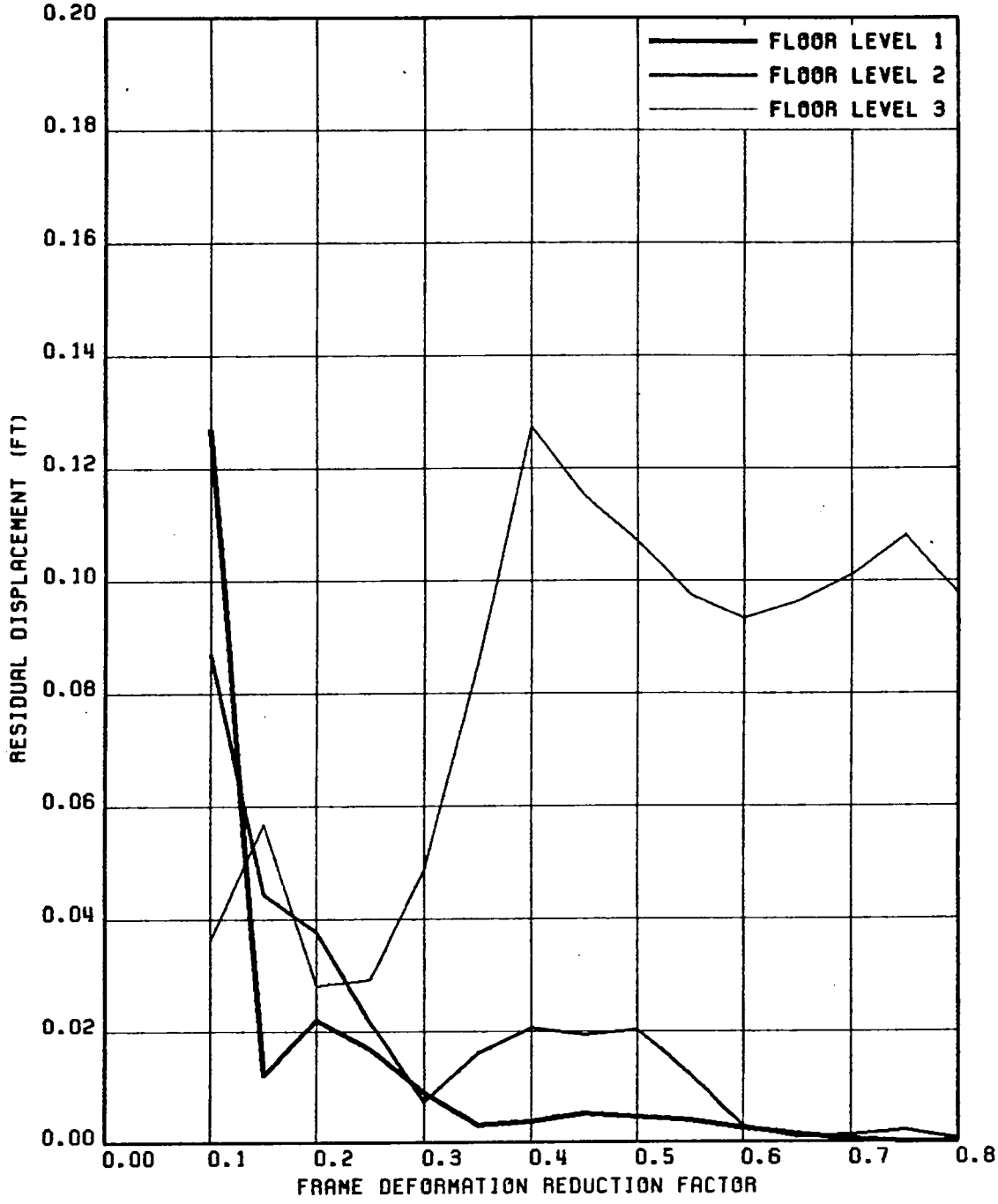

FIG. 5.72 VARIATION OF RESIDUAL SLAB SLIDING DISPLACEMENTS WITH FRAME DEFORMATION REDUCTION FACTOR; STRUCTURE 1, GR MOTION 2-HZ & VT COMP

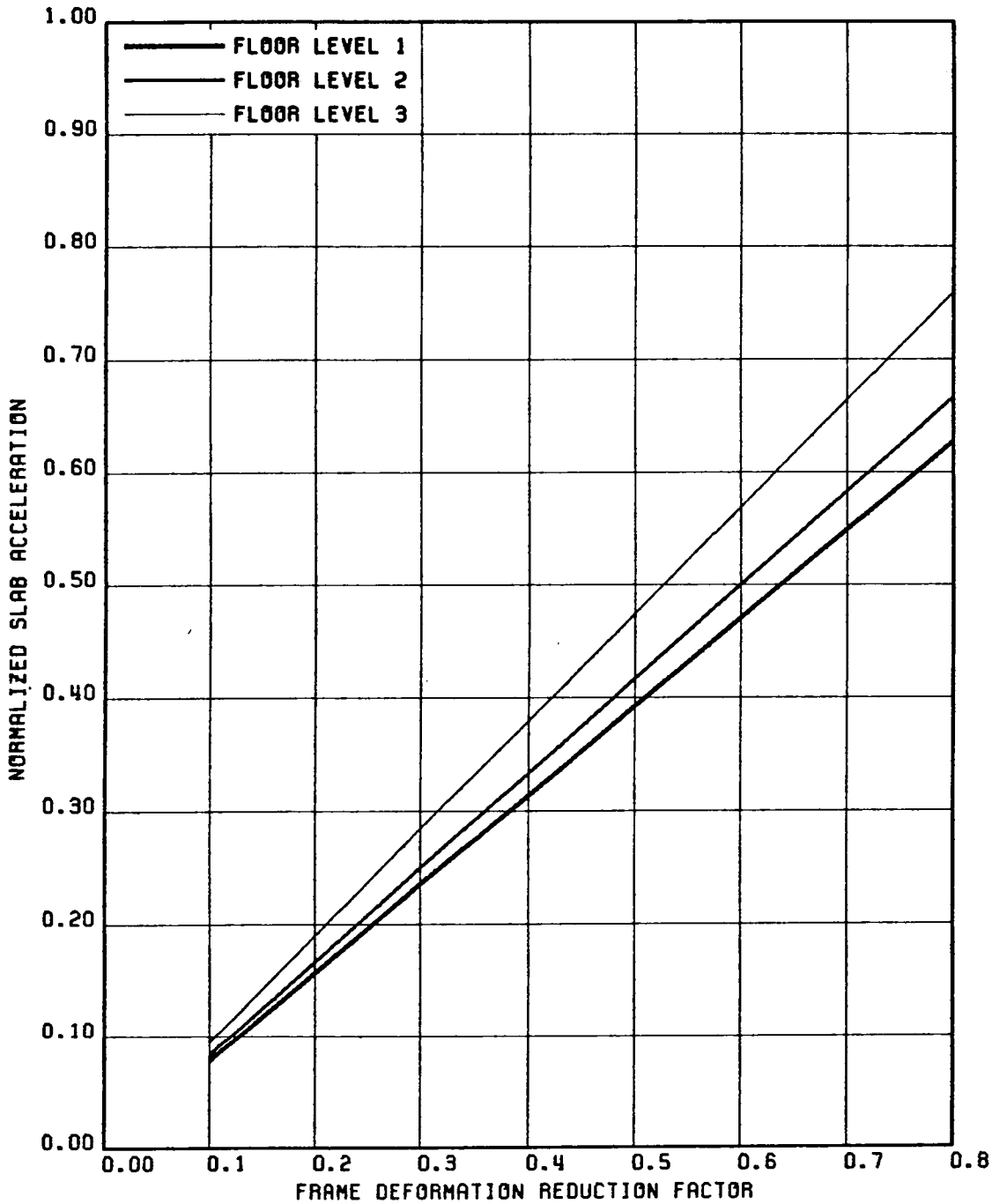

FIG. 5.73 VARIATION OF NORMALIZED SLAB ACCELERATION (NORMALIZED W.R.T. THE CORRESPONDING NON-SLIDING ACCELERATION RESPONSE) WITH FRAME DEFORMATION REDUCTION FACTOR; STRUCTURE 1, GR MOTION 3-HZ COMPONENT

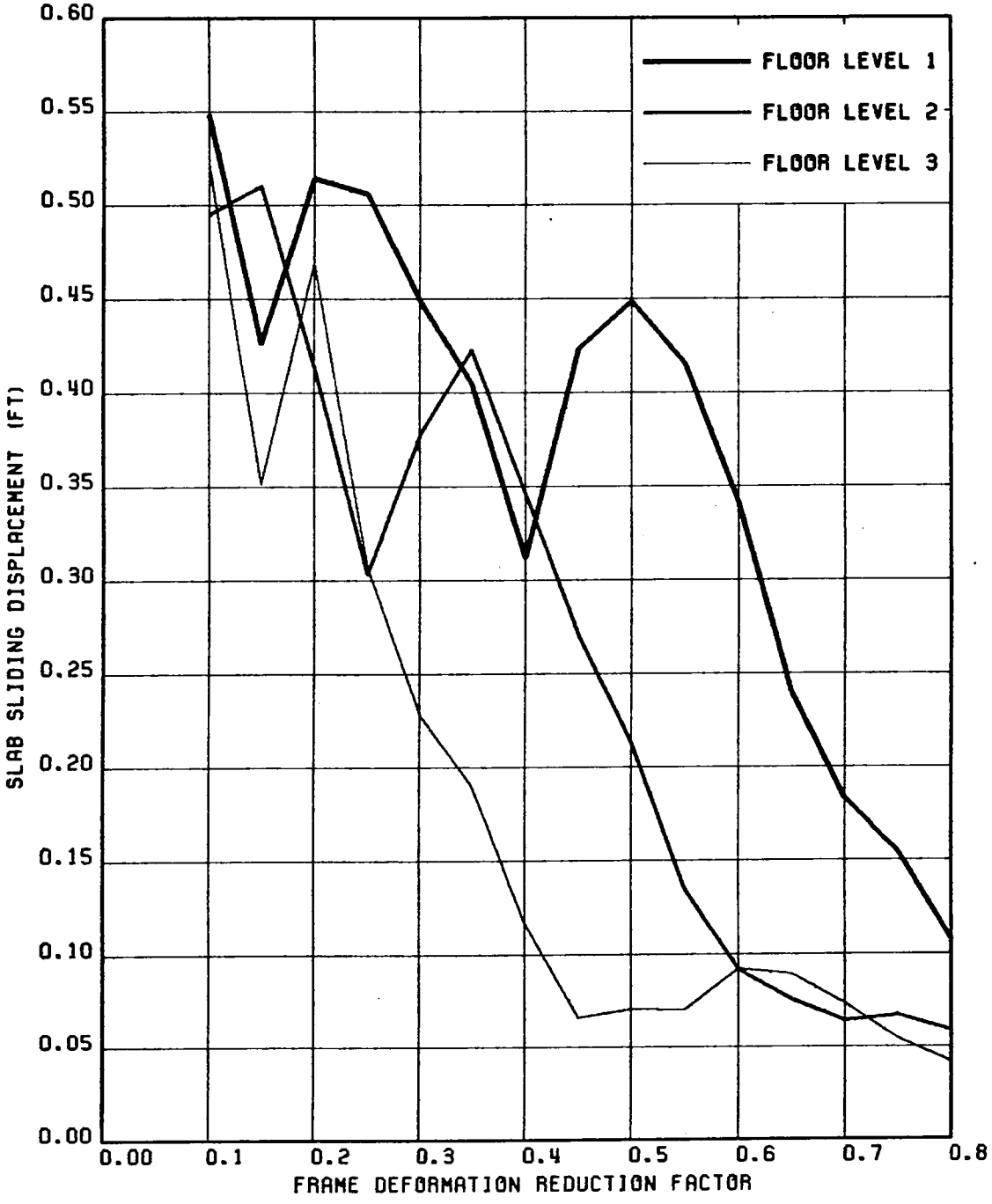

FIG. 5.74 VARIATION OF MAXIMUM SLAB SLIDING DISPLACEMENTS WITH FRAME DEFORMATION REDUCTION FACTOR; STRUCTURE 1, GR MOTION 3-HZ COMPONENT

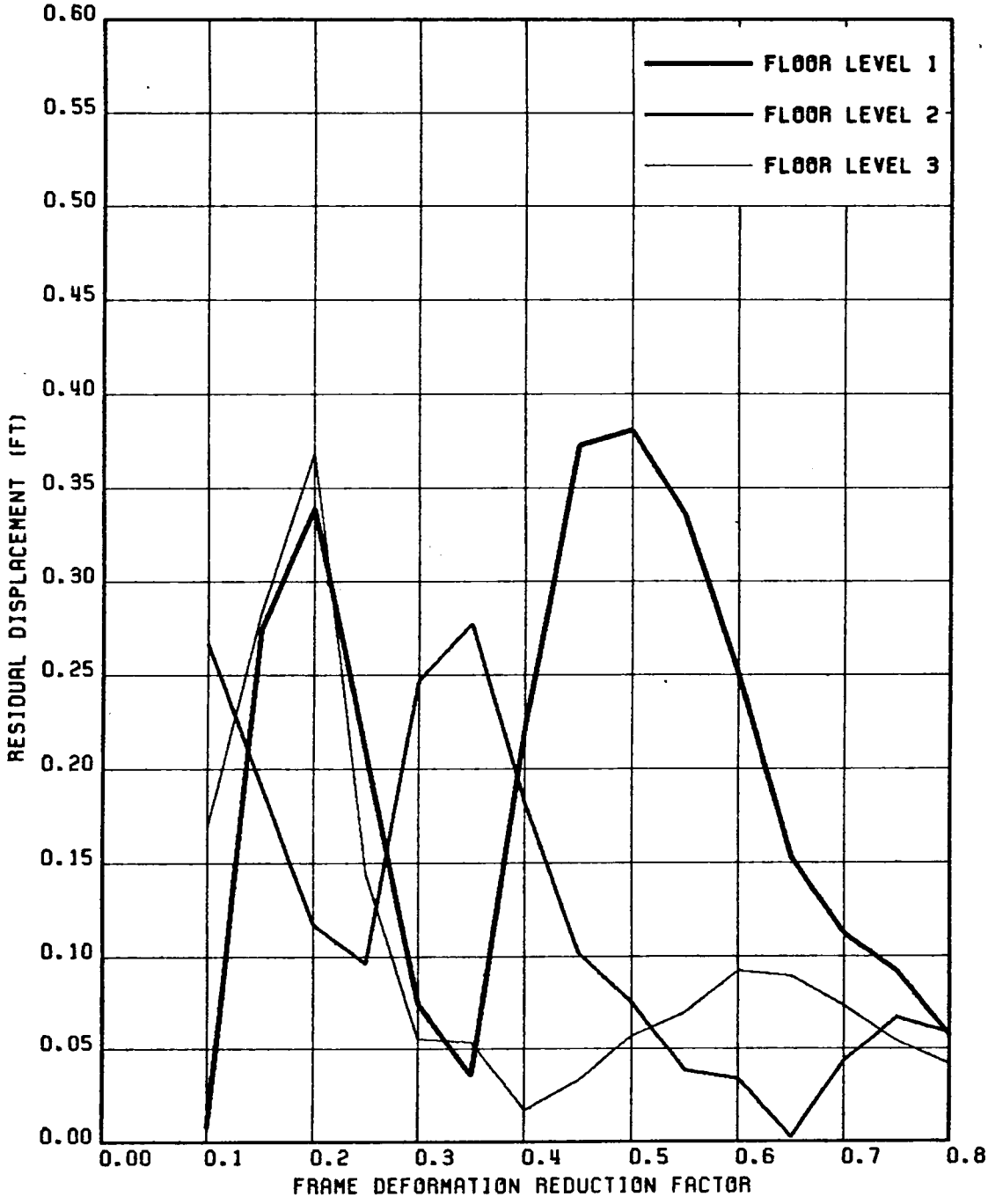

FIG. 5.75 VARIATION OF RESIDUAL SLAB SLIDING DISPLACEMENTS WITH FRAME DEFORMATION REDUCTION FACTOR; STRUCTURE 1, GR MOTION 3-HZ COMPONENT

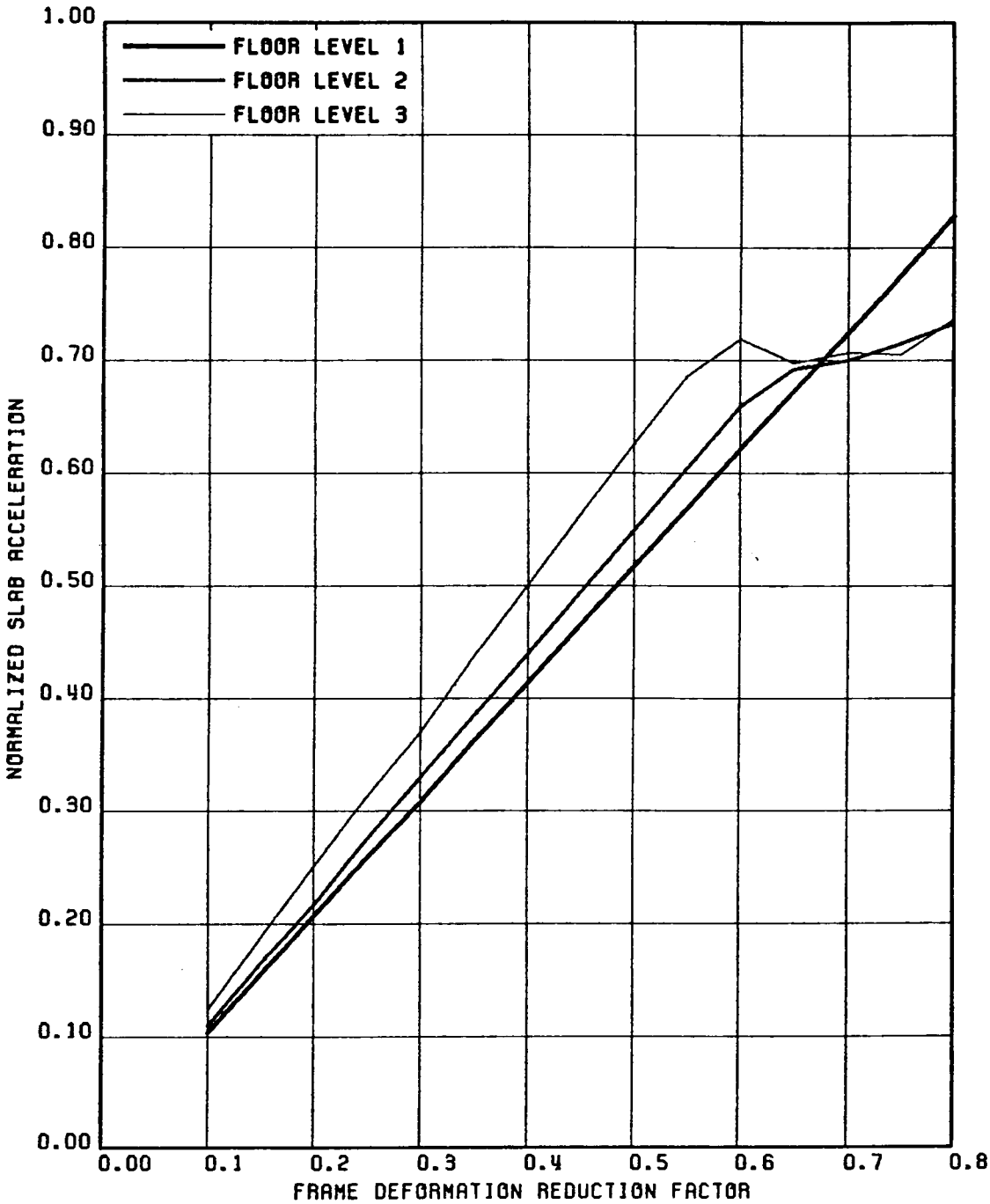

FIG. 5.76 VARIATION OF NORMALIZED SLAB ACCELERATION (NORMALIZED W.R.T. THE CORRESPONDING NON-SLIDING ACCELERATION RESPONSE) WITH FRAME DEFORMATION REDUCTION FACTOR; STRUCTURE 1, GR MOTION 3-HZ & VT COMP

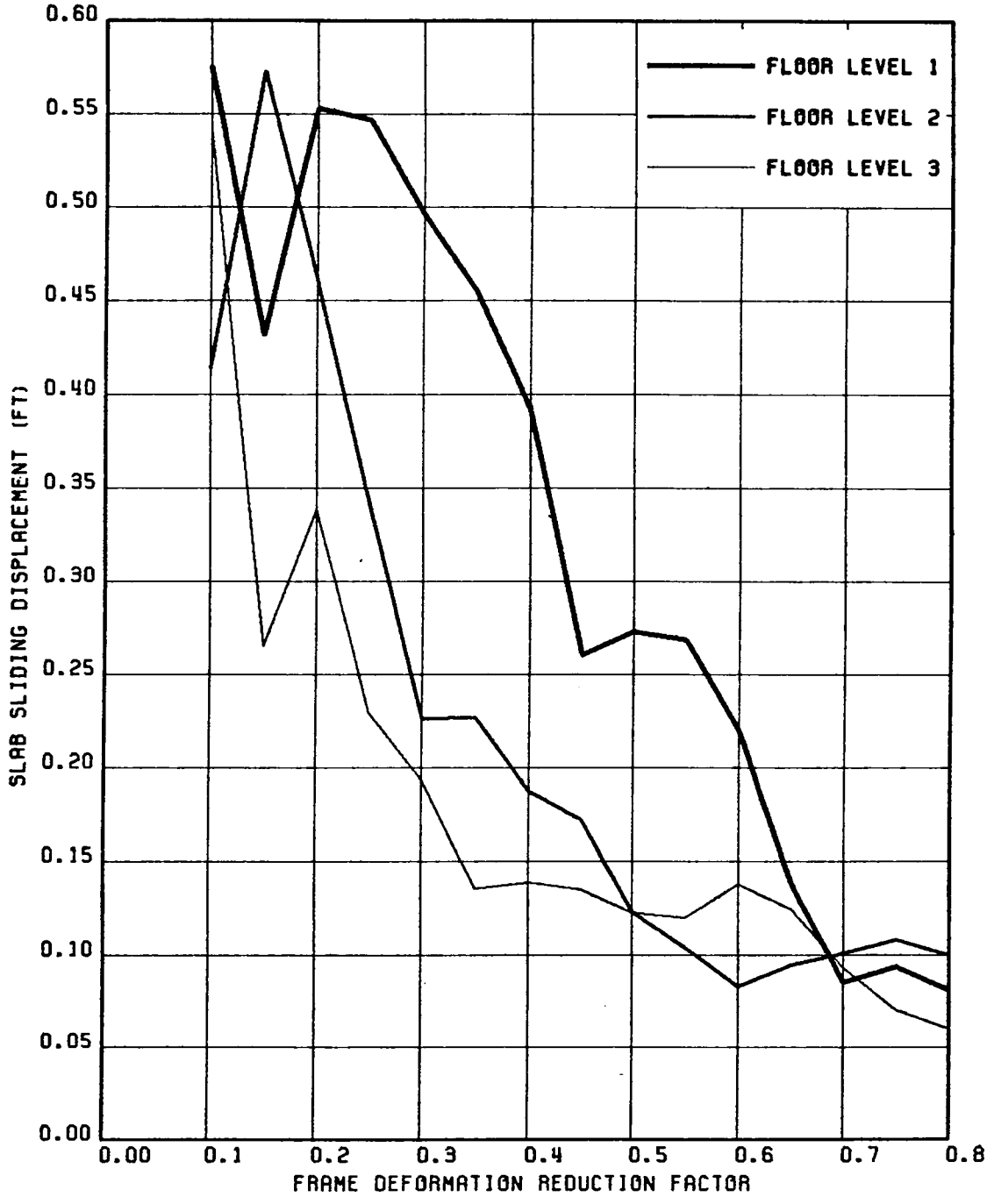

FIG. 5.77 VARIATION OF MAXIMUM SLAB SLIDING DISPLACEMENTS WITH FRAME DEFORMATION REDUCTION FACTOR; STRUCTURE 1, GR MOTION 3-HZ & VT COMP

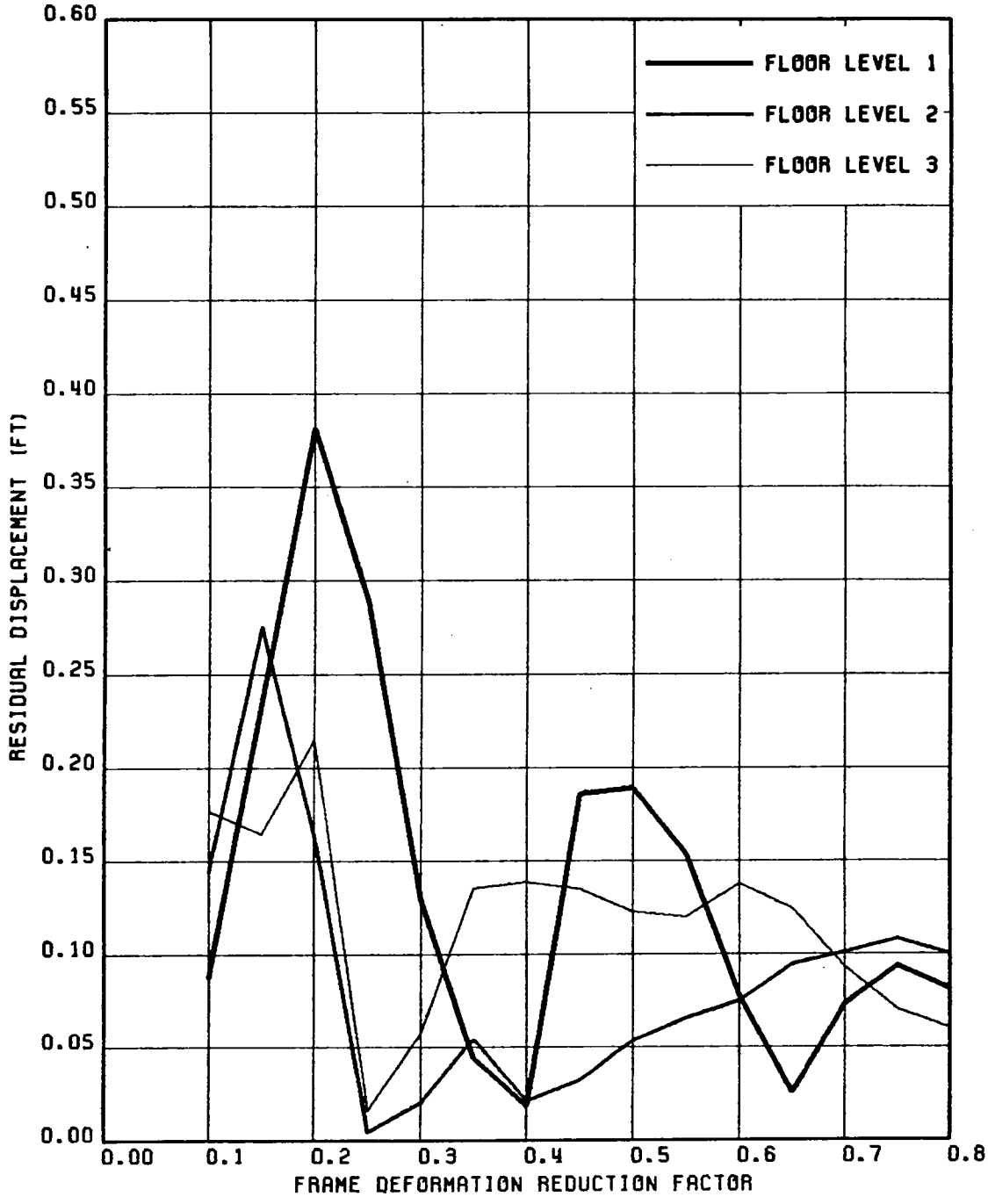

FIG. 5.78 VARIATION OF RESIDUAL SLAB SLIDING DISPLACEMENTS WITH FRAME DEFORMATION REDUCTION FACTOR; STRUCTURE 1, GR MOTION 3-HZ & VT COMP

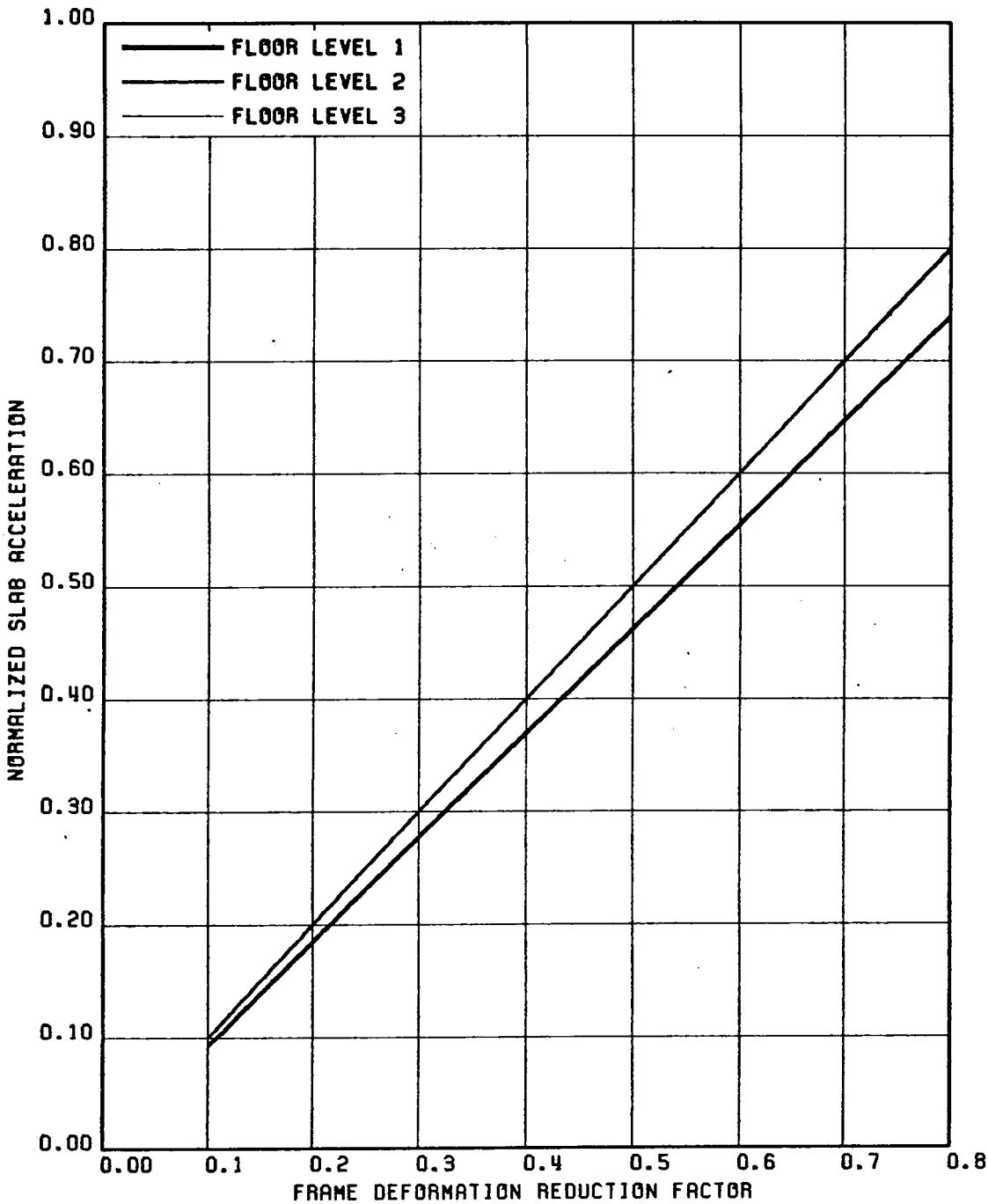

FIG. 5.79 VARIATION OF NORMALIZED SLAB ACCELERATION (NORMALIZED W.R.T. THE CORRESPONDING NON-SLIDING ACCELERATION RESPONSE) WITH FRAME DEFORMATION REDUCTION FACTOR; STRUCTURE 2, GR MOTION 1-HZ COMPONENT

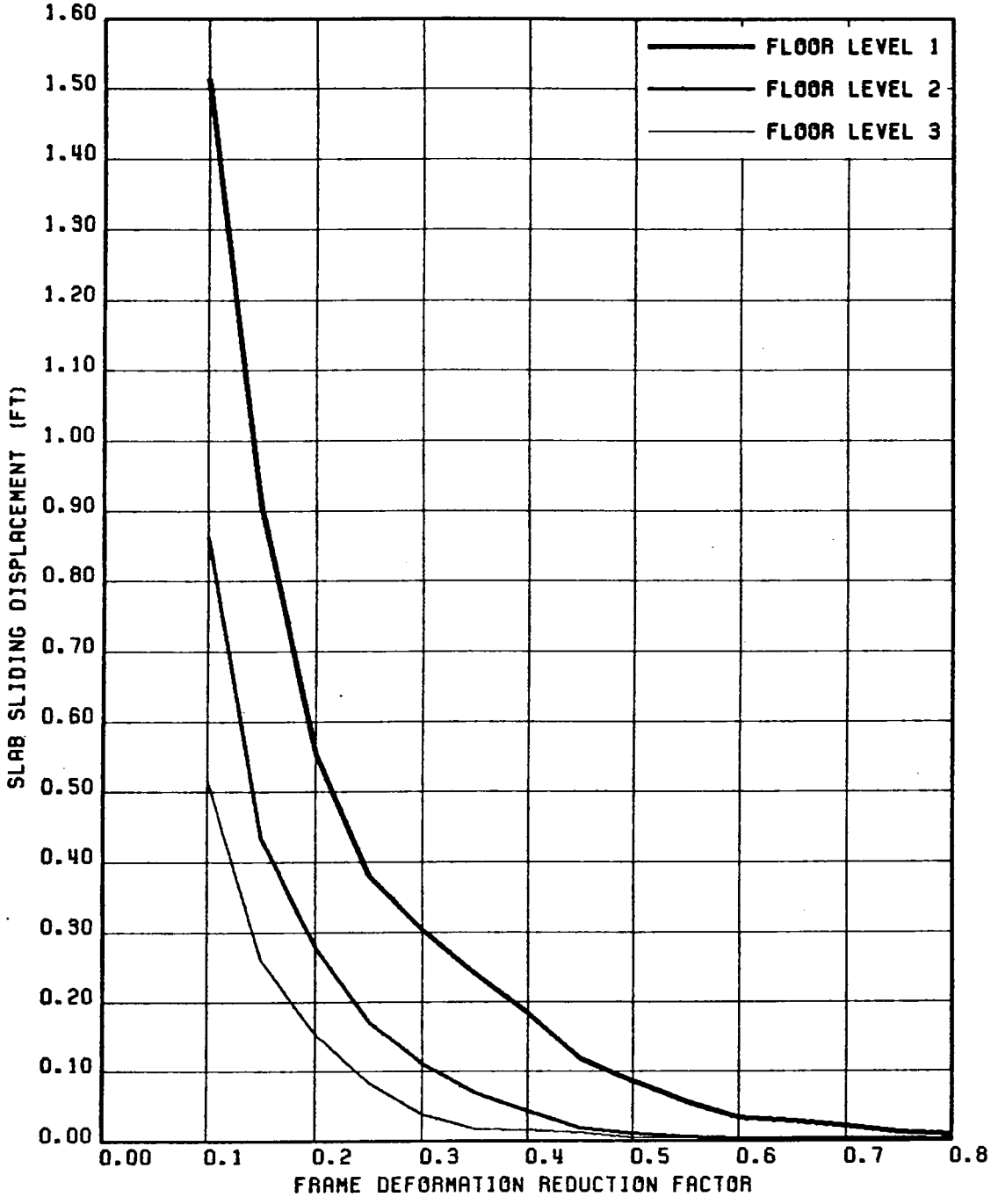

FIG. 5.80 VARIATION OF MAXIMUM SLAB SLIDING DISPLACEMENTS WITH FRAME DEFORMATION REDUCTION FACTOR; STRUCTURE 2, GR MOTION 1-HZ COMPONENT

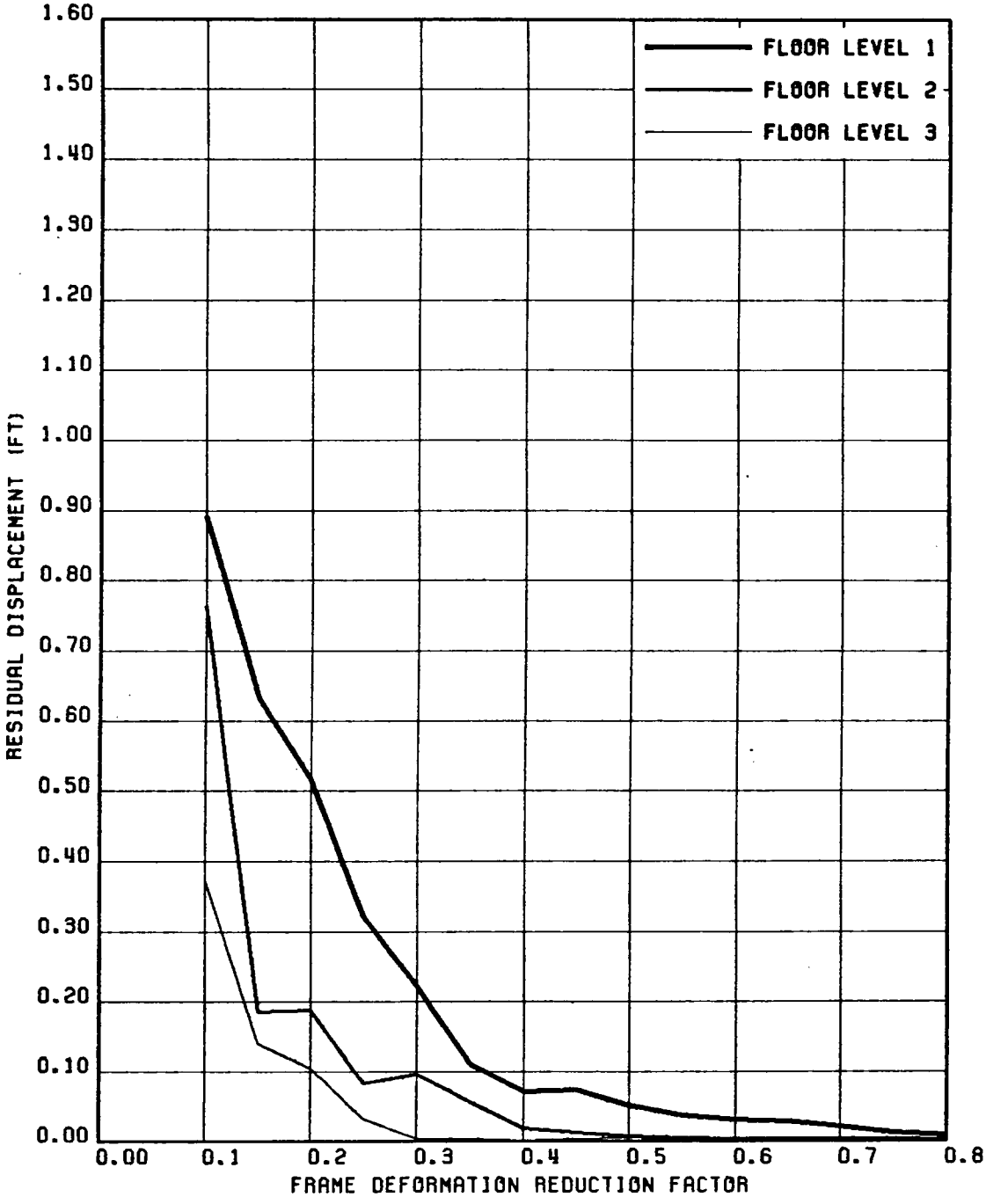

FIG. 5.81 VARIATION OF RESIDUAL SLAB SLIDING DISPLACEMENTS WITH FRAME DEFORMATION REDUCTION FACTOR; STRUCTURE 2, GR MOTION 1-HZ COMPONENT

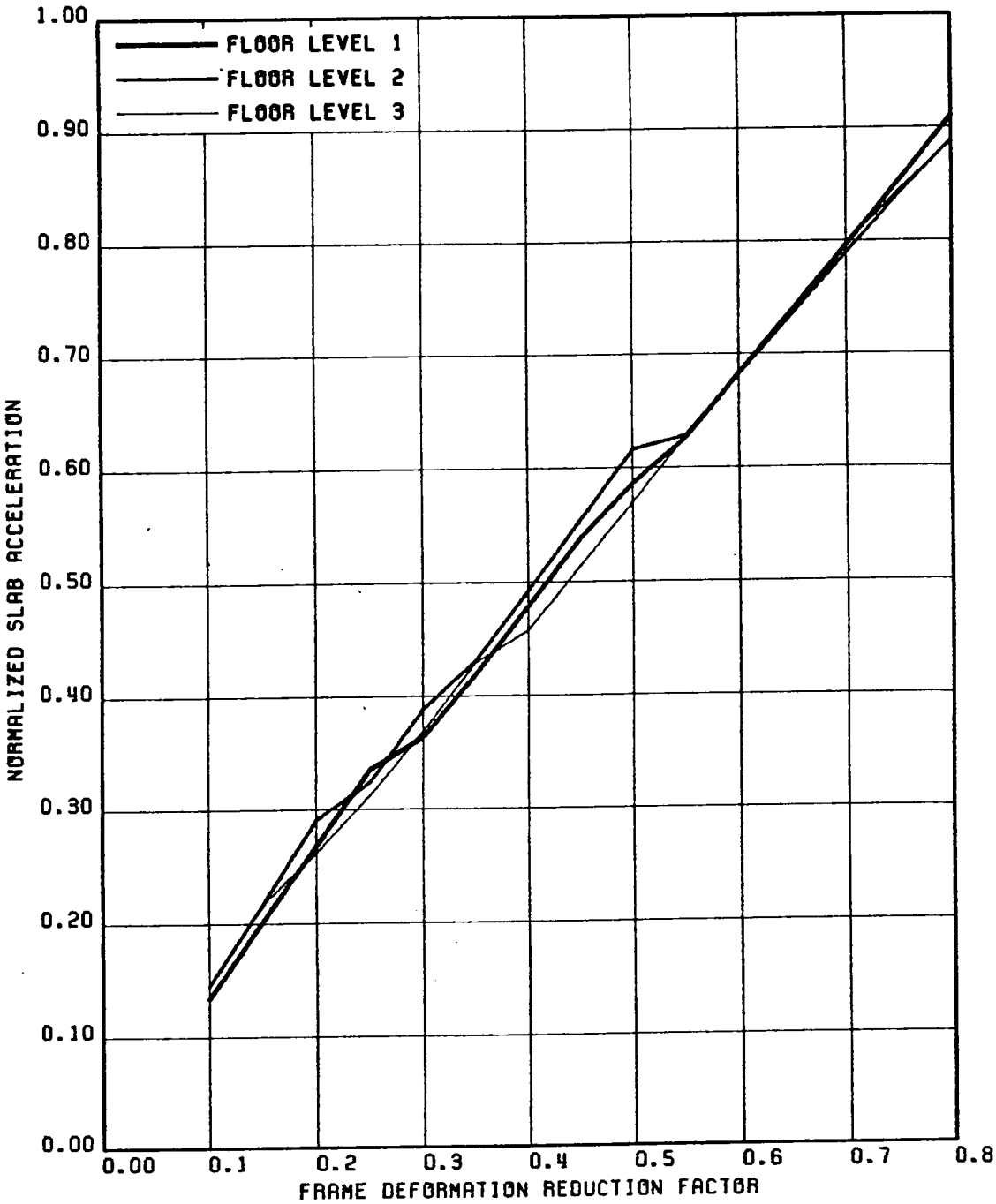

FIG. 5.82 VARIATION OF NORMALIZED SLAB ACCELERATION (NORMALIZED W.R.T. THE CORRESPONDING NON-SLIDING ACCELERATION RESPONSE) WITH FRAME DEFORMATION REDUCTION FACTOR; STRUCTURE 2, GR MOTION 1-HZ & VT COMP

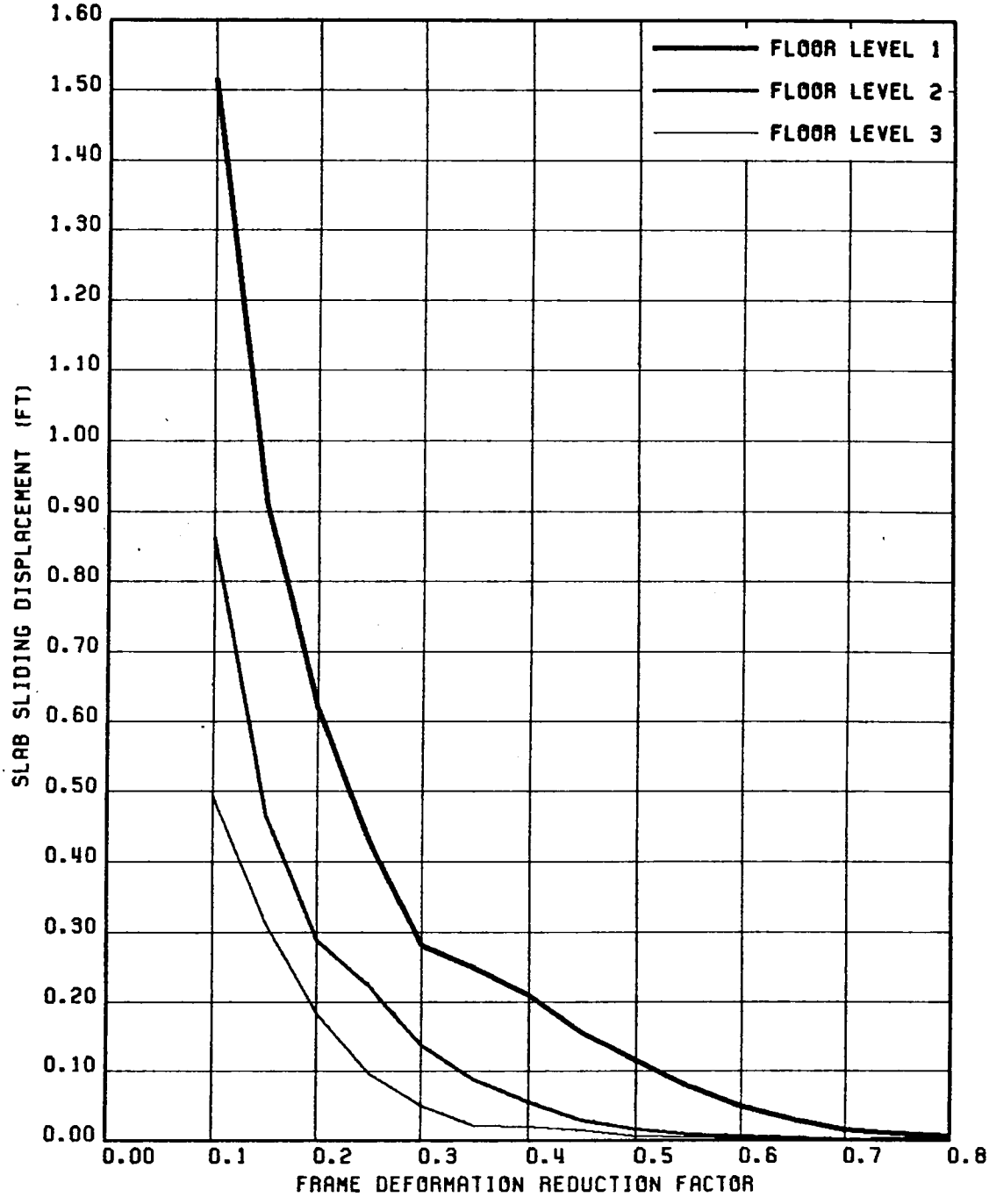

FIG. 5.83 VARIATION OF MAXIMUM SLAB SLIDING DISPLACEMENTS WITH FRAME DEFORMATION REDUCTION FACTOR; STRUCTURE 2, GR MOTION 1-HZ & VT COMP

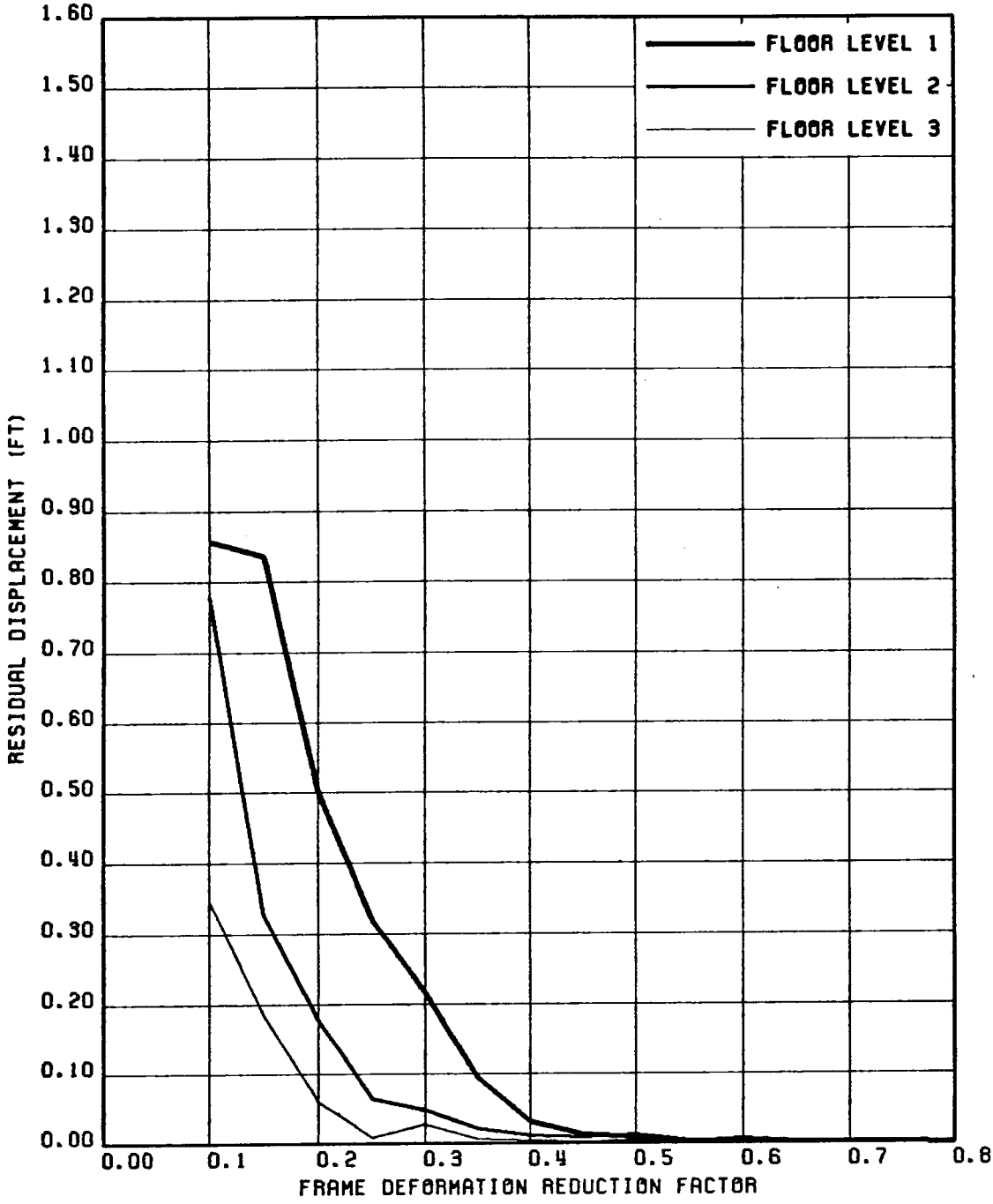

FIG. 5.84 VARIATION OF RESIDUAL SLAB SLIDING DISPLACEMENTS WITH FRAME DEFORMATION REDUCTION FACTOR; STRUCTURE 2, GR MOTION 1-HZ & VT COMP

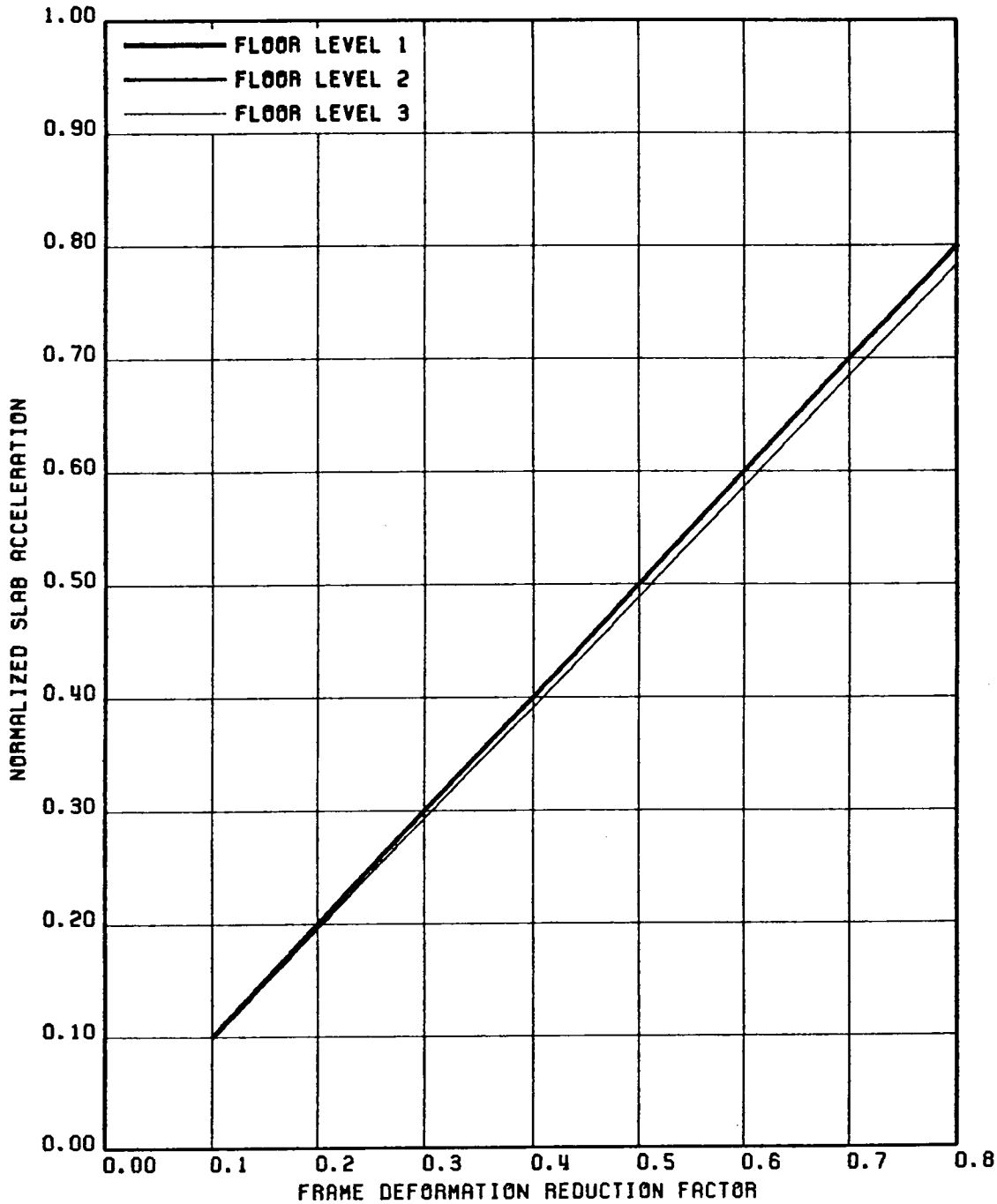

FIG. 5.85 VARIATION OF NORMALIZED SLAB ACCELERATION (NORMALIZED W.R.T. THE CORRESPONDING NON-SLIDING ACCELERATION RESPONSE) WITH FRAME DEFORMATION REDUCTION FACTOR; STRUCTURE 2, GR MOTION 2-HZ COMPONENT

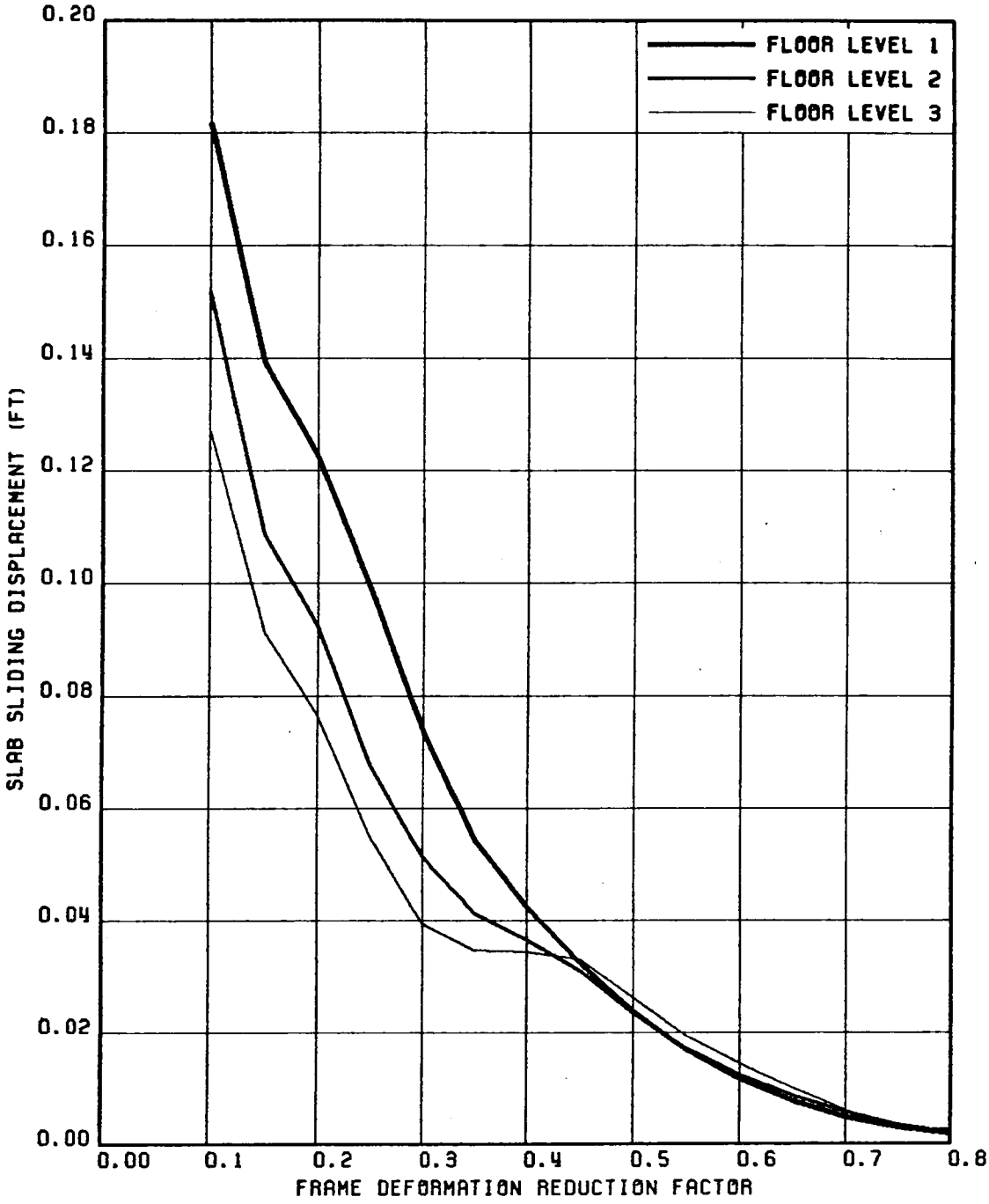

FIG. 5.86 VARIATION OF MAXIMUM SLAB SLIDING DISPLACEMENTS WITH FRAME DEFORMATION REDUCTION FACTOR; STRUCTURE 2, GR MOTION 2-HZ COMPONENT

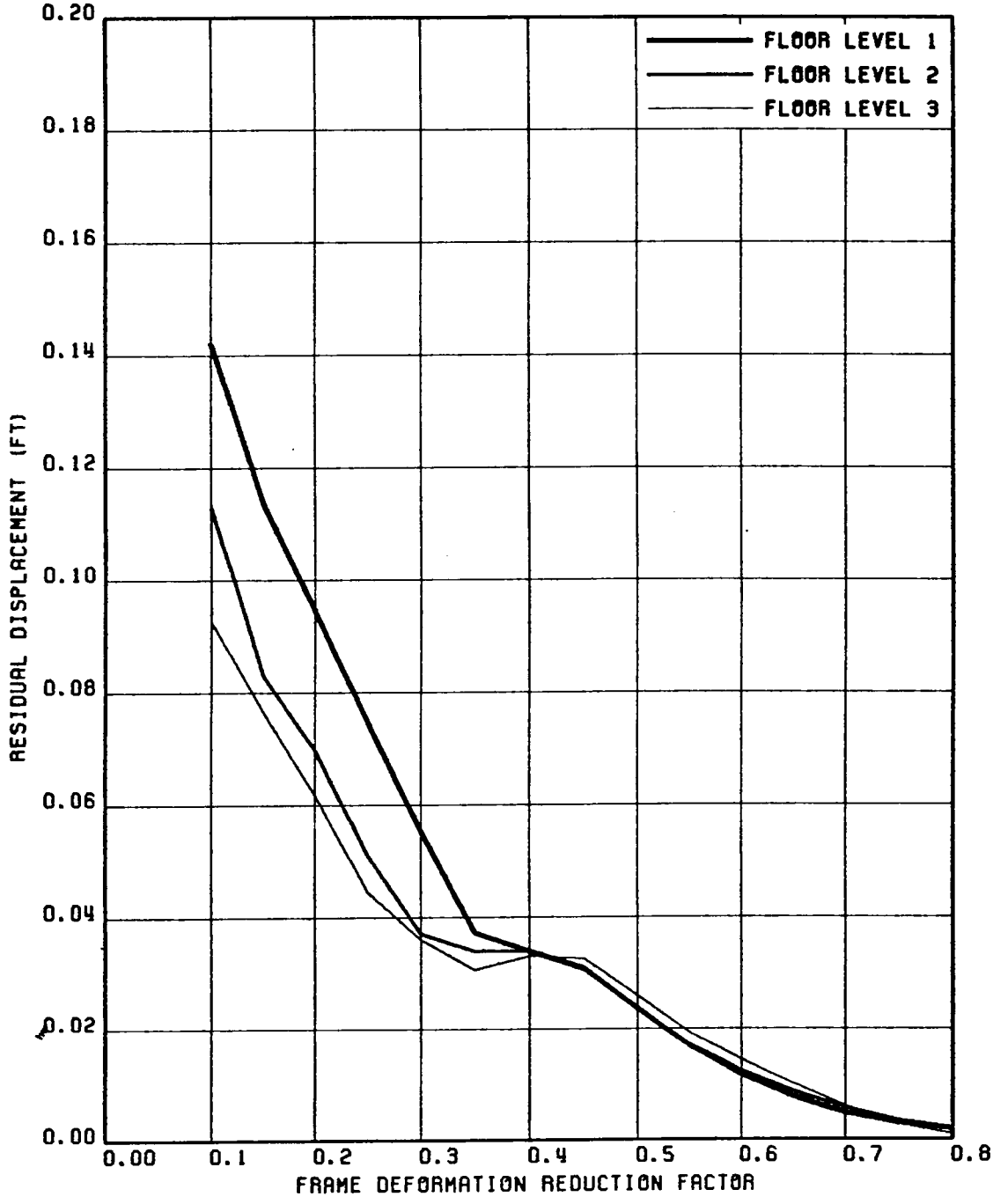

FIG. 5.87 VARIATION OF RESIDUAL SLAB SLIDING DISPLACEMENTS WITH FRAME DEFORMATION REDUCTION FACTOR; STRUCTURE 2, GR MOTION 2-HZ COMPONENT

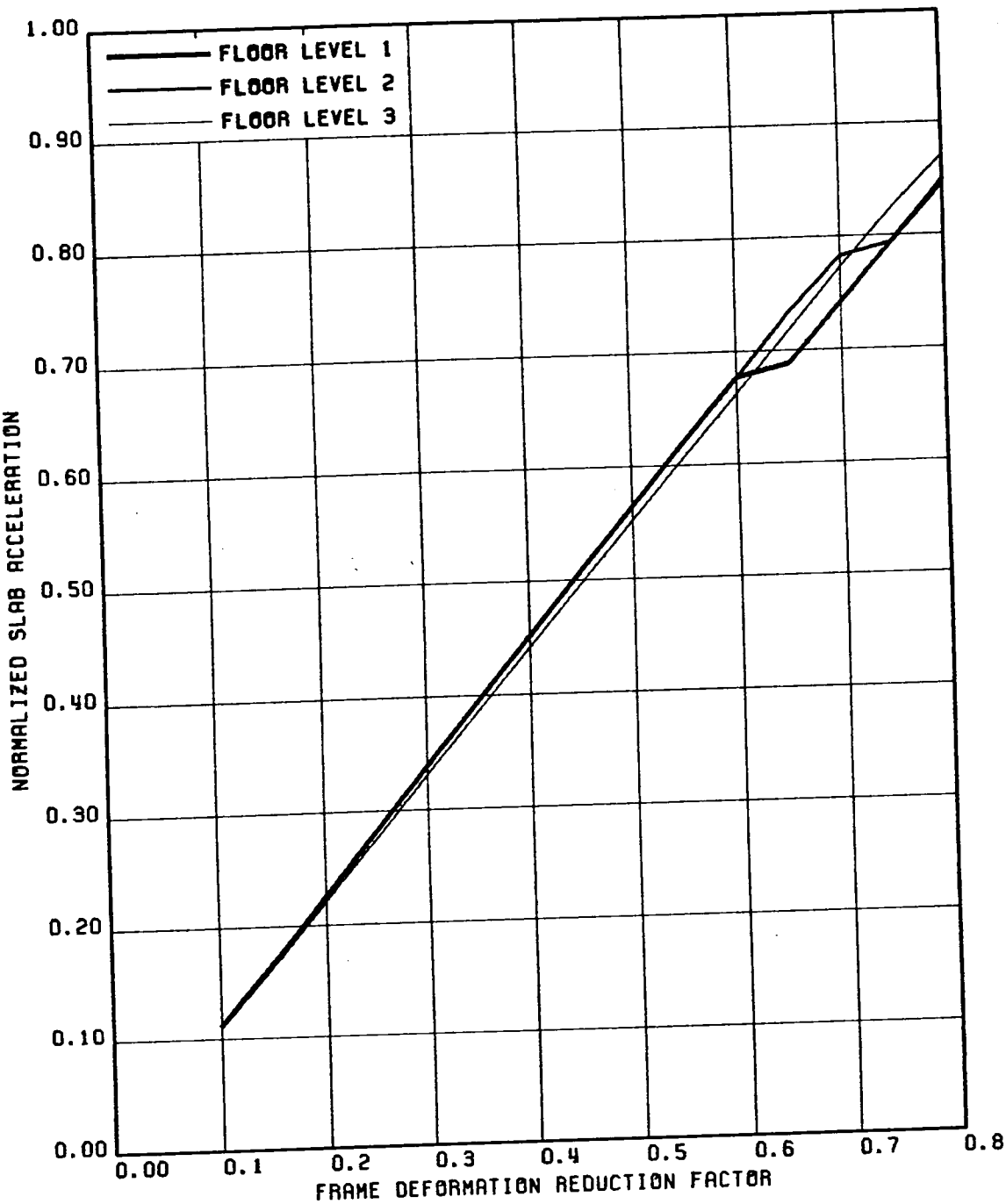

FIG. 5.88 VARIATION OF NORMALIZED SLAB ACCELERATION (NORMALIZED W.R.T. THE CORRESPONDING NON-SLIDING ACCELERATION RESPONSE) WITH FRAME DEFORMATION REDUCTION FACTOR; STRUCTURE 2, GR MOTION 2-HZ & VT COMP

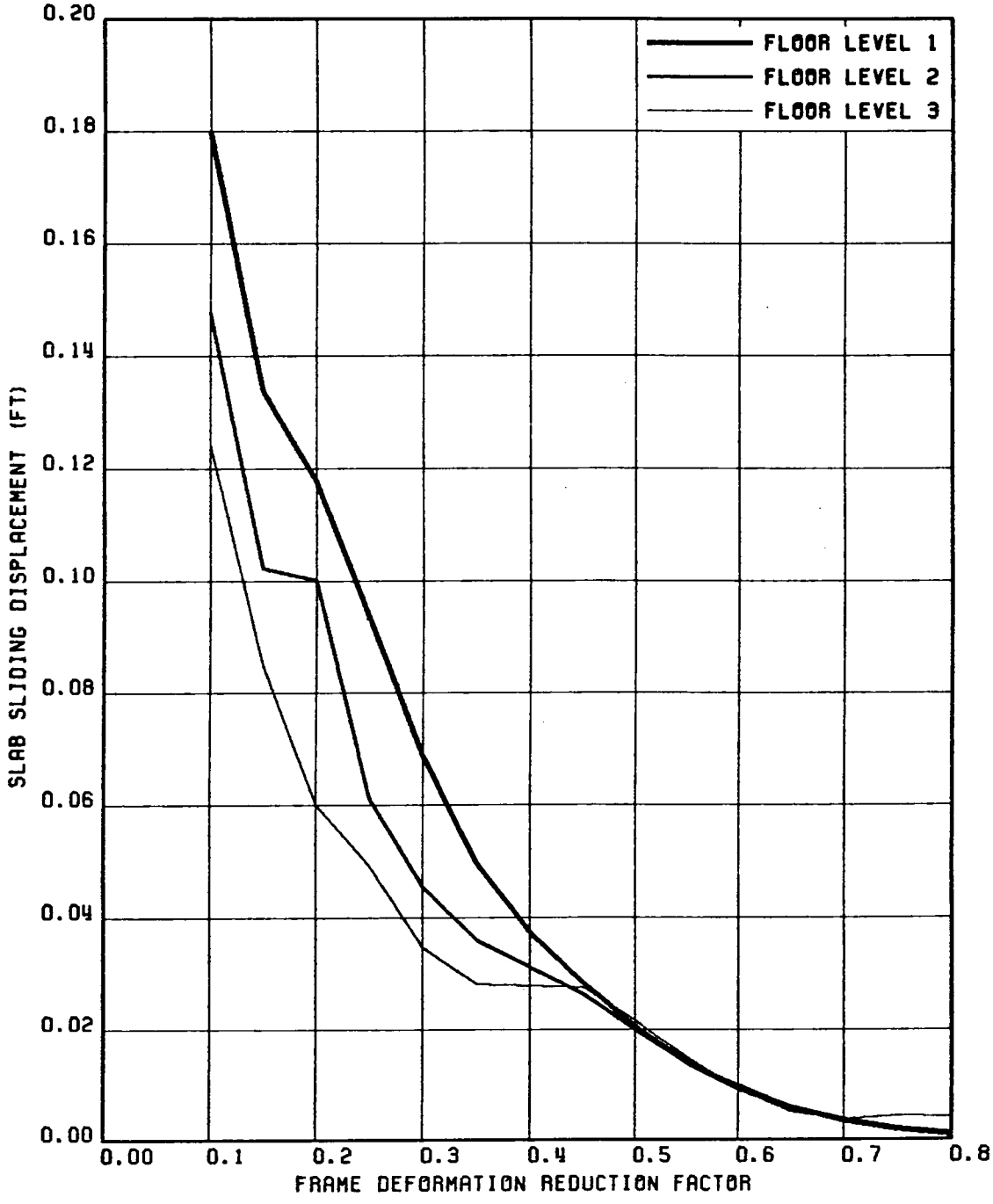

FIG. 5.89 VARIATION OF MAXIMUM SLAB SLIDING DISPLACEMENTS WITH FRAME DEFORMATION REDUCTION FACTOR; STRUCTURE 2, GR MOTION 2-HZ & VT COMP

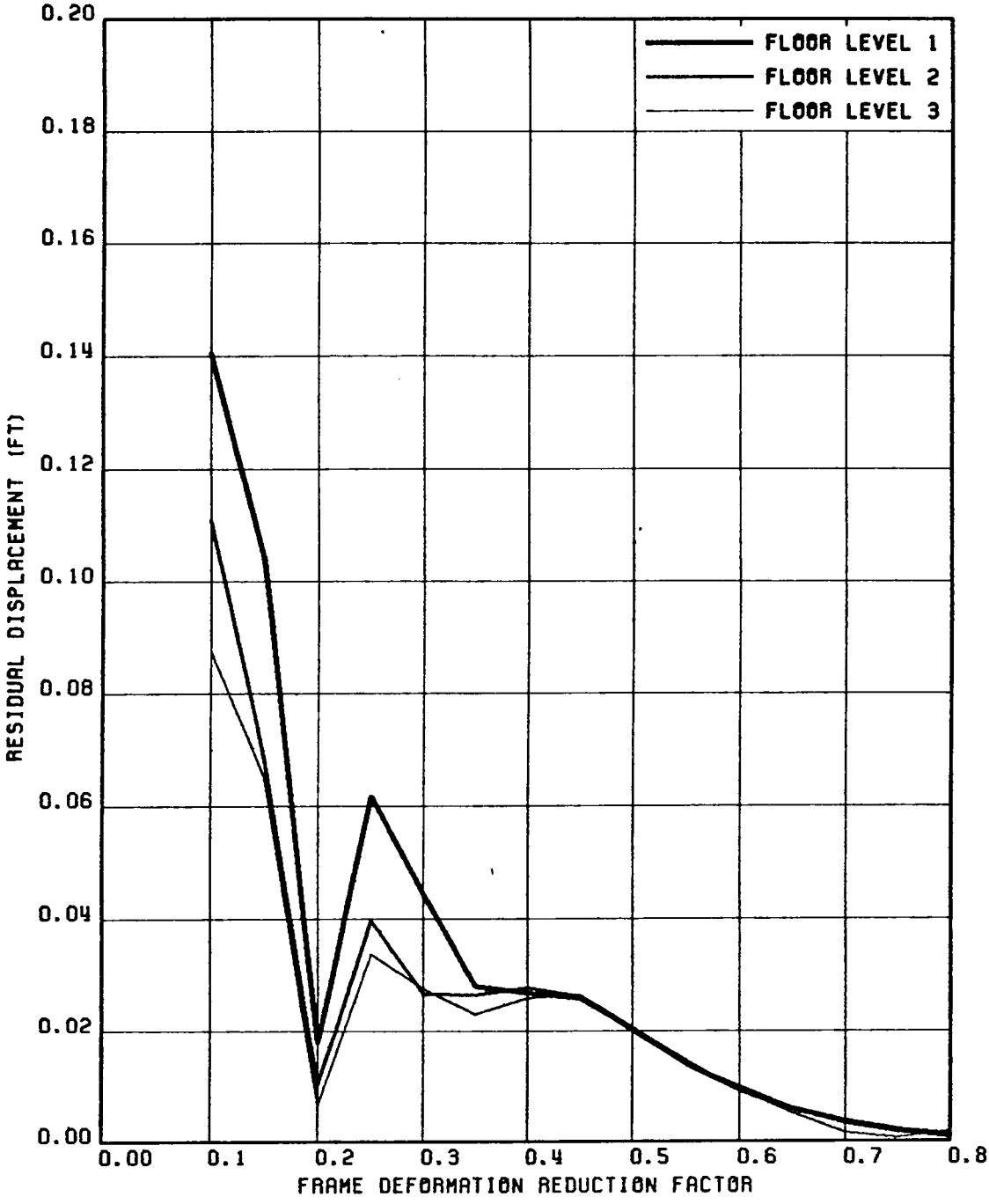

FIG. 5.90 VARIATION OF RESIDUAL SLAB SLIDING DISPLACEMENTS WITH FRAME DEFORMATION REDUCTION FACTOR; STRUCTURE 2, GR MOTION 2-HZ & VT COMP

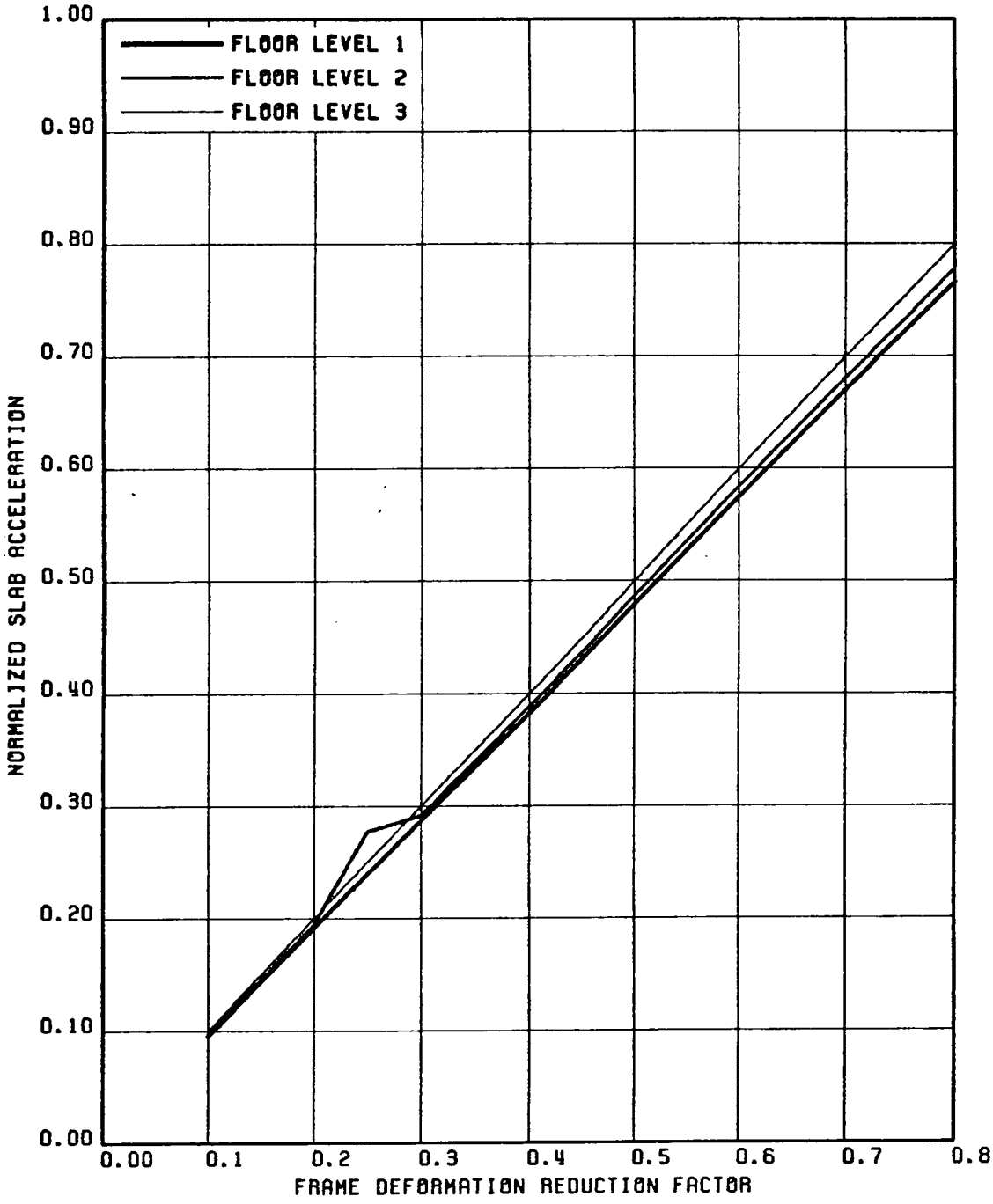

FIG. 5.91 VARIATION OF NORMALIZED SLAB ACCELERATION (NORMALIZED W.R.T. THE CORRESPONDING NON-SLIDING ACCELERATION RESPONSE) WITH FRAME DEFORMATION REDUCTION FACTOR; STRUCTURE 2, GR MOTION 3-HZ COMPONENT

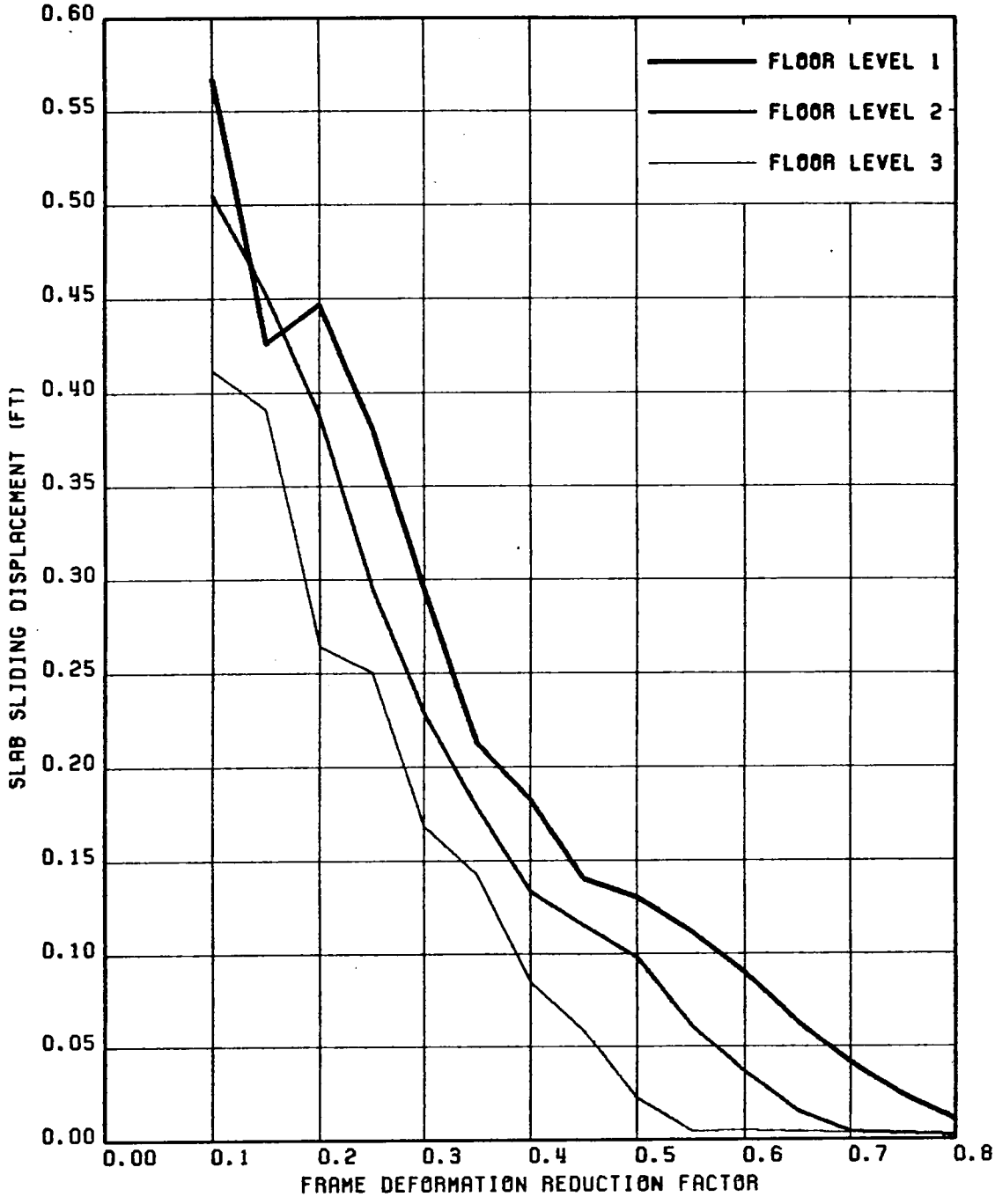

FIG. 5.92 VARIATION OF MAXIMUM SLAB SLIDING DISPLACEMENTS WITH FRAME DEFORMATION REDUCTION FACTOR; STRUCTURE 2, GR MOTION 3-HZ COMPONENT

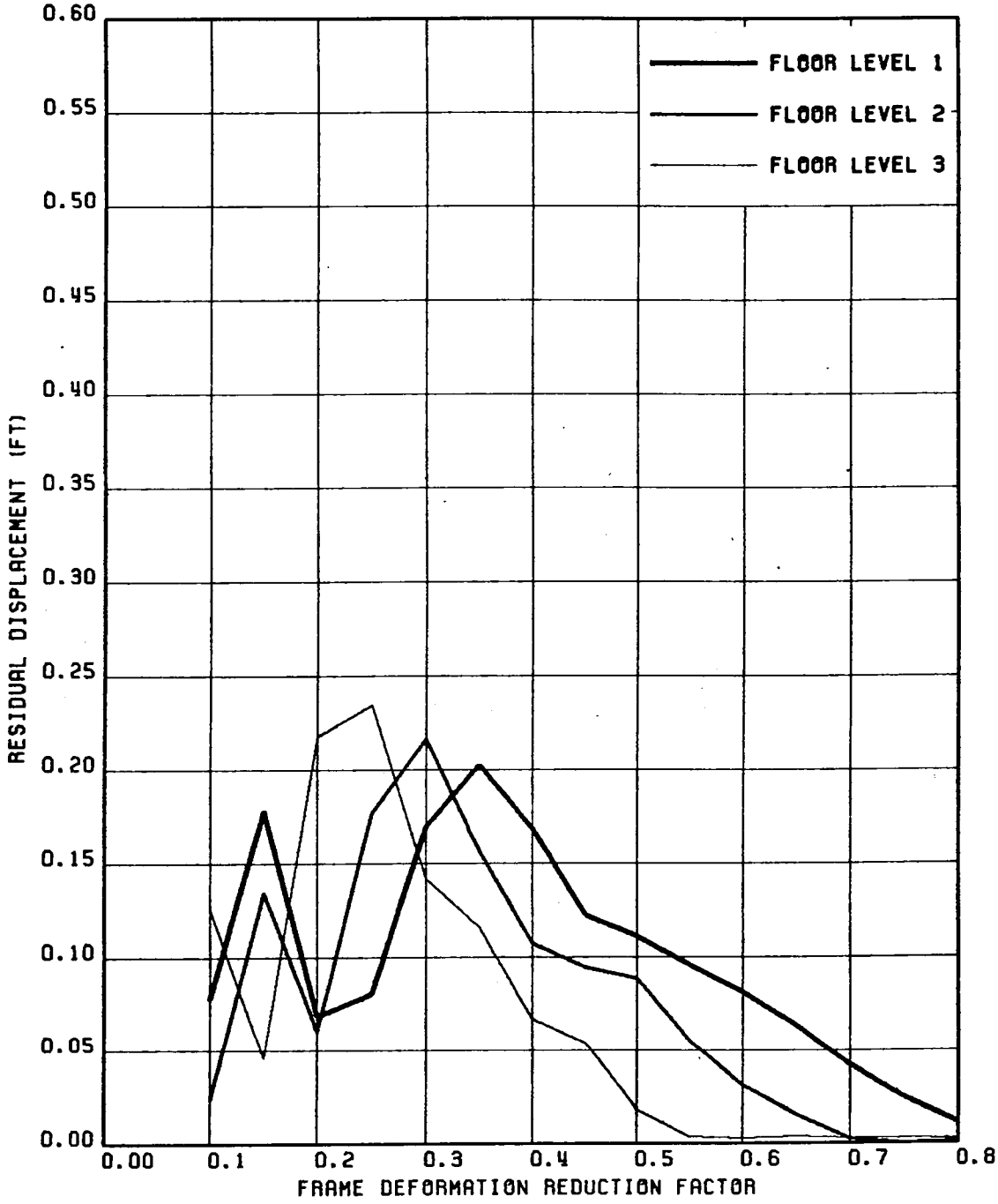

FIG. 5.93 VARIATION OF RESIDUAL SLAB SLIDING DISPLACEMENTS WITH FRAME DEFORMATION REDUCTION FACTOR; STRUCTURE 2, GR MOTION 3-HZ COMPONENT

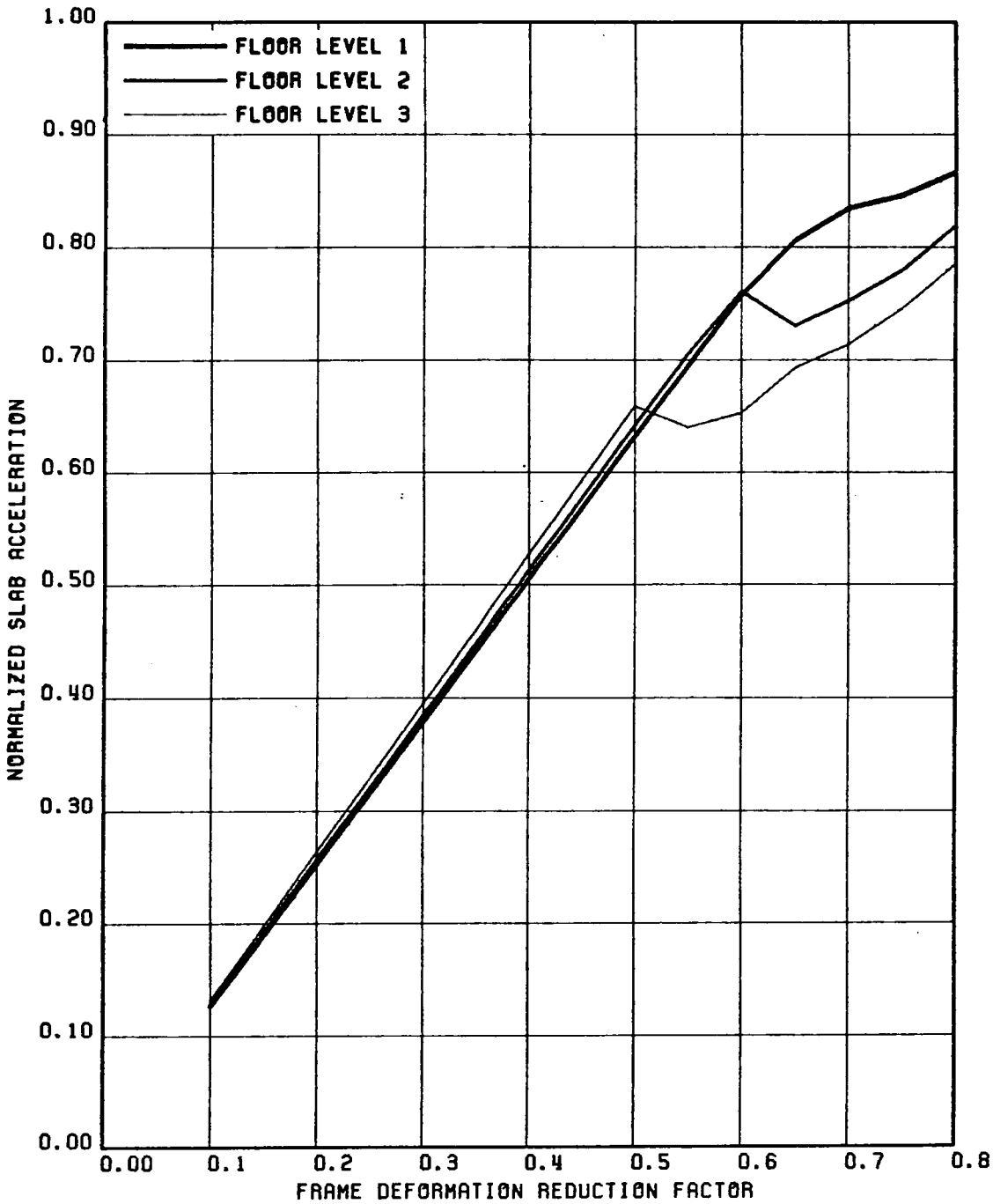

FIG. 5.94 VARIATION OF NORMALIZED SLAB ACCELERATION (NORMALIZED W.R.T. THE CORRESPONDING NON-SLIDING ACCELERATION RESPONSE) WITH FRAME DEFORMATION REDUCTION FACTOR; STRUCTURE 2, GR MOTION 3-HZ & VT COMP

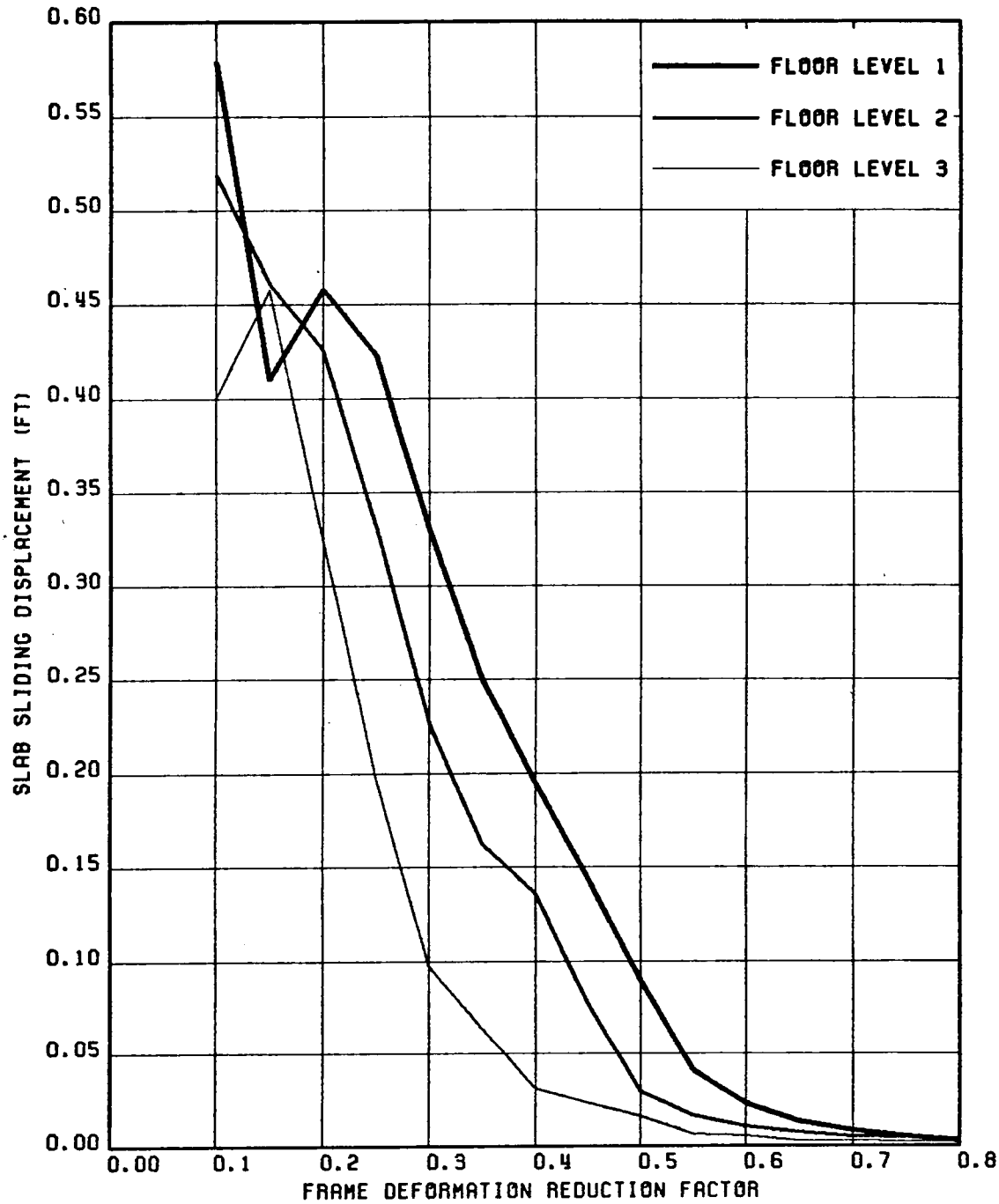

FIG. 5.95 VARIATION OF MAXIMUM SLAB SLIDING DISPLACEMENTS WITH FRAME DEFORMATION REDUCTION FACTOR; STRUCTURE 2, GR MOTION 3-HZ & VT COMP

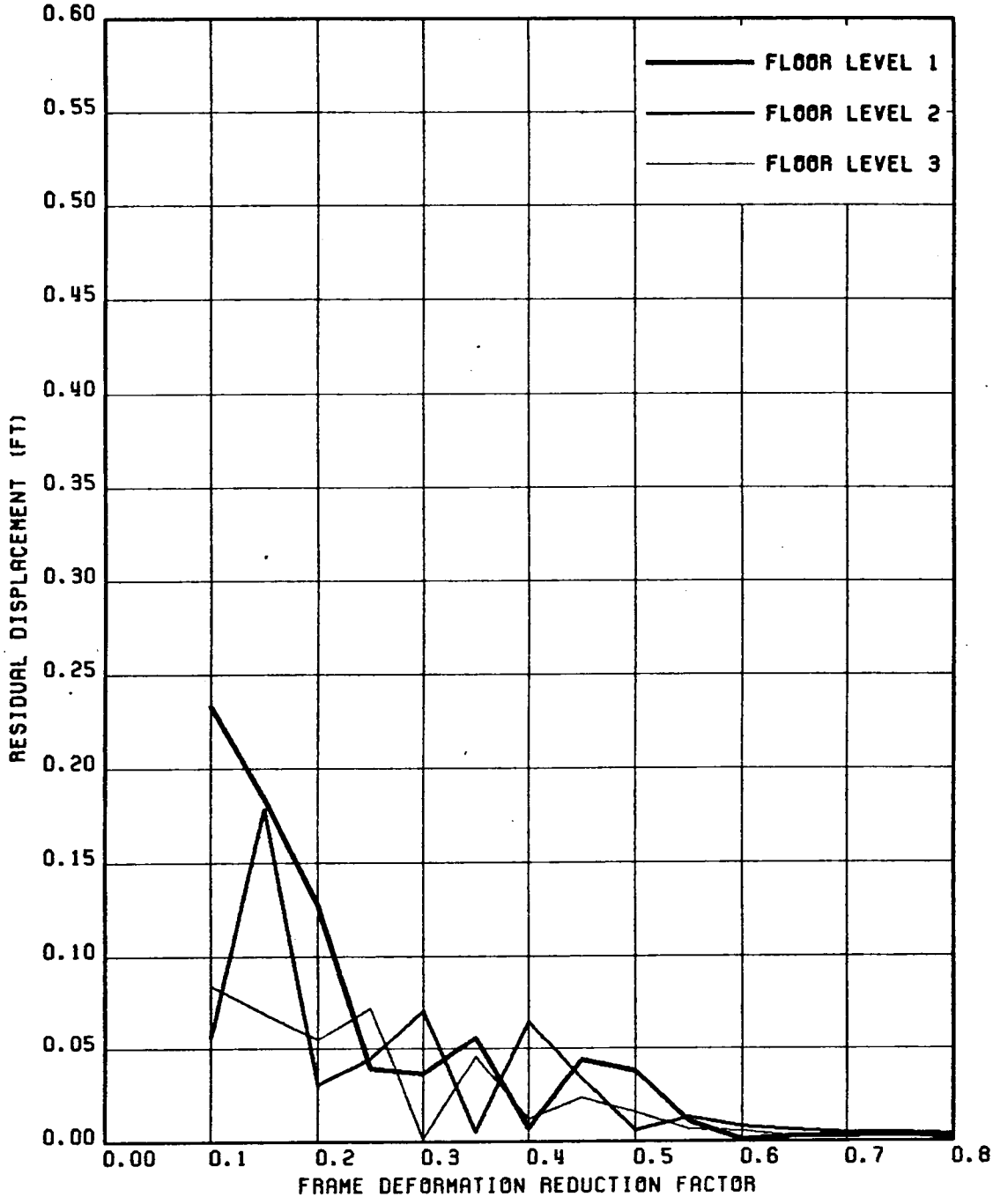

FIG. 5.96 VARIATION OF RESIDUAL SLAB SLIDING DISPLACEMENTS WITH FRAME DEFORMATION REDUCTION FACTOR; STRUCTURE 2, GR MOTION 3-HZ & VT COMP

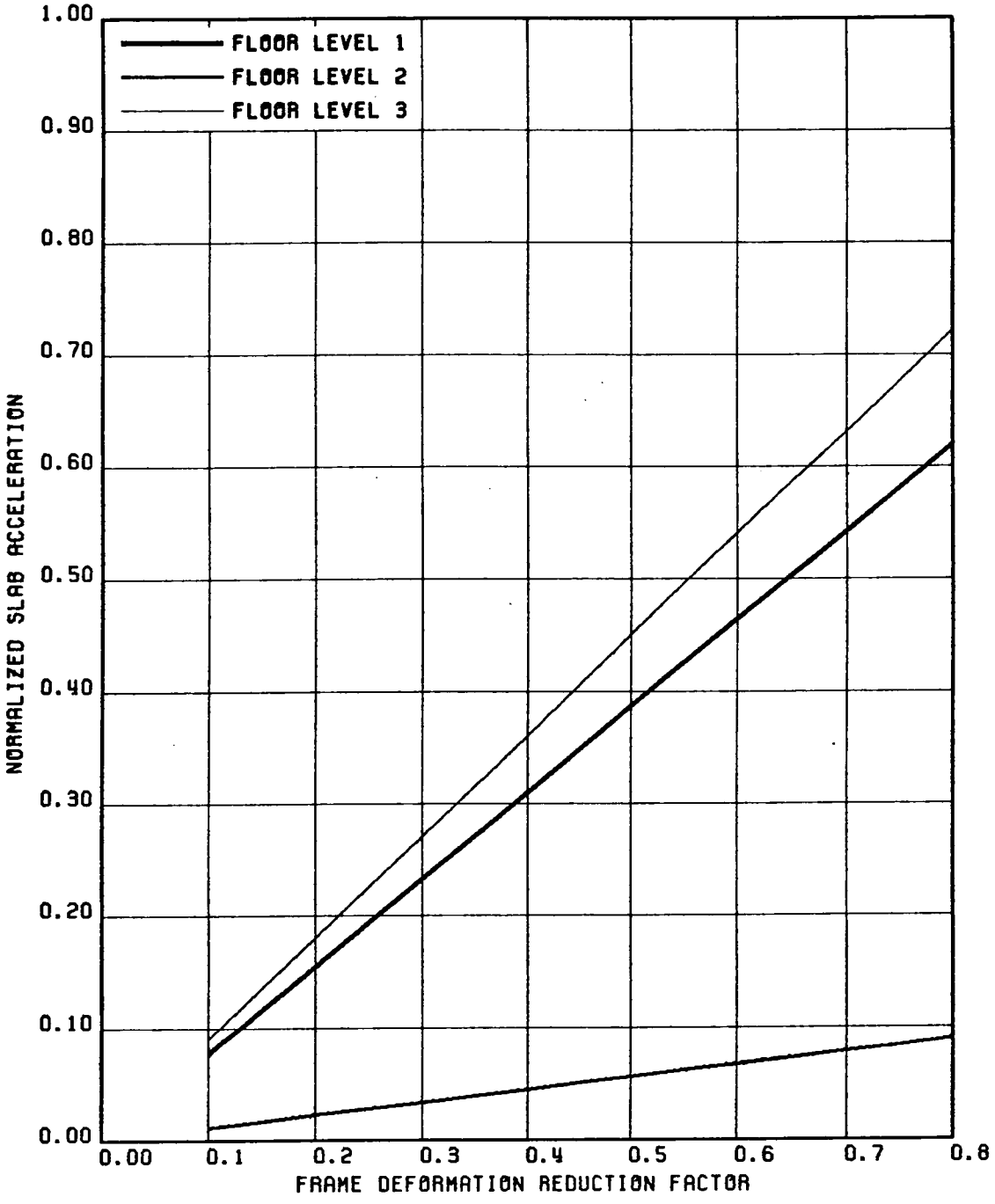

FIG. 5.97 VARIATION OF NORMALIZED SLAB ACCELERATION (NORMALIZED W.R.T. THE CORRESPONDING NON-SLIDING ACCELERATION RESPONSE) WITH FRAME DEFORMATION REDUCTION FACTOR; STRUCTURE 3, GR MOTION 1-HZ COMPONENT

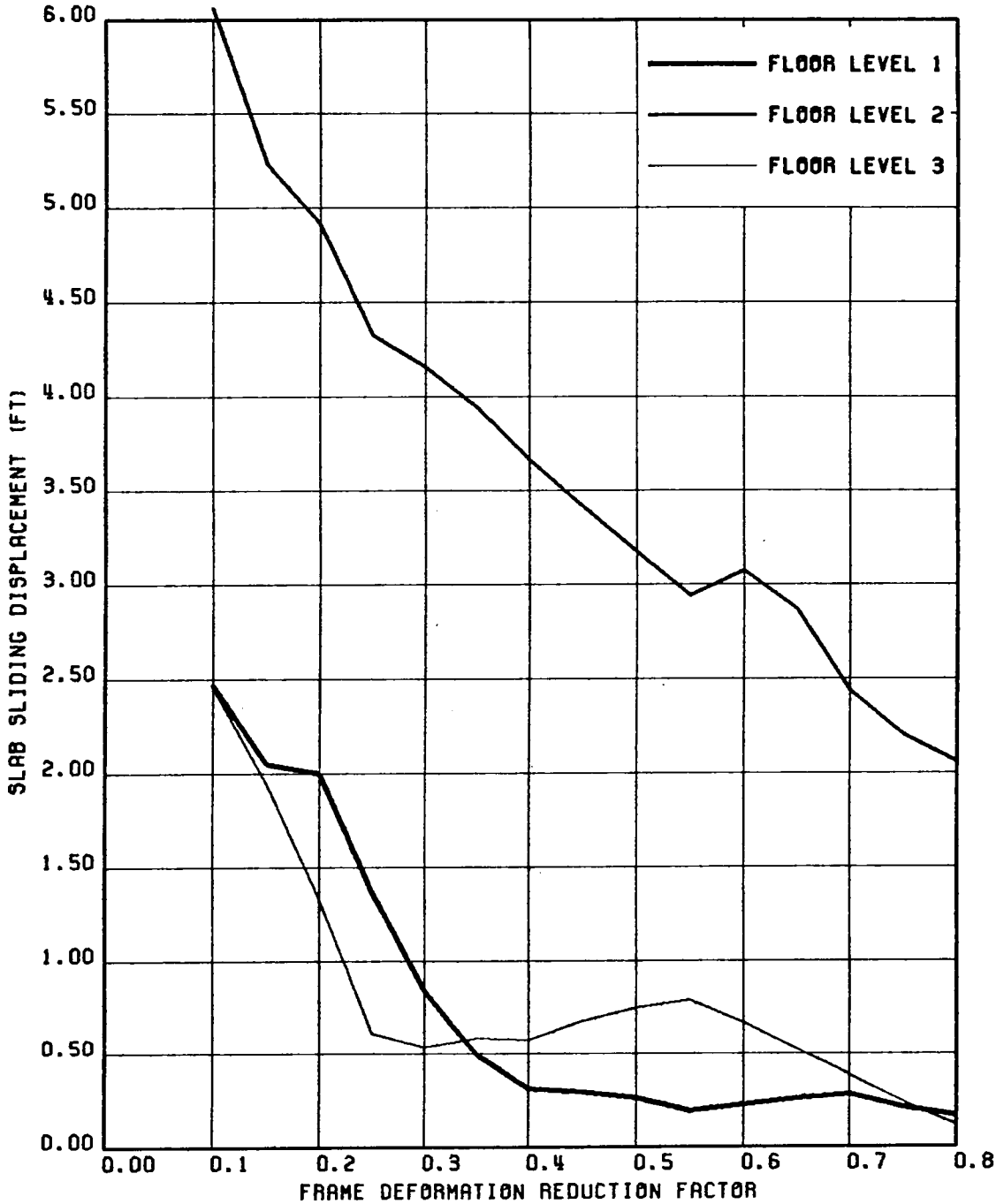

FIG. 5.98 VARIATION OF MAXIMUM SLAB SLIDING DISPLACEMENTS WITH FRAME DEFORMATION REDUCTION FACTOR; STRUCTURE 3, GR MOTION 1-HZ COMPONENT

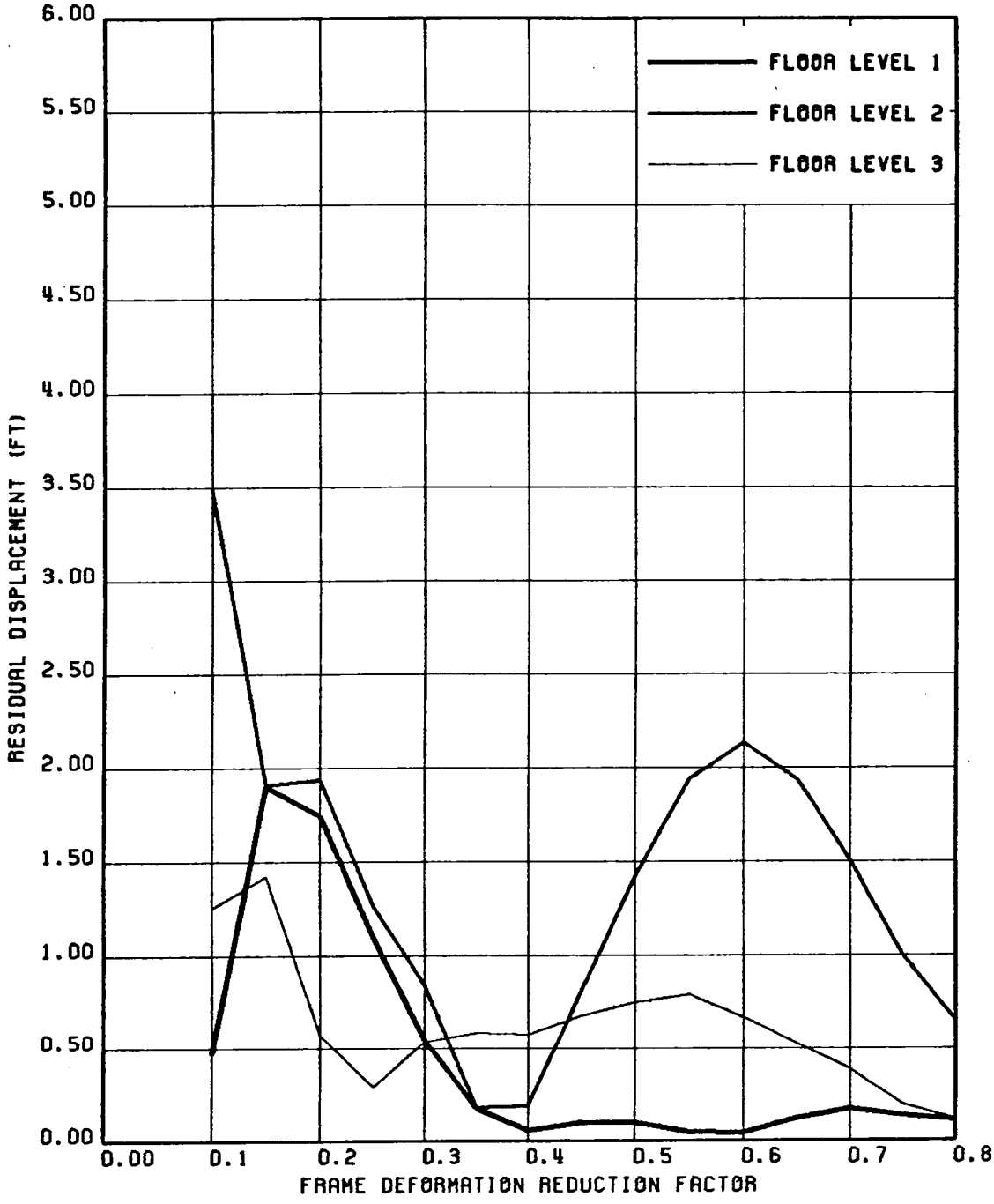

FIG. 5.99 VARIATION OF RESIDUAL SLAB SLIDING DISPLACEMENTS WITH FRAME DEFORMATION REDUCTION FACTOR; STRUCTURE 3, GR MOTION 1-HZ COMPONENT

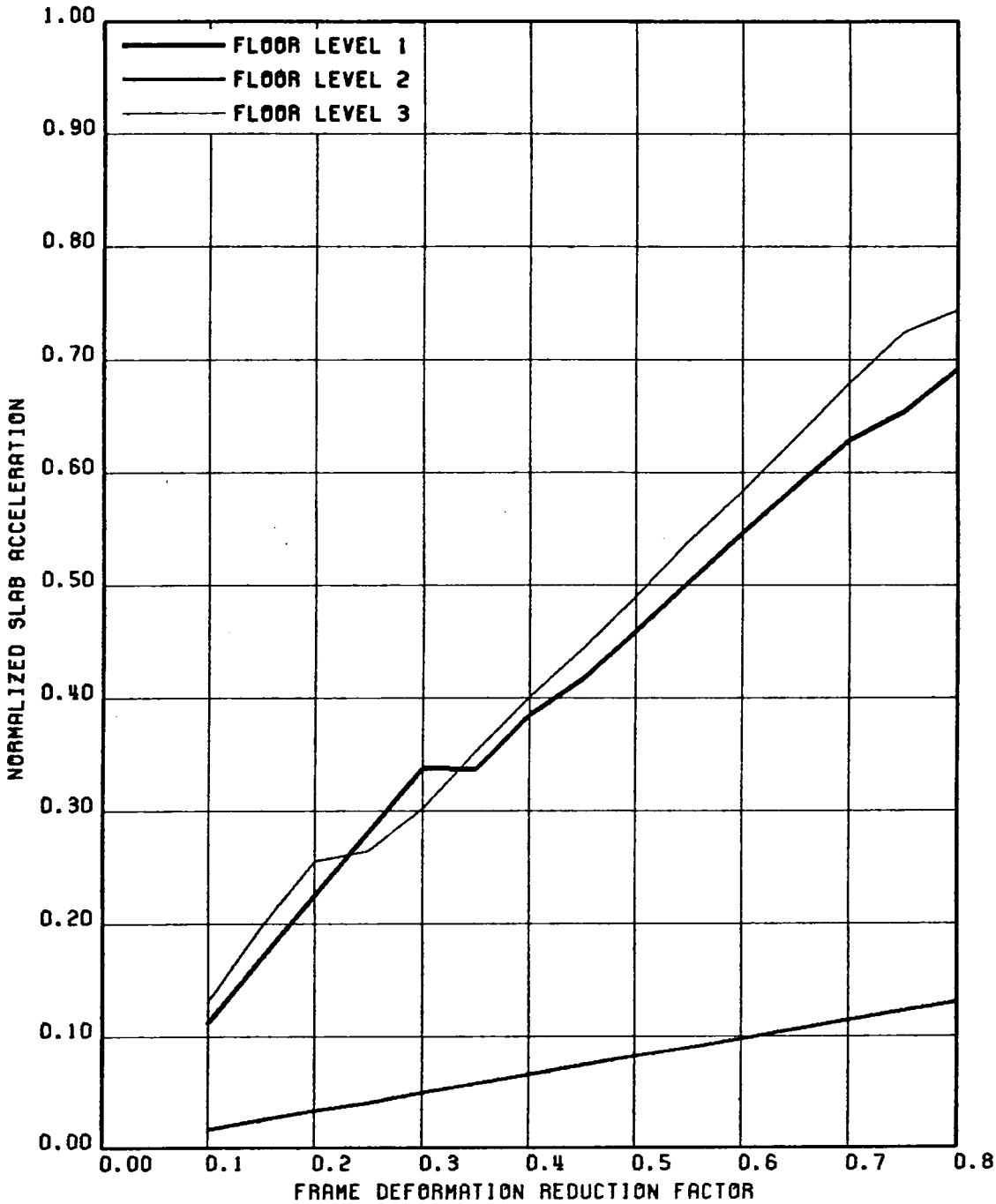

FIG. 5.100VARIATION OF NORMALIZED SLAB ACCELERATION (NORMALIZED W.R.T. THE CORRESPONDING NON-SLIDING ACCELERATION RESPONSE) WITH FRAME DEFORMATION REDUCTION FACTOR; STRUCTURE 3, GR MOTION 1-HZ & VT COMP

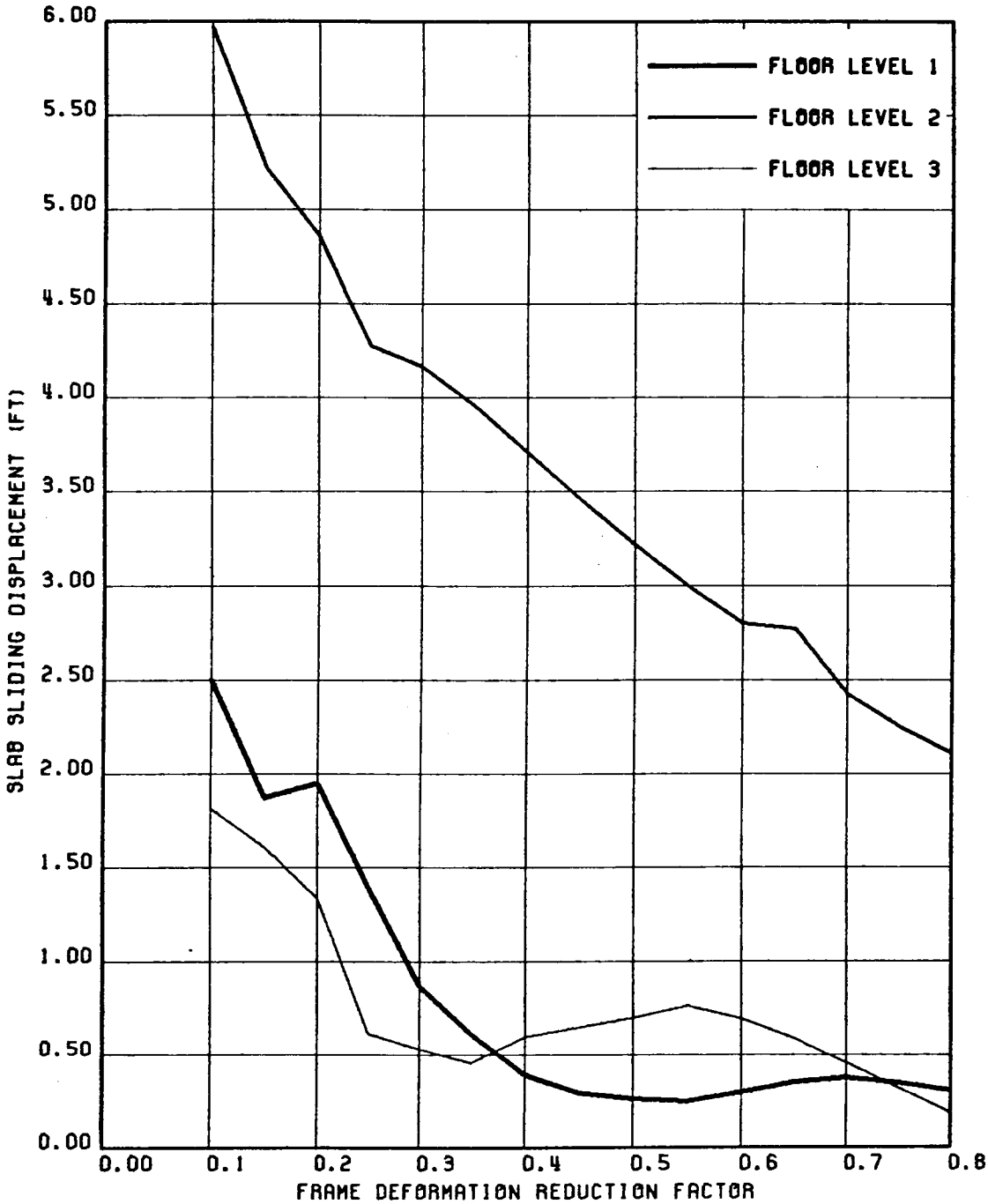

FIG. 5.101VARIATION OF MAXIMUM SLAB SLIDING DISPLACEMENTS WITH FRAME DEFORMATION REDUCTION FACTOR; STRUCTURE 3, GR MOTION 1-HZ & VT COMP

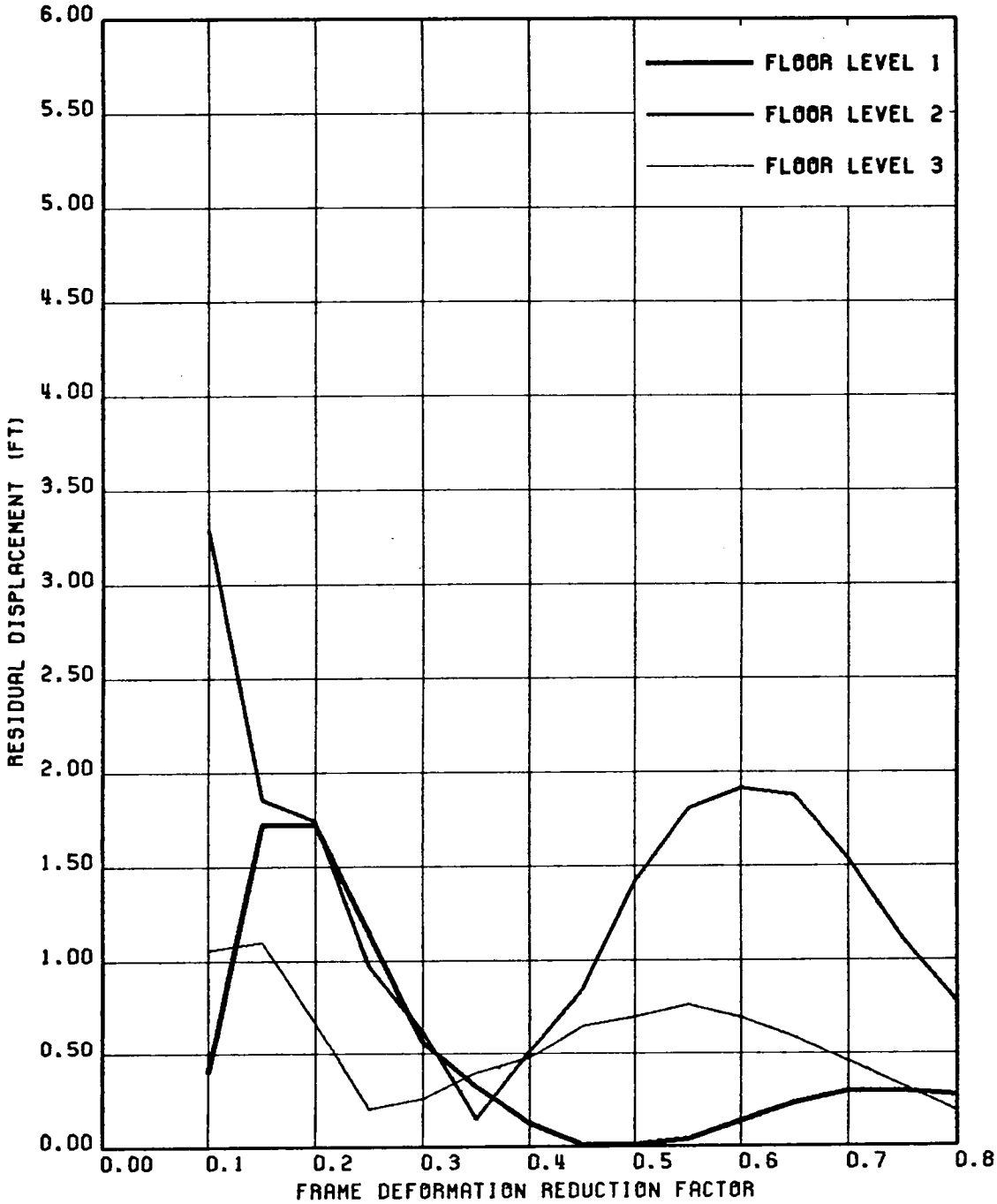

FIG. 5.102VARIATION OF RESIDUAL SLAB SLIDING DISPLACEMENTS WITH FRAME DEFORMATION REDUCTION FACTOR; STRUCTURE 3, GR MOTION 1-HZ & VT COMP

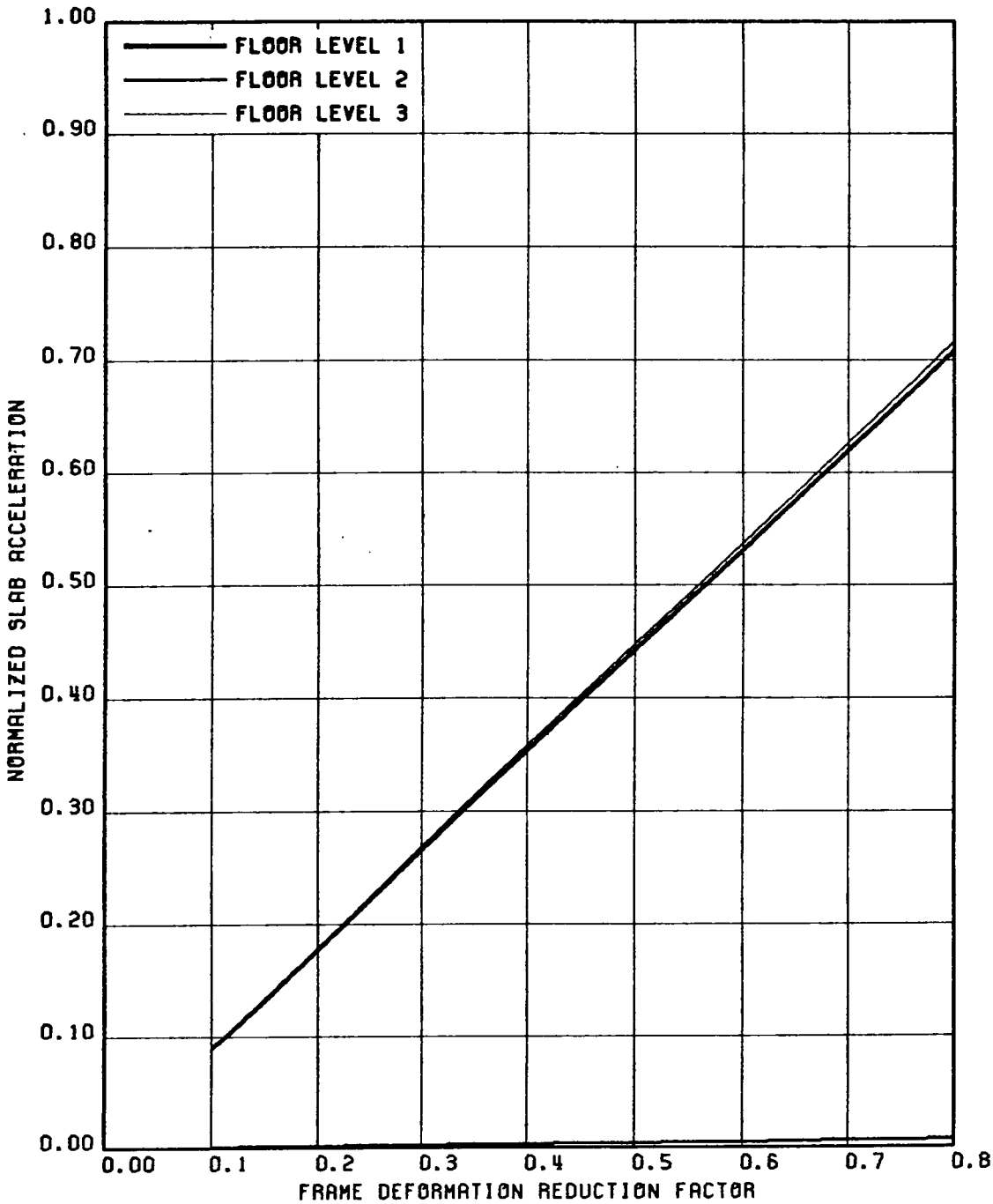

FIG. 5.103VARIATION OF NORMALIZED SLAB ACCELERATION (NORMALIZED W.R.T. THE CORRESPONDING NON-SLIDING ACCELERATION RESPONSE) WITH FRAME DEFORMATION REDUCTION FACTOR; STRUCTURE 3, GR MOTION 2-HZ COMPONENT

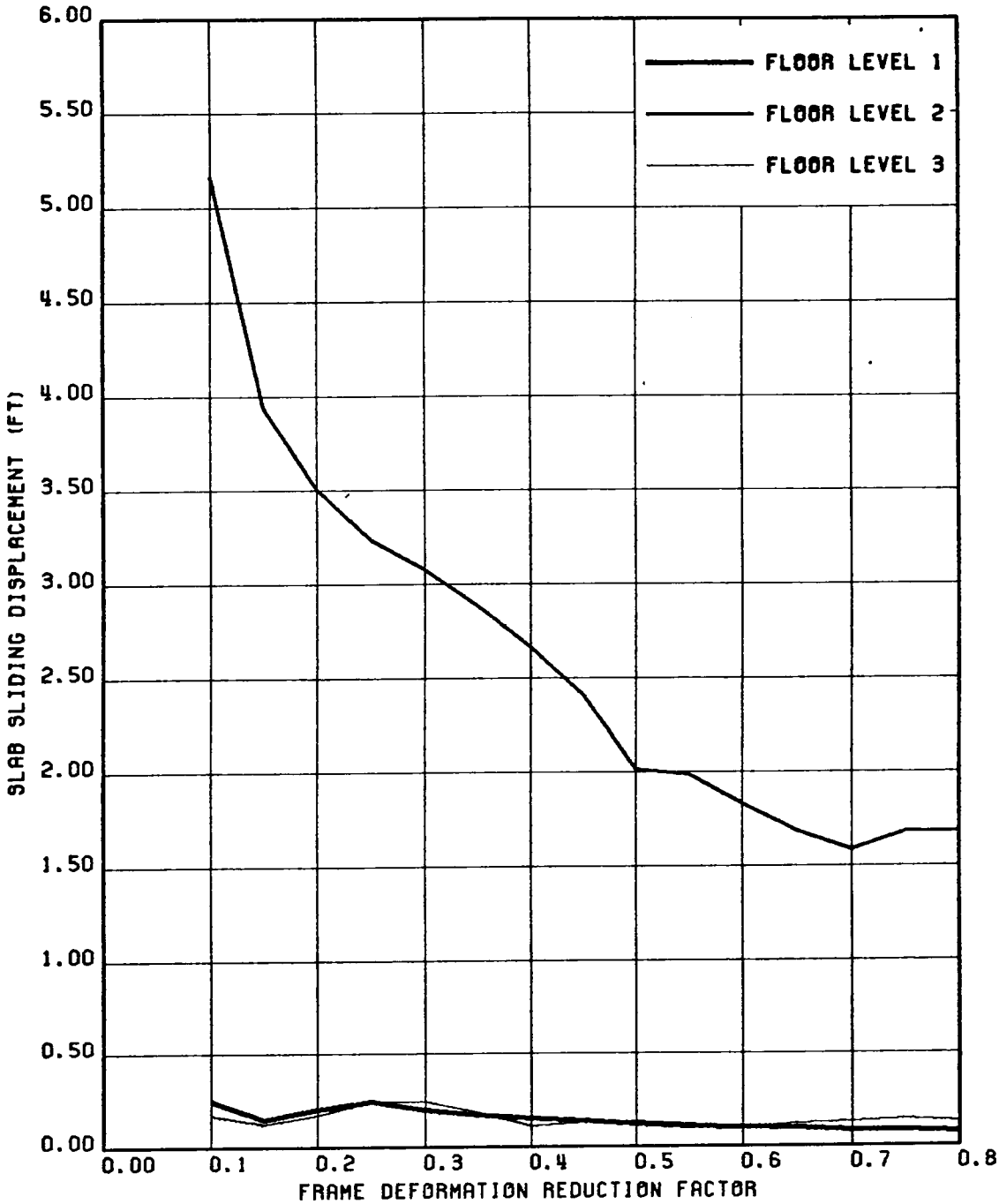

FIG. 5.104VARIATION OF MAXIMUM SLAB SLIDING DISPLACEMENTS WITH FRAME DEFORMATION REDUCTION FACTOR; STRUCTURE 3, GR MOTION 2-HZ COMPONENT

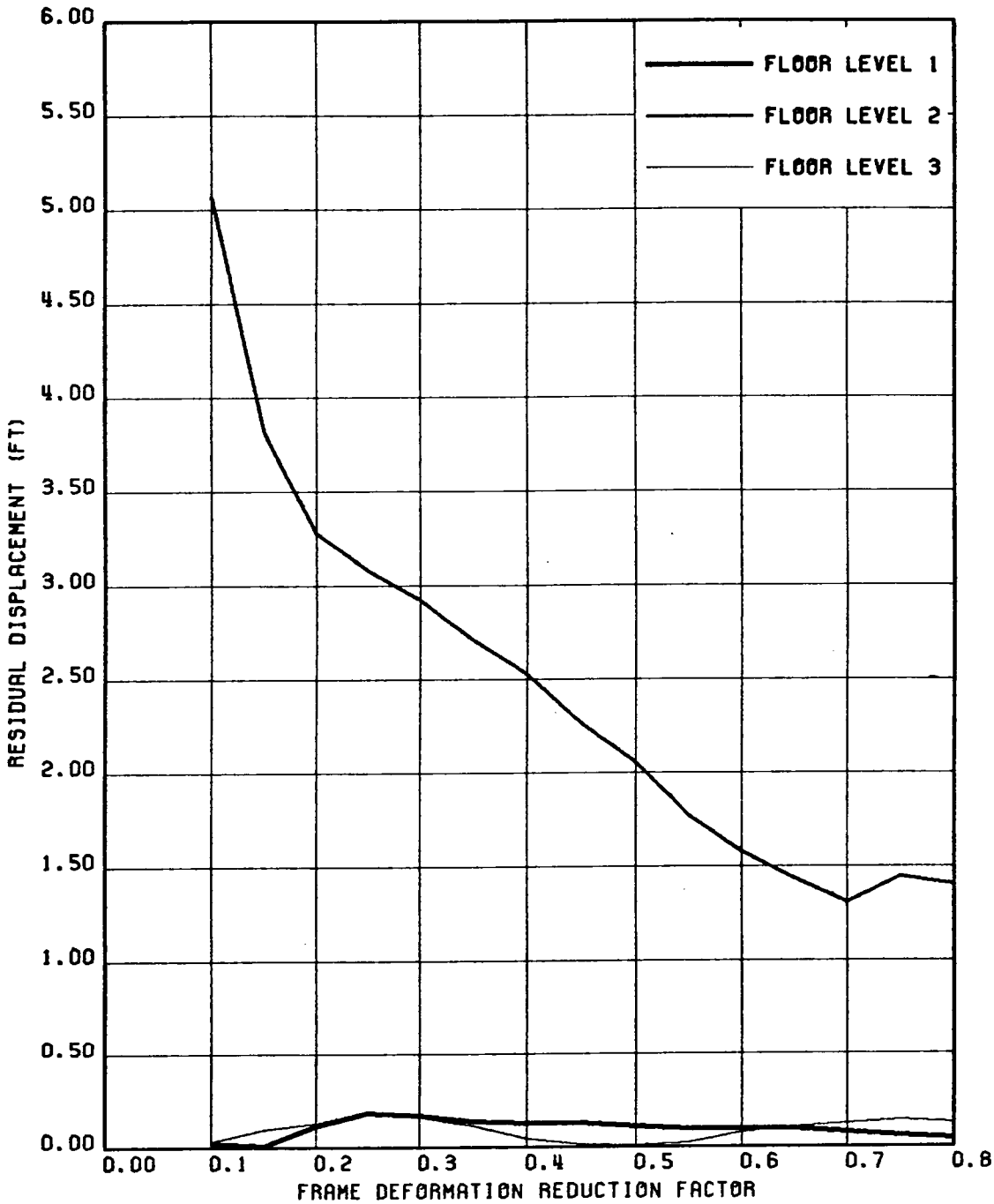

FIG. 5.105VARIATION OF RESIDUAL SLAB SLIDING DISPLACEMENTS WITH FRAME DEFORMATION REDUCTION FACTOR; STRUCTURE 3, GR MOTION 2-HZ COMPONENT

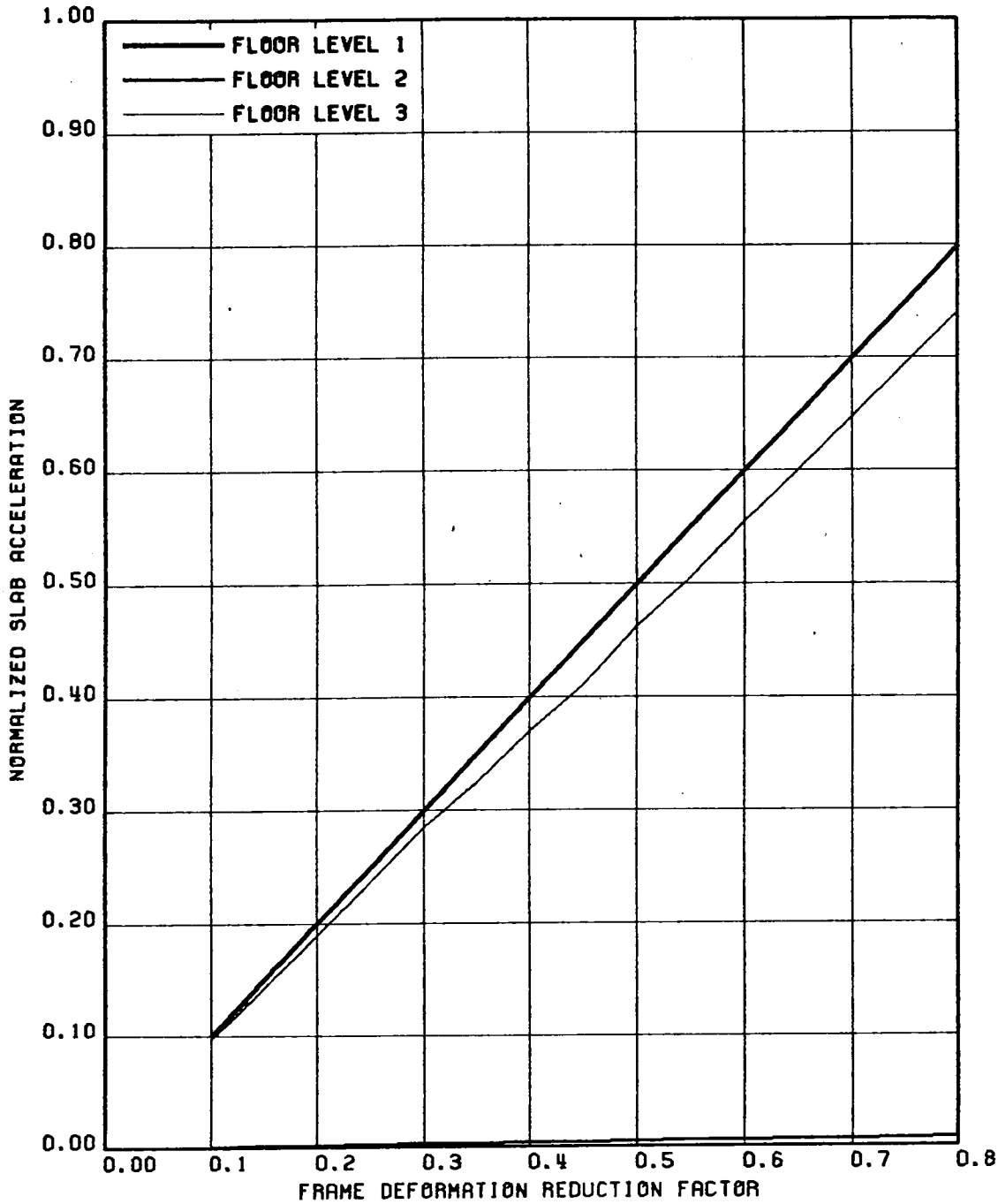

FIG. 5.106VARIATION OF NORMALIZED SLAB ACCELERATION (NORMALIZED W.R.T. THE CORRESPONDING NON-SLIDING ACCELERATION RESPONSE) WITH FRAME DEFORMATION REDUCTION FACTOR; STRUCTURE 3, GR MOTION 2-HZ & VT COMP

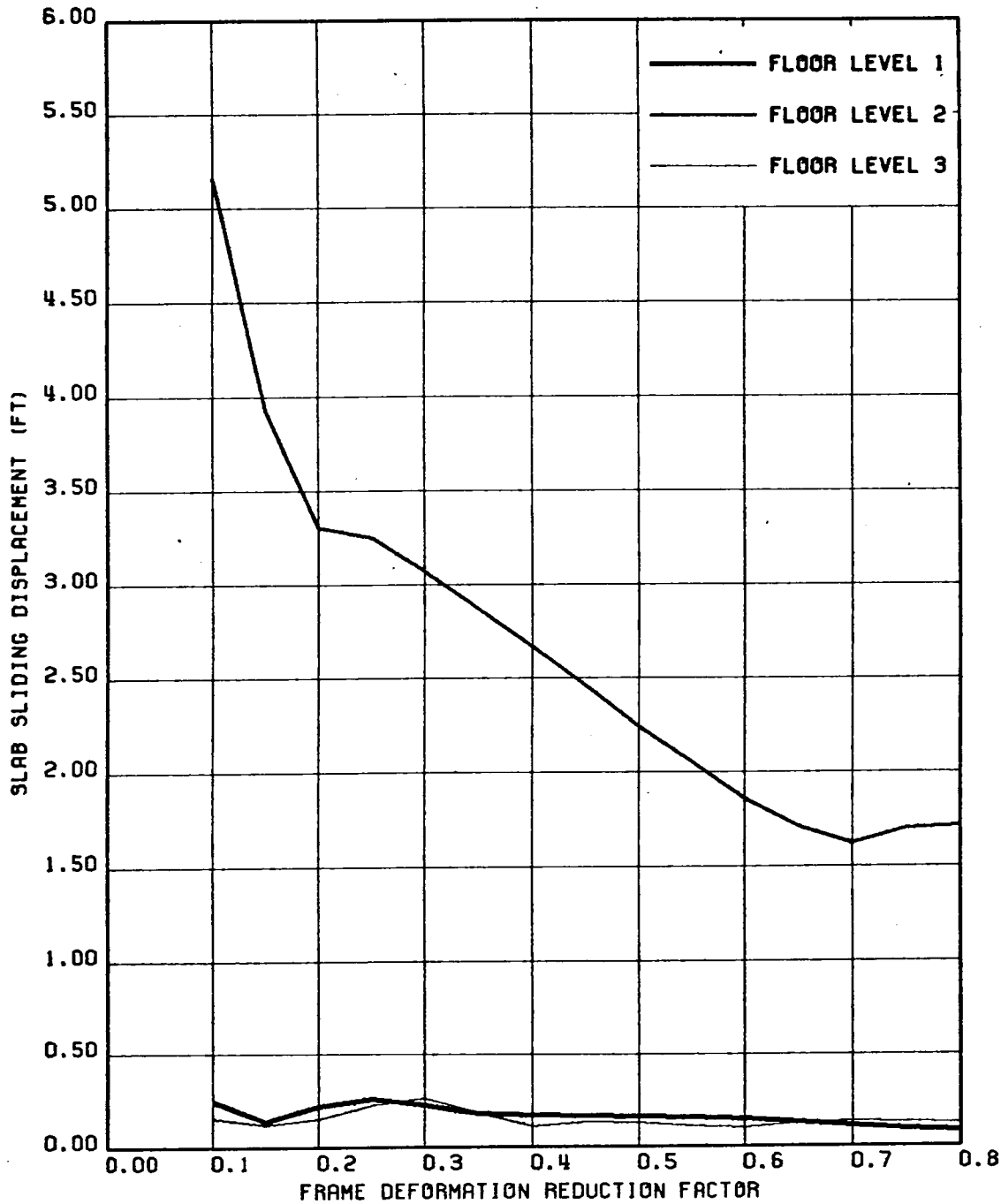

FIG. 5.107VARIATION OF MAXIMUM SLAB SLIDING DISPLACEMENTS WITH FRAME DEFORMATION REDUCTION FACTOR; STRUCTURE 3, GR MOTION 2-HZ & VT COMP

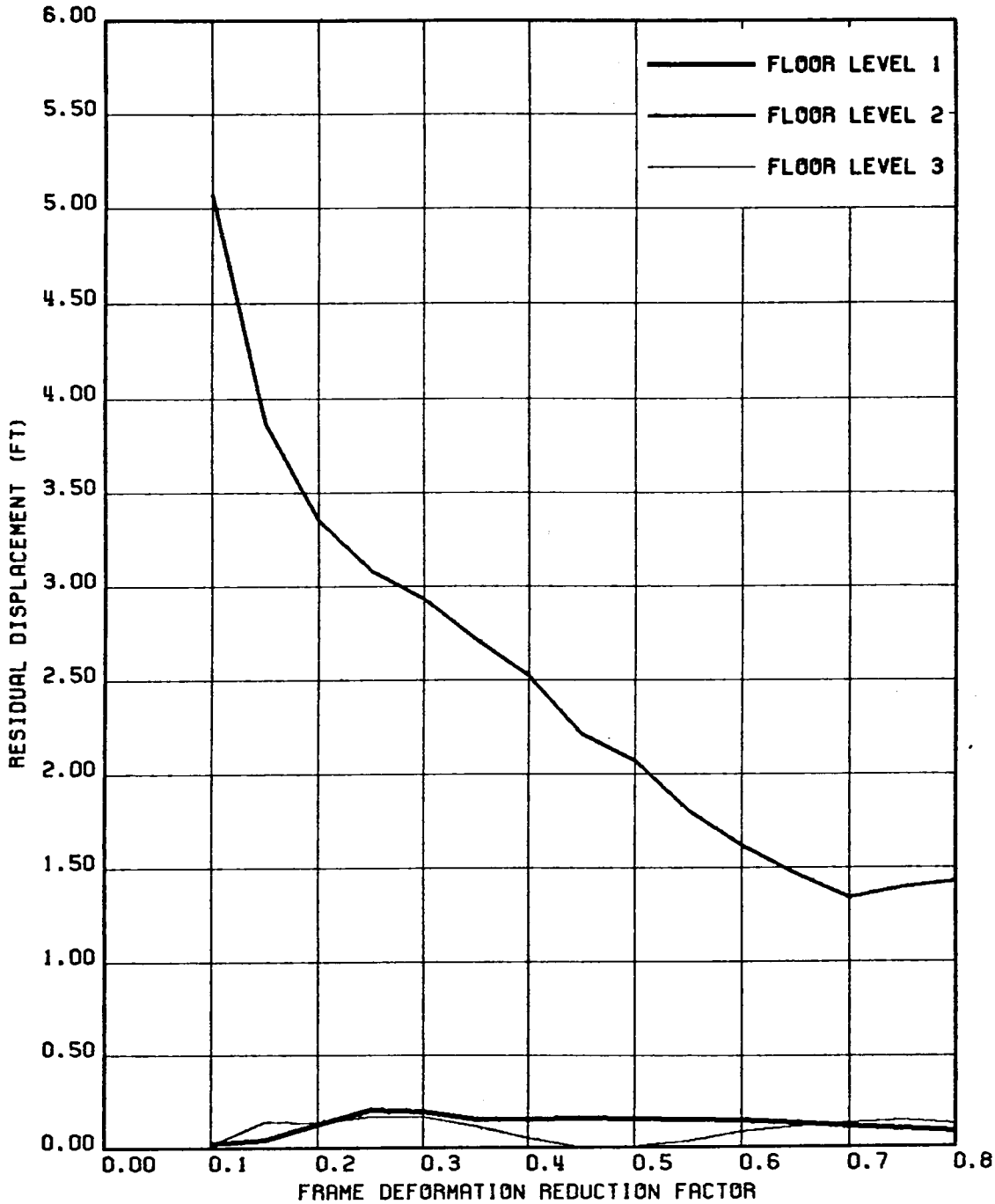

FIG. 5.108VARIATION OF RESIDUAL SLAB SLIDING DISPLACEMENTS WITH FRAME DEFORMATION REDUCTION FACTOR; STRUCTURE 3, GR MOTION 2-HZ & VT COMP

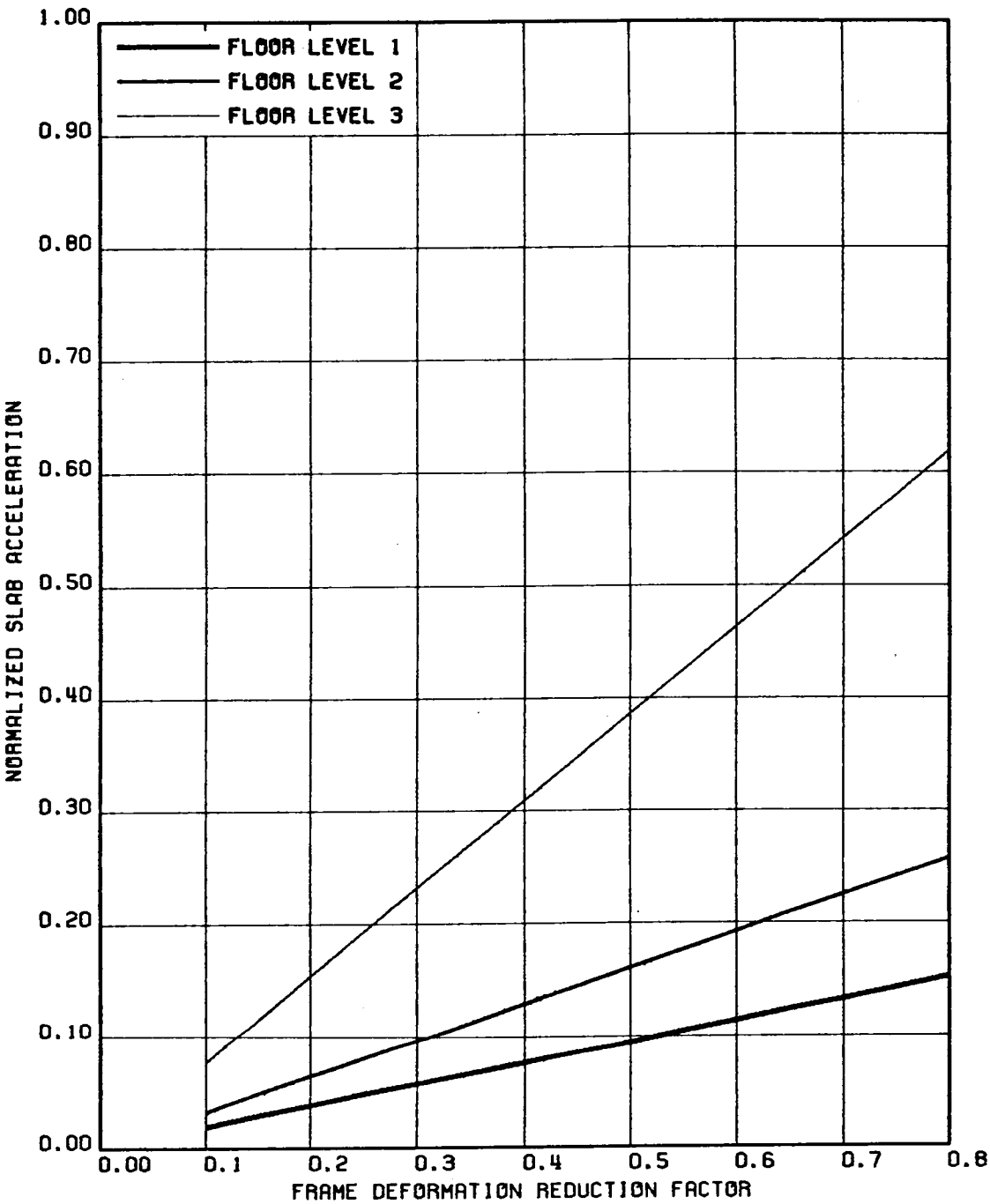

FIG. 5.109VARIATION OF NORMALIZED SLAB ACCELERATION (NORMALIZED W.R.T. THE CORRESPONDING NON-SLIDING ACCELERATION RESPONSE) WITH FRAME DEFORMATION REDUCTION FACTOR; STRUCTURE 3, GR MOTION 3-HZ COMPONENT

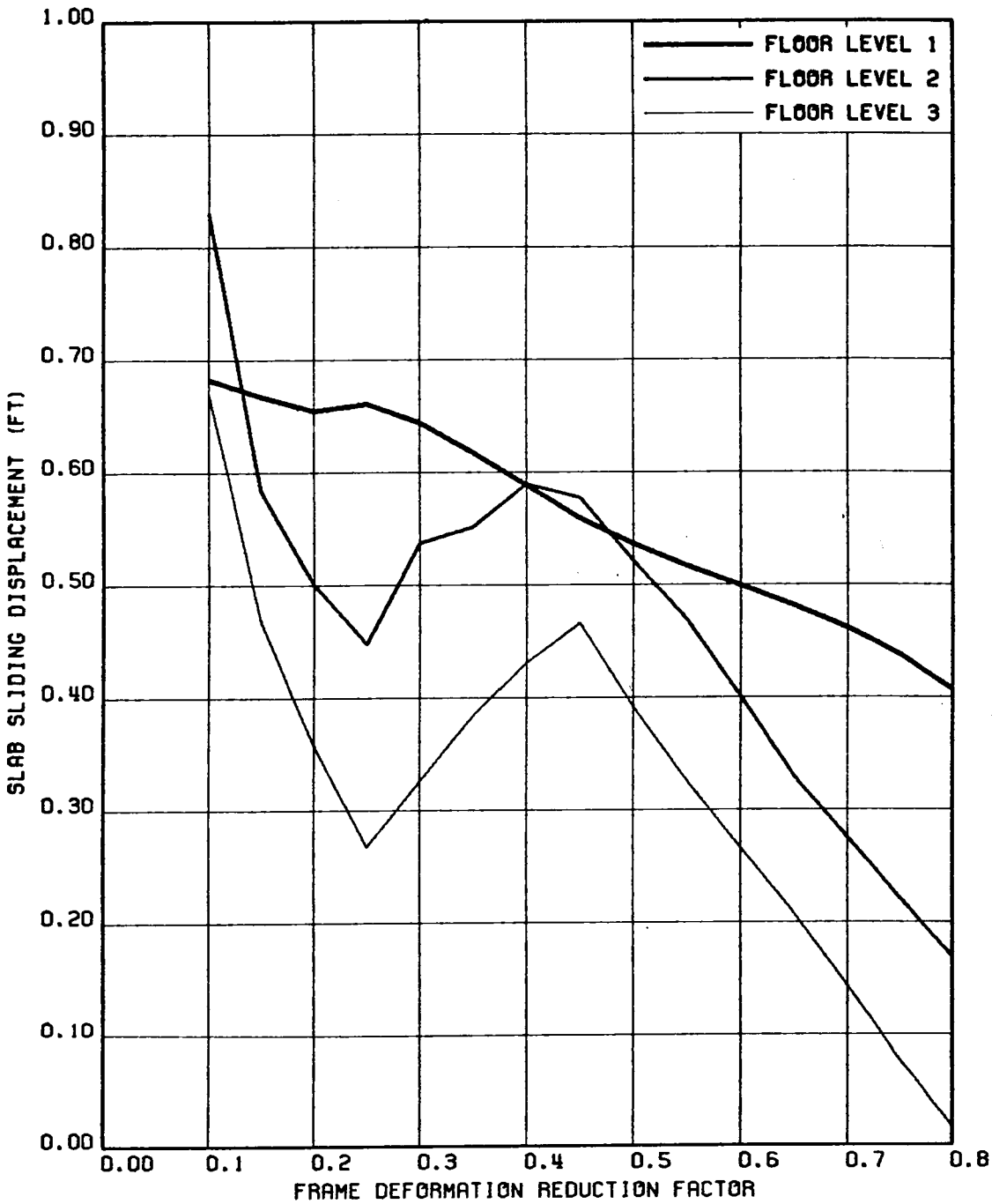

FIG. 5.110VARIATION OF MAXIMUM SLAB SLIDING DISPLACEMENTS WITH FRAME DEFORMATION REDUCTION FACTOR; STRUCTURE 3, GR MOTION 3-HZ COMPONENT

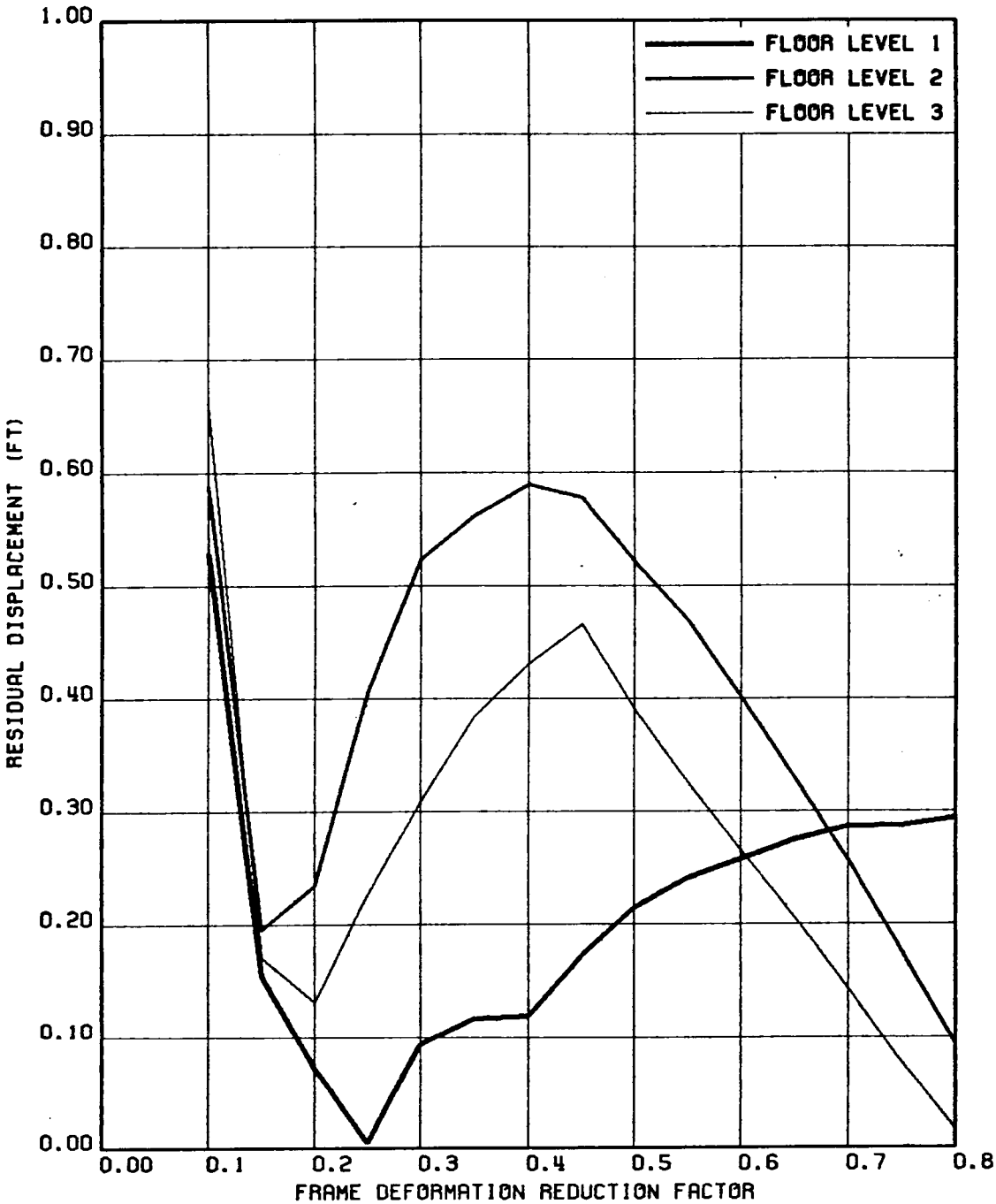

FIG. 5.111VARIATION OF RESIDUAL SLAB SLIDING DISPLACEMENTS WITH FRAME DEFORMATION REDUCTION FACTOR; STRUCTURE 3, GR MOTION 3-HZ COMPONENT

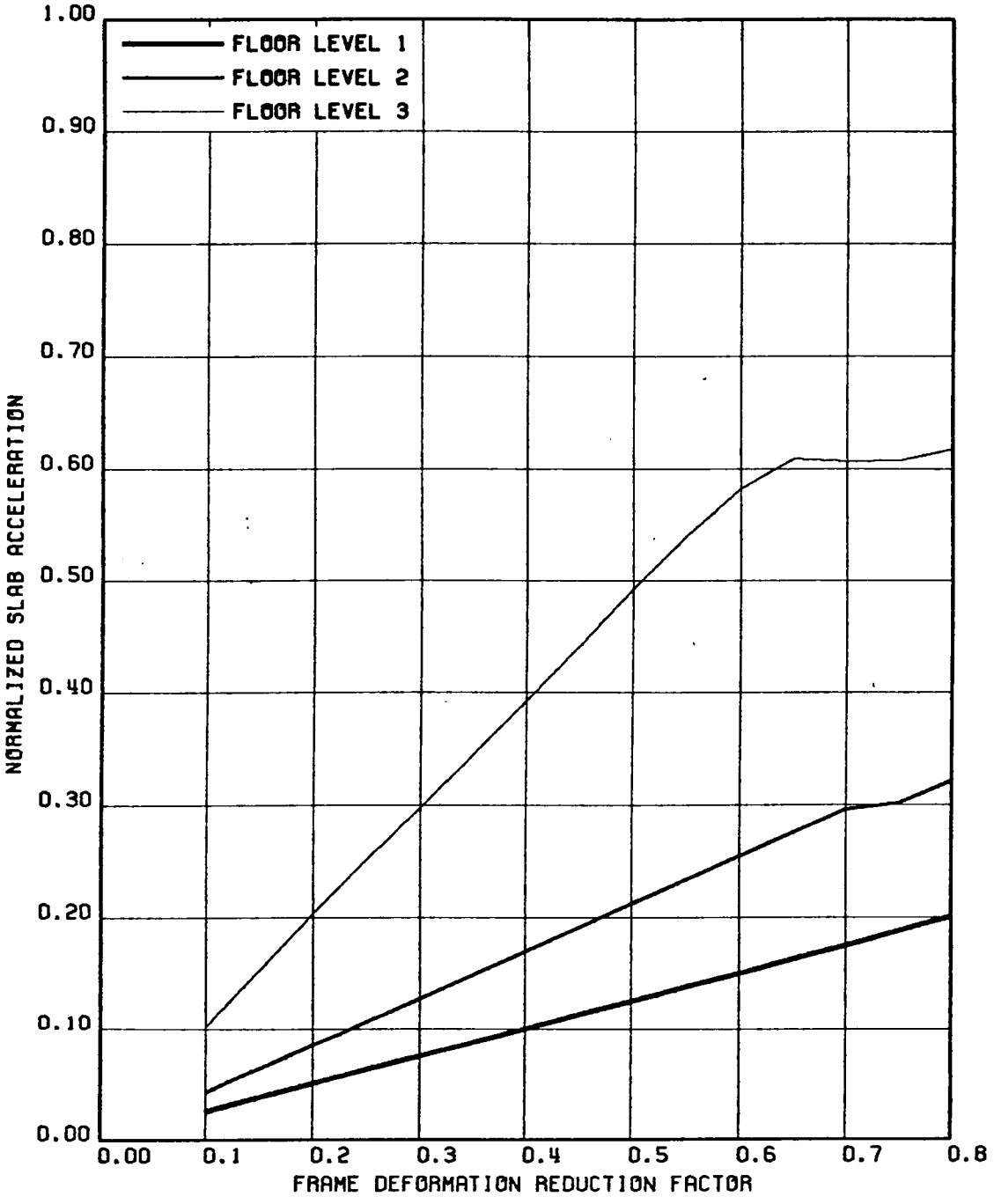

FIG. 5.112VARIATION OF NORMALIZED SLAB ACCELERATION (NORMALIZED W.R.T. THE CORRESPONDING NON-SLIDING ACCELERATION RESPONSE) WITH FRAME DEFORMATION REDUCTION FACTOR; STRUCTURE 3, GR MOTION 3-HZ & VT COMP

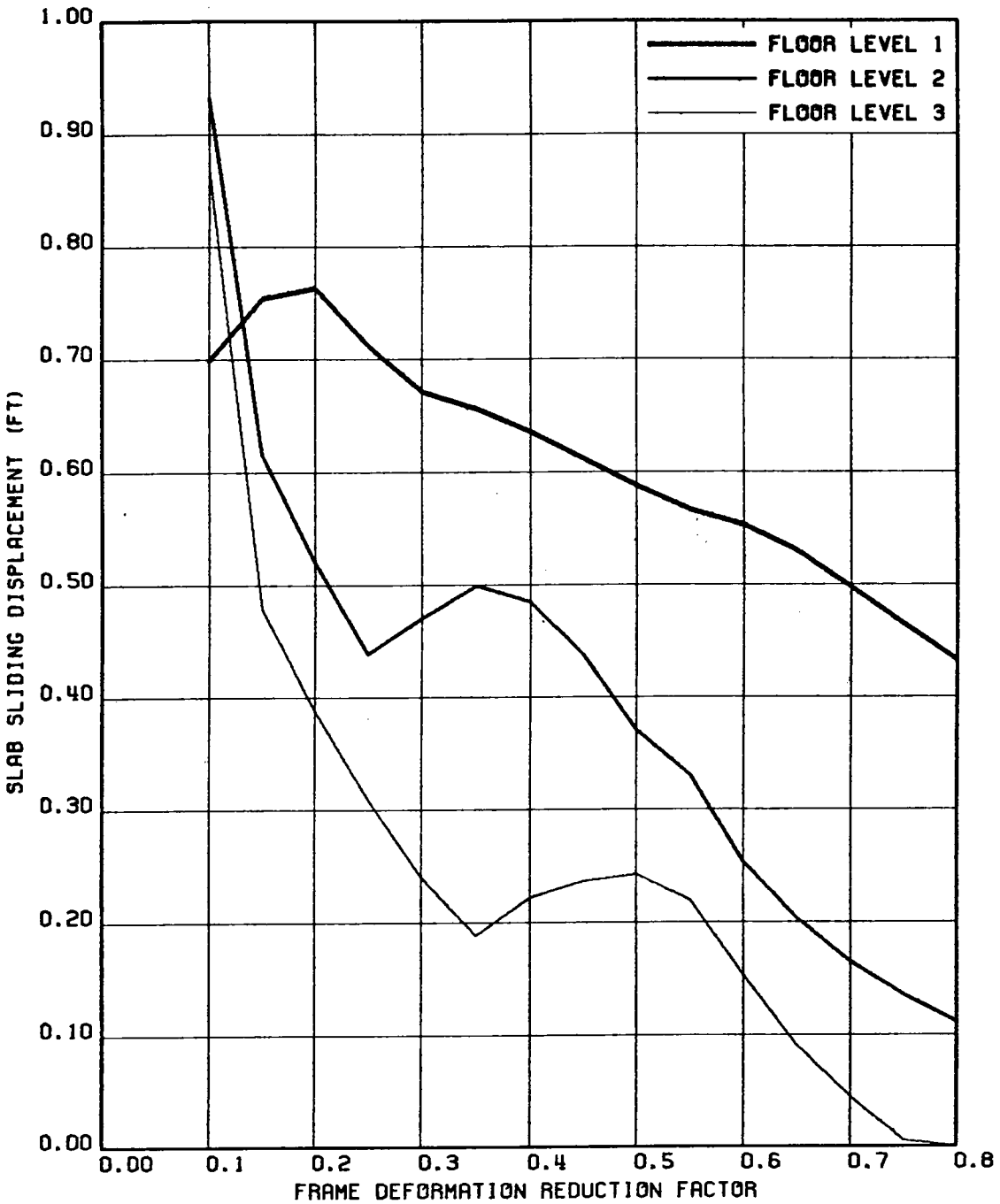

FIG. 5.113VARIATION OF MAXIMUM SLAB SLIDING DISPLACEMENTS WITH FRAME DEFORMATION REDUCTION FACTOR; STRUCTURE 3, GR MOTION 3-HZ & VT COMP

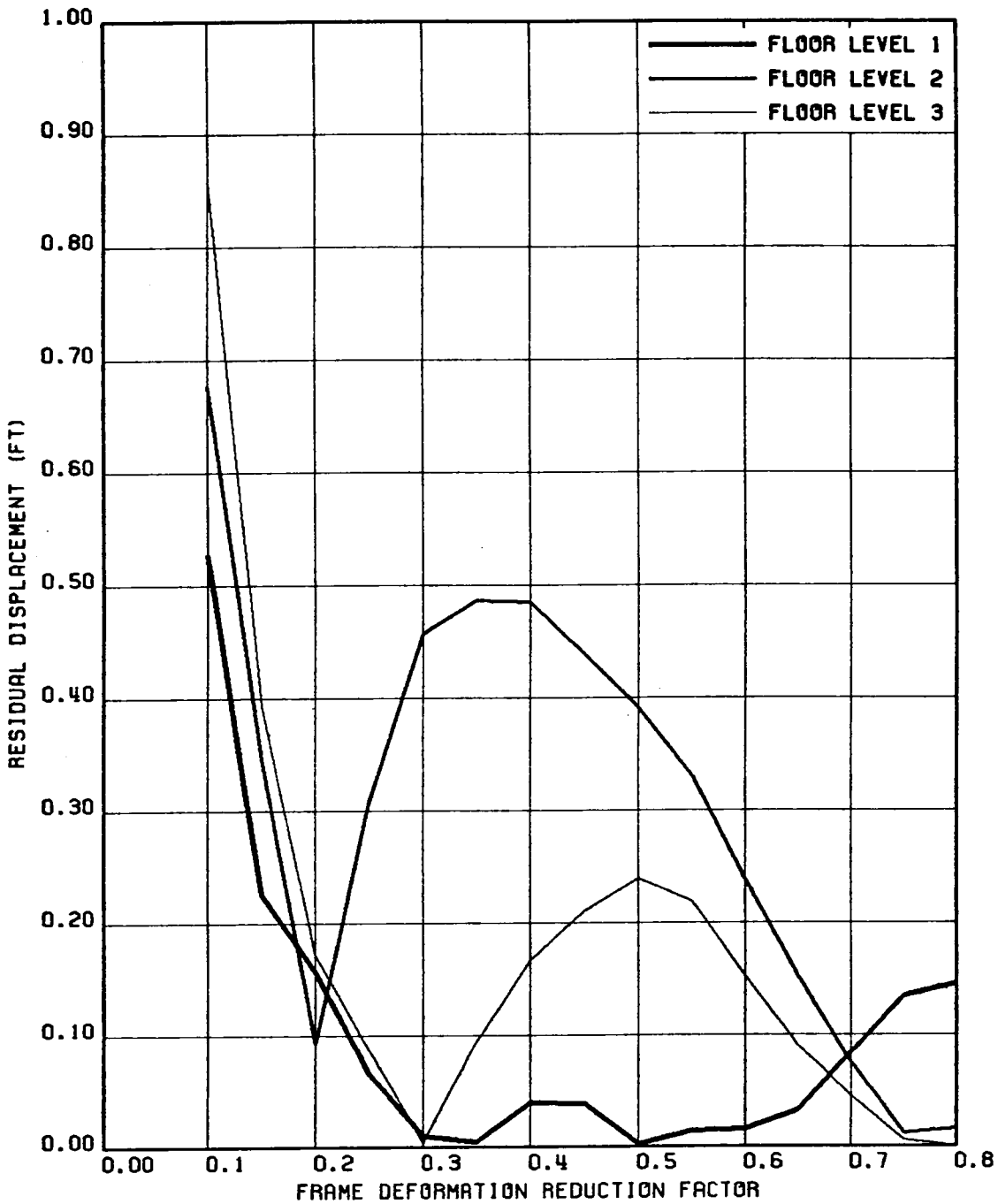

FIG. 5.114VARIATION OF RESIDUAL SLAB SLIDING DISPLACEMENTS WITH FRAME DEFORMATION REDUCTION FACTOR; STRUCTURE 3, GR MOTION 3-HZ & VT COMP

Chapter VI

Summary and Conclusions

This study was carried out to investigate the effectiveness of Coulomb damping for the purpose of seismic isolation and energy dissipation in structures subjected to earthquake induced ground motions. It is proposed to introduce a sliding interface under the slab of a structure. The performance of a single-story structure provided with this type of sliding arrangement has been studied and compared with the performance of the corresponding base sliding and hysteretic structures. The latter types of structures have been studied extensively in the past. The idea of introducing sliding in the floor slabs has also been extended to multi-story structures. Several examples of these structures have been studied to evaluate the usefulness of the proposed multiple-slab-sliding (multi-sliding) arrangement.

In Chapter 1, we have studied the response characteristics of a simple single-story shear structure. It is shown that for a one-story structure, the maximum frame deformation can be controlled to any desired level by properly choosing the value of the friction coefficient. Here the concept of a normalized friction coefficient,

chosen with respect to the known non-sliding response has been introduced as a convinient parameter. Several structures of different frequencies have been analyzed and their results have been presented in the response spectrum form. It is observed that a slab slding structure provides better isolation than a base sliding or hystretic structure. The accompanying sliding displacements were observed to be small enough to be accomodated in practice, particularly for medium and high frequency structures. However for more flexible structures, the sliding displacements are observed to be generally on the high side. Also, it is observed that in both base sliding and the proposed slab sliding structures, the magnitudes of the residual displacements that are about the same as those of the maximum sliding displacements. This is probably due to a lack of any recovery mechanism in the sliding structures.

To reduce the extents of residual and sliding displacements, it is, therefore proposed to use a lateral spring supported against the main frame of the structure. The analysis and response results for such an arrangement are presented in Chapter 3. From these results, it is observed that for flexible structures, the spring is generally effective in reducing the residual and sliding displacements without attracting large accelerations or forces on the frame. However, for high frequency structures, it is observed that the introduction of a lateral spring in the system causes rather high slab accelerations and frame deformations as well as increased levels of secondary spectra. Thus a lateral spring is detrimental to high frequency structures. However, as it was observed in Chapter 2, the high frequency structures did not have large sliding displacements. Thus there is no need to reduce them any furthe to start with. The problem existed only in the flexible structures where, as observed in Chapter 3, the provision of a lateral spring is successful in reducing the sliding and sliding displacements without any problems

In Chapter 4, the effect of the vertical acceleration on various sliding structures is investigated. It is observed that the responses of base sliding and spring-assisted sliding structures remained relatively unaffected in the presence of the vertical acceleration. Increased levels of accelerations and frame deformations are, however, noted in the pure slab sliding structures. This increase was shown to be directly related to the maximum positive acceleration value in the vertical acceleration time-history. However, it was shown that such increases in acceleration levels did not lead to any increase in the magnitudes of the secondary floor spectra.

Finally, in Chapter 5, the effectiveness of the slab sliding arrangement for multi-story structures has been investigated. The responses of three-story slab sliding structures with three different frequency characteristics have been examined. The study shows that in the multi-story structures, incorporation of many slab sliding interfaces is much more effective in reducing the structural response than the case when only a base sliding arrangement is provided. The numerical results for the normalized frame deformations, slab accelerations, secondary floor spectra and sliding and residual displacements indicate that a multiple-slab-sliding arrangement can indeed provide a substantial reduction in slab accelerations and frame deformations without causing large displacements in general. Also, the analytical formulation shows that it is possible to select friction coefficient values at different floor levels for a predetermined level of reduction in frame deformations or slab accelerations without performing a detailed dynamic analysis of the slab sliding structure. This is thought to be useful from design viewpoint. Also, it is shown that the acceleration and deformation responses of the structure can be estimated fairly accurately even in the presence of vertical acceleration. It is found that the vertical acceleration does not change the response of base sliding structures, but it leads to increased levels of floor acceleration and frame deformations for the multi-sliding

arrangement. However, the corresponding secondary spectra were again found to be relatively unchanged. In general, it is observed that the response characteristics of a multi-story sliding structure are similar to those of single-story sliding structure. However, this is not true for the residual displacement response. The residual displacements for multi-story structures with multiple-slab-sliding arrangement were observed to be significantly smaller than the corresponding maximum sliding displacements, this being especially true for stiff structures. This is an important observation, since the residual displacements are indicative of the work needed to restore the slabs to their original positions after the seismic event is over.

The stiffness of the site on which the ground motion is recorded seems to be significantly influencing the slding displacement characteristics. In general, it was observed that the ground motion from a soft site caused larger displacements. This is probably due to the fact that a soft site record is dominated by low frequncy content. It is however mentioned that a more detailed study utilizing several recorded ground motions is probably needed to establish useful guidelines for the design of such sliding structures.

In conclusion, this study indicates that the Coulomb damping is a viable option for isolating structures from detrimental effects of earthquake induced ground motions.

References

1. Ahmadi, G., "Stochastic Earthquake Response of Structures on Sliding Foundation", International Journal of Engineering Science, Vol. 21, No.2, 1983, pp 93-102.

2. Ashour, S. A. and Hanson, R. D., "Elastic Seismic Response of Buildings with Supplemental Damping", Department of Civil Engineering, University of Michigan Report No. UMCE 87-1, January 1987.

3. Chopra, A. K., Clough, D. P. and Clough, R. W., "Earthquake Resistance of Buildings with a 'Soft' First Story", Earthquake Engineering and Structural Dynamics, Vol. 1, 1973.

4. Constantinou, M. C. and Tadjabaksh, I. G., "Response of a Sliding Structure to Filtered Random Excitation", Journal of Structural Mechanics, Vol. 12(3), 1984, pp 401-418.

5. Constantinou, M. C. and Tadjabaksh, I. G., "The Optimum Design of a Base Isolation System With Frictional Elements", Earthquake Engineering and Structural Dynamics, Vol. 12, 1984, pp 203-214.

6. Crandall, S. H., Lee, S. S. and Williams, J. H., Jr., "Accumulated Slip of a Friction-Controlled Mass Excited by Earthquake Motions", Transactions of the ASME, December 1974, pp 1094-1098.

7. Den Hartog, J. P., "Forced Vibrations With Combined Coulomb and Viscous Friction", Transactions of the ASME, Vol. 53-9, 1931, pp 107-115.

8. Fintel, M. and Khan, F. R., "Shock Absorbing Soft Story Concept Concept for Multistory Earthquake Structures", Proceedings of the ACI Journal, Vol. 67, No. 29, 1969.

9. Hundal, M. S., "Response of a Base Excited System With Coulomb and Viscous Friction", Journal of Sound and Vibration, 64(3), 1979, pp 371-378.

10. Kelly, J. M. and Beucke, K. E., "A Friction Damped Base Isolation System With Fail-Safe Characteristics", Earthquake Engineering and Structural Dynamics, Vol. 11, 1982, pp 33-56.

11. Lee, S. S., "Accumulated Slip of a Continuous Structure Driven by Friction Under Earthquake Excitation", Technical Report No. 80463-1, Submitted to the National

Science Foundation under Grant No. GI-34945, Mechanical Engineering Department, MIT, May 1974.

12. Levitan, E. S., "Forced Oscillation of a Spring-Mass System Having Combined Coulomb and Viscous Damping", Journal of the Acoustical Society of America, Vol. 32, 1960, pp 1265-1269.

13. Lin, B. C. and Tadjabakhsh, I., "Effect of Vertical Motion on Friction-Driven Isolation Systems", Earthquake Engineering and Structural Dynamics, Vol. 14, 1986, pp 609-622.

14. Malushte, S. R. and Singh, M. P., "Seismic Response of Simple Nonlinear Hysteretic Structures", Technical Report No. VPI-E-87-4, Submitted to the National Science Foundation under Grants No. CEE-8214070 and CEE-8412830, Department of Engineering Science & Mechanics, VPI&SU, April 1987.

15. Malushte, S. R. and Singh, M. P., "Seismic Response of Simple Structures With Coulomb Damping", Proceedings of the Sixth ASCE-Structures Congress held in Orlando, FL, August 1987.

16. Malushte, S. R. and Singh, M. P., "Prediction of Seismic Design Response Spectra Using Ground Characteristics", Technical Report No. VPI-E-87-31, Submitted to the National Science Foundation under Grants No. CEE-8214070 and CEE-8412830, Department of Engineering Science & Mechanics, VPI&SU, September 1987.

17. Malushte, S. R. and Singh, M. P., "A Study of Seismic Response Characteristics of Structures With Friction Damping", Earthquake Engineering and Structural Dynamics, (in press).

18. Meirovitch, L. and Silverberg, L. M., "Control of Structures Subjected to Seismic Excitation", Journal of Engineering Mechanics, ASCE, Vol. 109, No. 2, April 1983, pp 604-618.

19. Mostaghel, N., Hejazi, M. and Tanbakuchi, J., "Response of Sliding Structures to Harmonic Support Motion", Earthquake Engineering and Structural Dynamics, Vol. 11, 1983, pp 355-366.

20. Mostaghel, N. and Tanbakuchi, J., "Response of Sliding Structures to Earthquake Support Motion", Earthquake Engineering and Structural Dynamics, Vol. 11, 1983, pp 729-748.

21. Nigam, N. C. and Jennings, P. C., "Calculation of Response Spectra from Strong-Motion Earthquake Records", Bulletin of the Seismological Society of America, Vol. 59, No. 2, April 1969.

22. Noguchi, T., "The Responses of a Building on Sliding Pads to Two Earthquake Models", Journal of Sound and Vibration, Vol. 103(3), 1985, pp 437-442.

23. Pall, A. S. and Marsh, C., "Seismic Response of Friction Damped Braced Structures", Journal of the Structural Division, Proceedings of the ASCE, June 1982, pp 1313-1323.

24. Pan, T-C. and Kelly, J. M., "Seismic Response of Base-Isolated Structures with Vertical-Rocking Coupling", Earthquake Engineering and Structural Dynamics, Vol. 14, 1984, pp 681-702.

25. Pratt, T. K. and Williams, R., "Non-linear Analysis of Stick/Slip Motion", Journal of Sound and Vibration, Vol. 74, No. 4, April 1981, pp 531-542.

26. Qamaruddin, M., Arya, A. S. and Chandra, B., "Seismic Response of Brick Buildings With Sliding Substructure", Journal of Structural Engineering, ASCE, Vol 112, No. 3, March 1986, pp 558-572.

27. Singh, M. P. and Malushte, S. R., "Seismic Response of Structures With Coulomb Damping", Proceedings of the Seventh ASCE-EMD Conference held in Blacksburg, VA, May 1988.

28. Skinner, R. I., Beck, J. L. and Bycroft, G. N., "A Practical System For Isolating Structures From Earthquake Attack", Earthquake Engineering and Structural Dynamics, Vol. 3, 1975, pp 297-309.

29. Skinner, R. I., Kelly, J. M. and Heine, A. J., "Hysteretic Dampers for Earthquake-Resistant Structures", Earthquake Engineering and Structural Dynamics, Vol. 3, 1975.

30. Westermo, B. and Udwadia, F., "Periodic Response of a Sliding Oscillator System to Harmonic Excitation", Earthquake Engineering and Structural Dynamics, Vol. 11, 1983, pp 135-146.

31. Williams, A., "Flexible 'First-Story' Construction For Earthquake Resistance", Discussion in Transactions of the ASCE, Vol. 100, 1935.

32. Williams, J. H., Jr., "Designing Earthquake-Resistant Structures", Technology Review, MIT Press, October/November 1973.

33. Yao, J. T. P. and Sae-Ung, S., "Active Control of Building Structures", Journal of the Engineering Mechanics Division, ASCE, Vol. 104, No. EM2, April 1978, pp 335-350.

34. Younis, C. J. and Tadjabakhsh, I. G., "Response of Sliding Rigid Structure to Base Excitation", Journal of Engineering Mechanics, ASCE, Vol. 110, No. 3, March 1984, pp 417-432.

APPENDIX I

Information About the Recorded Ground Motions Used in the Study

In this appendix, we present some relevant information about the five ground motions used in this study. First, the information about the site location and stiffness, epicentral distance and the recorded duration is given in Table A1.1. In Table A1.2, the peak ground motion characteristics of the time histories for the horizontal and vertical components of the ground motions listed in Table A1.1 are given. Finally, the plots of the time histories of the horizontal component of the ground motions are given in Figs. A1.1 to A1.5. It is noted that these plots are drawn after normalizing the available time histories to a peak acceleration value of 0.50 G. The information about the seismic inputs was obtained from the tapes supplied by the Earthquake Engineering Research Laboratory (EERL) at the California Institute of Technonlogy (also see reference 16).

TABLE A1.1

Location and Other Relevant Data About the Selected Ground Motions

No.	Recording Station	Long. (N) ° ' "	Lat. (N) ° ' "	Site Type	Year of Record	Epicentral Distance (kms)
1	El Centro Site Imperial Valley Irrigation Dist.	115 32 55	32 47 43	Soft	May 1940	11.56
2	Ferndale City Hall	124 15 00	40 34 00	Medium	Oct 1951	56.47
3	Lake Hughes, Array Station No. 01, California	118 26 24	34 40 30	Hard	Feb 1971	30.98
4	Lake Hughes, Array Station No. 04, California	118 28 48	34 38 30	Hard	Feb 1971	27.94
5	Lake Hughes, Array Station No. 09, California	118 33 42	34 36 30	Hard	Feb 1971	27.79

TABLE A1.2

Duration and Peak Ground Motion Characteristics of the Input

No.	Duration (sec)	Component Direction	Max. Disp. (inches)	Max. Vel. (ft/sec)	Max. Acc. (G-Units)
1	53.48	S90W	7.788	1.2113	0.214
1	53.48	VERT	2.188	0.3555	0.210
2	55.90	N21E	2.636	0.5157	0.156
2	55.90	VERT	0.637	0.0724	0.027
3	60.20	N21E	1.350	0.5890	0.148
3	60.20	VERT	1.122	0.3826	0.095
4	37.02	S21W	0.686	0.2827	0.146
4	37.02	VERT	0.632	0.2345	0.154
5	35.02	N69W	0.950	0.1477	0.112
5	35.02	VERT	0.872	0.1000	0.073

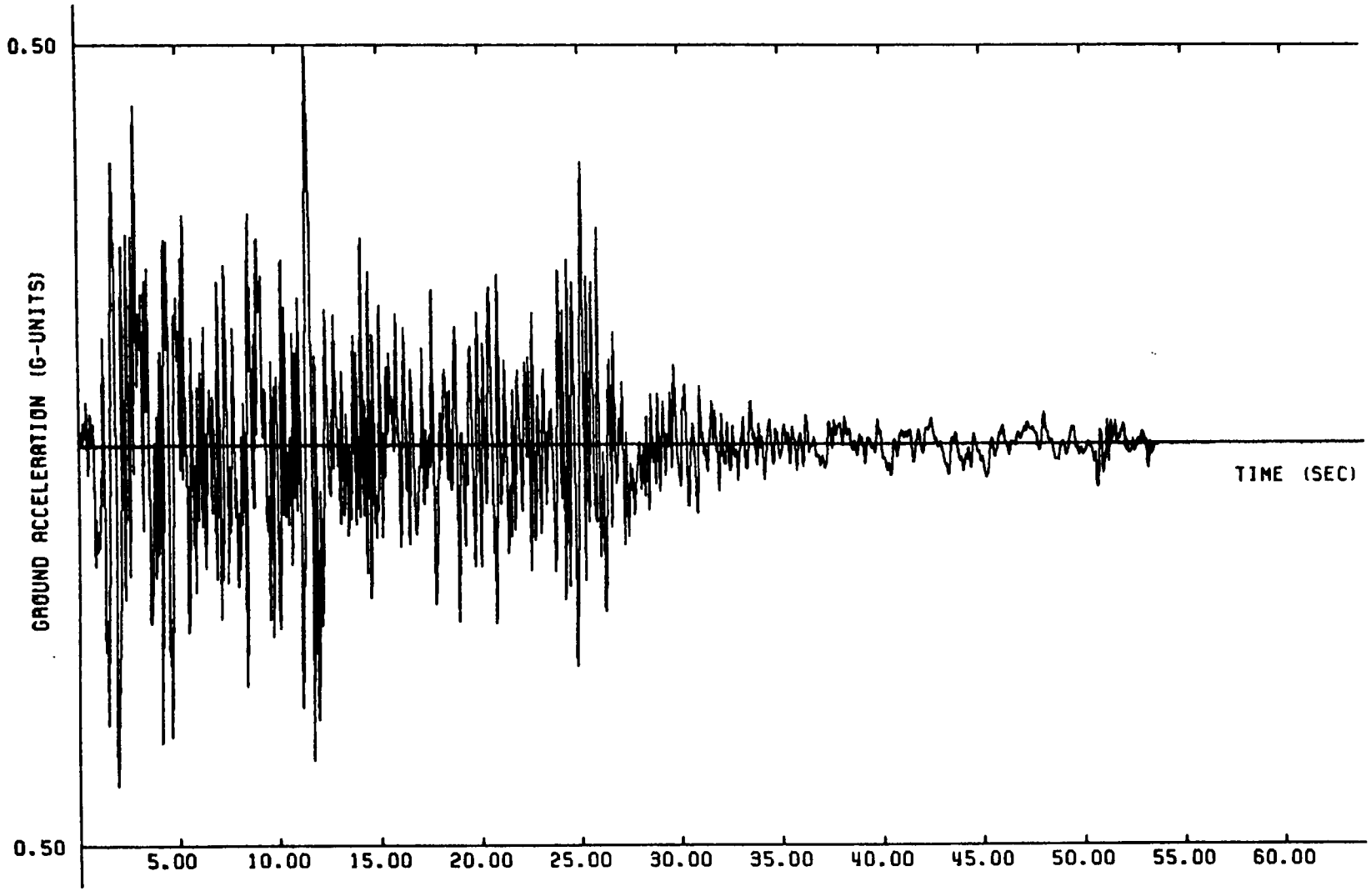

FIG. A1.1 ACCELERATION TIME HISTORY OF GROUND MOTION 1 - HORZ. COMPONENT

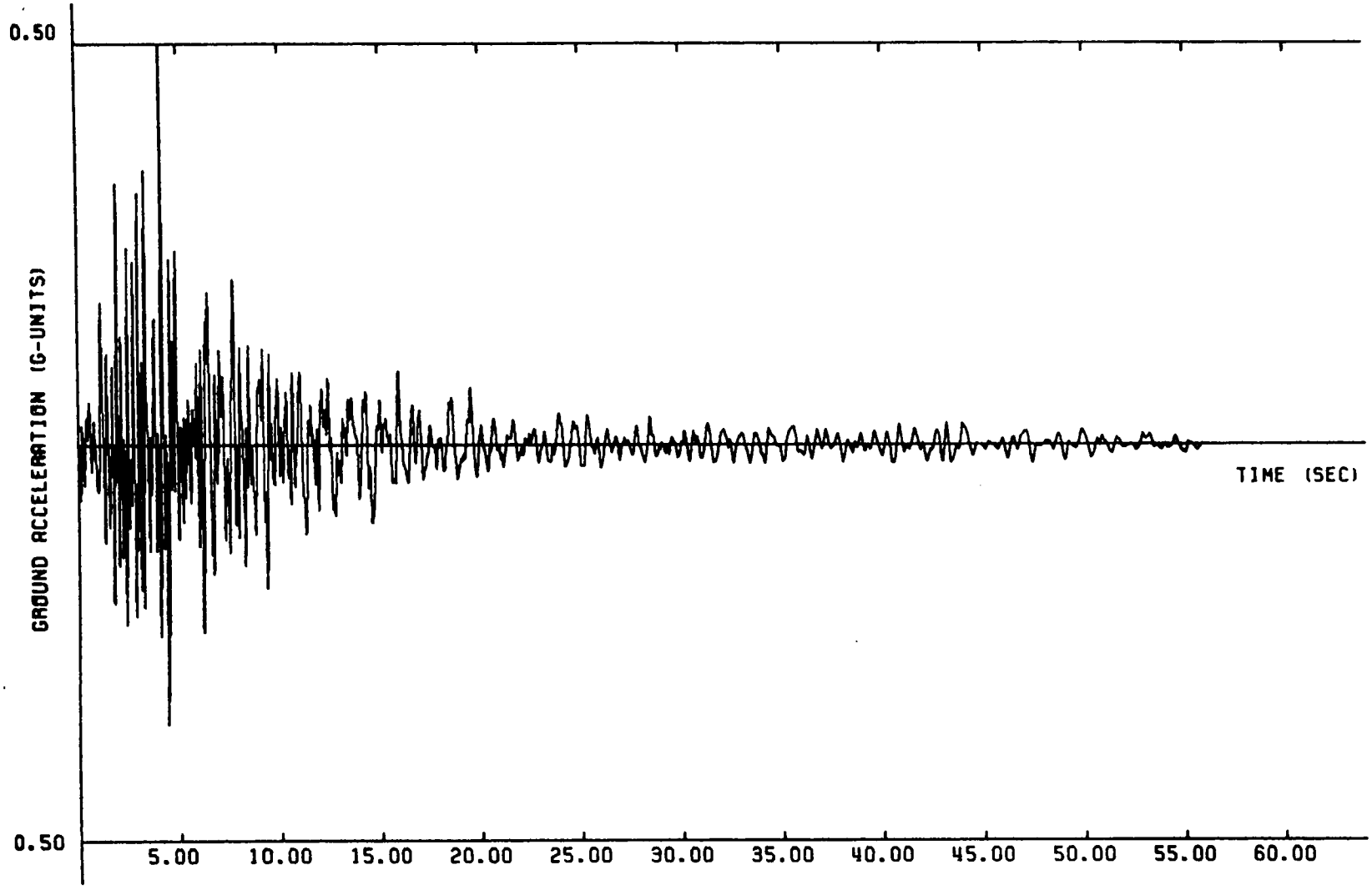

FIG. A1.2 ACCELERATION TIME HISTORY OF GROUND MOTION 2 - HORZ. COMPONENT

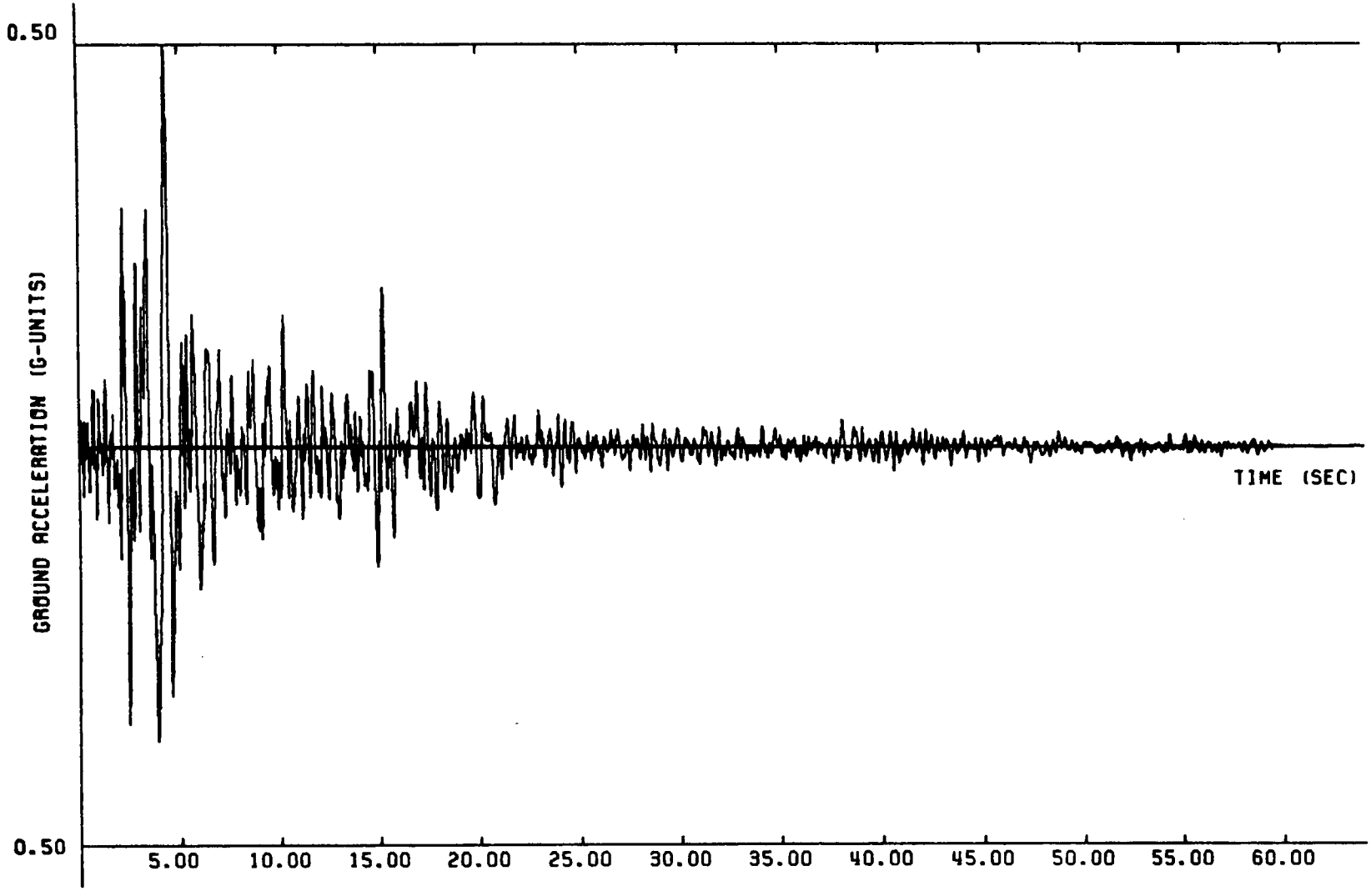

FIG. A1.3 ACCELERATION TIME HISTORY OF GROUND MOTION 3 - HORZ. COMPONENT

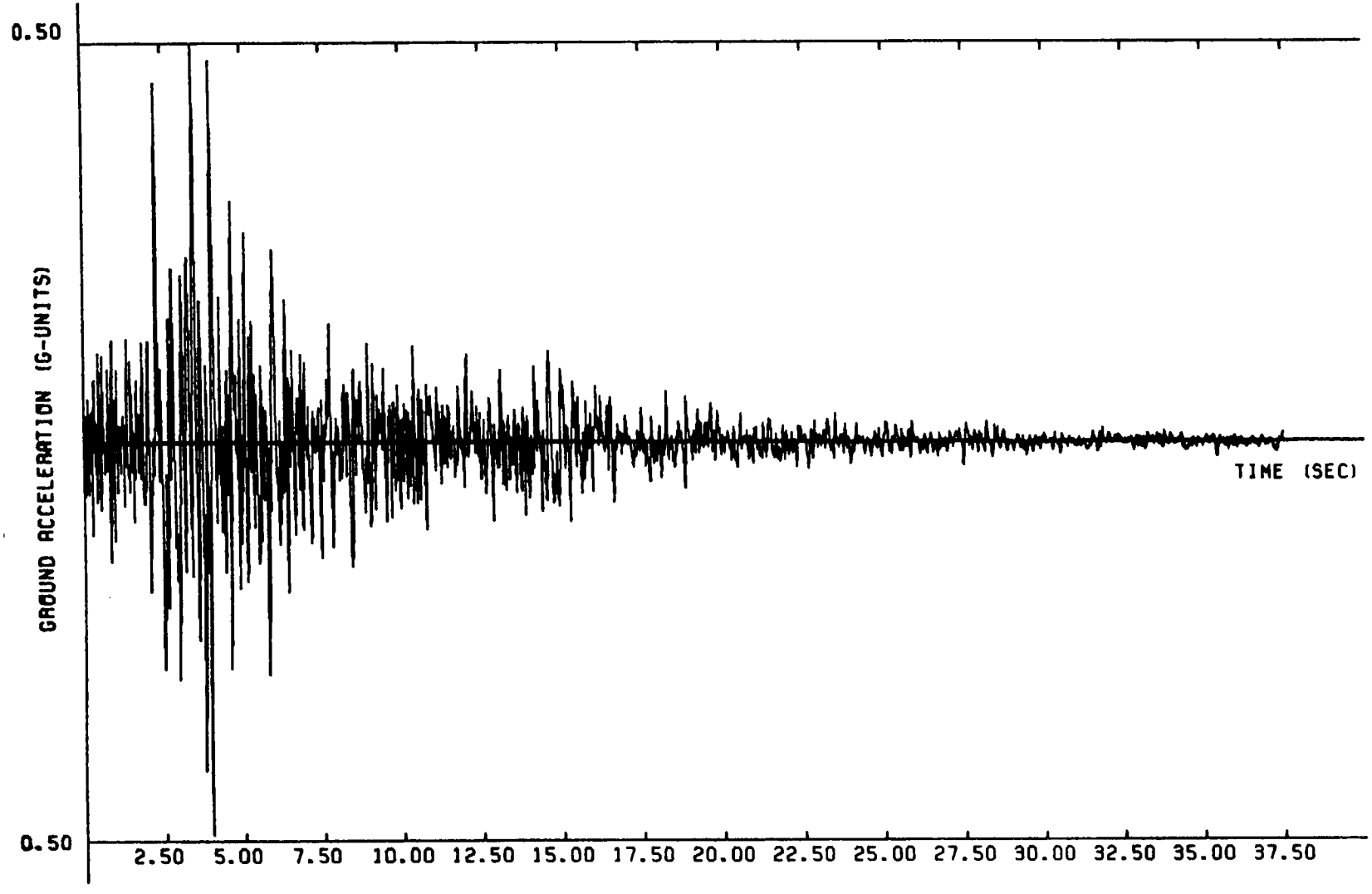

FIG. A1.4 ACCELERATION TIME HISTORY OF GROUND MOTION 4 - HORZ. COMPONENT

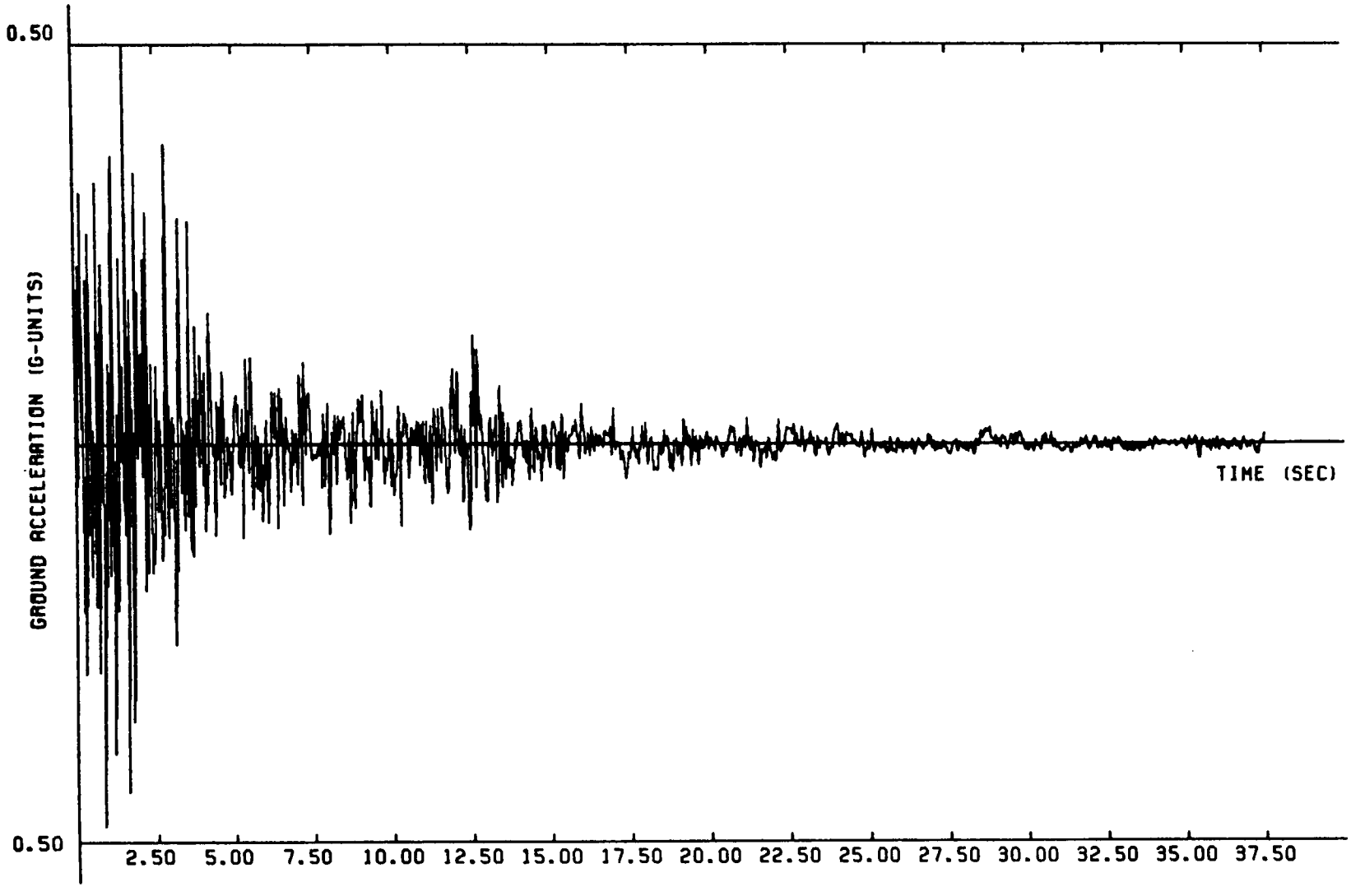

FIG. A1.5 ACCELERATION TIME HISTORY OF GROUND MOTION 5 - HORZ. COMPONENT

APPENDIX II

Expressions Mass & Stiffness Matrices and Load Vector of Eq. (5.2)

The following are the expressions for the mass matrix [M], stiffness matrix [K] and the load vector { $\ddot{X}_g$ } quantities that appear in Eq. (5.2). The expressions are valid for a shear beam structure.

$$[M] = \begin{bmatrix} m_1 & 0 & 0 & . & . & . \\ 0 & m_2 & . & . & . & . \\ . & . & m_3 & . & . & . \\ . & . & . & . & . & . \\ . & . & . & . & m_{n-1} & 0 \\ . & . & . & . & 0 & m_n \end{bmatrix} \tag{A2.1}$$

$$[K] = \begin{bmatrix} k_1 + k_2 & -k_2 & 0 & . & . & . \\ -k_2 & k_2 + k_3 & -k_3 & . & . & . \\ 0 & -k_3 & k_3 + k_4 & . & . & . \\ . & 0 & . & . & . & . \\ . & . & . & . & k_{n-1} + k_n & -k_n \\ . & . & . & . & -k_n & k_n \end{bmatrix} \tag{A2.2}$$

$$\{ \ddot{X}_g \} = [M] \begin{Bmatrix} 1 \\ 1 \\ 1 \\ . \\ . \\ 1 \\ 1 \end{Bmatrix} \ddot{x}_g \qquad (A2.3)$$

The vita has been removed from the scanned document